NPS67-82-012

NAVAL POSTGRADUATE SCHOOL
Monterey, California

THESIS

AERODYNAMICALLY EFFICIENT
GRADIENT REFRACTIVE INDEX
MISSILE SEEKER LENS

by

Herbert M. Carr III

October 1982

Thesis Advisor: A. E. Fuhs

Approved for public release; distribution unlimited.

Prepared for: Defense Advanced Research Projects Agency
1400 Wilson Boulevard
Arlington, VA 22209

NAVAL POSTGRADUATE SCHOOL
Monterey, California

Rear Admiral J. J. Ekelund
Superintendent

David A. Schrady
Provost

This thesis prepared in conjunction with research supported in part by Defense Advanced Research Projects Agency under DARPA Order 4035.

REPORT DOCUMENTATION PAGE

READ INSTRUCTIONS BEFORE COMPLETING FORM

1. REPORT NUMBER: NPS67-82-012	2. GOVT ACCESSION NO.
3. RECIPIENT'S CATALOG NUMBER	
4. TITLE (and Subtitle): Aerodynamically Efficient Gradient Refractive Index Missile Seeker Lens	5. TYPE OF REPORT & PERIOD COVERED: Master's Thesis; October, 1982
6. PERFORMING ORG. REPORT NUMBER	
7. AUTHOR(s): Herbert M. Carr III	8. CONTRACT OR GRANT NUMBER(s): DARPA ORDER 4035
9. PERFORMING ORGANIZATION NAME AND ADDRESS: Naval Postgraduate School, Monterey, California 93940	10. PROGRAM ELEMENT, PROJECT, TASK AREA & WORK UNIT NUMBERS
11. CONTROLLING OFFICE NAME AND ADDRESS: Naval Postgraduate School, Monterey, California 93940	12. REPORT DATE: October, 1982
	13. NUMBER OF PAGES: 483
14. MONITORING AGENCY NAME & ADDRESS (if different from Controlling Office): LTC. Rene Larriva, Defense Advanced Research Projects Agency, 1400 Wilson Blvd., Arlington, VA 22209	15. SECURITY CLASS. (of this report): Unclassified
	15a. DECLASSIFICATION/DOWNGRADING SCHEDULE

16. DISTRIBUTION STATEMENT (of this Report)

Approved for public release; distribution unlimited.

17. DISTRIBUTION STATEMENT (of the abstract entered in Block 20, if different from Report)

18. SUPPLEMENTARY NOTES

19. KEY WORDS (Continue on reverse side if necessary and identify by block number)

Missile Sensors
Missile Aerodynamics
Projectile Aerodynamics
Gradient Refractive Index
Lens Design
Conical Optics
Conical Lens
Guided Projectile

20. ABSTRACT (Continue on reverse side if necessary and identify by block number)

This thesis explores the use of a pointed seeker lens designed using a spherically symmetric gradient refractive index (GRIN). The design helps to solve the current design conflict between optical quality and aerodynamic drag inherent in hemispherical seeker lenses. Equations for lens design and the evaluation of off-axis lens performance have been developed for both a homogeneous version and a GRIN version of the pointed

#20 - ABSTRACT - (CONTINUED)

seeker lens. The homogeneous lens is used as a comparison and a check for the GRIN lens. A FORTRAN program (GISL) has been written and employed to evaluate and compare both the homogeneous lens and many different configurations of possible GRIN lens designs. Results indicate that the GRIN lens has highly superior off-axis imaging performance as compared to the homogeneous lens. The best results were obtained for the GRIN lens with a fifty percent, positive, spherically symmetric gradient index with center of symmetry interior to the lens. Only very slightly inferior performance was observed with a five percent version of the same lens; such a lens possible can be manufactured today. GRIN lens performance also indicates that for objects off-axis by more than 17.2 degrees a large scale, multiple element sensor array may be required; with such a sensor array, objects off-axis by more than 37.2 degrees may require mirror elements to compensate for image movement.

Approved for public release; distribution unlimited.

Aerodynamically Efficient Gradient Refractive Index Missile Seeker Lens

by

Herbert M. Carr III
Captain, United States Army
B.S., University of Texas, 1971

Submitted in partial fulfillment of the
requirements for the degree of

MASTER OF SCIENCE IN ENGINEERING SCIENCE

from the

NAVAL POSTGRADUATE SCHOOL
October 1982

ABSTRACT

This thesis explores the use of a pointed seeker lens designed using a spherically symmetric gradient refractive index (GRIN). The design helps to solve the current design conflict between optical quality and aerodynamic drag inherent in hemispherical seeker lenses. Equations for lens design and the evaluation of off-axis lens performance have been developed for both a homogeneous version and a GRIN version of the pointed seeker lens. The homogeneous lens is used as a comparison and a check for the GRIN lens. A FORTRAN program (GISL) has been written and employed to evaluate and compare both the homogeneous lens and many different configurations of possible GRIN lens designs. Results indicate that the GRIN lens has highly superior off-axis imaging performance as compared to the homogeneous lens. The best results were obtained for the GRIN lens with a fifty percent, positive, spherically symmetric gradient index with center of symmetry interior to the lens. Only very slightly inferior performance was observed with a five percent version of the same lens; such a lens possibly can be manufactured today. GRIN lens performance also indicates that for objects off-axis by more than 17.2 degrees a large scale, multiple element sensor array may be required; with such a sensor array, objects off-axis by more than 37.2 degrees may require mirror elements to compensate for image movement.

TABLE OF CONTENTS

LIST OF TABLES

LIST OF FIGURES

LIST OF SYMBOLS

Symbol in Equations	FORTRAN Symbol	Equation Number Where First Introduced	Definition	Units
a	A	113	Parameter of gradient index function	Nondimensional
a		41	Defined by Equation 44	
A		24	Defined by Equation 25	
A		137	Defined by Equation 138	
A_1		161	Defined by Equation 164	
A_2		160	Defined by Equation 161	
A_3		169	Defined by Equation 170	
A_5		179	Defined by Equation 184	
A_6		178	Defined by Equation 181	
AB	AB	30	Line segment from A to B, from nose to apex of cone	Nondimensional
b	B	113	Parameter of gradient index function	Nondimensional
b		41	Defined by Equation 45	
B		24,137	Defined by Equation 26	
B_1		161	Defined by Equation 165	
B_2		160	Defined by Equation 162	
B_5		179	Defined by Equation 185	
B_6		178	Defined by Equation 182	
BF	BF	2	Line segement from B to F, focal length	Nondimensional
c		41	Defined by Equation 46	

C		24	Defined by Equation 27	
C		137	Defined by Equation 139	
C_1		161	Defined by Equation 166	
C_2		160	Defined by Equation 163	
C_6		178	Defined by Equation 183	
d		41	Defined by Equation 47	
d	ERROR	142	Error parameter in meridian plane ray intercept with outside surface	Nondimensional
D	D2	72	Geometrical length of skew ray in homogeneous lens	Nondimensional
D'	D3	95	Geometrical length of skew ray from cone to image plane	Nondimensional
DYDXN(J)	DYDXN(J)	20	Slope of normal to outside surface in the meridian plane at the Jth point	Nondimensional
DYDXT(J)	DYDXT(J)	21	Slope of outside surface tangent in the meridian plane at the Jth point	Nondimensional
$DYDXN_{PIM}$		51	Slope of normal to outside surface in the meridian plane. Interpolated value	Nondimensional
e	E	108	Spherical GRIN scalar invariant	Nondimensional
e		41	Defined by Equation 48	
f(x,y,z)			General function of x, y, and z	
f_x		82	Partial derivative of function f with respect to x	

f_y		82	Partial derivative of function f with respect to y	
f_z		82	Partial derivative of function f with respect to z	
i		186	Summation index	
$\hat{i}$		53	Unit vector in the x direction	
I	I	3	Number of angular increments in lens design algorithm	
I_A			Fraction of absorbed radiant energy during transmission through the lens	Nondimensional
I_1	I1	17	Angle of incidence with respect to local normal at outside surface	Radians
I_1'	I1P	16	Angle of refraction with respect to the local normal at the outside surface	Radians
I_2	I2	12	Angle of incidence with respect to the local normal at the inside surface	Radians
I_2'	I2P	10	Angle of refraction with respect to the local normal at the inside surface	Radians
I_R		102	Fraction of reflected radiant energy at the surface interface	Nondimensional
I_T	NINCTY	102	Fraction of transmitted radiant energy at the interface	Nondimensional
I_i	NINCTY(G)	190	Intensity element of intensity summation	Nondimensional

I_{av}	XMAVE	190	Average value of ray intensity	Nondimensional
$\hat{j}$		53	Unit vector in the x-direction	
J	J	4	Ray Number index	
k	LK	63	Direction cosine, x-direction, of outside surface normal	
k'	LKP	83	Direction cosine, z-direction, of inside surface normal	
$\hat{k}$		55	Unit vector in y-direction	
K	CK	58	x-direction cosine of ray exterior to lens surface	
K'	CKP	63	x-direction cosine of ray inside the lens	
K"	CKPP	92	x-direction cosine of the ray after refraction by the lens	
l	LL	64	y-direction cosine of outside surface normal	
l'	LLP	84	y-direction cosine of inside surface normal	
L	CL	58	y-direction cosine of the ray external to the lens	
L'	CLP	64	y-direction cosine of the ray internal to the lens	
L"	CLPP	93	y-direction cosine of the ray after diffraction by the lens	

l_0		122	Generalized z-direction cosine of the initial ray direction in GRIN	
m	LM	65	z-direction cosine of outside surface normal	
m		38	Generalized slope of a line segment	
m'	LMP	85	z-direction cosine of inside surface normal	
M	CM	58	z-direction cosine of ray external to the lens	
M'	CMP	65	z-direction cosine of ray internal to the lens	
M"	CMPP	94	z-direction cosine of ray after refraction by the lens	
n		108	Generalized local value of the gradient refractive index	Nondimensional
n_0		109	Generalized value of the gradient index at the initial intercept point	Nondimensional
n_2	N2	125	Local lens interior value of the GRIN	Nondimensional
N		186	Generalized nth value of summation index	
N_1	N1	1	Homogeneous index of refraction of medium 1, exterior to lens	Nondimensional
N_2	N2	1	Homogeneous index of refraction of medium 2, interior to lens	Nondimensional
N_3	N3	12	Homogeneous index of refraction of medium 3, behind the lens	Nondimensional
$\bar{N}'$		55	Normal vector at the point of intersection at the outside surface	

$\bar{N}_m$		53	Normal vector in the meridian plane corresponding to $\bar{N}'$	
$\hat{N}_i$		80	Generalized surface normal unit vector	
N_{ti}		104	Ratio of indices of refraction at an interface	Nondimensional
$\hat{N}_{po}$		148	Unit normal vector to plane of skew ray	
N_{pox}	NPOX	149	Defined by Equation 150	
N_{poy}	NPOY	149	Defined by equation 151	
N_{poz}	NPOZ	149	Defined by Equation 152	
OB	OSYMB	126	Line segment from the center of symmetry of the GRIN function, O_s, to B, the origin	Nondimensional
O_s		112	Location of the GRIN center of symmetry on the lens axis	Nondimensional
P_0		120	Generalized initial x-direction cosine of the GRIN ray	
P_1		76	Defined by Equation 77	
P_2		76	Defined by Equation 78	
P_3		76	Defined by Equation 79	
PAR1	PAR1	40	Defined by Equation 41	
PAR2	PAR2	40	Defined by Equation 42	
PAR3	PAR3	40	Defined by Equation 43	
q_0		121	Generalized y-direction cosine of initial GRIN ray direction	
Q		5	Perpendicular distance between ray and line parallel to ray through the origin at B in Figure 3	Nondimensional

QP		37	Line segment defined by Figure 5	Nondimensional
QP'		37	Line segment defined by Figure 5	Nondimensional
r	RAD	108	Radial coordinate in GRIN from O_s	Nondimensional
r_0	R0	108	Initial value of r at ray intercept point	Nondimensional
$\hat{r}_0$		146	Unit vector in direction from O_s to intercept point on outside surface	
r_{ox}	R0X	151	x-direction cosine of $\hat{r}_0$	
r_{oy}	ROY	150	y-direction cosine of $\hat{r}_0$	
r_{oz}	ROZ	150	z-direction cosine of $\hat{r}_0$	
$\hat{r}_{iH}$		156	Unit vector from O_s to point of homogeneous intercept on inside surface	
r_g	RADH	160	Geometrical radius from O_s to cone during iteration for the inside surface intercept	Nondimensional
r_{PI}	RAD	174	Radius to inside surface intercept as found by interation	Nondimensional
r_{ll}		103	Reflection coefficient for parallel E vector	Nondimensional
r		104	Reflection coefficient for perpendicular E vector	Nondimensional
R	R	2	Maximum inside radius of cone measured from the lens axis	Meters
R	RAD	33	Radius of circle in the y-z plane	Nondimensional
$\hat{R}$		57	Unit vector in the ray direction	

$\bar{R}'$		62	Vector in the direction of refracted ray	
R_z	RZERO	113	Maximum possible radius in GRIN	Nondimensional
S	S	51	Line segment in the meridian plane; see Figure 5	Nondimensional
ST	ST	51	Inclusive line segment in the meridian plane; see Figure 5	Nondimensional
T	T	14	Edge thickness of the lens	Nondimensional
U	U	17	Direction of the ray with respect to the lens axis in the meridian plane	Radians
U'	UP	13	Direction of the ray inside the lens with respect to the lens axis in the meridian plane	Radians
U"	UDP	4	Angle between ray and lens axis at the focal point in the meridian plane	Radians
v		115	Integration variable	Nondimensional
x		22	General x-coordinate along lens axis	Nondimensional
x'		30	General x-coordinate in the grid plane (tilted)	Nondimensional
$\|x\|$		2	Absolute value of any quantity x	
x_0	XO	40	x-coordinate of outside surface skew ray intercept	Nondimensional
x_i	XI	69	x-coordinate of inside surface intercept	Nondimensional

x_{im}	XIM	95	x-coordinate in the image plane (Spot Diagram)	Nondimensional
x_{1H}	X1H	130	First x-coordinate of imaginary homogeneous intercept in GRIN design	Nondimensional
x_p	XP	135	x-coordinate of the first intermediate point on the GRIN ray during iteration in the design algorithm	Nondimensional
x'_{1H}	X1HP	141	Second x-coordinate of imaginary homogeneous intercept in GRIN design	Nondimensional
$x'''_p \cdots$	XP	143	Successive values of x_p during iteration	Nondimensional
x_{PIM}		52	x-coordinate of ray intercept in meridian plane	Nondimensional
$X_1(J)$	X1(J)	14	x-coordinate of the Jth ray on the outside surface in the meridian plane	Nondimensional
$X_2(J)$	X2(J)	5	x-coordinate of the Jth ray on the inside surface in the meridian plane	Nondimensional
y		22	General y-coordinate (vertical)	Nondimensional
y'		31	y-coordinate in the tilted grid plane	Nondimensional
Y_0	Y0	49	y-coordinate of outside surface skew ray intercept	Nondimensional
Y_i	YI	170	y-coordinate of inside surface skew ray intercept	Nondimensional

y_{im}	YIM	96	y-coordinate of the skew ray in the image plane (Spot Diagram)	Nondimensional
y_{1H}	Y1H	131	First y-coordinate of imaginary HIN intercept in GRIN design (iteration)	Nondimensional
y'_{1H}	Y1HP	137	Second y-coordinate of imaginary HIN intercept in GRIN design (iteration)	Nondimensional
y_p	YP	136	x-coordinate of the first intermediate point on the GRIN ray during iteration in the design algorithm	Nondimensional
y_p ...	YP	144	Successive values of y_p during iteration	Nondimensional
y_c	YCENTR	186	y-coordinate of the image centroid in the Spot Diagram	Nondimensional
Y_i	YIM(G)	186	Individual y-coordinates of image plane ray intercept	Nondimensional
$y_1(J)$	Y1(J)	15	y-coordinate of the Jth ray on the outside surface in the meridian plane	Nondimensional
$y_2(J)$	J2(J)	5	y-coordinate of the ray on the inside surface in the meridian plane	Nondimensional
z		32	General z-coordinate (horizontal)	Nondimensional
z'		32	z-coordinate in the grid plane (tilted)	Nondimensional
z_0	ZO	50	z-coordinate of the skew ray on the outside surface	Nondimensional
z_i	ZI	71	z-coordinate of the skew ray on the inside surface (cone)	Nondimensional

z_{im}	ZIM	97	z-coordinate of the skew ray in the image plane (Spot Diagram)	Nondimensional
α	ALPHA	2	Cone half-angle	Radians
α_p	ALFAP	30	Grid plane tilt angle with respect to the lens axis	Radians/Degrees
β	BETA	2	Total angle between lens axis and the point of maximum radius of the cone; measured at the focal point	Radians
γ	GAMMA	29	Nose half-angle (opaque region)	Radians
δ		120	Defined by Equation 124	
$\Delta U''$	DLUDP	3	Angle between successive rays at the focal point	Radians
Δx		52	Incremental change in x; see Figure 5	
Δy		52	Incremental change in y; see Figure 5	
ε	EPSILON	109	Sign function (± 1)	
ζ	ZETA	134	Angle between instantaneous GRIN ray direction and the lens axis in the meridian plane	Radians
η		120	Defined by Equation 123	
θ		108	Generalized angular coordinate of GRIN ray in the plane of the ray	Radians
θ_1		1	Generalized angle of incidence with respect to the local normal	Radians
θ_2		1	Generalized angle of refraction with respect to the local normal	Radians
θ_0	THETA0	108	Reference (at surface intercept) in GRIN	Radians

θ_H	THETAH	125	Iteration trial value of θ	Radians
θ_T		125	Total angular GRIN coordinate	Radians
θ_p	THETAP	173	Trial values of θ during iteration	Radians
θ'_p	XNEW	173	Revised trial value of θ during iteration	Radians
μ		54	Angle between meridian plane and the point of intersection on the outside surface	Radians
π	PI	13	Proportionality factor between the circumference and the diameter of a circle; 3.14159...	Radians
σ_r	RMSRAD	189	Spot size; RMS radius of image	Nondimensional
σ_y	SIGMAY	188	Standard deviation of y-coordinates of rays in the Spot Diagram	Nondimensional
σ_z	SIGMAZ	187	z-standard deviation of rays in the Spot Diagram	Nondimensional
ϕ	PHI	57	Angle between skew ray and the outside surface with respect to the surface normal	Radians
ϕ'	PHIP	61	Refraction angle between skew ray and the outside surface normal	Radians
ϕ_i	PHII	90	Angle of skew ray intercept with respect to the inside surface normal	Radians
ϕ'_i	PHIIP	91	Refraction angle of skew ray with respect to the inside surface normal	Radians

ψ	PSI	118	Angle between skew ray direction and radial direction from O_s	Radians
ψ_0	PSI0	109	Initial value of angle ψ at point of intercept at outside surface	Radians

ACKNOWLEDGEMENTS

The author would like to express his sincere appreciation to Distinguished Professor Allen E. Fuhs for his invaluable guidance, friendship, and time away from sabbatical. Without him this thesis would not have been possible.

The author would also like to thank Dr. Oded Amichai for his friendship and his assistance in many areas most notably in the intricacies of the IBM 3033.

I. INTRODUCTION

Historically, the design of tactical missiles employing passive or semiactive infrared (IR) seekers has involved a difficult compromise between aerodynamic requirements and optical or seeker requirements. Whereas aerodynamically the missile nose region should be sharp in order to reduce drag, optically it should be hemispherically shaped for image quality and as large as possible to increase aperture and therefore acquisition or tracking range. Some IR homing missiles designed for very short range anti-armor missions have totally ignored nose drag in order to optimize seeker performance while other designs for longer range missiles requiring high cruise velocities and greater aerodynamic efficiency have used the blunted ogive as a compromise. There have not been any IR designs which have ignored optics in favor of aerodynamics; nor has there been employed a pointed seeker lens with the desired optical qualities.

In order to increase the performance of optically guided missiles beyond the current state of development, the conflict between aerodynamic requirements and optical restrictions must be resolved. Significant improvement in missile performance by increasing thrust is not likely due to the highly advanced state of propulsion today. One way to resolve the aerodynamics-optics problem is to design a pointed lens which has, if not

imaging quality, enough optical performance to allow the reduction of tracking data.

The lens must be in the general shape of a cone or ogive with half angle compatible with the design free stream Mach number in order to maintain an attached shock wave. Such a spike-shaped lens might also be used in the diffuser portion of an optically guided ramjet with nose inlet to conserve stagnation pressure. A diffuser-lens may benefit by a semi-isentropic spike shaped lens.

Poor optical performance due to the pointed shape of sharp lenses has precluded their use. Gradient Refractive Index (GRIN) materials, however, permit the lens designer the freedom to spatially vary the lens index of refraction to compensate for a traditionally poor optical shape. Although the use of GRIN has seen widespread use in fiber optics technology, it has been used infrequently in lens applications until recently. Lens designers are discovering that multiple-element photographic objectives may be redesigned using a two-element gradient lens [1]. It should be noted, however, that such GRIN lens have not yet been successfully fabricated even though large index changes in glass have been accomplished by the diffusion of doped electropolarizable ions [2]. Extensive research is being conducted in the creation of ever larger and more precise gradients. A total change in refractive index of approximately five percent is currently attainable.

At the Naval Postgraduate School, Frazier [3], Terrell [4], and Amichai [5] have studied GRIN as applied to the sharp lens problem. The brief introduction by Frazier was followed by Terrell who designed a sharp lens having a conical outside surface and a variable inner surface using a homogeneous index (HIN) and then also briefly touched on the GRIN application. Amichai extended Terrell's lens to the GRIN case and included preliminary results from this thesis in a computer routine intended as a framework for lens optimization by following researchers.

This thesis investigates the design and off-axis performance (skew rays) of a GRIN seeker lens having a variable outer surface and a fixed right circular cone as an inside surface. The variable outside surface is determined by the character of the spherical gradient employed and varies from a pseudo ogive to an approximate isentropic spike as shown in Figure 1. First, the theory of the HIN lens is developed, followed by the design of a homogeneous lens intended both as a comparison and a check for the GRIN lens theory and the design which follows. Lens performance parameters are discussed and results presented for both the HIN and GRIN lenses.

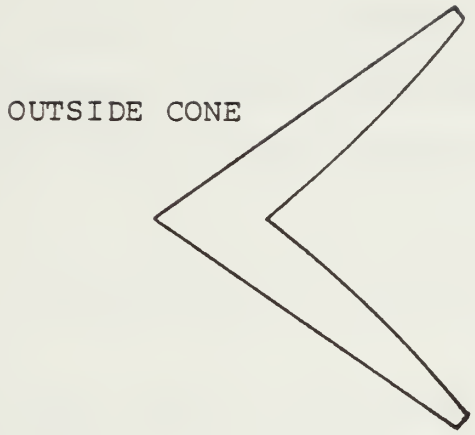

(a) Terrell's Lens With Conical Outer Surface

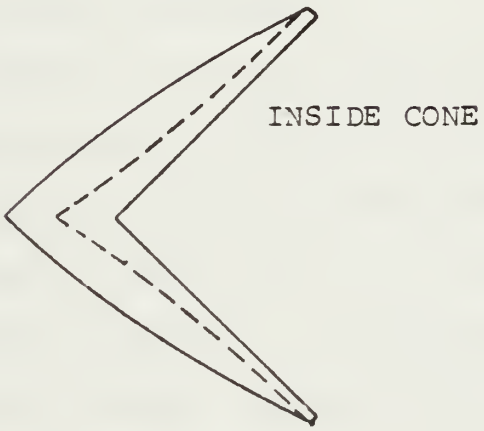

(b) Lens Shapes In This Thesis With Conical Inner Surface.

Figure 1. Lens Shapes

II. THE HOMOGENEOUS LENS

A. THEORY

Snell's law is the cornerstone of contemporary lens design in homogeneous optical materials. In the HIN case Snell's law is used in the familiar form

$$N_1 \sin \theta_1 = N_2 \sin \theta_2 \qquad (1)$$

where N_i is the index of refraction of the material corresponding to surface intercept angle θ_i, with respect to the surface normal, at the interface between surfaces. Lens geometry and the relative values of N_i determine the resultant optical behavior.

B. ASSUMPTIONS AND SIGN CONVENTION

In order to simplify the design and analysis of the seeker lens problem, certain assumptions have been introduced. Although energy loss upon transmission through the lens at each surface is calculated, it is assumed that the light is monochromatic radiation, time dependent electric and magnetic fields. Light impinging upon the lens is assumed to have a planar wave front as if propagating from an object at infinity. The presence of a shock wave attached to the lens is ignored as are any other regions of expansion or compression in the flow field about the lens [6]. Furthermore, the index of refraction of the free stream is assumed

to be equal to that of the interior space behind the lens even though computer routines were written with the flexibility to process unequal values.

The sign convention used is a right handed system with spatial coordinates positive to the right, up, and out of the page as seen by the reader. All angles are assumed positive counterclockwise from point of reference unless otherwise noted. All linear dimensions are implicitly non-dimensionalized with respect to the maximum radius of the right circular cone forming the inside surface of the lens.

C. HIN LENS DESIGN

The lens design procedure consists of calculating both the loci of points forming the outside surface and the slope of the surface at each point in the meridian plane. It is convenient to approach the problem by placing a point source of light at the design focal point F and calculating successive refracted ray paths U' using Snell's law at points D_i on the inside surface in Figure 2. Points E_i are formed by the intercept of the refracted ray and the slope of the outside surface as extended from the previous point E_{i-1}. The tangent to the surface which will refract the ray in the desired direction, U, may again be found from Snell's law. The accuracy of the calculated surface increases as the spacing between points decreases or as angle $\Delta U"$ becomes very small. The final ray is parallel to the lens axis and point D_n corresponds to point B, which is the origin. The area

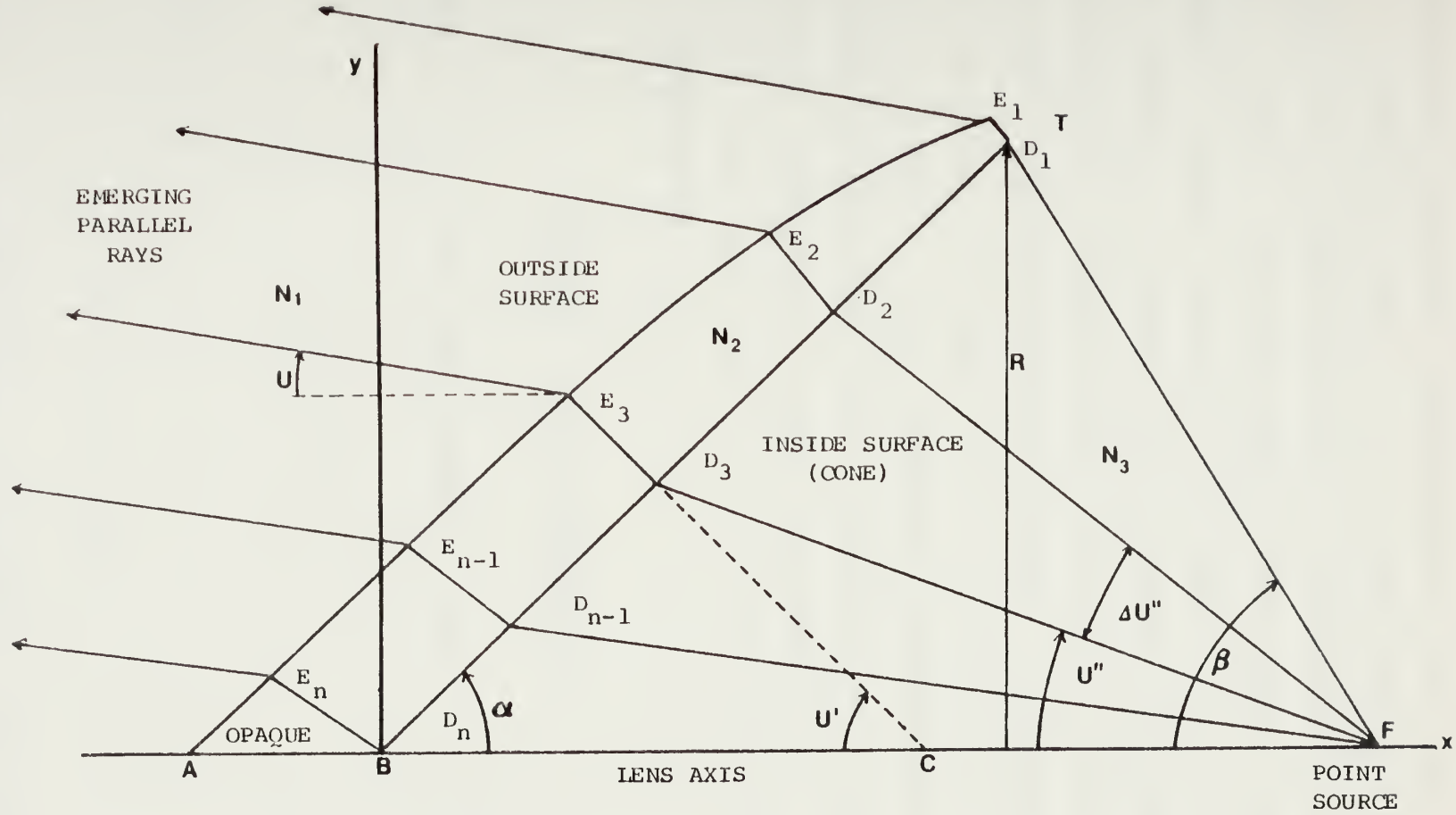

Figure 2. Conceptual Drawing and Coordinate System of Outer Surface Solution

formed by the triangle ABE_n is opaque to prevent rays from scattering through the opposite side of the lens.

A particular lens is begun by specifying the focal length BF, the cone half-angle α, the indices of refraction N_1, N_2, and N_3, the cone radius at the edge R, the ray direction angle U, and the total number of rays to be traced. The thickness, T, of the lens at the edge (E_1D_1) must also be specified in order to define which of the family of possible outer surfaces will be calculated. In general, angle U will be taken to be zero in order to investigate objects on-axis at infinity. R will always be set equal to one and to nondimensionalize all linear dimensions every length is implicitly expressed as a ratio with respect to R. The angle β at the focal point is measured from the lens axis to D_1 and is expressed as

$$\tan |\beta| = \frac{R}{(BF - R \cdot \operatorname{cotan} \alpha)} \qquad (2)$$

Thus, if I+1 is the total number of rays to be traced, then

$$\Delta U'' = \beta / I \qquad (3)$$

and

$$U'' = \beta - J \cdot \Delta U'' \qquad (4)$$

where J is the ray number. To begin the lens design the

coordiantes $x_2(J), y_2(J)$ of point D_J must be found. Here the subscript 2 refers to the inside surface where $x_1(J)$, $y_1(J)$ are the coordinates of E_J on the outside surface.

Following Kingslake [7], Q in Figure 3 may be expressed as

$$Q = BF \sin U'' = x_2(J) \sin U'' + y_2(J) \cos U'' \quad (5)$$

But,

$$y_2(J) = x_2(J) \tan \alpha \quad (6)$$

so that

$$BF \sin U'' = x_2(J)[\sin U'' + \tan \alpha \cos U''] \quad (7)$$

Now, $x_2(J)$ and $y_2(J)$ are

$$x_2(J) = \frac{BF \sin U''}{[\sin U'' + \tan \alpha \cos U'']} \quad (8)$$

$$y_2(J) = \frac{BF \sin U'' \tan \alpha}{[\sin U'' + \tan \alpha \cos U'']} \quad (9)$$

Looking now to find the incident angle I_2' which the ray forms with the inside surface at D_J it can be seen that

$$\tan (\alpha + I_2') = \frac{BF - x_2(J)}{y_2(J)} \quad (10)$$

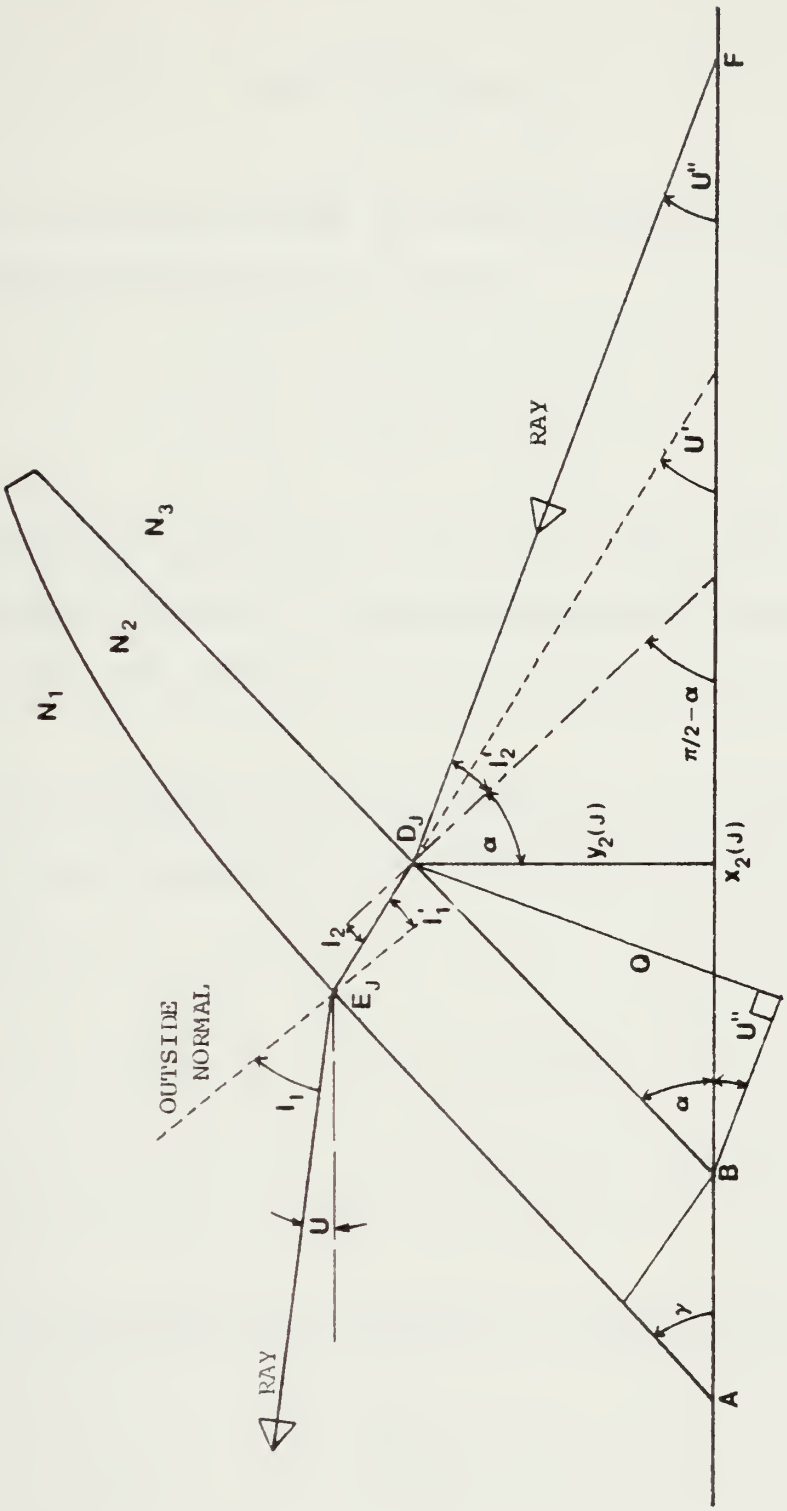

Figure 3. Ray Trace Geometry

Substituting into Equation (1), Snell's law, the refraction angle I_2 can now be written as

$$I_2 = \sin^{-1}[(\frac{N_3}{N_2}) \sin I_2'] \tag{12}$$

The path of the ray inside the lens may now be expressed in the form of the angle U' where

$$U' = (\frac{\pi}{2} - \alpha) - I_2 \tag{13}$$

To this stage all rays are treated the same. Now, however, a differentiation must be made between the outermost ray which defines the edge of the lens and all other subsequent rays.

For the outermost ray the thickness, T, of the lens at the edge can be specified which yields $x_1(1)$ and $y_1(1)$ immediately:

$$x_1(1) = x_2(1) - T \cos U' \tag{14}$$

$$y_1(1) = y_2(1) + T \cos U' \tag{15}$$

At point E_1 we may write Equation (1) again to obtain

$$I_1' = \sin^{-1}[(\frac{N_1}{N_2}) \sin I_1] \tag{16}$$

where angles I_1 and I_1' are the incident and refracted angles at the outside surface and are not yet known. Angles I_1 and I_1' may be found by first noting that

$$U + I_1 = U' + I_1' \tag{17}$$

then substituting Equation (16) into (17) and rearranging terms to obtain

$$I_1 = U' - U + \sin^{-1}[(\frac{N_1}{N_2})\sin I_1] \tag{18}$$

It can be shown after some algebraic manipulation that Equation (18) may be solved for the angle I_1 in the form

$$I_1 = \sin^{-1}\{\frac{\sin^2(U' - U)}{[\cos(U'-U) - N_1/N_2]^2 + \sin^2(U' - U)}\}^{1/2} \tag{19}$$

Angle I_1' may be found, if desired, by substitution of Equation (19) into Equation (16). Of more importance, however, is the determination of the slope of the outer surface and the surface normal. Now that angle I_1 is known these slopes may be written as

$$DYDXN(J) = \frac{dy}{dx}\Big|_{normal} = -\tan(U + I_1) \tag{20}$$

and

$$DYDXT(J) = \left.\frac{dy}{dx}\right|_{\substack{\text{surface}\\\text{tangent}}} = \cot an(U + L_1) \qquad (21)$$

Equations (20) and (21) may be evaluated by using Equation (19) for I_1.

Now that all the parameters are known for the first ray, the remainder of the points E_J and the respective slopes may be found. Each successive ray is traced as before by Equations (4) through (13). Equations (14) and (15), however, may not now be used since the lens thickness along the ray can not be specified. Instead, the intersection of the ray and the surface slope from the previous ray is used to define the new point E_{J+1}. The intersection is found by first writing the equations of lines representing the ray and the surface tangent. For the ray:

$$y = -x \tan U' + y_2(J) + x_2(J) \tan(U') \qquad (22)$$

For the surface tangent:

$$y = x \cot(I_1 + U) + y_1(J-1) - x_1(J-1) \cot(I_1 + U) \qquad (23)$$

Equations (22) and (23) are solved simultaneously to yield the coordinates of E_J which are

$$y_1(J) = \{\frac{A + B}{C}\} \qquad (24)$$

where:

$$A = \cot(I_1+U)\ \cot(U')\ [y_2(J)+x_2(J)\tan(U')] \qquad (25)$$

$$B = y_1(J-1) - x_1(J-1)\ \cot(I_1 + U) \qquad (26)$$

$$C = 1 + \cot(I_1 + U)\ \cot(U') \qquad (27)$$

and

$$x_1(J) = \cot(U')\ [-y_1(J)+y_2(J)+x_2(J)\tan(U')] \qquad (28)$$

Now Equations (19), (20), and (21) are used to calculate I_1 and the slopes at E_J. Therefore, the remainder of the lens surface may be generated. The opaque region at the surface is formed by extending the slope of the surface at E_K to intersect the lens axis. Here, K refers to the last ray. The nose half-angle, γ, thus formed is given by

$$\tan\gamma = \left.\frac{dy}{dx}\right|_{\text{surface, } E_K} \qquad (29)$$

D. SKEW RAYS

A skew ray is one that begins from an off-axis object point and enters the lens either in front of or behind the meridian plane (z = 0). For every skew ray, there is a corresponding mirror image skew ray on the opposite side of the meridian plane so that two skew rays are traced at the

expense of only one calculation. These two skew rays intersect at the same diapoint.

Large numbers of skew rays are traced through a lens in order to study lens performance at different obliquities. The procedure is to superimpose a grid over the lens aperture and to trace rays through the intersections of the grid, through the lens and onto the image plane. An image plane spot diagram and an energy density plot are then constructed for study.

To accomplish this, the aperture grid has been attached to the nose (opaque region) of the seeker lens at station A; see Figure 3. The plane of the aperture grid is tilted relative to the lens by a variable angle. A transformation between the grid coordinates and the lens coordinates has been derived to connect skew rays from grid to intercept with the outside surface of the lens. Referring to Figure 4, it can easily be seen that

$$x' = [x + AB]\cos \alpha_p - y \sin \alpha_p \tag{30}$$

$$y' = [x + AB]\sin \alpha_p + y \cos \alpha_p \tag{31}$$

$$z' = z \tag{32}$$

where α_p is the tilt of the grid plane, AB is the length of the opaque nose portion on the x-axis. Both z and z' are positive out of the page.

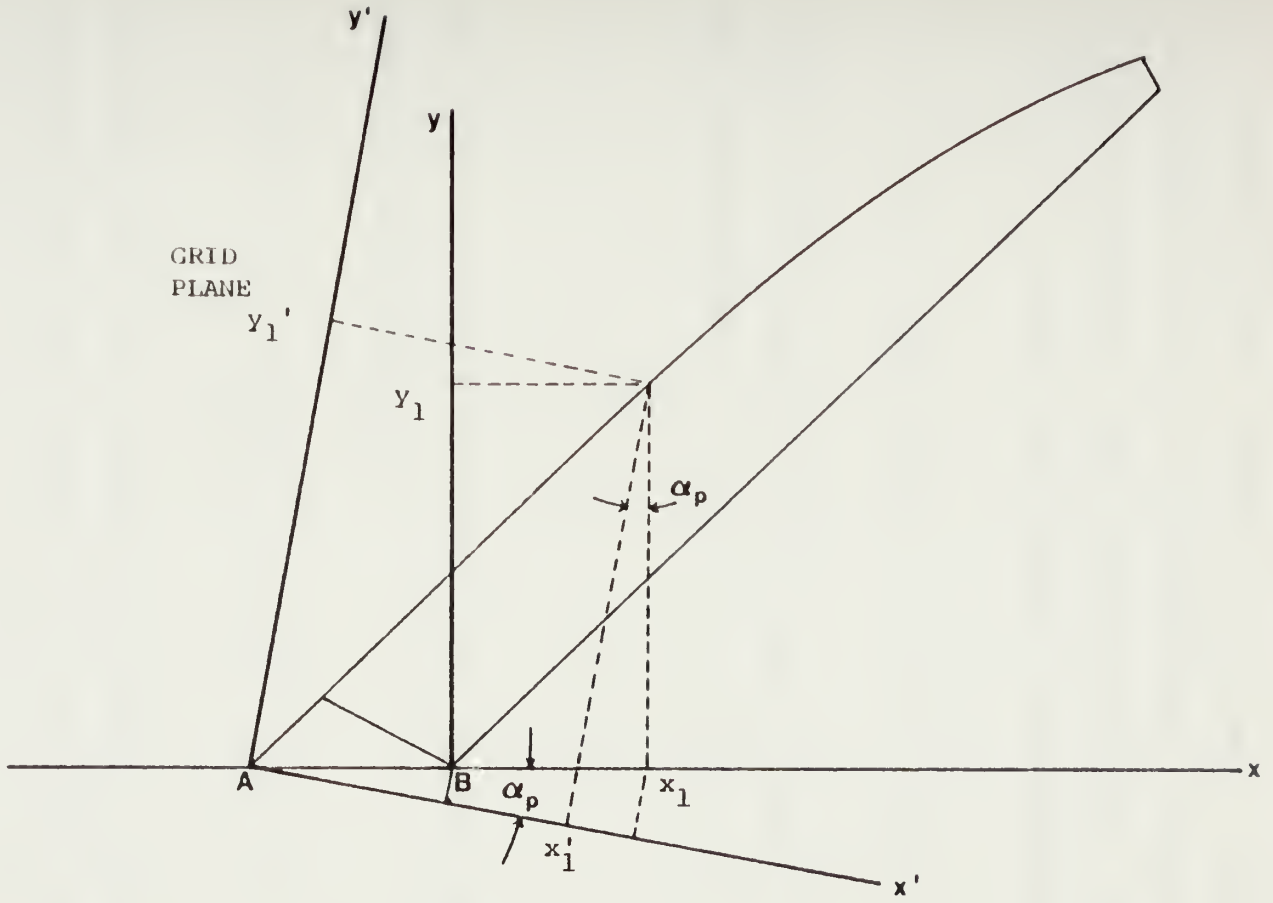

Figure 4. Coordinate Transformation (z and z' are out of the page)

The three dimensional lens outer surface is generated by rotating the array of outer surface coordinates in the meridian plane through 2π about the lens axis. Each pair of coordinates $x_1(J), y_1(J)$ thus describe a circle in the y-z plane of the lens. This circle transforms, however, to an ellipse in the grid plane given by the equation

$$y' = [x + AB] \sin \alpha_p \pm \sqrt{R^2 - z'^2} \cos \alpha_p \qquad (33)$$

where R is the radius of the circle in the x-y plane. R may be expressed by the familiar equation of a circle

$$R^2 = y^2 + z^2 \qquad (34)$$

in the y-z plane of the lens, or by solving Equation (33) for R in the grid plane

$$R^2 = z'^2 + \left(\frac{y'}{\cos \alpha_p} - (x + AB) \tan \alpha_p\right)^2 \qquad (35)$$

With the aid of the foregoing groundwork, the x,y,z coordinates of the ray intercept with the outer surface may be found. To see how this is accomplished, first refer to Figure 5. The skew ray will pass outside the circle formed by rotating some point $x_1(J), y_1(J)$ and inside the next circle formed by rotating $x_1(J-1), y_1(J-1)$. In so doing the skew ray will

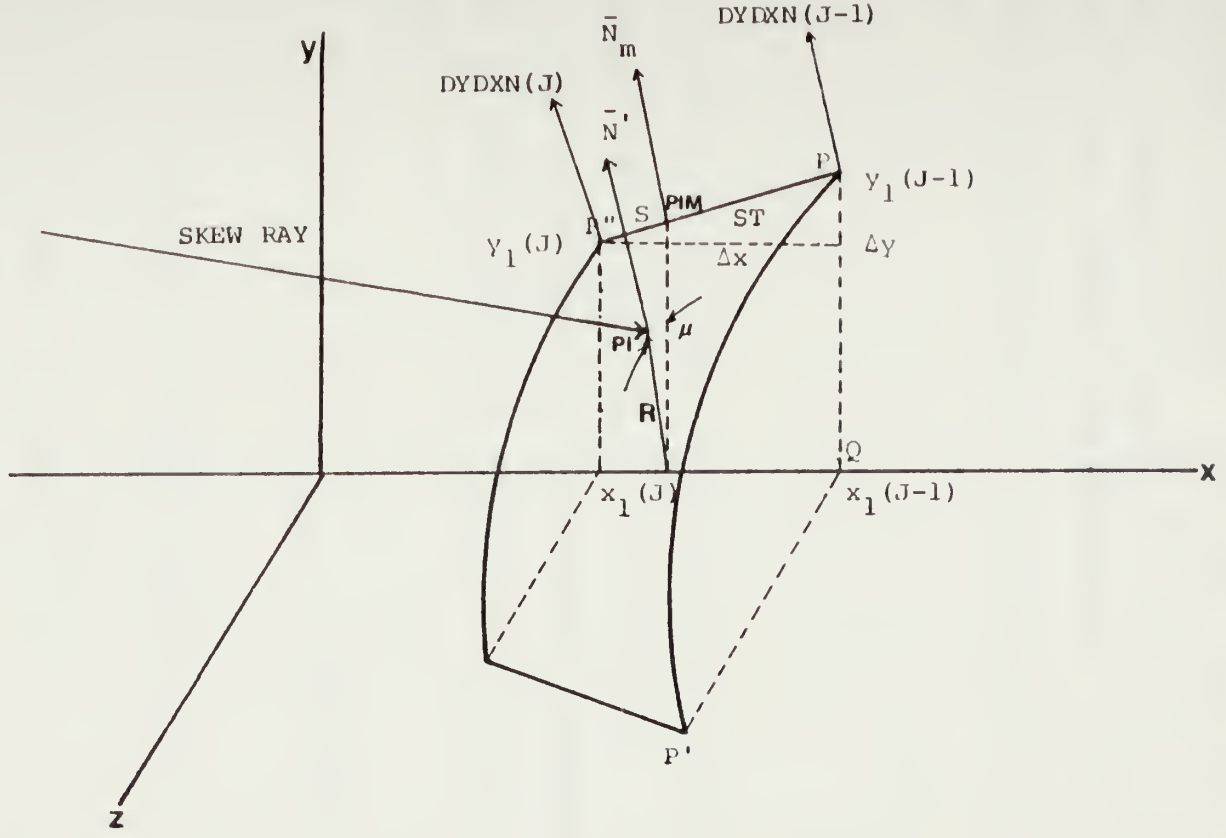

Figure 5. Geometry of Skew Ray Intercept With Outside Surface. X, Y Plane is the Meridian Plane. $\bar{N}_m$ is the Surface Normal in the Meridian Plane; $\bar{N}'$ the Surface Normal at the Point of Intercept, PI.

intercept an imaginary cone formed by the two circles.[1] Now, the y',z' of the skew ray in the grid plane and a trial value $x_1(J)$ from the array of surface points are substituted into Equation (35) and a value for R is calculated. If R is greater than $y_1(J)$ but less than $y_1(J-1)$ than the appropriate circles have been found. If not, another trial value of $x_1(J)$ is picked. In practice the $x_1(J)$ corresponding to

$$y_1(J) = z' \tag{36}$$

is chosen as the first trial value and subsequent trial values are $x_1(J-1)$, $x_1(J-2)$ and so forth.

The equation of the cone passing through the two circles may be derived by again referring to Figure 5 and noting that

$$QP = QP' = \sqrt{y^2 + z^2} = R \tag{37a}$$

$$QP = y = m[x - x_1(J)] + y_1(J) \tag{37b}$$

where the slope m is given by

---

[1]Recall that a straight line between points E_J was used to form the outer surface in the meridian plane. These approximations are valid only if the spacing between points or circles is very small.

$$m = \frac{y_1(J-1) - y_1(J)}{x_1(J-1) - x_1(J)} \tag{38}$$

and therefore

$$R^2 = \{[\frac{y_1(J-1) - y_1(J)}{x_1(J-1) - x_1(J)}][X - X(j)] + y_1(J)\}^2 \tag{39}$$

By equating Equation (39) to Equation (35) and solving for x, the expression for the x-coordinate, x_0, of the outside surface ray intercept may be found. After some algebra, this reduces to the complicated relationship

$$x_0 = \frac{PAR1}{PAR2} \pm \sqrt{\frac{PAR1}{PAR2} - \frac{PAR3}{PAR2}} \tag{40}$$

where:

$$PAR1 = ab + ce - b^2AB - c^2d \tag{41}$$

$$PAR2 = b^2 - c^2 \tag{42}$$

$$PAR3 = a^2 + b^2(AB)^2 - 2abAB + z' - (e-cd)^2 \tag{43}$$

and where

$$a = y'/\cos \alpha_p \tag{44}$$

$$b = \tan \alpha_p \tag{45}$$

$$c = \left[\frac{y_1(J-1) - y_1(J)}{x_1(J-1) - x_1(J)}\right] \tag{46}$$

$$d = x_1(J) \tag{47}$$

$$e = y_1(J) \tag{48}$$

It has been found that the plus sign in Equation (40) gives the correct values until PAR1/PAR2 becomes greater than $x_1(1)$ at which time the negative sign must be used. It now follows from Equations (31), (32) and (40) that the y_0 and z_0 coordinates of the intercept are

$$y_0 = \frac{y'}{\cos \alpha_p} - (x_0 + AB) \tan \alpha_p \tag{49}$$

and

$$z_0 = z' \tag{50}$$

The next step in tracing the skew ray is to ascertain the direction cosines of the ray inside the lens after refraction at the outside surface. This is accomplished in a series of steps beginning with the determination of the angle ϕ which the skew ray makes with the normal to the surface at the point of intercept. Angle ϕ may be found by taking the scalar product of the direction cosines of the

skew ray and the surface normal. Thus to find ϕ, the surface normal must first be obtained.

As might be surmised by the reader, the direction cosines of the surface normal can be found by taking the gradient of Equation (39) with Equation (37) substituted for R. Several orders of magnitude may be gained in accuracy, however, if the normal $\bar{N}_m$ is found by interpolation in the meridian plane and then rotated to the point of intercept by angle μ as in Figure 5. This interpolation procedure involves multiplying the ratio S/ST with the difference between DYDXN(J) and DYDXN(J-1) and adding the product to DYDXN(J).

$$DYDXN_{PIM} = \frac{S}{ST}(DYDXN(J-1) - DYDXN(J)) + DYDXN(J) \qquad (51)$$

where subscript PIM refers to point of intersection, meridian. Values of the slopes of the normals in the meridian plane, DYDXN(J), are given by Equation (20) and S and ST are the linear separation of points P", PIM and P", P respectively. S/ST is given by

$$\frac{S}{ST} = \frac{[(R - y_1(J))^2 + (x_{PIM} - x_1(J))^2]^{1/2}}{(\Delta x^2 + \Delta y^2)^{1/2}} \qquad (52)$$

Therefore, the normal vector, $\bar{N}_m$, in the meridian plane is

$$\bar{N}_m = \left(\frac{1}{DYDXN_{PIM}}\right)\hat{i} + \hat{j} \qquad (53)$$

and since

$$\tan \mu = \frac{z'}{y_0} = \frac{z_0}{y_0} \tag{54}$$

the normal vector at the point of intersection on the outside surface becomes

$$\bar{N}' = \left(\frac{1}{DYDXN_{PIM}}\right)\hat{i} + \cos\left(\tan^{-1}\frac{z_0}{y_0}\right)\hat{j} + \sin\left(\tan^{-1}\frac{z_0}{y_0}\right)\hat{k} \tag{55}$$

and

$$|\bar{N}'| = [DYDXN_{PIM}^{-2} + 1]^{1/2} \tag{56}$$

Now the scalar product of the skew ray vector, $\hat{R}$, and surface normal, $\bar{N}'$, may be performed to find ϕ. Since the acute angle between these vectors is required, the dot product must be written

$$\hat{R}\cdot\bar{N}' = |\bar{N}'| \cos(\pi-\phi) \tag{57}$$

Substituting Equation (55) for $\bar{N}'$ and noting that

$$\hat{R} = K\hat{i} + L\hat{j} + M\hat{k} = \cos\alpha_p\hat{i} - \sin\alpha_p\hat{j} \tag{58}$$

the left side of Equation (56) may be expanded to

$$\hat{R}\cdot\bar{N}' = \frac{\cos\alpha_p}{DYDXN_{PIM}} - \sin\alpha_p \cos\left(\tan^{-1}\frac{z_0}{y_0}\right) \tag{59}$$

Solving Equation (56) for the angle ϕ and introducing Equation (58), the expression for angle ϕ becomes

$$\phi = \pi - \cos^{-1}\left\{\frac{\frac{\cos\alpha_p}{DYDXN_{PIM}} - \sin\alpha_p \cos(\tan^{-1}\frac{z_0}{y_0})}{[DYDXN_{PIM}^{-2} + \cos^2(\tan^{-1}\frac{z_0}{y_0}) + \sin^{-2}(\tan^{-1}\frac{z_0}{y_0})]^{1/2}}\right\} \tag{60}$$

Now that the acute angle, ϕ, between the ray and the outside surface normal is known, ϕ', the angle between the refracted ray inside the lens and the surface normal may be found using Snell's law.

$$\phi' = \sin^{-1}(\frac{N_1}{N_2}\sin\phi) \tag{61}$$

The next step is to ascertain the direction cosines K', L', M' of the refracted ray inside the lens. Following Kingslake [7], Figure 6 shows the optical vector relationship between $\bar{R}$, the skew ray, $\bar{R}'$, the refracted skew ray, $\bar{N}'$, the surface normal, and the indices of refraction of the two media. Algebraically this relationship is written as

$$N_2\bar{R}' = N_1\bar{R} + (N_2\cos\phi' - N_1\cos\phi)\bar{N}' \tag{62}$$

By resolving Equation (61) into component form, the direction cosines of $\bar{R}'$ may be found. After rearranging, K', L', and M' become

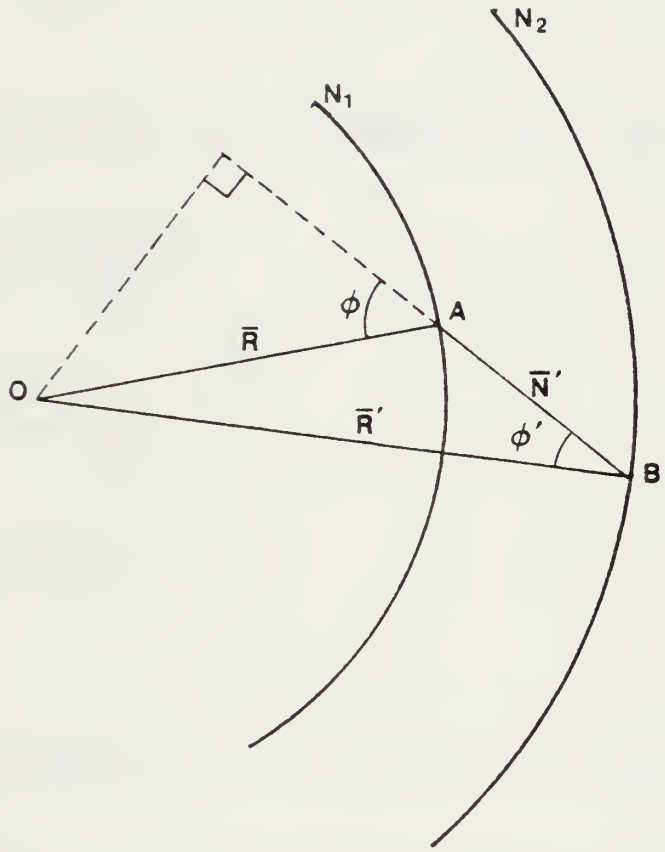

Figure 6. Kingslake's Skew Ray Diffraction Diagram

$$K' = \frac{N_1}{N_2} K + (\cos \phi' - \frac{N_1}{N_2} \cos \phi) k \tag{63}$$

$$L' = \frac{N_1}{N_2} L + (\cos \phi' - \frac{N_1}{N_2} \cos \phi) \ell \tag{64}$$

$$M' = \frac{N_1}{N_2} M + (\cos \phi' - \frac{N_1}{N_2} \cos \phi) m \tag{65}$$

where K, L, and M are given by Equation (57) and k, ℓ, m are

$$k = \frac{DYDXN_{PIM}^{-1}}{|\bar{N}'|} \tag{66}$$

$$\ell = \frac{\cos(\tan^{-1} \frac{z_0}{y_0})}{|\bar{N}'|} \tag{67}$$

$$m = \frac{\sin(\tan^{-1} \frac{z_0}{y_0})}{|\bar{N}'|} \tag{68}$$

Again, $|\bar{N}'|$ in Equations (66) through (68) is expressed by Equation (56).

At this stage in the process of tracing the skew ray, the coordinates of the external ray intercept x_0, y_0, z_0 are known as are the direction cosines K', L', M' of the skew ray inside the lens. The next step is, of course, to find the ray intercept with the inside surface (cone) and the direction of the ray subsequent to refraction. The intermediate steps are similar to, if not identical with,

the foregoing. One major difference, however, is that the inside conical surface may be expressed analytically and the intercept coordinates x_i, y_i, z_i may be found exactly without approximation. Proceeding, it can be seen that if x_i, y_i, z_i were already known, Equations (63), (64), and (65) could be rewritten as

$$K' = \frac{x_i - x_0}{D} \tag{69}$$

$$L' = \frac{y_i - y_0}{D} \tag{70}$$

$$M' = \frac{z_i - z_0}{D} \tag{71}$$

where D is the distance between surface intercept points. Upon rearranging:

$$x_i = DK' + x_0 \tag{72}$$

$$y_i = DL' + y_0 \tag{73}$$

$$z_i = DM' + z_0 \tag{74}$$

Furthermore, there exists a relationship between x_i, y_i, and z_i which is given by the expression for the inside conical surface:

$$y_i^2 + z_i^2 - x_i^2 \tan^2 \alpha = 0 \tag{75}$$

where α is the half-angle of the cone. Substituting Equations (72), (73), and (74) into Equation (75) and solving for D, it is seen that

$$D = \frac{-P_1}{P_2} \pm \frac{\sqrt{P_1^2 - P_2 P_3}}{P_2} \tag{76}$$

where

$$P_1 = L'y_0 + M'z_0 - K'x_0 \tan^2 \alpha \tag{77}$$

$$P_2 = L'^2 + M'^2 - K'^2 \tan^2 \alpha \tag{78}$$

and

$$P_3 = y_0^2 + z_0^2 - x_0^2 \tan^2 \alpha \tag{79}$$

Correct values for D are obtained by using the minus sign in Equation (76). Now that D is known, values for K', L', M', x_0, y_0, and z_0 are substituted into Equations (72), (73), and (74) to yield the coordinates of the inside surface intercept point.

In the case of the inside surface, the gradient may be used to obtain the surface normal at the point of intercept since this surface has been expressed analytically. If Equation (75) is denoted by f(x,y,z) then

$$\hat{N}_i = \left. \frac{\nabla f}{|\nabla f|} \right|_{x_i, y_i, z_i} \tag{80}$$

where $\hat{N}_i$ is the unit vector in the direction of the surface normal at the point of intercept. Here,

$$\bar{\nabla} f = \frac{\partial f}{\partial x} \hat{i} + \frac{\partial f}{\partial y} \hat{j} + \frac{\partial f}{\partial z} \hat{k} \tag{81}$$

or alternately,

$$\bar{\nabla} f = f_x \hat{i} + f_y \hat{j} + f_z \hat{k} \tag{82}$$

Thus, the direction cosines of the normal k', ℓ', m' may be expressed as

$$k' = \frac{f_x}{|\bar{\nabla} f|} \tag{83}$$

$$\ell' = \frac{f_y}{|\bar{\nabla} f|} \tag{84}$$

$$m' = \frac{f_z}{|\bar{\nabla} f|} \tag{85}$$

where:

$$f_x = - 2x_i \tan^2 \alpha \tag{86}$$

$$f_y = 2y_i \tag{87}$$

$$f_z = 2z_i \tag{88}$$

and

$$|\bar{\nabla}f| = 2[x_i^2 \tan^4 \alpha + y_i^2 + z_i^2]^{1/2} \qquad (89)$$

Now that the two unit vectors $\hat{R}'$ and $\hat{N}'$ are known the incident acute angle of the skew ray with the inside surface, ϕ_i, may be ascertained by again taking the scalar product as in Equation (57). Thus,

$$\phi_i = \pi - \cos^{-1}[K'k' + L'\ell' + M'm'] \qquad (90)$$

and using Equation (1) again

$$\phi_i' = \sin^{-1}[\frac{N_2}{N_3} \sin \phi_i] \qquad (91)$$

where ϕ_i' is the acute angle between the skew ray and the surface normal after refraction at the inside surface. Direction cosines K", L", M" of the skew ray after refraction are found analogously to K', L', and M' in Equations (63), (64) and (65). Here, however, N_2, N_3, K', L', M', Φ_i, Φ_i', and k', ℓ', m' are substituted for N_1, N_2, K, L, M, Φ, Φ', and k, ℓ, m respectively. Thus

$$K'' = \frac{N_2}{N_3} K' + (\cos \phi_i' - \frac{N_2}{N_3} \cos \phi_i)k' \qquad (92)$$

$$L'' = \frac{N_2}{N_3} L' + (\cos \phi_i' - \frac{N_2}{N_3} \cos \phi_i)\ell' \qquad (93)$$

and

$$M'' = \frac{N_2}{N_3} M' + (\cos \phi_i' - \frac{N_2}{N_3} \cos \phi_i) m' \qquad (94)$$

Finally, the skew ray intercept with the image plane may be found. The image plane is treated as another surface along the path of the skew ray, and the intercept coordinates x_{im}, y_{im}, z_{im} are easy to find. Equations (72), (73) and (74) may be used again in the form

$$x_{im} = D'K'' + x_i \qquad (95)$$

$$y_{im} = D'L'' + y_i \qquad (96)$$

$$z_{im} = D'M'' + z_i \qquad (97)$$

where D', in this instance, is the linear separation between coordinates x_i, y_i, z_i at the inside surface and x_{im}, y_{im}, z_{im} of the image plane. Furthermore,

$$x_{im} = BF \qquad (98)$$

is the equation of the image plane. It follows that

$$D' = \frac{(BF - x_i)}{K''} \qquad (99)$$

after substitution of Equation (98) into Equation (95). Therefore,

$$y_{im} = \left[\frac{BF - x_i}{K''}\right]L'' + y_i \qquad (100)$$

and

$$z_{im} = \left[\frac{BF - x_i}{K''}\right]M'' + z_i \qquad (101)$$

Hence, the skew ray has been traced onto the image plane at the focal point of the lens. The y_{im} coordinate of the corresponding mirror image skew ray is the same as Equation (100). The z_{im} coordinate, however, is the negative of Equation (101) since the mirror image ray is behind (when viewed along the z-axis) the meridian plane. After tracing a complete set of skew rays through the lens a spot diagram may be plotted. Clearly, the number of rays to be traced depends entirely upon the incremental size of the aperture grid chosen. According to Kingslake [7], at least 100 rays must be traced to give a fair approximation of the actual image. In addition to the spot diagram, an energy density plot may now be constructed by counting the number of rays within progressively larger radii from the image centroid and then plotting the number of rays as a function of radius. Here, each ray is assumed to contain a unit, nondimensional, an amount of radiant energy for convenience.

E. RADIANT ENERGY LOSS

In reality, each ray loses intensity upon transmission at each interface. Of the total amount of energy contained in each ray, a fraction I_T will be transmitted, a fraction I_R will be reflected, and a fraction I_A will be absorbed by the medium into which the ray is propagating. Since it has been assumed that absorption is negligible, it must be true that

$$I_T + I_R = 1 \tag{102}$$

Furthermore, the relative amounts of transmitted and reflected electromagnetic energy may be calculated by the well-known Fresnel Equations which state the dependency of I_T and I_R upon the angle of incidence and the indices of refraction at the interface. That I_T and I_R are further dependent upon the orientation of the electric vector with respect to the geometry of ray incidence is fundamental to the boundary conditions which govern the form of the Fresnel relations as derived in Hecht-Zajac [8]. Since this thesis examines lens response to monochromatic radiation, the indices of refraction are not considered as a function of wavelength; further, the electric vector orientation is assumed to be rapidly and randomly changing with time. By time averaging field components, it may be seen that the reflectance is

$$I_R = \frac{1}{2}(r_{\perp}^2 + r_{\parallel}^2) \tag{103}$$

where

$$r_{\perp} = \frac{\cos \phi - (N_{ti}^2 - \sin^2\phi)^{1/2}}{\cos \phi + (N_{ti}^2 - \sin^2\phi)^{1/2}} \tag{104}$$

and

$$r_{\parallel} = \frac{N_{ti}^2 \cos \phi - (N_{ti}^2 - \sin^2\phi_i)^{1/2}}{N_{ti}^2 \cos \phi + (N_{ti}^2 - \sin^2\phi)^{1/2}} \tag{105}$$

Here, N_{ti} is the ratio of the index of refraction of the transmission side of the interface to the index of refraction of the incident side. From Equation (102) it now follows that the transmittance through the interface is

$$I_t = 1 - I_R \tag{106}$$

The total transmittance through the lens is simply the product of I_t at the outside surface with that of the inside surface where ϕ_i is substituted for ϕ in Equations (104) and (105).

Total internal reflection of the ray may occur at the inside surface if the incident angle becomes too large. Following Reference (7), this occurs when angle ϕ_i is equal to or greater than $\pi/2$. Thus, Snell's law becomes

$$\sin \phi_i = \frac{N_3}{N_2} \tag{107}$$

and any ray with ϕ_i equal to or greater than this will be

totally internally reflected. In this thesis such rays are labeled "failed rays" since they fail to intersect the image plane. If N_2 is 1.5 and N_3 is 1.0, the incident angle for total internal reflection is 41.81°, or greater.

F. OPTICAL PATH LENGTH (OPL)

The optical path length of a skew ray is an analytical tool with which the researcher may ascertain the phase of a ray at the end of the path. By so doing, the image diffraction pattern may be constructed which shows the addition or subtraction of amplitude depending upon relative phase. Since each ray must begin with the same phase, monochromatic radiation is used for diffraction experiments. OPL is included here only as a matter of interest. The calculation of optical path length is simply the sum of the geometrical path segments of a ray multiplied by the corresponding index of refraction of the medium for that segment.

III. THE GRIN LENS

A. THEORY

This thesis assumes a spherically symmetric, inhomogeneous, isentropic medium in which the refractive index varies from point to point but is independent of direction at each point. The refractive index is a function of the coordinates of the points of the region being considered. The problem of describing the resulting curved paths of rays in such GRIN materials has been solved long ago in the form of a single second order vectorial differential equation. Marchand [9] has shown that the solution to the differential equation in the case of spherical gradients can be written in polar coordinates in the plane of the ray as

$$\theta = \theta_0 + e \int_{r_0}^{r} \frac{dr}{r[n^2 r^2 - e^2]^{1/2}} \qquad (108)$$

Here r_0 and θ_0 are values of r and θ at a convenient reference point on the ray and $|e|$ is a scalar constant along the ray given by

$$e = \varepsilon\, n_0\, r_0 \sin \psi_0 \qquad (109)$$

Referring to Figure 7, r is measured from the center of symmetry of the index function; angles θ and θ_0 are measured

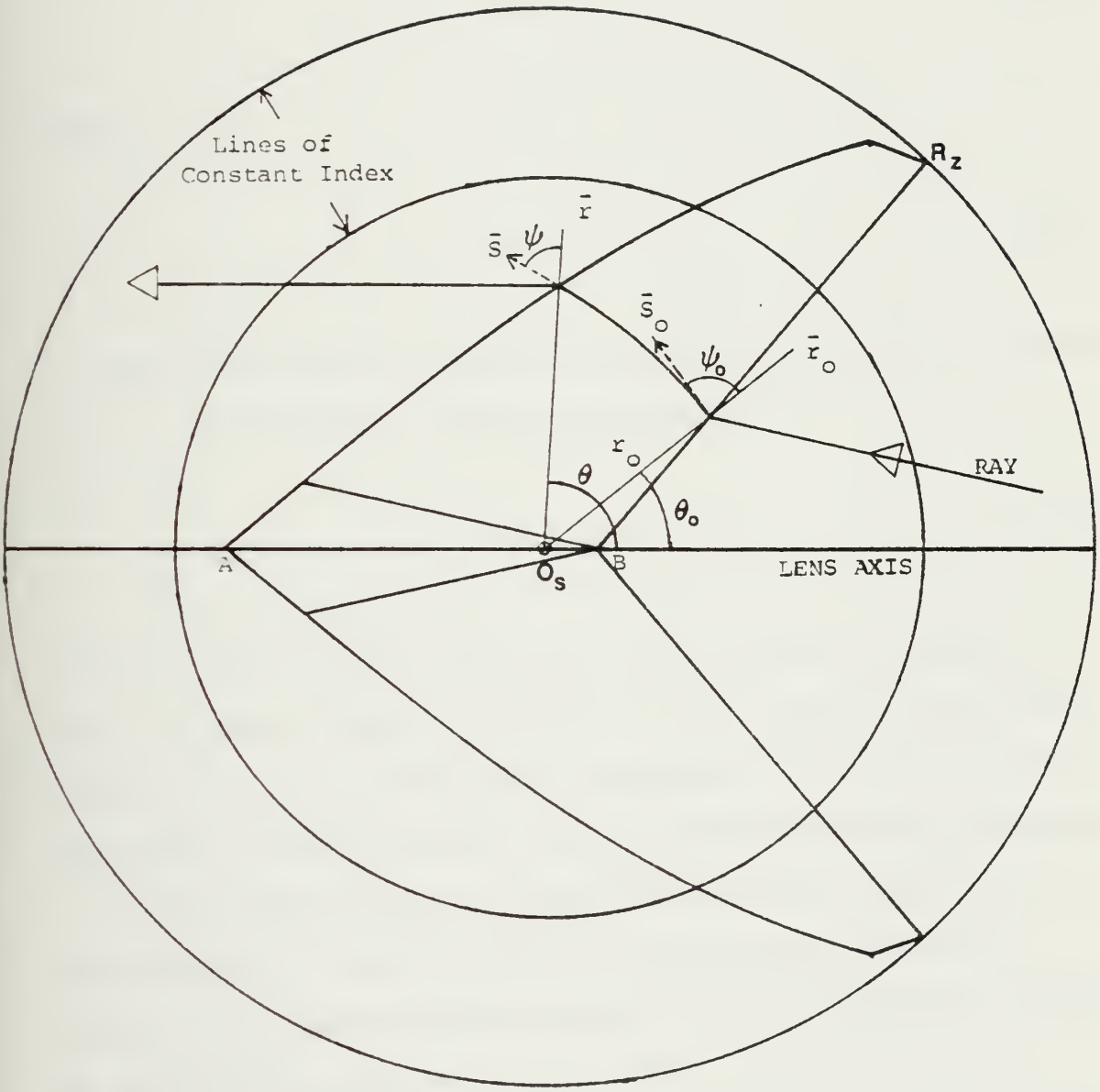

Figure 7. Grin Lens Geometry

counterclockwise from the lens axis; angles ψ and ψ_0 are measured counterclockwise from the radius vector to the instantaneous ray direction vector. ε is the sign function expressed as

$$\varepsilon = \text{sgn } |\psi_0| = \pm 1 \tag{110}$$

where

$$|\psi_0| \gtrless \pi/2 \tag{111}$$

In Equation (109), n_0 refers to the index function n evaluated at r_0. The form of n has been chosen as

$$n = n(O_s, r) \tag{112}$$

where O_s denotes the position of the center of symmetry on the lens axis (shown in Figure 7) and r is the radial coordinate from O_s to the point in question. This form allows the study of the effects on lens performance as O_s is changed.

More specifically, in order to allow the analytical integration of Equation (108), the expression used for $n(O_s, r)$ is a generalized version of that employed by Luneburg as described by Marchand [9]. Here

$$n = [a + b(\frac{r}{R_Z})^2]^{1/2} \tag{113}$$

whereas Luneburg used specific values for a and b. Generalizing the index function enables the strength, or percent change of the gradient to be varied as well as the algebraic sign of the gradient. If the parameter b is negative, a decreasing parabolic gradient results; conversely a positive b yields an increasing parabolic gradient. By visualizing a plane wave front passing through a spherical gradient, it may be seen that the negative gradient results in light rays bending forward at the center, as shown in Figure 7, whereas a positive gradient has the opposite effect. This principle was used by Wood, as related by Marchand [9], in constructing simple lenses having plane faces and a radial index. The Wood lens acted as a converging or diverging lens depending upon the sign of the gradient used.

Additionally, it must be noted that if the parameter b is equal to zero, Equation (113) reduces to

$$n = \sqrt{a} \tag{114}$$

which is a HIN lens having constant index of refraction. This fact has facilitated the correlation of GRIN and HIN computer trace algorithms.

Equation (108) may be integrated by a change of variable using the relation

$$v = \left(\frac{r_0}{r}\right)^2 \tag{115}$$

which leads to the solution

$$\theta = \theta_0 - \frac{\varepsilon}{2}\left\{\sin^{-1}\left[\frac{2e^2/r^2 - a}{\sqrt{a^2 + 4be^2/R_Z^2}}\right] - \sin^{-1}\left[\frac{2e^2/r_0^2 - a}{\sqrt{a^2 + 4be^2/R_Z^2}}\right]\right\} \tag{116}$$

Equation (116) gives θ as a function of r. This equation can be easily solved for r as a function of θ in the form

$$r = \frac{\sqrt{2}\,|e|}{\left\{a + \sqrt{a^2 + \frac{4be^2}{R_Z^2}}\sin\left[-2\varepsilon(\theta-\theta_0) + \sin^{-1}\left[\frac{2e^2/r_0^2 - a}{\sqrt{a^2+4be^2/R_Z^2}}\right]\right]\right\}^{1/2}} \tag{117}$$

The instantaneous direction of the ray at any point r,θ may be ascertained by using the invariance of e. Hence,

$$e = \varepsilon n r \sin\psi = \varepsilon n_0 r_0 \sin\psi_0 \tag{118}$$

and

$$\psi = \sin^{-1}\left[\frac{n_0 r_0 \sin\psi_0}{nr}\right] \tag{119}$$

Furthermore, the orientation of the plane of the ray may be easily deduced since every ray in a spherical medium is a plane curve lying in a plane through the center of symmetry.

Using this fact, Marchand [9] has shown that a suitable conversion from coordinates r and θ in the plane of the ray to global Cartesian coordinates may be written in the form

$$x = r(\delta \frac{x_0}{r_0} + \eta\ p_0) \tag{120}$$

$$y = r(\delta \frac{y_0}{r_0} + \eta\ q_0) \tag{121}$$

$$z = r(\delta \frac{z_0}{r_0} + \eta\ \ell_0) \tag{122}$$

Here p_0, q_0, ℓ_0 are the initial direction cosines of the ray at r_0, θ_0; x_0, y_0, and z_0 are the Cartesian coordinates corresponding to r_0, θ_0. The parameters δ and η are given by Marchand as

$$\eta = \sin \theta / \sin \psi_0 \tag{123}$$

$$\delta = \cos \theta - \eta \cos \psi_0 \tag{124}$$

It should be noted that Equation (117) may become singular for certain rays where ψ or ψ_0 become very close to zero or π. This singularity may be more easily seen in Equation (123) where η becomes indeterminate as both θ and ψ_0 approach zero and/or π. In practice these conditions occur when O_s is located either far out in object space, coincident with B, or on the image side of the lens; see Figure 8. Positioning

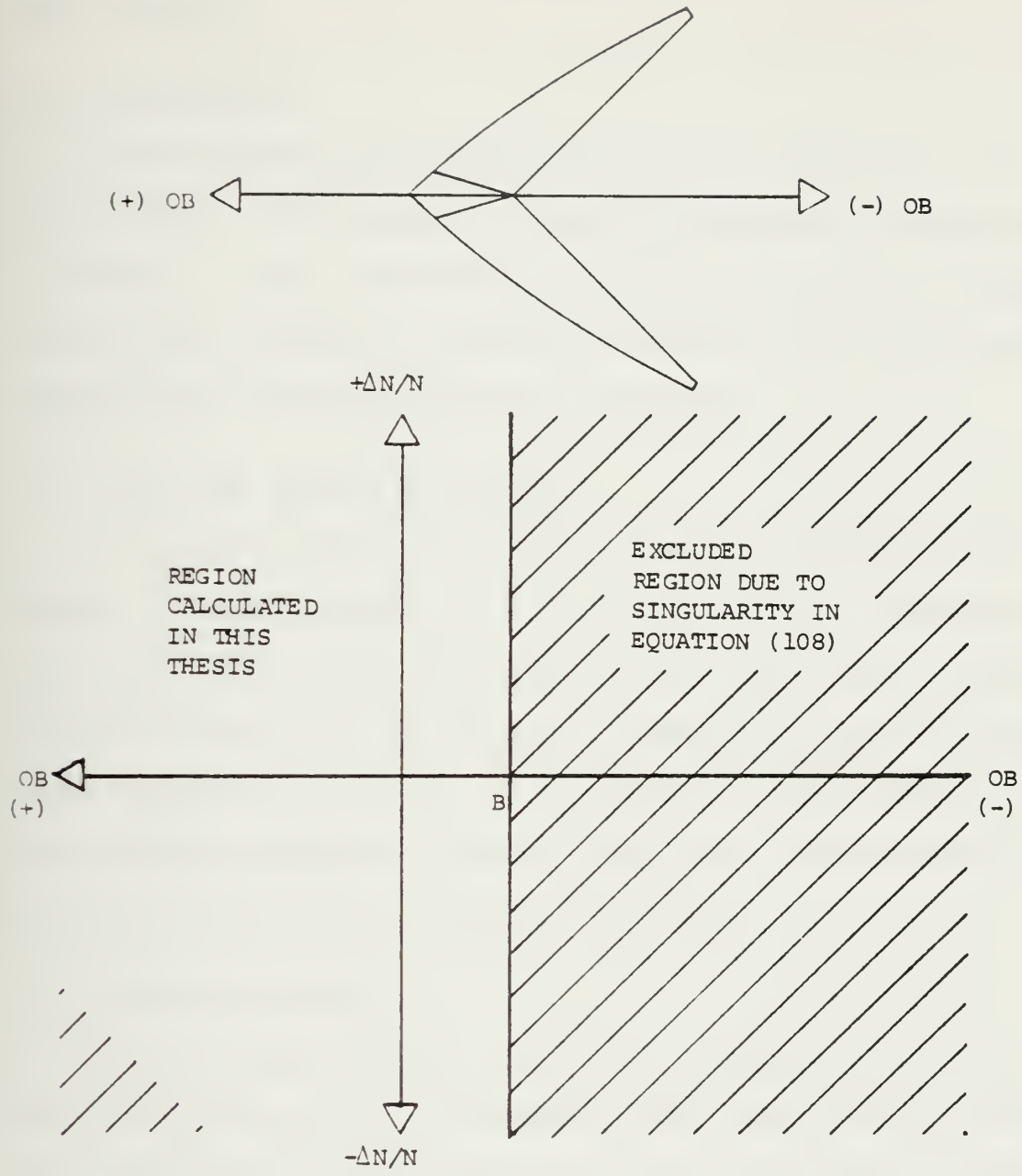

Figure 8. Excluded Regions for Center of Symmetry Due to Singularities

the center of symmetry at these locations has therefore been avoided.

B. ASSUMPTIONS

The aforementioned assumptions for the HIN case also apply here. Additionally, it must be assumed, as depicted in Figure 7, that the GRIN lens could or soon may be fabricated from a sphere of dielectric material with the required spherically symmetric parabolic gradient.

C. GRIN LENS DESIGN PARAMETERS

In the HIN lens, the available design parameters are basic. These include: F, R, T, α, U, and N_2. Parameters available for varying the design of the GRIN lens, however, include those of the HIN case but expand the index of refraction variable N_2 into O_s, a, +b, and -b. These additional lens design parameters greatly expand the lens designer's power to bend radiant energy to his will.

D. GRIN LENS DESIGN

The GRIN lens design procedure, although paralleling that of the HIN case, is somewhat more complicated in that the rays are now curved and the index of refraction varies. Accordingly, the same design process is used but with more intermediate calculations required.

The additional calculations arise since the intercept of the GRIN ray with the surface tangent cannot be solved in closed form, and an iterative solution must be used.

The reader will note that Equation (117) will yield r if $(\theta-\theta_0)$ is known. Hence the iterative procedure is to "guess" $(\theta-\theta_0)$ based on the HIN coordinates x_{1H},y_{1H} which are calculated as in the homogeneous lens. Thus

$$\theta_H = \theta_T - \theta_0 \tag{125}$$

in Figure 9 is used in Equation (117) to find point p. The tangent to the ray path at point p is now extended to intercept the surface tangent again using the homogeneous intercept relations to find x'_{1H},y'_{1H}. The prime superscripts indicate successive iteration values. The distance d is employed as a measure of the error of point p. If d is not within an acceptable margin then θ'_H is calculated based on x'_{1H},y'_{1H} and the procedure repeated to find p' in Figure 9. If d' is not within allowable error then the iteration continues until it is acceptable. In practice, this iteration procedure has proved to be extremely rapid, rarely requiring more than three iterative steps before converging. Slight modifications, however, must be introduced to handle a positive gradient. Furthermore, if O_s is located outside the lens proper, a decreasing angular increment must be subtracted from θ_H to ensure that each radial vector r_H, r'_H, ... intersects the ray during iteration. These modifications to the intercept iteration procedure are recorded in the program listing for program GISL (for Gradient Index Seeker Lens). Refer to Appendices A, B, and C for a full description of GISL.

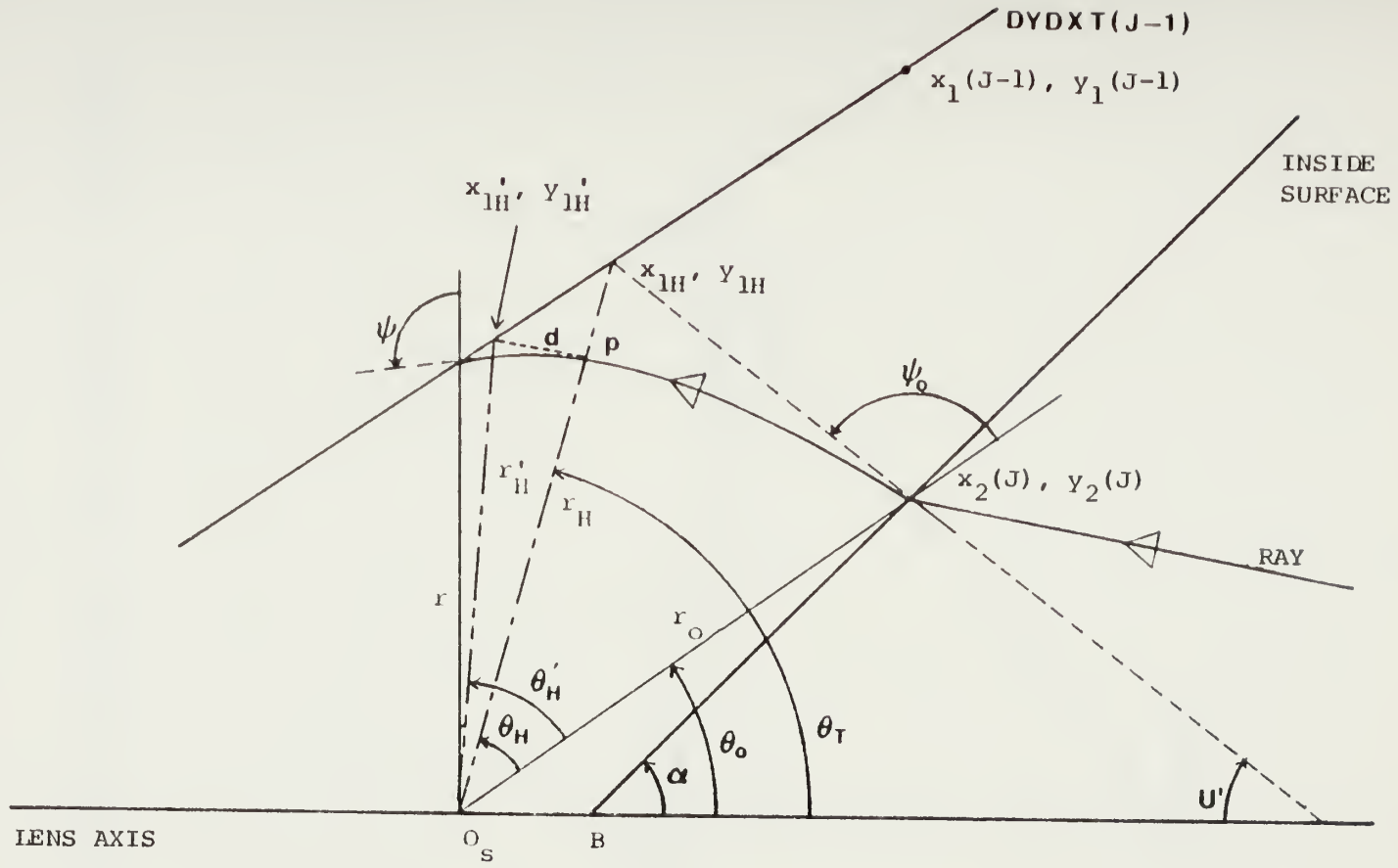

Figure 9. Grin Ray Intercept Geometry

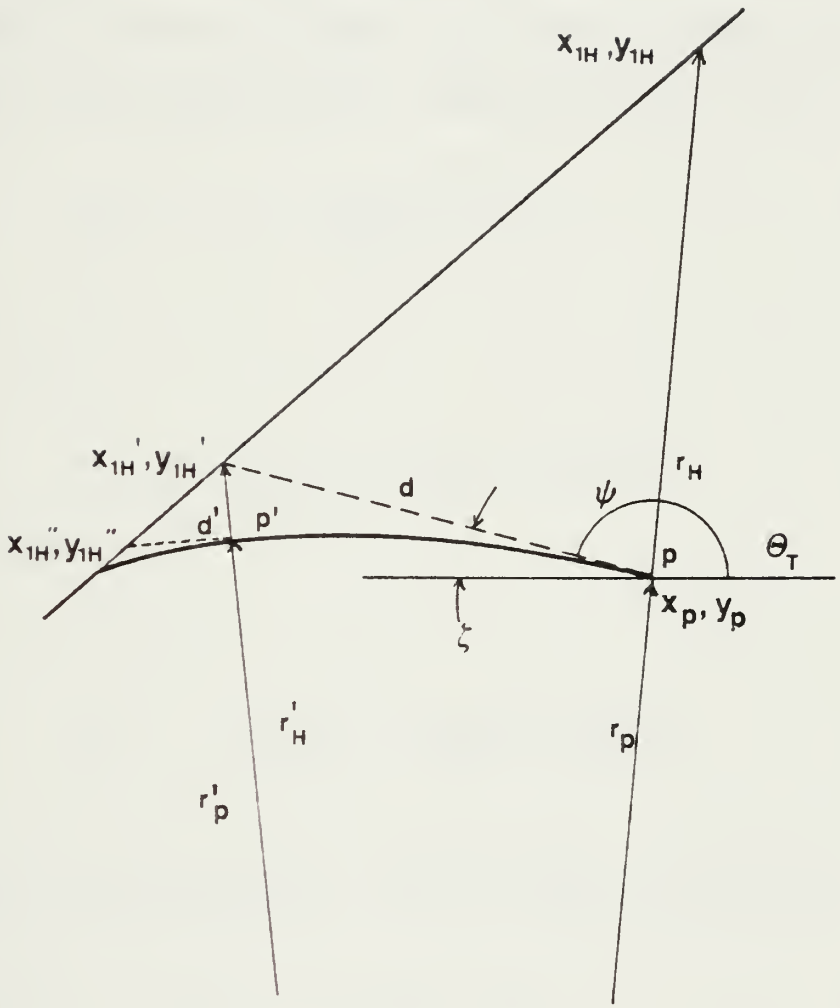

Figure 10. Expanded View, Intercept Geometry

With the overall iterative intercept procedure now being clear, the mathematical details of the GRIN lens design follow. Referring again to Figure 9, the GRIN ray is traced as in the HIN design procedure to obtain the coordinates $x_2(J), y_2(J)$ on the inside surface in the meridian plane. Now, before Snell's law can be used, the index of refraction must be found at these coordinates. Using Equation (113)

$$n_2 = [a + b(\frac{r_0}{R_Z})^2]^{1/2} \tag{125}$$

where

$$r_0 = \sqrt{(x_2(J) + OB)^2 + y_2(J)^2} \tag{126}$$

and where

$$R_Z = \sqrt{(x_2(1) + OB)^2 + y_2(1)^2} \tag{127}$$

Furthermore, by inspection it can be easily seen that

$$\psi_0 = \pi - U' - \theta_0 \tag{128}$$

U' is identical to the HIN case[1] and

---

[1]Here Equation (125) must be substituted for N_2 in Equation (12).

$$\theta_0 = \tan^{-1}\left[\frac{y_2(J)}{y_2(J) + OB}\right] \tag{129}$$

In Equations (126) through (129) OB is the line segment from O_s to B and is defined as a positive quantity to the left of B for algebraic ease of manipulation. By substitution into Equation (109) the scalar constant, e, of the ray can now be found. Furthermore, since angle U' is now known coordinates x_{1H}, y_{1H} may be calculated using Equations (14) and (15) or Equations (24) through (28).

For the first ray defining the edge of the lens, Equations (14) and (15) are employed, and, since no iteration is required, angle $(\theta_T - \theta_0)$ is used in Equation (117) to find r immediately. Here

$$\cos \theta_T = \frac{x_{1H} + OB}{r_H} \tag{130}$$

and

$$r_H = \sqrt{(x_{1H} + OB)^2 + y_{1H}^2} \tag{131}$$

Thus

$$x_1(1) = r \cos \theta_T - OB \tag{132}$$

and

$$y_1(1) = r \sin \theta_T \tag{133}$$

are the coordinates of the first point on the outside surface. Since e is known, Equation (119) is employed to find the angle ψ. Angle ζ in Figure 10 is employed to translate ψ into the ray direction with respect to the lens axis by the relation

$$\zeta = \pi - (\psi + \theta_T) \tag{134}$$

Therefore, by substituting ζ for U' in Equations (19), (20), and (21), DYDXN(1) and DYDXT(1) may be found. Here again, N_2 in Equation (19) must be replaced by n_2 as given by Equation (113) evaluated at $x_1(1), y_1(1)$.

Now that the first point on the outside surface is known, along with the surface tangent, the remainder of the K number of rays may be processed to yield the balance of the outside surface. Each subsequent intercept between ray and tangent must be iterated. Thus, unlike the first ray, once x_{1H}, y_{1H}, r_H, r_p, ψ, and ζ are known, x_{1H}' and y_{1H}' are ascertained by the substitution of the coordinates of point p for $x_2(J), y_2(J)$ in Equations (24) through (28) with U' replaced by ζ. The coordinates of point p are

$$x_p = r_p \cos \theta_T - OB \tag{135}$$

$$y_p = r_p \sin \theta_T \tag{136}$$

Therefore

$$y_{1H}' = \{\frac{A + B}{C}\} \tag{137}$$

where

$$A = \cot(I_1 + U) \cot \zeta [y_p + x_p \tan \zeta] \tag{138}$$

$$B = y_1(J-1) - x_1(J-1) \cot[I_1 + U] \tag{26}$$

$$C = 1 + \cot(I_1 + U) \cot \zeta \tag{139}$$

and

$$I_1 = \sin^{-1} \left\{ \frac{\sin^2(\zeta-U)}{[\cos(\zeta-U) - N_1/n_2]^2 + \sin^2(\zeta-U)} \right\} \tag{140}$$

Note that n_2 in Equation (140) is found from Equation (113) evaluated at r_p.

Additionally,

$$x_{1H}' = \cot \zeta [-y_{1H}' + y_p + x_p \tan \zeta] \tag{141}$$

Now the error, d, may be evaluated as

$$d = \sqrt{(x_p - x_{1H}')^2 + (y_{1H}' - y_p)^2} \tag{142}$$

Here d is compared to 1×10^{-5}. If d is larger than this value then the entire procedure is repeated by substituting x_{1H}', y_{1H}' for x_{1H}, y_{1H} and so forth. Once the error criteria are satisfied

$$x_1(J) = x_p \quad (143)$$

$$y_1(J) = y_p \quad (144)$$

and the next ray is processed. Correlation between GRIN (with b set equal to zero) and HIN design procedures run with identical parameters has shown agreement to the fifth and sixth decimal places.

E. SKEW RAYS IN GRIN

GRIN skew rays are handled analogously to the homogeneous case with the same coordinate transformation from grid plane to global coordinates being required. It is only after the initial directions cosines of the GRIN skew ray K', L', M' are found that the differences between GRIN and HIN appear. The only exception to this being the use of Equation (113) in Snell's law for refraction at the interface. Since the GRIN skew rays display curvature in a plane through O_s, K', L', and M' are constantly changing until intercept with the inside conical surface. Therefore, not only must the plane of the skew ray be analytically described, but the final values of K', L', M' must be found. Due to the nature of

GRIN rays, the procedure for finding the ray intercept with the conical inside surface is different from both the HIN case and the iteration procedure employed in the meridian plane due to the multiplicity of the geometry encountered. The Newton-Raphson iteration routine has been found to be ideal for this purpose.

To begin, the magnitude and direction of the initial radius vector $\bar{r}_0$ from O_s for x_0, y_0, z_0 must be ascertained. The magnitude is given by

$$r_0 = [(x_0 + OB)^2 + y_0^2 + z_0^2]^{1/2} \tag{145}$$

Therefore the unit vector in the direction of the intercept is

$$\hat{r}_0 = \frac{x_0 + OB}{r_0} \hat{i} + \frac{y_0}{r_0} \hat{j} + \frac{z_0}{r_0} \hat{k} \tag{146}$$

The plane of the ray may be fully described by the vector normal to the plane. Two vectors, $\hat{r}_0$ and $\hat{R}$ lie in the plane of the ray. $\hat{R}$ is the unit vector in the initial direction of the ray after refraction and described using direction cosines as

$$\hat{R} = K'\hat{i} + L'\hat{j} + M'\hat{k} \tag{147}$$

Thus, the plane of the ray may be described by the cross product

$$\hat{N}_{p_0} = \hat{r}_0 \times \hat{R} \tag{148}$$

or

$$\hat{N}_{p_0} = N_{p_{0x}} \hat{i} + N_{p_{0y}} \hat{j} + N_{p_{0z}} \hat{k} \tag{149}$$

where

$$N_{p_{0x}} = r_{0y}M' - r_{0z}L' \tag{150}$$

$$N_{p_{0y}} = r_{0z}K' - r_{0x}M' \tag{151}$$

and

$$N_{p_{0z}} = r_{0x}L' - r_{0y}K' \tag{152}$$

In Equations (150), (151), and (152) r_{0x}, r_{0y}, and r_{0z} refer to the x, y, and z components of $\hat{r}_0$ in Equation (146). Furthermore, the angle ψ_0 between $\hat{r}_0$ and $\hat{R}$ may be found from the dot product as

$$\psi_0 = \cos^{-1}[r_{0x}K' + r_{0y}L' + r_{0z}M'] \tag{153}$$

Now the scalar invariant e may be found. Substituting known values into Equation (109):

$$e = \varepsilon\left[a + b\left(\frac{r_0}{R_Z}\right)^2\right]^{1/2} r_0 \sin \psi_0 \qquad (154)$$

where R_Z is unchanged from that found during previous calculations for the lens shape by Equation (127).

With the foregoing groundwork established, the intercept of the ray with the inside surface may be calculated. The Newton-Raphson iteration scheme requires the calculation of the radius vector from O_s to the cone by geometrical methods and the radius to the ray by GRIN theory. The difference between the two radii is then divided by the difference between the derivatives of the two functions. The resulting quantity is subtracted from the trial angle, θ_p, in the plane of the ray, to give a new trial angle θ_p'. The process is continued until the difference between radii is less than 1×10^{-5}. The first trial angle is measured to a reference HIN intercept as if the material were homogeneous since the actual GRIN ray curves only slightly. The coordinates of this HIN intercept point are designated x_{iH}, y_{iH}, z_{iH} and are derived using the HIN equations as before. To obtain the first trial angle, the scalar product between $\hat{r}_0$ and $\hat{r}_{iH}$ is used. Here

$$r_{iH} = \left[(x_{iH} + OB)^2 + y_{iH}^2 + z_{iH}^2\right]^{1/2} \qquad (155)$$

and

$$\hat{r}_{iH} = \frac{x_{iH} + OB}{r_{iH}} \hat{i} + \frac{y_{iH}}{r_{iH}} \hat{j} + \frac{z_{iH}}{r_{iH}} \hat{k} \qquad (156)$$

Thus,

$$\theta_p = \cos^{-1}[r_{0x}r_{iHx} + r_{0y}r_{iHy} + r_{0z}r_{iHz}] \qquad (157)$$

where r_{iHx}, r_{iHy}, and r_{iHz} are the x, y, and z components of r_{iH}, respectively.

In Equation (117) θ_p is substituted for $(\theta-\theta_0)$ to yield r as required by the iteration procedure. The geometrical radius, r_g, is not so easily acquired. First, note that the equation of the plane of the ray inside the lens is given by

$$N_{p0x}(x-x_0) + N_{p0y}(y-y_0) + N_{p0z}(z-z_0) = 0 \qquad (158)$$

Secondly, the equation of the conical surface is given by Equation (75). The combination of the plane of the ray and the cone yield the loci of possible intercept points on the inside surface. In Cartesian coordinates, the sum of Equations (75) and (158) is

$$x(N_{p0x} - x\tan^2\alpha) + y[N_{p0y} + y] + z[N_{p0z} + z] - N_{p0x}x_0$$

$$- N_{p0y}y_0 - N_{p0z}z_0 = 0 \qquad (159)$$

Equation (159) must be transformed into coordinates r and θ_p

in the plane of the ray. The transformation is made possible using Equations (120) through (124). Upon substitution, and after solving for r_g, Equation (159) becomes

$$r_g = \frac{-B_2}{2A_2} \pm \sqrt{\frac{B_2^2}{4A_2^2} + \frac{C_2}{A_2}} \tag{160}$$

where

$$A_2 = B_1^2 + C_1^2 - A_1^2 \tan^2\alpha \tag{161}$$

$$B_2 = B_1 N_{poy} + C_1 N_{poz} + A_1 N_{pox} + 2A_1 OB \tan^2\alpha \tag{162}$$

$$C_2 = OBN_{pox} + OB^2 \tan^2\alpha + N_{pox} x_0 + N_{poy} y_0 + N_{poz} z_0 \tag{163}$$

and

$$A_1 = \frac{\delta}{r_0}(x_0 + OB) + \eta K' \tag{164}$$

$$B_1 = \frac{\delta y_0}{r_0} + \eta L' \tag{165}$$

$$C_1 = \frac{\delta z_0}{r_0} + \eta M' \tag{166}$$

Here, δ and η are found from

$$\eta = \sin\theta_p / \sin\psi_0 \tag{167}$$

and

$$\delta = \cos \theta_p - \cos \psi_0 \tag{168}$$

which follow from Equations (123) and (124). The plus sign in Equation (160) yields the correct values. Now that r of the ray and r_g of the surface are known, the derivatives of r and r_g with respect to θ at θ_p must be found. It can be shown that for the ray

$$\left.\frac{dr}{d\theta}\right|_{\theta_p} = \frac{\varepsilon r^3}{2e^2} \cos[-2\varepsilon\theta_p + \sin^{-1}(A_3)] \tag{169}$$

where

$$A_3 = \frac{2e^2/r_0^2 - a}{\sqrt{a^2 + 4be^2/R_z^2}} \tag{170}$$

The derivative of r_g is somewhat more complicated. With persistence, however, it can be shown that

$$\frac{dr_g}{d\theta} = -\frac{1}{2A_2^2}\left[A_2 \frac{dB_2}{d\theta} - B_2 \frac{dA_2}{d\theta}\right] + \frac{1}{2}\left[\frac{B_2^2}{4A_2^2} + \frac{C_2}{A_2}\right]^{-1/2} [C_3] \tag{171}$$

where A_2, B_2, and C_2 are given by Equations (161) through (168) and

$$C_3 = \left[\frac{1}{2A_2^4}\left(A_2^2 B_2 \frac{dB_2}{d\theta} - B_2^2 A_2 \frac{dA_2}{d\theta}\right) - \frac{C_2}{A_2^2}\frac{dA_2}{d\theta}\right] \tag{172}$$

Therefore, the r and θ_p to the intercept are found by iteration of revised trial values

$$\theta_p' = \theta_p - \frac{(r - r_g)}{(\frac{dr}{d\theta} - \frac{dr_g}{d\theta})} \tag{173}$$

In practice the quotient of differences in Equation (173) is reduced by a factor of 1.3 to slow convergence and provide stability. The number of iterations, however, rarely exceeds five.

Values for r and θ_p are now transformed into Cartesian coordinates x_i, y_i, z_i by substitution into Equations (120) through (124). Next, the values of the direction cosines K', L', and M' at the intercept are needed. The angle ψ between the radius vector and the tangent to the ray at intercept may first be deduced from the scalar invariant, e. Hence

$$\psi = \sin^{-1}(\frac{e}{n_2 r_{PI}}) \tag{174}$$

Where e is known, n_2 is evaluated at r_{PI}; r_{PI} is the radius to the intercept as found by the iteration above. Three constraints on the direction cosines may be written. These are:

1) The scalar product of the radius vector, $\hat{r}_{PI}$, and the instantaneous ray direction vector, $\hat{R}$, at intercept.

2) The scalar product of the normal to the plane of the ray $\hat{N}_{p0}$ and $\hat{R}$.

3) The sum of the squares of the direction cosines must sum to unity.

Mathematically, the above constraints are written as

$$\frac{(x_i + OB)}{r_{PI}} K' + \frac{y_i}{r_{PI}} L' + \frac{z_i}{r_{PI}} M' = \cos \psi \tag{175}$$

$$N_{P0x}K' + N_{p0y}L' + N_{p0z}M' = 0 \tag{176}$$

$$K'^2 + L'^2 + M'^2 = 1 \tag{177}$$

To find K', L', and M', Equations (175), (176) and (177) are solved simultaneously. It can be shown that the solution leads to

$$M' = \frac{-B_6}{2A_6} \pm \sqrt{\frac{B_6^2}{4A_6^2} - \frac{C_6}{A_6}} \tag{178}$$

$$L' = A_5 - B_5M' \tag{179}$$

$$K' = (1 - L'^2 - M'^2)^{1/2} \tag{180}$$

where

$$A_6 = [1 + (\frac{N_{P0z}}{N_{p0x}})^2]B_5^2 - \frac{2 N_{p0y} N_{p0z}}{N_{p0x}^2} B_5 + (\frac{N_{p0z}}{N_{p0x}})^2 + 1 \tag{181}$$

$$B_6 = \frac{2 N_{p0y} N_{p0z}}{N_{p0x}} A_5 -][1 + (\frac{N_{p0z}}{N_{p0x}})^2]A_5 B_5 \quad (182)$$

$$C_6 = [1 + (\frac{N_{p0z}}{N_{p0x}})^2]A_5^2 - 1 \quad (183)$$

and

$$A_5 = \frac{N_{p0x} \cos \psi}{N_{p0x} B_4 - N_{p0y} A_4} \quad (184)$$

$$B_5 = \frac{N_{p0x} C_4 - N_{p0z} A_4}{N_{p0x} B_4 - N_{p0y} A_4} \quad (185)$$

Furthermore, in Equations (184) and (185), A_4, B_4, and C_4 are the coefficients of K', L' and M' in Equation (175).

Now that the direction cosines of the ray are known at the point of intersection with the inside surface, the index of refraction, n_2, is computed by substituting r_{PI} into Equation (113). The remainder of the skew ray trace to the image plane is identical to the homogeneous procedure.

IV. LENS PERFORMANCE PARAMETERS

The function of the seeker lens is to focus electromagnetic energy either reflected from or emitted by the target onto a detector. Angular displacement of the target with respect to the missile body axes as well as target angular rate information are both desired outputs from the seeker. Hence, it is not only important just to be able to detect the target by focusing energy into a spot on the detector, it is equally important that this spot be as small as possible to enable the precise position of the spot on the detector to be discerned.

The ability of a lens to focus an object to a small spot does not guarantee the quality of the image. For a FLIR optical system extensive effort is expended to obtain an image with minimum aberration [10]. Seeker optics, however, are generally non-imaging devices where the pressure of the different aberrations does not detract from the function of the seeker as long as a tight image is maintained [11].

Accordingly, the most important parameter by which seeker lens performance is judged is that of spot size at different obliquities. Since the image found at the focal point is not necessarily circular nor equally dense, the standard deviation in the y and z directions with respect to image centroid is used to define spot size.

Therefore, once the coordinate pairs of all the skew rays have been calculated in the image plane, the first step in

the analysis of lens performance is to calculate the image centroid [12]. If the spot diagram is composed of N rays, the centroid location, y_c is

$$y_c = \frac{1}{N} \sum_{i=1}^{N} Y_i \tag{186}$$

Since there is symmetry about the x-y plane, the z coordinate of the centroid will always be zero.

The next step in finding the spot size is to find the standard deviations of the spot diagram in the y and z directions. This is accomplished by summing the squares of the differences of the intercept coordinates with respect to the centroid and then dividing by the number of rays. The standard deviations then, are given by

$$\sigma_z^2 = \frac{1}{N} \sum_{i=1}^{N} Z_i^2 \tag{187}$$

and

$$\sigma_y^2 = \frac{1}{N} \sum_{i=1}^{N} (Y_i - y_c)^2 \tag{188}$$

The spot size, σ_r, is now defined by

$$\sigma_r = \sqrt{\sigma_z^2 + \sigma_y^2} \tag{189}$$

Of further interest in appraising lens performance is the energy density of the image as a function of radius from the centroid. In nondimensional form, this is simply the number of rays in the spot diagram within a succession of circles of increasing size overlaid about the centroid. Here, each ray is assumed to carry a unit amount of radiant energy. This type of plot facilitates the comparison of different lens designs by detailing the distribution of energy within each image. Clearly, it is desirable to have as much energy as possible concentrated very close to the image centroid. Between two lenses with equal spot sizes, the preferred lens has more energy concentrated within a smaller radius.

Every ray, however, does not deliver an equal amount of energy to the focal plane. It is prudent, therefore, to include as a performance parameter the average ray intensity. Again, for N rays, the intensity I of each ray is summed and normalized by N to yield

$$I_{av} = \frac{1}{N} \sum_{i=1}^{N} I_i \qquad (190)$$

Finally, each lens design is checked for "failed rays". The reader will recall that these rays fail to intercept the image plane due to total internal reflection, total external reflection, or failure to intercept the inside surface within the bounds of the lens. Hence, a lens design with fewer "failed rays" or no "failed rays" at all is a preferred lens.

Although there are many other performance criteria by which lenses are compared, the foregoing parameters are more than sufficient to judge the merit of preliminary seeker lens designs. It should be noted, however, that notwithstanding the fact that the image centroid and standard deviations were used as stepping stones to obtain image spot size, they have significant meaning of their own. The standard deviations σ_y and σ_z inform the lens designer as to the horizontal and vertical spread of the image. Image centroid location, y_c, at increasing obliquities is of obvious importance since excessive displacement will cause the image to miss the detector entirely and would dictate the necessity for a second lens element to dampen the movement. Furthermore, since Line of Sight (LOS) measurement accuracy to the target is highly dependent upon the linearity of y_c as a function of the lens tilt angle, lens designs which exhibit a greater degree of such linear behavior are the preferred designs.

To summarize, it is sufficient to note that although spot size is the most important of the performance parameters, every other parameter has a significant impact on the performance of a particular lens.

V. RESULTS FOR THE HOMOGENEOUS LENS

The performance of the homogeneous lens is presented primarily as a comparison with which to compare the performance of the GRIN lens. Here, the relationship of spot size to increasing lens obliquity and lens thickness are presented as well as the image centroid movement as a function of obliquity. Additionally, the reader is introduced to the four basic computer plots used to display the results: lens shape, object plane with superimposed skew ray grid, image plane or spot diagram, and energy density. These plots were generated on the VERSATEC Plotter using arrays of data points produced by program GISL on the IBM 3033 mainframe computer.

To begin, Figure 11 shows the homogeneous lens shape. The first of the four basic plots, the lens shape plot, presents the lens side view in the meridian plane. The outer surface (curved) and the inner surface (cone) are constructed by connecting the points $x_1(J)$, $y_1(H)$ and $x_2(J)$,$y_2(J)$, respectively, by straight lines. At the apex of the lens about the lens axis is a trapezoidal region which represents the opaque nose area. In the legend are listed the lens design parameters and the significant calculated dimensions of the lens. Since all linear dimensions are implicitly normalized with respect to the maximum inside radius, R, the lens may be scaled up or down by multiplying each dimension by a factor of R_{new}/R. Beginning at the top, the parameters listed in the legend are explained in Table 1.

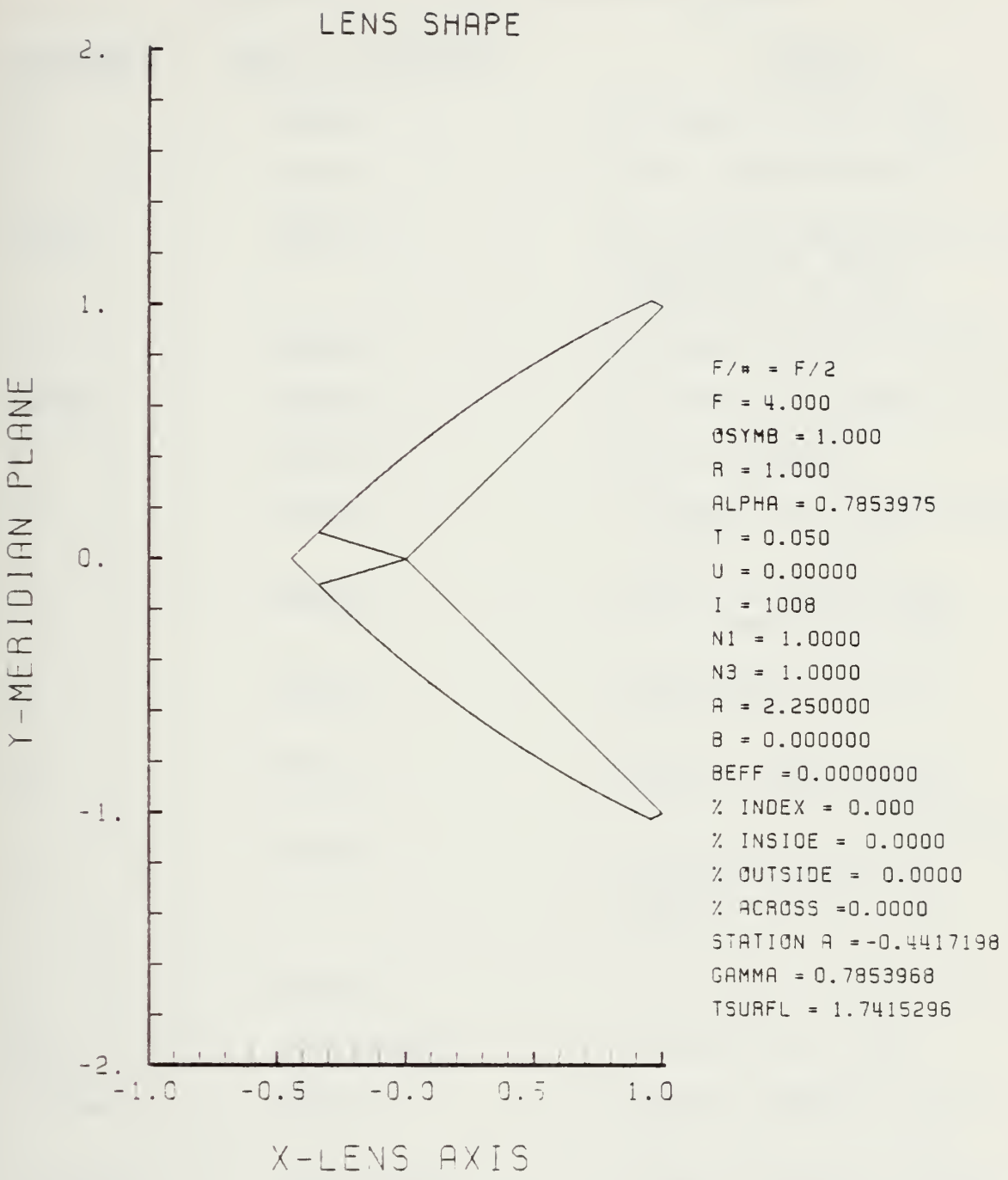

Figure 11. Homogeneous Lens Shape for $N_2 = 1.5$

TABLE 1

Explanation of Lens Shape Plot Legend

PARAMETER	TYPE OF PARAMETER	MEANING
F/#	DESIGN	F number. F/# = F/2R
F	DESIGN	Focal length from B.*
OSYMB	DESIGN	OB. Line segment O_s to B (positive to left).* Immaterial in HIN
R	DESIGN	Maximum radius of cone*
ALPHA	DESIGN	α--cone half-angle,* radians
T	DESIGN	Edge thickness*
U	DESIGN	Incident ray offset angle (design)*, radians
I	DESIGN	Number of iterations. I+1 = number of rays
N_1	DESIGN	Free stream index of refraction
N_3	DESIGN	Index of refraction of interior lens cavity
A	DESIGN	a in $n_2(r) = \sqrt{a + b(r^2/R_Z^2}$, gradient refractive index function. $N_2 = \sqrt{a}$ in HIN.
B	DESIGN	b in $n_2(r)$. Zero in HIN
B_{EFF}	CALCULATED	b effective = b/R_Z^2
% Index	DESIGN	Percent change in $n_2(r)$ from r = 0 to r = R_Z^2
% Inside	CALCULATED	Percent change in $n_2(r)$ along inside surface from lens axis to edge
% Outside	CALCULATED	Percent change in $n_2(r)$ along outside surface from opaque region to edge

Table 1 (Continued)

PARAMETER	TYPE OF PARAMETER	MEANING*
% Across	CALCULATED	Percent change in $n_2(r)$ across lens from lens axis to outside surface at the thickest point
STATION A	CALCULATED	x-coordinate at nose of lens*
GAMMA	CALCULATED	γ--nose half-angle of opaque nose region,* radians
TSURFL	CALCULATED	Total outside surface length from Station A to the edge

*Refer to Figure 2 for clarification

The HIN lens shape has a convex outer surface with maximum thickness on axis of almost ten times the edge thickness. Although the lens has a good aerodynamic shape resembling an ogive, the outer surface is not a circular arc nor can a single analytical function be fitted to the array of points describing the surface. Note that the nose half-angle, γ, is almost identical to the cone half-angle, α.

All lenses have been designed with a cone half-angle of 45° which is approximately the maximum angle for which aerodynamically efficient lens shapes may be designed, considering a free stream Mach Number not to exceed three. Without exception, overall lens performance is more severely degraded as angle α is reduced.

Table 2 explains the legend of Figure 12, which is the second basic plot. Here the lens is depicted as seen from the skew ray grid plane. The lens tilt angle, α_p, causes the equally spaced (in J) circles descriging the surface of the lens to appear as ellipses. In Figure 12, the grid spacing has been reduced from 0.1, which is normally used, to 0.3 to allow identification of individual rays for correlation with the image plane spot diagram. Although the small number of rays used is not sufficient to given an accurate definition of spot size, the number is sufficient to describe where rays in the object plane are being focused in the image plane by the HIN lens. The skew rays in Figure 12 have been numbered in the order in which they were processed. Actually, only rays 1 through 19 were actually traced; 20 through 33 are

TABLE 2

Explanation of OBJECT PLANE Plot Legend

PARAMETER	TYPE OF PARAMETER	MEANING
ALFAP	Analysis	α_p. Lens tilt angle, radians
Rays	Analysis	Total number of rays processed
Failed Rays	Analysis	Total number of rays failing to pass through the lens*

*Failed Rays are indicated on the plot by a diamond superimposed on the grid location of the ray.

mirror image skew rays. Ray 30 corresponds to ray 14, for example, Here, the lens has been tilted by 0.4 radians, or 22.9 degrees, and 33 rays have been processed of which none have failed to intercept the image plane. The staircase pattern has been added in this case in order to show the resulting distortion present in the image plane (Figure 13).

The Spot Diagram in Figure 13 is an example of the third basic computer plot; see Table 3. Unlike most Spot Diagrams, this example has the individual rays numbered for comparison with Figure 12; also the resulting distorted staircase pattern is sketched. By cross-referencing individual rays between Figures 12 and 13, it is possible to recognize where certain areas of the lens are focusing rays in the image plane. Rays 1, 4, 20, and 22 about the opaque nose region form a coma tail which contributes most of the image spread. Rays 33,

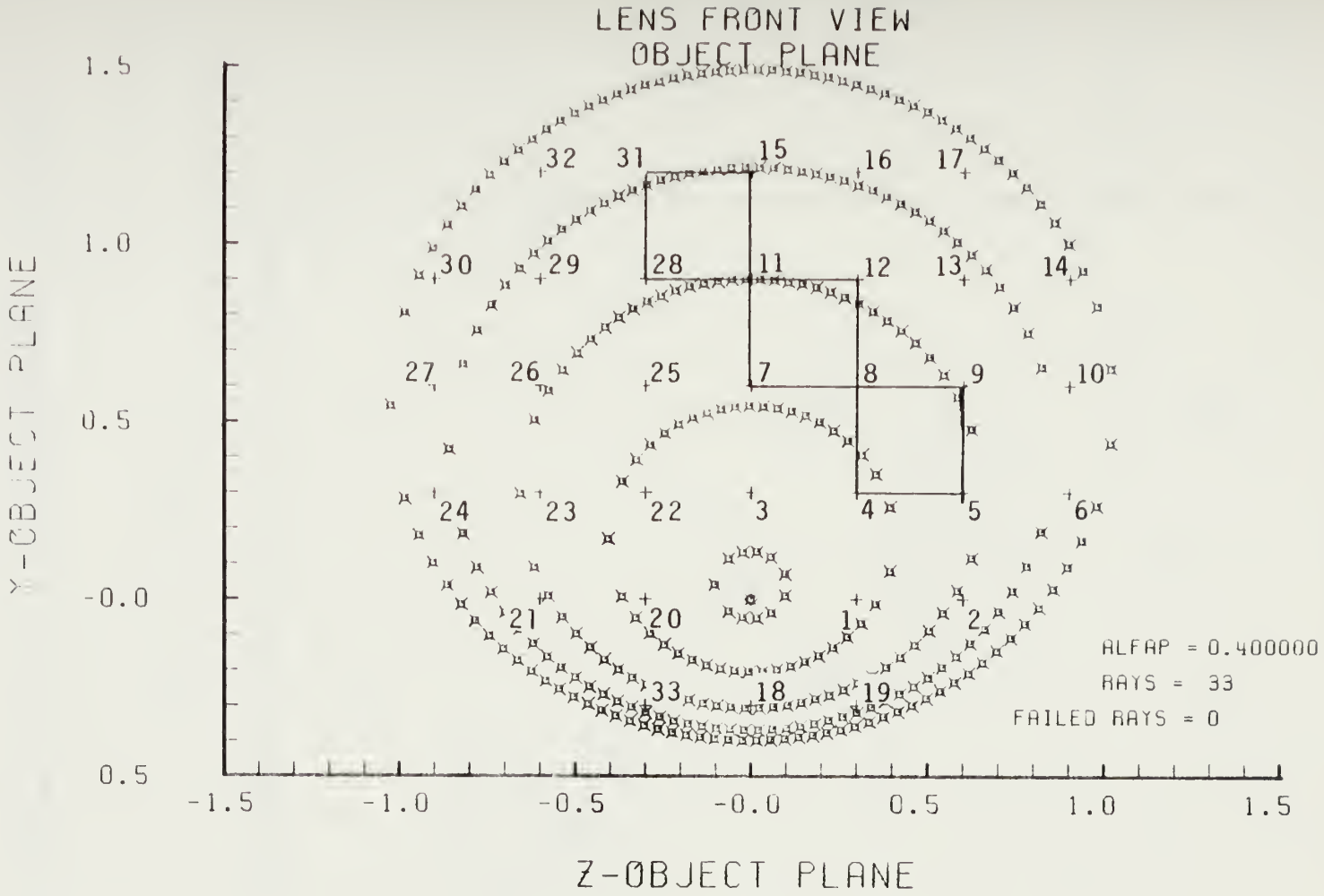

Figure 12. Example Object Plane

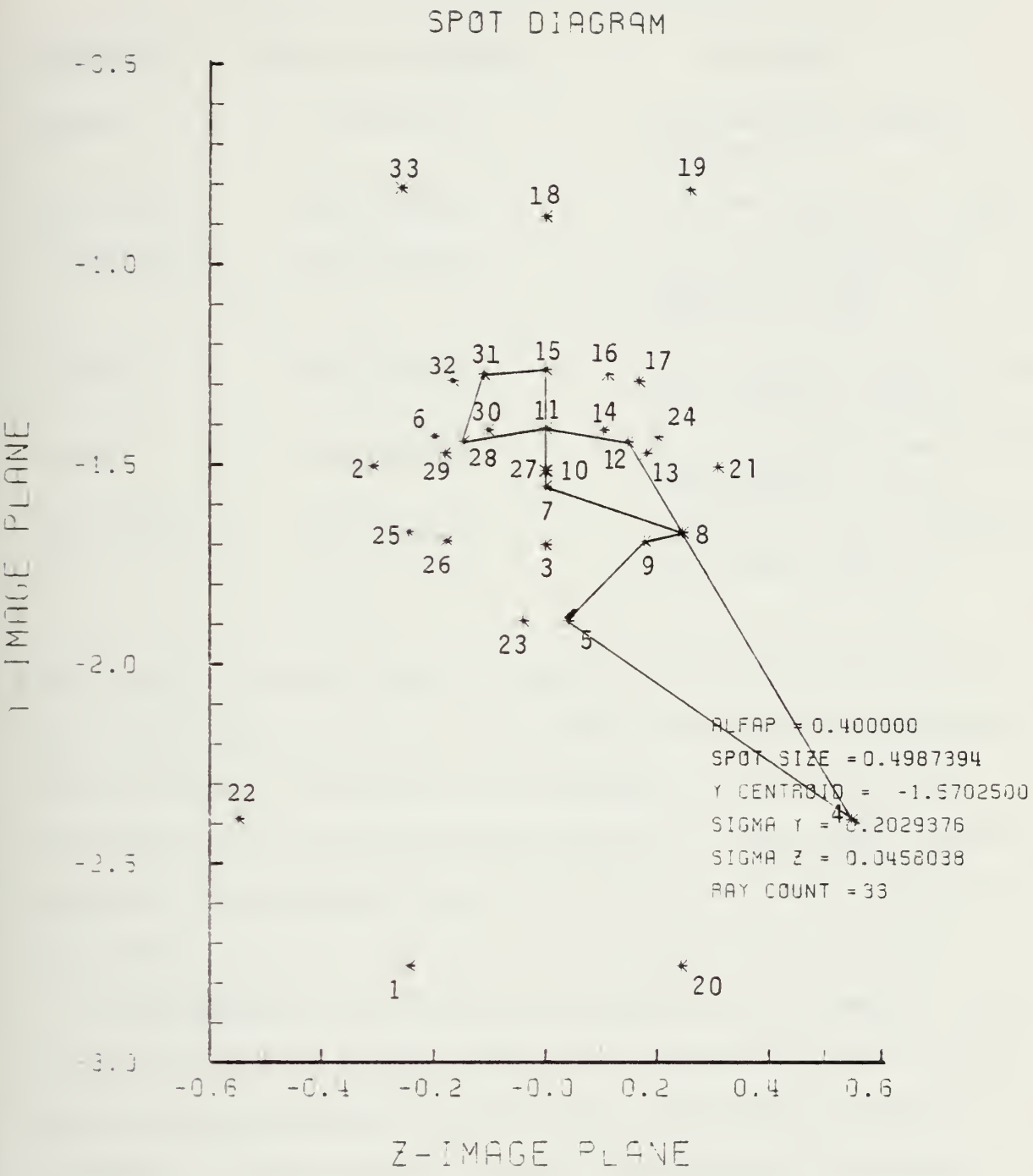

Figure 13. Spot Diagram for HIN Lens Design Shown in Figure 11

TABLE 3

Explanation of Spot Diagram Legend

PARAMETER	TYPE OF PARAMETER	MEANING
ALFAP	Analysis	α_p, lens tilt angle, radians
SPOT SIZE	Performance	σ_r, see Equation (189)
Y-CENTROID	Performance	y_c, y-coordinate of image centroid; see Equation (186)
SIGMA Y	Performance	σ_y, y-standard deviation; see Equation (188)
SIGMA Z	Performance	σ_z, z-standard deviation; see Equation (187)
RAY COUNT	Performance	Number of rays striking the image plane

18, and 19 from the bottom portion of the homogeneous lens are imaged at the top and are widely separated from the core of the image. In general, the regions of the lens which have been found to contribute the bulk of the widely spaced rays are the immediate nose region and the lower portion of the lens.

Furthermore, the distortion present in the image of the staircase pattern clearly shows that regions closest to the nose yield the greatest distortion. Horizontal lines are switched end for end and tilted approximately 45 degrees.

The upper portion of the lens performs the best. Rays 3, 7, 11, and 15 in the meridian plane are focused on the y_{IM} axis in a fairly tight region; rays 10, 14, 17, 27, 30,

and 32 about the upper periphery in the object plane are all focused within the image core.

Table 3 explains the legend of the spot diagram. It is seen that the standard deviation in the y-direction is approximately five times that of the z-direction. This elongation of the image is not readily evident in the spot diagram since the ordinate and abscissa have not been plotted with equal increments. This results from the great disparity between Spot Diagrams of the various lens designs studied. It is important, therefore, for the reader to take careful note of the relative sizes of the y_{IM} and z_{IM} axes.

Of primary importance is the spot size in Figure 13. The value for spot size is adversely affected by the poorest performing regions of the lens. Were it not for these errant rays, the spot size would be considerably smaller. The image intensity pattern is benefitted, however, by the fact that the rays spread the farthest from the centroid contribute significantly less energy per ray than those being focused in the core of the image. Table 4 lists the relative intensities of the primary skew rays plotted in Figure 13. It is seen that the high intercept angles experienced by the rays closest to the bottom of the lens and, to a lesser extent, those near the nose, result in higher reflectivity and lower transmission through the lens.

In the legend of Figure 14, the average of ray intensity is given. The Spot Diagram Energy Density distribution may be seen at a glance. The fraction of energy (number of rays)

TABLE 4

Skew Ray Intensities of HIN Lens

a) Numberical Order

Ray	Intensity	Ray	Intensity
1	0.746	11	0.919
2	0.789	12	0.918
3	0.921	13	0.910
4	0.892	14	0.887
5	0.877	15	0.918
6	0.811	16	0.916
7	0.920	17	0.910
8	0.917	18	0.640
9	0.904	19	0.576
10	0.870		

b) In order of Descending Intensity

Intensity	Ray(s)	Intensity	Ray(s)
0.921	3	0.887	14
0.920	7	0.877	5
0.919	11	0.870	10
0.918	12,15	0.811	6
0.917	8	0.789	2
0.916	16	0.746	1
0.910	13,17	0.640	18
0.904	9	0.576	19
0.892	4		

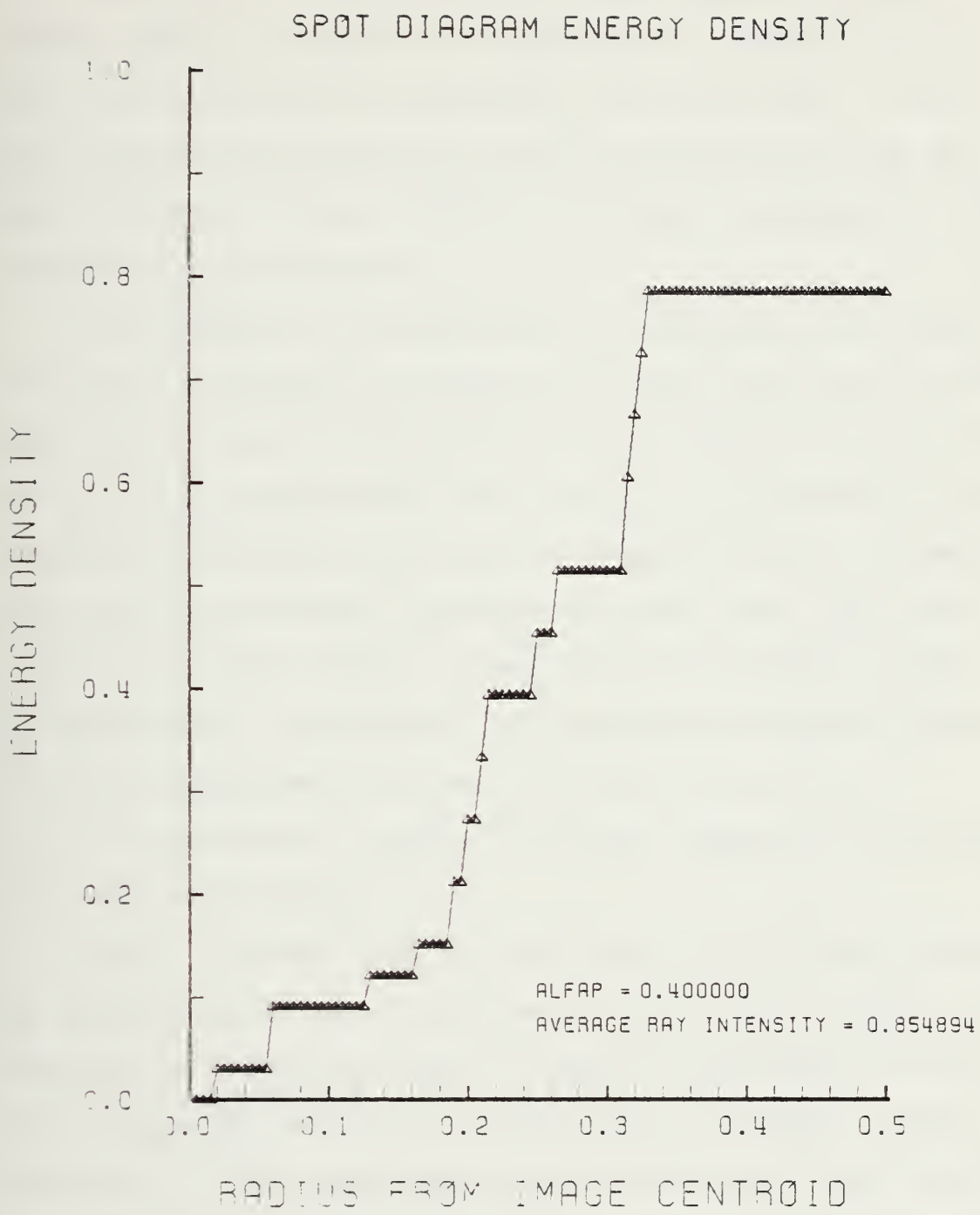

Figure 14. Nondimensional Encircled Energy Plot for HIN Lens Design of Figure 11

shown as a function of radius from the Spot Diagram centroid is normalized with respect to the total number of rays traces (Rays, in Figure 12) regardless of whether all of the rays successfully intercepted the image plane. Thus the fourth basic plot may be used in conjunction with the Spot Diagram to further define the image concentration with respect to the centroid.

The response of the HIN lens to increasing tilt angles is given in Figures D-1 through D-23 where the index of refraction of the lens has been set at 1.5. Whereas the spot size at $\alpha_p = 0.0$ is very small, that at $\alpha_p = 0.7$ radians is quite large at 67% of the lens radius. Figures 15 and 16 summarize spot size and centroid locations for the lens. Spot size growth, although somewhat irregular at the higher angles, is pronounced. Furthermore, the centroid movement is seen to be an approximately linear function of α_p until $\alpha_p \cong 0.3$ and easily exceeds the radial dimension of the lens at higher tilt angles.

Figure 17 shows that the HIN lens may be slightly improved by increasing the edge thickness, T, by a small amount. The lens may be otherwise tuned to improve performance at certain tilt angles by designing the lens with U slightly greater than zero. These performance improvements are practically insignificant, however, and neither lens tuning by the parameter U nor T produce improvement across the spectrum of tilt angles. Instead, an improvement at one α_p usually has resulted in a degradation at others.

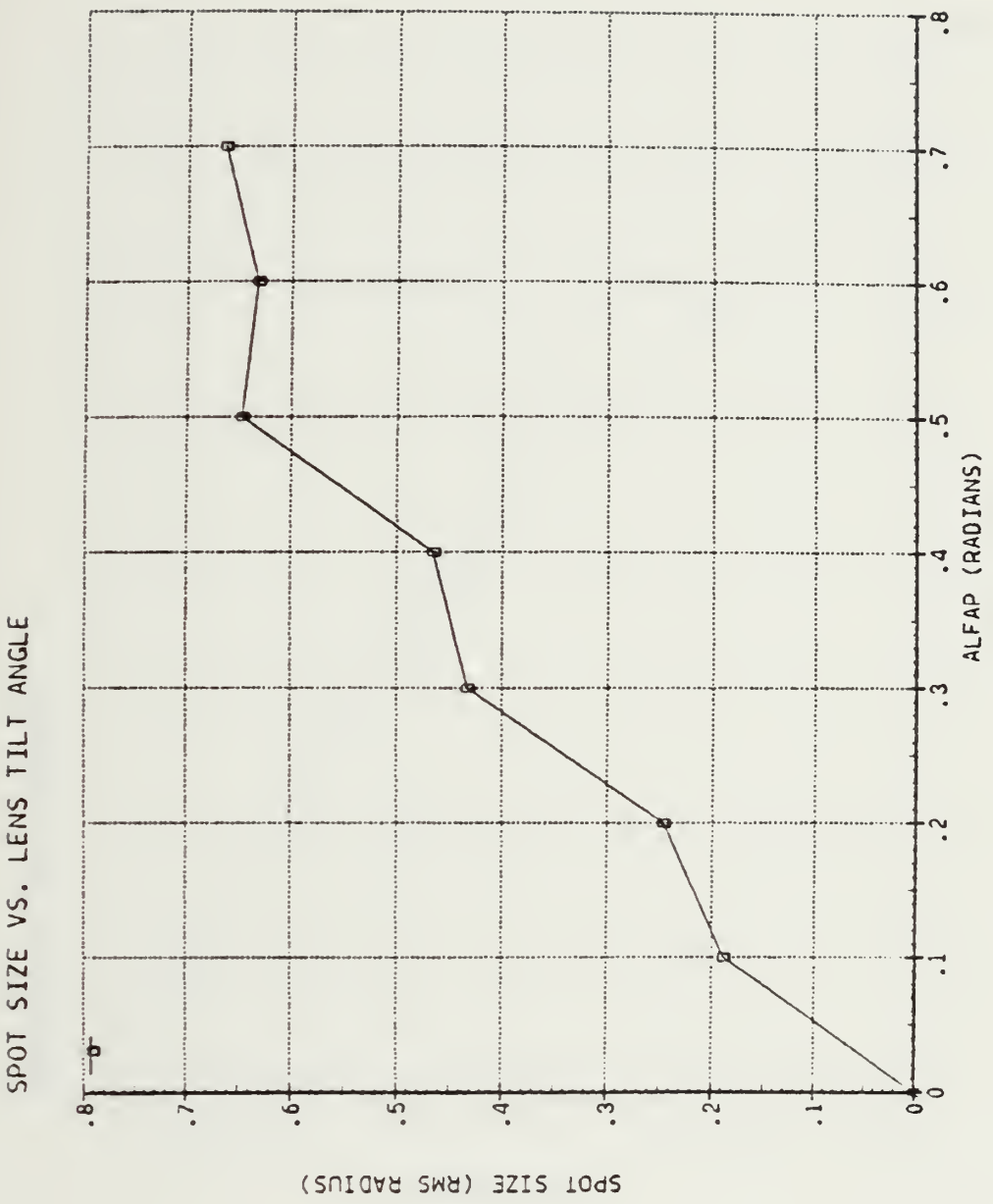

Figure 15. HIN Lens Spot Size versus α_p for $N_2 = 1.5$

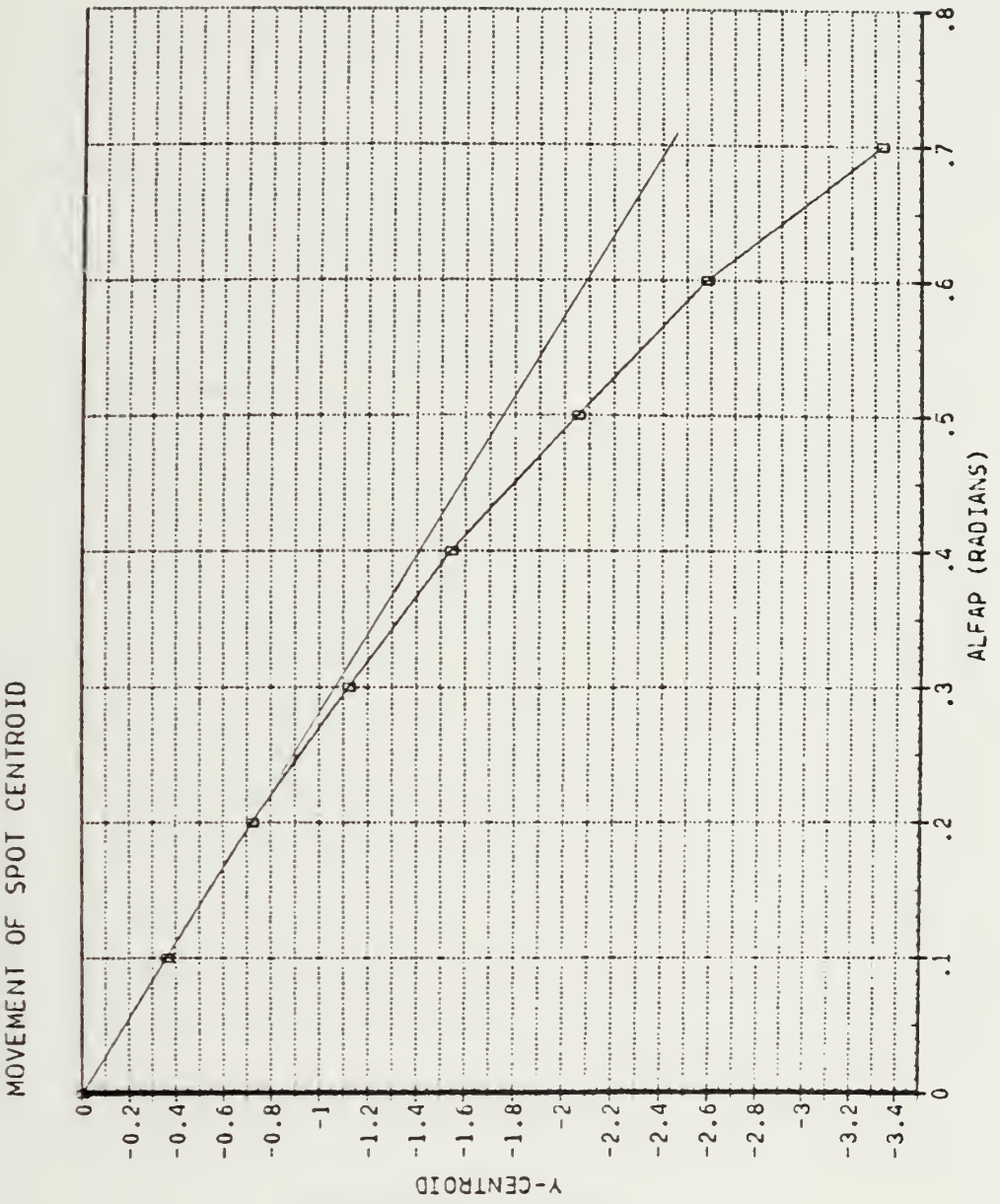

Figure 16. HIN Lens Centroid Movement versus α_p at $N_2 = 1.5$

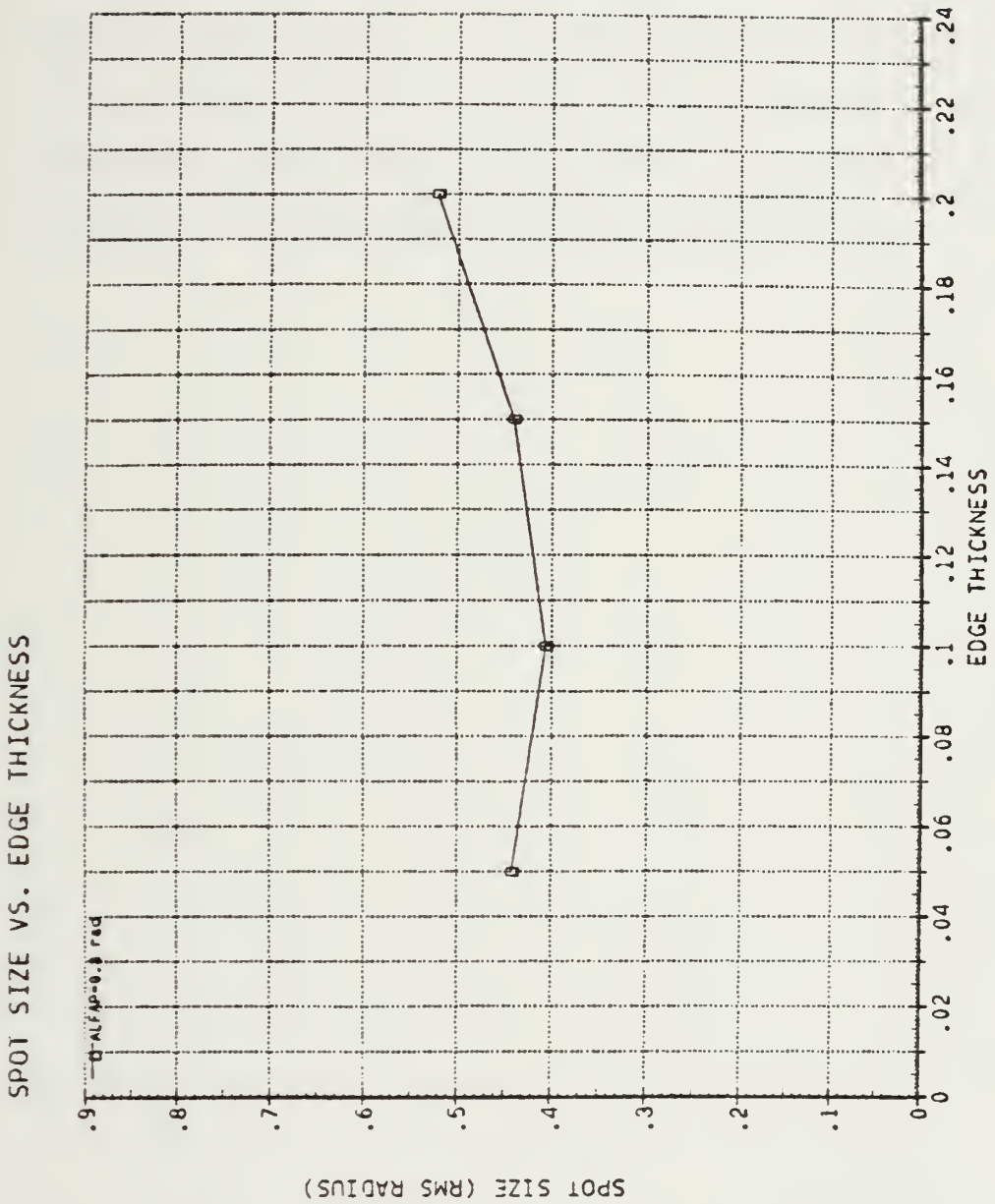

Figure 17. HIN Lens Spot Size versus Edge Thickness at α_p = 0.3 Radians and N_2 = 1.5

Finally, the homogeneous lens is shown with index of refraction of three at the intermediate tilt angle of 0.3 radians in Figures D-24 through D-27. The lens shape required to accommodate the higher index of refraction is seen to be thinner and displays less outside surface curvature than the HIN lens with $N_2 = 1.5$. Spot size is significantly reduced. Since infrared lenses such as germanium generally have fairly high refractive indices, improved lens performance at these higher values is encouraging.

VI. GRIN LENS RESULTS

The performance of the GRIN lens is similar in many respects to the homogeneous lens. The relationship between characteristic regions of the GRIN lens, such as the lower lens portion, and where these regions image bundles of rays is identical to the HIN lens as depicted in Figures 11 and 12. The growth of spot size with increasing α_p and the respective movement of image centroid typical of the homogeneous lens is clearly displayed by the GRIN lens as well.

The measure of the superiority of the GRIN lens, therefore, lies in the successful correction or improvement of the deficiencies seen in the HIN lens. Here, the reduction of spot size is of primary concern.

As a modest example of the ability of the gradient refractive index to reduce spot size, the GRIN lens design shown in Figure 18 is examined. This lens is very similar in shape to the homogeneous lens with $N_2 = 1.5$. Note, however, that unlike the HIN lens, the nose half-angle, γ, is slightly larger than that of the cone, indicating more outside surface curvature. The object plane for this lens, at $\alpha_p = 0.4$, is shown in Figure 19. Here, the error in focusing rays present in the image plane has been superimposed over the grid plane. y_{IM} coordinate error contours (with respect to the centroid) are shown in the left half of the plane and z_{IM} contours in the right. These contours vividly show that the largest

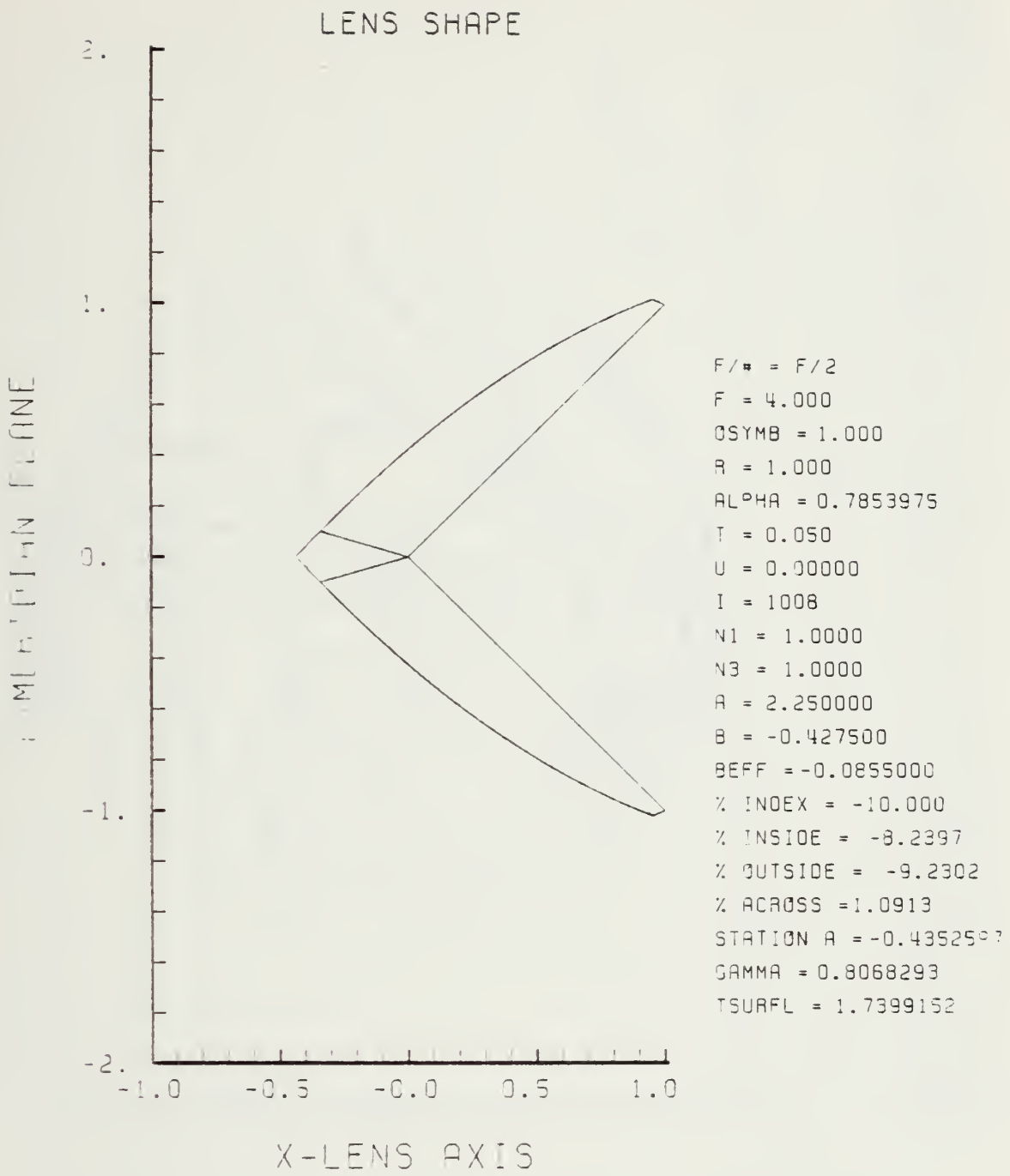

Figure 18. Example GRIN Lens Design with 10% Negative Gradient at OB = 1.0

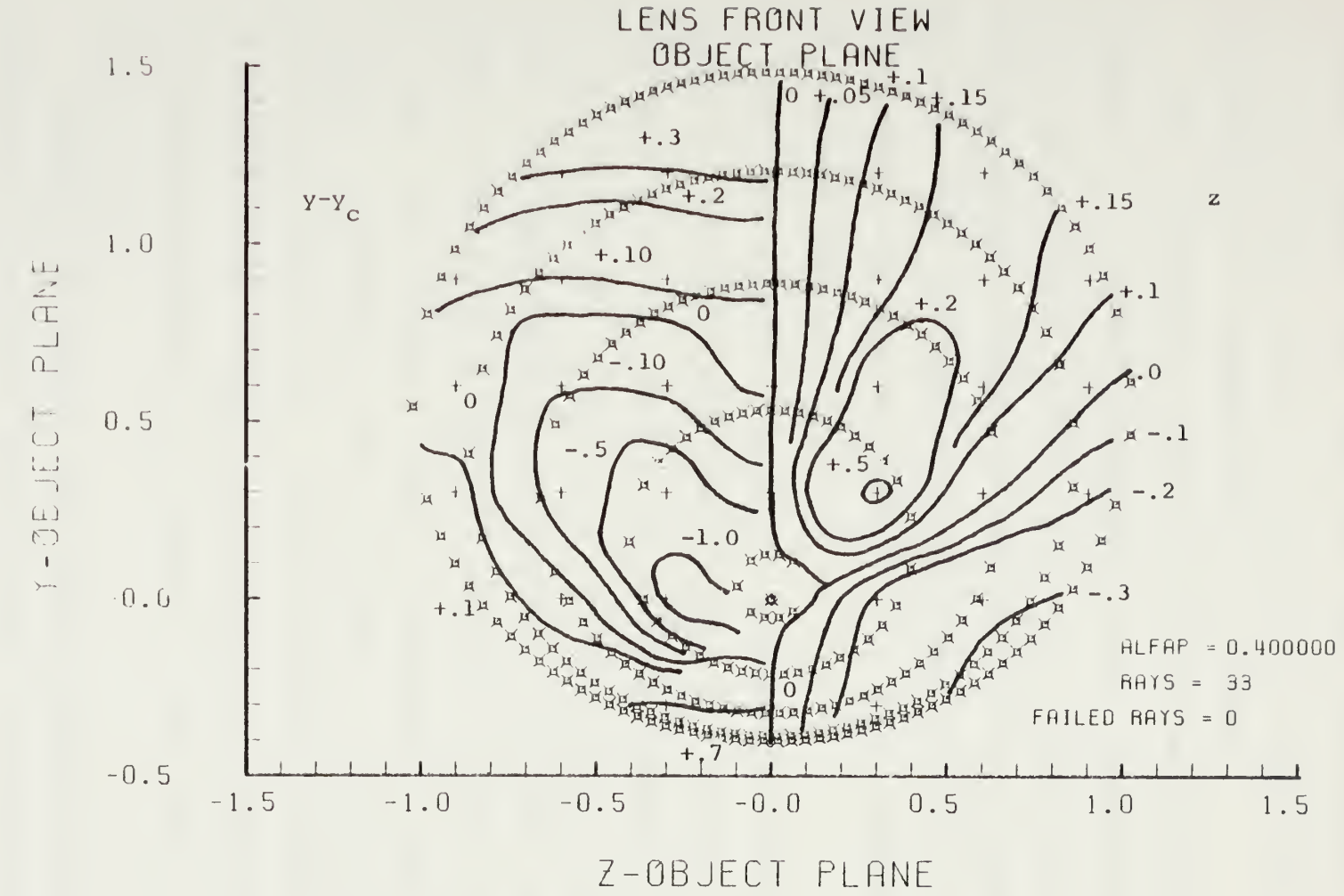

Figure 19. Example GRIN Lens Object Plane. Contours in the Left Half Depict the Difference Between the y Coordinate in the Image Plane and Image Centroid. The Right Hand Contour Shows the Corresponding z Displacement in the Image Plane.

errors in both y and z stem from the nose and bottom of the lens. The best performance is contributed by the upper central region. The reader will note that negative errors in z occur below the $y_0 = 0$ plane of the lens and that negative errors in y straddle the $y_0 = 0$ plane.

The corresponding intensity contours are displayed in Figure 20. Of significance here is that regions which perform relatively well in y and z error also perform well in transmitting energy. Regions of the lens which are characterized by relatively high angles of incidence, therefore, perform the poorest and have the most to gain from better combinations of gradient index and O_S

The Spot Diagram, Figure 21, displays an image pattern virtually identical with the HIN lens in Figure 11. The GRIN spot size, σ_r, however, is slightly smaller by approximately 2% and both σ_y and σ_z are correspondingly smaller which indicates superior performance by the GRIN version. Image centroid for the GRIN is displaced further than that for HIN. The average intensity transmitted by the GRIN lens compares favorably at 0.88 as opposed to the average intensity of the HIN at 0.85. Further evidence of superiority of the GRIN lens is seen in the form of a steeper slope to the Encircled Energy Plot (Figure 22) than that of the HIN lens in Figure 13.

Although the example GRIN design displays marginal superiority, some GRIN designs do not. In particular, it

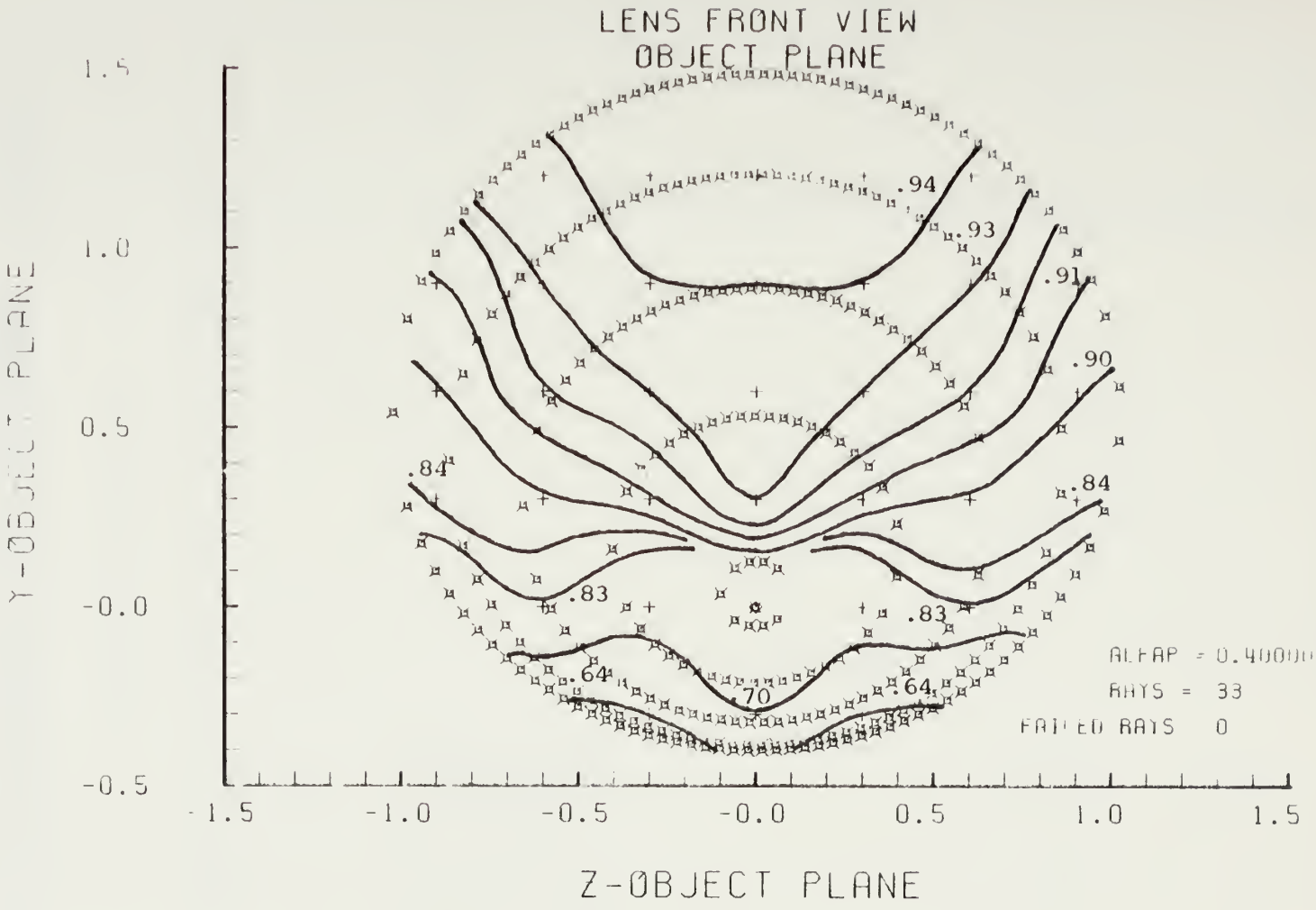

Figure 20. Intensity Contours of the Example GRIN Lens Shown in Figure 45

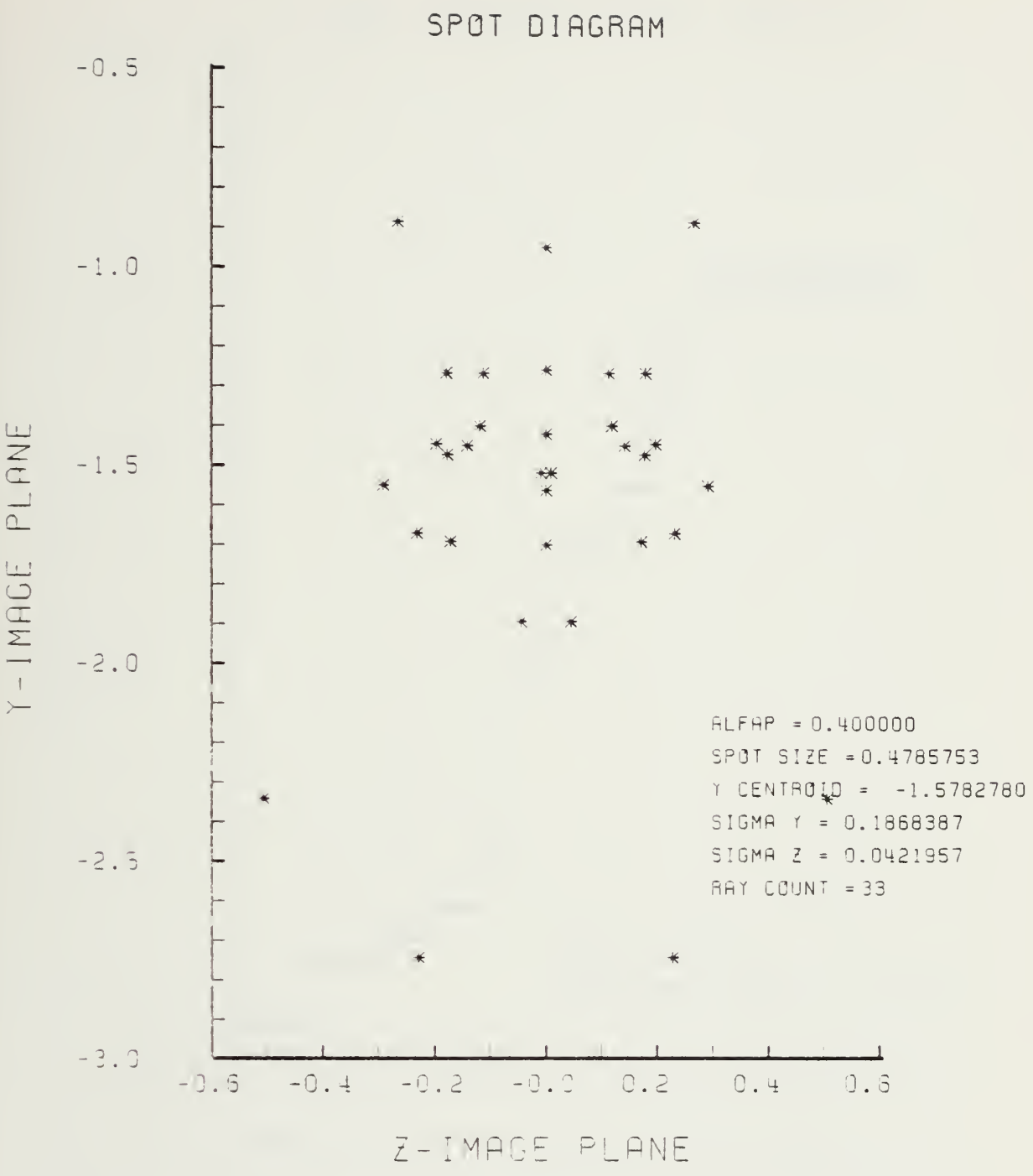

Figure 21. Example GRIN Spot Diagram at α_p = 0.4 Radians for GRIN Lens Design Shown in Figure 18

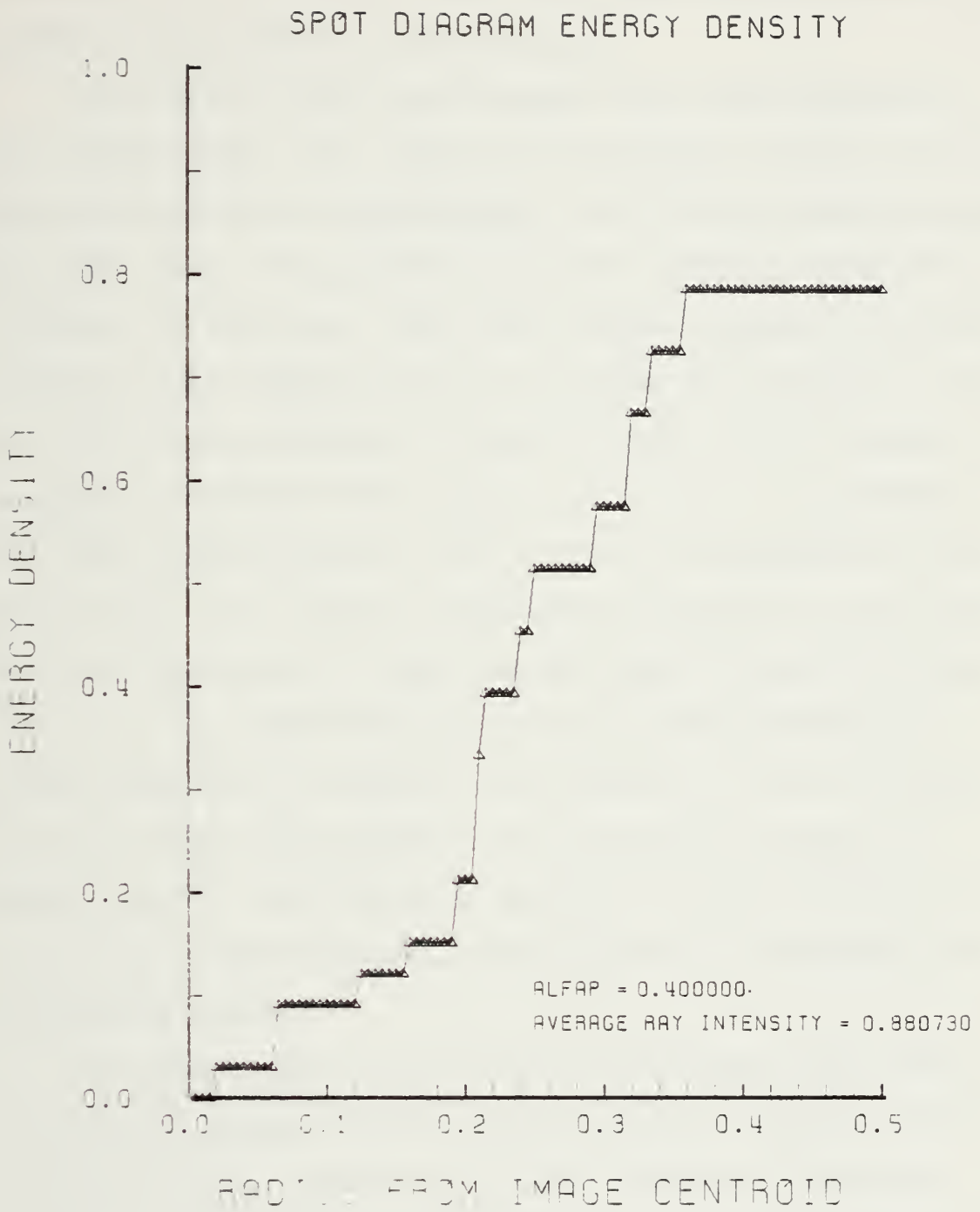

Figure 22. Example GRIN Encircled Energy Plot Corresponding to Figure 21

has been found that as the center of symmetry of the index function, O_s, is moved further away from the interior of the GRIN lens, performance deteriorates.

Two series of GRIN lens designs have been examined at the intermediate tilt angle of 0.3 radians in order to define the spectrum of lens performance. Both design series explore the GRIN lens for O_S inside, outside, and far outside the interior of the lens. The first series, Figures E-1 through E-92, are GRIN designs in the "low range" of refractive index with the index parameter "a" set at 2.25. This first set is compared to the HIN lens with $N_2 = \sqrt{a} = 1.5$. The second, or "high range" series is for a = 9.0, as compared to the HIN at $N_2 = 3.0$, and are displayed in Figures F-1 to F-128. Both the high and low range lenses exploit gradient changes of 5, 10, 25, and 50 percent both positive and negative, where possible. A negative 50% gradient in the low range is, of course, not possible since an index of below 1.0 would result. The center of symmetry was not located at $x \geq 0$ due to the aforementioned singularity encountered at very small angles.

The lens shapes of the GRIN designs shown vary widely. The outside surface may be either convex or concave and exhibits a thinner profile at higher values of refractive index. Although all of the resultant GRIN lens shapes are superior aerodynamically to the hemispherical seeker lenses currently in use, the convex version of the lens has more

obvious applications for a Sidewinder type tactical missile, whereas the concave lens shape is more applicable to the diffuser of a ramjet with nose inlet.

Object plane diagrams show that for lens designs exhibiting smaller spot size, fewer or none of the skew rays failed. This fact underscores the success of GRIN in controlling image deterioration contributed by the nose region of the lenses. Although the lower lens and nose regions still create the largest of the image spread, the extent is reduced.

Figures 23 and 24 are contour diagrams summarizing spot size performance of GRIN lens designs in the low and high range respectively. From these diagrams, it can be seen immediately that the best performance is obtained from lenses having the center of symmetry inside the lens. From this fact, it may be deduced that large changes in refractive index are desired along the surface of the lens rather than across. Except for isolated regions at -5%, increasing gradients produce smaller spot sizes. The positive gradient in the high range, however, has an almost constant spot size from +5% to +50% where an improvement of only 0.6% is seen. In both the low and high ranges the positive gradient at 50% and at OB = 0.05 has proved to be the best performing combination. Again, as in the HIN lens the high range exhibits the smaller spot size.

The best GRIN lens is now further examined over the range of obliquities up to 0.8 radians. Furthermore, since it has

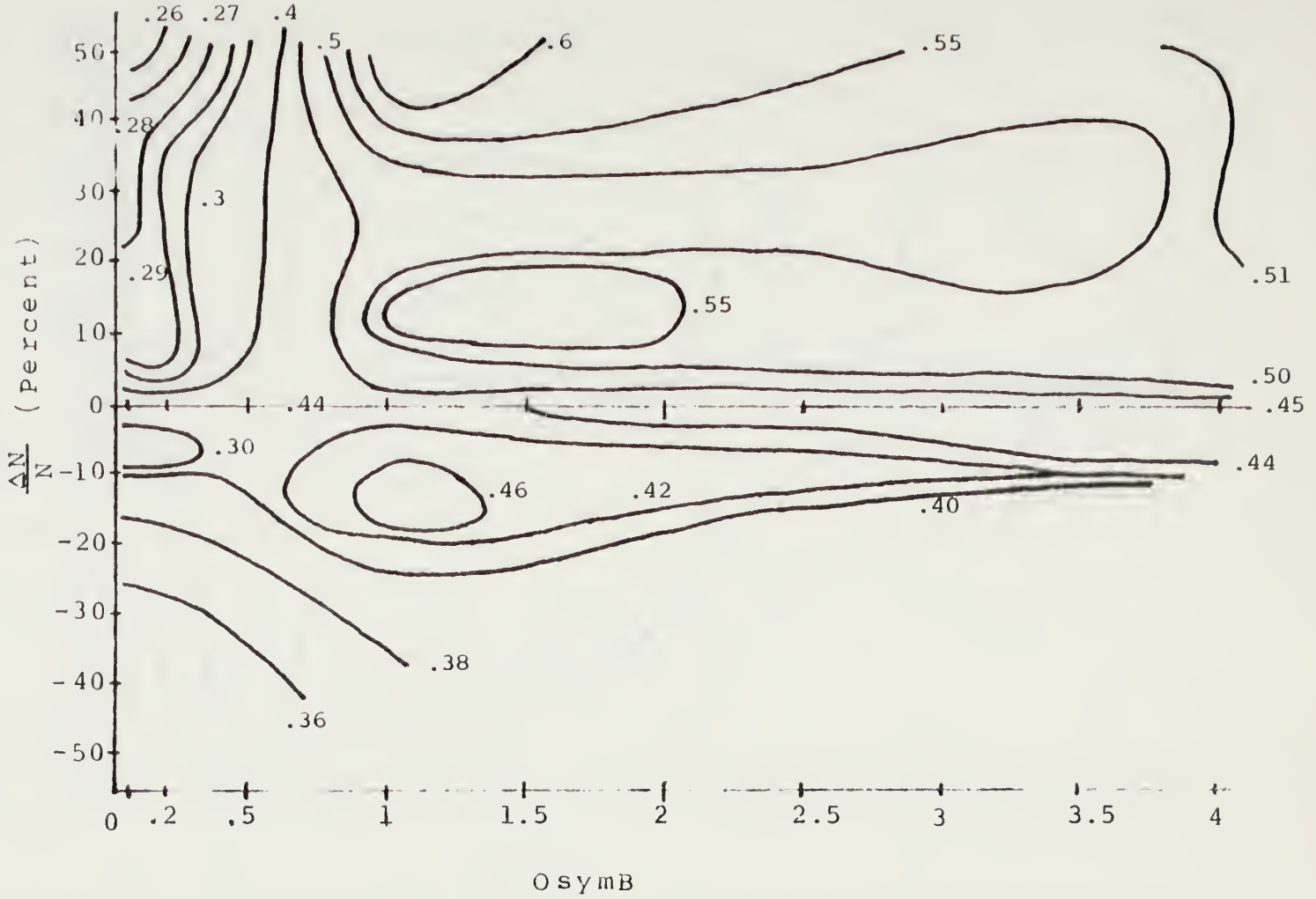

Figure 23. Contour Plot Summary of GRIN Lens Spot Size Performance for α_p = 0.3 radians, a = 2.25

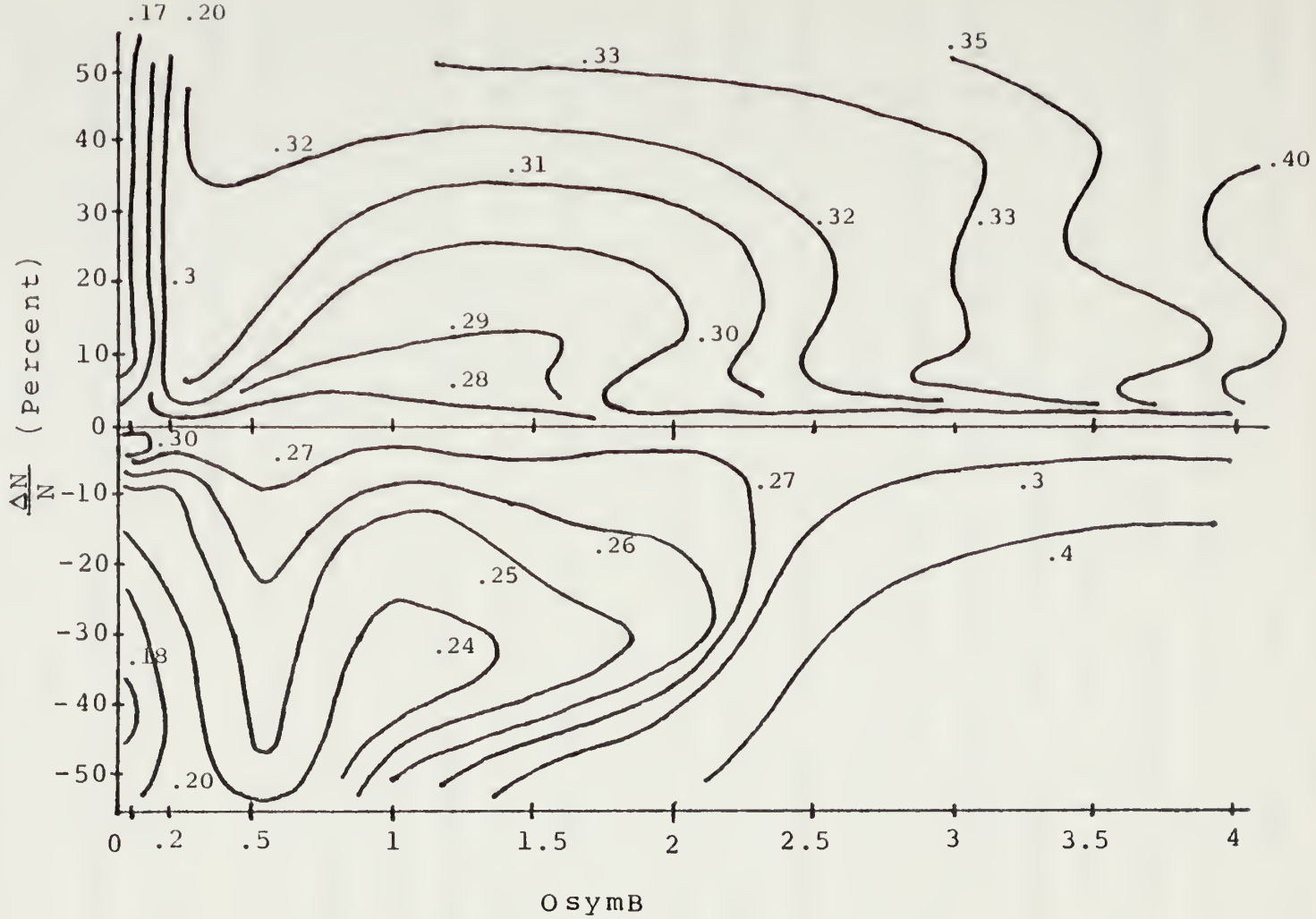

Figure 24. Contour Plot Summarizing GRIN Lens Spot Size Performance at α_p = 0.3 radians, a = 9.0

been determined that placing the focal point at x = 2.0, improves spot size performance at lower values of α_p, another series of plots is given for F/1. With the focal point at x = 1.5, severe degradation results; for F = 3.0 only modest differences with F/2 are evident. Appendices G and H show the performance of the "best" GRIN lens at F/1 and F/2.

Here it may be fully recognized that the resulting behavior of a "good" gradient refractive index seeker lens is far superior to that of the HIN lens for $\alpha_p \leq 0.6$ radians; see Table 5. The reader will note that there are no failed rays even at 0.8 radians (45.8 degrees). Although centroid movement at F/2 is slightly greater than the HIN lens, by changing to F/1, this can be corrected; see Figure 25. The F/1 version, moreover, displays a range of spot sizes significantly smaller than that for the F/2 lens below $\alpha_p \cong 0.54$ radians or the HIN lens below 0.68 radians; see Figure 26. That the lens displays more desirable performance with a shorter focal length is a surprising but highly desired result. Since seeker optics systems are volumn limited, any reduction in the lens focal length is beneficial to the final design and packaging requirements.

It is significant for the reader to note that centroid movement beyond a value of ±1.0 exceeds the physical dimensions of the lens radius. If the interior of the lens mount is of similar dimension, it follows that the requirement for y_{CENTR} to be less than ±1.0 restricts the F/1 lens to approximately 0.65 radians of tilt whereas the F/2 lens is further restricted to less than 0.3 radians. The superior performance

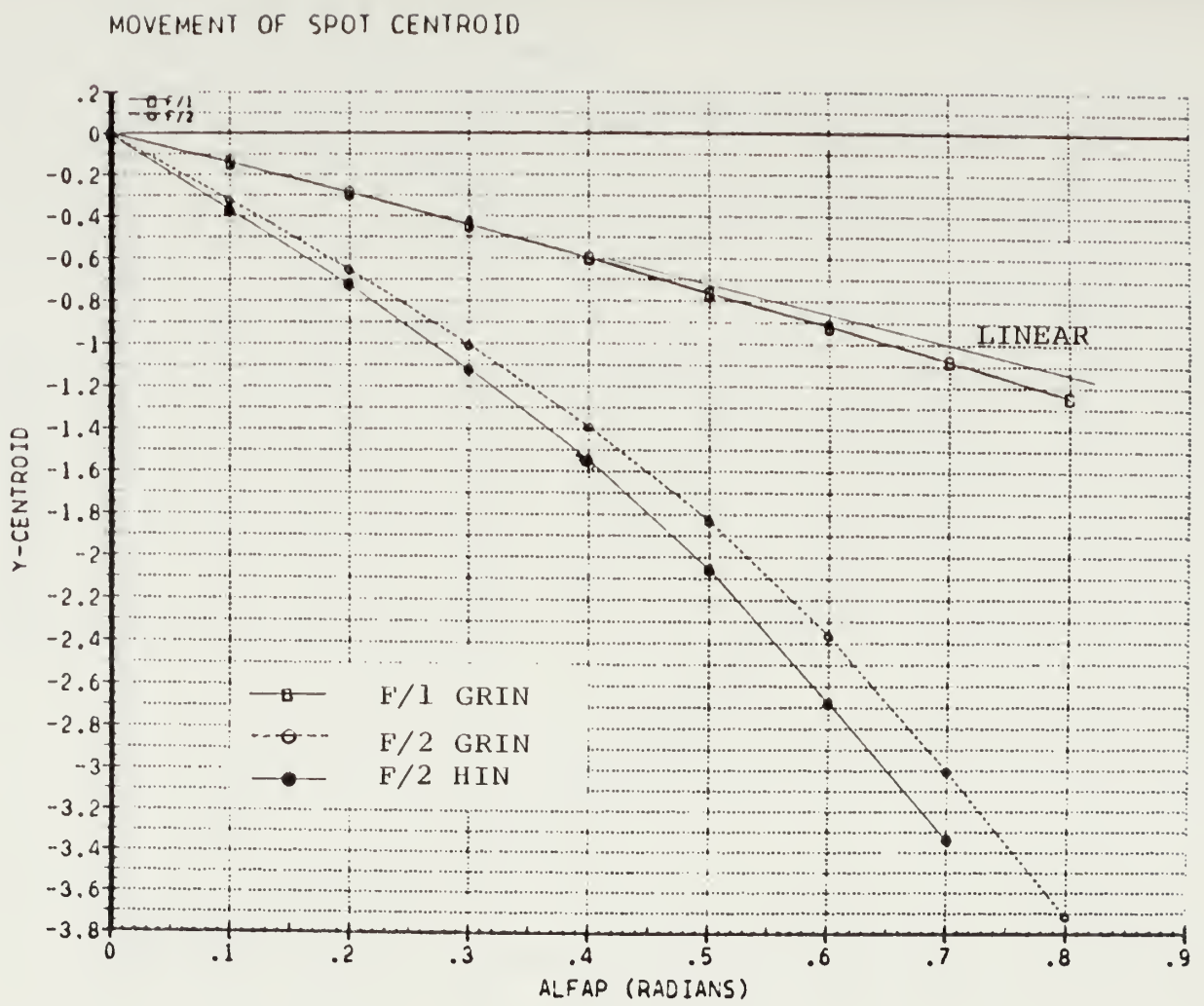

Figure 25. "Best" GRIN Lens Centroid Moment for F/Numbers of F/1 and F/2

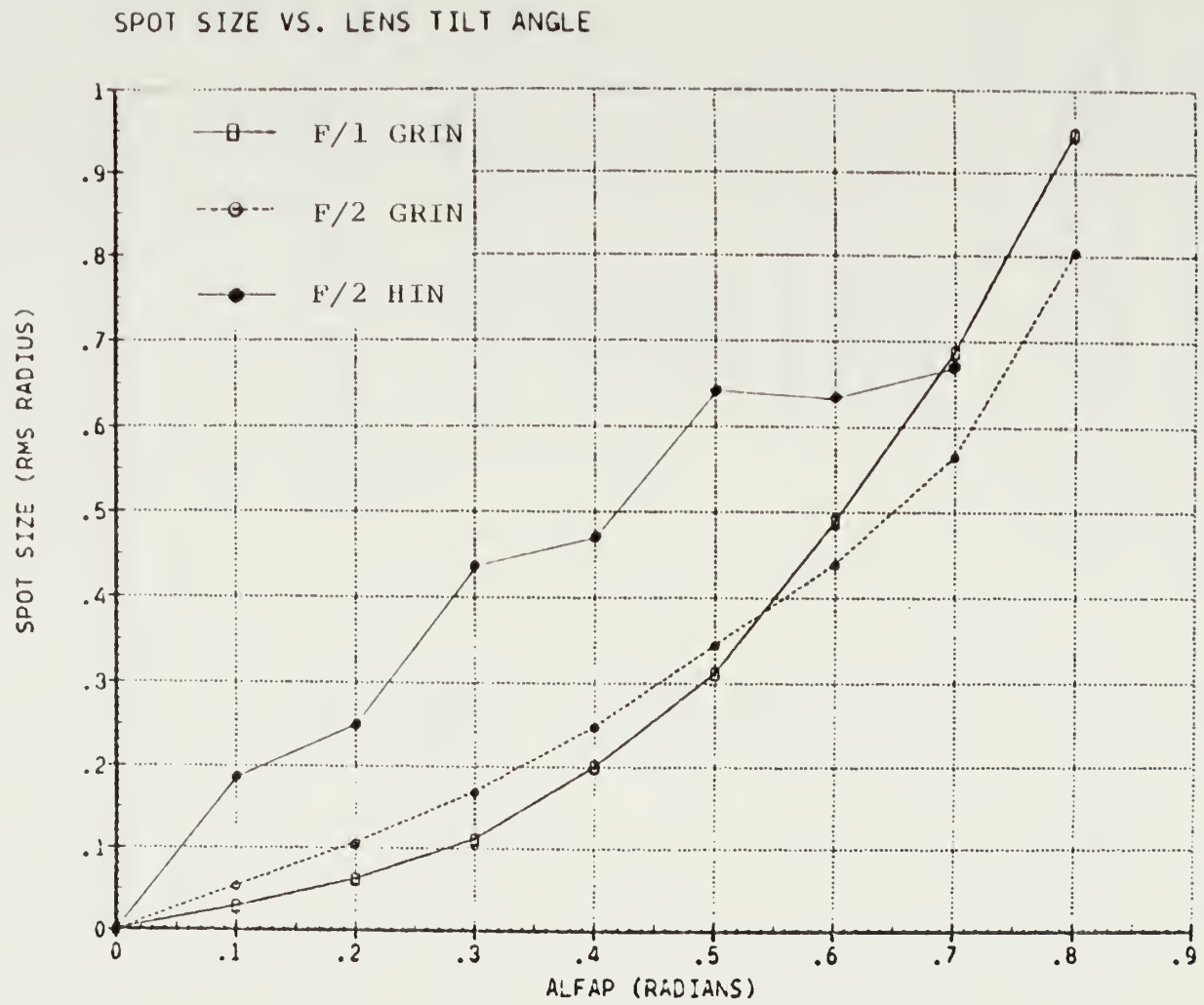

Figure 26. "Best" GRIN Lens Spot Size Performance for F/Numbers of F/1 and F/2

TABLE 5

Comparison of HIN and GRIN Lens Designs

Performance Parameter or Feature	HIN	GRIN*
Shape of Outer Surface	Convex	Concave
Fraction of Failed Rays at α_p = 0.7 radians	0.143	0.0
Linearity of Centroid Motion; α_p for $\Delta y/y$ deviation of 10%	0.4 radians	0.8 radians
Spot Size for α_p		
α_p = 0.1 radians	0.190	0.029
α_p = 0.2 radians	0.247	0.063
α_p = 0.3 radians	0.442	0.112
α_p = 0.4 radians	0.466	0.201
α_p = 0.5 radians	0.637	0.313
α_p = 0.6 radians	0.632	0.490
α_p = 0.7 radians	0.667	0.688
α_p = 0.8 radians	N/A	0.947
Spot radius for 80% of energy @ α_p = 0.4 radians	Does not attain 80% within 0.50	0.28
Average relative intensity of skew rays @ α_p = 0.4 radians	0.82	0.44

*"Best" GRIN lens with 50% positive gradient, O_S = 0.05, in the F/1 configuration.

of the F/2 lens above 0.54 radians is, therefore, unusable. Attempts to improve upon this performance by increasing the edge thickness, T, or by slightly adjusting the parameter U, as with the homogeneous lens only produced uniformly degraded performance in every respect.

Although the "best" GRIN lens resulted from a positive 50% gradient change in refractive index, it has been noted that this configuration was only slightly better than the same lens with a positive 5% change. Furthermore, since refractive index gradients of five percent or better have already been produced, it is entirely feasible that if the precise parabolic change could be controlled, this lens could be produced today.

Despite the obvious success of GRIN in controlling spot size growth and image centroid movement, a penalty in the form of reduced ray intensity has been paid. That increasing spot size performance is tempered by a loss of intensity may be seen by comparing "good" GRIN encircled energy plots with that of the HIN lens. Note that the HIN lens with $N_2 = 3.0$ also loses ~ 50% to intensity; see Figure 44. This loss in intensity is partially offset, however, by the GRIN lens with an increased number of rays transmitted and by the reduced spot size.

One drawback to the use of the GRIN lens as a self sufficient, single element lens is still that of the relative sizes of image and detector. Hence, even though GRIN has

significantly reduced spot size below $\alpha_p \cong 0.6$, that size is still significant at tilt angles above 0.3 radians. In order to use the lens without a secondary focusing element or mirror arrangement, a large composite sensor array would be required.

VII. CONCLUSION

Gradient refractive index materials may be employed to design a pointed seeker lens which exhibits optical performance far superior to that obtainable with conventional homogeneous optical material. A fifty percent, positive, parabolic gradient index with center of symmetry interior to the lens was found to yield the best performance although a five percent version of the same lens was only very slightly inferior; this lens may possibly be fabricated today.

For objects off-axis by more than 0.3 radians (~17.2 degrees) a secondary lens element may be required unless a large scale multiple element sensor array is employed. With such arrays, objects off-axis by more than 0.65 radians (37.2 degrees) may require Cassegrainian or other mirror elements to compensate image movement.

VIII. RECOMMENDATIONS FOR FUTURE WORK

This thesis investigated a spherically symmetric GRIN seeker lens with inside conical surface. Future studies should investigate:

a) The elimination of the singularity problem by modification of the theoretical equations for GRIN using numerical techniques. See Reference 13.

b) The optimization of the GRIN lens with both inside and outside curvature.

c) The effect on lens performance due to an attached shock wave.

d) The effect on lens performance when the object is no longer in the far field and wave front curvature must be taken into account.

e) The performance of the lens using wavelengths corresponding to atmospheric windows.

f) The effect of a radially symmetric gradient index on lens performance.

g) The feasibility of adding an anamorphic gradient-index lens located on the missile body to increase off-axis tracking/acquisition capability to 90° and beyond. See Figure 1 of Reference 14.

APPENDIX A

COMPUTER LOGIC FLOW DIAGRAM FOR PROGRAM GISL

This appendix together with Appendices B and C describe the FORTRAN program GISL. GISL may be used to design either a homogeneous (B = 0), or a GRIN lens to the user's specifications by changing the design parameter where indicated by comments in the input section of the program. Additional software required to run GISL and plot the results are not described since these system-dependent procedures do not apply elsewhere.

The flow diagrams which follow provide the reader with the information necessary to follow the fundamental logic of the main program and subroutines of GISL. Not shown is Subroutine DIRECT which has been derived from Subroutine DIRECT as described by Amichai [5] with only slight modifications.

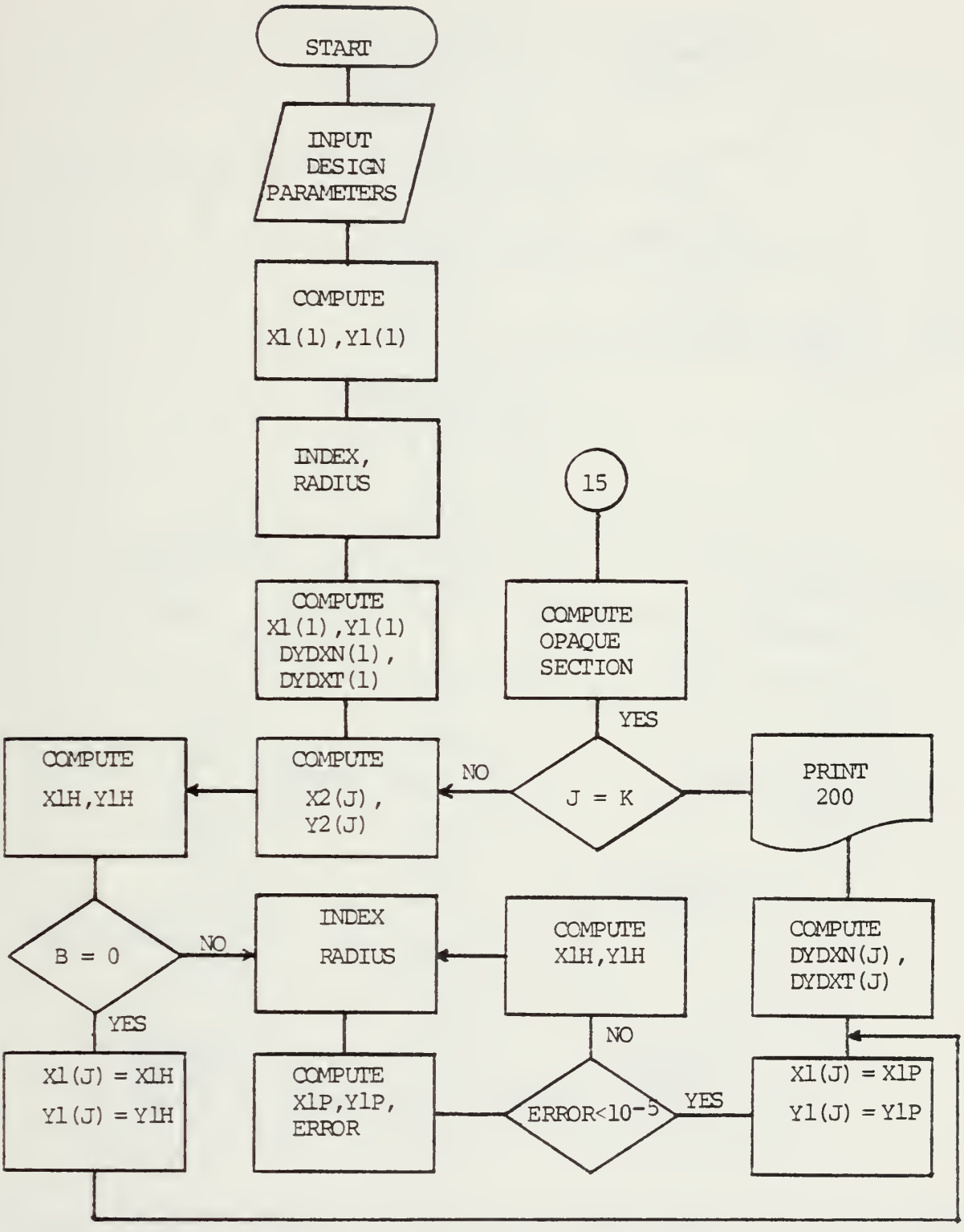
START
INPUT DESIGN PARAMETERS
COMPUTE X1(1),Y1(1)
INDEX, RADIUS
COMPUTE X1(1),Y1(1) DYDXN(1), DYDXT(1)
15
COMPUTE OPAQUE SECTION
YES
J = K
NO
PRINT 200
COMPUTE X2(J), Y2(J)
COMPUTE X1H,Y1H
B = 0
NO
YES
INDEX RADIUS
COMPUTE X1H,Y1H
COMPUTE DYDXN(J), DYDXT(J)
X1(J) = X1H
Y1(J) = Y1H
COMPUTE X1P,Y1P, ERROR
NO
ERROR<10-5
YES
X1(J) = X1P
Y1(J) = Y1P

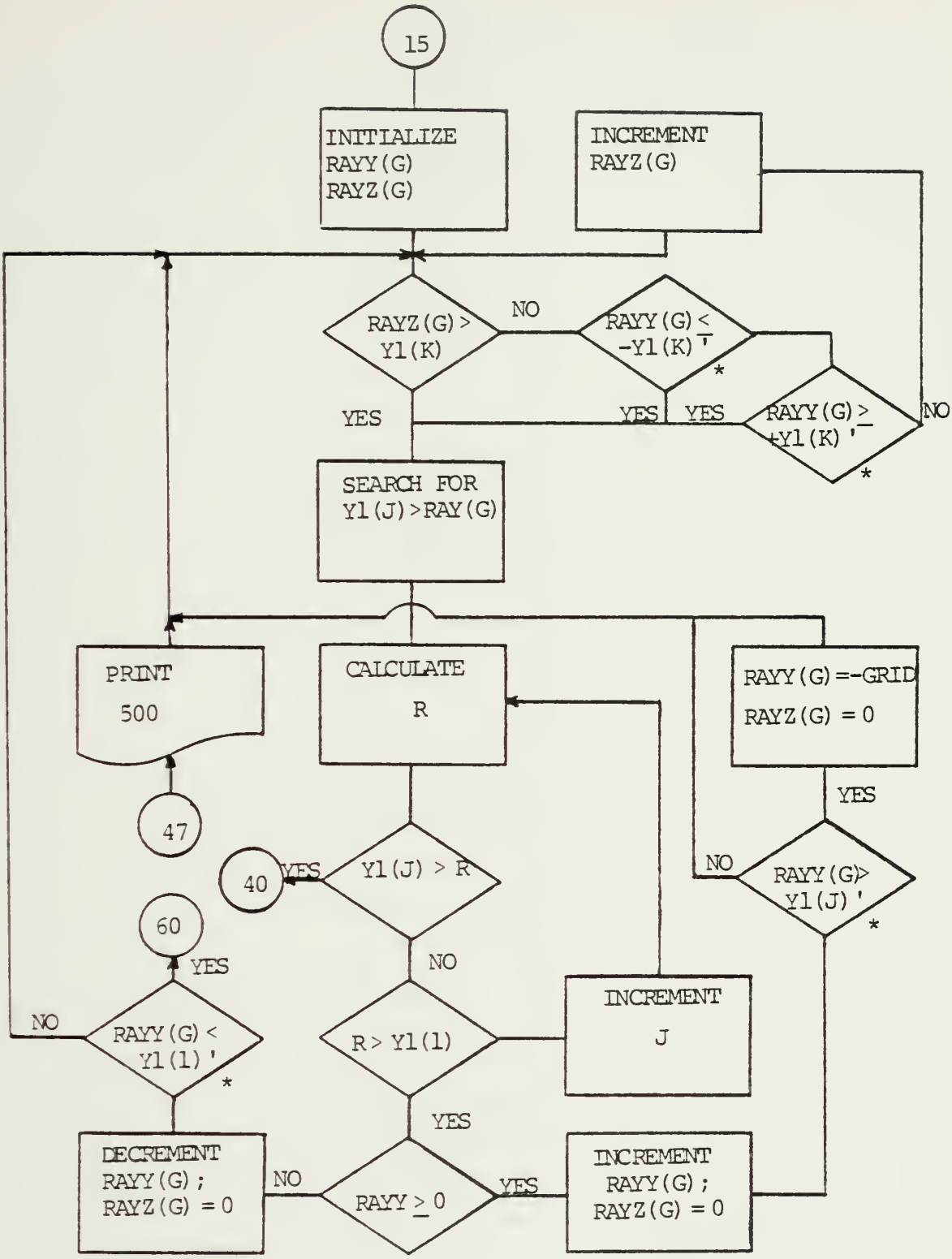

*Here, the prime indicates Y-coordinate as transformed into the grid plane.

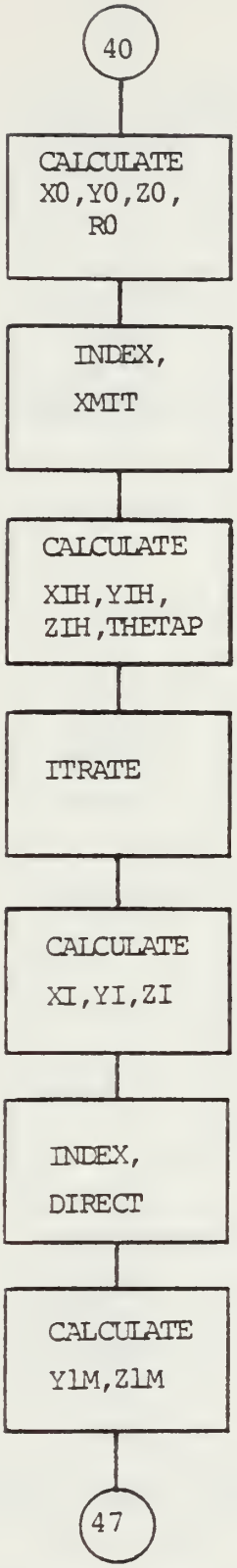
40
CALCULATE
X0,Y0,Z0,
R0
INDEX,
XMIT
CALCULATE
XIH,YIH,
ZIH,THETAP
ITRATE
CALCULATE
XI,YI,ZI
INDEX,
DIRECT
CALCULATE
YLM,ZLM
47

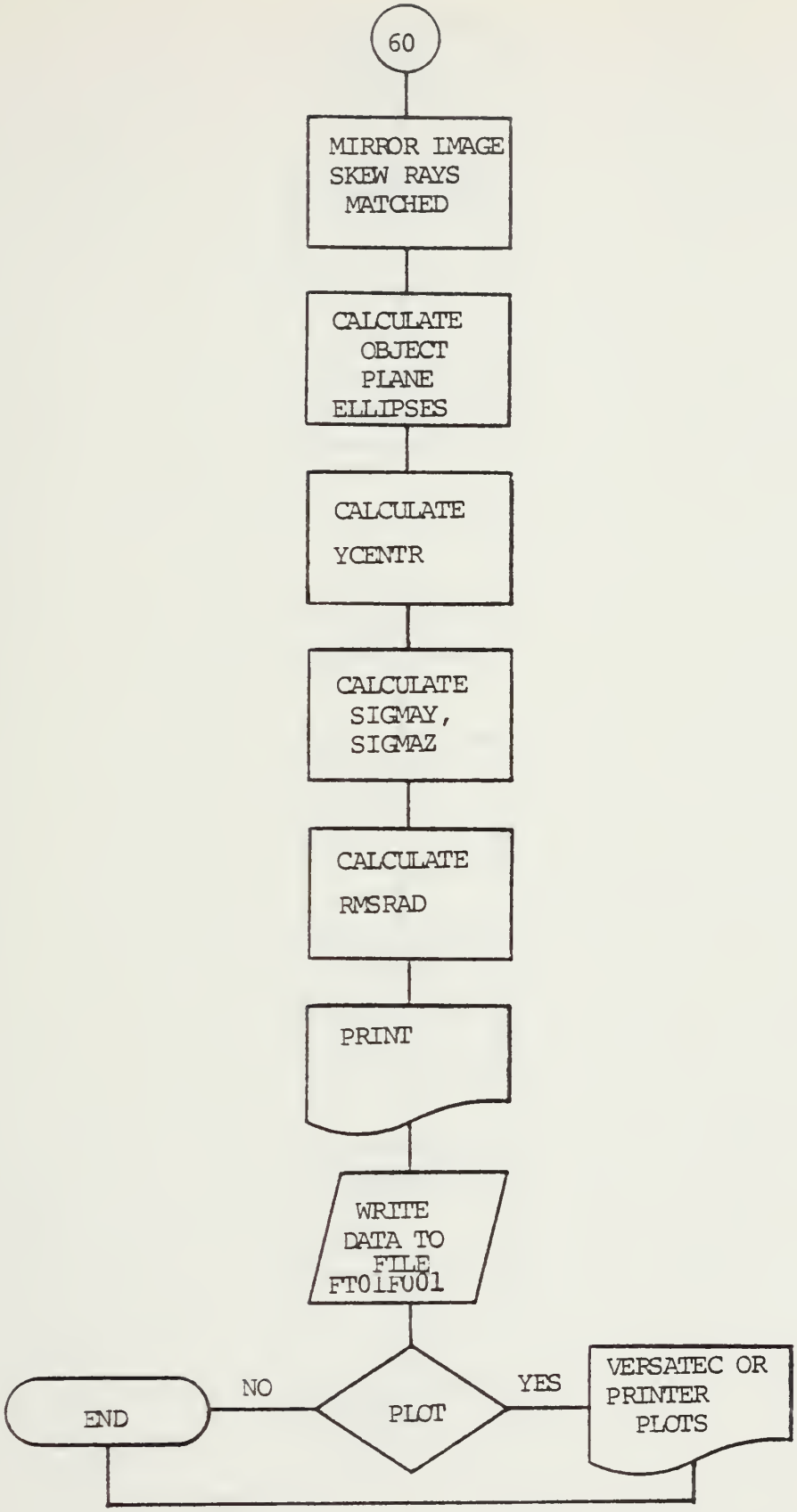
60
MIRROR IMAGE SKEW RAYS MATCHED
CALCULATE OBJECT PLANE ELLIPSES
CALCULATE YCENTR
CALCULATE SIGMAY, SIGMAZ
CALCULATE RMSRAD
PRINT
WRITE DATA TO FILE FT01F001
PLOT
NO
END
YES
VERSATEC OR PRINTER PLOTS

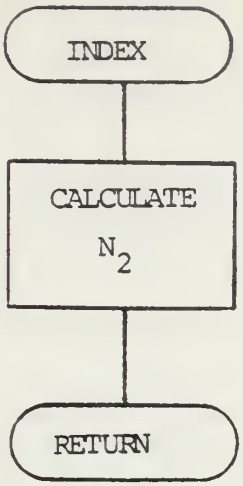
INDEX
CALCULATE
N_2
RETURN

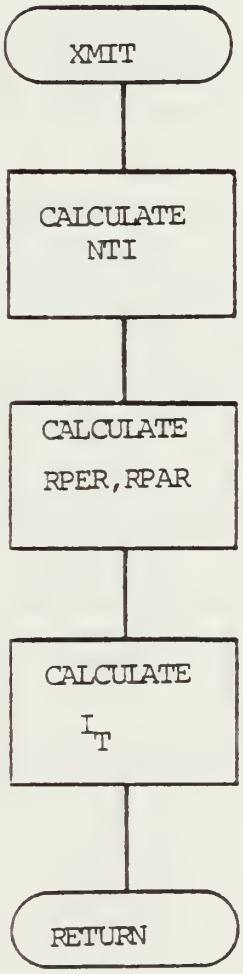
XMIT
CALCULATE
NTI
CALCULATE
RPER,RPAR
CALCULATE
I_T
RETURN

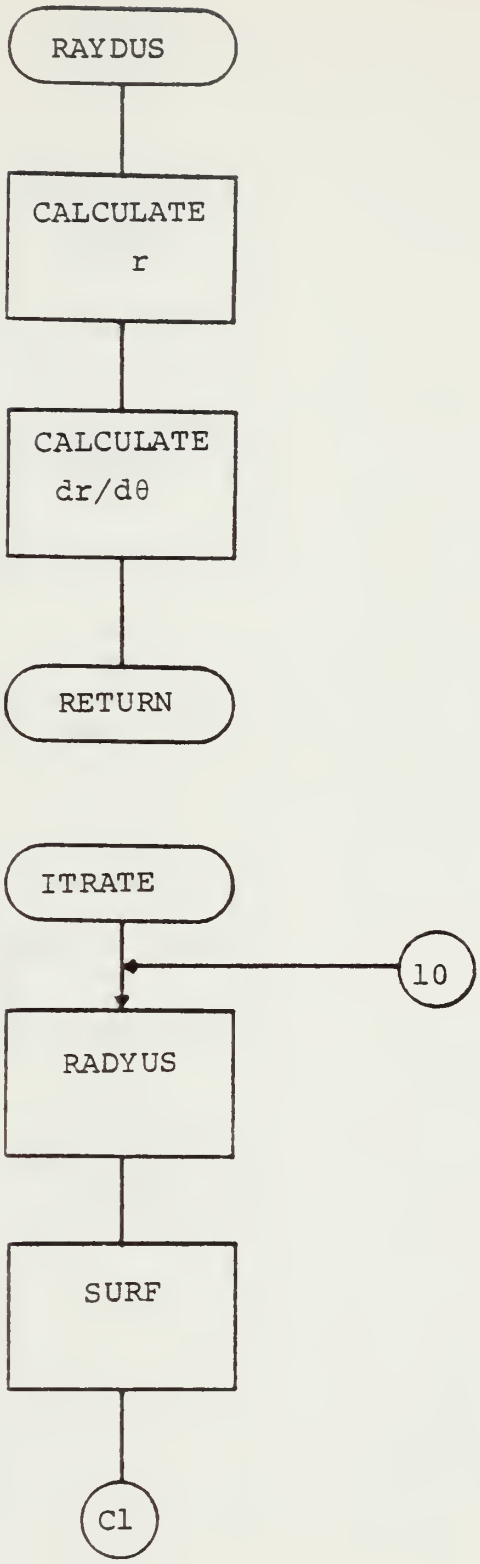
RAYDUS
CALCULATE
r
CALCULATE
dr/dθ
RETURN
ITRATE
10
RADYUS
SURF
C1

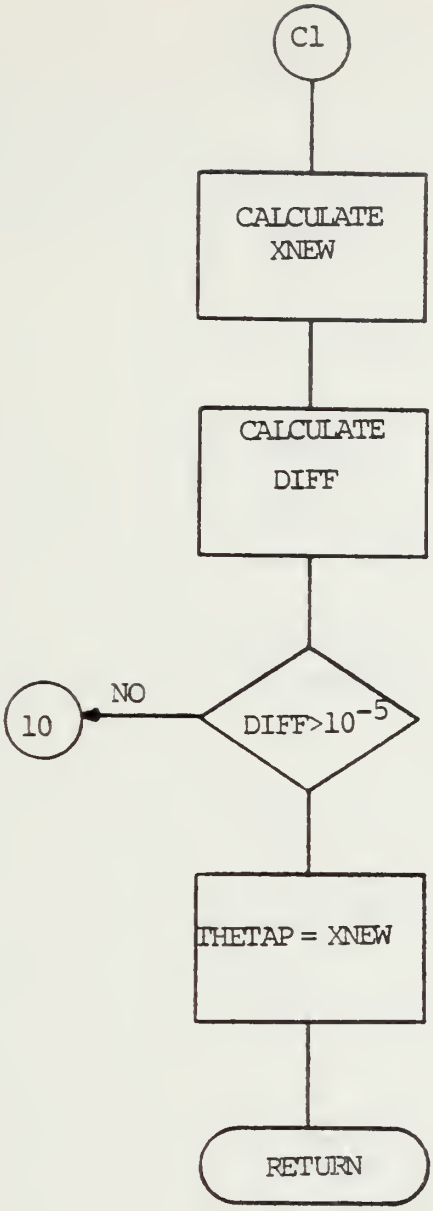
C1
CALCULATE XNEW
CALCULATE DIFF
NO
10
DIFF>10^-5
THETAP = XNEW
RETURN

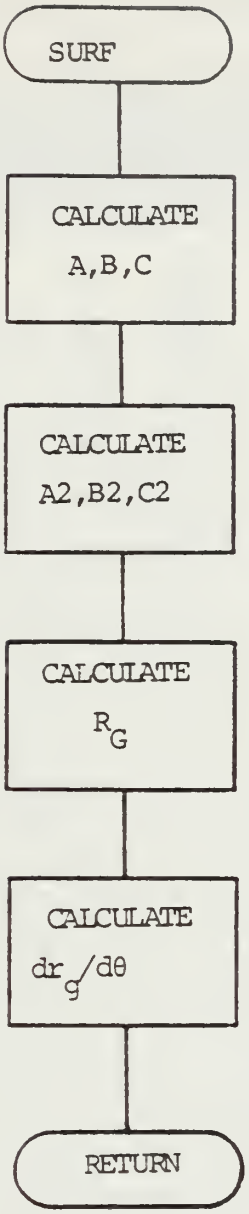
SURF
CALCULATE
A,B,C
CALCULATE
A2,B2,C2
CALCULATE
R_G
CALCULATE
$dr_g/d\theta$
RETURN

```
C     ************************************************************GIS00040
C     *                                                          *GIS00050
C     *                  GRADIENT INDEX SEEKER LENS              *GIS00060
C     *                                                          *GIS00070
C     *                                                          *GIS00080
C     ************************************************************GIS00090
C                                                                 GIS00100
C                                                                 GIS00110
C                                                                 GIS00120
      INTEGER I,J,K,L,G,H,M,N,P,FLAG(1000),Q,RAYS,S,DRAYS,ELLNUM,  GIS00130
     1NUMBR,COORD,ENUM,NUMB,IANGLE,THICK,GG,HH,COUNT,SHAPE,GGT,   GIS00140
     1COOR(500),NUMBT,VARY,ELLIPS,SQURAY,THKNES,TRIP,FILTER,COORT, GIS00150
     1FACE                                                       GIS00160
      REAL BF,UDP(1010),ALPHA,U,BETA,R,DLUDP,F,I2P(1010),ED,     GIS00170
     1I2(1010),ARSIN,COTAN,SIN,COS,TAN,ATAN,SQRT,ARCOS,          GIS00180
     1UP(1010),I1(1010),X1(1010),Y1(1010),X2(1010),Y2(1010),     GIS00190
     1DYDXN(1010),DYDXT(1010),I1P(1010),GAMMA,AB,ONP,            GIS00200
     1N1,N2,N3,T,ALFAP,GRID,RAYY(1000),RAYZ(1000),CENI,TORBI,BOTI,TOPI, GIS00210
     1RADIUS,CEN,TOP,BOT,TORB,DELTAX,DELTAY,SP,ST,RATIO,DYDXNP,LK,LL GIS00220
      REAL CL,NPI,NPJ,NPK,THETA,PHI,PHIP,AO,BO,CO,DO,EO,PAR1,     GIS00230
     1PAR2,XO,YO,ZO,NUM,CKP,CLP,CMP,NUM1,NUM2,NUM3,NUM4,D2,XI,YI,ZI, GIS00240
     1NUM5,CKPP,CLPP,CMPP,D3,OPL(1000),D1,NUM6,NUM7,NTNCTY(1000), GIS00250
     1YIM(1000),ZIM(1000),ELL,ELY(7,1000),ELZ(7,1000),ELZZ,LM,CK,ZOYO, GIS00260
     1PAR3,NUM8,LKP,LLP,LMP,THETAI,XDIAPT(1000),YDIAPT(1000),SUM1, GIS00270
     1SUM2,SUM3,SIGMAZ(10,500),SIGMAY(10,500),RMSRAD(10,500)     GIS00280
      REAL ROC(300),SUM4(300),FRACTN(300),SDRAD(1000),YCENTR(20,500), GIS00290
     1RO,PI,THETAE,EPSLON,PI2,PSIO,E,A,B,OSYMB,THETAO,RAD,PSI,PSIP,X1H, GIS00300
     1Y1H,ZIH,THETAH(50),X1P,Y1P,ZETA,X1HP,Y1HP,ERROR,N20,XP,YP,ZP,RH, GIS00310
     1PCY,ROZ,NPOX,NPOY,NPOZ,D2T,CPHX,OPHY,OPHZ,OSYMPH,THETAP,    GIS00320
     1RZERO,ABS,TCRIT,ROX,EONR,X1PP,A1,B1,C1                     GIS00330
      REAL Y1PP,ZETAP,BASE,BAS1,BEFF,ROOO,N2X21,N2X1K,N2X2K,      GIS00340
     1PRCNTE,PRCNTT,PRCNTO,SURFL,TSURFL,SLINCR,ARKCOS,CHEKRO,CALIBR, GIS00350
     1KKLLMM,CKKP,CLLP,CMMP,THTAP,BETAO,ALFAO,RDOTG,RDOTS,RADH,  GIS00360
     1SIGN,DIFFOR,XMAVE,XMAVET                                   GIS00370
      COMMON A,B,E,RZERO,EPSLON,PI2,J                            GIS00380
      COMMON/DIR/A1,B1,C1,NPOX,NPOY,NPOZ,PSIP                    GIS00390
      COMMON/SUR/PSIO,XO,OSYMB,YO,ZO,RO,CKKP,CLLP,CMMP,N2O,ALPHA GIS00400
      COMMON/XM/N1,N3                                            GIS00410
C                                                                 GIS00420
C                                                                 GIS00430
C     OUTPUT OPTIONS:                                             GIS00440
C                                                                 GIS00450
C     CAUTION. OUTPUT OPTIONS MUST BE CHOSEN WITH CARE TO AVOID   GIS00460
C     EXCESSIVE PRINTING AND VOLUMOUS OUTPUT. OPTIONS "VARY" AND  GIS00470
C     "THKNES" WILL MULTIPLY THE PAGES OF OUTPUT. IN GENERAL      GIS00480
C     NO MORE THAN ONE SUCH REPEAT PARAMETER SHOULD BE USED       GIS00490
C     IN THE SAME RUN.                                            GIS00500
C                                                                 GIS00510
```

```
C       TO HAVE LENS SHAPE DATA PRINTED SET "SHAPE" TO 1. OTHERWISE          GIS00520
C       SET "SHAPE"=0.                                                       GIS00530
        SHAPE=1                                                              GIS00540
C                                                                            GIS00550
C       TO HAVE SKEW RAY AND MIRROR IMAGE SKEW RAY DATA PRINTED SET          GIS00560
C       "SQURAY" TO 1. ELSE SET "SQURAY" TO 0. (INTEGER)                     GIS00570
        SQURAY=1                                                             GIS00580
C                                                                            GIS00590
C       TO HAVE ELLIPSE SHAPE DATA PRINTED SET "ELLIPS" TO 1. OTHERWISE      GIS00600
C       SET "ELLIPS"=0.                                                      GIS00610
        ELLIPS=0                                                             GIS00620
C                                                                            GIS00630
C     INPUT KNOWNS FOR GLM LENS SHAPE:                                       GIS00640
C                                                                            GIS00650
C       FOCAL LENGTH:                                                        GIS00660
        F=4.0                                                                GIS00670
C       INSIDE SURFACE CONE HALF-ANGLE:                                      GIS00680
        ALPHA=0.7853982                                                      GIS00690
C       INCIDENT RAY OFFSET ANGLE:                                           GIS00700
        U=0.000000                                                           GIS00710
C       NUMBER OF ITERATIONS (MUST BE AN EVEN INTEGER GT 750)                GIS00720
        I=100                                                                GIS00730
C       MAXIMUM RADIUS OF INSIDE SURFACE CONE:                               GIS00740
        R=1.0                                                                GIS00750
C       THICKNESS OF LENS AT THE EDGE:                                       GIS00760
        T=0.05                                                               GIS00770
C       OR, IF IT IS DESIRED TO HAVE THE THICKNESS BE CHANGED FROM T=0.05    GIS00780
C       TO T=0.55 BY A 0.05 STEP INCREMENT, SET "THKNES" TO 1. ELSE ENSURE   GIS00790
C       THAT "THKNES"=0. (INTEGER)                                           GIS00800
        THKNES=0                                                             GIS00810
C                                                                            GIS00820
C       INDICES OF REFRACTION                                                GIS00830
        N1=1.0                                                               GIS00840
C       THE FOLLOWING ARE CONSTANTS A & B FOR N2(R). SEE SUBR INDEX.         GIS00850
C       NOTE THAT IF B=0.0, N2(R) NO LONGER VARIES AS A FUNCTION OF R        GIS00860
C       WHICH CORRESPONDS TO THE HOMOGENEOUS LENS WITH N2=SQRT(A).           GIS00870
        A=9.00                                                               GIS00880
        B=+11.25                                                             GIS00890
C       THE FOLLOWING IS THE DISTANCE FROM 0,0 TO THE CENTER OF              GIS00900
C       SYMMETRY OF THE GRADIENT INDEX ALONG THE X-AXIS. THE                 GIS00910
C       POSITIVE SENSE IMPLIES THAT OSYM IS TO THE LEFT OF 0,0.              GIS00920
C       CONVERSELY, THE NEGATIVE SENSE IMPLIES THAT OSYM IS TO               GIS00930
C       THE RIGHT OF 0,0.                                                    GIS00940
        OSYMB=+0.05                                                          GIS00950
        N3=1.0                                                               GIS00960
        BETA=ATAN(R/(F-R*COTAN(ALPHA)))                                      GIS00970
        PI=3.1415926535897 93                                                GIS00980
        PI2=PI/2.0                                                           GIS00990
```

```
C                                                                       GIS01000
C     INPUT KNOWNS FOR TRACE RAY:                                       GIS01010
C                                                                       GIS01020
C       INCLINATION OF OBJECT PLANE (RADIANS)                           GIS01030
        ALFAP=0.4                                                       GIS01040
C       OR IF IT IS DESIRED TO HAVE ALFAP VARY BETWEEN 0.0 AND 0.7:     GIS01050
C       SET VARY = 1, OTHERWISE SET VARY = 0                            GIS01060
        VARY = 0                                                        GIS01070
C       SIZE OF GRID INCREMENT:                                         GIS01080
        GRID=0.3                                                        GIS01090
        ELLNUM=4                                                        GIS01100
C       NUMBER OF ELLIPSES = ENUM. ELLNUM MUST BE EVEN AND              GIS01110
C       I/ELLNUM MUST BE AN INTEGER WITH NO REMAINDER                   GIS01120
        ENUM=ELLNUM+1                                                   GIS01130
C       ELL IS THE Z COORDINATE INCREMENT FOR ELLIPSE PLOTS             GIS01140
        ELL=GRID/7.5                                                    GIS01150
C                                                                       GIS01160
CCC                                                                     GIS01170
CCC                                                                     GIS01180
C     ALGORITHM GLM LENS SHAPE (SEE INPUT ABOVE)                        GIS01190
CCC                                                                     GIS01200
CCCC                                                                    GIS01210
CCC     AT THIS POINT, IF "THKNES" IS 1, THE REMAINDER OF THE PROGRAM   GIS01220
C       WILL BE REPEATED FOR T=0.05 TO T=0.55 BY A 0.05 INCREMENT STEP. GIS01230
        IF(THKNES .EQ. 1) T=0.05                                        GIS01240
          GO TO 3                                                       GIS01250
      2 CONTINUE                                                        GIS01260
        T=T+0.05                                                        GIS01270
      3 CONTINUE                                                        GIS01280
        DLUDP=BETA/I                                                    GIS01290
        BF=F/R                                                          GIS01300
        WRITE(6,1900)                                                   GIS01310
        IF(SHAPE .EQ. 1) WRITE(6,100) ALPHA,BETA,R,U,I,T,N1,            GIS01320
       1N3,BF,DLUDP                                                     GIS01330
C     START AT THE EDGE _ 1ST RAY                                       GIS01340
        FILTER=0                                                        GIS01350
        J=1                                                             GIS01360
        UDP(J)=BETA                                                     GIS01370
        X2(J)=(BF*SIN(UDP(J)))/(SIN(UDP(J))+(TAN(ALPHA))*COS(UDP(J)))   GIS01380
        Y2(J)=(X2(J))*TAN(ALPHA)                                        GIS01390
        I2P(J)=-ALPHA+ATAN((BF-X2(J))/Y2(J))                            GIS01400
        RO=SQRT((X2(J)+OSYMB)**2+Y2(J)**2)                              GIS01410
        RZERO=RO                                                        GIS01420
        IF(OSYMB .LT. 0.0) RZERO=2.0*RO                                 GIS01430
        CALL INDEX(RO,N20)                                              GIS01440
        I2(J)=ARSIN((N3/N20)*SIN(I2P(J)))                               GIS01450
        UP(J)=PI2-ALPHA-I2(J)                                           GIS01460
        BASE=X2(J)+CSYMB                                                GIS01470
```

```
      IF(BASE .EQ. 0.0) OSYMB=1.0000001*OSYMB                                  GIS01480
      BASE=X2(J)+OSYMB                                                         GIS01490
      THETAO=ATAN(Y2(J)/BASE)                                                  GIS01500
      IF(BASE .LT. 0.0)THETAO=PI+THETAO                                        GIS01510
      ED=T/R                                                                   GIS01520
      X1H=X2(J)-ED*COS(UP(J))                                                  GIS01530
      Y1H=Y2(J)+ED*SIN(UP(J))                                                  GIS01540
      BAS1=X1H+OSYMB                                                           GIS01550
      IF(BAS1 .EQ. 0.0)OSYMB=1.0000001*OSYMB                                   GIS01560
      BAS1=X1H+OSYMB                                                           GIS01570
      THETAE=ATAN(Y1H/BAS1)-THETAO                                             GIS01580
      IF(BAS1 .LT. 0.0)THETAE=PI+THETAE                                        GIS01590
      PSIO=PI-UP(J)-THETAO                                                     GIS01600
      EPSLON=1.0                                                               GIS01610
      IF(PSIO .GT. PI2) EPSLON=-1.0                                            GIS01620
      E=EPSLON*N20*RO*SIN(PSIO)                                                GIS01630
      CALL SWITCH(RO,TCRIT)                                                    GIS01640
      CALL RADYUS(RO,THETAE,RAD,ROOTG,FILTER)                                  GIS01650
      IF(FILTER .EQ. 1)WRITE(6,1800)                                           GIS01660
      IF(FILTER .EQ. 1)GO TO 82                                                GIS01670
      X1(J)=RAD*COS(THETAE+THETAO)-OSYMB                                       GIS01680
      Y1(J)=RAD*SIN(THETAE+THETAO)                                             GIS01690
      CALL INDEX(RAD,N2)                                                       GIS01700
C     HERE TAKE PI-PSI  INSTEAD OF PSI AS IN THE TEXT SINCE 'ARSIN'            GIS01710
C     RETURNS AN ANGLE  ALWAYS LE PI2:                                         GIS01720
      PSI=PI-ARSIN(E/(EPSLON*N2*RAD))                                          GIS01730
      IF(THETAE .GE. TCRIT)PSI=PI-PSI                                          GIS01740
      IF(EPSLON .GT. 0)PSI=PI-PSI                                              GIS01750
      ZETA=PI-PSI-THETAE-THETAO                                                GIS01760
      I1(J)=ARSIN(SQRT(((SIN(ZETA-U))**2)/((COS(ZETA-U)-(N1/N2))**2+           GIS01770
     1(SIN(ZETA-U))**2)))                                                      GIS01780
      I1P(J)=ARSIN((N1/N2)*SIN(I1(J)))                                         GIS01790
      DYDXN(J)=-TAN(I1(J)+U)                                                   GIS01800
      DYDXT(J)=COTAN(I1(J)+U)                                                  GIS01810
      IF(SHAPE .EQ. 0) GO TO 5                                                 GIS01820
      WRITE(6,200) J,X1(J),Y1(J),X2(J),Y2(J),UDP(J),I2P(J),I2(J),UP(J),        GIS01830
     1I1P(J),I1(J),DYDXT(J)                                                    GIS01840
    5 CONTINUE                                                                 GIS01850
C   END OF TRACE FOR 1ST RAY                                                   GIS01860
      K=I+1                                                                    GIS01870
      SURFL=0.0                                                                GIS01880
      DO 10 J=2,K                                                              GIS01890
         L=J-1                                                                 GIS01900
         UDP(J)=BETA-(L)*DLUDP                                                 GIS01910
         X2(J)=(BF*SIN(UDP(J)))/(SIN(UDP(J))+(TAN(ALPHA))*COS(UDP(J)))         GIS01920
         Y2(J)=(X2(J))*TAN(ALPHA)                                              GIS01930
         RO=SQRT((X2(J)+OSYMB)**2+Y2(J)**2)                                    GIS01940
         IF(J .EQ. K) ROOO=RO                                                  GIS01950
```

```
      I2P(J)=-ALPHA+ATAN((BF-X2(J))/Y2(J))                                  GIS01960
      CALL INDEX(RO,N20)                                                    GIS01970
      I2(J)=ARSIN((N3/N20)*SIN(I2P(J)))                                     GIS01980
      UP(J)=PI2-ALPHA-I2(J)                                                 GIS01990
      THETAO=ARCOS((X2(J)+OSYMB)/RO)                                        GIS02000
      PSIO=PI-UP(J)-THETAO                                                  GIS02010
      EPSLON=1.0                                                            GIS02020
      IF(PSIO .GT. PI2) EPSLON=-1.0                                         GIS02030
      E=EPSLON*N20*RO*SIN(PSIO)                                             GIS02040
      Y1H=((COTAN(I1(L)+U))*(COTAN(UP(J)))*(Y2(J)+                          GIS02050
     1  X2(J)*TAN(UP(J)))+Y1(L)-X1(L)*COTAN(I1(L)+U))/(1.0+                 GIS02060
     1  (COTAN(I1(L)+U))*COTAN(UP(J)))                                      GIS02070
      X1H=(COTAN(UP(J)))*(-Y1H+Y2(J)+X2(J)*TAN(UP(J)))                      GIS02080
      IF(B .EQ. 0.0) GO TO 8                                                GIS02090
      IF(PSIO .LE. 0.05 .AND. PSIO .GE. -0.15) GO TO 8                      GIS02100
      TRIP=0                                                                GIS02110
      ZETAP=3.14                                                            GIS02120
      X1PP=X1H                                                              GIS02130
      Y1PP=Y1H                                                              GIS02140
      IF(B .GT. 0.0 .AND. PSIO .GT. 0.0) X1H=X1(L)                          GIS02150
      IF(B .GT. 0.0 .AND. PSIO .GT. 0.0) Y1H=Y1(L)                          GIS02160
    6 CONTINUE                                                              GIS02170
      RH=SQRT((X1H+OSYMB)**2+Y1H**2)                                        GIS02180
      ARKCOS=ARCOS((X1H+OSYMB)/RH)                                          GIS02190
      TRIP=TRIP+1                                                           GIS02200
      THETAH(TRIP)=ARKCOS-THETAO                                            GIS02210
      IF(OSYMB .GT. 0.4) THETAH(TRIP)=THETAH(TRIP)*(1.0-.1+.020*TRIP)       GIS02220
      THTHT=THETAH(TRIP)                                                    GIS02230
      IF(B.GT.0.0 .AND. TRIP.GT.1 .AND. PSIO .GT. 0.0) THETAH(TRIP)=        GIS02240
     1  THETAH(TRIP-1)+(THETAH(TRIP)-THETAH(TRIP-1))/(3.5-0.0416*TRIP)      GIS02250
      IF(B .GT. 0.0 .AND. PSIO .LT. 0.0) THETAH(TRIP)=THETAH(TRIP)*         GIS02260
     1  (1.0-0.01/TRIP)                                                     GIS02270
      CALL SWITCH(RO,TCRIT)                                                 GIS02280
      CALL RADYUS(RO,THETAH(TRIP),RAD,RDOTG,FILTER)                         GIS02290
      IF(FILTER .EQ. 1) WRITE(6,1800)                                       GIS02300
      IF(FILTER .EQ. 1) GO TO 82                                            GIS02310
      X1P=RAD*COS(THETAH(TRIP)+THETAO)-OSYMB                                GIS02320
      Y1P=RAD*SIN(THETAH(TRIP)+THETAO)                                      GIS02330
      CALL INDEX(RAD,N2)                                                    GIS02340
C     WE TAKE PI-PSIP VICE PSIP BECAUSE OF THE CHARACTER OF                 GIS02350
C     THE 'ARSIN' FUNCTION IN FORTRAN.                                      GIS02360
      EONR=E/(EPSLON*N2*RAD)                                                GIS02370
      IF(EONR .GT. 1.0) WRITE(6,9978)EONR                                   GIS02380
 9978 FORMAT(10X,'EONR =',F19.16)                                           GIS02390
      IF(EONR .GT. 1.0)EONR=1.0                                             GIS02400
      PSIP=PI-ARSIN(EONR)                                                   GIS02410
      IF(THETAH(TRIP).GE.TCRIT.OR.PSIO.LT.PI2.AND.PSIO.GT.-PI2)PSIP=        GIS02420
     1  PI-PSIP                                                             GIS02430
```

```
      ZETA=PI-PSIP-THETAN(TRIP)-THETAO                                  GIS02440
      IF(B .LE. 0 .AND. ZETA .GT. ZETAP) X1P=X1PP                       GIS02450
      IF(B .LE. 0 .AND. ZETA .GT. ZETAP) Y1P=Y1PP                       GIS02460
      IF(B .LE. 0 .AND. ZETA .GT. ZETAP) GO TO 7                        GIS02470
      IF(X1P .EQ. X1PP .AND. Y1P .EQ. Y1PP) GO TO 7                     GIS02480
      ZETAP=ZETA                                                        GIS02490
      X1PP=X1P                                                          GIS02500
      Y1PP=Y1P                                                          GIS02510
      Y1HP=((COTAN(I1(L)+U))*(COTAN(ZETA))*(Y1P+                        GIS02520
     1    X1P*TAN(ZETA))+Y1(L)-X1(L)*COTAN(I1(L)+U))/(1.0+              GIS02530
     1    (COTAN(I1(L)+U))*COTAN(ZETA))                                 GIS02540
      X1HP=(COTAN(ZETA))*(-Y1HP+Y1P+X1P*TAN(ZETA))                      GIS02550
      ERROR=SQRT((X1HP-X1P)**2+(Y1HP-Y1P)**2)                           GIS02560
      IF(ERROR .LE. 0.0000100) GO TO 7                                  GIS02570
      X1H=X1HP                                                          GIS02580
      Y1H=Y1HP                                                          GIS02590
      GO TO 6                                                           GIS02600
    7 CONTINUE                                                          GIS02610
      X1(J)=X1P                                                         GIS02620
      Y1(J)=Y1P                                                         GIS02630
      GO TO 9                                                           GIS02640
    8 CONTINUE                                                          GIS02650
      X1(J)=X1H                                                         GIS02660
      Y1(J)=Y1H                                                         GIS02670
      ZETA=UP(J)                                                        GIS02680
    9 CONTINUE                                                          GIS02690
      IF(Y1(J) .LE. 0.0) GO TO 11                                       GIS02700
        I1(J)=ARSIN(SQRT((SIN(ZETA-U))**2/((COS(ZETA-U)-(N1/N2))**2+    GIS02710
     1    (SIN(ZETA-U))**2)))                                           GIS02720
        I1P(J)=ARSIN((N1/N2)*SIN(I1(J)))                                GIS02730
        DYDXN(J)=(-TAN(I1(J)+U))                                        GIS02740
        DYDXT(J)=COTAN(I1(J)+U)                                         GIS02750
      SLINCR=SQRT((X1(J)-X1(L))**2+(Y1(L)-Y1(J))**2)                    GIS02760
      SURFL=SURFL+SLINCR                                                GIS02770
        IF(SHAPE .EQ. 0) GO TO 10                                       GIS02780
        WRITE(6,200)J,X1(J),Y1(J),X2(J),Y2(J),UDP(J),I2P(J),I2(J),      GIS02790
     1    UP(J),I1P(J),I1(J),DYDXT(J)                                   GIS02800
   10 CONTINUE                                                          GIS02810
      GO TO 12                                                          GIS02820
C                                                                       GIS02830
CC    END OF TRACE FOR RAY (I+1)                                        GIS02840
CC    OPAQUE NOSE SECTION FOLLOWS                                       GIS02850
C                                                                       GIS02860
   11 CONTINUE                                                          GIS02870
      K=J-1                                                             GIS02880
   12 CONTINUE                                                          GIS02890
      AB=(-X1(K))+(Y1(K))/DYDXT(K)                                      GIS02900
      STATNA=-AB                                                        GIS02910
```

```
      GAMMA=ATAN(DYDXT(K))                                                    GIS02920
      CNP=(Y1(K))/SIN(GAMMA)                                                  GIS02930
      TSURFL=ONP+SURFL                                                        GIS02940
      WRITE(6,300) GAMMA,STATNA,ONP,SURFL,TSURFL                              GIS02950
C                                                                             GIS02960
CC    LENS INDEX OF REFRACTION DATA -- N2(R) --                               GIS02970
C                                                                             GIS02980
      BEFF=B/(RZERO**2)                                                       GIS02990
      N2X21=SQRT(A+BEFF*RZERO**2)                                             GIS03000
      IF(OSYMB .LT. 0.0)N2X21=SQRT(A+BEFF*((RZERO/2.0)**2))                   GIS03010
      CALL INDEX(RAD,N2X1K)                                                   GIS03020
      CALL INDEX(ROOO,N2X2K)                                                  GIS03030
      PRCNTE=-((N2X2K-N2X21)/N2X2K)*100.0                                     GIS03040
      PRCNTT=-((N2X2K-N2X1K)/N2X2K)*100.0                                     GIS03050
      PRCNTO=-((N2X1K-N2X21)/N2X1K)*100.0                                     GIS03060
      WRITE(6,170C)A,BEFF,OSYMB,PRCNTE,PRCNTT,PRCNTO                          GIS03070
C    END GLM LENS SHAPE                                                       GIS03080
C                                                                             GIS03090
CC    ALGCRITHM TRACE RAY (SEE INPUTS;X1(J),Y1(J),DYDXN(J),X2(J))             GIS03100
CCC                                                                           GIS03110
C     IF VARY IS "1" TRACE RAY WILL BE REPEATED FOR ALFAP = 0.0 TO 0.7        GIS03120
      IF(VARY .EQ. 0) GO TO 15                                                GIS03130
      ALFAP=0.0                                                               GIS03140
      GO TO 15                                                                GIS03150
   14 ALFAP=ALFAP+0.1                                                         GIS03160
   15 CONTINUE                                                                GIS03170
      G=1                                                                     GIS03180
      CCUNT=0                                                                 GIS03190
      RAYY(G)=0.0                                                             GIS03200
      RAYZ(G)=0.0                                                             GIS03210
      NTNCTY(G)=1.0                                                           GIS03220
      XMAVET=0.0                                                              GIS03230
      XMAVE=0.0                                                               GIS03240
      IF(SQURAY .EQ. 1) WRITE(6,400) ALFAP,GRID                               GIS03250
   20 CONTINUE                                                                GIS03260
      IF(RAYZ(G) .GE. Y1(K)) GO TO 30                                         GIS03270
        CENI=(AB+X1(K))*SIN(ALFAP)                                            GIS03280
        TORBI=SQRT(Y1(K)**2-RAYZ(G)**2)                                       GIS03290
        BOTI=CENI-TORBI                                                       GIS03300
        IF(RAYY(G) .LE. BOTI) GO TO 30                                        GIS03310
          TOPI=CENI+TORBI                                                     GIS03320
          IF(RAYY(G) .GE. TOPI) GO TO 30                                      GIS03330
            RAYZ(G)=RAYZ(G)+GRID                                              GIS03340
            GO TO 20                                                          GIS03350
   30 CONTINUE                                                                GIS03360
C  SEARCH FOR Y1(J) JUST GT RAYZ(G); RETRIEVE X1(J)                           GIS03370
      M=K/2                                                                   GIS03380
      IF(Y1(M) .LT. RAYZ(G)) GO TO 32                                         GIS03390
```

```
      IF(RAYY(G) .GT. 1.15) GO TO 32                                    GIS03400
        N=K-1                                                           GIS03410
   31 CONTINUE                                                          GIS03420
      IF(Y1(N) .GT. RAYZ(G)) GO TO 36                                   GIS03430
        N=N-1                                                           GIS03440
        IF(N .EQ. 0) GO TO 34                                           GIS03450
        GO TO 31                                                        GIS03460
   32 CONTINUE                                                          GIS03470
      N=M                                                               GIS03480
   33 CONTINUE                                                          GIS03490
      IF(Y1(N) .GT. RAYZ(G)) GO TO 36                                   GIS03500
        N=N-1                                                           GIS03510
        IF(N .EQ. 0) GO TO 34                                           GIS03520
          GO TO 33                                                      GIS03530
   34 CONTINUE                                                          GIS03540
      RAYZ(G)=0.0                                                       GIS03550
      IF(RAYY(G) .LT. 0.0) GO TO 35                                     GIS03560
        RAYY(G)=RAYY(G)+GRID                                            GIS03570
        GO TO 20                                                        GIS03580
   35 CONTINUE                                                          GIS03590
      RAYY(G)=RAYY(G)-GRID                                              GIS03600
      GO TO 20                                                          GIS03610
   36 CONTINUE                                                          GIS03620
      RADIUS=SQRT(RAYZ(G)**2+((RAYY(G)/COS(ALFAP))-(X1(N)+AB)*          GIS03630
     1TAN(ALFAP))**2)                                                   GIS03640
      IF(Y1(N) .GT. RADIUS) GO TO 40                                    GIS03650
        IF(RADIUS .GT.Y1(1)) GO TO 37                                   GIS03660
        N=N-1                                                           GIS03670
        GO TO 36                                                        GIS03680
   37 CONTINUE                                                          GIS03690
      N=N-1                                                             GIS03700
      IF(N .GT. 0) GO TO 36                                             GIS03710
      CEN=(X1(1)+AB)*SIN(ALFAP)                                         GIS03720
      TORB=Y1(1)*COS(ALFAP)                                             GIS03730
      RAYZ(G)=0.0                                                       GIS03740
      IF(RAYY(G) .GE. 0.0) GO TO 38                                     GIS03750
        RAYY(G)=RAYY(G)-GRID                                            GIS03760
        BOT=CEN-TORB                                                    GIS03770
C       CHECK FOR BOTTOM EDGE OF LENS, GO TO MIRROR IMAGE RAYS          GIS03780
        IF(RAYY(G) .LT. BOT) GO TO 60                                   GIS03790
          GO TO 20                                                      GIS03800
   38 CONTINUE                                                          GIS03810
      RAYY(G)=RAYY(G)+GRID                                              GIS03820
      TOP=CEN+TORB                                                      GIS03830
      IF(RAYY(G) .GT. TOP) GO TO 39                                     GIS03840
        GO TO 20                                                        GIS03850
   39 CONTINUE                                                          GIS03860
      RAYY(G)=-GRID                                                     GIS03870
```

```
      GO TO 20                                                          GIS03880
   40 CONTINUE                                                          GIS03890
      P=N+1                                                             GIS03900
C     CALCULATE INTERCEPT POINT ON OUTER SURFACE                        GIS03910
      AC=RAYY(G)/COS(ALFAP)                                             GIS03920
      BO=TAN(ALFAP)                                                     GIS03930
      CO=(Y1(N)-Y1(P))/(X1(N)-X1(P))                                    GIS03940
      DO=X1(P)                                                          GIS03950
      EO=Y1(P)                                                          GIS03960
      PAR1=(AO*BO+CO*EO-(CO**2)*DO-AB*(BO**2))                          GIS03970
      PAR2=(BO**2-CO**2)                                                GIS03980
      PAR3=(AO**2+AB*(BO**2)*AB-2.0*AO*BO*AB+                           GIS03990
     1RAYZ(G)**2-(EO-CO*DO)**2)                                         GIS04000
      XO=(PAR1/PAR2)+SQRT((PAR1/PAR2)**2-PAR3/PAR2)                     GIS04010
      IF((PAR1/PAR2).GT.X1(1))XO=XO-2.0*SQRT((PAR1/PAR2)**2-PAR3/PAR2)  GIS04020
      YO=(RAYY(G)/COS(ALFAP))-(XO+AB)*TAN(ALFAP)                        GIS04030
      ZO=RAYZ(G)                                                        GIS04040
C     CALCULATE THE DIRECTION COSINES OF OUTSIDE SURFACE NORMAL         GIS04050
      DELTAX=X1(N)-X1(P)                                                GIS04060
      DELTAY=Y1(N)-Y1(P)                                                GIS04070
      SP=SQRT((RADIUS-Y1(P))**2+(XO-X1(P))**2)                          GIS04080
      ST=SQRT(DELTAX**2+DELTAY**2)                                      GIS04090
      RATIO=SP/ST                                                       GIS04100
      DYDXNP=RATIO*(DYDXN(N)-DYDXN(P))+DYDXN(P)                         GIS04110
      NPI=1.0/DYDXNP                                                    GIS04120
      IF(YO .EQ. 0.0) GO TO 41                                          GIS04130
        ZOYO=(ZO/YO)                                                    GIS04140
        IF(ZOYO .GE. 8235000) GO TO 41                                  GIS04150
        IF(ZOYO .LE. -8235000) GO TO 42                                 GIS04160
          NPJ=COS(ATAN(ZO/YO))                                          GIS04170
          NPK=SIN(ATAN(ZO/YO))                                          GIS04180
          GO TO 43                                                      GIS04190
   41 CONTINUE                                                          GIS04200
      NPJ=0.0                                                           GIS04210
      NPK=1.0                                                           GIS04220
      GO TO 43                                                          GIS04230
   42 CONTINUE                                                          GIS04240
      NPJ=0.0                                                           GIS04250
      NPK=-1.0                                                          GIS04260
   43 CONTINUE                                                          GIS04270
C     DIRECTION COSINES OF EXTERNAL RAY                                 GIS04280
      CK=COS(ALFAP)                                                     GIS04290
      CL=-SIN(ALFAP)                                                    GIS04300
C     DIRECTION COSINES OF OUTSIDE SURFACE NORMAL                       GIS04310
      LK=NPI/(SQRT(NPI**2+NPJ**2+NPK**2))                               GIS04320
      LL=(NPJ*LK)/NPI                                                   GIS04330
      LM=(NPK*LK)/NPI                                                   GIS04340
      IF(YO .LT. 0.0) GO TO 44                                          GIS04350
```

```
      GO TO 45                                                          GIS04360
   44 CONTINUE                                                          GIS04370
      LL=-LL                                                            GIS04380
      LM=-LM                                                            GIS04390
   45 CONTINUE                                                          GIS04400
      THETA=ARCOS(CK*LK+CL*LL)                                          GIS04410
C     ANGLES OF INCIDENCE AND REFRACTION OUTSIDE SURFACE                GIS04420
      PHI=PI-THETA                                                      GIS04430
      RO=SQRT((XO+OSYMB)**2+YO**2+ZO**2)                                GIS04440
      CALL INDEX(RO,N20)                                                GIS04450
      PHIP=ARSIN((N1/N20)*SIN(PHI))                                     GIS04460
C     CALCULATION OF TRANSMITED INTENSITY AT OUTSIDE SURFACE            GIS04470
      FACE=1                                                            GIS04480
      CALL XMIT(PHI,N20,XMTNC,FACE)                                     GIS04490
      IF(FACE .EQ. 3) GO TO 53                                          GIS04500
      NUM=COS(PHIP)-(N1/N20)*COS(PHI)                                   GIS04510
C     INITIAL DIRECTION COSINES OF INTERNAL REFRACTED RAY               GIS04520
      CKP=(N1/N20)*CK-NUM*LK                                            GIS04530
      CLP=(N1/N20)*CL-NUM*LL                                            GIS04540
      CMP=-NUM*LM                                                       GIS04550
      CKKP=CKP                                                          GIS04560
      CLLP=CLP                                                          GIS04570
      CMMP=CMP                                                          GIS04580
C     INTERNAL RAY LENGTH AND INSIDE SURFACE INTERCEPT                  GIS04590
      ROX=(XO+OSYMB)/RO                                                 GIS04600
      ROY=YO/RO                                                         GIS04610
      ROZ=ZO/RO                                                         GIS04620
      NPOX=ROY*CMP-ROZ*CLP                                              GIS04630
      NPOY=ROZ*CKP-ROX*CMP                                              GIS04640
      NPOZ=ROX*CLP-ROY*CKP                                              GIS04650
      NPO=SQRT(NPOX**2+NPOY**2+NPOZ**2)                                 GIS04660
      NPOX=NPOX/NPO                                                     GIS04670
      NPOY=NPOY/NPO                                                     GIS04680
      NPOZ=NPOZ/NPO                                                     GIS04690
      PSIO=ARCOS(ROX*CKP+ROY*CLP+ROZ*CMP)                               GIS04700
      EPSLON=1.0                                                        GIS04710
      IF(PSIO .GE. PI2) EPSLON=-1.0                                     GIS04720
      E=EPSLON*N2C*RO*SIN(PSIO)                                         GIS04730
      NUM1=(CLP*YO+CMP*ZO-CKP*XO*(TAN(ALPHA)**2))                       GIS04740
      NUM2=(CLP**2+CMP**2-(CKP**2)*(TAN(ALPHA)**2))                     GIS04750
      NUM3=(YO**2+ZO**2-(XO**2)*(TAN(ALPHA)**2))                        GIS04760
      NUM4=NUM1**2-NUM2*NUM3                                            GIS04770
C     CHECK FOR INTERCEPT WITH INSIDE SURFACE                           GIS04780
      IF(NUM4 .LT. 0.0) GO TO 50                                        GIS04790
        D2=-NUM1/NUM2-SQRT(NUM4)/NUM2                                   GIS04800
          XIH=D2*CKP+XO                                                 GIS04810
          YIH=D2*CLP+YO                                                 GIS04820
          ZIH=D2*CMP+ZO                                                 GIS04830
```

```
      IF(ZIH .LT. 0.0) GO TO 50                                          GIS04840
      IF(PSIO .GE. (PI-0.05)) GO TO 455                                  GIS04850
      OSYMPH=SQRT((CSYMB+XIH)**2+YIH**2+ZIH**2)                          GIS04860
      OPHX=(OSYMB+XIH)/OSYMPH                                            GIS04870
      OPHY=YIH/OSYMPH                                                    GIS04880
      OPHZ=ZIH/OSYMPH                                                    GIS04890
      THETAP=ARCOS(ROX*OPHX+ROY*OPHY+ROZ*OPHZ)                           GIS04900
      XINT=XO+CSYMP+*CKP                                                 GIS04910
      XINTO=-OSYMB-XINT                                                  GIS04920
      IF(OSYMB .LT. 0.0 .AND. XINTO .GT. 0.0) THETAP=-THETAP             GIS04930
      SIGN=+1.0                                                          GIS04940
      IF(THETAP .LT. 0.0) SIGN=-1.0                                      GIS04950
      IF(THETAP .LT. 0.0) PSIO=-PSIO                                     GIS04960
      CALL SURF(THETAP,RADD,RDOT,SIGN,FILTER)                            GIS04970
      IF(RADD .LT. 0.0) SIGN=-SIGN                                       GIS04980
      CALL ITRATE(SIGN,THETAP,RAD,THTAP,FILTER)                          GIS04990
      IF(PSIO.GT.PI2.AND.OSYMB.LT.0.0.AND.FILTER.EQ.2)GO TO 455          GIS05000
      IF(FILTER .EQ. 2 .OR. FILTER .EQ. 1) GO TO 51                      GIS05010
      IF(FILTER .EQ. 3) GO TO 50                                         GIS05020
      BETAO=SIN(THTAP)/SIN(PSIO)                                         GIS05030
      ALFAO=COS(THTAP)-BETAO*COS(PSIO)                                   GIS05040
      XI=RAD*(ALFAO*((XO+OSYMB)/RO)+BETAO*CKKP)-OSYMB                    GIS05050
      YI=RAD*(ALFAO*(YO/RO)+BETAO*CLLP)                                  GIS05060
      ZI=RAD*(ALFAO*(ZO/RO)+BETAO*CMMP)                                  GIS05070
      CALL INDEX(RAD,N2)                                                 GIS05080
      CALL SWITCH((RO),TCRIT)                                            GIS05090
      EONR=E/(EPSLON*N2*RAD)                                             GIS05100
      IF(EONR .GT. 1.0) WRITE(6,9978)EONR                                GIS05110
      IF(EONR .GT. 1.0) EONR=1.0                                         GIS05120
      PSIP=ARSIN(EONR)                                                   GIS05130
      IF(PSIO .LT. 0.0 .AND. (ABS(PSIO-PSIP)) .GT. PI2)PSIP=PI-PSIP      GIS05140
      IF(PSIO .LT. 0.0) PSIP=-PSIP                                       GIS05150
      IF(THTAP .GT. 0.6 .AND. TCRIT .GT. THTAP)PSIP=PI-PSIP              GIS05160
      A1=(XI+OSYMB)/RAD                                                  GIS05170
      B1=YI/RAD                                                          GIS05180
      C1=ZI/RAD                                                          GIS05190
      CALL DIRECT(CKP,CLP,CMP)                                           GIS05200
      GO TO 456                                                          GIS05210
  455 CONTINUE                                                           GIS05220
      XI=XIH                                                             GIS05230
      YI=YIH                                                             GIS05240
      ZI=ZIH                                                             GIS05250
  456 CONTINUE                                                           GIS05260
        IF(XI .LT. 0.0 .OR. XI .GT. X2(1)) GO TO 51                      GIS05270
        NUM5=SQRT((XI**2)*(TAN(ALPHA)**4)+YI**2+ZI**2)                   GIS05280
C       DIRECTION COSINES OF INSIDE NORMAL                               GIS05290
        LKP=-XI*(TAN(ALPHA)**2)/NUM5                                     GIS05300
        LLP=YI/NUM5                                                      GIS05310
```

```
      LMP=ZI/NUM5                                                        GIS05320
      KKLLMM=CKP*LKP+CLP*LLP+CMP*LMP                                     GIS05330
      IF(KKLLMM .GE. 1.0)THETAI=0.0                                      GIS05340
      IF(KKLLMM .LE. -1.0)THETAI=PI                                      GIS05350
      IF((ABS(KKLLMM)) .GE. 1.0) GO TO 457                               GIS05360
      THETAI=ARCOS((CKP*LKP)+(CLP*LLP)+(CMP*LMP))                        GIS05370
  457 CONTINUE                                                           GIS05380
C     ANGLES OF INCIDENCE AND TOTAL INTERNAL REFLECTION                  GIS05390
C     AT THE INSIDE SURFACE:                                             GIS05400
      PHII=PI-THETAI                                                     GIS05410
      TIRA=ARSIN(N3/N2)                                                  GIS05420
C     CHECK FOR TOTAL INTERNAL REFLECTION:                               GIS05430
      IF(PHII .GE. TIRA) GO TO 52                                        GIS05440
        PHIIP=ARSIN((N2/N3)*SIN(PHII))                                   GIS05450
C       CALCULATION OF TRANSMITTED INTENSITY AT INSIDE SURFACE           GIS05460
        FACE=2                                                           GIS05470
        CALL XMIT(PHII,N2,XMTNCP,FACE)                                   GIS05480
        NTNCTY(G)=XMTNC*XMTNCP                                           GIS05490
        XMAVET=XMAVET+NTNCTY(G)                                          GIS05500
        XMAVE=XMAVET/(G*1.0)                                             GIS05510
        NUM8=COS(PHIIP)-(N2/N3)*COS(PHII)                                GIS05520
C       DIRECTION COSINES OF INSIDE EXTERNAL REFRACTED RAY               GIS05530
        CKPP=(N2/N3)*CKP-NUM8*LKP                                        GIS05540
        CLPP=(N2/N3)*CLP-NUM8*LLP                                        GIS05550
        CMPP=(N2/N3)*CMP-NUM8*LMP                                        GIS05560
C       LENGTH OF INSIDE EXTERNAL REFRACTED RAY                          GIS05570
        D3=(BF-XI)/CKPP                                                  GIS05580
        NUM6=((XO+AB)*CK+YO*CL)                                          GIS05590
        NUM7=((XO+AB)*(-CL)+YO*CK)                                       GIS05600
C       LENGTH OF OUTSIDE INCIDENT RAY                                   GIS05610
        D1=SQRT((XO-NUM6)**2+(YO-NUM7)**2)                               GIS05620
C       TOTAL OPTICAL PATHLENGTH:                                        GIS05630
        OPL(G)=N1*D1+N2*D2+N3*D3                                         GIS05640
C       INTERSECTION WITH THE IMAGE PLANE:                               GIS05650
        YIM(G)=((BF-XI)/CKPP)*CLPP+YI                                    GIS05660
        ZIM(G)=((BF-XI)/CKPP)*CMPP+ZI                                    GIS05670
        IF(CMPP .LT. 0.000000000001 .AND. CMPP .GT. -0.000000000001)GIS05680
     1    GO TO 46                                                      GIS05690
          XDIAPT(G)=(-ZIM(G)/CMPP)*CKPP+AB                               GIS05700
          YDIAPT(G)=(-ZIM(G)/CMPP)*CLPP+YIM(G)                           GIS05710
          GO TO 47                                                       GIS05720
   46 CONTINUE                                                           GIS05730
        XDIAPT(G)=99999.                                                 GIS05740
        YDIAPT(G)=99999.                                                 GIS05750
   47 CONTINUE                                                           GIS05760
        IF(SQURAY .EQ. 1) WRITE(6,500)G,RAYY(G),RAYZ(G),XO,YO,XI,        GIS05770
     1  YI,ZI,OPL(G),YIM(G),ZIM(G),NTNCTY(G),XDIAPT(G),YDIAPT(G)         GIS05780
        FLAG(G)=0                                                        GIS05790
```

```
   49 CONTINUE                                                          GIS05800
      H=G                                                               GIS05810
      G=H+1                                                             GIS05820
      NTNCTY(G)=1.0                                                     GIS05830
      RAYY(G)=RAYY(H)                                                   GIS05840
      RAYZ(G)=RAYZ(H)+GRID                                              GIS05850
      IF(FLAG(H) .EQ. 0) COUNT=COUNT+1                                  GIS05860
      GO TO 30                                                          GIS05870
C     END OF RAY TRACE                                                  GIS05880
   50 CONTINUE                                                          GIS05890
      NTNCTY(G)=0.0                                                     GIS05900
      FLAG(G)=1                                                         GIS05910
      IF(SQURAY .EQ. 1) WRITE(6,600)G,RAYY(G),RAYZ(G)                   GIS05920
      GO TO 49                                                          GIS05930
   51 CONTINUE                                                          GIS05940
      NTNCTY(G)=0.0                                                     GIS05950
      FLAG(G)=2                                                         GIS05960
      IF(SQURAY .EQ. 1) WRITE(6,700)G,RAYY(G),RAYZ(G)                   GIS05970
      GO TO 49                                                          GIS05980
   52 CONTINUE                                                          GIS05990
      NTNCTY(G)=0.0                                                     GIS06000
      FLAG(G)=3                                                         GIS06010
      IF(SQURAY .EQ. 1) WRITE(6,800)G,RAYY(G),RAYZ(G)                   GIS06020
      GO TO 49                                                          GIS06030
   53 CONTINUE                                                          GIS06040
      NTNCTY(G)=0.0                                                     GIS06050
      FLAG(G)=4                                                         GIS06060
      IF(SQURAY .EQ. 1) WRITE(6,802) G,RAYY(G),RAYZ(G)                  GIS06070
      GO TO 49                                                          GIS06080
C                                                                       GIS06090
CC    MIRROR IMAGE RAY MATCHING FOLLOWS                                 GIS06100
C                                                                       GIS06110
   60 CONTINUE                                                          GIS06120
      IF(SQURAY .EQ.1) WRITE(6,401)                                     GIS06130
      Q=G-1                                                             GIS06140
      S=G-Q                                                             GIS06150
   61 CONTINUE                                                          GIS06160
      IF(RAYZ(S) .EQ. 0.0) S=S+1                                        GIS06170
        IF(S .GT. Q) GO TO 70                                           GIS06180
          FLAG(G)=FLAG(S)                                               GIS06190
          IF(FLAG(G) .EQ. 0) COUNT=COUNT+1                              GIS06200
          RAYY(G)=RAYY(S)                                               GIS06210
          RAYZ(G)=-RAYZ(S)                                              GIS06220
          IF(FLAG(S) .GE. 1) GO TO 63                                   GIS06230
            XDIAPT(G)=XDIAPT(S)                                         GIS06240
            YDIAPT(G)=YDIAPT(S)                                         GIS06250
            YIM(G)=YIM(S)                                               GIS06260
            ZIM(G)=-ZIM(S)                                              GIS06270
```

```
            OPL(G)=OPL(S)                                                       GIS06280
            NTNCTY(G)=NTNCTY(S)                                                 GIS06290
            IF(SQURAY .EQ. 1) WRITE(6,501)G,S,RAYY(G),RAYZ(G),OPL(G),           GIS06300
     1      YIM(G),ZIM(G),NTNCTY(G)                                             GIS06310
   62 CONTINUE                                                                  GIS06320
      S=S+1                                                                     GIS06330
      G=G+1                                                                     GIS06340
      GO TO 61                                                                  GIS06350
   63 CONTINUE                                                                  GIS06360
      IF(FLAG(S) .GE. 2 ) GO TO 64                                              GIS06370
        IF(SQURAY .EQ. 1) WRITE(6,601)G,S,RAYY(G),RAYZ(G)                       GIS06380
        GO TO 62                                                                GIS06390
   64 CONTINUE                                                                  GIS06400
      IF(FLAG(S) .GE. 3 ) GO TO 65                                              GIS06410
        IF(SQURAY .EQ. 1) WRITE(6,701)G,S,RAYY(G),RAYZ(G)                       GIS06420
        GO TO 62                                                                GIS06430
   65 CONTINUE                                                                  GIS06440
      IF(FLAG(S) .EQ. 4 ) GO TO 67                                              GIS06450
      IF(SQURAY .EQ. 1) WRITE(6,801)G,S,RAYY(G),RAYZ(G)                         GIS06460
      GO TO 62                                                                  GIS06470
   67 CONTINUE                                                                  GIS06480
      IF(SQURAY .EQ. 1)WRITE(6,803)G,S,RAYY(G),RAYZ(G)                          GIS06490
      GO TO 62                                                                  GIS06500
   70 CONTINUE                                                                  GIS06510
      RAYS=G-1                                                                  GIS06520
      DRAYS=RAYS-C                                                              GIS06530
      IF(SQURAY .EQ. 1) WRITE(6,900)RAYS,DRAYS,COUNT                            GIS06540
C                                                                               GIS06550
C     GENERATE OBJECT PLANE ELLIPSES:                                           GIS06560
C                                                                               GIS06570
      IF(ELLIPS .EQ. 1) WRITE(6,1000)ENUM                                       GIS06580
      NUMBR=1                                                                   GIS06590
      NUMB=1                                                                    GIS06600
   71 CONTINUE                                                                  GIS06610
      COORD=1                                                                   GIS06620
      ELZ(NUMB,COORD)=-Y1(NUMBR)                                                GIS06630
   72 CONTINUE                                                                  GIS06640
      ELY(NUMB,COORD)=(X1(NUMBR)+AB)*SIN(ALFAP)+SQRT((Y1(NUMBR))**2-            GIS06650
     1(ELZ(NUMB,COORD))**2)*COS(ALFAP)                                          GIS06660
      ELZZ=ELZ(NUMB,COORD)                                                      GIS06670
      IF(ELLIPS .EQ. 1) WRITE(6,1100)NUMBR,COORD,ELY(NUMB,COORD),               GIS06680
     1ELZ(NUMB,COORD)                                                           GIS06690
      COORD=COORD+1                                                             GIS06700
      ELZ(NUMB,COORD)=ELZZ+ELL                                                  GIS06710
      IF(ELZ(NUMB,COORD) .GE. Y1(NUMBR)) GO TO 73                               GIS06720
        GO TO 72                                                                GIS06730
   73 CONTINUE                                                                  GIS06740
      ELZZ=ELZ(NUMB,COORD)                                                      GIS06750
```

```
   74 CONTINUE                                                                  GIS06760
      ELZ(NUMB,COORD)=ELZZ-ELL                                                  GIS06770
      IF(ELZ(NUMB,COORD) .LE. -Y1(NUMBP)) GO TO 75                              GIS06780
      ELY(NUMB,COORD)=(X1(NUMBR)+AB)*SIN(ALFAP)-SQRT((Y1(NUMBR))**2-            GIS06790
     1(ELZ(NUMB,COORD))**2)*COS(ALFAP)                                          GIS06800
      ELZZ=ELZ(NUMB,COORD)                                                      GIS06810
      IF(ELLIPS .EQ. 1) WRITE(6,1100)NUMBR,COORD,ELY(NUMB,COORD),               GIS06820
     1ELZ(NUMB,COORD)                                                           GIS06830
      COOR(NUMB)=COORD                                                          GIS06840
      COORD=COORD+1                                                             GIS06850
      GO TO 74                                                                  GIS06860
   75 CONTINUE                                                                  GIS06870
      NUMBR=NUMBR+(K-1)/ELLNUM                                                  GIS06880
      NUMB=NUMB+1                                                               GIS06890
      IF(NUMBR .GT. K) GO TO 76                                                 GIS06900
      GO TO 71                                                                  GIS06910
   76 CONTINUE                                                                  GIS06920
      IF(ELLIPS .EQ. 1) WRITE(6,1200)                                           GIS06930
      NUMBT=NUMB-1                                                              GIS06940
C                                                                               GIS06950
C     IMAGE PLANE SPOT DIAGRAM STATISTICAL ANALYSIS:                            GIS06960
C                                                                               GIS06970
      SUM1=0.0                                                                  GIS06980
      DO 77 G=1,RAYS                                                            GIS06990
        IF(FLAG(G) .GT. 0) GO TO 77                                             GIS07000
          SUM1=YIM(G)+SUM1                                                      GIS07010
   77 CONTINUE                                                                  GIS07020
C     REFERENCE EACH ITERATION TO INCIDENT ANGLE & THICKNESS BY:                GIS07030
      IANGLE=ALFAP*10+1                                                         GIS07040
      THICK=(T/R)*100                                                           GIS07050
C     CENTROID OF SPOT:                                                         GIS07060
      YCENTR(IANGLE,THICK)=SUM1/COUNT                                           GIS07070
C     STANDARD DEVIATIONS:                                                      GIS07080
      SUM2=0.0                                                                  GIS07090
      SUM3=0.0                                                                  GIS07100
      DO 78 G=1,RAYS                                                            GIS07110
        IF(FLAG(G) .GT. 0) GO TO 78                                             GIS07120
        SUM2=ZIM(G)**2+SUM2                                                     GIS07130
        SUM3=(YCENTR(IANGLE,THICK)-YIM(G))**2+SUM3                              GIS07140
   78 CONTINUE                                                                  GIS07150
      SIGMAZ(IANGLE,THICK)=SUM2/COUNT                                           GIS07160
      SIGMAY(IANGLE,THICK)=SUM3/COUNT                                           GIS07170
C     ROOT MEAN SQUARE SPOT SIZE:                                               GIS07180
      RMSRAD(IANGLE,THICK)=SQRT(SIGMAZ(IANGLE,THICK)+SIGMAY(IANGLE,             GIS07190
     1THICK))                                                                   GIS07200
      WRITE(6,1300) T,U,ALFAP,R,YCENTR(IANGLE,THICK),                           GIS07210
     1SIGMAY(IANGLE,THICK),SIGMAZ(IANGLE,THICK),RMSRAD(IANGLE,THICK)            GIS07220
C                                                                               GIS07230
```

```
C      SPOT DIAGRAM ENERGY DENSITY VS. RADIUS FROM CENTROID:                    GIS07240
C                                                                               GIS07250
       DO 79 G=1,RAYS                                                           GIS07260
         IF(FLAG(G) .GT. 0) GO TO 79                                            GIS07270
         SDRAD(G)=SQRT((YCENTR(IANGLE,THICK)-YIM(G))**2+ZIM(G)**2)              GIS07280
    79 CONTINUE                                                                 GIS07290
       GG=1                                                                     GIS07300
       ROC(GG)=0.005                                                            GIS07310
       SUM4(GG)=0.0                                                             GIS07320
    80 CONTINUE                                                                 GIS07330
       DO 81 G=1,RAYS                                                           GIS07340
         IF(FLAG(G) .GT. 0) GO TO 81                                            GIS07350
         IF(SDRAD(G) .LE. ROC(GG)) SUM4(GG)=1+SUM4(GG)                          GIS07360
    81 CONTINUE                                                                 GIS07370
       FRACTN(GG)=SUM4(GG)/RAYS                                                 GIS07380
       WRITE(6,1400) GG,ROC(GG),FRACTN(GG)                                      GIS07390
       HH=GG                                                                    GIS07400
       GG=GG+1                                                                  GIS07410
       ROC(GG)=ROC(HH)+0.005                                                    GIS07420
       SUM4(GG)=0.0                                                             GIS07430
       IF(ROC(GG) .GT. 0.5) GO TO 82                                            GIS07440
       GO TO 80                                                                 GIS07450
    82 CONTINUE                                                                 GIS07460
       GGT=GG-1                                                                 GIS07470
       IF(VARY .EQ. 1 .AND. ALFAP .LT. 0.65) GO TO 14                           GIS07480
       WRITE(6,1500)                                                            GIS07490
       IF(T .LT. 0.5 .AND. THKNES .EQ. 1) GO TO 2                               GIS07500
       WRITE(6,1600)                                                            GIS07510
C                                                                               GIS07520
CCC                                                                             GIS07530
CCC    PLOT OUTPUT                                                              GIS07540
CCC                                                                             GIS07550
CCCC   WRITE OUTPUT FOR PLOT INTO FILE FT01F001                                 GIS07560
CCC                                                                             GIS07570
C                                                                               GIS07580
       WRITE(1,83)F,ALPHA,U,I,R,T,N1,N2,N3,ALFAP,GRID,STATNA,GAMMA,RAYS,        GIS07590
      1COUNT,K,GGT,IANGLE,THICK,OSYMB,TSURFL,BEFF,PRCNTO,PRCNTE,PRCNTT,         GIS07600
      1XMAVE,A,B                                                                GIS07610
    83 FORMAT(' ',3F9.7,I4,4F9.7/' ',3F9.7,F9.5,F9.7/' ',6I4,4F11.7/1X,         GIS07620
      15F11.7)                                                                  GIS07630
       DO 85 J=1,K                                                              GIS07640
          WRITE(1,84)X1(J),Y1(J),X2(J),Y2(J)                                    GIS07650
    84    FORMAT(' ',4F10.7)                                                    GIS07660
    85 CONTINUE                                                                 GIS07670
       DO 88 G=1,RAYS                                                           GIS07680
          WRITE(1,86)RAYY(G),RAYZ(G),FLAG(G)                                    GIS07690
    86    FORMAT(' ',2F10.7,3X,I1)                                              GIS07700
          IF(FLAG(G) .GT. 0) GO TO 88                                           GIS07710
```

```
      WRITE(1,87)YIM(G),ZIM(G)                                          GIS07720
87    FORMAT(' ',2F10.7)                                                GIS07730
88 CONTINUE                                                             GIS07740
   DO 90 GG=1,GGT                                                       GIS07750
      WRITE(1,89)ROC(GG),FRACTN(GG)                                     GIS07760
89    FORMAT(' ',F10.7,2X,F10.7)                                        GIS07770
90 CONTINUE                                                             GIS07780
   WRITE(1,91)YCENTR(IANGLE,THICK),SIGMAY(IANGLE,THICK),                GIS07790
  1SIGMAZ(IANGLE,THICK),RMSRAD(IANGLE,THICK),NUMBT                      GIS07800
91 FORMAT(' ',4F10.7,I4)                                                GIS07810
   DO 96 NUMB=1,NUMBT                                                   GIS07820
      WRITE(1,92)COOR(NUMB)                                             GIS07830
92    FORMAT(' ',I3)                                                    GIS07840
      COORT=COOR(NUMB)                                                  GIS07850
      DO 95 COORD=1,COORT                                               GIS07860
         WRITE(1,94)ELY(NUMB,COORD),ELZ(NUMB,COORD)                     GIS07870
94       FORMAT(' ',F11.8,3X,F11.8)                                     GIS07880
95    CONTINUE                                                          GIS07890
96 CONTINUE                                                             GIS07900
   WRITE(1,97)                                                          GIS07910
97 FORMAT(' ','/*')                                                     GIS07920
   WRITE(6,98)                                                          GIS07930
98 FORMAT(' ','TO OBTAIN PLOTS FROM THE PLOTTER OR THE PRINTER,'/' ',   GIS07940
  1'ISSUE THE FOLLOWING COMMAND: '/' ',8X,'FOR PRINTER PLOTS',          GIS07950
  1T36,'ENTER "CHARTS PRINTER"'/' ',8X,'FOR PLOTTER GRAPHS',T36,        GIS07960
  1'ENTER "CHARTS PLOTTER"')                                            GIS07970
   WRITE(6,99)                                                          GIS07980
99 FORMAT(' ','END OF PROGRAM')                                         GIS07990
   STOP                                                                 GIS08000
100 FORMAT('1',' LENS PARAMETERS:'///5X,'ALPHA = ',F9.7,2X,             GIS08010
   1'BETA = ',F9.7,2X,'RADIUS = ',F7.5//5X,'INCIDENT ANGLE = ',         GIS08020
   1F9.6,2X,'ITERATIONS = ',I5//5X,'EDGE THICKNESS = ',F9.7,2X,         GIS08030
   1'INDICES OF REFRACTION: N1 = ',F7.5//5X,'N3 = ',                    GIS08040
   1F7.5,2X,'FOCAL LENGTH FROM STATION ZERO = ',F7.5,2X,                GIS08050
   1'DELTA UDP = ',F7.5///                                              GIS08060
   11X,'  J        X1          Y1          X2          Y2          UDP        I2PGIS08070
   1        I2'//25X,'UP          I1P         I1       DYDXT'//)        GIS08080
200 FORMAT(1X,I4,7F10.7/20X,4F10.7/)                                    GIS08090
300 FORMAT('0'/1X,'NOSE SECTION DATA:'//2X,'NOSE HALF ANGLE = ',        GIS08100
   1F7.5,2X,'STATION A = ',F9.5/2X,'OPAQUE SURFACE LENGTH = ',F7.5/2X,GIS08110
   1'TRANSPARENT SURFACE LENGTH =',F7.5/2X,'TOTAL LENS SURFACE LENGTH GIS08120
   1=',F7.5///)                                                         GIS08130
400 FORMAT('1',' SKEW RAY TRACE PARAMETERS:'///5X,'ALPAP= ',F9.7,2X,    GIS08140
   1'GRID= ',F9.7,2X,'SEE LENS PARAMETERS ABOVE.'///2X,'RAY      RAYY   GIS08150
   1    RAYZ        XO          YO          XI          YI          ZI'//14X,'OGIS08160
   1PL         YIM         ZIM     NTNCTY      XDIAPT      YDIAPT'///)GIS08170
500 FORMAT(1X,I4,7F10.7/8X,F13.9,3F10.7,2E13.3/)                        GIS08180
600 FORMAT(1X,I4,2F10.7,' NO INTERCEPT WITH 2ND SURFACE'/)              GIS08190
```

```
  700 FORMAT(1X,I4,2F10.7,' INTERCEPT OUTSIDE BOUNDARY OF 2ND SURFACE'/)GIS08200
  800 FORMAT(1X,I4,2F10.7,2X,'TOTAL INTERNAL REFLECTION AT 2ND SURFACE'/GIS08210
     1)                                                                 GIS08220
  401 FORMAT('1'/////'MIRROR IMAGE SKEW RAYS FOLLOW'///1X,'IMAGE'/2X,'RAGIS08230
     1Y   RAY    RAYY       RAYZ         OPL          YIM          ZIM       NTNCTGIS08240
     1Y'//)                                                             GIS08250
  501 FORMAT(I4,1X,I4,2F10.7,F13.9,3F10.7/)                             GIS08260
  601 FORMAT(I4,1X,I4,2F10.7,' NO INTERCEPT WITH 2ND SURFACE'/)         GIS08270
  701 FORMAT(I4,1X,I4,2F10.7,' INTERCEPT OUTSIDE OF BOUNDARY OF 2ND SURFGIS08280
     1ACE'/)                                                            GIS08290
  801 FORMAT(I4,1X,I4,2F10.7,' TOTAL INTERNAL REFLECTION'/)             GIS08300
  802 FORMAT(1X,I4,2F10.7,2X,'TOTAL EXTERNAL REFLECTION'/)              GIS08310
  803 FORMAT(I4,1X,I4,2F10.7,'TOTAL EXTERNAL REFLECTION'/)              GIS08320
  900 FORMAT(1X,'END OF  SKEW RAY TRACE.'//3X,'TOTAL NUMBER OF RAYS TRACEGIS08330
     1D = ',I4/3X,'TOTAL NUMBER OF MIRROR IMAGE RAYS = ',I4/3X,'TOTAL NUGIS08340
     1MBER OF RAYS STRIKING IMAGE PLANE = ',I4///)                      GIS08350
 1000 FORMAT('1','TWO DIMENSIONAL PROJECTION OF 3-DIM LENS'///3X,'GENERAGIS08360
     1TED ELLIPSES ARE REFERENCED TO THE CORRESPONDING JTH COORD'/3X,'INGIGIS08370
     1THE MERIDIAN PLANE AS COMPUTED IN THE ABOVE'/3X,'GLM LENS SHAPEAL GIS08380
     1GORITHM. INSIDE/OUTSIDE ELLIPSES DEFINE THE '/3X,'LIMITS OF THE TRGIS08390
     1ANSPARENT/OPAQUE PARTS.'/3X,'THE NUMBER OF ELLIPSES =  ',I3//1X,' GIS08400
     1 J    COORD     ELY        ELZ'//)                                GIS08410
 1100 FORMAT(1X,I4,3X,I4,2F10.7)                                        GIS08420
 1200 FORMAT(1X/'CALCULATION OF ELLIPSE COORDINATES COMPLETE.')         GIS08430
 1300 FORMAT('1'////'IMAGE PLANE SPOT DIAGRAM ANALYSIS:'///1X,'THICKNESSGIS08440
     1 =',F9.7,'  U =',F9.7,'  ALFAP =',F9.7,'  R =',F9.7//1X,'CENTROID:GIS08450
     1 ZCENTR = 0.0,  YCENTR = ',F10.7//1X,'STANDARD DEVIATIONS:  SIGMAYGIS08460
     1 = ',F10.7,2X,'SIGMAZ = ',F10.7//1X,'RMS SPOT SIZE: RMSRAD = ',   GIS08470
     1F10.7//1X,'SPOT DIAGRAM ENERGY DENSITY VS. RADIUS FROM CENTROID:'GIS08480
     1//1X,' GG     RADIUS     FRACTION'//)                             GIS08490
 1400 FORMAT(I4,2F11.7)                                                 GIS08500
 1500 FORMAT(1X/'SPOT DIAGRAM CALCULATIONS COMPLETE.'////)              GIS08510
 1600 FORMAT(1X/'END OF  PROGRAM'////)                                  GIS08520
 1700 FORMAT(1X,'LENS INDEX OF REFRACTION DATA'/2X,'THE INDEX GRADIENT IGIS08530
     1S: N2(R) = SQRT((',F4.2,')+(',F6.3,')*R**2)'/2X,'WITH THE CENTER OGIS08540
     1F SYMMETRY LOCATED AT ',F7.3/2X,'(MINUS IMPLIES THE CSYM IS ON THEGIS08550
     1 IMAGE SIDE).'/2X,'PERCENT CHANGE OF THE LENS INDEX GRADIENT:'/    GIS08560
     14X,'INSIDE SURFACE FROM CENTER TO EDGE :',F10.5/4X,'INSIDE SURFACEGIS08570
     1 TO OUTSIDE SURFACE AT THICKEST POINT :',F10.5/4X,'OUTSIDE SURFACEGIS08580
     1 FROM CENTER TO EDGE :',F10.5////)                                GIS08590
 1800 FORMAT(1X,'IMAGINARY RADIUS DUE TO IMPROPER A TO B RATIO IN N2(R) GIS08600
     1FOR THIS RAY')                                                    GIS08610
 1900 FORMAT(1X,'**********************************************************GIS08620
     1**********'/1X,'*',68X,'*'/1X,'*',25X,'GISL TABULAR OUTPUT',2GIS08630
     14X,'*'/1X,'*',68X,'*'/1X,'**********************************************GIS08640
     1**********'///)                                                   GIS08650
      END                                                               GIS08660
C                                                                       GIS08670
```

```
C                                                                       GIS08680
C     SUBROUTINE INDEX CALCULATES THE INDEX OF REFRACTION AS A FUNCTION GIS08690
C      OF RADIUS FROM THE CENTER OF SYMMETRY. THE VALUES OF THE INDEX   GIS08700
C      CONSTANTS A AND B ARE USER INPUTS.                               GIS08710
C                                                                       GIS08720
      SUBROUTINE INDEX(R,N)                                             GIS08730
      REAL R,N,A,B,RZERO,E,EPSLON,SQRT                                  GIS08740
      COMMON A,B,E,RZERO,EPSLON,PI2,J                                   GIS08750
      N=SQRT(A+B*(R/RZERO)**2)                                          GIS08760
      RETURN                                                            GIS08770
      END                                                               GIS08780
C                                                                       GIS08790
C                                                                       GIS08800
C     SUBROUTINE TRANSMIT CALCULATES THE TRANSMITTED INTENSITY OF       GIS08810
C      EACH RAY AT BOTH THE OUTSIDE AND INSIDE SURFACES USING THE       GIS08820
C      FRESNEL EQUATIONS.                                               GIS08830
C                                                                       GIS08840
      SUBROUTINE XMIT(PHI,N2,XM1,FACE)                                  GIS08850
      REAL PHI,N3,XM1,NTI,N1,N2,SQRT,COS                                GIS08860
      INTEGER FACE                                                      GIS08870
      COMMON/XM/N1,N3                                                   GIS08880
C                                                                       GIS08890
      NTI=N2/N1                                                         GIS08900
      IF(FACE .EQ. 2) NTI=N3/N2                                         GIS08910
      VALUE=NTI**2-(SIN(PHI)**2)                                        GIS08920
      IF(VALUE .LT. 0.0) GO TO 10                                       GIS08930
      SQ=SQRT(VALUE)                                                    GIS08940
      COSP=COS(PHI)                                                     GIS08950
      RPER=(COSP-SQ)/(COSP+SQ)                                          GIS08960
      RPAR=((NTI**2)*COSP-SQ)/((NTI**2)*COSP+SQ)                        GIS08970
      XM1=1.0-0.5*(RPER**2+RPAR**2)                                     GIS08980
      RETURN                                                            GIS08990
   10 CONTINUE                                                          GIS09000
      FACE=3                                                            GIS09010
      RETURN                                                            GIS09020
      END                                                               GIS09030
C                                                                       GIS09040
C                                                                       GIS09050
C     SUBROUTINE RADYUS CALCULATES THE RADIAL DIMENSION FROM THE CENTER GIS09060
C      OF SYMMETRY TO THE RAY AT THE ANGLE SPECIFIED.                   GIS09070
C      RADYUS ALSO FINDS D(R)/D(THETA) FOR SUBR ITRATE.                 GIS09080
C                                                                       GIS09090
      SUBROUTINE RADYUS(RC,ANGLE,R,DRDTHG,FILTER)                       GIS09100
      REAL ANGLE,R,E,RAT,A,B,EPSLON,ARCSYN,FRACTN,RC,SQRT,COS,SIN,ARSIN GIS09110
      INTEGER J,FILTER                                                  GIS09120
      COMMON A,B,E,RZERO,EPSLON,PI2,J                                   GIS09130
      RAT=SQRT(A**2+4.*B*(E**2)/RZERO**2)                               GIS09140
      ARCSYN=ARSIN((2.0*(E/RC)**2-A)/RAT)                               GIS09150
```

```
      IF(ANGLE .LT. 0.0) ARCSYN=2*PI2-ARCSYN                                    GIS09160
      FRACTN=SIN(-EPSLON*2.0*ANGLE+ARCSYN)                                      GIS09170
      IF((A+RAT*FRACTN) .LE. 0.0) GO TO 10                                      GIS09180
      R=SQRT(2.0)*ABS(E)/SQRT(A+RAT*FRACTN)                                     GIS09190
      IF(FRACTN .LE. (-0.989)) GO TO 10                                         GIS09200
      DRDTHG=((EPSLON*R**3)/(2.0*E**2))*COS(-2.0*EPSLON*ANGLE+ARCSYN)           GIS09210
   10 CONTINUE                                                                  GIS09220
      FILTER=0                                                                  GIS09230
      IF(FRACTN .LE. (-0.989))FILTER=2                                          GIS09240
      IF((A+RAT*FRACTN) .LT. 0.0) FILTER=1                                      GIS09250
      RETURN                                                                    GIS09260
      END                                                                       GIS09270
C                                                                               GIS09280
CCCC                                                                            GIS09290
CCCC  SUBROUTINE SWITCH CALCULATES THE POINT ON THE RAY WHERE                   GIS09300
CCCC   D(R)/D(THETA) IS ZERO. THIS ENABLES THE MAIN ROUTINE TO                  GIS09310
CCCC   DETERMINE WHETHER PSIP SHOULD BE EVALUATED IN THE 1ST OR 2ND             GIS09320
CCCC   QUADRANT.                                                                GIS09330
C                                                                               GIS09340
      SUBROUTINE SWITCH(RC,THTACR)                                              GIS09350
      REAL THTACR,RAT,E,EPSLON,A2B,PI2,RO,SQRT,ARSIN                            GIS09360
      COMMON A,B,E,RZERO,EPSLON,PI2,J                                           GIS09370
      RAT=SQRT(A**2+4.*B*(E**2)/RZERO**2)                                       GIS09380
      THTACR=0.5*(PI2-ARSIN((2.0*(E**2/RO**2)-A)/RAT))                          GIS09390
C     IF(THTACR .LT. 0.0) THTACR=THTACR+2.0*PI2                                 GIS09400
      RETURN                                                                    GIS09410
      END                                                                       GIS09420
C                                                                               GIS09430
CCCC                                                                            GIS09440
CCCC   SUBROUTINE SURF CALCULATES BOTH THE RADIUS TO THE                        GIS09450
CCCC  LOCUS OF THE INTERCEPT OF THE RAY PLANE AND THE IN-                       GIS09460
CCCC  SIDE SURFACE AND THE DERIVATIVE OF THE RADIUS WRT THETA                   GIS09470
CCCC  GIVEN THE ANGLE THETA. SURF IS DESIGNED PRIMARILY                         GIS09480
CCCC  FOR USE WITH SUBROUTINE ITRATE.                                           GIS09490
C                                                                               GIS09500
      SUBROUTINE SURF(THETA,R,RDOT,SIGN,FILTER)                                 GIS09510
      COMMON/SUR/PSIO,XC,OSYMB,YO,ZO,RO,CKKP,CLLP,CMMP,N2O,ALPHA                GIS09520
      COMMON/DIR/A1,B1,C1,NPOX,NPOY,NPOZ,PSIP                                   GIS09530
      REAL N2O,OSYMB,NPOX,NPOY,NPOZ,SIN,COS,TAN,COTAN,SQRT,ATAN                 GIS09540
      INTEGER FILTER                                                            GIS09550
C                                                                               GIS09560
      ALFA=COS(THETA)-SIN(THETA)*COTAN(PSIO)                                    GIS09570
      BETA=SIN(THETA)/SIN(PSIO)                                                 GIS09580
      A=ALFA*(XO+OSYMB)/RO+BETA*CKKP                                            GIS09590
      B=ALFA*YO/RO+BETA*CLLP                                                    GIS09600
      C=ALFA*ZO/RO+BETA*CMMP                                                    GIS09610
      A2=B**2+C**2-(A**2)*(TAN(ALPHA)**2)                                       GIS09620
      B2=B*NPOY+C*NPOZ+A*NPOX+2.0*A*OSYMB*(TAN(ALPHA)**2)                       GIS09630
```

```
      C2=CSYMB*NPOX+(OSYMB*TAN(ALPHA))**2+NPOX*XO+NPOY*YO+NPOZ*ZO          GIS09640
      SQUARE=0.25*(B2/A2)**2+C2/A2                                        GIS09650
      IF(SQUARE .LT. 0.0) FILTER=3                                        GIS09660
      IF(FILTER .EQ. 3) RETURN                                            GIS09670
      R=-B2/(2.0*A2)+SIGN*SQRT(SQUARE)                                    GIS09680
C     CALCULATE DR/DTHETA                                                 GIS09690
      DAL=-SIN(THETA)-COS(THETA)*COTAN(PSIO)                              GIS09700
      DBE=COS(THETA)/SIN(PSIO)                                            GIS09710
      DA=DAL*(XO+CSYMB)/RO+DBE*CKKP                                       GIS09720
      DB=DAL*YO/RO+DBE*CLLP                                               GIS09730
      DC=DAL*ZO/RO+DBE*CMMP                                               GIS09740
      DA2=2.0*B*DB+2.0*C*DC-2.0*A*DA*(TAN(ALPHA)**2)                      GIS09750
      DB2=DB*NPOY+DC*NPOZ+DA*NPOX+2.0*DA*CSYMB*(TAN(ALPHA)**2)            GIS09760
      A3=-0.5*(A2*DB2-B2*DA2)/(A2**2)                                     GIS09770
      B3=SIGN/(2.0*SQRT(0.25*(B2/A2)**2+C2/A2))                           GIS09780
      C3=0.25*((A2**2)*2.0*B2*DB2-(B2**2)*2.0*A2*DA2)/(A2**4)-            GIS09790
     1C2*DA2/(A2**2)                                                      GIS09800
      RDOT=A3+B3*C3                                                       GIS09810
      RETURN                                                              GIS09820
      END                                                                 GIS09830
C                                                                         GIS09840
CC                                                                        GIS09850
CCC   SUBROUTINE DIRECT CALCULATES THE VECTOR DIRECTION COSINES OF        GIS09860
CC     A SKEW RAY AT THE POINT OF INTERCEPT WITH THE INSIDE SURFACE.      GIS09870
C                                                                         GIS09880
      SUBROUTINE DIRECT(CKP,CLP,CMP)                                      GIS09890
      COMMON/DIR/RRX,RRY,RRZ,NPFX,NPFY,NPFZ,PSIR                          GIS09900
      REAL RRX,RRY,RRZ,NPFX,NPFY,NPFZ,PSIR,CKP,CLP,CMP,COS,SQRT           GIS09910
      EPS=1.0E-06                                                         GIS09920
      SIGN=+1.0                                                           GIS09930
      IF((ABS(NPFX)) .GT. EPS) GO TO 50                                   GIS09940
      IF((ABS(NPFY)) .GT. EPS) GO TO 30                                   GIS09950
      IF((ABS(RRY)) .LT. EPS) GO TO 25                                    GIS09960
        CMP=0.0                                                           GIS09970
      APP=1.0+(RRX/RRY)**2                                                GIS09980
      BPP=COS(PSIR)*RRX/RRY**2                                            GIS09990
      CPP=(COS(PSIR)/RRY)**2-1.0                                          GIS10000
        CKP=BPP/APP+SIGN*SQRT(BPP**2-APP*CPP)/APP                         GIS10010
        CLP=(COS(PSIR)-RRX*CKP)/RRY                                       GIS10020
        RETURN                                                            GIS10030
   25 CONTINUE                                                            GIS10040
        CMP=0.0                                                           GIS10050
        CKP=COS(PSIR)/RRX                                                 GIS10060
        CLP=SIGN*SQRT(1.0-CKP**2)                                         GIS10070
        RETURN                                                            GIS10080
   30 CONTINUE                                                            GIS10090
      IF((ABS(NPFZ)) .GT. EPS) GO TO 40                                   GIS10100
      IF((ABS(RRZ)) .LT. EPS) GO TO 35                                    GIS10110
```

```
      CLP=0.0                                                          GIS10120
      APP=1.0+(RRX/RRZ)**2                                             GIS10130
      BPP=COS(PSIR)*RRX/RRZ**2                                         GIS10140
      CPP=(COS(PSIR)/RRZ)**2-1.0                                       GIS10150
      CKP=BPP/APP+SQRT(BPP**2-APP*CPP)/APP                             GIS10160
      CMP=(COS(PSIR)-RRX*CKP)/RRZ                                      GIS10170
      RETURN                                                           GIS10180
   35 CONTINUE                                                         GIS10190
      CLP=0.0                                                          GIS10200
      CKP=COS(PSIR)/RRX                                                GIS10210
      CMP=SIGN*SQRT(1.0-CKP**2)                                        GIS10220
      RETURN                                                           GIS10230
   40 CONTINUE                                                         GIS10240
      IF((ABS(RRX)) .GT. EPS) GO TO 45                                 GIS10250
      CLP=COS(PSIR)/(RRY-NPFY/NPFZ*RRZ)                                GIS10260
      CMP=-NPFY/NPFZ*CLP                                               GIS10270
      CKP=SIGN*SQRT(1.0-CLP**2-CMP**2)                                 GIS10280
      RETURN                                                           GIS10290
   45 CONTINUE                                                         GIS10300
      IF((ABS(RRY-NPFY/NPFZ*RRZ)) .GT. EPS) GO TO 47                   GIS10310
      CKP=COS(PSIR)/RRX                                                GIS10320
      CLP=SIGN*SQRT((1.0-CKP**2)/(1.0+(NPFY/NPFZ)**2))                 GIS10330
      CMP=-NPFY/NPFZ*CLP                                               GIS10340
      RETURN                                                           GIS10350
   47 CONTINUE                                                         GIS10360
      SIGN=-1.0                                                        GIS10370
      IF(RRY .LT. 0.0 .OR. RRX .LT. 0.0) SIGN=+1.0                     GIS10380
      IF(RRY .LT. 0.0 .AND. RRX .LT. 0.0) SIGN=-1.0                    GIS10390
      APP=((RRY-NPFY/NPFZ*RRZ)/RRX)**2+1.0+(NPFY/NPFZ)**2              GIS10400
      BPP=2.0*COS(PSIR)/(RRX**2)*(RRY-NPFY/NPFZ*RRZ)                   GIS10410
      CPP=(COS(PSIR)/RRX)**2-1.0                                       GIS10420
      CLP=BPP/(2.0*APP)+SIGN*SQRT(BPP**2-4.0*APP*CPP)/(2.0*APP)        GIS10430
      CMP=-NPFY/NPFZ*CLP                                               GIS10440
      CKP=(COS(PSIR)-(RRY-NPFY/NPFZ*RRZ)*CLP)/RRX                      GIS10450
      RETURN                                                           GIS10460
   50 CONTINUE                                                         GIS10470
      SIGN=-1.0                                                        GIS10480
      IF(RRY .LT. 0.0)SIGN=+1.0                                        GIS10490
      IF(RRY .LT. 0.0 .AND. NPFZ .LT. 0.0) SIGN=-1.0                   GIS10500
      AA=NPFX*RRY-NPFY*RRX                                             GIS10510
      BB=NPFX*RRZ-NPFZ*RRX                                             GIS10520
      CC=NPFX*COS(PSIR)                                                GIS10530
      IF((ABS(BB)) .GT. EPS)GO TO 60                                   GIS10540
      CLP=CC/AA                                                        GIS10550
      APP=(NPFZ/NPFX)**2+1.0                                           GIS10560
      BPP=NPFY*NPFZ/NPFX**2*CLP                                        GIS10570
      CPP=((NPFY/NPFX)**2+1.0)*CLP**2-1.0                              GIS10580
      CMP=-BPP/APP+SIGN*SQRT(BPP**2-APP*CPP)/APP                       GIS10590
```

```
        CKP=(-NPFY*CLP-NPFZ*CMP)/NPFX                                          GIS10600
        RETURN                                                                 GIS10610
   60 CONTINUE                                                                 GIS10620
      IF(BB .GT. 0.0) SIGN=-1.0                                                GIS10630
      AP=(NPFY/NPFX)**2+1.0                                                    GIS10640
      BP=(NPFZ/NPFX)**2+1.0                                                    GIS10650
      CP=2.0*NPFY*NPFZ/NPFX**2                                                 GIS10660
      APP=AP+BP*(AA/BB)**2-CP*AA/BB                                            GIS10670
      BPP=2.0*AA*CC*BP/BB**2-CP*CC/BB                                          GIS10680
      CPP=BP*(CC/BB)**2-1.0                                                    GIS10690
        CLP=BPP/(2.0*APP)+SIGN*SQRT(BPP**2-4.0*APP*CPP)/(2.0*APP)              GIS10700
        CMP=CC/BB-AA/BB*CLP                                                    GIS10710
        CKP=(-NPFY*CLP-NPFZ*CMP)/NPFX                                          GIS10720
        RETURN                                                                 GIS10730
      END                                                                      GIS10740
C                                                                              GIS10750
CC                                                                             GIS10760
CC    SUBROUTINE ITRATE PERFORMS ITERATION TO FIND R AND THETAP                GIS10770
CC   OF THE INTERCEPT OF THE GRIN SKEW-RAY AND THE INSIDE CONICAL              GIS10780
CC   SURFACE USING THE NEWTON-RAPHSON ITERATION PROCEDURE.                     GIS10790
C                                                                              GIS10800
      SUBROUTINE ITRATE(SIGN,THETA,R,THETAP,FILTER)                            GIS10810
      COMMON A,B,E,RZERO,EPSLON,PI2,J                                          GIS10820
      COMMON/DIR/A1,B1,C1,NPOX,NPOY,NPOZ,PSIP                                  GIS10830
      COMMON/SUR/PSI0,X0,OSYMB,Y0,Z0,R0,CKKP,CLLP,CMMP,N20,ALPHA               GIS10840
      INTEGER LOOP,FILTER                                                      GIS10850
C                                                                              GIS10860
      LOOP=0                                                                   GIS10870
   10 CONTINUE                                                                 GIS10880
      CALL RADYUS(R0,THETA,RADG,RDOTG,FILTER)                                  GIS10890
      IF(FILTER .EQ. 1)RETURN                                                  GIS10900
      IF(FILTER .EQ. 2)RETURN                                                  GIS10910
      CALL SURF(THETA,RADH,RDOTS,SIGN,FILTER)                                  GIS10920
      IF(FILTER .EQ. 3)RETURN                                                  GIS10930
      FX=RADG-RADH                                                             GIS10940
      FXDOT=RDOTG-RDOTS                                                        GIS10950
      XNEW=THETA-(FX/FXDOT)/1.3                                                GIS10960
      DIFF=ABS(THETA-XNEW)                                                     GIS10970
      IF(DIFF .GT. 0.00001) GO TO 20                                           GIS10980
      THETAP=THETA                                                             GIS10990
      R=RADG                                                                   GIS11000
      RETURN                                                                   GIS11010
   20 CONTINUE                                                                 GIS11020
      IF(LOOP .GE. 90) GO TO 30                                                GIS11030
      LOOP=LOOP+1                                                              GIS11040
      THETA=XNEW                                                               GIS11050
      GO TO 10                                                                 GIS11060
   30 CONTINUE                                                                 GIS11070
```

```
      IF(LOOP .GE. 90) FILTER=3                                         GIS11080
      WRITE(6,6410)                                                     GIS11090
 6410 FORMAT(/1X,'SOLUTION NOT FOUND')                                  GIS11100
      RETURN                                                            GIS11110
      END                                                               GIS11120
```

```
**********************************************************************
*                                                                    *
*                        GISL TABULAR OUTPUT                         *
*                                                                    *
**********************************************************************

1 LENS PARAMETERS:

     ALPHA = 0.7853982   BETA = 0.3217505   RADIUS = 1.00000
     INCIDENT ANGLE =   0.0        ITERATIONS =    100
     EDGE THICKNESS = 0.0500000   INDICES OF REFRACTION: N1 = 1.00000
     N3 = 1.00000   FOCAL LENGTH FROM STATION ZERO = 4.00000   DELTA LOP = 0.00322

  J       X1          Y1          X2          Y2          UOP         I2P          I2
                                    UP          I1P         I1       DYDXT

  1 0.9616396 1.0320053 1.0000000 0.9999998 0.3217505 0.4636472 0.0995450
                                0.6858528 0.1720029 0.8769178 0.8318774
  2 0.9527428 1.0245905 0.9919431 0.9919429 0.3185330 0.4668649 0.1006271
                                0.6847707 0.1727901 0.8770413 0.8316687
  3 0.9438142 1.0171518 0.9838600 0.9838598 0.3153155 0.4700826 0.1017177
                                0.6836802 0.1735849 0.8771699 0.8314511
  4 0.9348540 1.0096884 0.9757503 0.9757501 0.3120980 0.4732993 0.1028165
                                0.6825813 0.1743850 0.8772871 0.8312529
  5 0.9258599 1.0022020 0.9676142 0.9676141 0.3088804 0.4765170 0.1039242
                                0.6814736 0.1751921 0.8774052 0.8310531
  6 0.9168330 0.9946885 0.9594508 0.9594507 0.3056630 0.4797347 0.1050406
                                0.6803573 0.1760102 0.8775480 0.8308118
  7 0.9077742 0.9871492 0.9512604 0.9512602 0.3024455 0.4829524 0.1061657
                                0.6792321 0.1768308 0.8776608 0.8306212
  8 0.8986831 0.9795850 0.9430425 0.9430423 0.2992280 0.4861692 0.1072993
                                0.6780985 0.1776611 0.8777914 0.8304005
```

9 0.8895560 0.9719930 0.9347960 0.9347959 0.2960104 0.4993869 0.1084422
0.6769556 0.1784965 0.8779076 0.8302040

10 0.8803961 0.9643753 0.9265221 0.9265219 0.2927930 0.4926046 0.1095940
0.6758038 0.1793403 0.8780314 0.8299952

11 0.8712009 0.9567289 0.9182188 0.9182186 0.2895755 0.4958213 0.1107548
0.6746430 0.1801909 0.8781521 0.8297914

12 0.8619708 0.9490560 0.9098864 0.9098862 0.2863579 0.4990390 0.1119250
0.6734728 0.1810462 0.8782556 0.8296165

13 0.8527024 0.9413573 0.9015246 0.9015244 0.2831404 0.5022567 0.1131043
0.6722935 0.1819105 0.8783699 0.8294234

14 0.8433996 0.9336274 0.8931330 0.8931329 0.2799229 0.5054744 0.1142931
0.6711047 0.1827840 0.8784947 0.8292129

15 0.8340593 0.9258732 0.8847126 0.8847124 0.2767054 0.5086921 0.1154910
0.6699068 0.1836621 0.8786031 0.8290300

16 0.8246826 0.9180898 0.8762615 0.8762614 0.2734879 0.5119098 0.1166985
0.6686993 0.1845482 0.8787155 0.8288405

17 0.8152681 0.9102768 0.8677794 0.8677792 0.2702704 0.5151275 0.1179156
0.6674823 0.1854381 0.8788039 0.8286913

18 0.8058172 0.9024346 0.8592664 0.8592662 0.2670529 0.5183452 0.1191421
0.6662558 0.1863384 0.8789114 0.8285100

19 0.7963278 0.8945618 0.8507230 0.8507228 0.2638354 0.5215619 0.1203781
0.6650197 0.1872448 0.8790098 0.8283439

20 0.7867995 0.8866592 0.8421465 0.8421463 0.2606179 0.5247796 0.1216241
0.6637738 0.1881607 0.8791218 0.8281551

21 0.7772329 0.8787258 0.8335392 0.8335391 0.2574005 0.5279973 0.1228797
0.6625181 0.1890816 0.8792174 0.8279940

22 0.7676280 0.8707618 0.8248989 0.8248987 0.2541829 0.5312141 0.1241450
0.6612529 0.1900077 0.8792992 0.8278561

23 0.7579840 0.8627660 0.8162262 0.8162261 0.2509654 0.5344318 0.1254203
0.6599776 0.1909401 0.8793746 0.8277292

24 0.7482984 0.8547372 0.8075203 0.8075202 0.2477480 0.5376495 0.1267056
0.6586922 0.1918799 0.8794488 0.8276040

25 0.7385736 0.8466769 0.7987810 0.7987808 0.2445304 0.5408671 0.1280009
0.6573970 0.1928259 0.8795164 0.8274904

26 0.7288064 0.8385835 0.7900075 0.7900074 0.2413129 0.5440839 0.1293058
0.6560920 0.1937829 0.8796067 0.8273380

27 0.7189997 0.8304576 0.7811996 0.7811995 0.2380954 0.5473016 0.1306210
0.6547768 0.1947386 0.8796439 0.8272754

28 0.7091515 0.8222976 0.7723581 0.7723579 0.2348779 0.5505193 0.1319463
0.6534515 0.1957040 0.8796960 0.8271877

29 0.6992603 0.8141024 0.7634806 0.7634804 0.2316604 0.5537370 0.1332816
0.6521162 0.1966770 0.8797513 0.8270944

30 0.6893276 0.8058743 0.7545682 0.7545680 0.2284429 0.5569547 0.1346271
0.6507707 0.1976526 0.8797790 0.8270478

31 0.6793501 0.7976097 0.7456194 0.7456192 0.2252254 0.5601724 0.1359826
0.6494152 0.1986350 0.8798047 0.8270046

32 0.6693305 0.7893112 0.7366352 0.7366350 0.2220079 0.5633891 0.1373481
0.6480498 0.1996242 0.8798310 0.8269601

33 0.6592678 0.7809767 0.7276143 0.7276142 0.2187904 0.5666068 0.1387237
0.6466741 0.2006130 0.8798138 0.8269892

34 0.6491598 0.7726042 0.7185560 0.7185559 0.2155729 0.5698245 0.1401095
0.6452883 0.2016122 0.8798180 0.8269823

35 0.6390076 0.7641952 0.7094607 0.7094606 0.2123554 0.5730422 0.1415054
0.6438924 0.2026151 0.8798057 0.8270029

36 0.6288099 0.7557480 0.7003270 0.7003269 0.2091379 0.5762599 0.1429113
0.6424865 0.2036191 0.8797619 0.8270767

37 0.6185674 0.7472628 0.6911556 0.6911554 0.2059204 0.5794767 0.1443270
0.6410708 0.2046333 0.8797413 0.8271113

38 0.6082788 0.7387393 0.6819450 0.6819448 0.2027029 0.5826944 0.1457528
0.6396450 0.2056431 0.8796603 0.8272479

39 0.5979443 0.7301762 0.6726955 0.6726953 0.1994854 0.5859120 0.1471885
0.6382093 0.2066600 0.8795860 0.8273730

40 0.5875602 0.7215751 0.6634064 0.6634063 0.1962678 0.5891297 0.1486340
0.6367638 0.2076797 0.8794951 0.8275260

41 0.5771319 0.7129317 0.6540776 0.6540775 0.1930503 0.5923465 0.1500890
0.6353088 0.2087043 0.8794014 0.8276839

42 0.5666530 0.7042491 0.6447080 0.6447079 0.1898329 0.5955642 0.1515539
0.6338440 0.2097281 0.8792736 0.8278992

43 0.5561299 0.6955217 0.6352974 0.6352973 0.1866153 0.5987819 0.1530283
0.6323695 0.2107540 0.8791294 0.8281425

44 0.5455577 0.6867517 0.6258453 0.6258451 0.1833978 0.6019996 0.1545120
0.6308858 0.2117817 0.8789694 0.8284122

45 0.5349353 0.6779414 0.6163516 0.6163515 0.1801803 0.6052173 0.1560050
0.6293928 0.2128095 0.8787854 0.8287225

46 0.5242630 0.6690865 0.6068150 0.6068149 0.1769629 0.6084350 0.1575071
0.6278907 0.2138370 0.8785779 0.8290725

47 0.5135422 0.6601877 0.5972365 0.5972363 0.1737453 0.6116517 0.1590179
0.6263800 0.2148613 0.8783325 0.8294867

48 0.5027711 0.6512430 0.5876139 0.5876138 0.1705278 0.6148694 0.1605376
0.6248602 0.2158903 0.8780947 0.8298882

49 0.4919505 0.6422523 0.5779477 0.5779476 0.1673103 0.6180871 0.1620658
0.6233320 0.2169136 0.8778104 0.8303685

50 0.4810801 0.6332145 0.5682372 0.5682371 0.1640928 0.6213048 0.1636023
0.6217955 0.2179340 0.8774970 0.8308981

51 0.4701589 0.6241291 0.5584818 0.5584816 0.1608753 0.6245225 0.1651468
0.6202511 0.2189507 0.8771533 0.8314793

52 0.4591874 0.6149944 0.5486809 0.5486808 0.1576578 0.6277393 0.1666989
0.6186990 0.2199641 0.8767840 0.8321041

53 0.4481649 0.6058107 0.5388345 0.5388344 0.1544403 0.6309569 0.1682587
0.6171392 0.2209763 0.8764024 0.8327499

54 0.4370912 0.5965770 0.5289415 0.5289414 0.1512228 0.6341746 0.1698255
0.6155723 0.2219762 0.8759543 0.8335092

55 0.4259651 0.5872923 0.5190016 0.5190015 0.1480053 0.6373923 0.1713992
0.6139987 0.2229703 0.8754758 0.8343204

56 0.4147875 0.5779552 0.5090140 0.5090139 0.1447878 0.6406100 0.1729792
0.6124186 0.2239618 0.8749874 0.8351490

57 0.4035584 0.5685652 0.4989785 0.4989784 0.1415703 0.6438268 0.1745651
0.6108327 0.2249327 0.8744001 0.8361464

58 0.3922781 0.5591206 0.4888944 0.4888943 0.1383528 0.6470445 0.1761568
0.6092411 0.2259064 0.8738380 0.8371021

59 0.3809454 0.5496220 0.4787614 0.4787613 0.1351352 0.6502622 0.1777536
0.6076442 0.2268587 0.8731809 0.8382204

60 0.3695607 0.5400661 0.4685786 0.4685785 0.1319178 0.6534799 0.1793550
0.6060428 0.2278067 0.8725201 0.8393459

61 0.3581234 0.5304537 0.4583452 0.4583451 0.1287003 0.6566976 0.1809607
0.6044372 0.2287461 0.8718379 0.8405095

62 0.3466337 0.5207836 0.4480610 0.4480609 0.1254827 0.6599143 0.1825695
0.6028283 0.2296700 0.8711029 0.8417643

63 0.3350886 0.5110562 0.4377257 0.4377256 0.1222652 0.6631320 0.1841817
0.6012161 0.2305866 0.8703625 0.8430304

64 0.3234909 0.5012694 0.4273381 0.4273379 0.1190478 0.6663497 0.1857961
0.5996017 0.2315134 0.8697081 0.8441503

65 0.3118377 0.4914232 0.4168978 0.4168977 0.1158302 0.6695674 0.1874124
0.5979854 0.2321913 0.8678473 0.8473423

66 0.3001441 0.4815053 0.4064043 0.4064041 0.1126127 0.6727841 0.1890293
0.5963685 0.2330918 0.8671477 0.8485447

67 0.2883955 0.4715261 0.3958564 0.3958563 0.1093952 0.6760018 0.1906468
0.5947511 0.2339365 0.8662193 0.8501430

68 0.2765932 0.4614829 0.3852540 0.3852539 0.1061777 0.6792195 0.1922638
0.5931340 0.2347438 0.8651602 0.8519691

69 0.2647396 0.4513741 0.3745971 0.3745970 0.1029602 0.6824372 0.1938794
0.5915185 0.2355235 0.8640264 0.8539279

70 0.2528339 0.4411972 0.3638837 0.3638836 0.0997427 0.6856549 0.1954927
0.5899051 0.2362607 0.8627505 0.8561365

71 0.2408782 0.4309509 0.3531137 0.3531135 0.0965252 0.6888726 0.1971030
0.5882948 0.2369844 0.8614810 0.8583391

72 0.2288720 0.4206347 0.3422866 0.3422865 0.0933077 0.6920894 0.1987091
0.5866887 0.2376738 0.8601224 0.8607012

73 0.2168158 0.4102467 0.3314016 0.3314016 0.0903902 0.6953071 0.2003103
0.5850875 0.2383270 0.8586721 0.8632289

74 0.2047106 0.3997850 0.3204582 0.3204581 0.0868727 0.6985248 0.2019055
0.5834923 0.2389493 0.8571633 0.8658658

75 0.1925563 0.3892483 0.3094552 0.3094551 0.0836552 0.7017425 0.2034936
0.5819042 0.2395362 0.8555795 0.8686407

76 0.1803538 0.3786361 0.2983926 0.2983925 0.0804377 0.7049602 0.2050733
0.5803245 0.2400801 0.8538936 0.8716030

77 0.1681040 0.3679463 0.2872689 0.2872688 0.0772201 0.7081769 0.2066433
0.5787545 0.2405922 0.8521645 0.8746502

78 0.1558043 0.3571798 0.2760841 0.2760840 0.0740027 0.7113946 0.2082030
0.5771948 0.2410619 0.8503491 0.8778595

79 0.1434576 0.3463323 0.2648367 0.2648366 0.0707852 0.7146123 0.2097508
0.5756471 0.2414904 0.8484600 0.8812100

80 0.1310653 0.3354030 0.2535262 0.2535262 0.0675676 0.7178300 0.2112853
0.5741125 0.2418711 0.8464741 0.8847443

81 0.1186289 0.3243900 0.2421523 0.2421522 0.0643501 0.7210477 0.2128052
0.5725926 0.2422076 0.8444154 0.8884209

82 0.1061490 0.3132926 0.2307140 0.2307140 0.0611327 0.7242644 0.2143090
0.5710889 0.2424974 0.8422785 0.8922517

83 0.0936257 0.3021082 0.2192101 0.2192100 0.0579152 0.7274821 0.2157956
0.5696022 0.2427363 0.8400525 0.8962579

84 0.0810609 0.2908359 0.2076402 0.2076401 0.0546976 0.7306998 0.2172634
0.5681344 0.2429250 0.8377470 0.9004240

85 0.0684555 0.2794743 0.1960034 0.1960033 0.0514801 0.7339175 0.2187108
0.5666870 0.2430628 0.8353659 0.9047449

86 0.0558102 0.2680214 0.1842988 0.1842987 0.0482626 0.7371352 0.2201362
0.5652616 0.2431462 0.8329000 0.9092394

87 0.0431264 0.2564759 0.1725258 0.1725258 0.0450451 0.7403520 0.2215379
0.5638599 0.2431734 0.8303474 0.9139132

88 0.0304019 0.2448380 0.1606832 0.1606832 0.0418276 0.7435697 0.2229148
0.5624831 0.2431445 0.8277161 0.9187540

```
 89 0.0176410 0.2331046 0.1487704 0.1487703 0.0386101 0.7467874 0.2242649
                0.5611330 0.2430580 0.8250054 0.9237653

 90 0.0048451 0.2212741 0.1367862 0.1367862 0.0352926 0.7500051 0.2255866
                0.5598112 0.2429150 0.8222255 0.9289307

 91-0.0079843 0.2093453 0.1247303 0.1247303 0.0321751 0.7532218 0.2268779
                0.5585199 0.2427126 0.8193703 0.9342635

 92-0.0208471 0.1973162 0.1126012 0.1126012 0.0289576 0.7564395 0.2281377
                0.5572602 0.2424498 0.8164404 0.9397660

 93-0.0337411 0.1851857 0.1003983 0.1003982 0.0257401 0.7596572 0.2293640
                0.5560338 0.2421274 0.8134441 0.9454245

 94-0.0466690 0.1729540 0.0881205 0.0881204 0.0225226 0.7628749 0.2305551
                0.5548428 0.2417436 0.8103788 0.9512465

 95-0.0596255 0.1606186 0.0757670 0.0757669 0.0193051 0.7660926 0.2317091
                0.5536888 0.2413010 0.8072599 0.9572054

 96-0.0726097 0.1481775 0.0633368 0.0633368 0.0160876 0.7693103 0.2328244
                0.5525734 0.2407974 0.8040817 0.9633141

 97-0.0856237 0.1356313 0.0508290 0.0508290 0.0128701 0.7725270 0.2338991
                0.5514987 0.2402332 0.8008499 0.9695645

 98-0.0986636 0.1229768 0.0382423 0.0382423 0.0096526 0.7757447 0.2349319
                0.5504659 0.2396098 0.7975732 0.9759415

 99-0.1117308 0.1102147 0.0255759 0.0255759 0.0064350 0.7789624 0.2359210
                0.5494769 0.2389274 0.7942556 0.9824401

100-0.1248229 0.0973431 0.0128291 0.0128291 0.0032176 0.7821801 0.2368645
                0.5485333 0.2381868 0.7909024 0.9890516

101-0.1379396 0.0843605 0.0000002 0.0000002 0.0000001 0.7853969 0.2377607
                0.5476371 0.2373897 0.7875214 0.9957625

0
 NOSE SECTION DATA:

  NOSE HALF ANGLE = 0.78327  STATION A =  -0.22266
  OPAQUE SURFACE LENGTH = 0.11956
  TRANSPARENT SURFACE LENGTH =1.45205
  TOTAL LENS SURFACE LENGTH =1.57160
```

LENS INDEX OF REFRACTION DATA
THE INDEX GRADIENT IS: N2(R) = SQRT((9.00)+(5.351)*R**2)
WITH THE CENTER OF SYMMETRY LOCATED AT 0.050
(MINUS IMPLIES THE OSYM IS ON THE IMAGE SIDE).
PERCENT CHANGE OF THE LENS INDEX GRADIENT:
INSIDE SURFACE FROM CENTER TO EDGE : 49.88858
INSIDE SURFACE TO OUTSIDE SURFACE AT THICKEST POINT : 0.36591
OUTSIDE SURFACE FROM CENTER TO EDGE : 49.34212

1SKEW RAY TRACE PARAMETERS:

ALFAP= 0.4C00000 GRID= 0.3000000 SEE LENS PARAMETERS ABOVE.

RAY	RAYY	RAYZ	XO	YO	XI	YI	ZI
	OPL	YIM	ZIM	NTNCTY	XDIAPT	YDIAPT	
1	0.0	0.3000000	0.1307886	-0.1494352	0.2557881	-0.1287202	0.2210370
	5.04583168	-2.1801453	-0.1453156	0.5102614	-0.126E+01	-0.137E+01	
2	0.0	0.6000000	0.5384317	-0.3217840	0.6207671	-0.3018253	0.5424452
	4.45595169	-1.4455128	-0.2271336	0.4481558	-0.775E+00	-0.111E+01	
3	0.0	0.9000000	0.9583030	-0.4993026	0.9974844	-0.4872602	0.8703845
	4.09892273	-1.1834154	-0.2429521	0.3635889	-0.433E+00	-0.103E+01	
4	0.3000000	0.0	0.0109681	0.2269354	0.1305237	0.1305212	0.0
	4.85042477	-1.6185007	0.0	0.5535472	0.100E+06	0.100E+06	
5	0.3000000	0.3000000	0.1424869	0.1713301	0.2579772	0.1139907	0.2314239
	4.93159103	-1.9860687	0.3676595	0.5334762	-0.988E+01	0.368E+01	
6	0.3000000	0.6000000	0.4431463	0.0442133	0.5327001	0.0265410	0.5320314
	4.60996151	-1.7169704	0.0316697	0.4739231	0.442E+00	-0.183E+01	
7	0.3000000	0.9000000	0.8111566	-0.1113788	0.8637780	-0.1123655	0.8564321
	4.27614594	-1.4330120	-0.1198373	0.3925338	-0.162E+00	-0.127E+01	
8	0.6000000	0.0	0.2600275	0.4473460	0.3610061	0.3610038	0.0

```
          4.66151619 -1.4761887 0.0        0.5169492     0.100E+06     0.100E+06

 9 0.6000000 0.3000000 0.3363692 0.4150693 0.4317581 0.3448501 0.2597798
          4.65313148 -1.5641460 0.1932485 0.5009179     0.106E+02    -0.711E+01

10 0.6000000 0.6000000 0.5420605 0.3281044 0.6192006 0.2887600 0.5477414
          4.53353596 -1.5893183 0.1321886 0.4537812     0.130E+01    -0.219E+01

11 0.6000000 0.9000000 0.8309218 0.2059760 0.8806287 0.1906774 0.8597310
          4.31594181 -1.4822788 0.0079514 0.3868141     0.252E+00    -0.150E+01

12 0.9000000 0.0        0.5180798 0.6639546 0.5948910 0.5948853 0.0
          4.56061363 -1.3724556 0.0        0.4602101     0.100E+06     0.100E+06

13 0.9000000 0.3000000 0.5713329 0.6414395 0.6435080 0.5810593 0.2765256
          4.53502178 -1.4060097 0.1153301 0.4473754     0.262E+01    -0.283E+01

14 0.9000000 0.6000000 0.7219925 0.5777416 0.7806184 0.5374358 0.5661314
          4.45209980 -1.4449883 0.1326690 0.4111363     0.121E+01    -0.205E+01

15 0.9000000 0.9000000 0.9483795 0.4820271 0.9865439 0.4622759 0.8715199
          4.30145073 -1.4332008 0.0648745 0.3594230     0.465E+00    -0.159E+01

16 1.1999998 0.0        0.7783279 0.8796349 0.8306387 0.8306248 0.0
          4.49608326 -1.3109426 0.0        0.3974670     0.100E+06     0.100E+06

17 1.1999998 0.3000000 0.8187981 0.8625243 0.8675712 0.8187382 0.2869341
          4.47258854 -1.3300571 0.0765226 0.3879091     0.136E+01    -0.211E+01

18 1.1999998 0.6000000 0.9357986 0.8130573 0.9743750 0.7823852 0.5807928
          4.40475750 -1.3604498 0.1072606 0.3611534     0.908E+00    -0.185E+01

19-0.3000000 0.0        0.4567428-0.6129578 0.5509578-0.5509512 0.0
          4.38281155 -0.9380237 0.0        0.4409877     0.100E+06     0.100E+06

20-0.3000000 0.3000000 0.6123005-0.6787266 0.6885747-0.6313385 0.2748162
          4.28067303 -0.9621467-0.2031004 0.4222168    -0.118E+01    -0.822E+00

21-0.3000000 0.6000000 0.9397941-0.8171884 0.9814265-0.7927174 0.5786383
          4.05062485 -0.9309339-0.2432328 0.3676401    -0.671E+00    -0.890E+00

1


MIRROR IMAGE SKEW RAYS FOLLOW
```

IMAGE RAY	RAY	RAYY	RAYZ	OPL	YIM	ZIM	NTNCTY
22	1	0.0	-0.3C00000	5.04583168	-2.1801453	C.1453156	0.5102614
23	2	0.0	-0.6C00000	4.45595169	-1.4455128	0.2271336	0.4481558
24	3	0.0	-0.9C00000	4.09892273	-1.1834154	0.2429521	0.3635889
25	5	0.3000000	-0.3C00000	4.93159103	-1.9860687	-0.3676595	0.5334762
26	6	0.3000000	-0.6CC0000	4.60996151	-1.7169704	-0.0316697	0.4739231
27	7	0.3000000	-0.9000000	4.27614594	-1.4330120	0.1158373	0.3925338
28	9	0.6000000	-0.3000000	4.65313148	-1.5641460	-0.1932485	0.5C09179
29	10	0.6000000	-0.6000000	4.53353596	-1.5893183	-0.1321886	0.4537812
3C	11	0.6000000	-0.9000000	4.31594181	-1.4822788	-0.0079514	0.3868141
31	13	C.9000000	-0.3C00000	4.53502178	-1.4060097	-0.1153301	0.4473754
32	14	0.9000000	-0.6000000	4.45209980	-1.4449883	-0.1326690	0.4111363
33	15	0.9000000	-0.9000000	4.30145073	-1.4332008	-0.0648745	0.3594230
34	17	1.1999998	-0.3C00000	4.47258854	-1.3300571	-0.0765226	0.3879091
35	18	1.1999998	-0.6C00000	4.40475750	-1.3604498	-0.1072606	0.3611534
36	20	-0.3000000	-0.3000000	4.28067303	-0.9621467	0.2031004	C.4222168
37	21	-0.3000000	-0.6C00000	4.05062485	-0.9309339	0.2432328	0.3676401

END OF SKEW RAY TRACE.

TOTAL NUMBER OF RAYS TRACED = 37
TOTAL NUMBER OF MIRROR IMAGE RAYS = 16
TOTAL NUMBER OF RAYS STRIKING IMAGE PLANE = 37

1

IMAGE PLANE SPOT DIAGRAM ANALYSIS:

THICKNESS =0.0500000 U =0.0 ALFAP =0.4000000 R =1.0000000

CENTROID: ZCENTR = 0.0, YCENTR = -1.4490051

STANDARD DEVIATIONS: SIGMAY = 0.0911858 SIGMAZ = 0.0264883

RMS SPOT SIZE: RMSRAD = 0.3430366

SPOT DIAGRAM ENERGY DENSITY VS. RADIUS FROM CENTROID:

GG	RADIUS	FRACTION
1	0.0050000	0.0
2	0.0100000	0.0
3	0.0150000	0.0
4	0.0200000	0.0
5	0.0250000	0.0
6	0.0300000	0.0270270
7	0.0350000	0.0810810
8	0.0400000	0.0810810
9	0.0450000	0.0810810
10	0.0500000	0.0810810
11	0.0550000	0.0810810
12	0.0600000	0.0810810
13	0.0649999	0.0810810
14	0.0699999	0.1351351
15	0.0749999	0.1351351
16	0.0799999	0.1621621
17	0.0849999	0.1621621
18	0.0899999	0.1621621
19	0.0949999	0.1621621
20	0.0999999	0.1621621
21	0.1049999	0.1621621
22	0.1099999	0.1621621
23	0.1149999	0.1621621
24	0.1199999	0.1621621
25	0.1249999	0.2702702
26	0.1299999	0.2702702
27	0.1349999	0.3243243
28	0.1399999	0.4054054
29	0.1449999	0.4594594
30	0.1499999	0.4594594

31	0.1549999	0.4594594
32	0.1599998	0.4594594
33	0.1649998	0.4594594
34	0.1699998	0.4864864
35	0.1749998	0.4864864
36	0.1799998	0.4864864
37	0.1849998	0.4864864
38	0.1899998	0.4864864
39	0.1949998	0.5405405
40	0.1999998	0.5405405
41	0.2049998	0.5405405
42	0.2099998	0.5405405
43	0.2149998	0.5405405
44	0.2199998	0.5405405
45	0.2249998	0.5945945
46	0.2299998	0.6486486
47	0.2349998	0.6486486
48	0.2399998	0.6486486
49	0.2449998	0.6486486
50	0.2499998	0.6486486
51	0.2549998	0.6486486
52	0.2599998	0.6486486
53	0.2649997	0.6486486
54	0.2699997	0.7027027
55	0.2749997	0.7027027
56	0.2799997	0.7027027
57	0.2849997	0.7027027
58	0.2899997	0.7027027
59	0.2949997	0.7027027
60	0.2999997	0.7027027
61	0.3049997	0.7027027
62	0.3099997	0.7027027
63	0.3149997	0.7027027
64	0.3199997	0.7027027
65	0.3249997	0.7027027
66	0.3299997	0.7027027
67	0.3349997	0.7027027
68	0.3399997	0.7027027
69	0.3449997	0.7027027
70	0.3499997	0.7027027
71	0.3549997	0.7027027
72	0.3599997	0.7567567
73	0.3649997	0.7567567
74	0.3699996	0.7567567
75	0.3749996	0.7567567
76	0.3799996	0.7567567
77	0.3849996	0.7567567
78	0.3899996	0.7567567

79	0.3949996	0.7567567
80	0.3999996	0.7567567
81	0.4049996	0.7567567
82	0.4099996	0.7567567
83	0.4149996	0.7567567
84	0.4199996	0.7567567
85	0.4249996	0.7567567
86	0.4299996	0.7567567
87	0.4349996	0.7567567
88	0.4399996	0.7567567
89	0.4449996	0.7567567
90	0.4499996	0.7567567
91	0.4549996	0.7567567
92	0.4599996	0.7567567
93	0.4649996	0.7567567
94	0.4699996	0.7567567
95	0.4749995	0.7567567
96	0.4799995	0.7567567
97	0.4849995	0.7567567
98	0.4899995	0.7567567
99	0.4949995	0.7567567
100	0.4999995	0.7567567

SPOT DIAGRAM CALCULATIONS COMPLETE.

END OF PROGRAM

TO OBTAIN PLOTS FROM THE PLOTTER OR THE PRINTER,
ISSUE THE FOLLOWING COMMAND:
FOR PRINTER PLOTS ENTER "CHARTS PRINTER"
FOR PLOTTER GRAPHS ENTER "CHARTS PLOTTER"
END OF PROGRAM

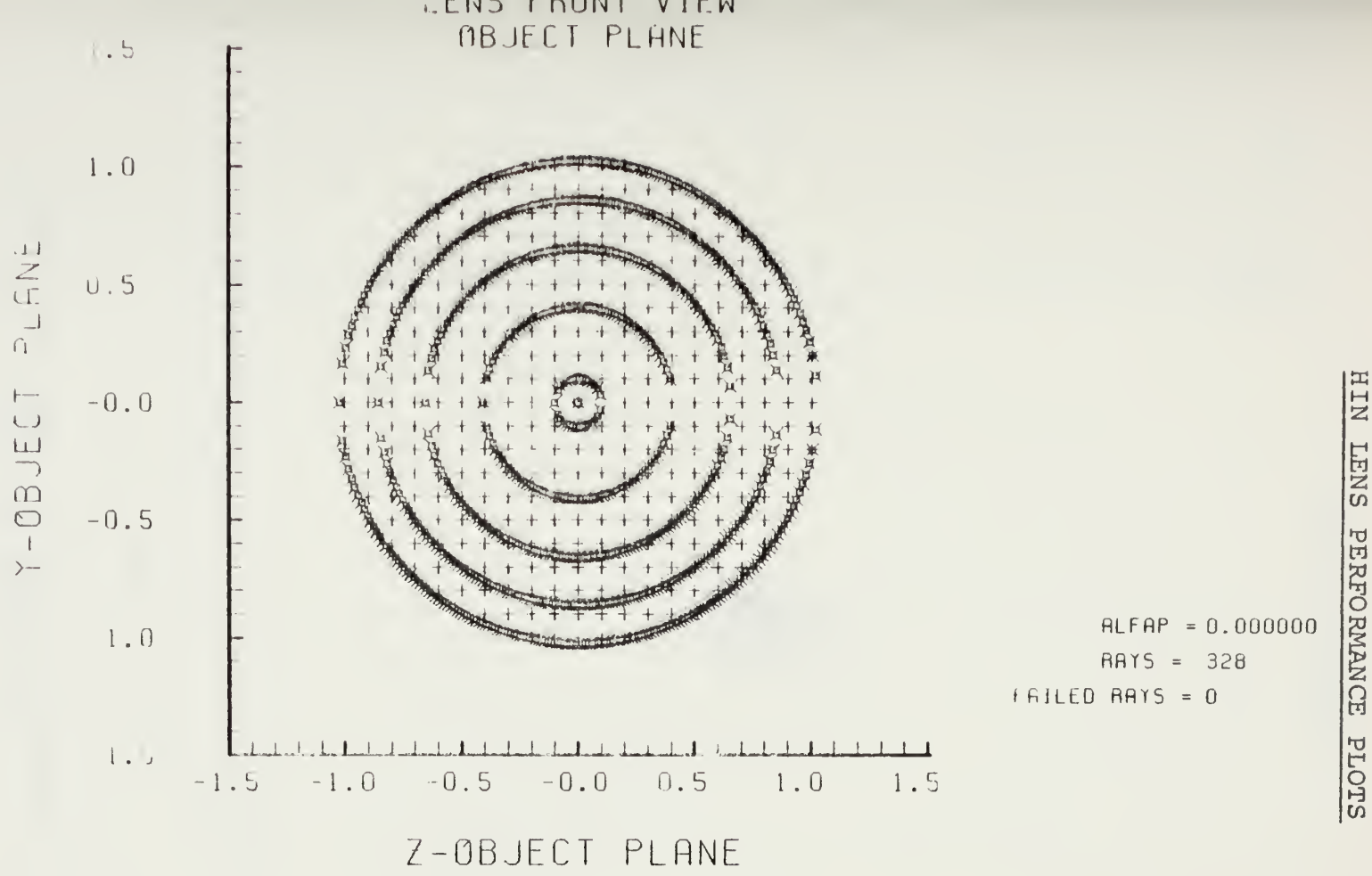

Figure D-1. Object Plane at α_p = 0.0 Radians for Hin Lens Design Shown in Figure 11

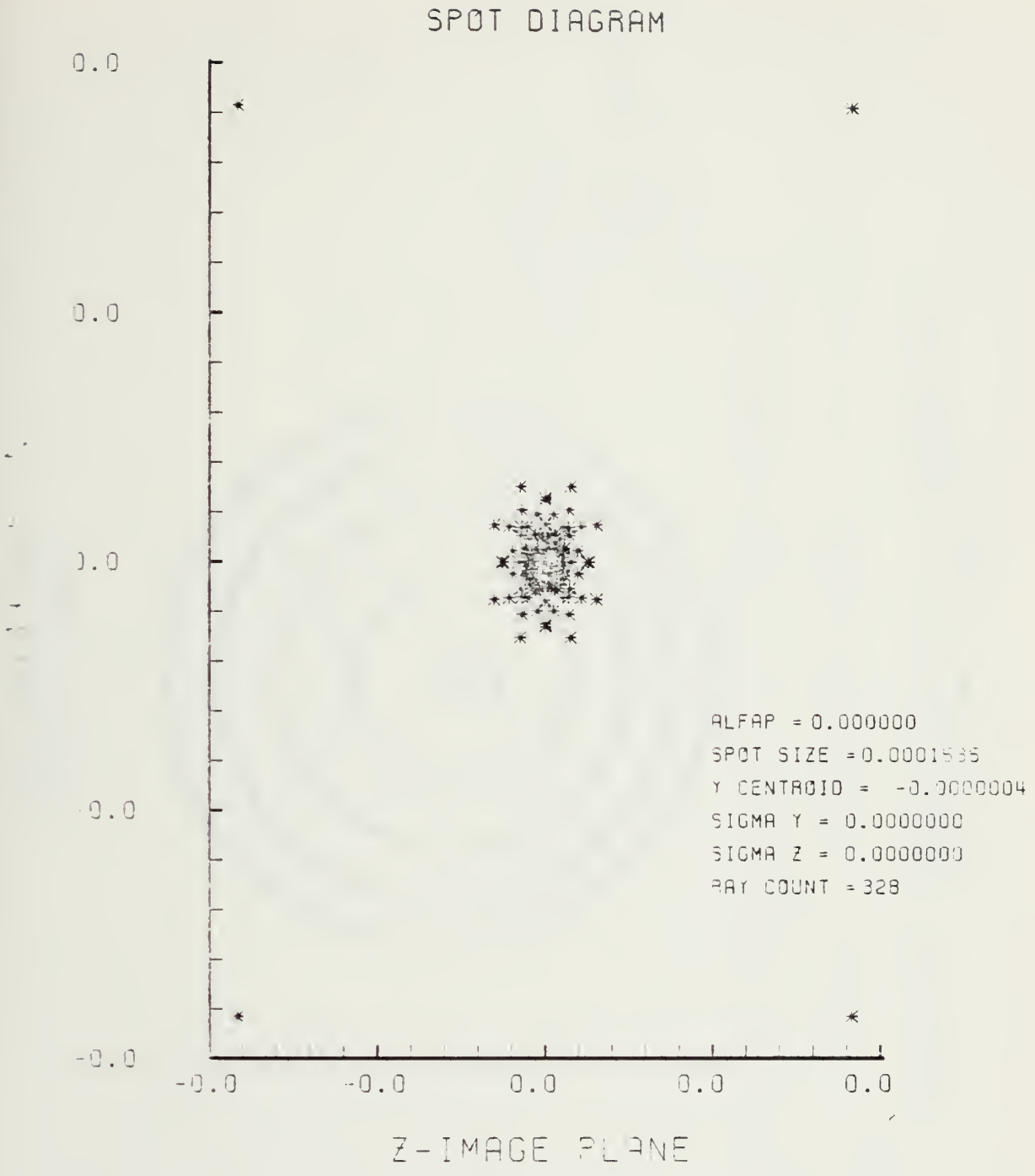

Figure D-2. Spot Diagram Corresponding to Object Plane of Figure D-1

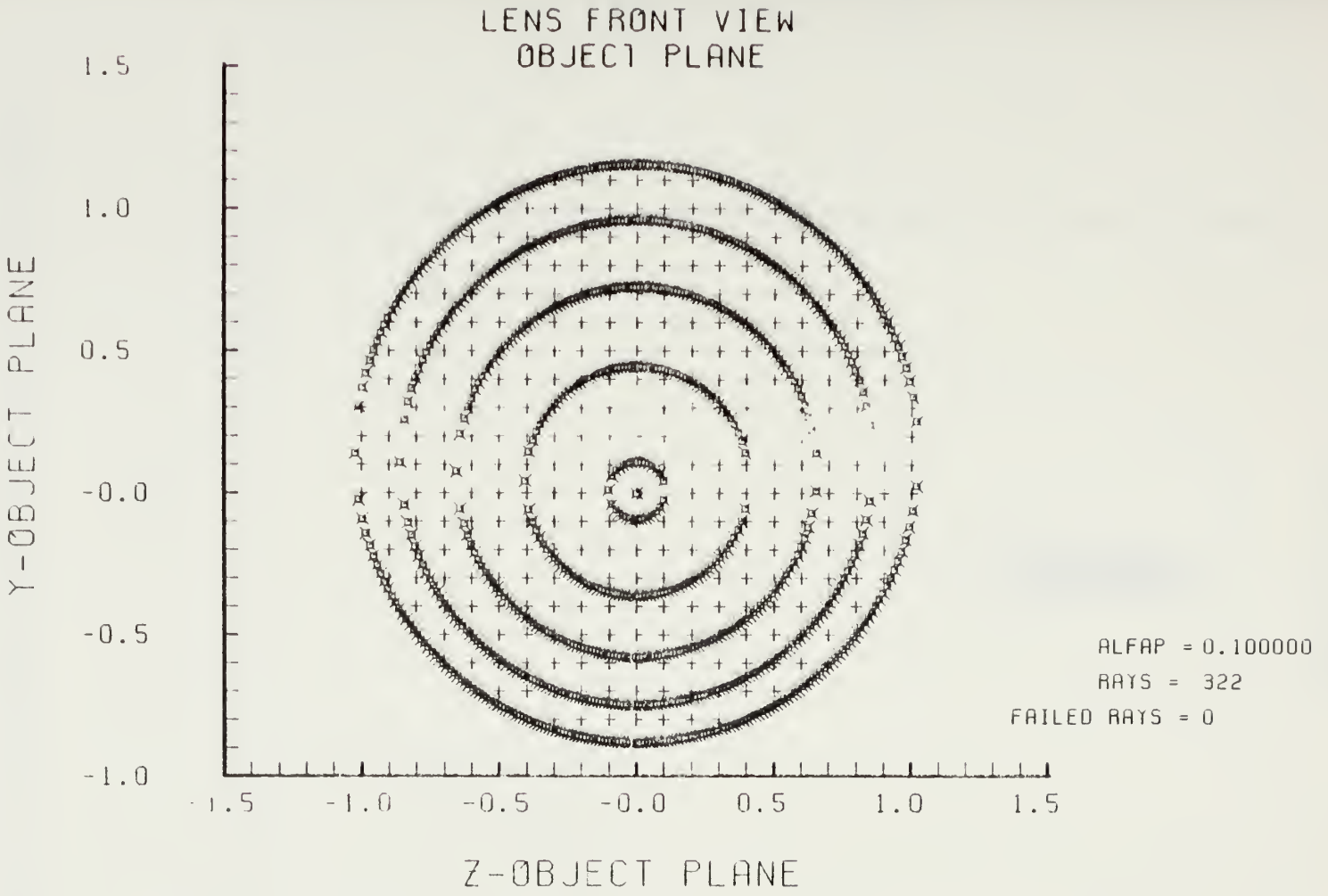

Figure D-3. Object Plane at α_p = 0.1 Radians for HIN Lens Shown in Figure 11

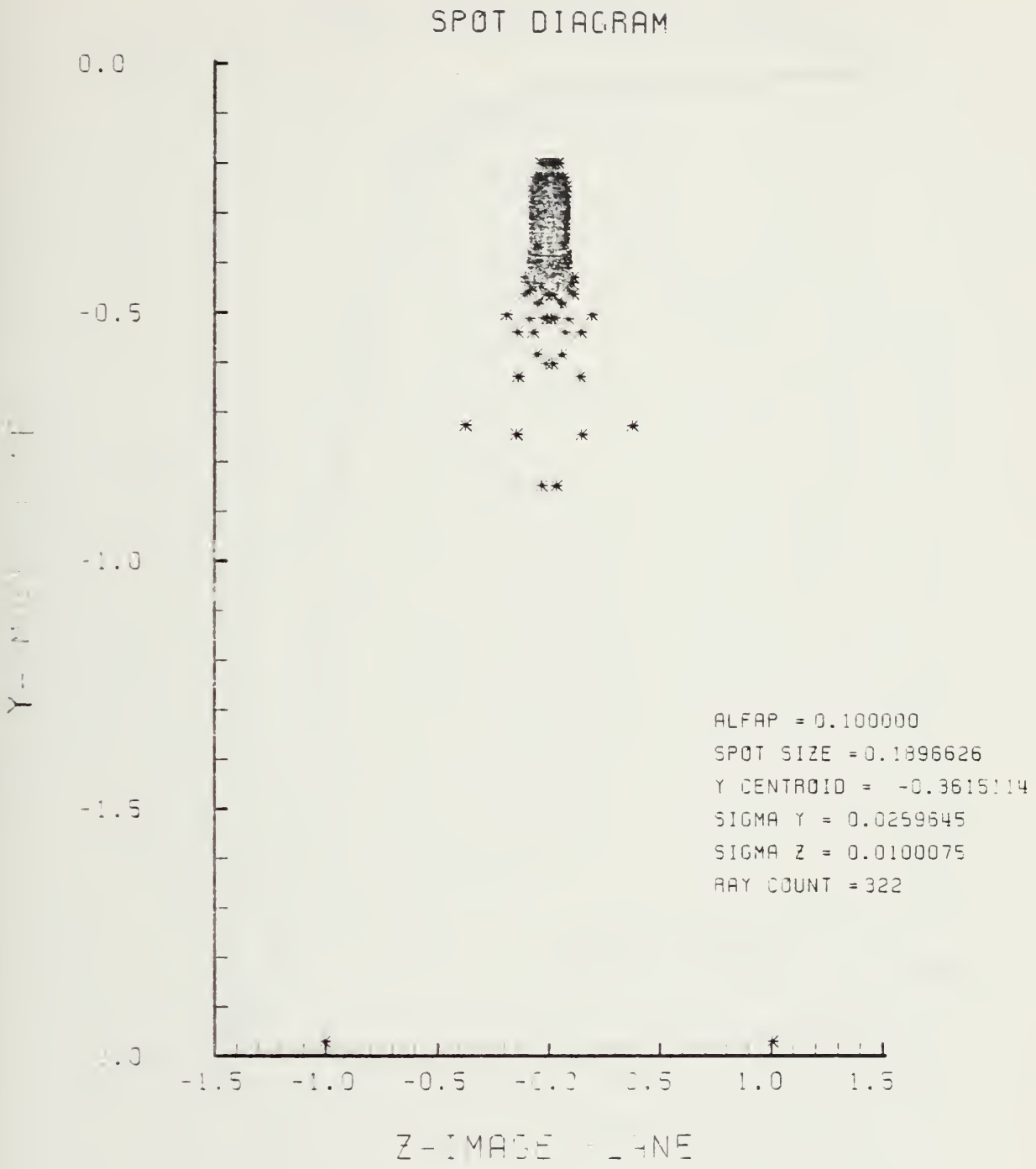

Figure D-4. Spot Diagram Corresponding to Figure D-3

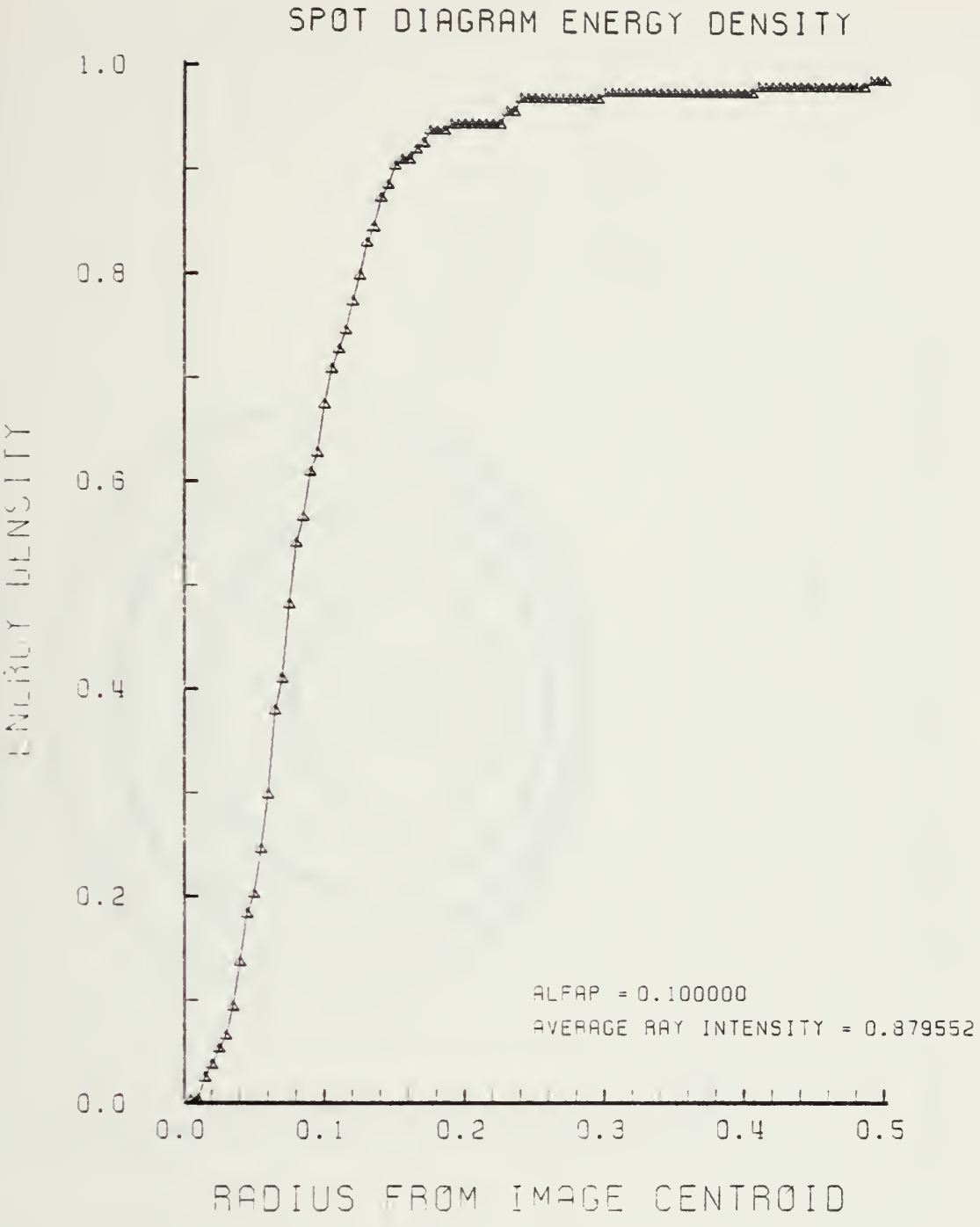

Figure D-5. Encircled Energy Plot for the Spot Diagram of Figure D-4

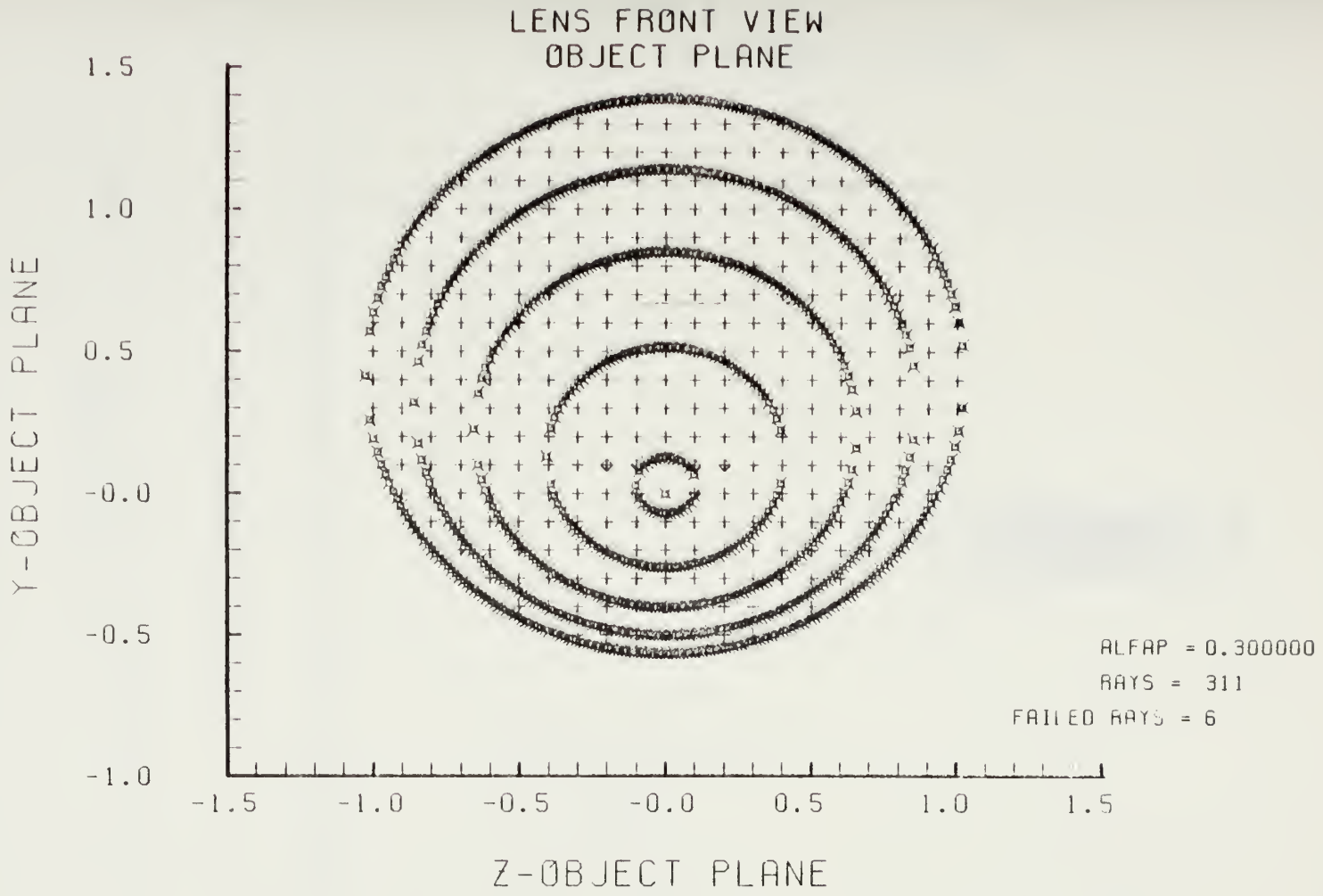

Figure D-6. HIN Object Plane at α_p = 0.2 Radians, N_2 = 1.5

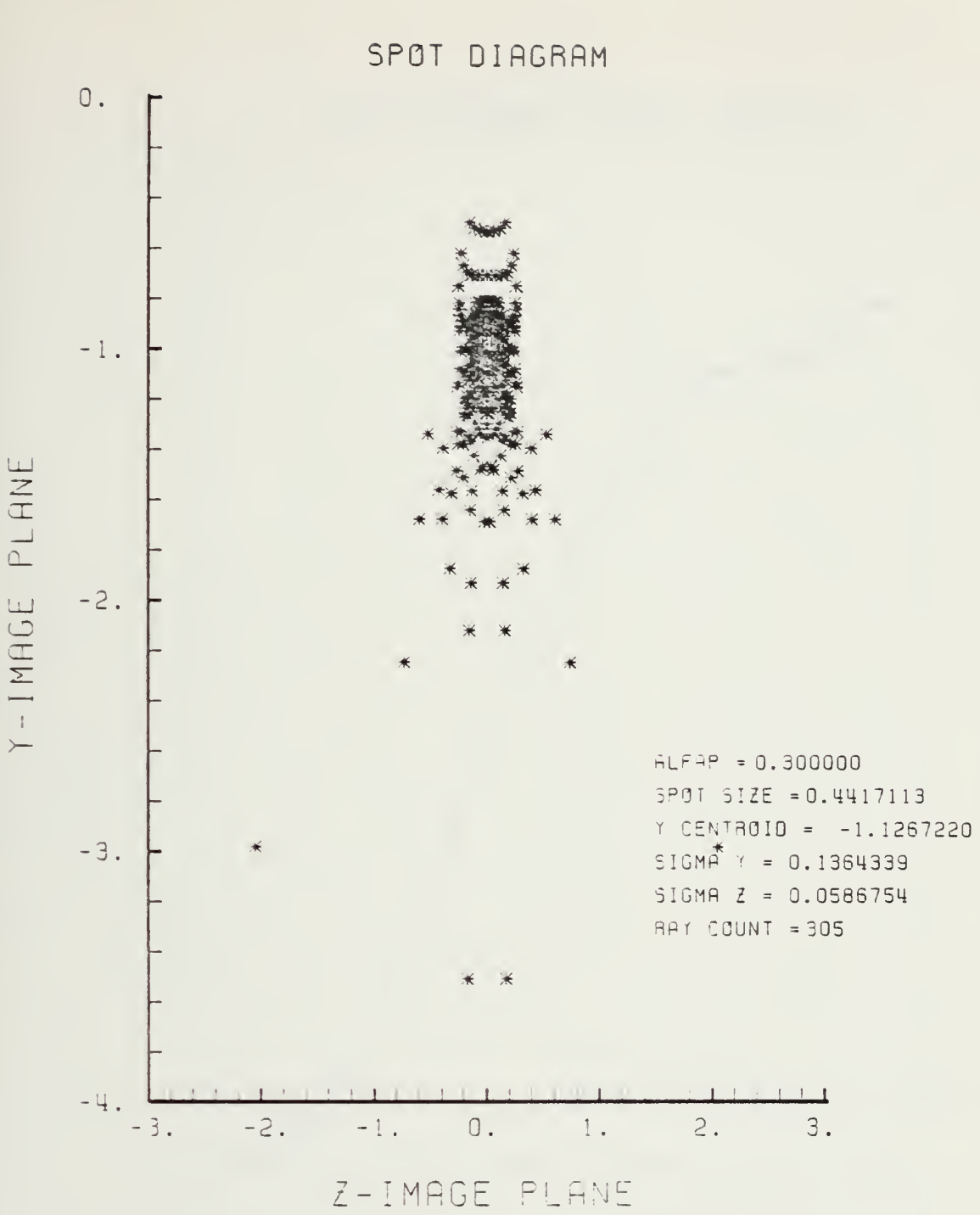

Figure D-7. Spot Diagram of HIN Lens at α_p = 0.2 Radians, N_2 = 1.5

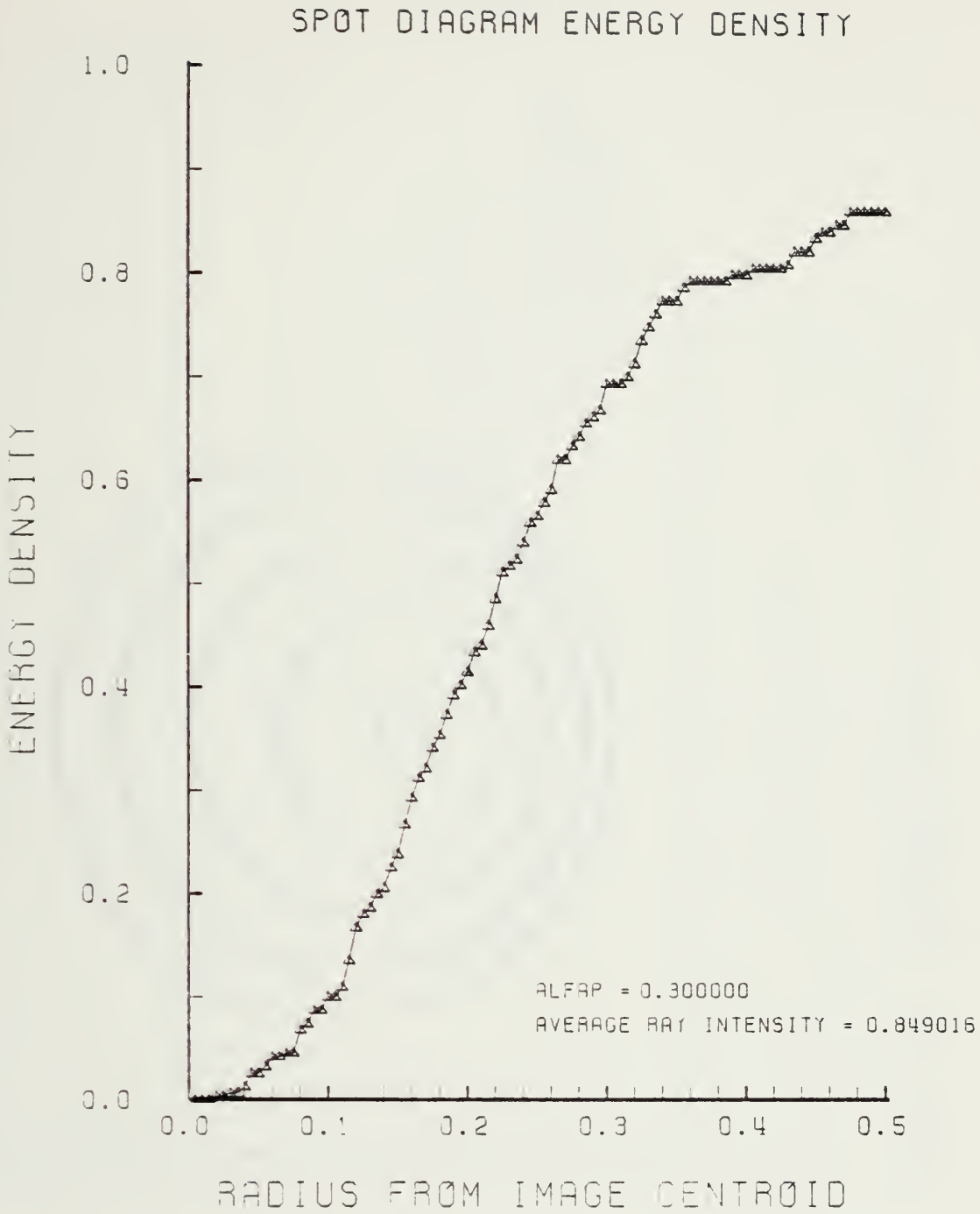

Figure D-8. Encircled Energy Plot of HIN Lens at α_p = 0.2 Radians, N_2 = 1.5

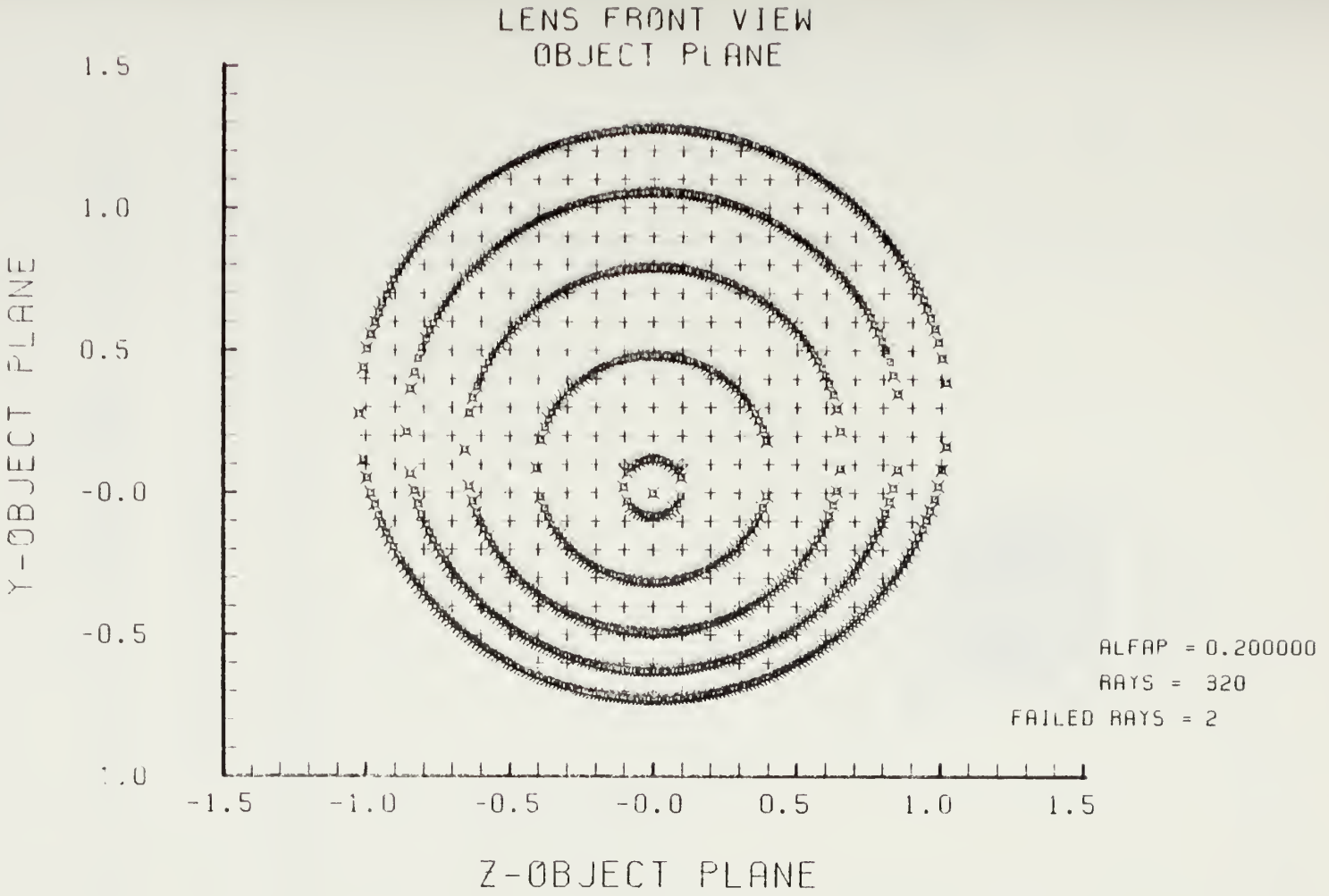

Figure D-9. HIN Object Plane at α_p = 0.3 Radians, N_2 = 1.5

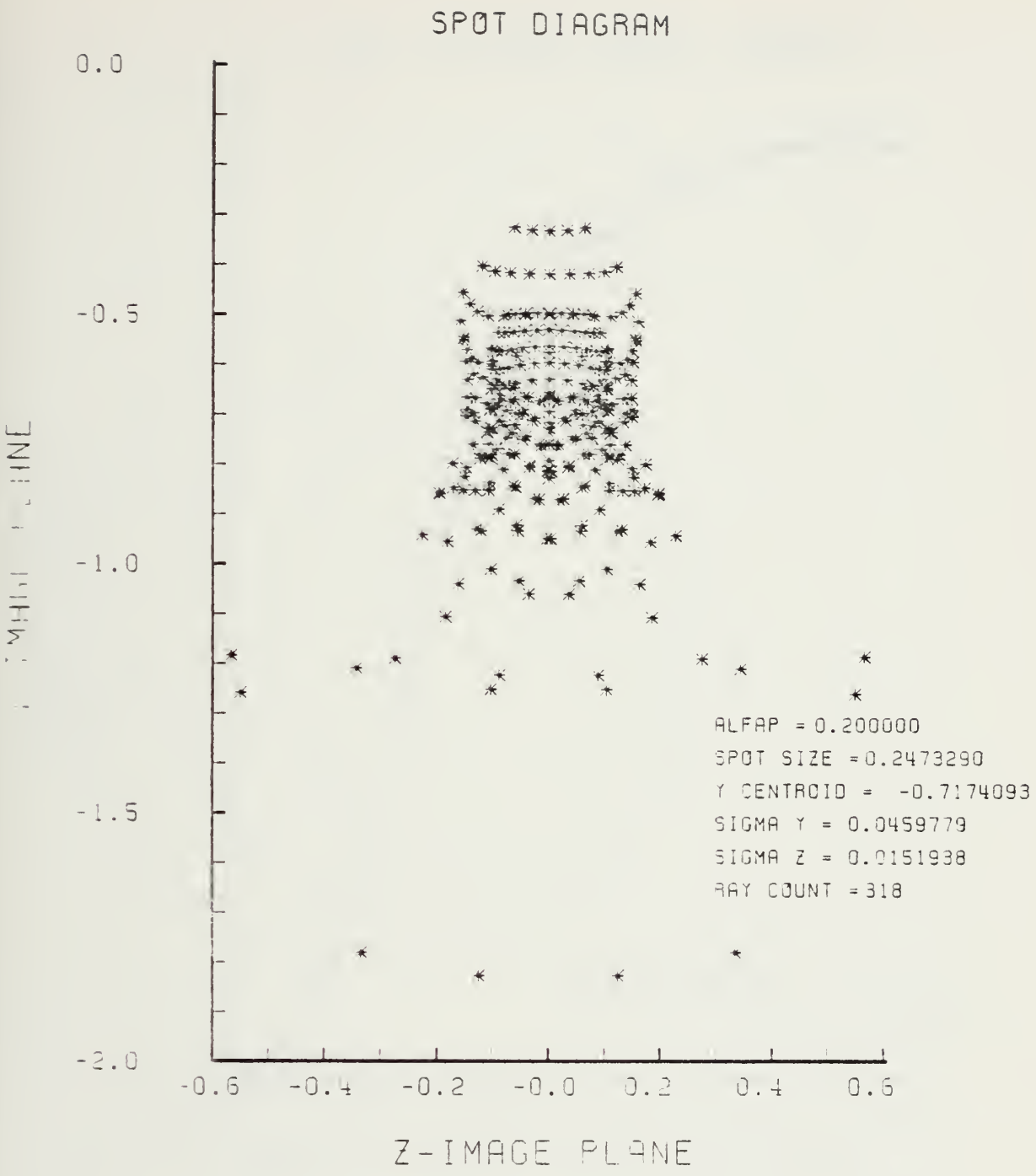

Figure D-10. Spot Diagram of HIN Lens at α_p = 0.3 Radians, N_2 = 1.5

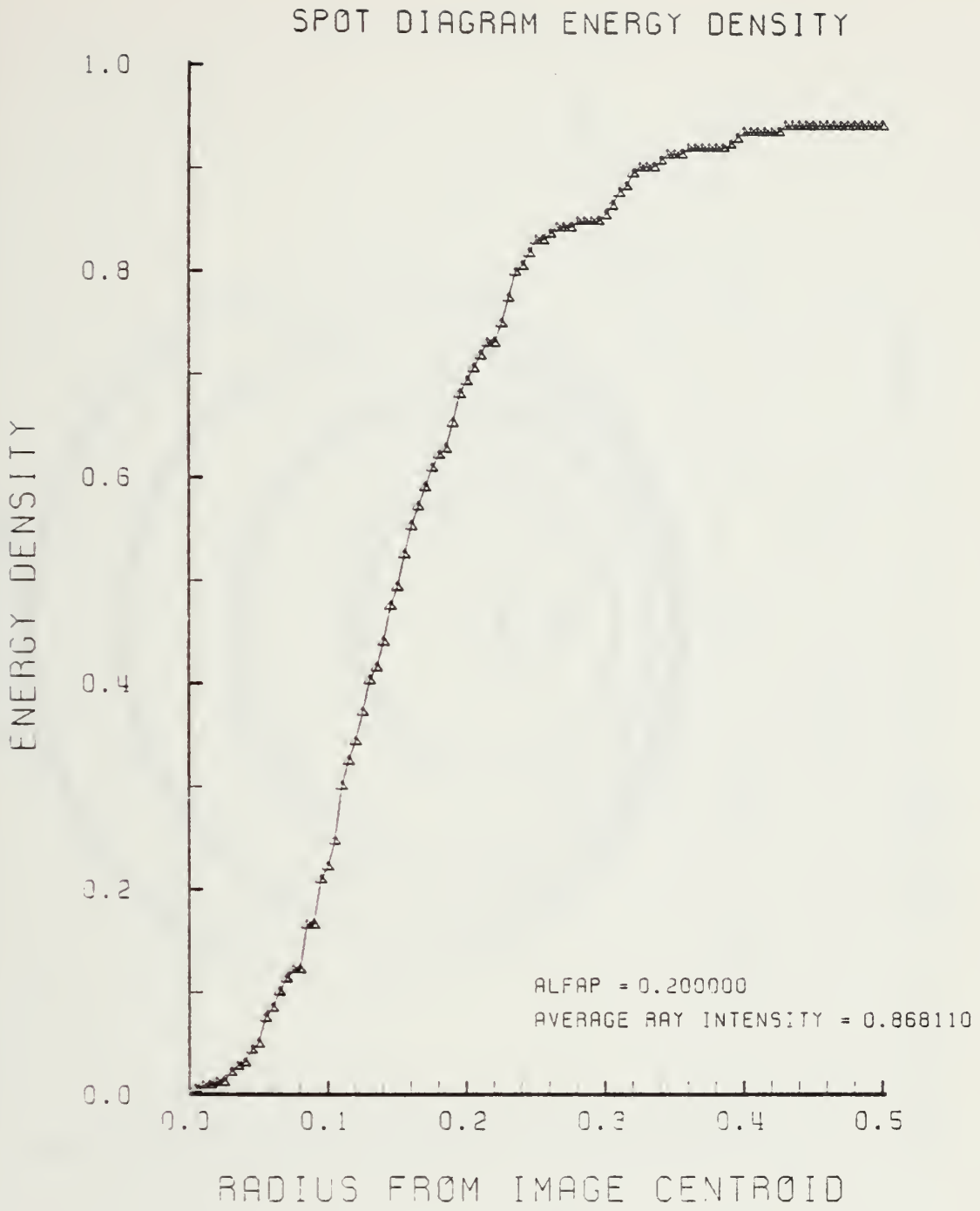

Figure D-11. HIN Lens Encircled Energy at α_p = 0.3 Radians, N_2 = 1.5

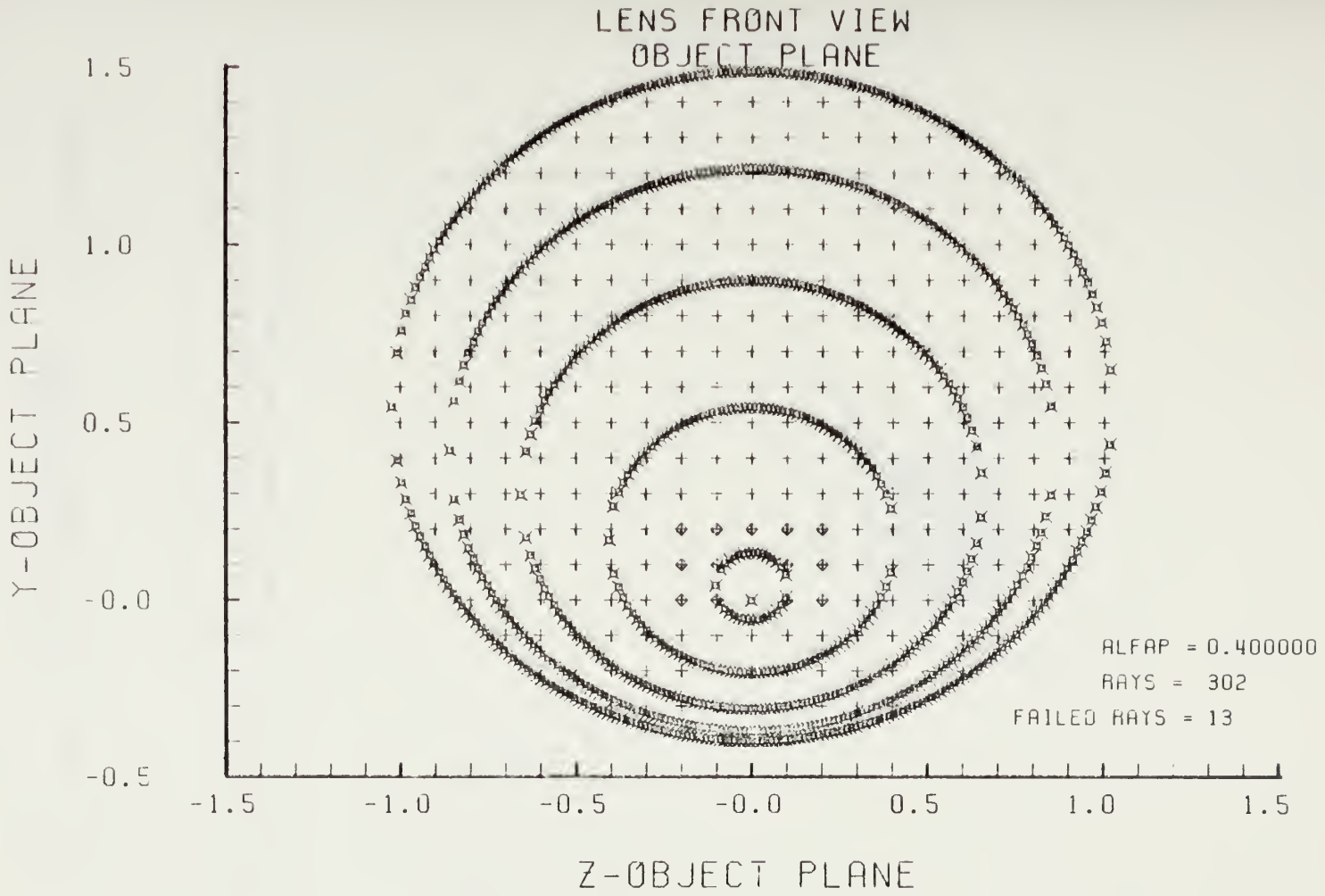

Figure D-12. HIN Object Plane at α_p = 0.4 Radians, N_2 = 1.5

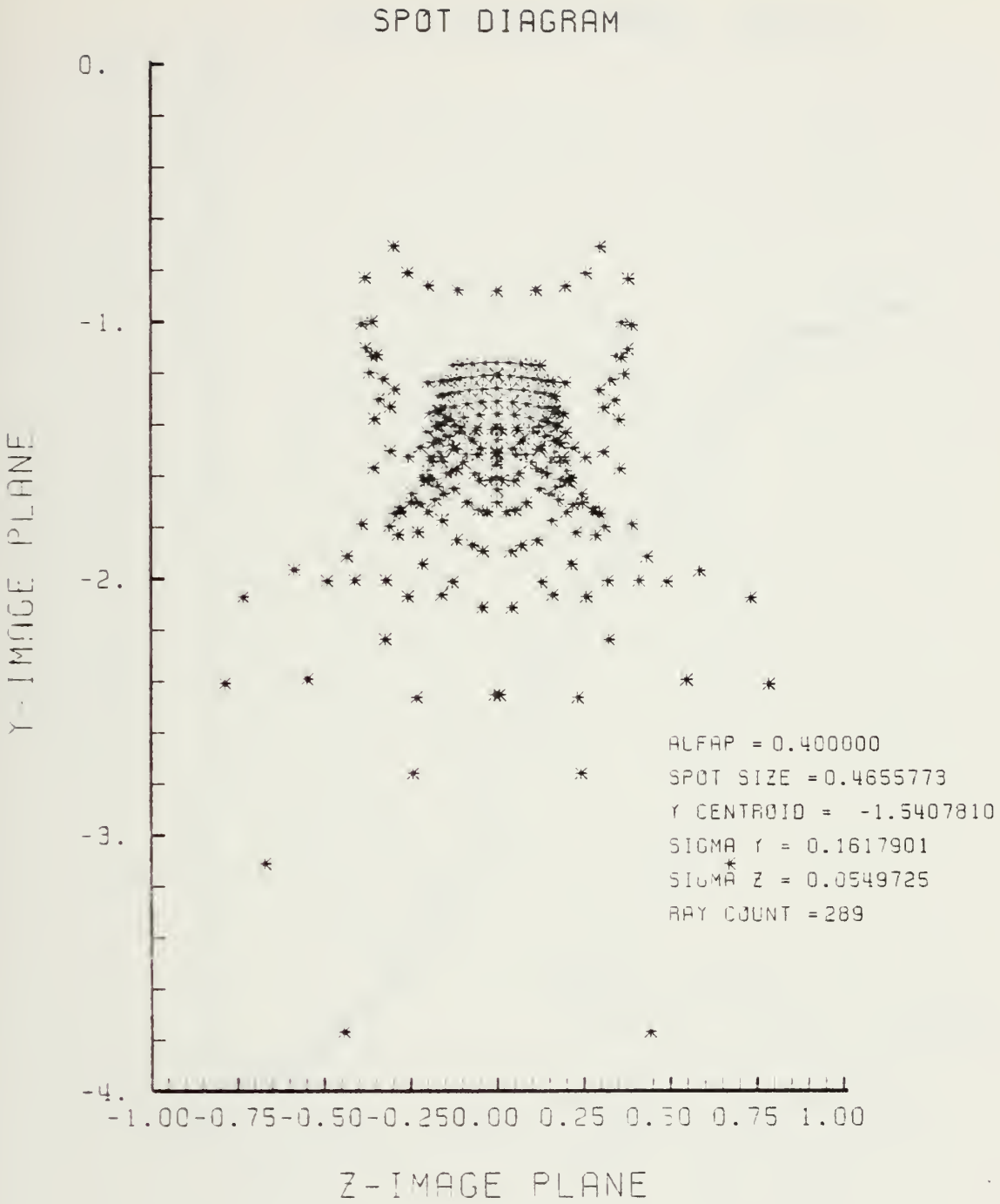

Figure D-13. Spot Diagram of HIN lens at α_p = 0.4 Radians, N_2 = 1.5

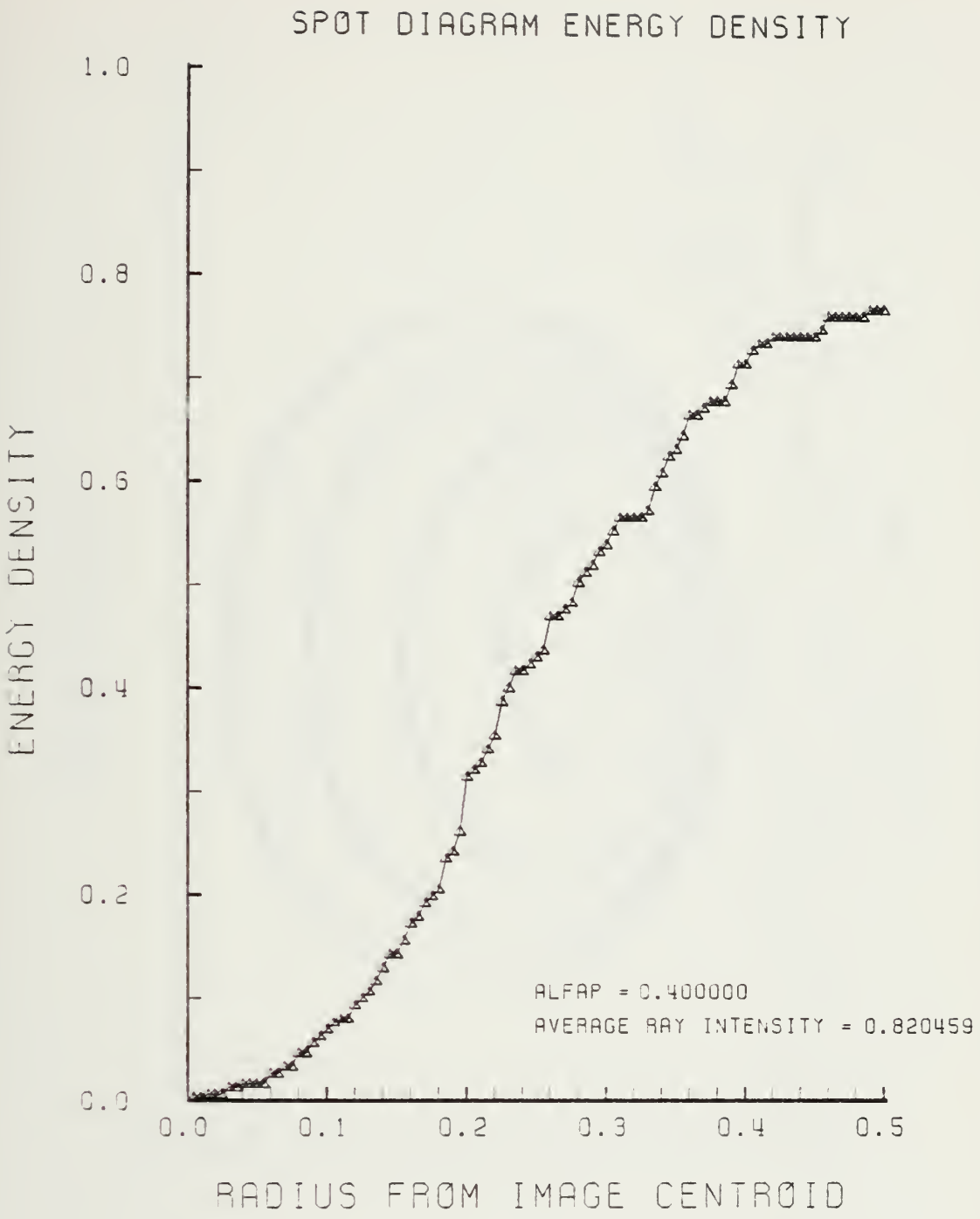

Figure D-14. Encircled Energy Plot at $\alpha_p = 0.4$ Radians, $N_2 = 1.5$

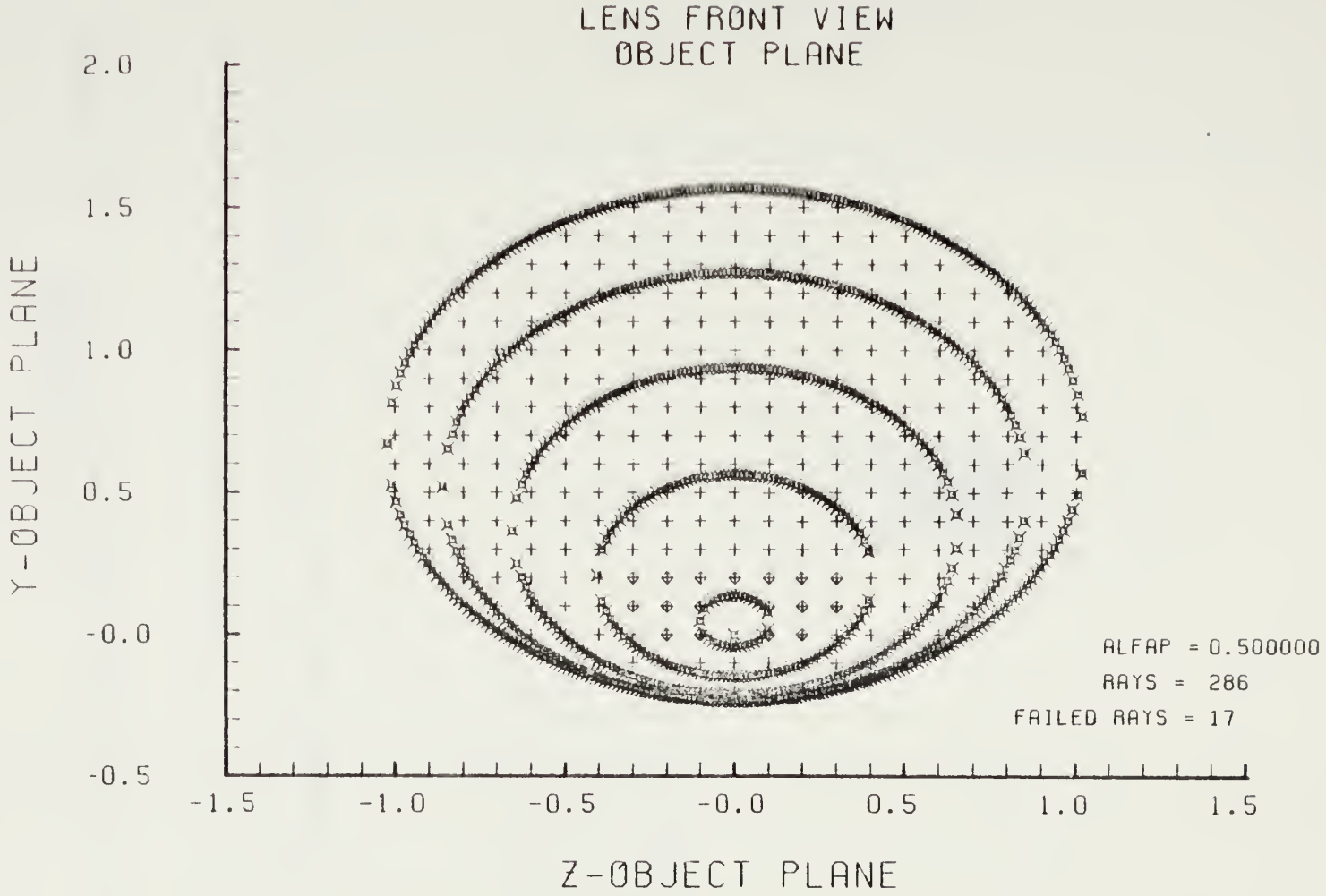

Figure D-15. HIN Lens Object Plane at α_p = 0.5 Radians, N_2 = 1.5

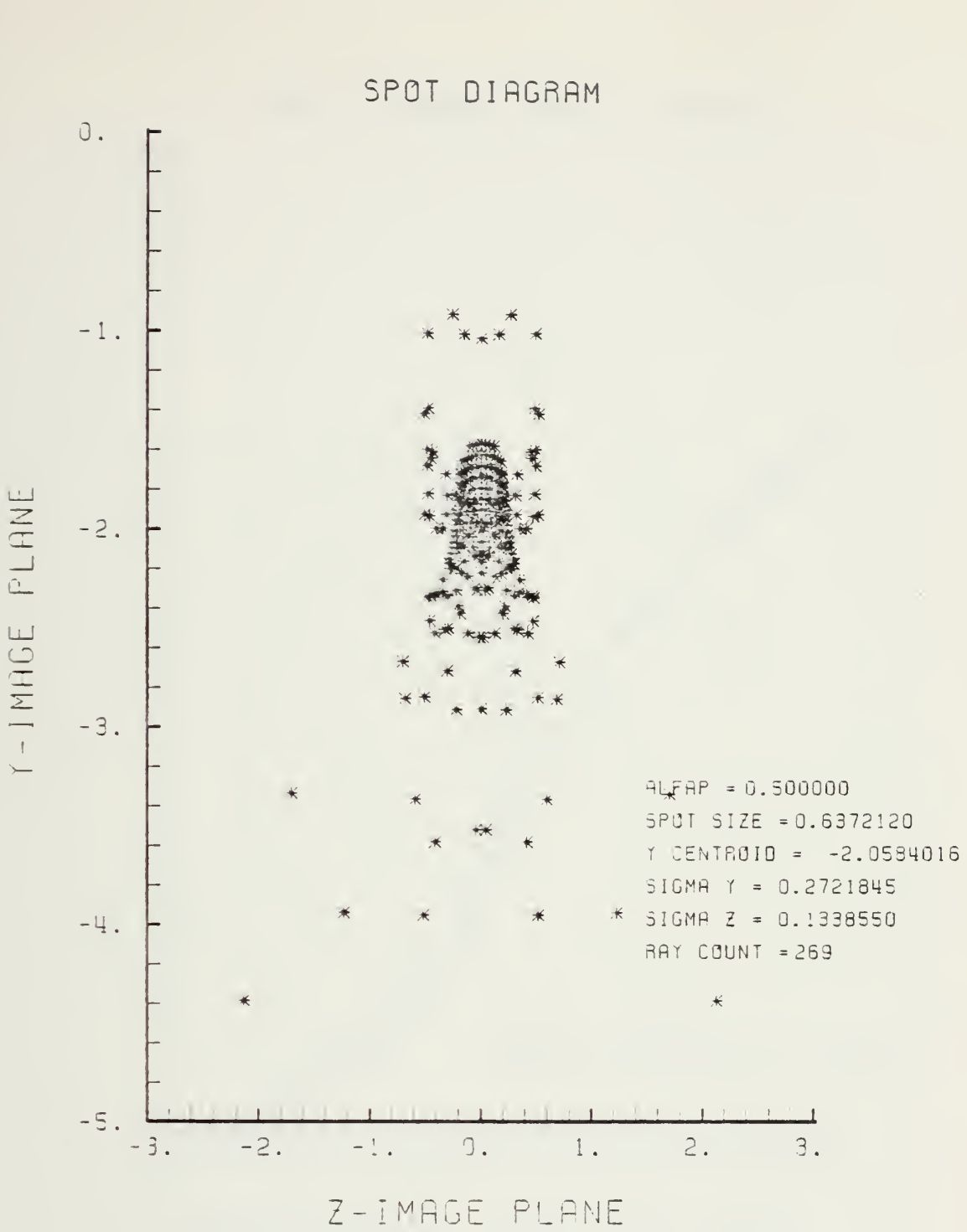

Figure D-16. Spot Diagram of HIN Lens at α_p = 0.5 Radians, N_2 = 1.5

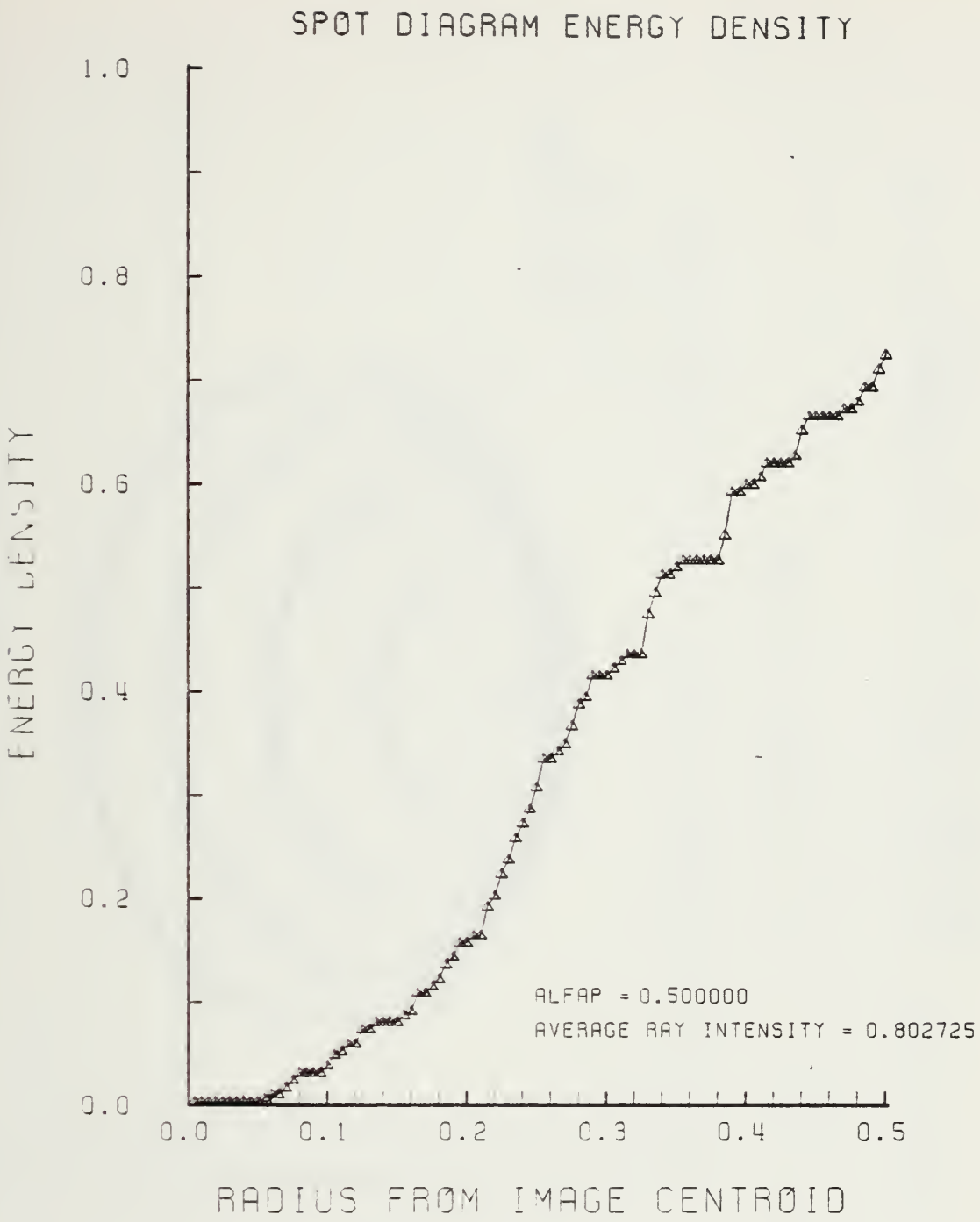

Figure D-17. Encircled Energy Plot at α_p = 0.5 Radians, N_2 = 1.5

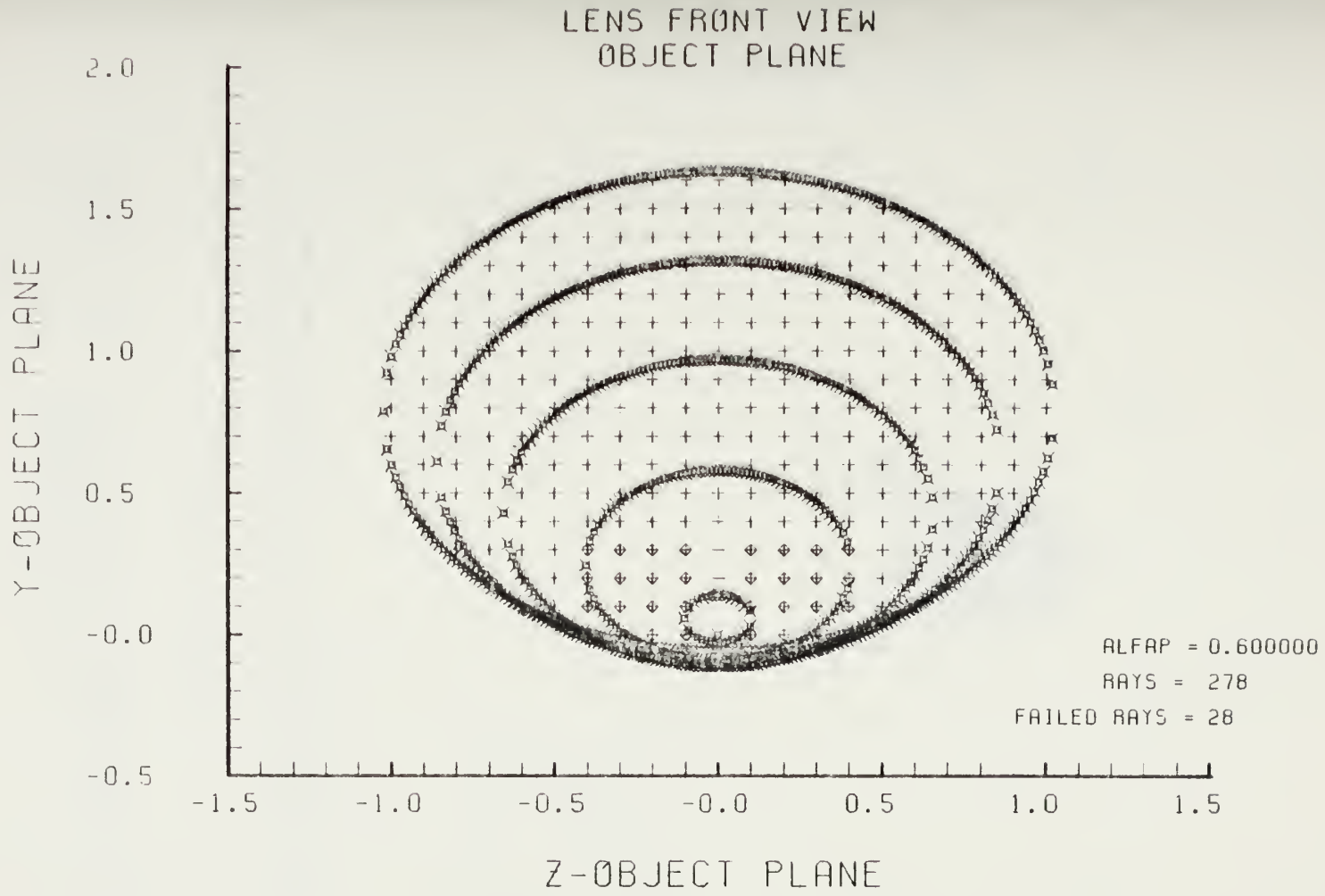

Figure D-18. HIN Object Plane at α_p = 0.6 Radians, N_2 = 1.5. Overlapping Portions of Inner Ellipses are hidden lines.

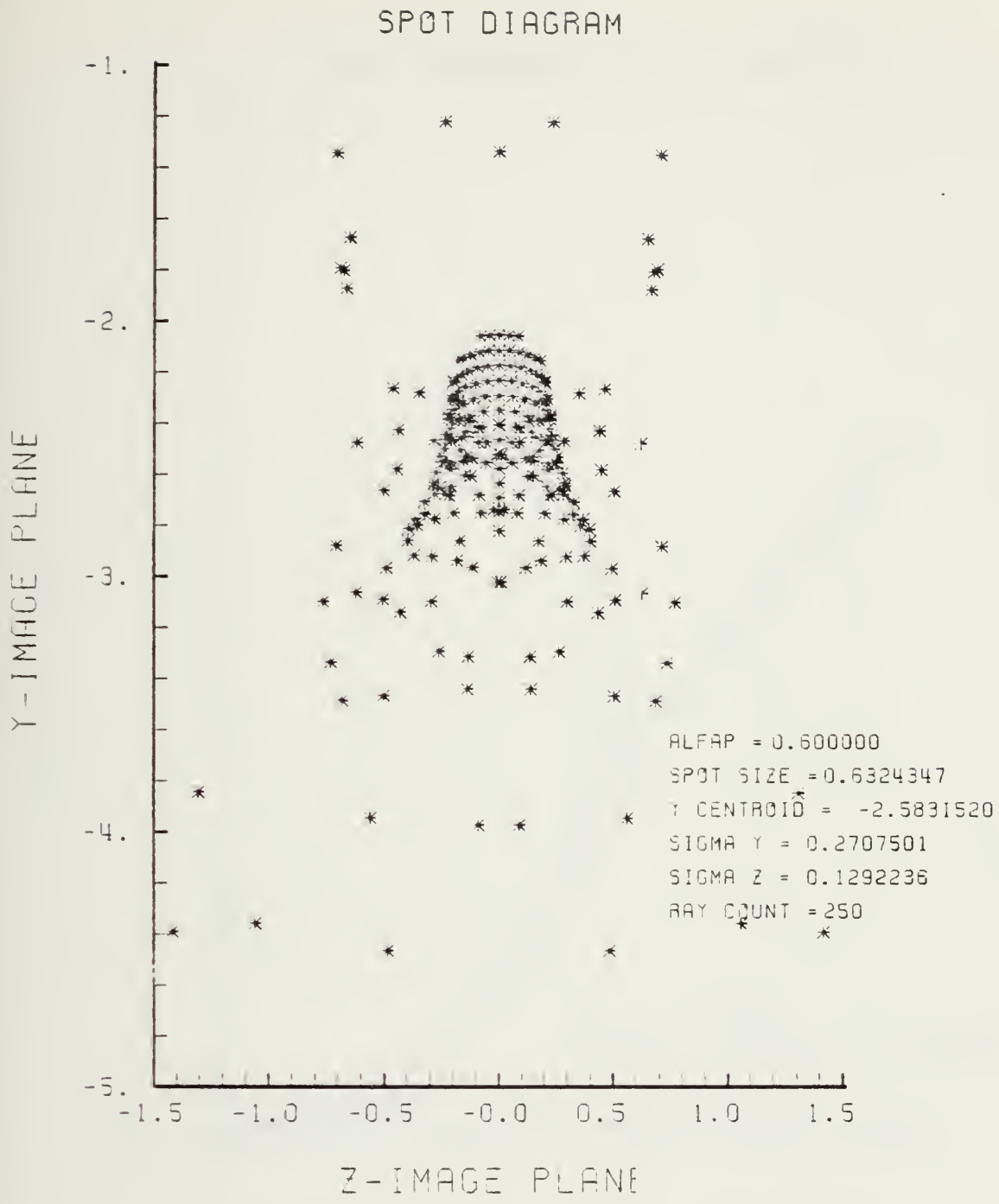

Figure D-19. Spot Diagram of HIN Lens at α_p = 0.6 Radians, N_2 = 1.5

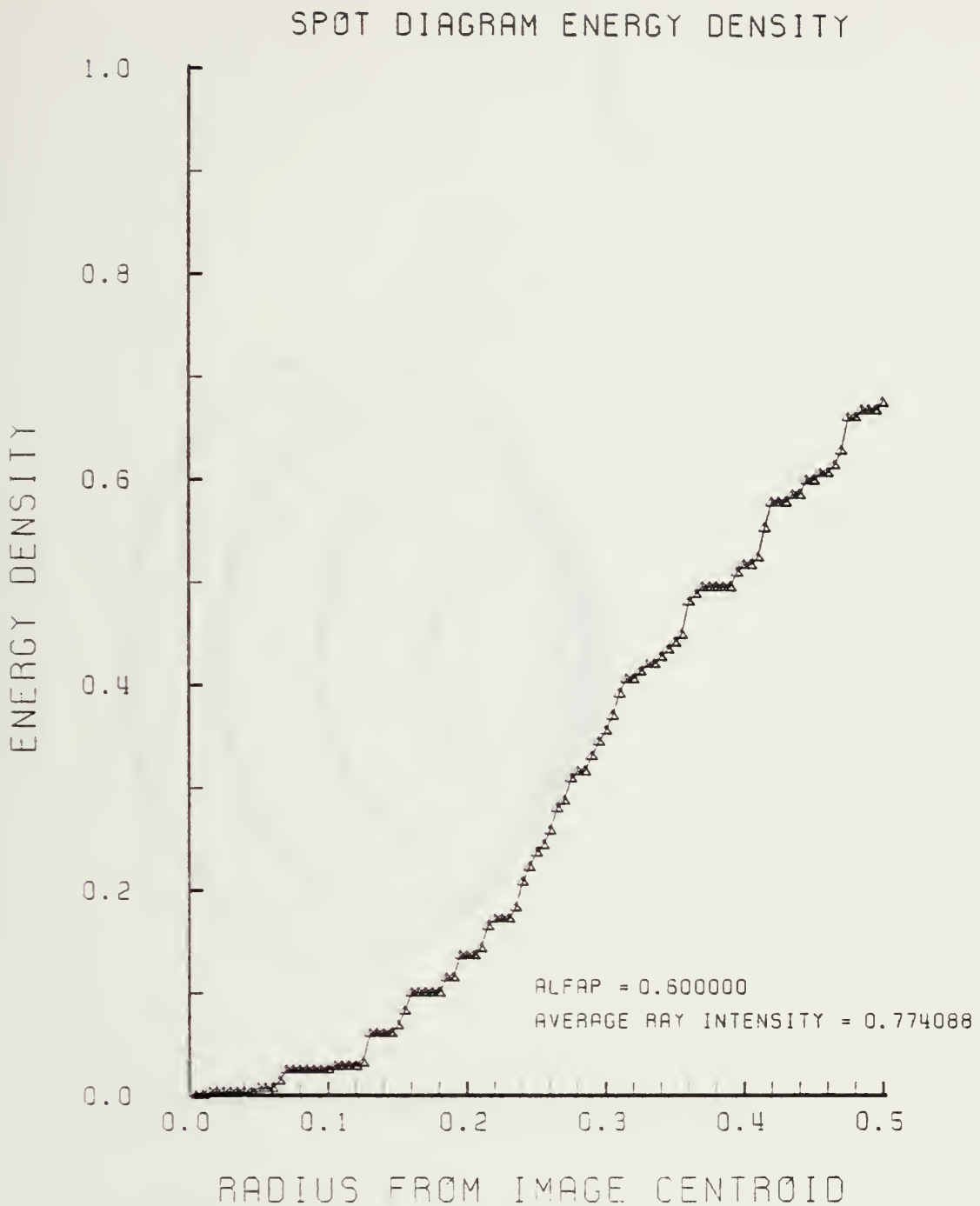

Figure D-20. Encircled Energy Plot at α_p = 0.6 Radians, N_2 = 1.5

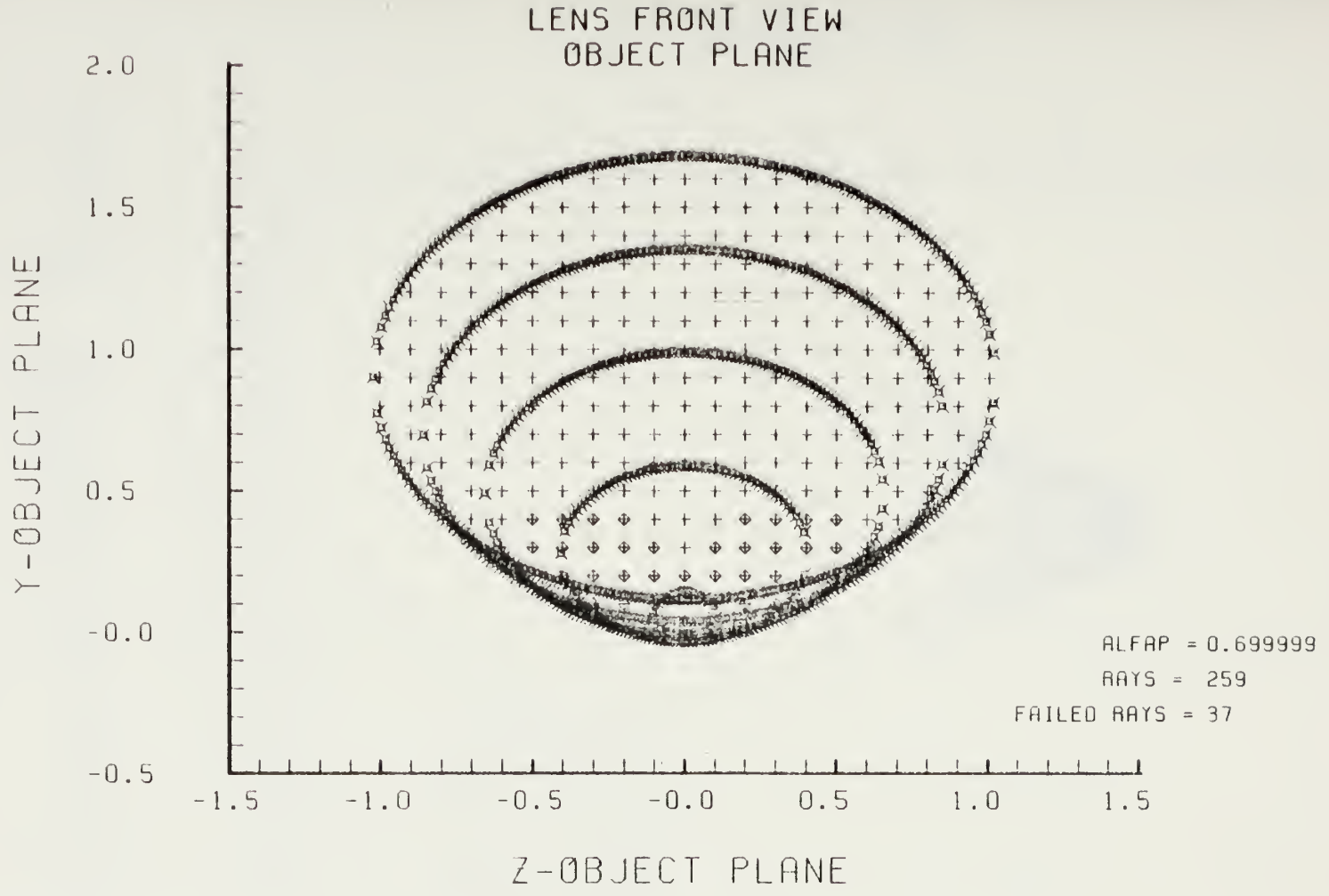

Figure D-21. HIN Object Plane at α_p = 0.7 Radians, N_2 = 1.5. Overlapping Portions of Inner Ellipses are Hidden Lines.

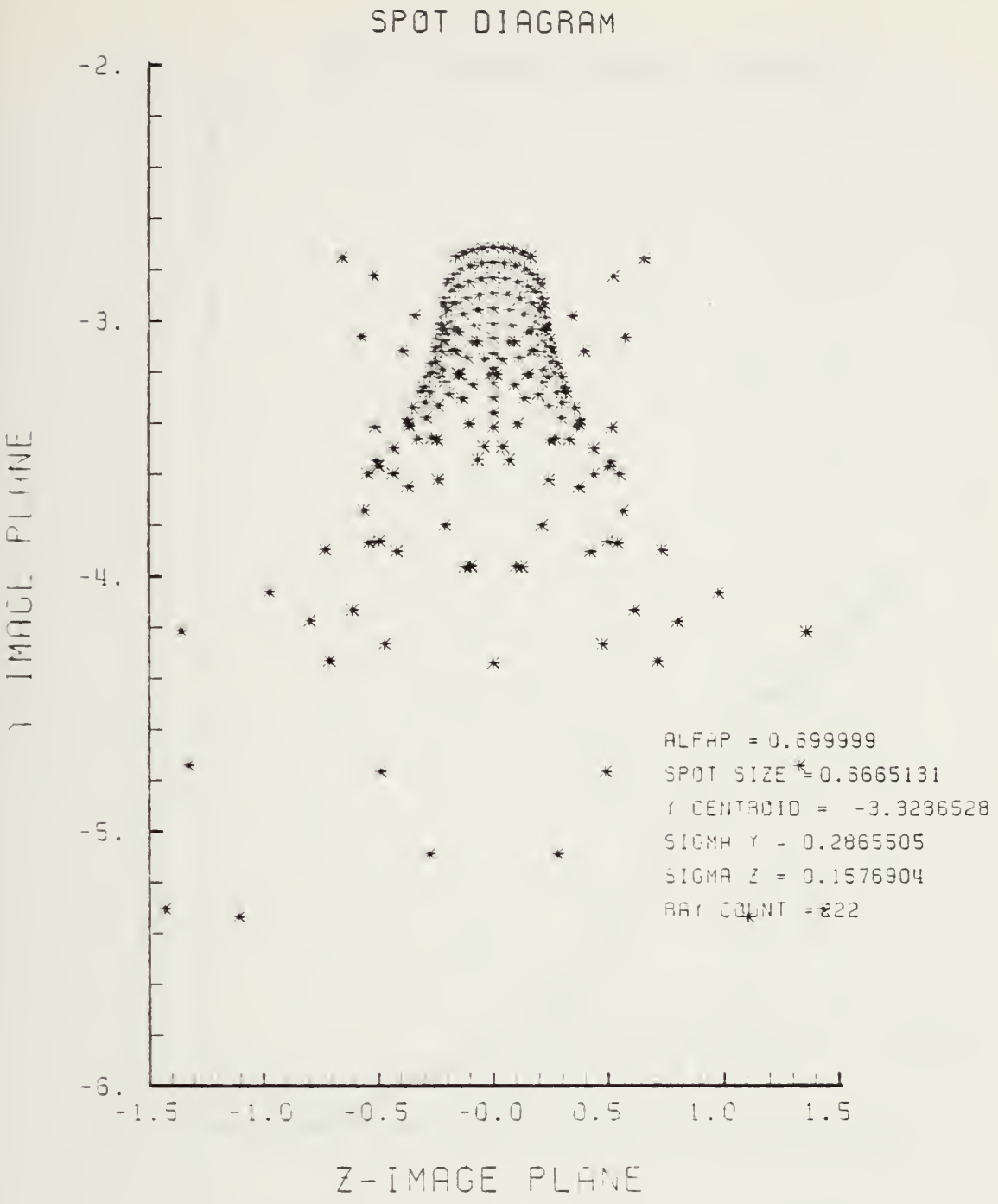

Figure D-22. Spot Diagram of HIN Lens at α_p = 0.7 Radians, N_2 = 1.5

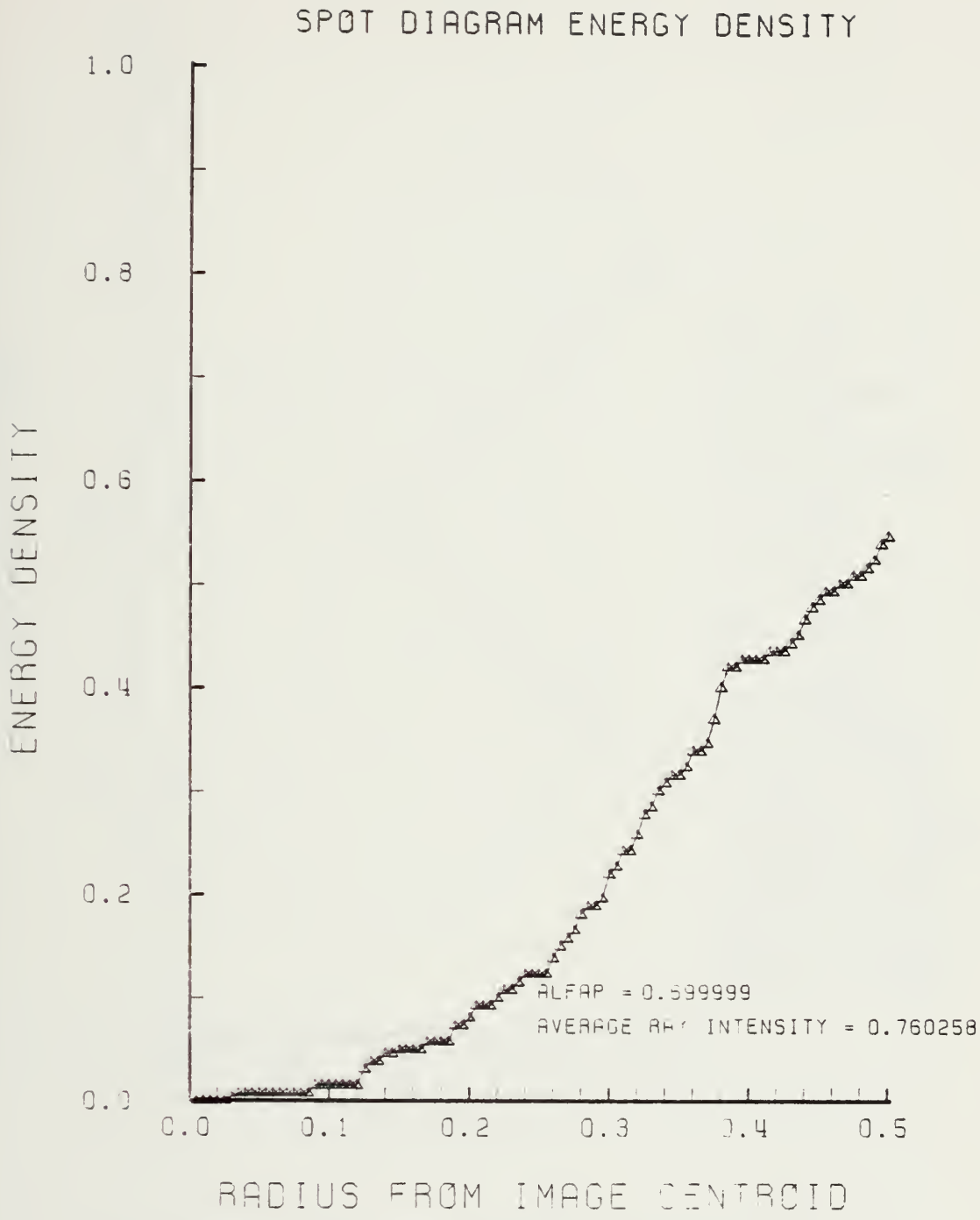

Figure D-23. Encircled Energy Plot at α_p = 0.7 Radians, N_2 = 1.5

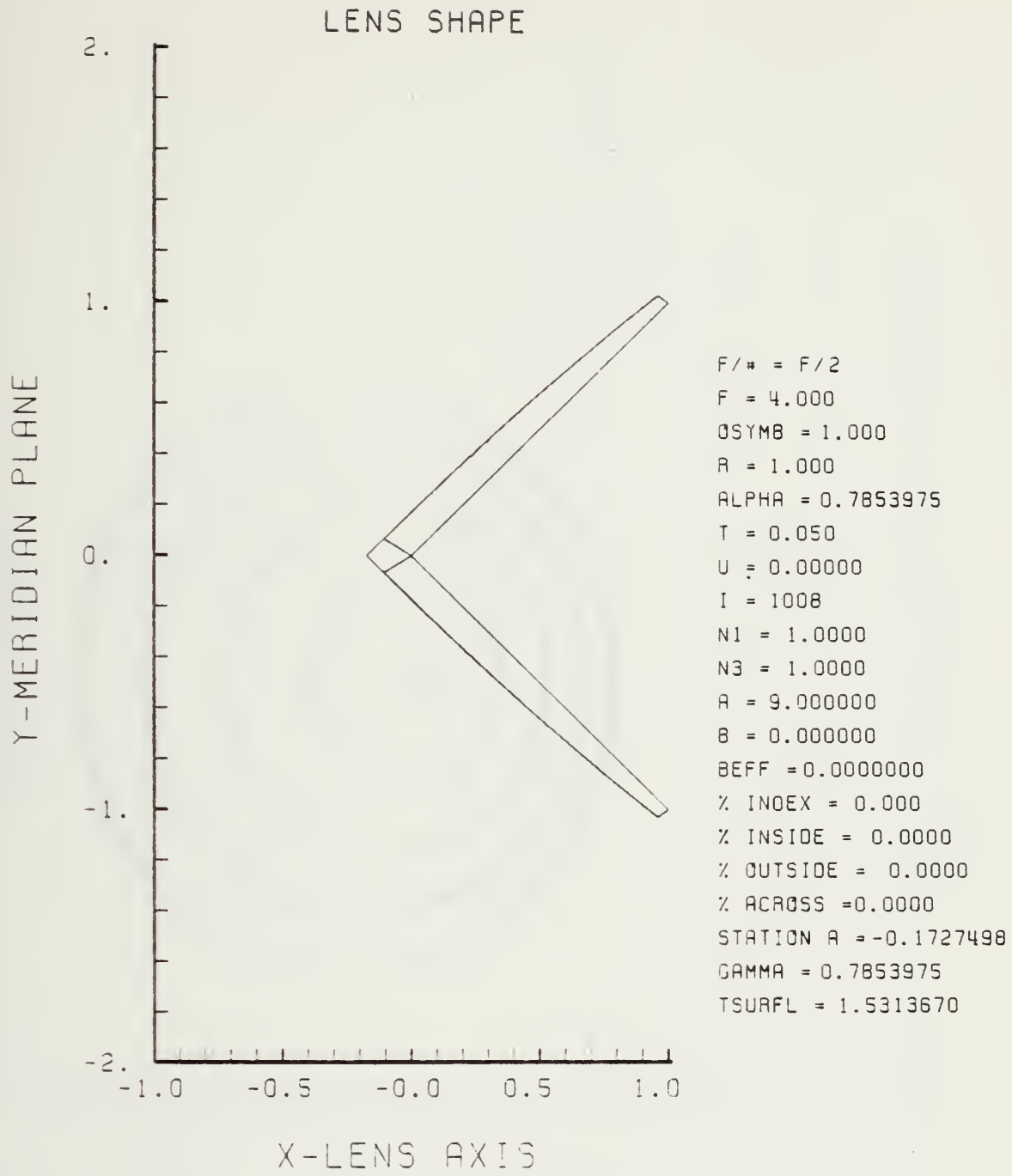

Figure D-24. HIN Lens Design for N_2 = 3.0

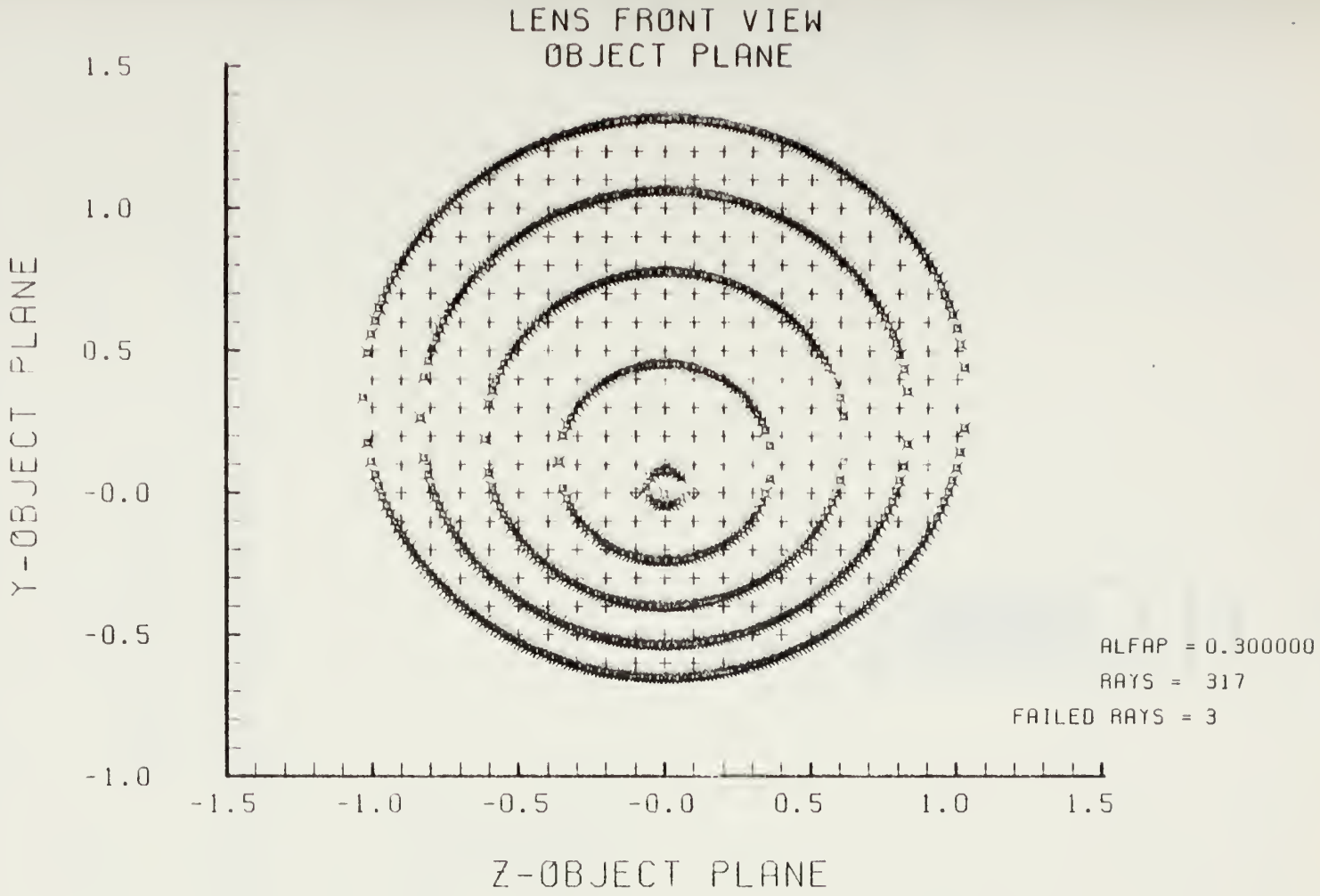

Figure D-25. Object Plane of HIN Lens in Figure D-24 at α_p = 0.3 Radians

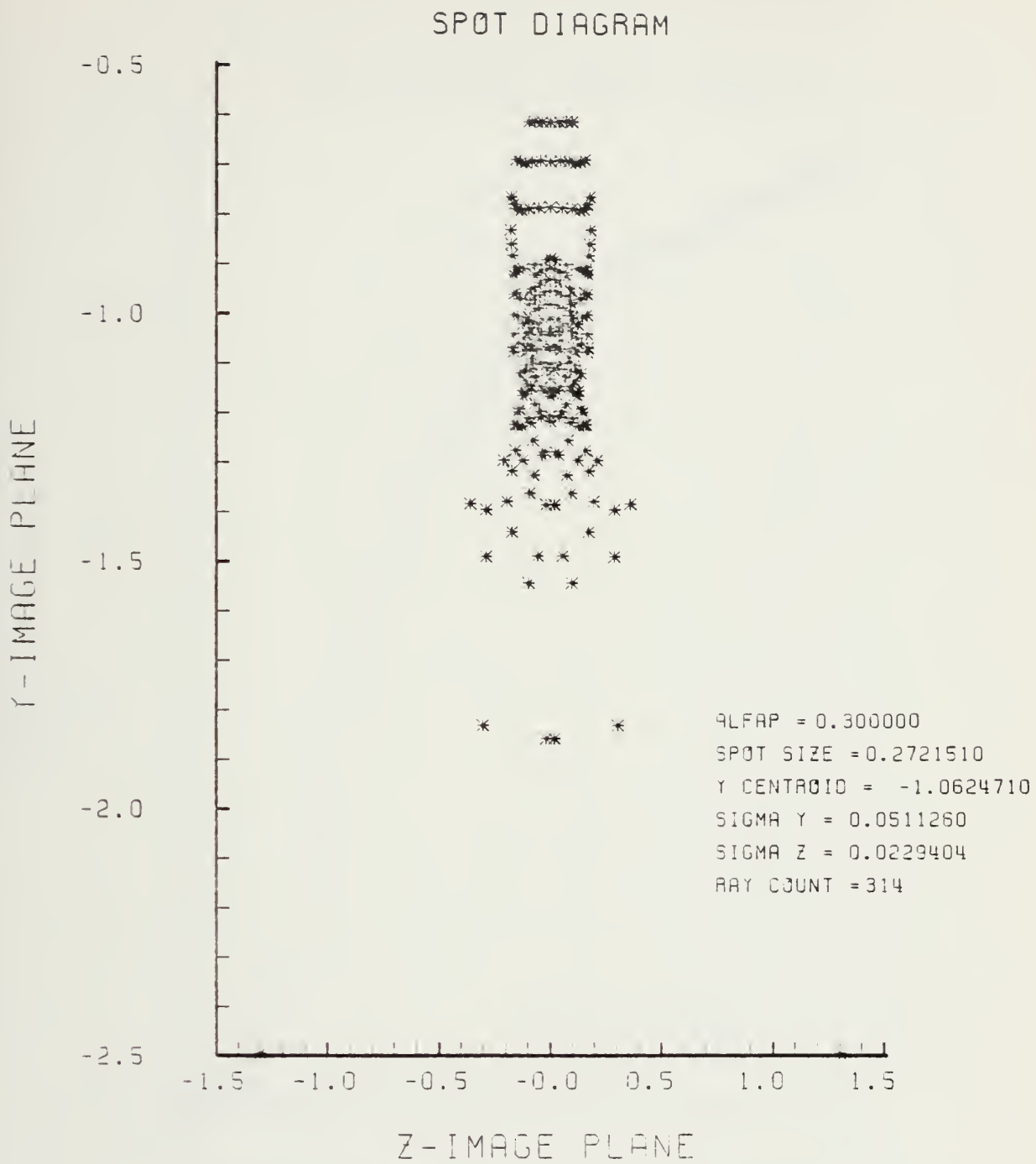

Figure D-26. Spot Diagram Corresponding to Figure D-25

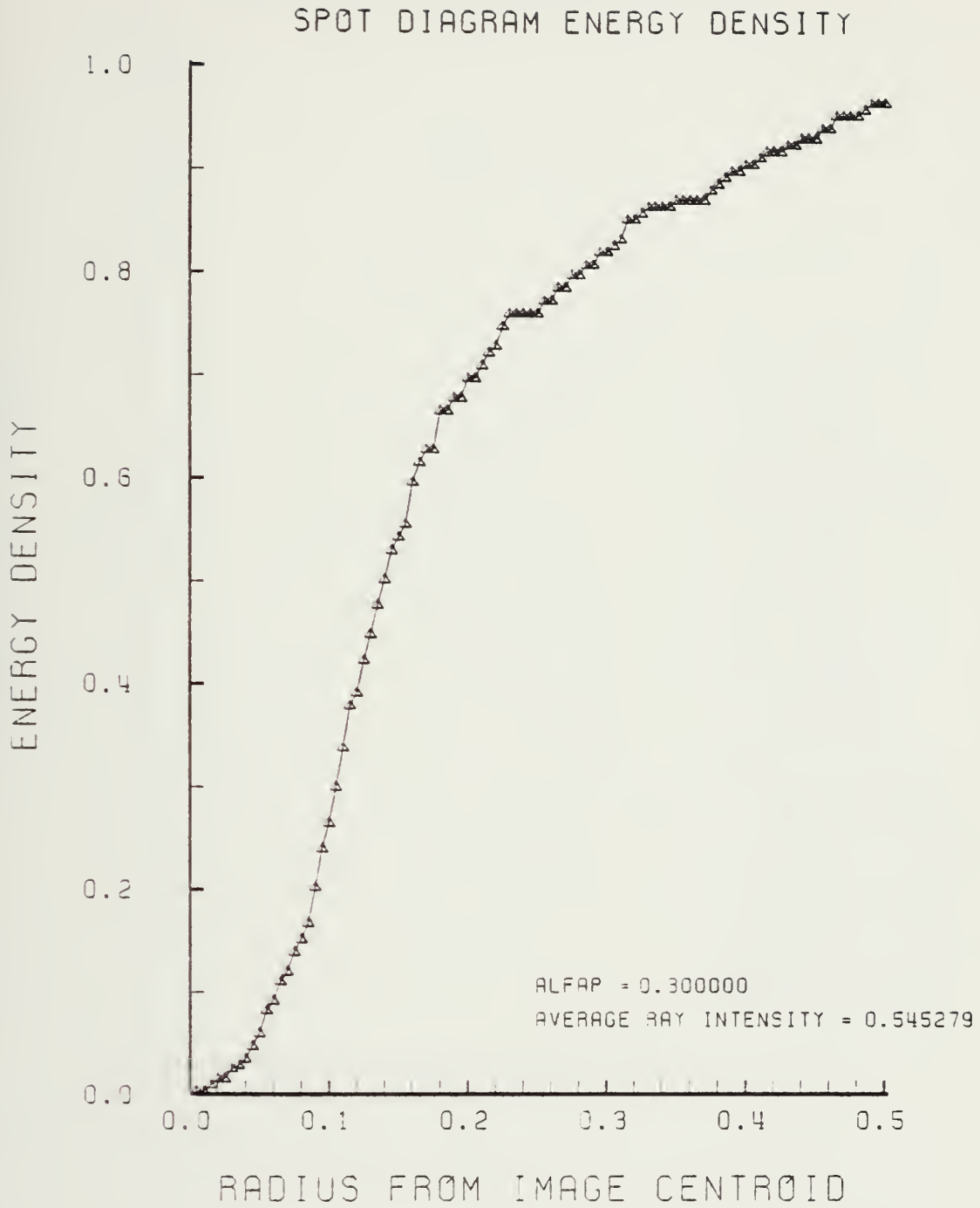

Figure D-27. Encircled Energy Plot for Spot Diagram of Figure D-26

APPENDIX E

GRIN LENS PERFORMANCE PLOTS IN THE LOW RANGE OF INDICES OF REFRACTION (a = 2.25)

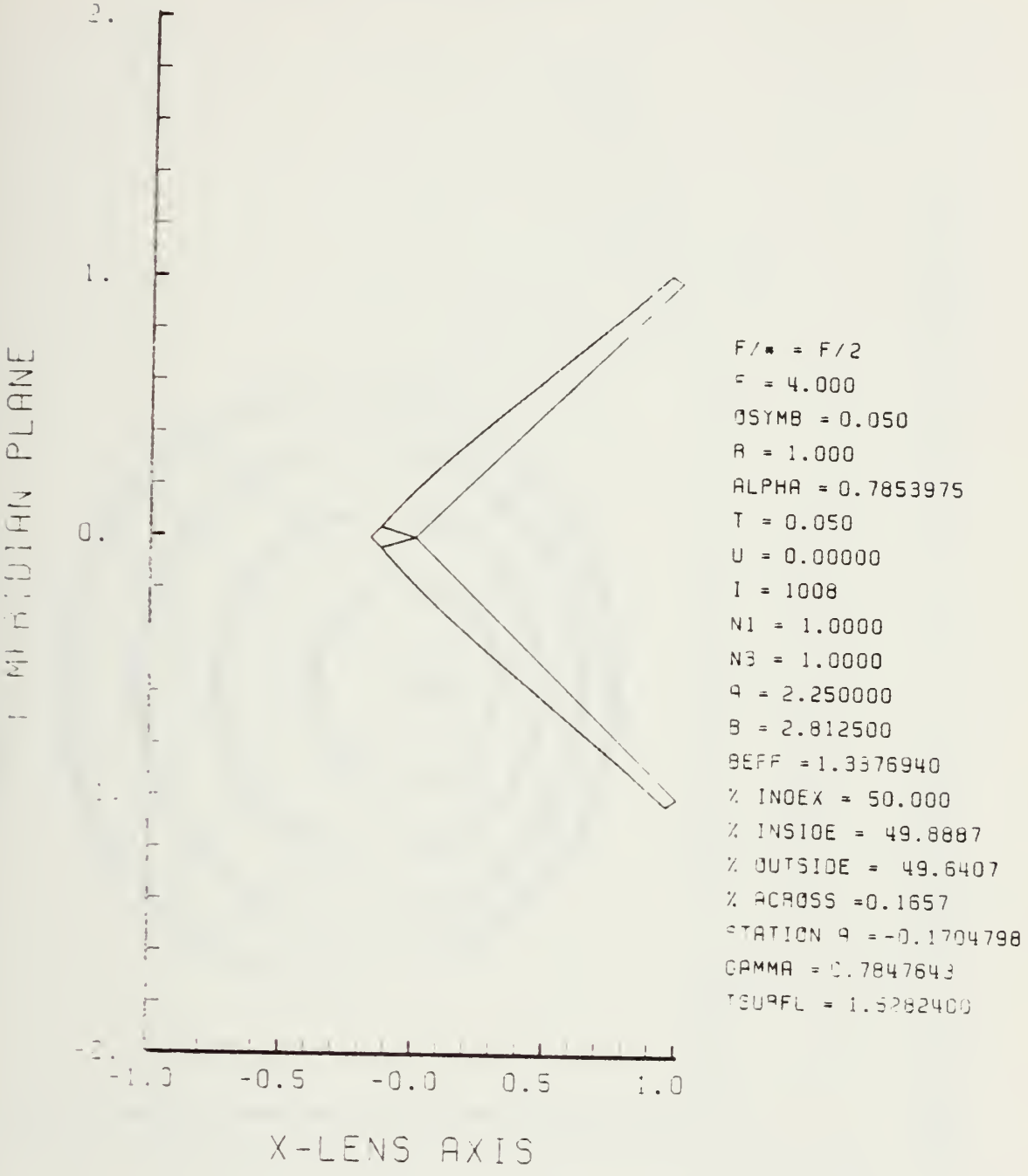

Figure E-1. GRIN Lens Shape at +50%, OB = 0.05, a = 2.25

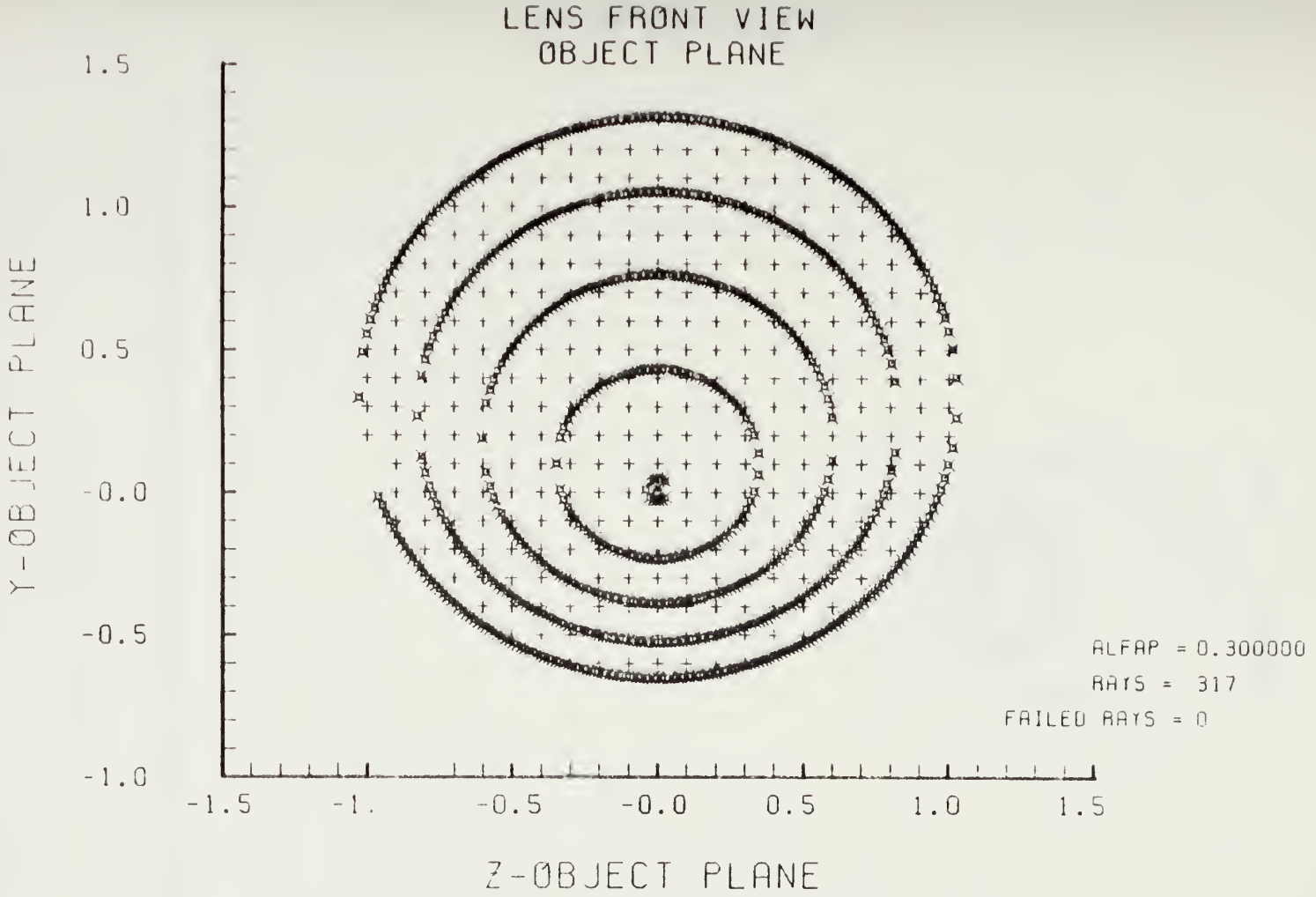

Figure E-2. Grid Plane at $\alpha_p = 0.3$ for Lens of Figure E-1

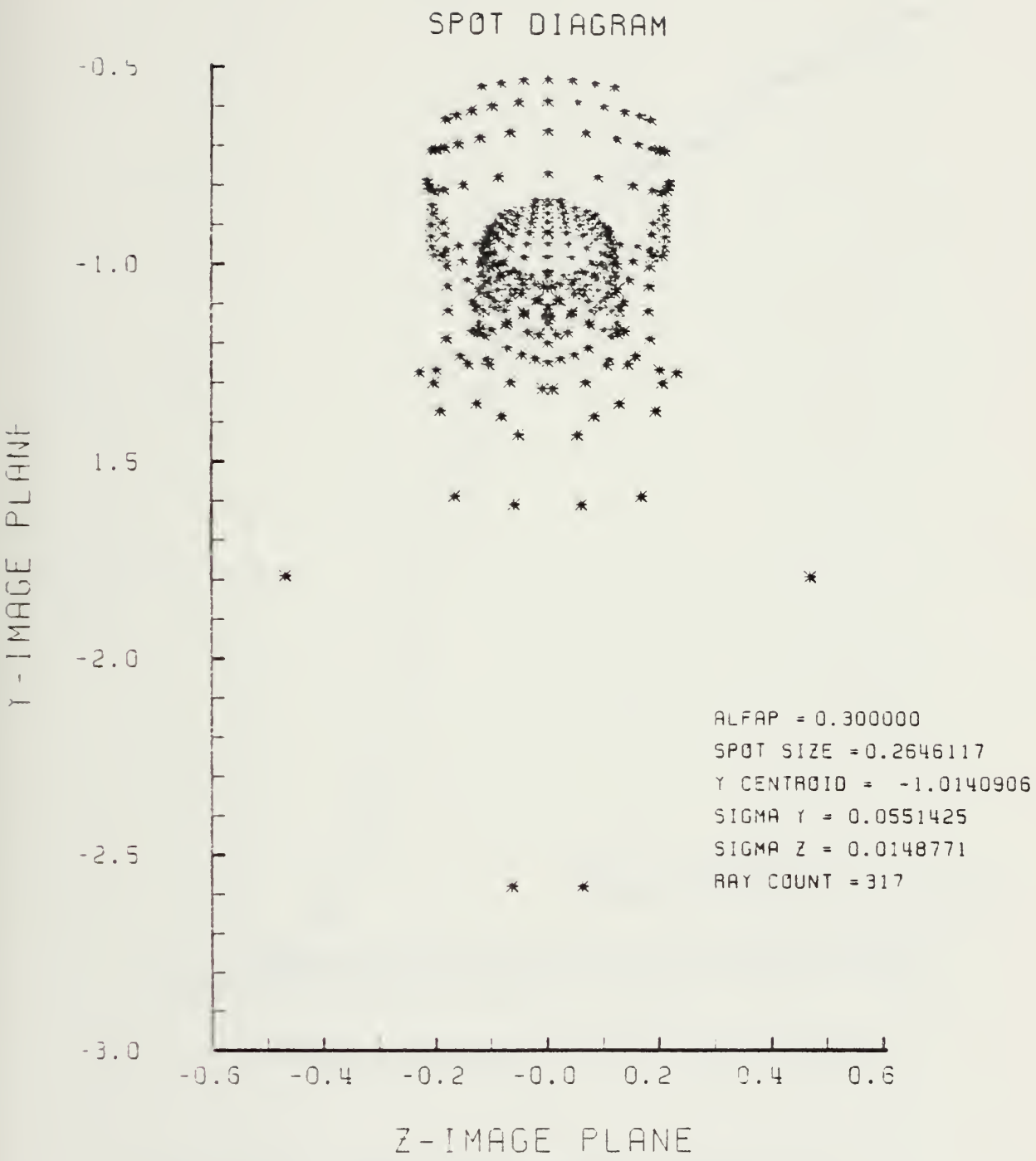

Figure E-3. Spot Diagram for Grid of Figure E-2

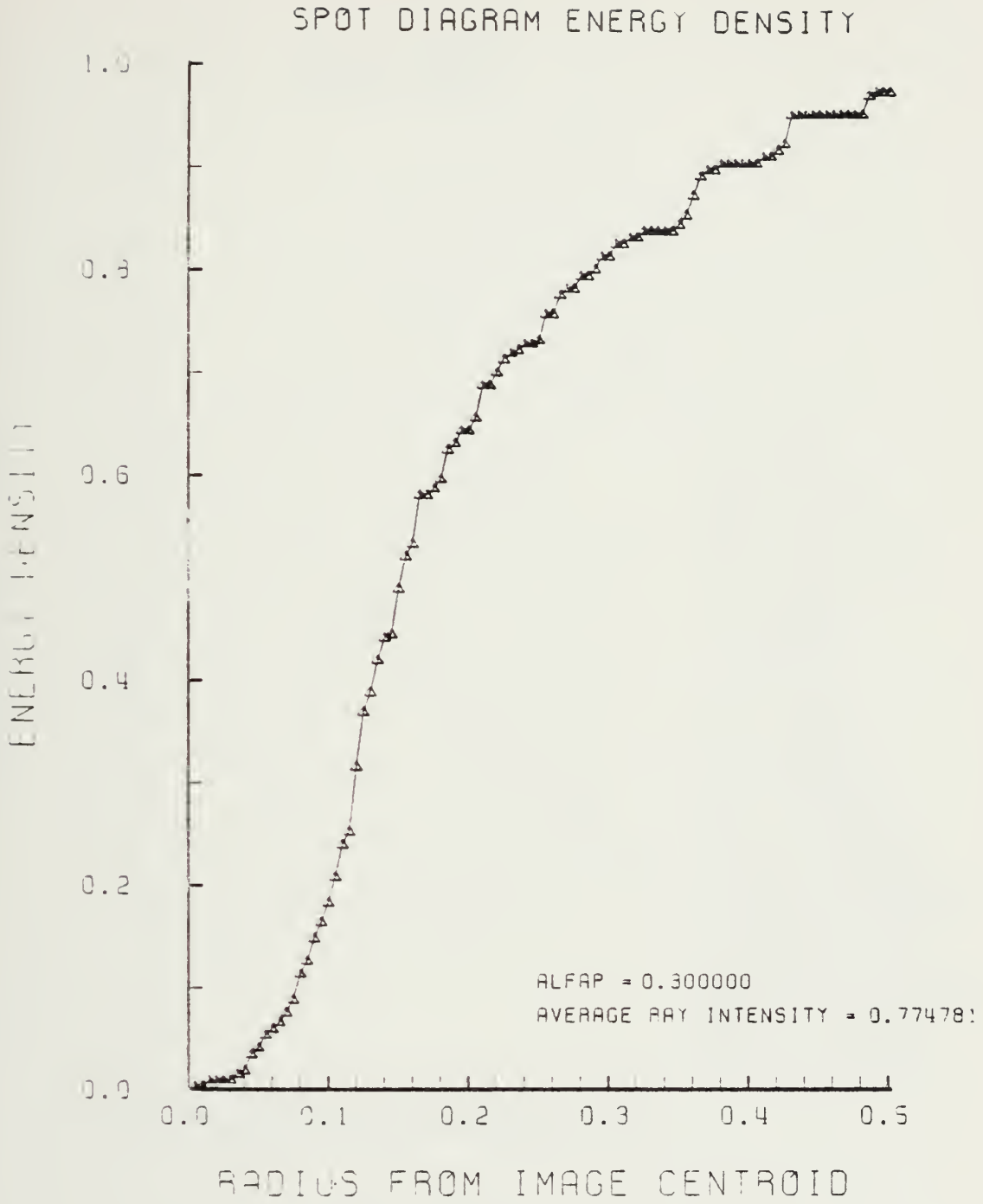

Figure E-4. Encircled Energy of Figure E-3

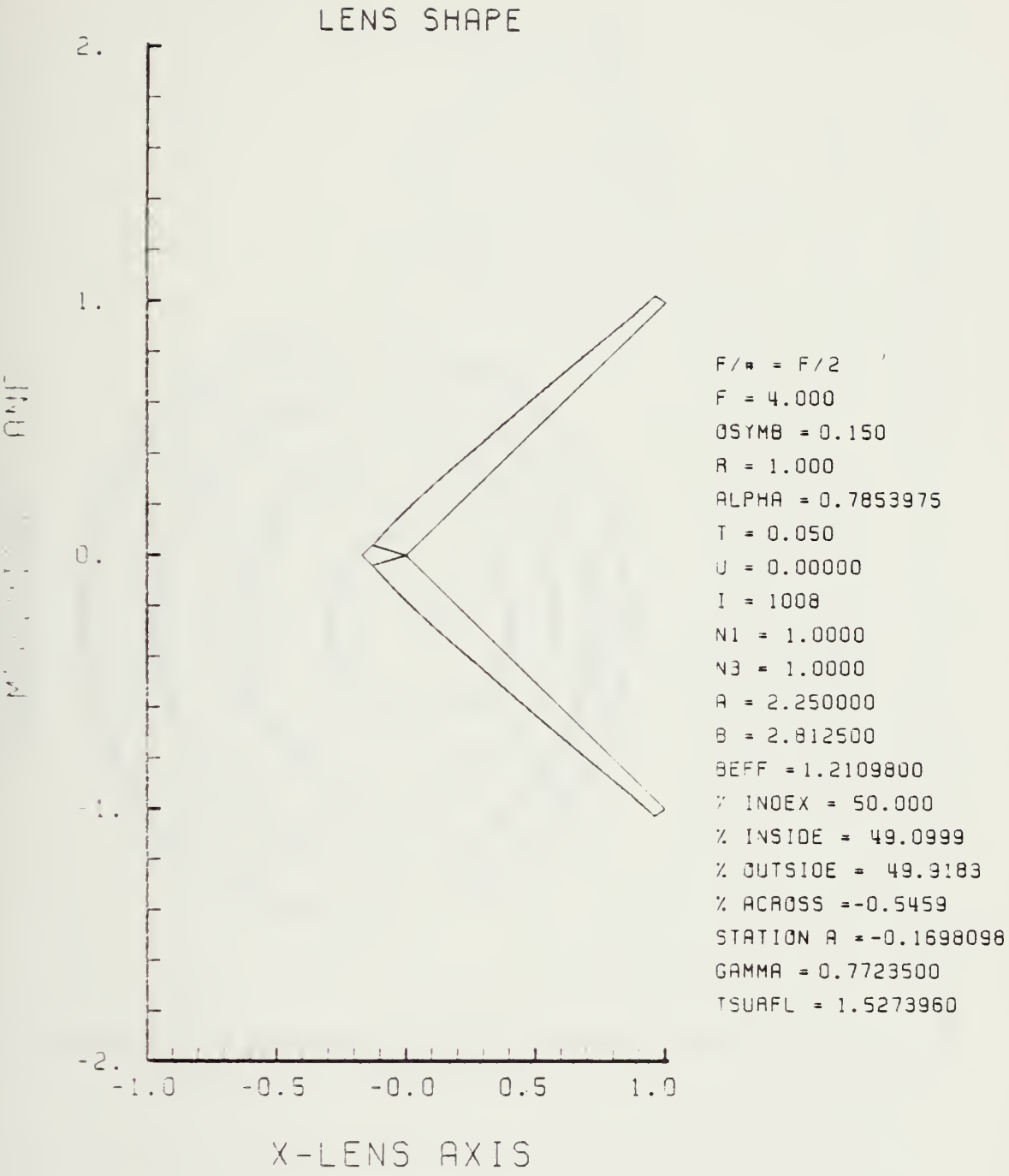

Figure E-5. GRIN Lens Shape at +50%, OB = 0.15, a = 2.25

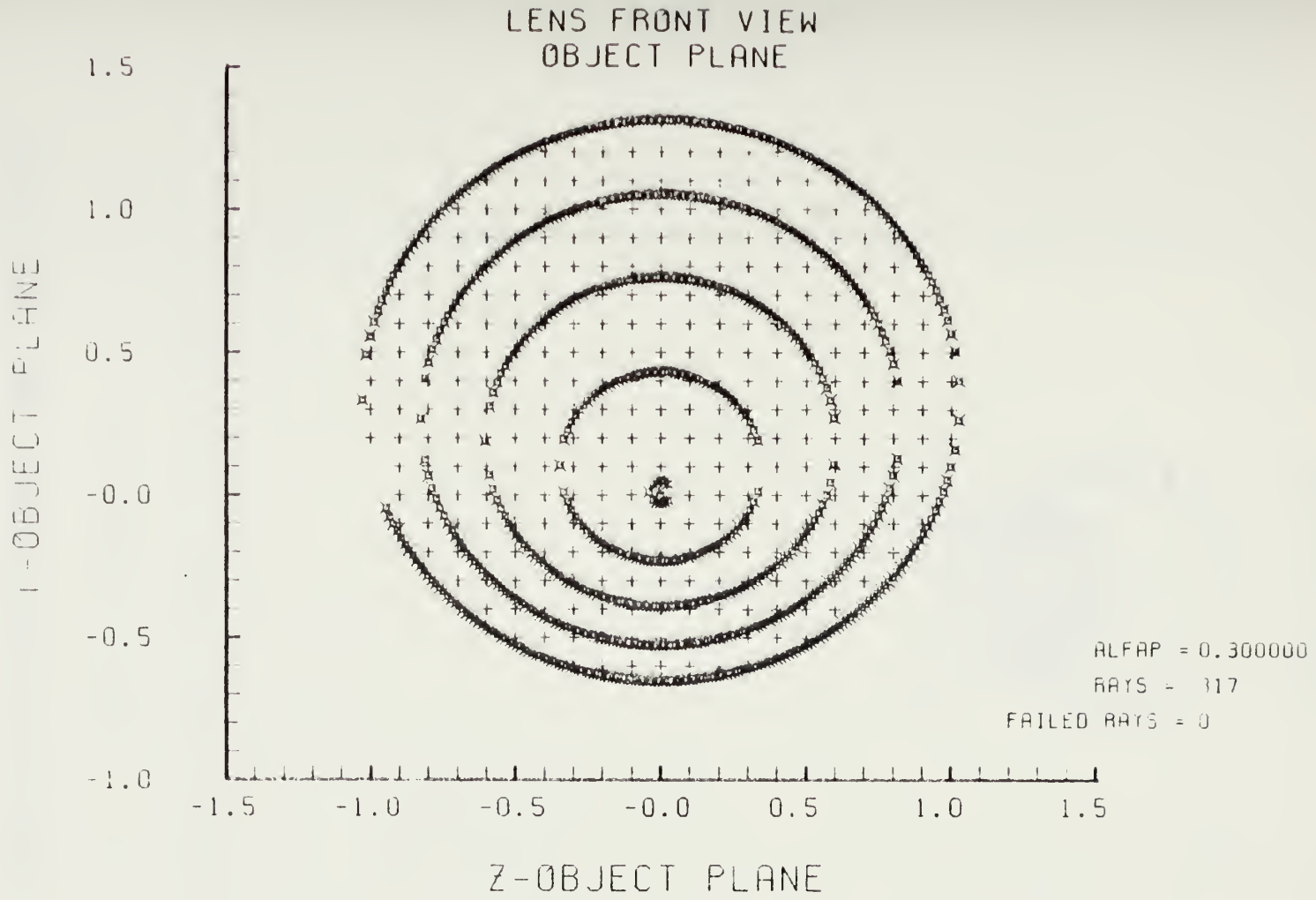

Figure E-6. Grid Plane at $\alpha_p = 0.3$ for Lens of Figure E-5

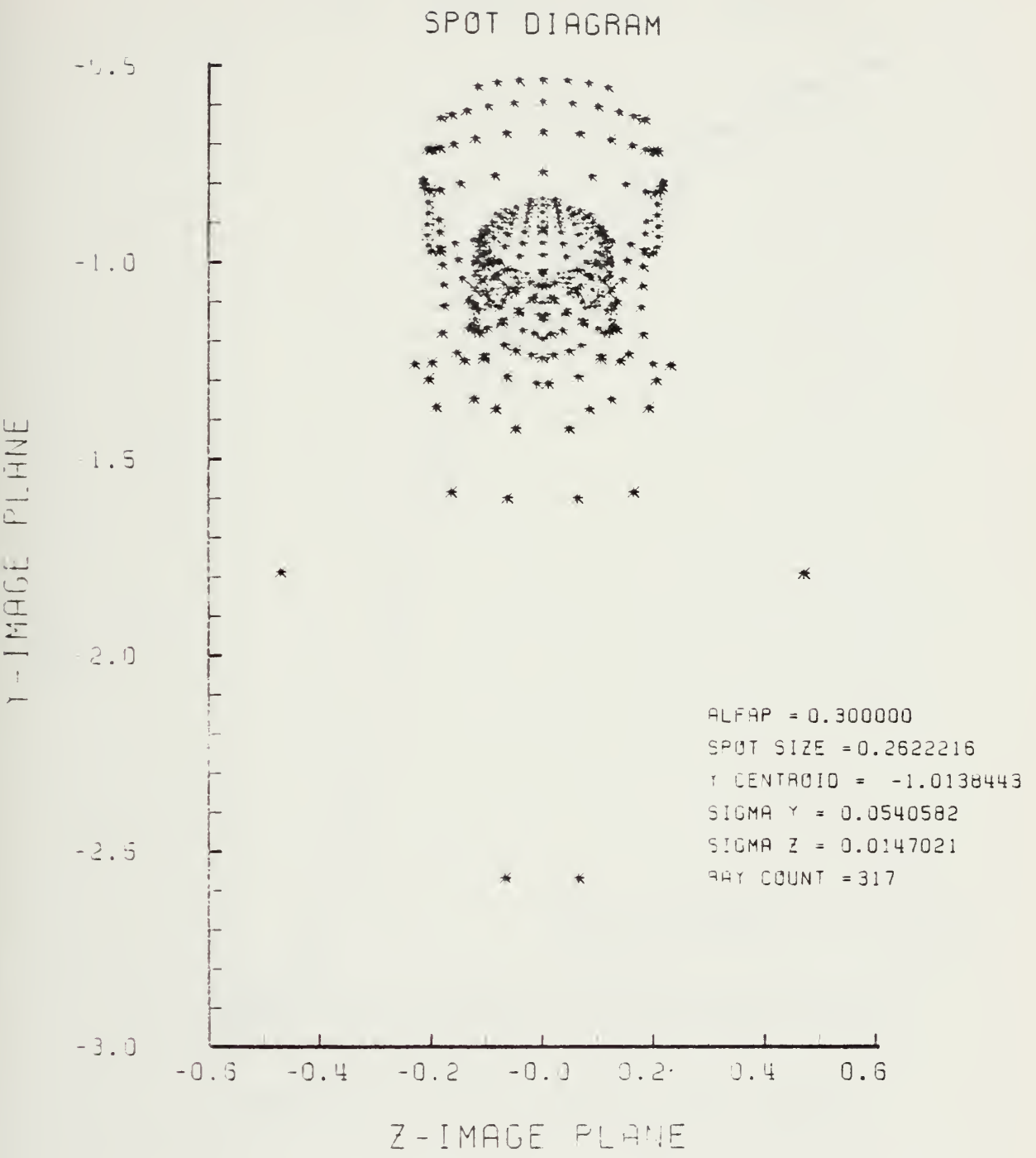

Figure E-7. Spot Diagram for Grid of Figure E-6

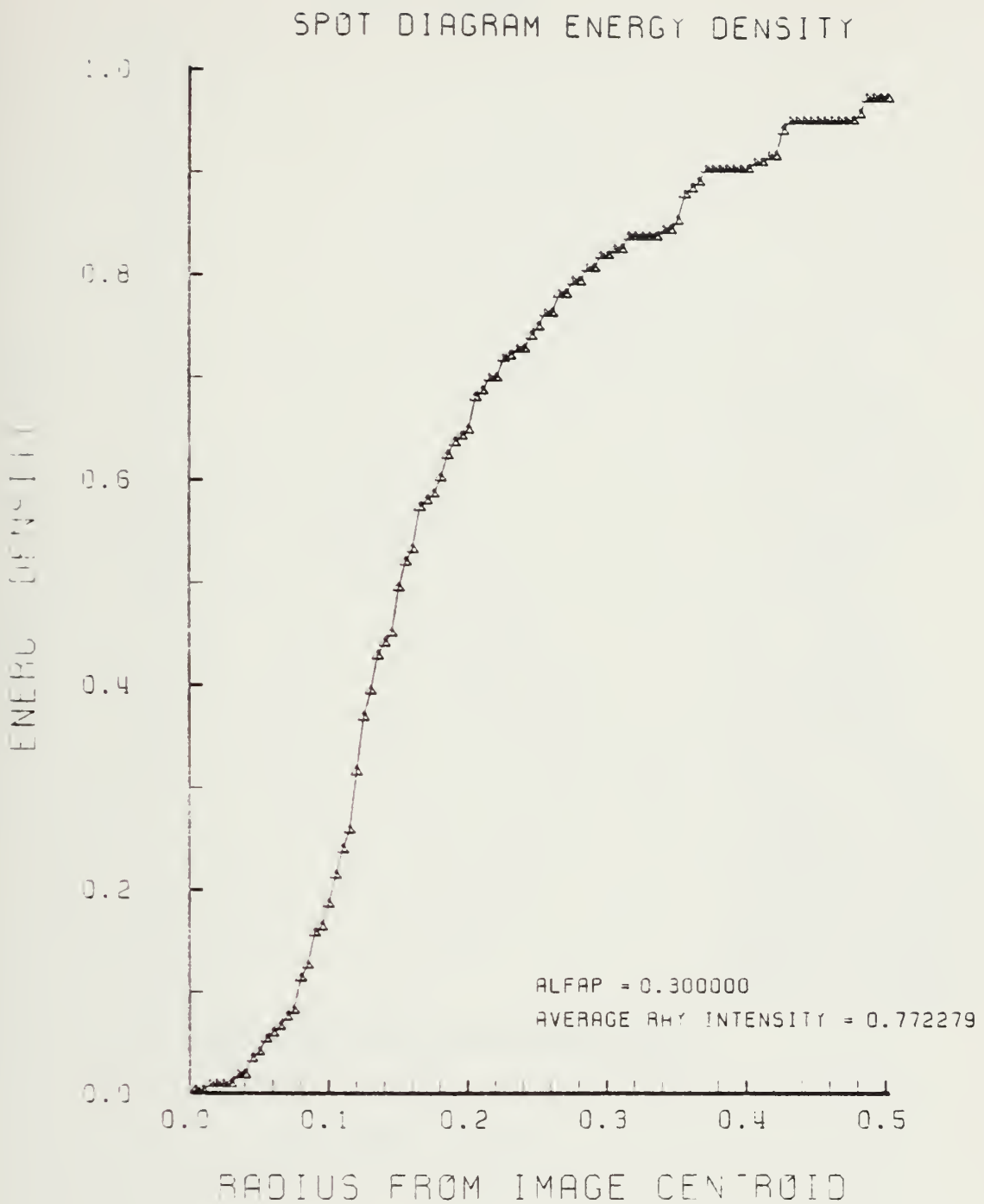

Figure E-8. Encircled Energy of Figure E-7

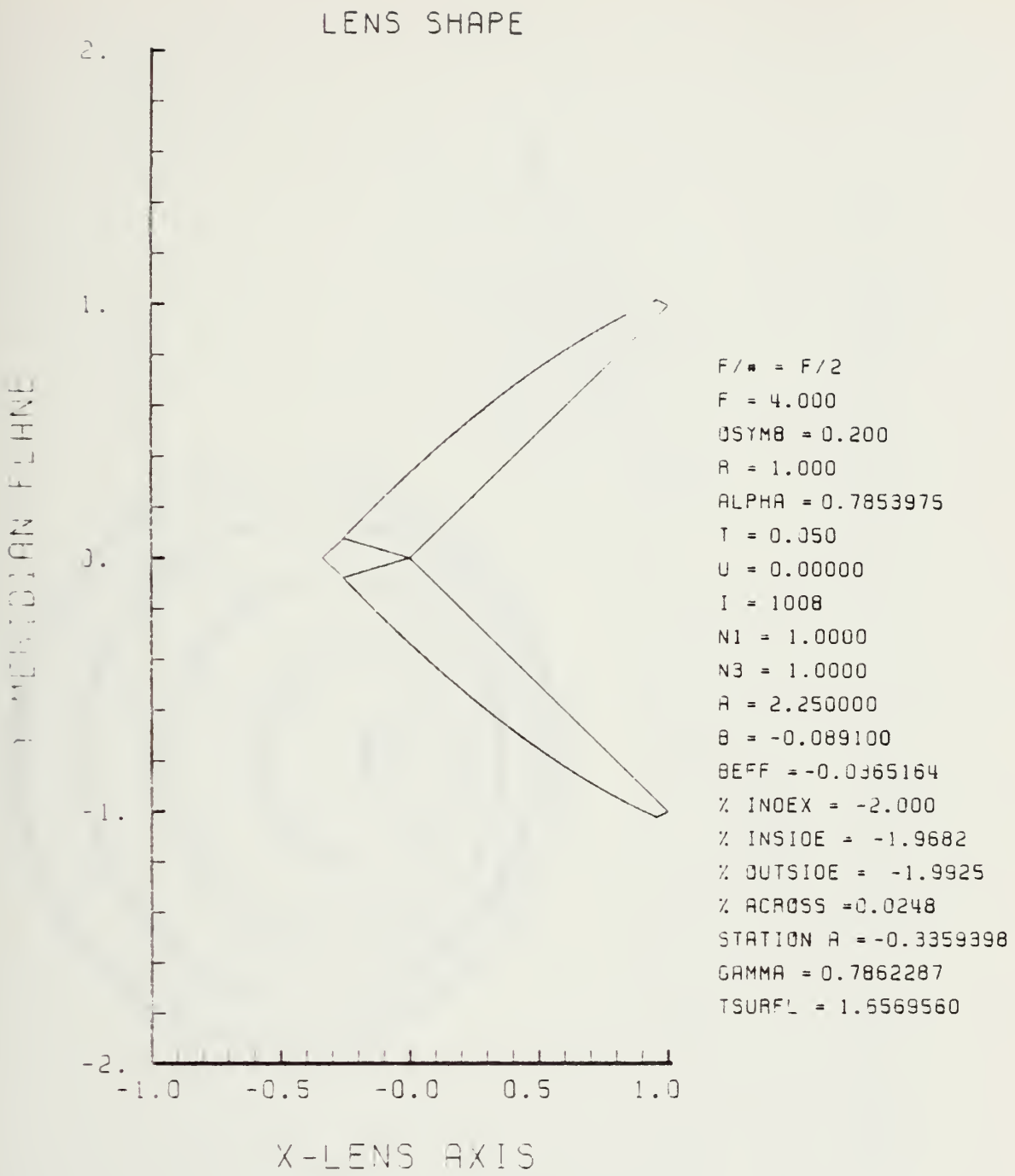

Figure E-9. GRIN Lens Shape at -2%, OB = 0.20, a = 2.25

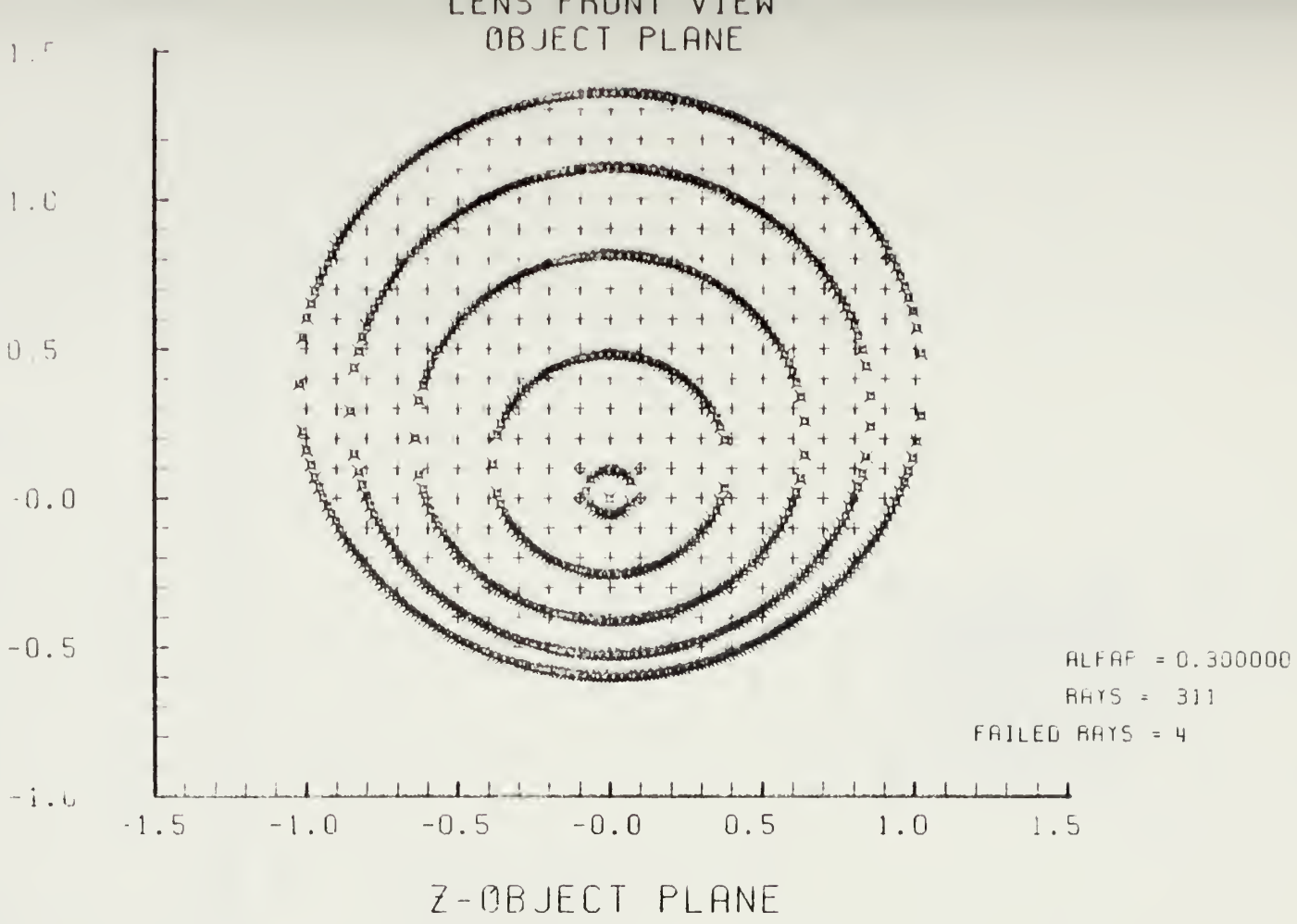

Figure E-10. Grid Plane at α_p = 0.3 for Lens of Figure E-9

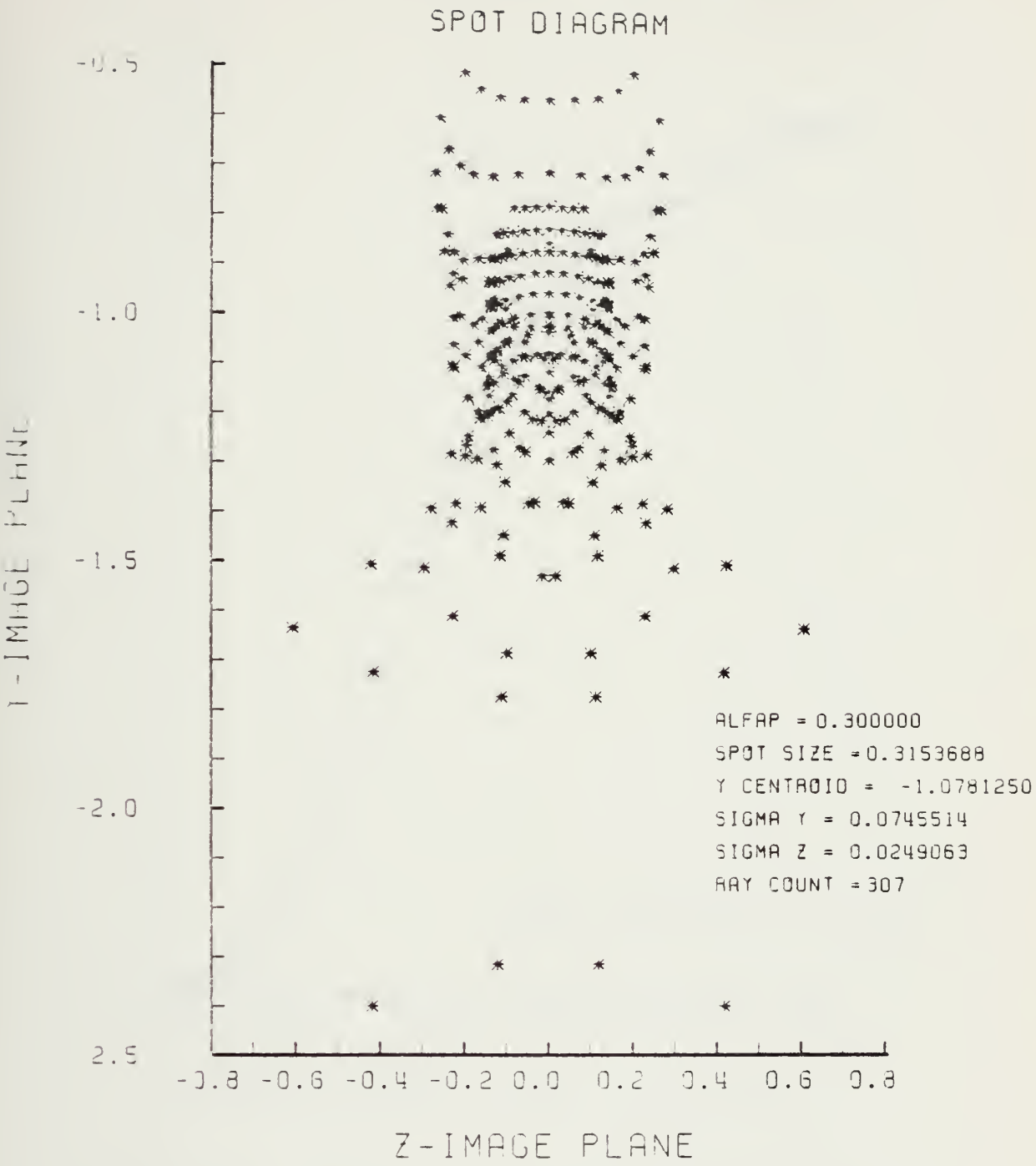

Figure E-11. Spot Diagram for Grid of Figure E-10

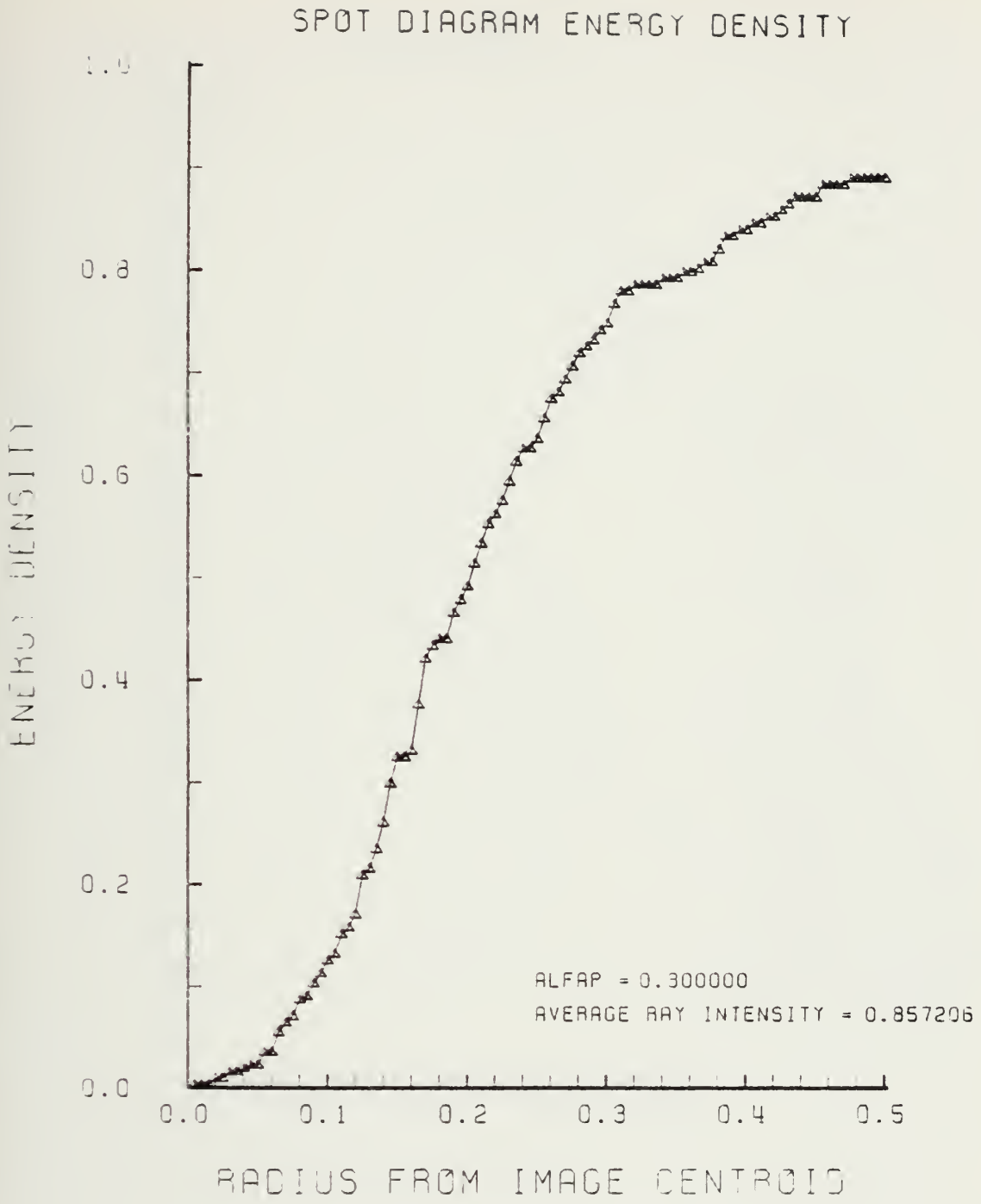

Figure E-12. Encircled Energy of Figure E-11

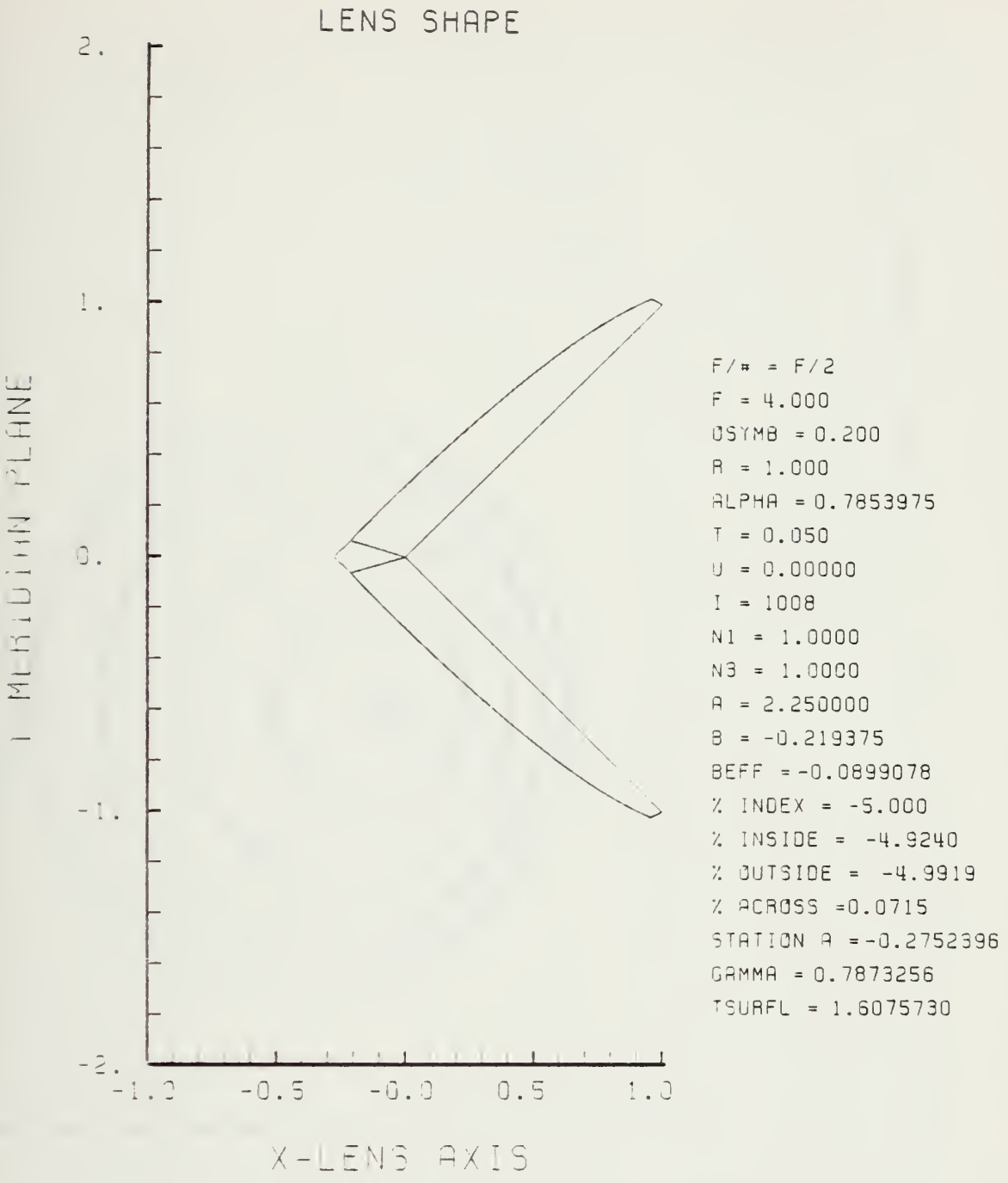

Figure E-13. GRIN Lens Shape at -5%, OB = 0.20, a = 2.25

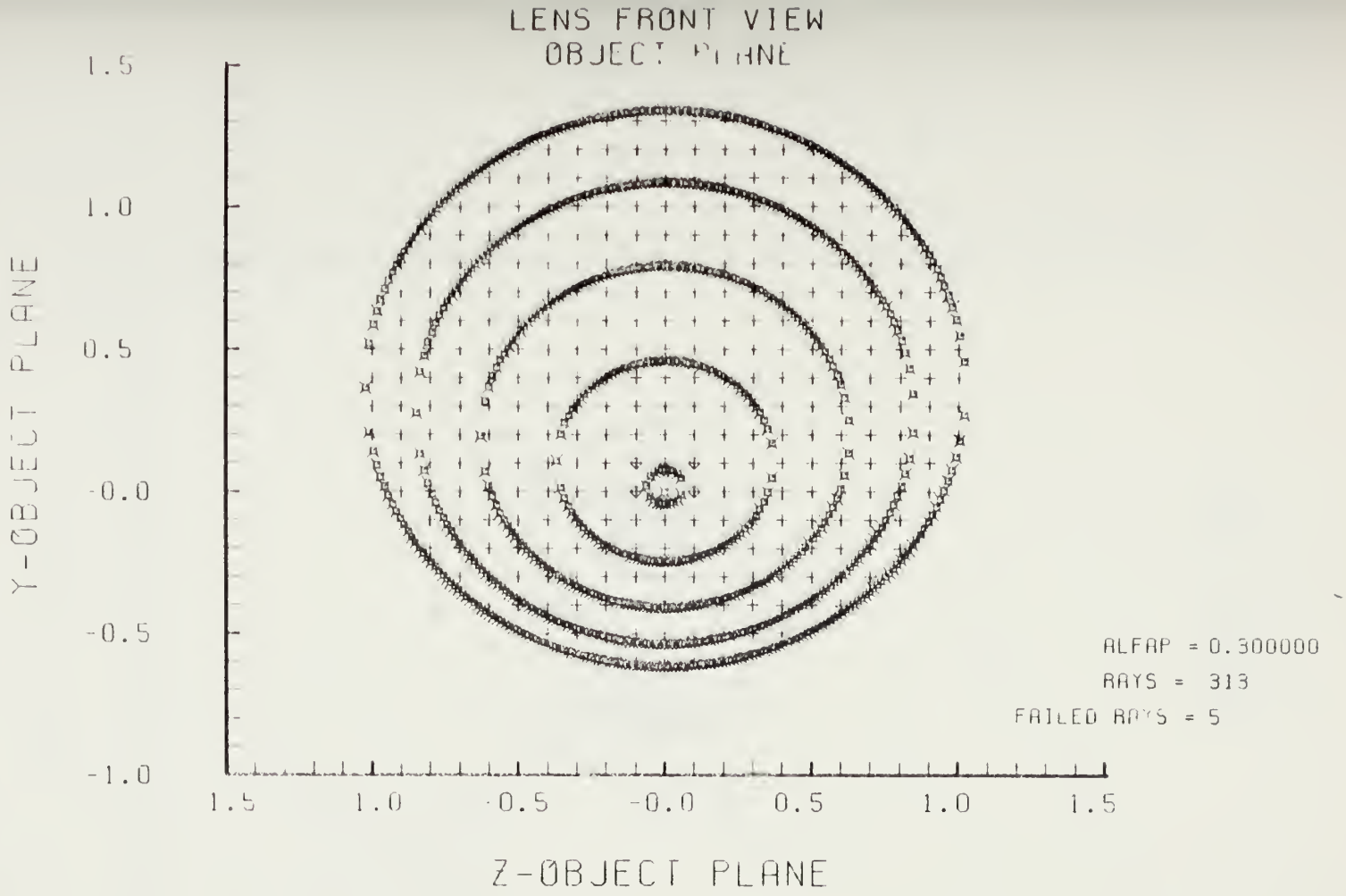

Figure E-14. Grid Plane at α_p = 0.3 for Lens of Figure E-13

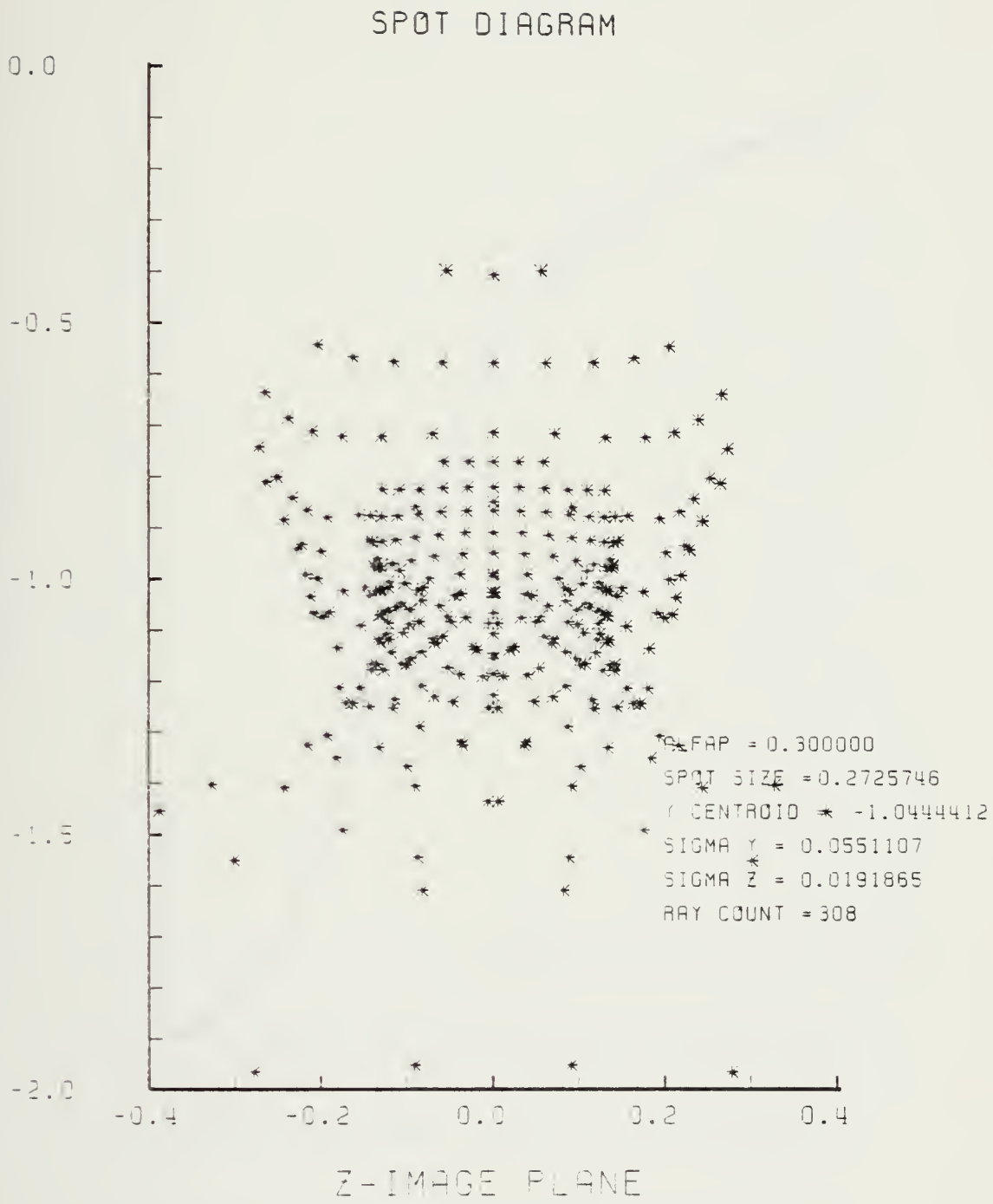

Figure E-15. Spot Diagram for Grid of Figure E-14

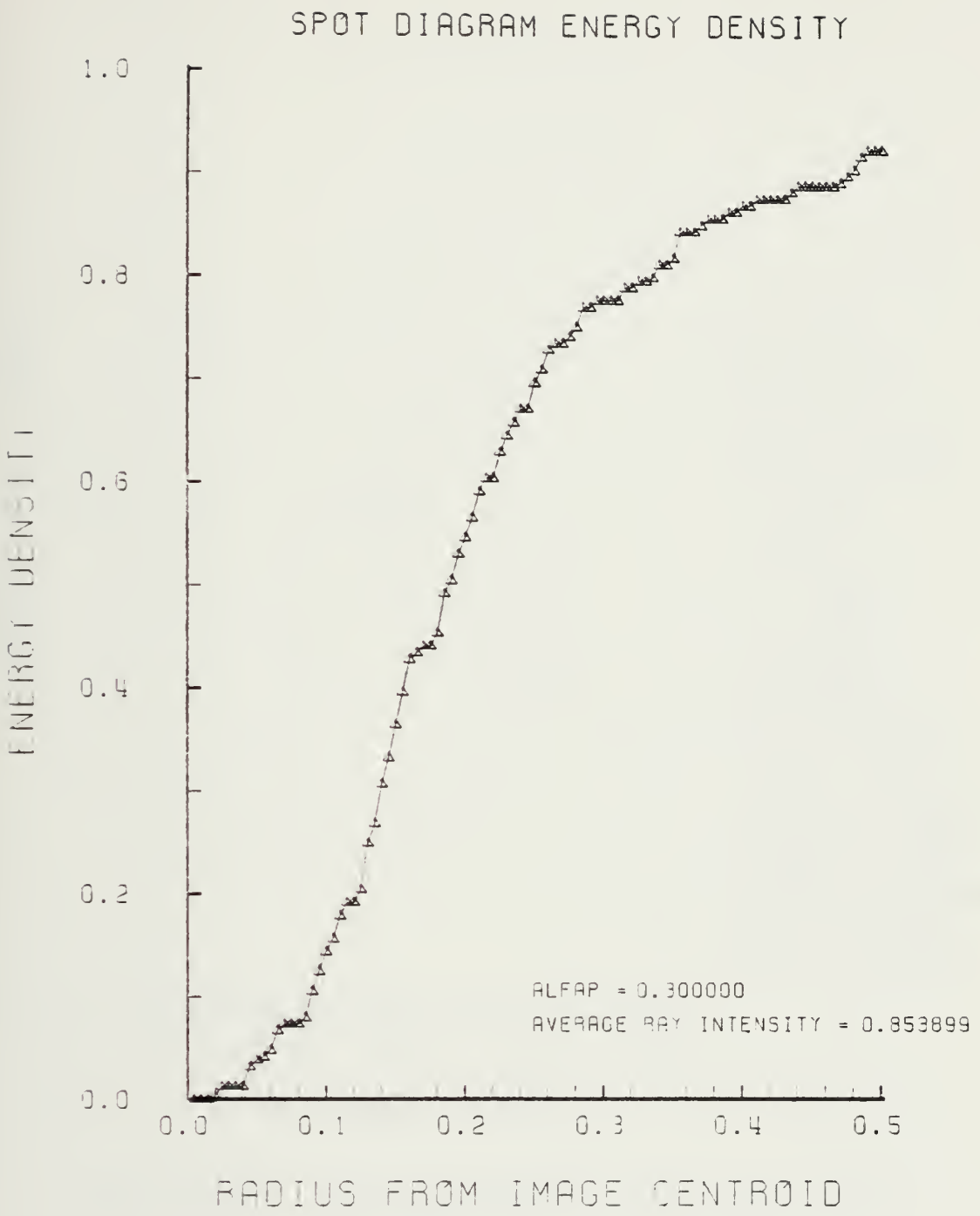

Figure E-16. Encircled Energy of Figure E-15

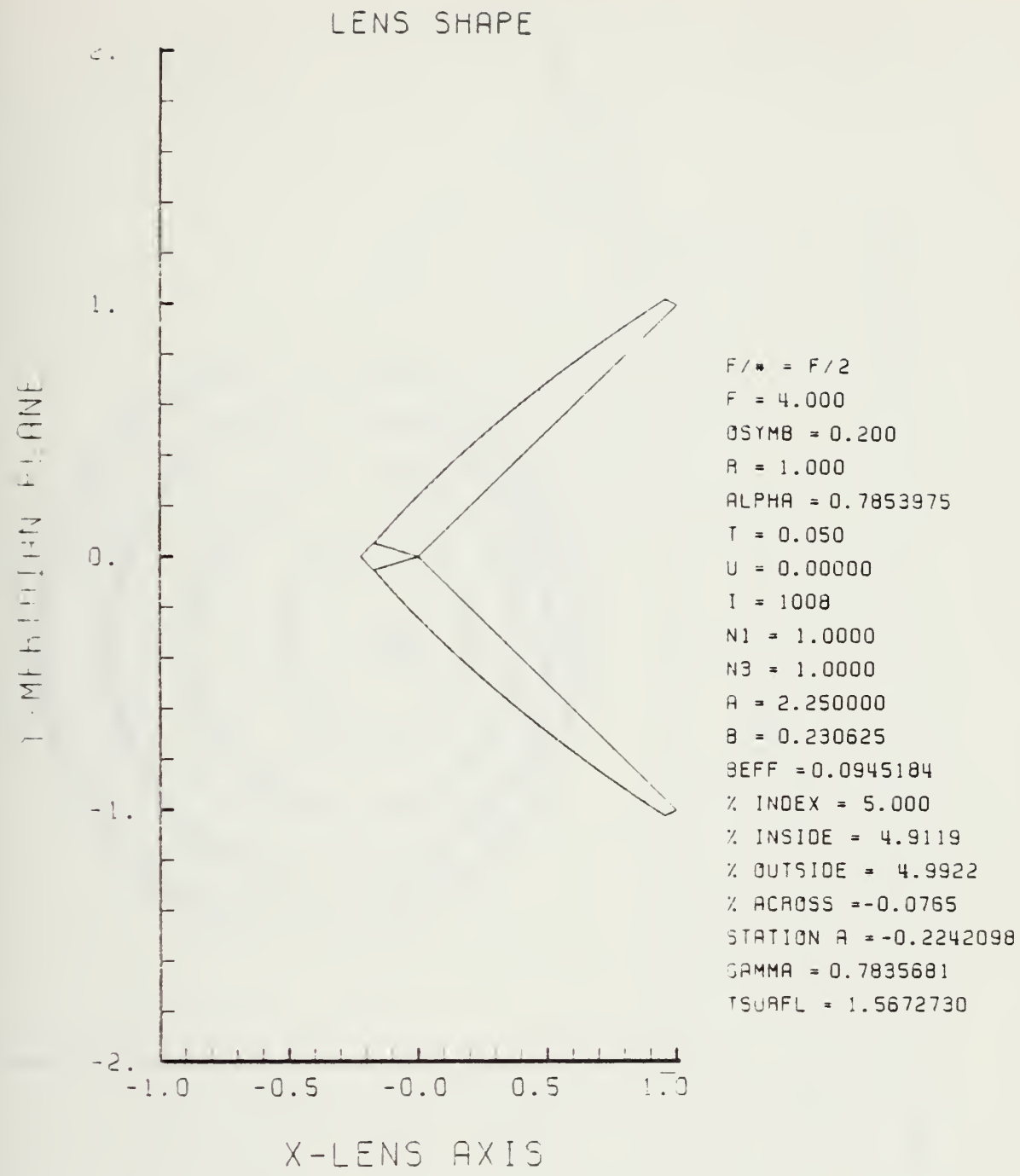

Figure E-17. GRIN Lens Shape at +5%, OB = 0.20, a = 2.25

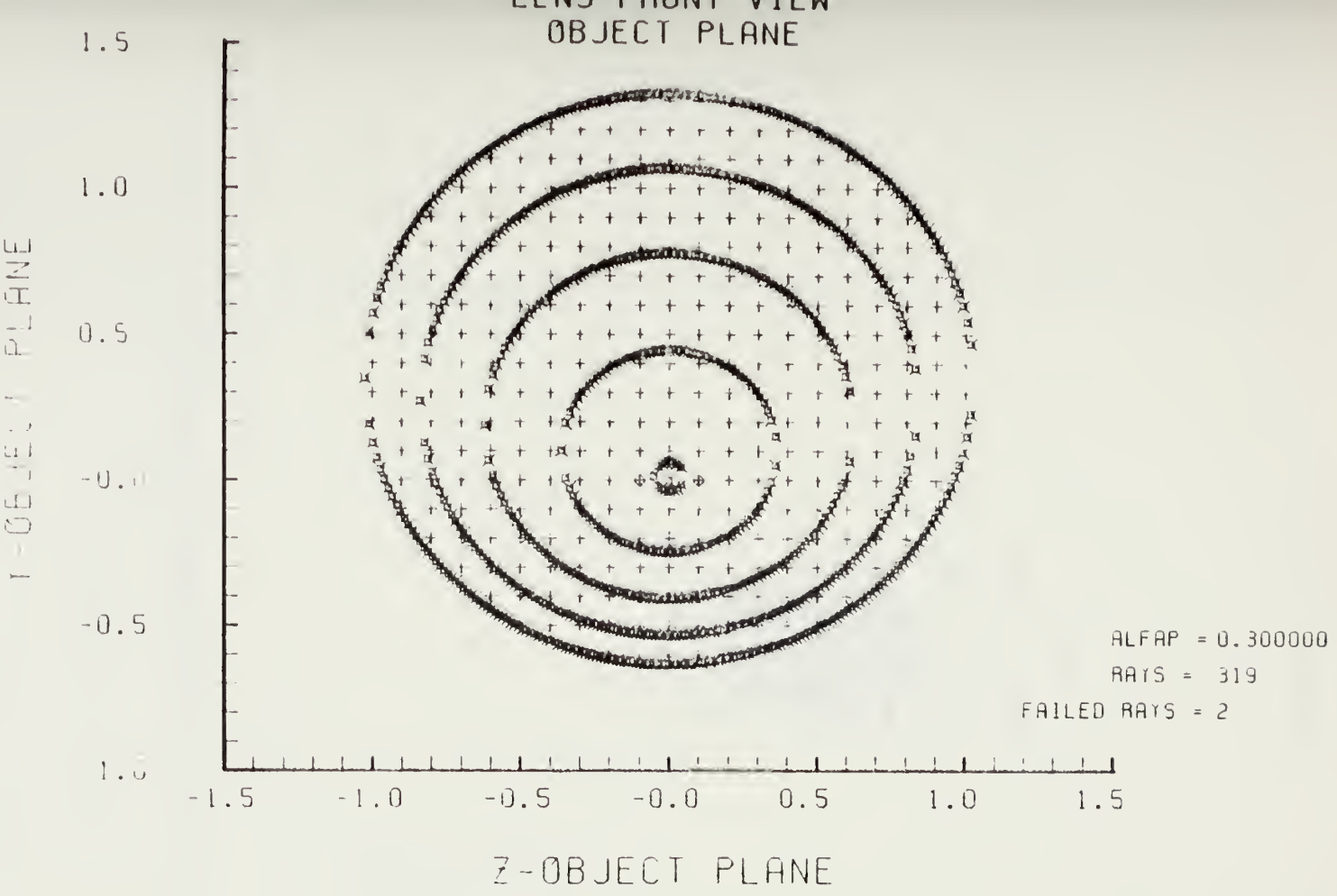

Figure E-18. Grid Plane at $\alpha_p = 0.3$ for Lens of Figure E-17

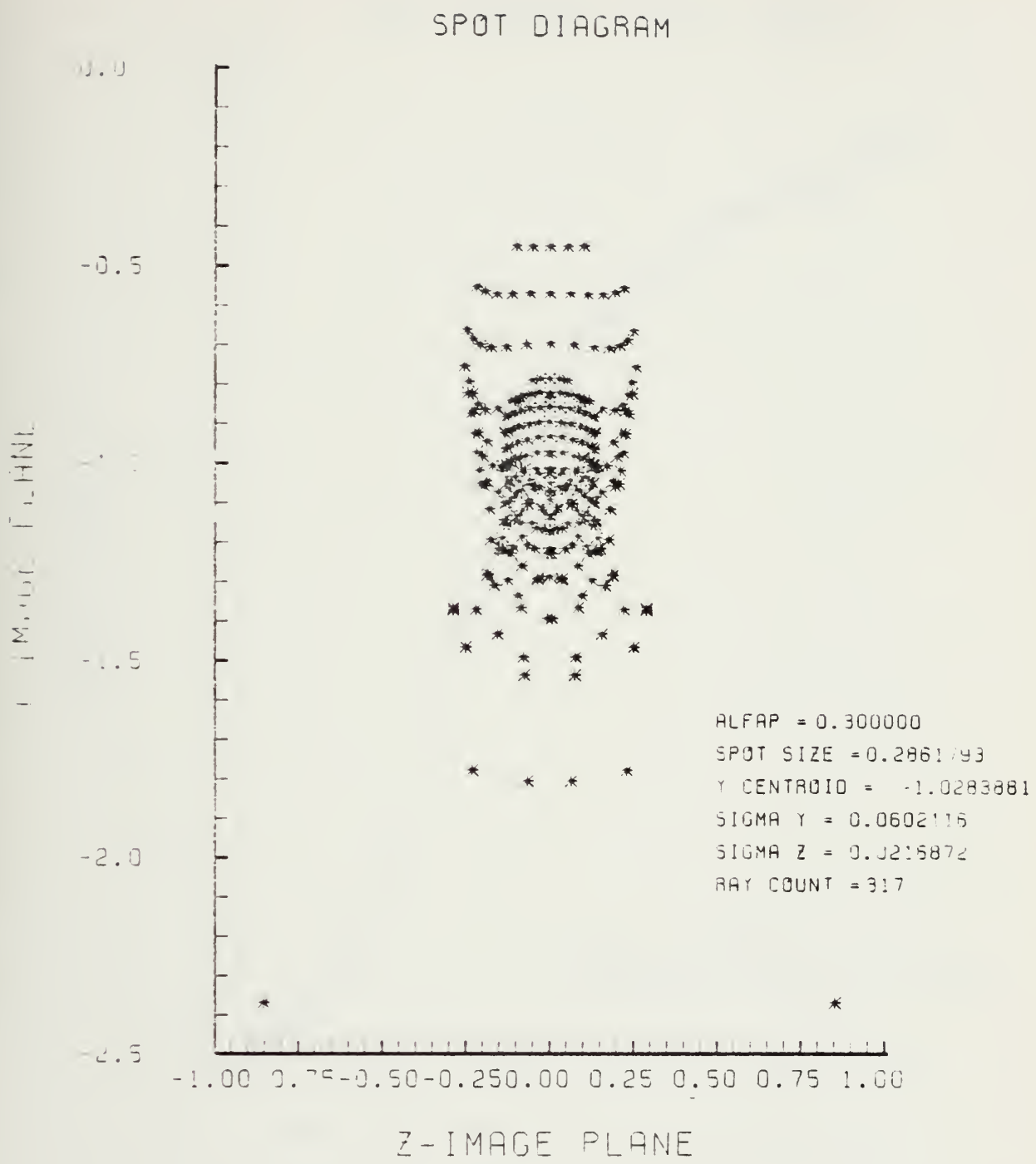

Figure E-19. Spot Diagram for Grid of Figure E-18

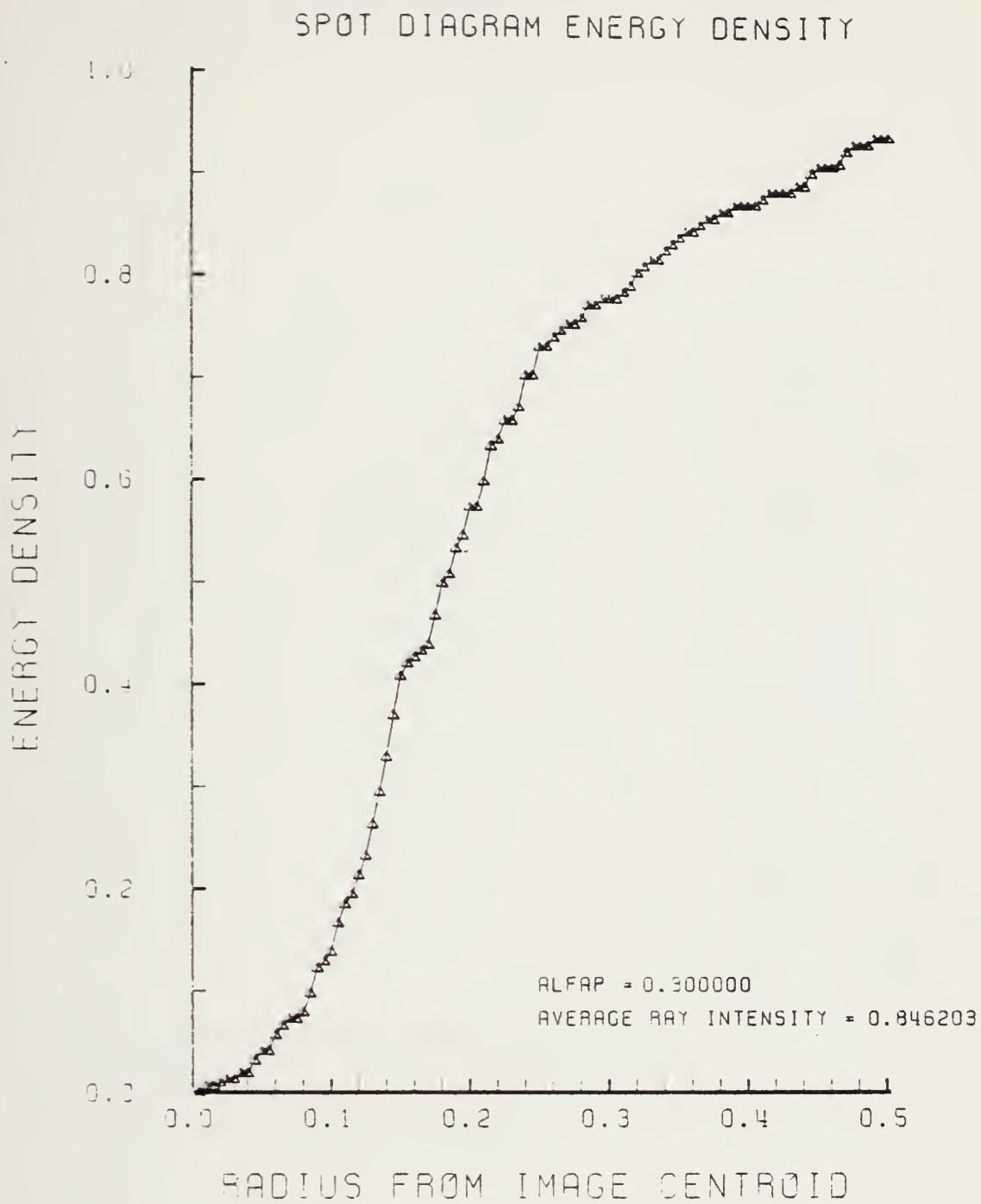

Figure E-20. Encircled Energy of Figure E-19

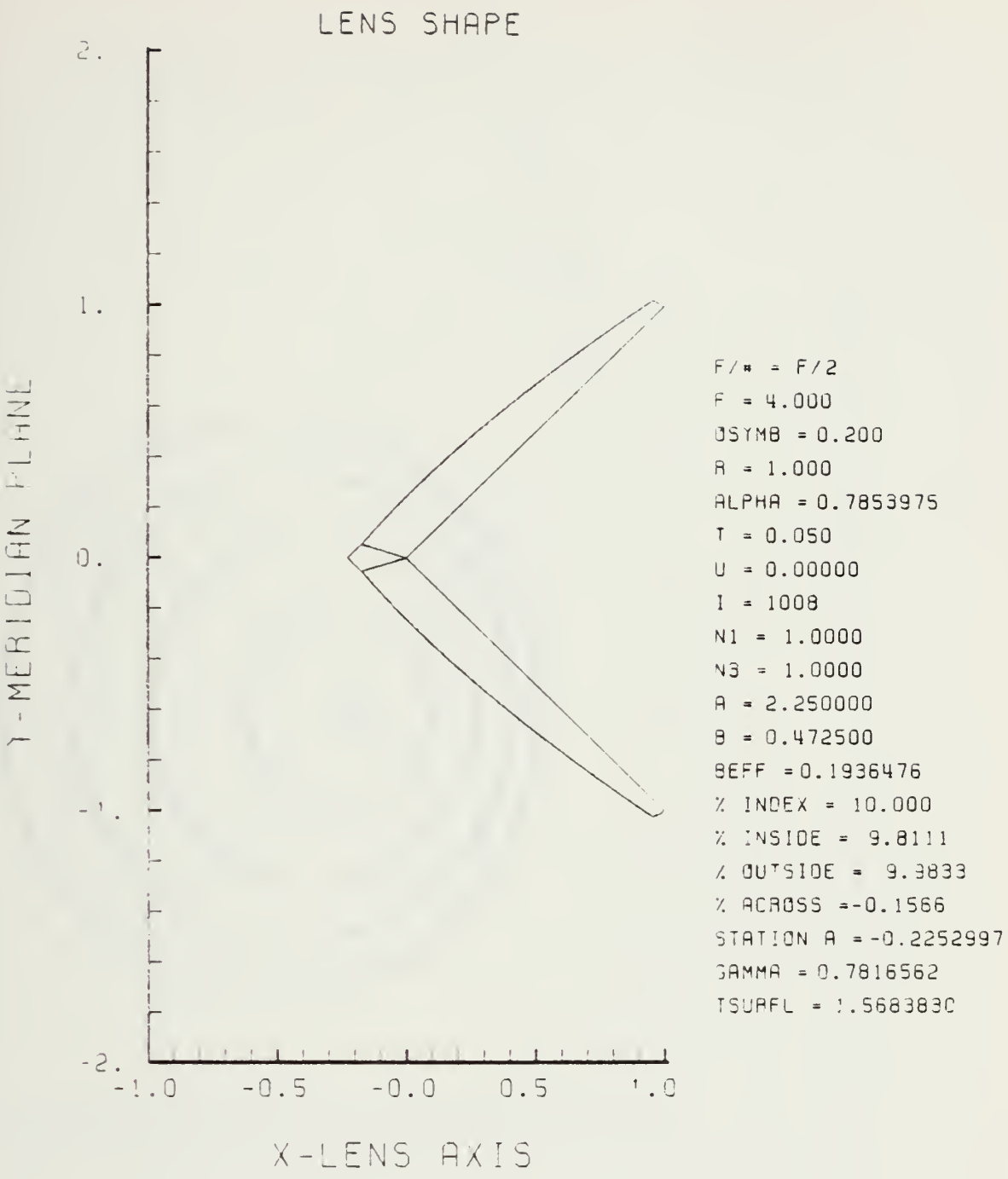

Figure E-21. GRIN Lens Shape at +10%, OB = 0.20, a = 2.25

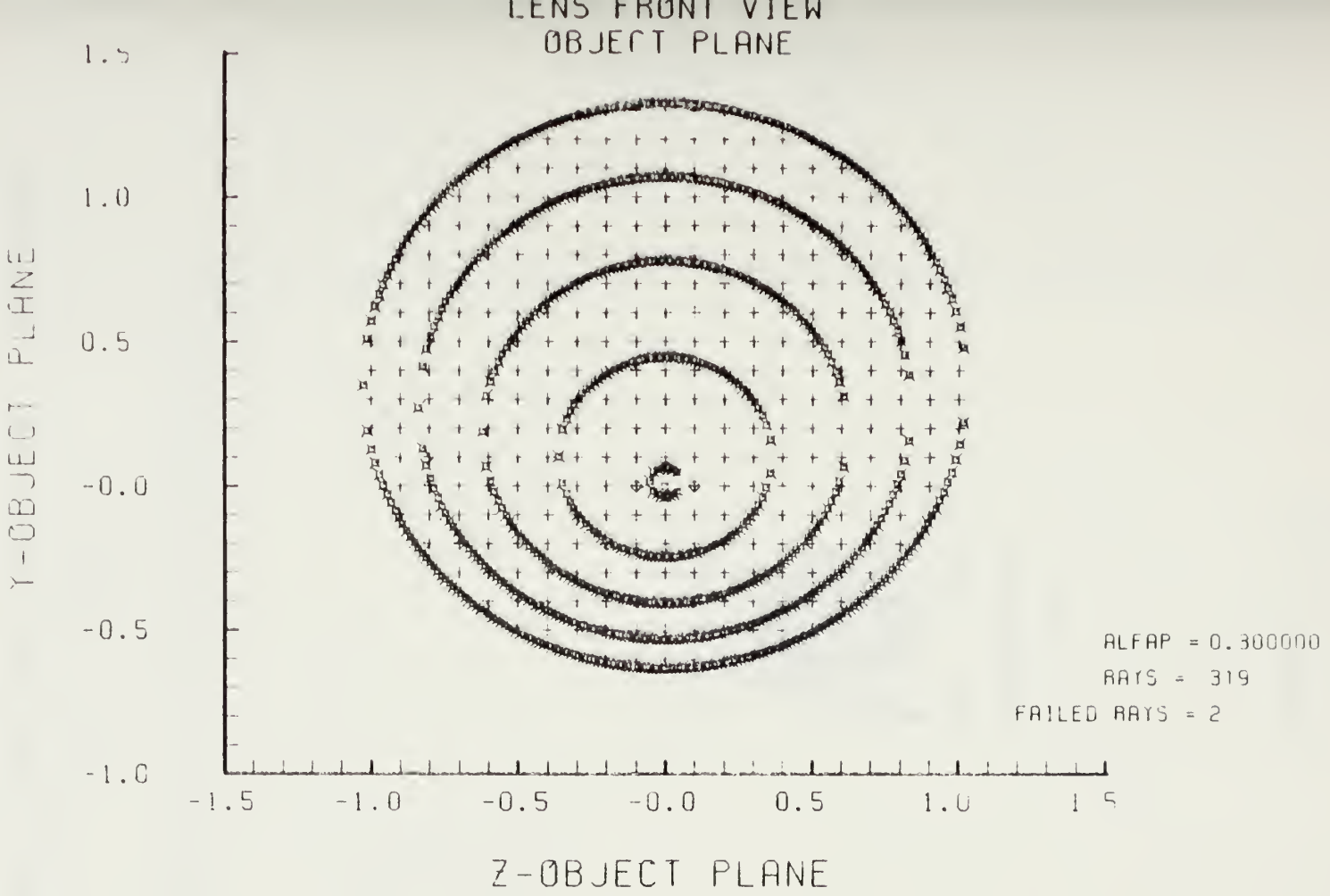

Figure E-22. Grid Plane at $\alpha_p = 0.3$ for Lens of Figure E-21

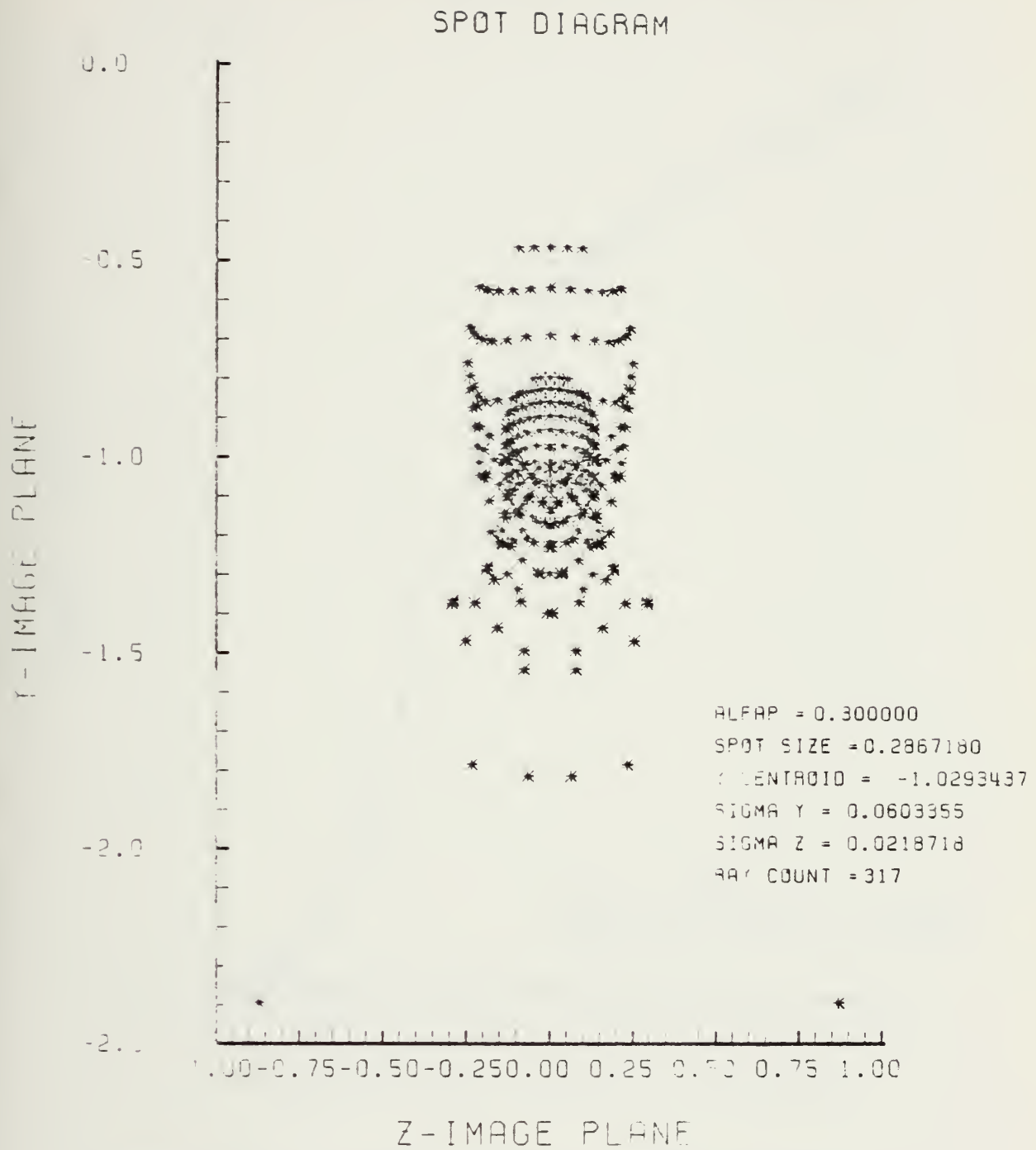

Figure E-23. Spot Diagram for Grid of Figure E-22

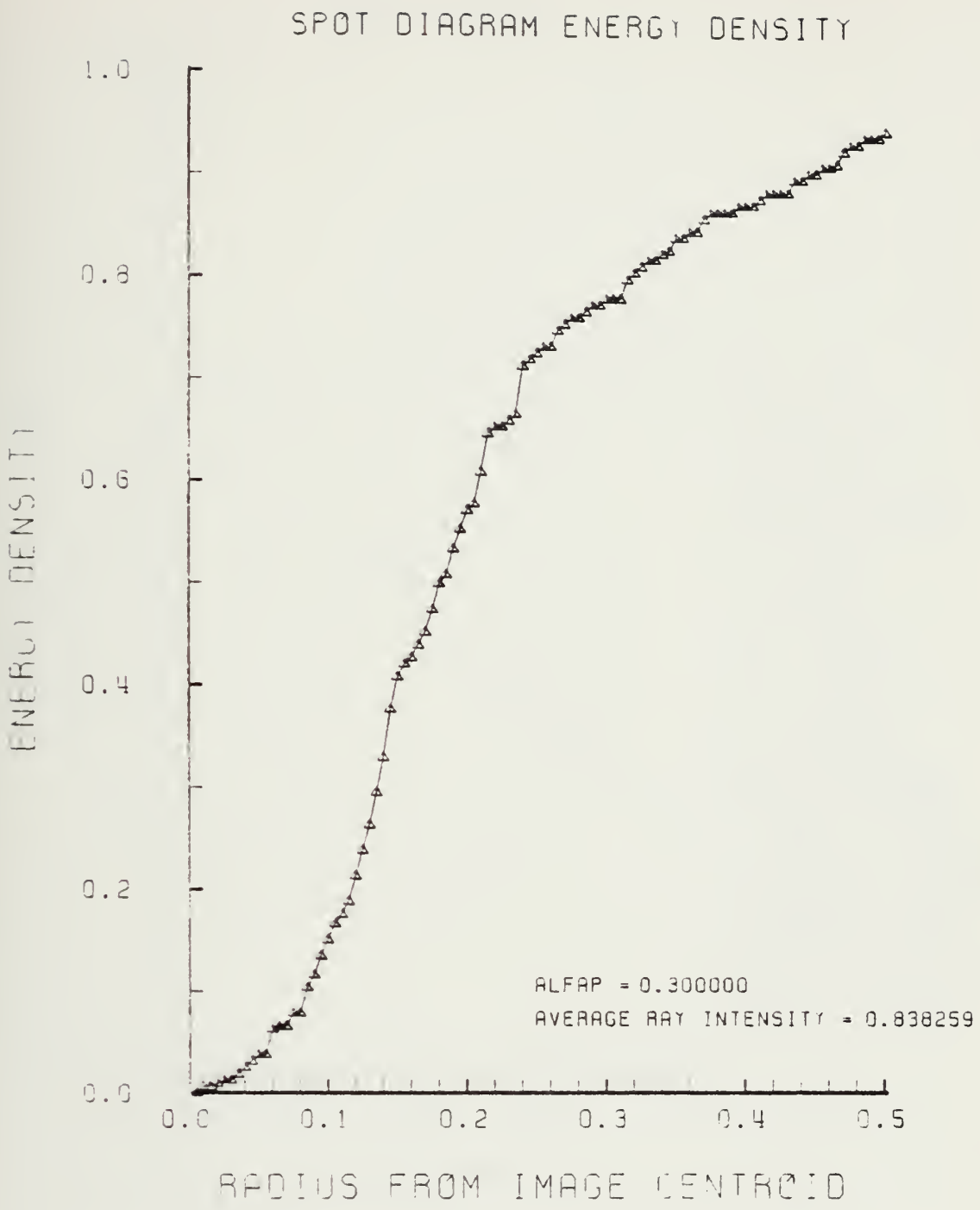

Figure E-24. Encircled Energy of Figure E-23

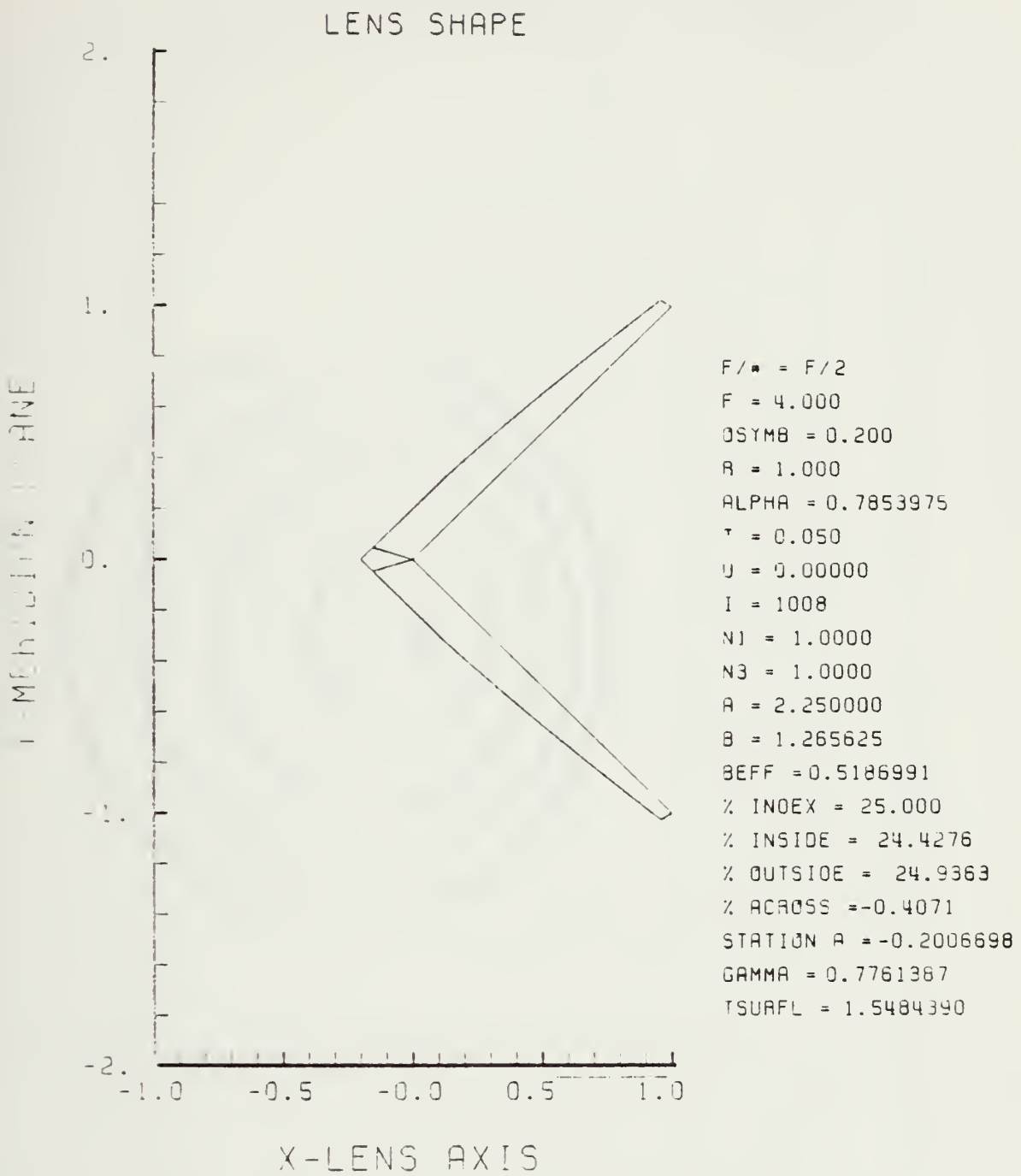

Figure E-25. GRIN Lens Shape at +25%, OB = 0.20, a = 2.25

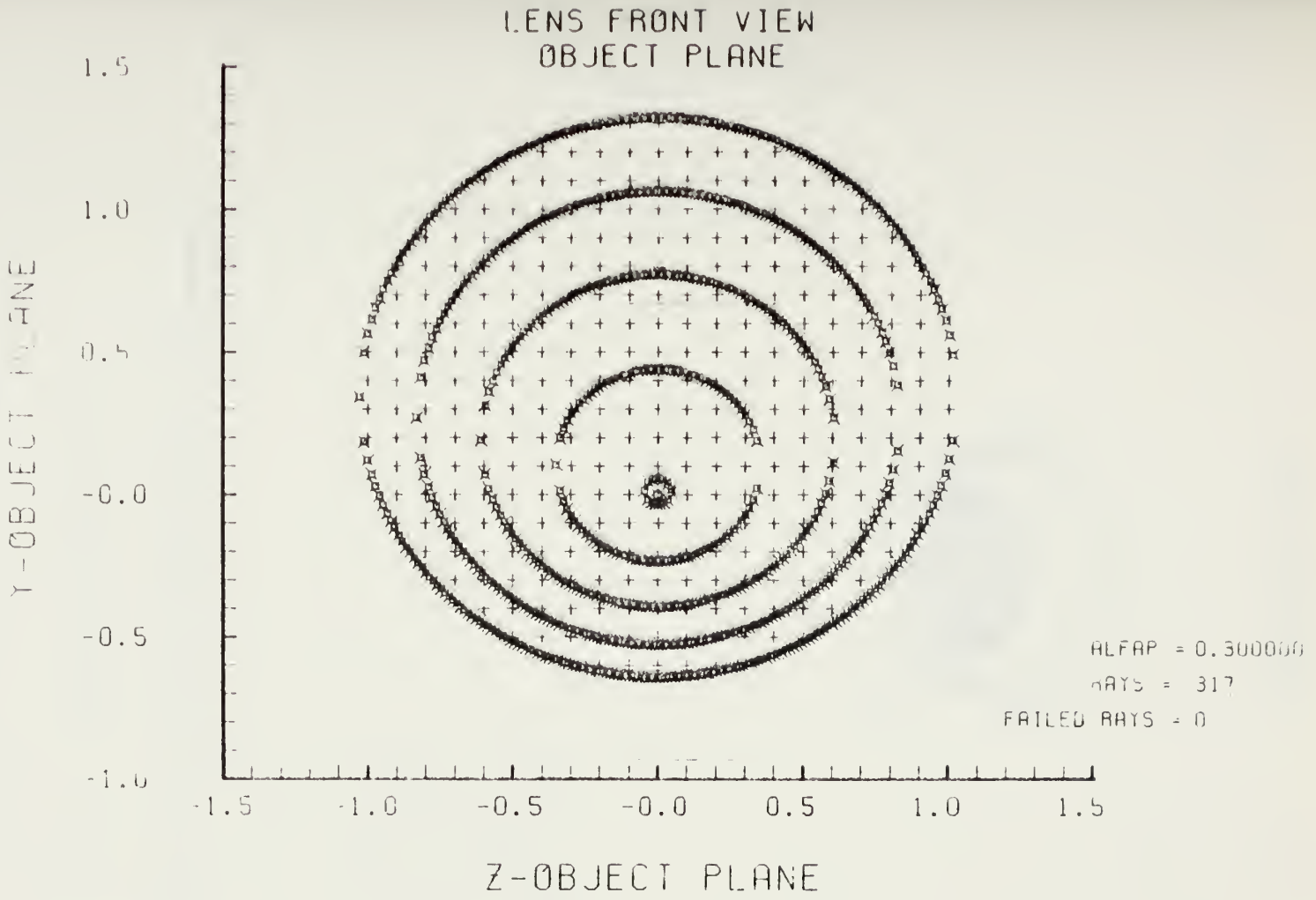

Figure E-26. Grid Plane at α_p = 0.3 for Lens of Figure E-25

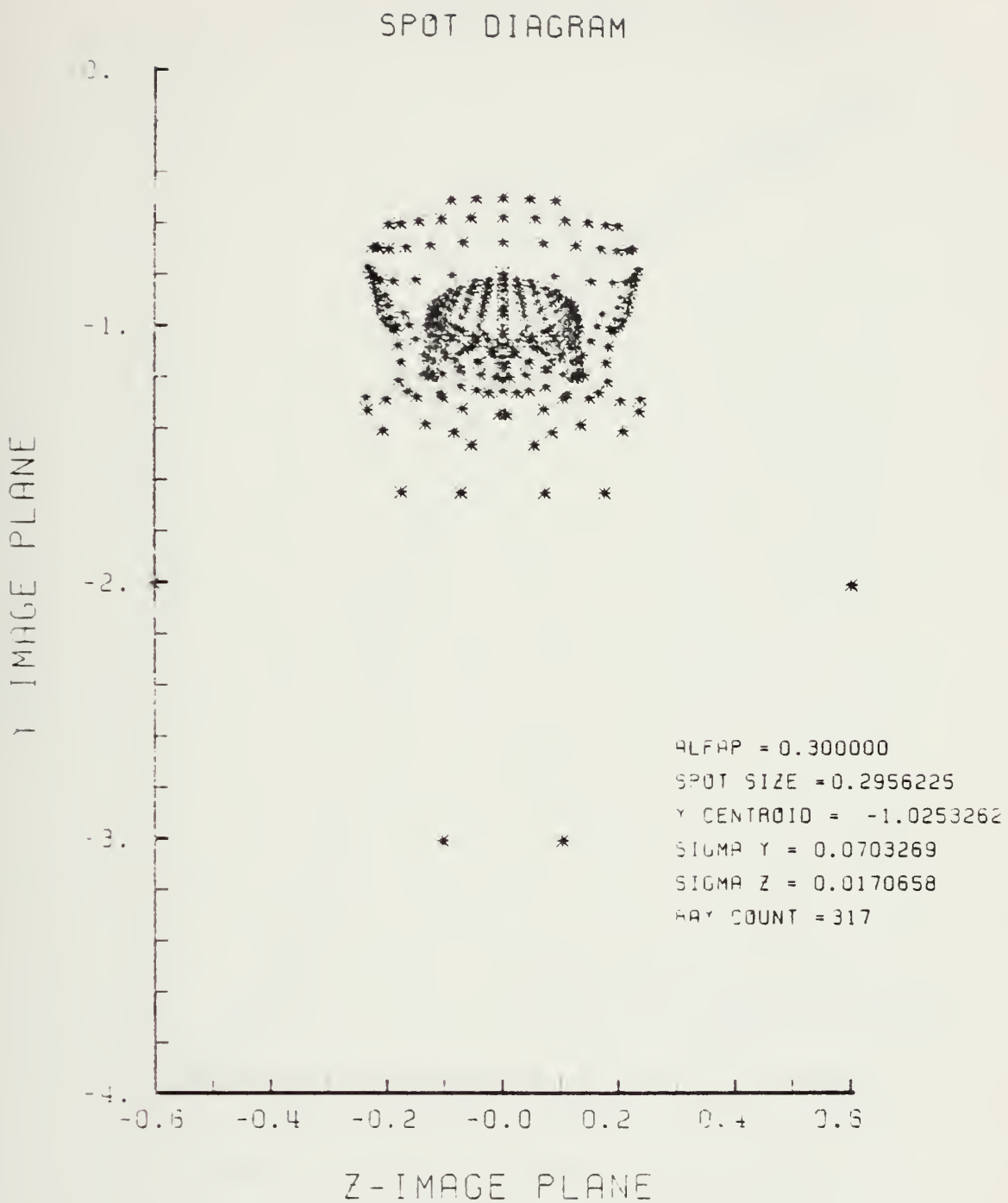

Figure E-27. Spot Diagram for Grid of Figure E-26

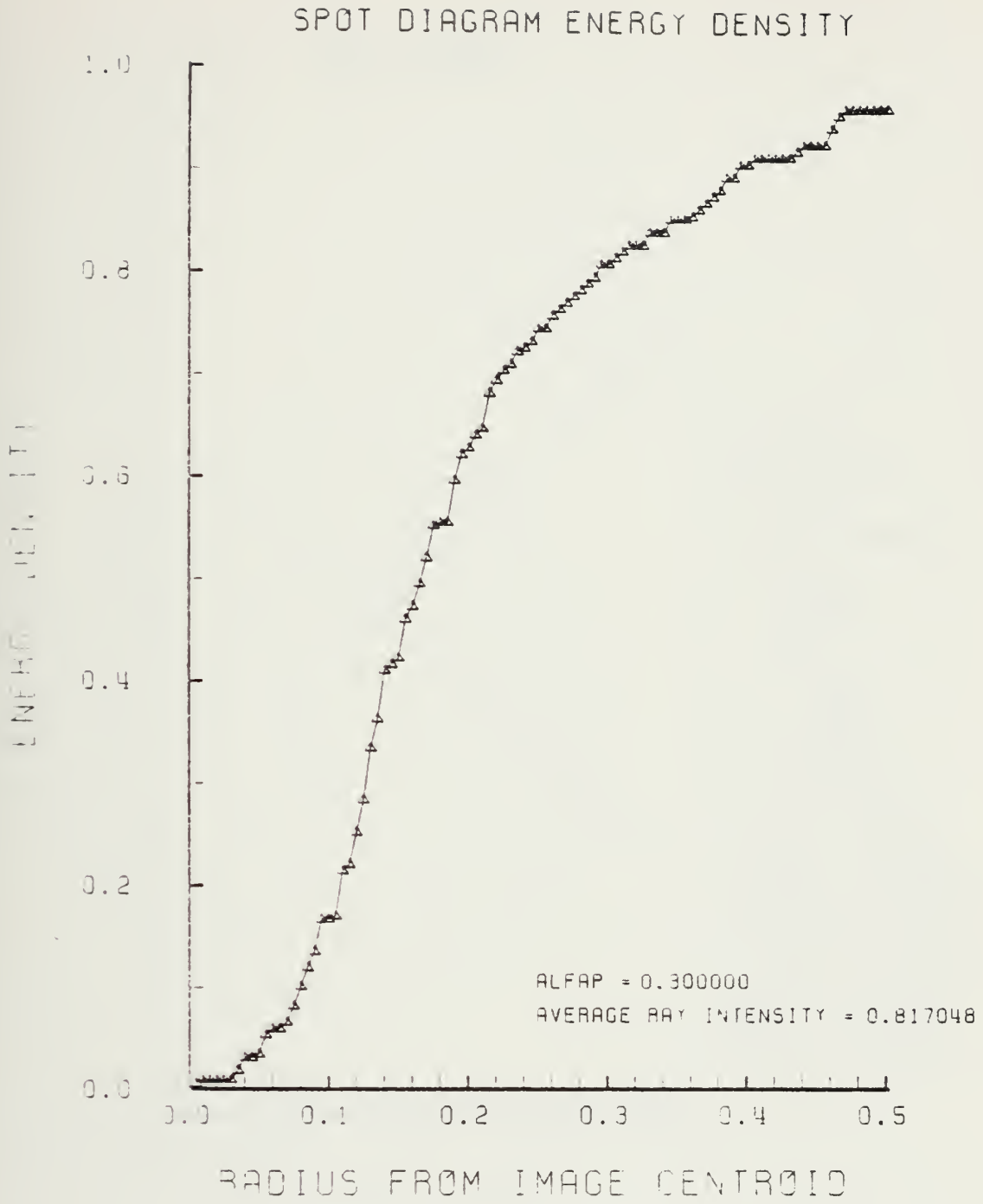

Figure E-28. Encircled Energy of Figure E-27

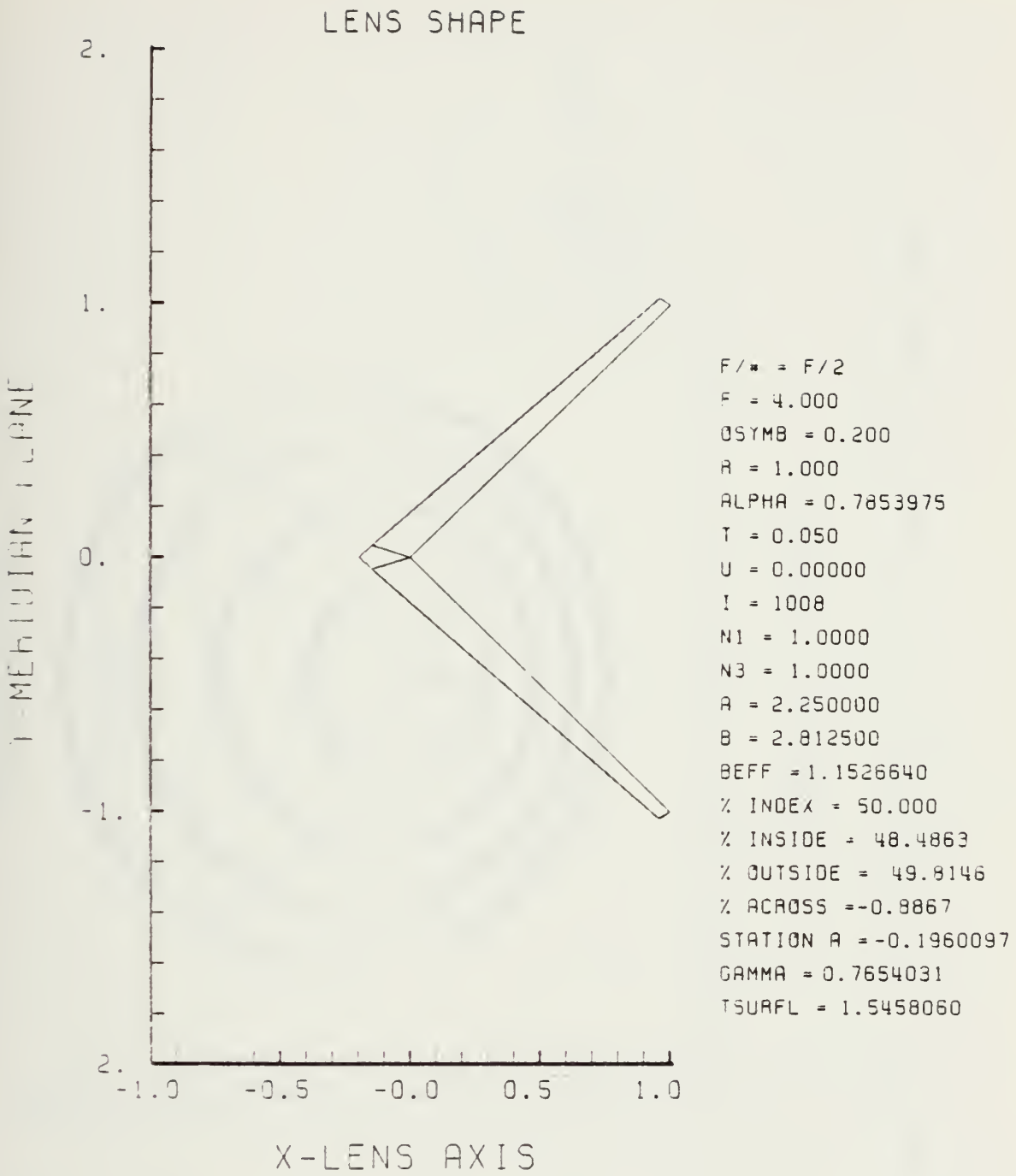

Figure E-29. GRIN Lens Shape at +50%, OB = 0.20, a = 2.25

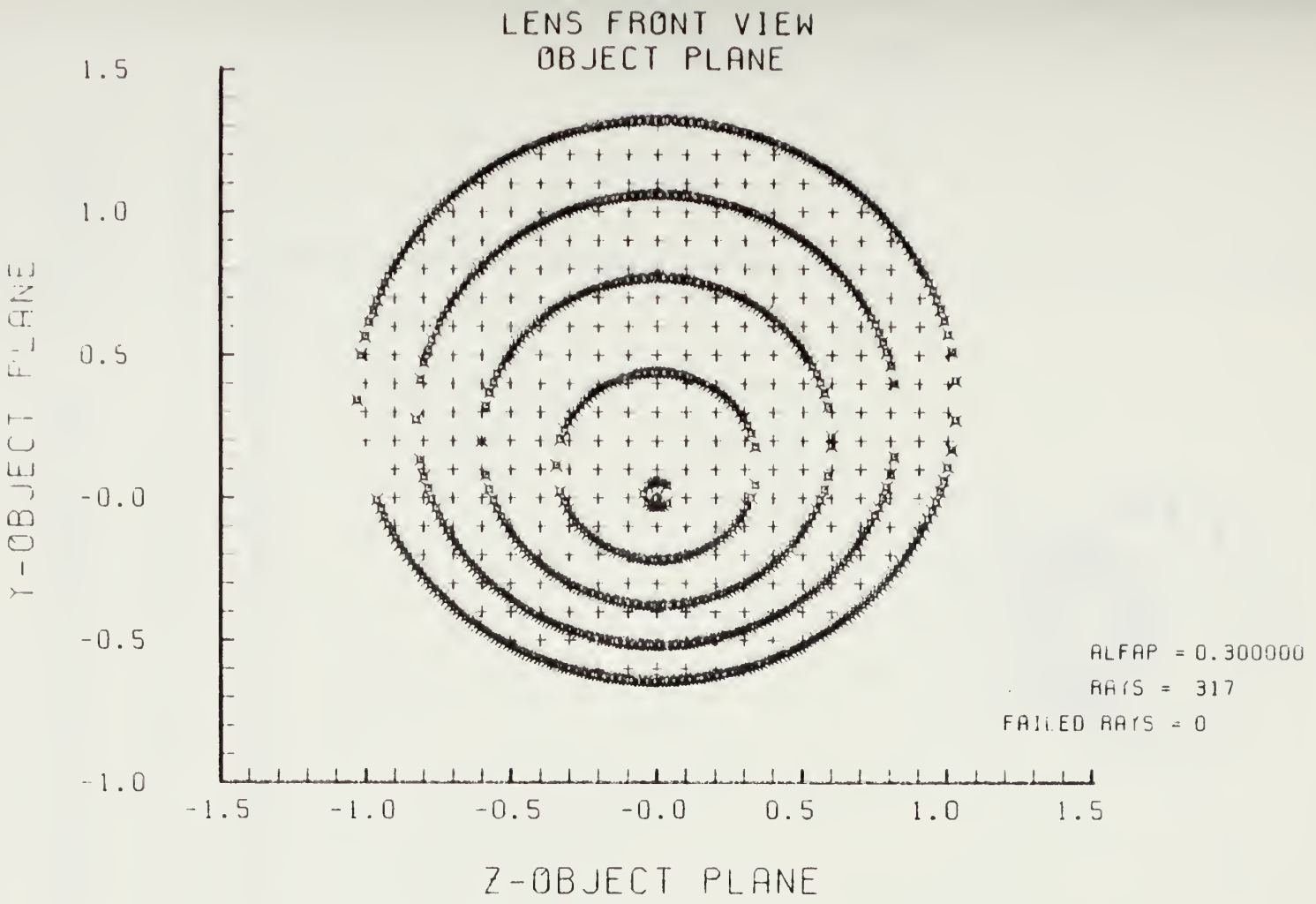

Figure E-30. Grid Plane at $\alpha_p = 0.3$ for Lens of Figure E-29

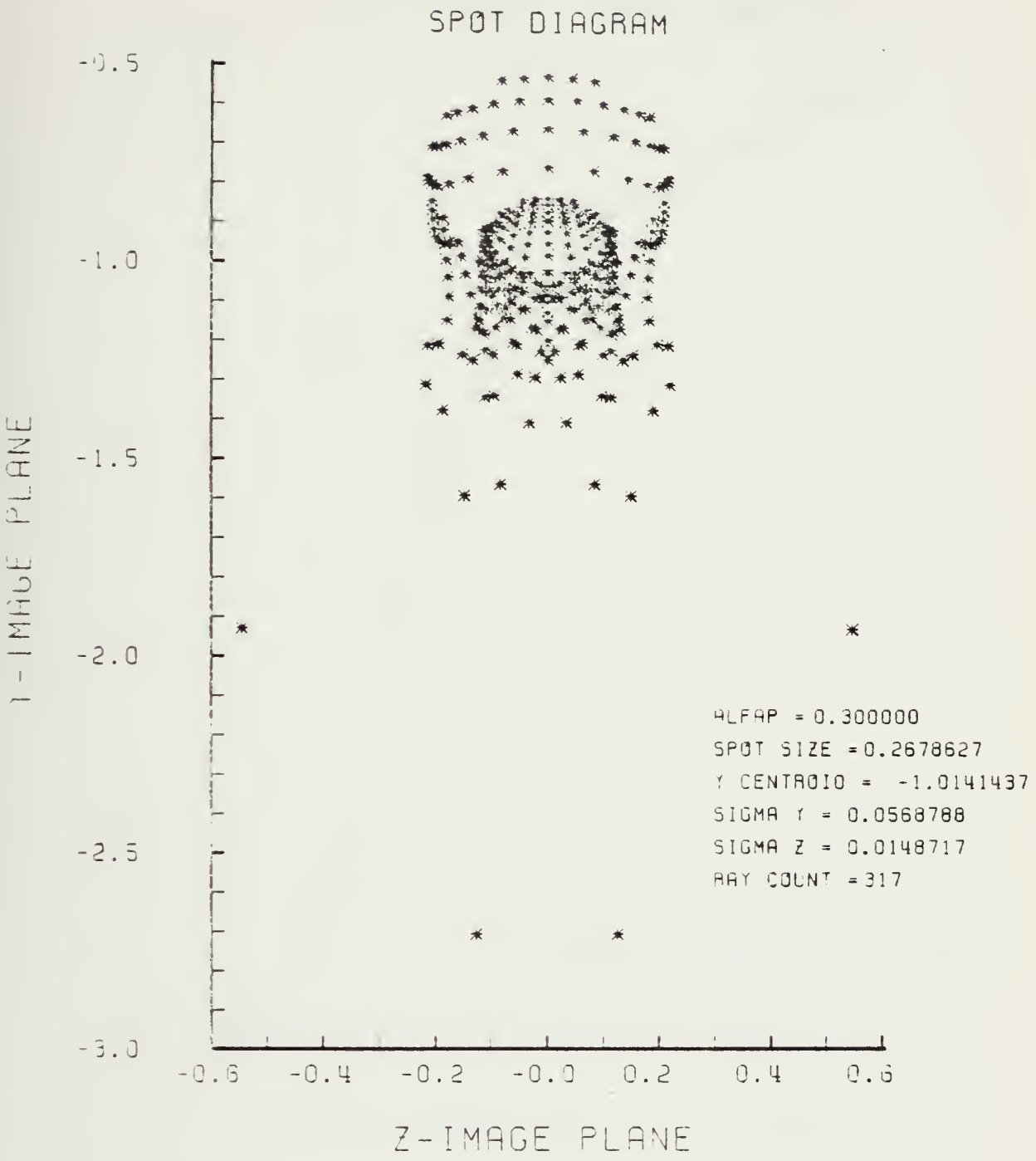

Figure E-31. Spot Diagram for Grid of Figure E-30

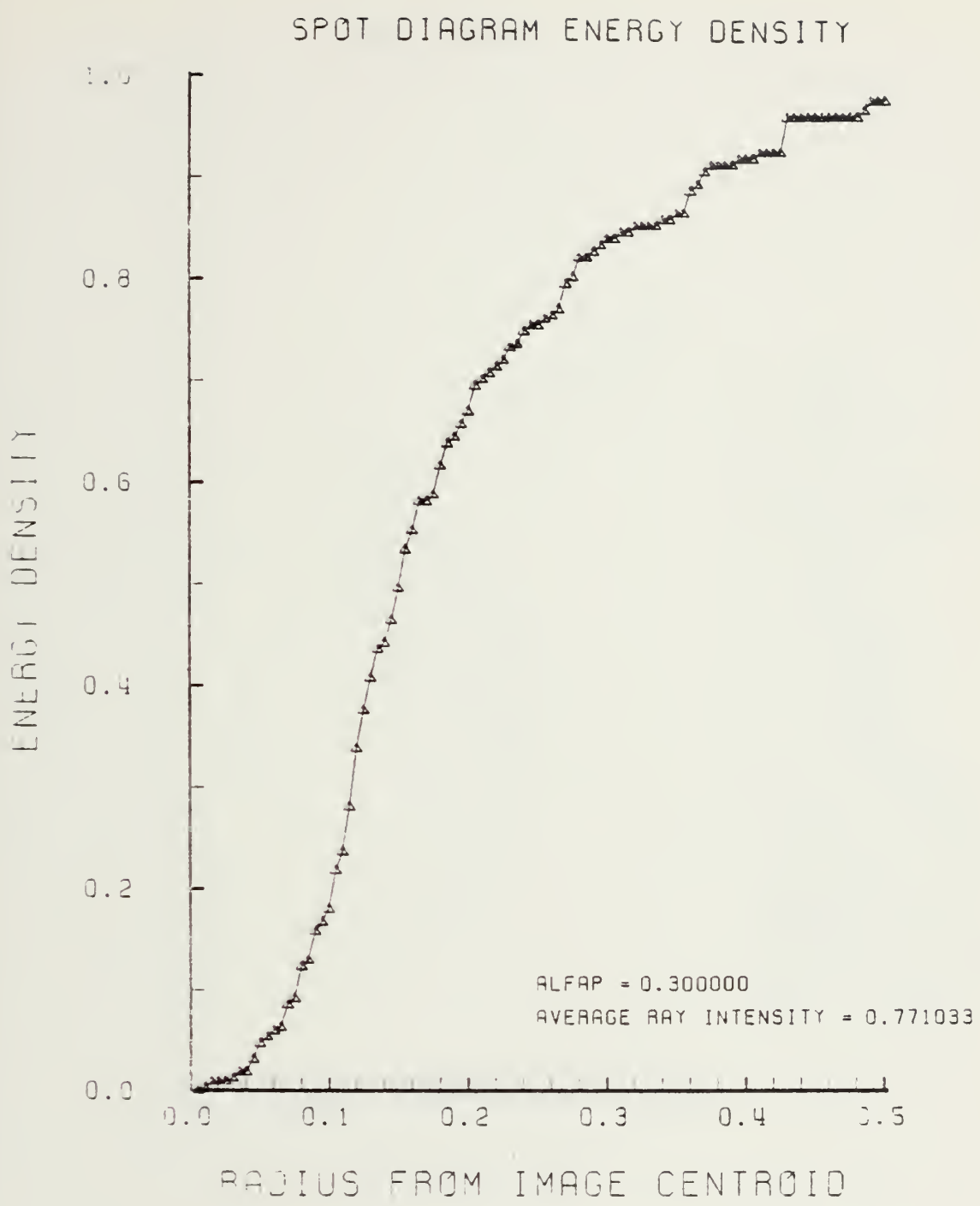

Figure E-32. Encircled Energy of Figure E-31

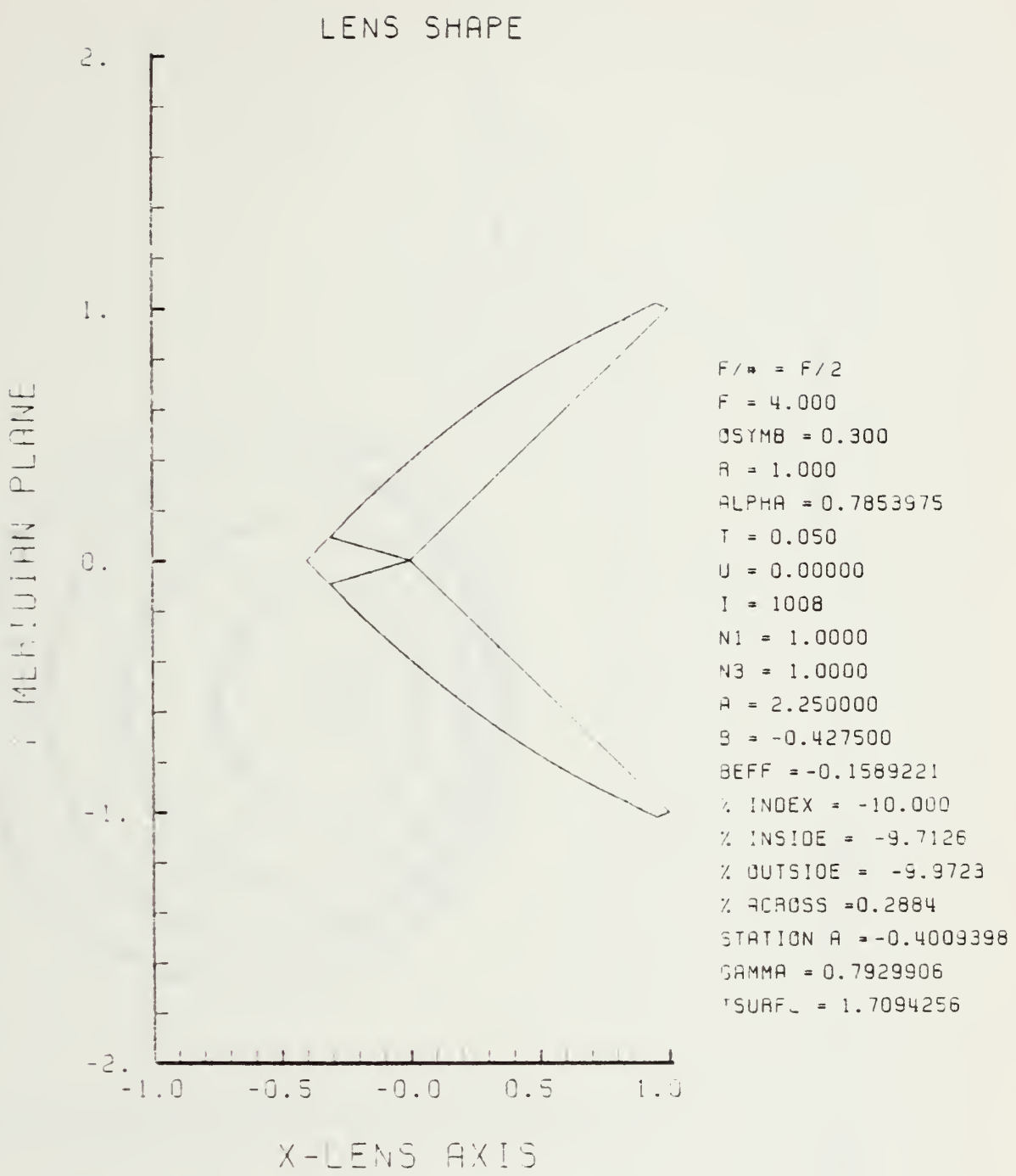

Figure E-33. GRIN Lens Shape at -10%, OB = 0.30, a = 2.25

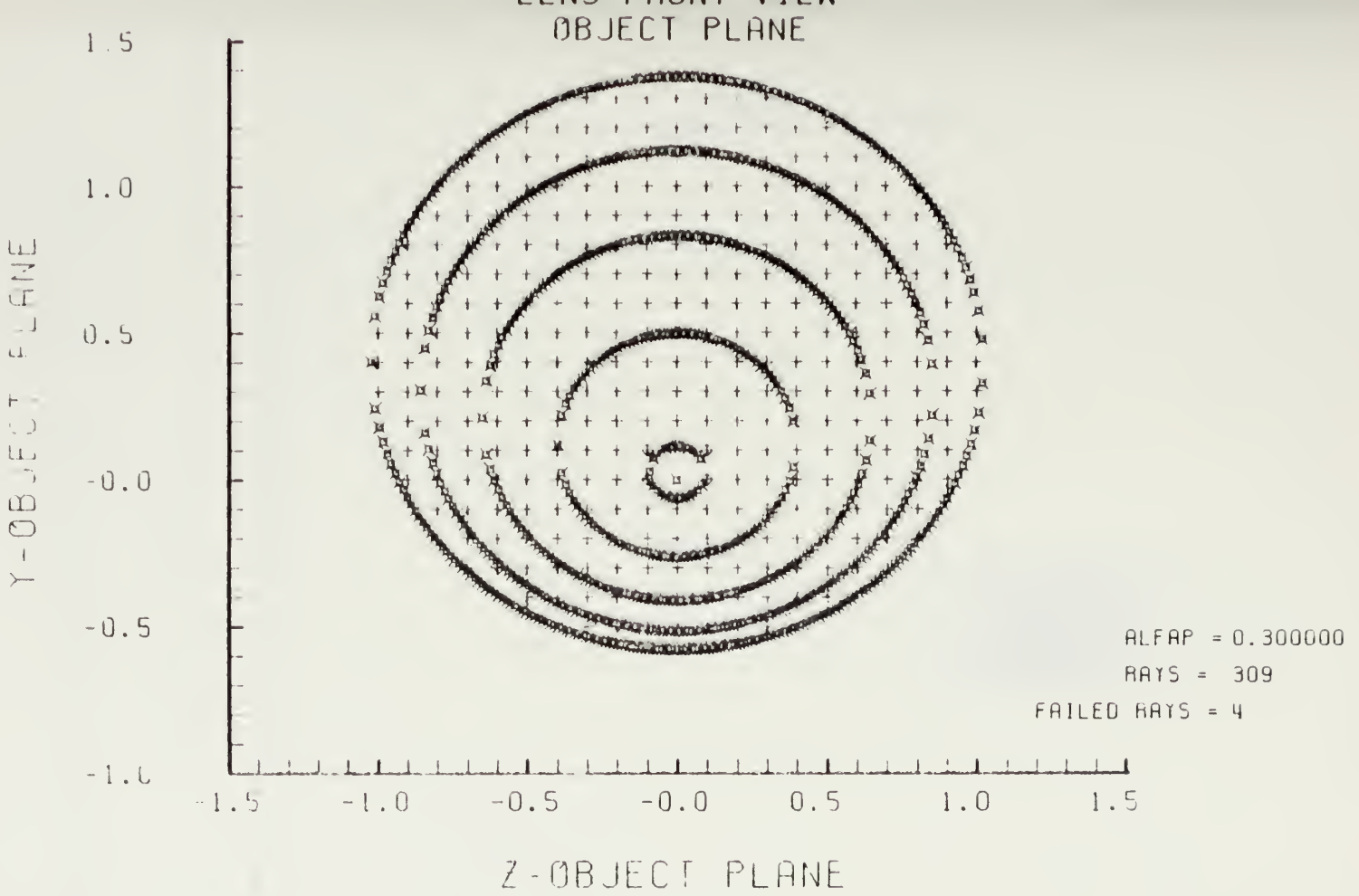

Figure E-34. Grid Plane at α_p = 0.3 for Lens of Figure E-33

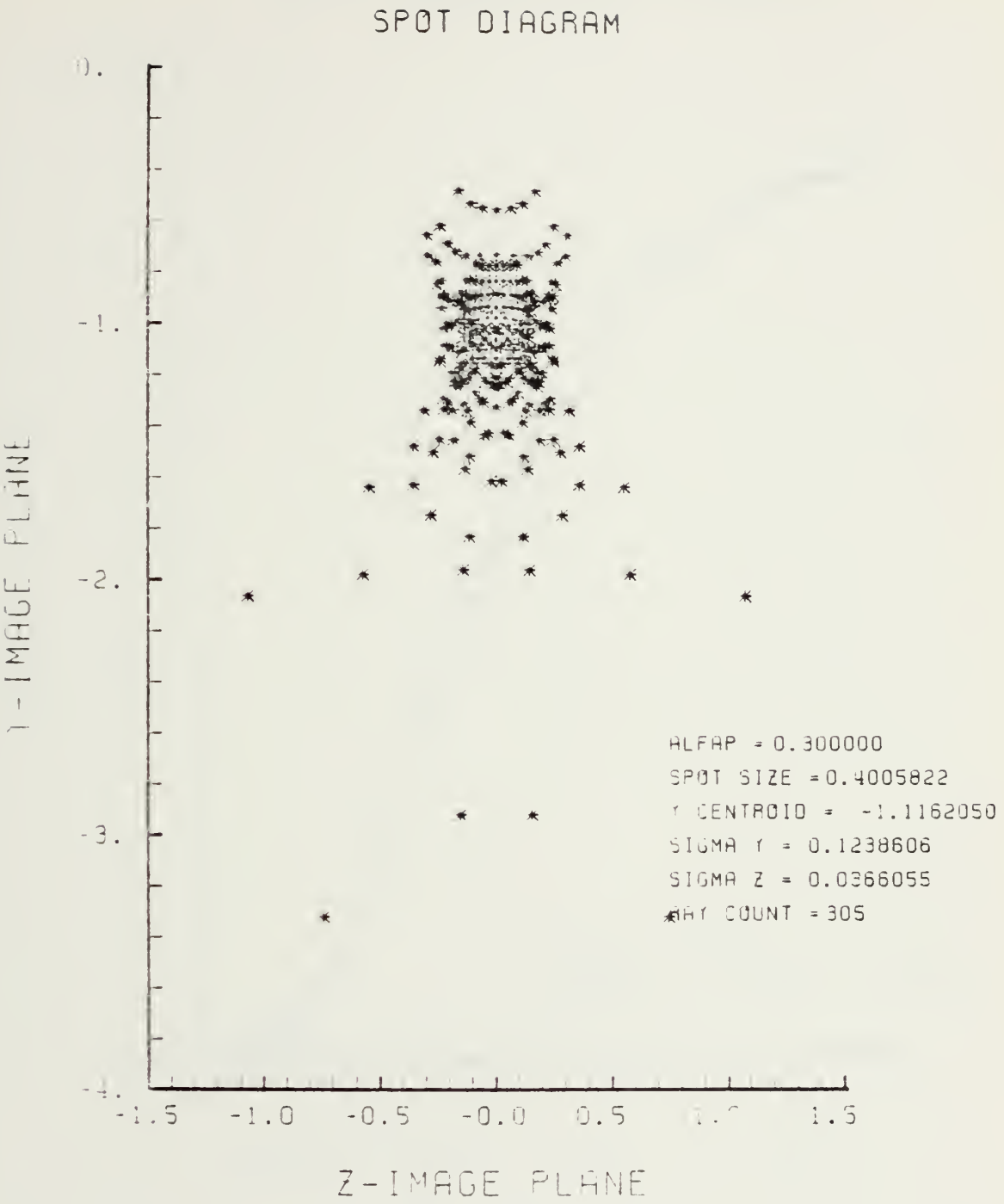

Figure E-35. Spot Diagram for Grid of Figure E-34

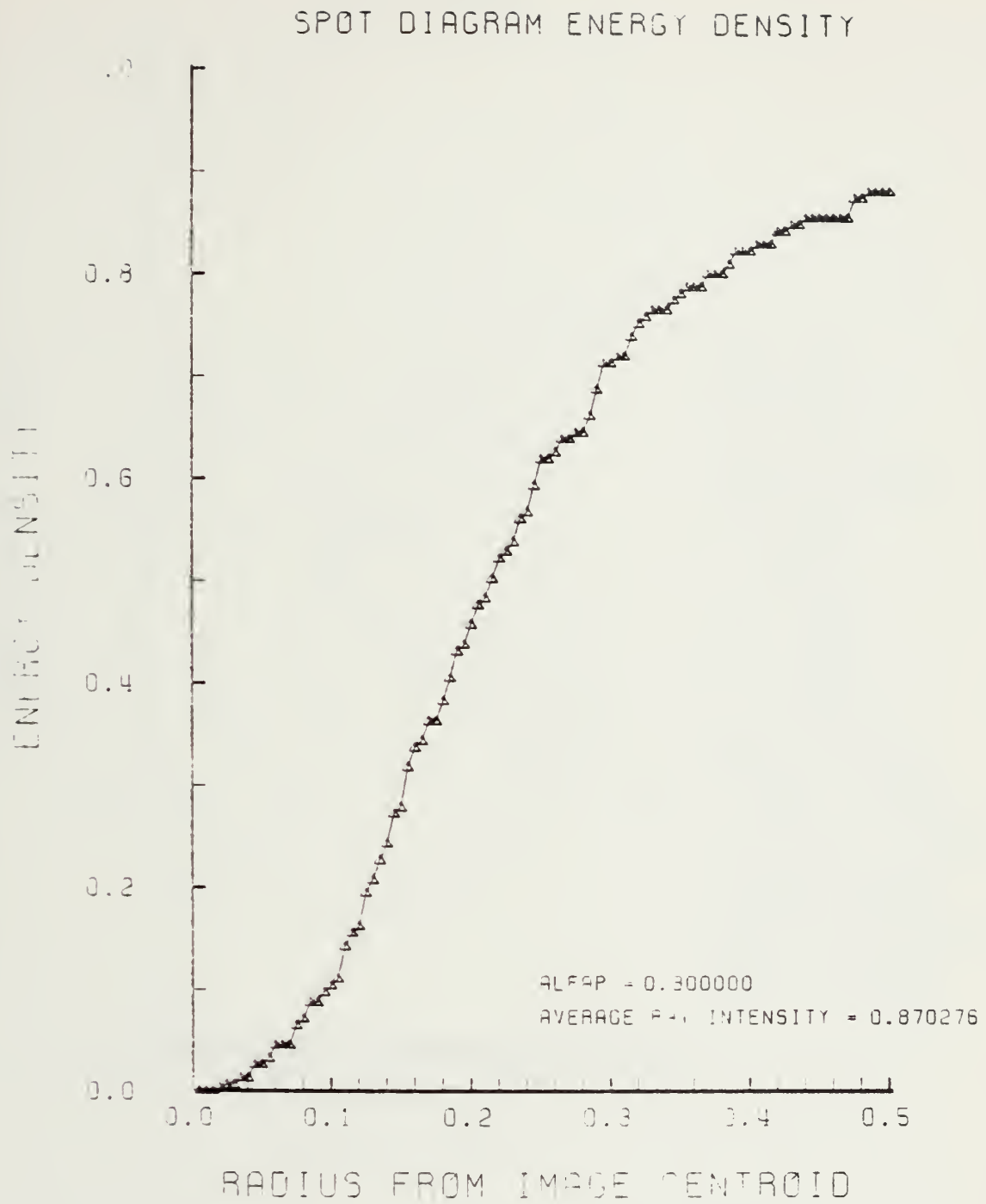

Figure E-36. Encircled Energy of Figure E-35

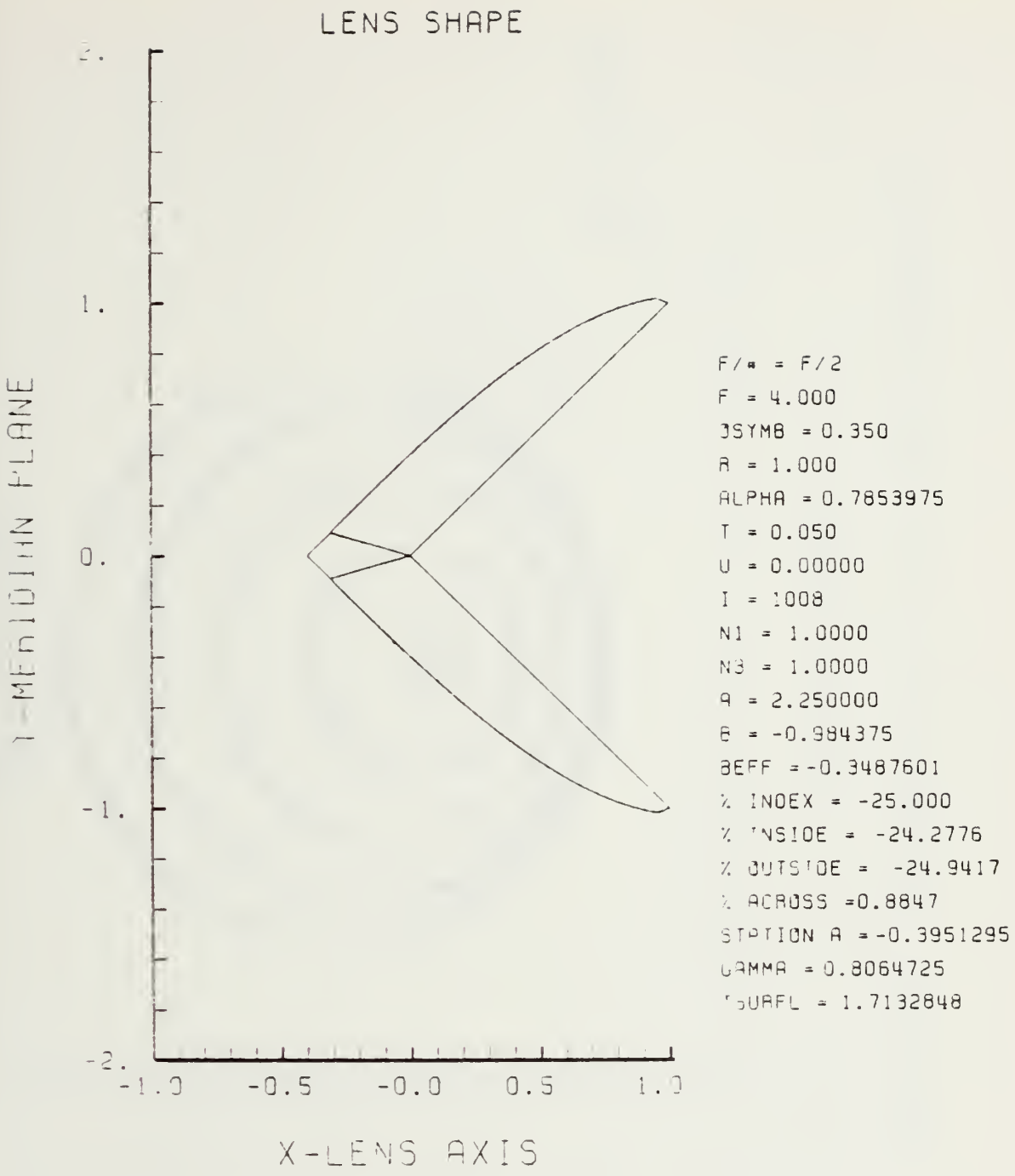

Figure E-37. GRIN Lens Shape at -25%, OB = 0.35, a = 2.25

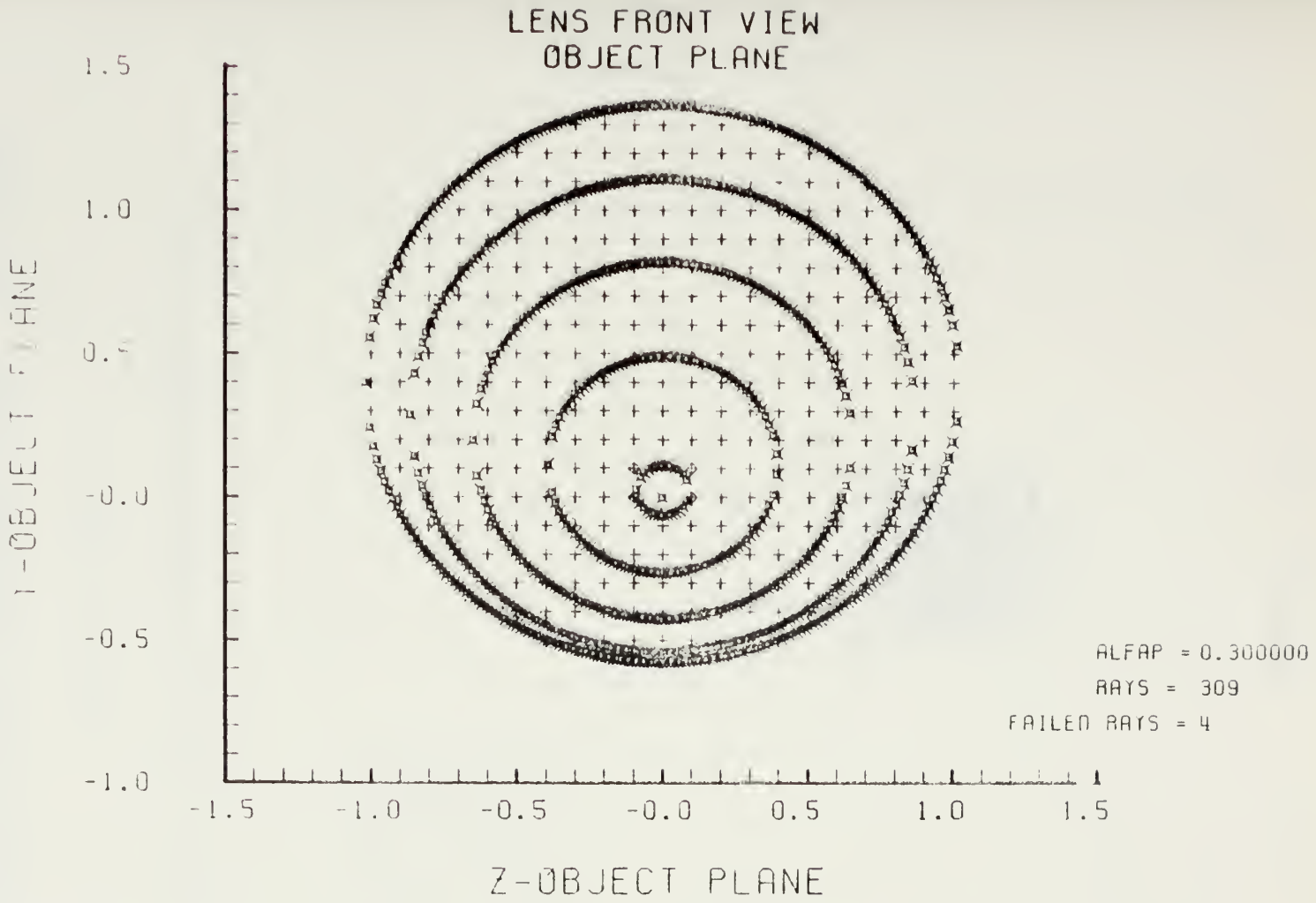

Figure E-38. Grid Plane at $\alpha_p = 0.3$ for Lens of Figure E-37

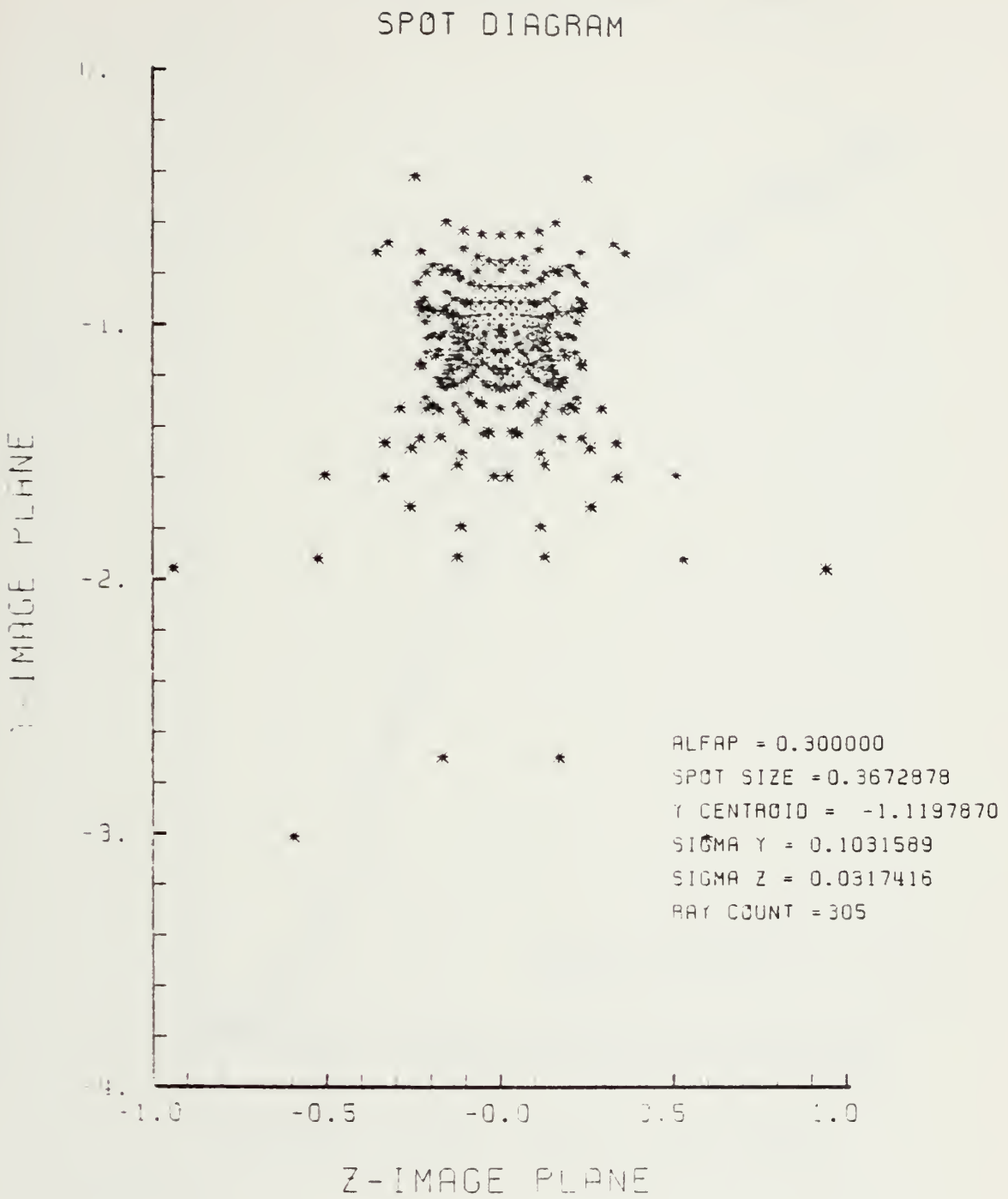

Figure E-39. Spot Diagram for Grid of Figure E-38

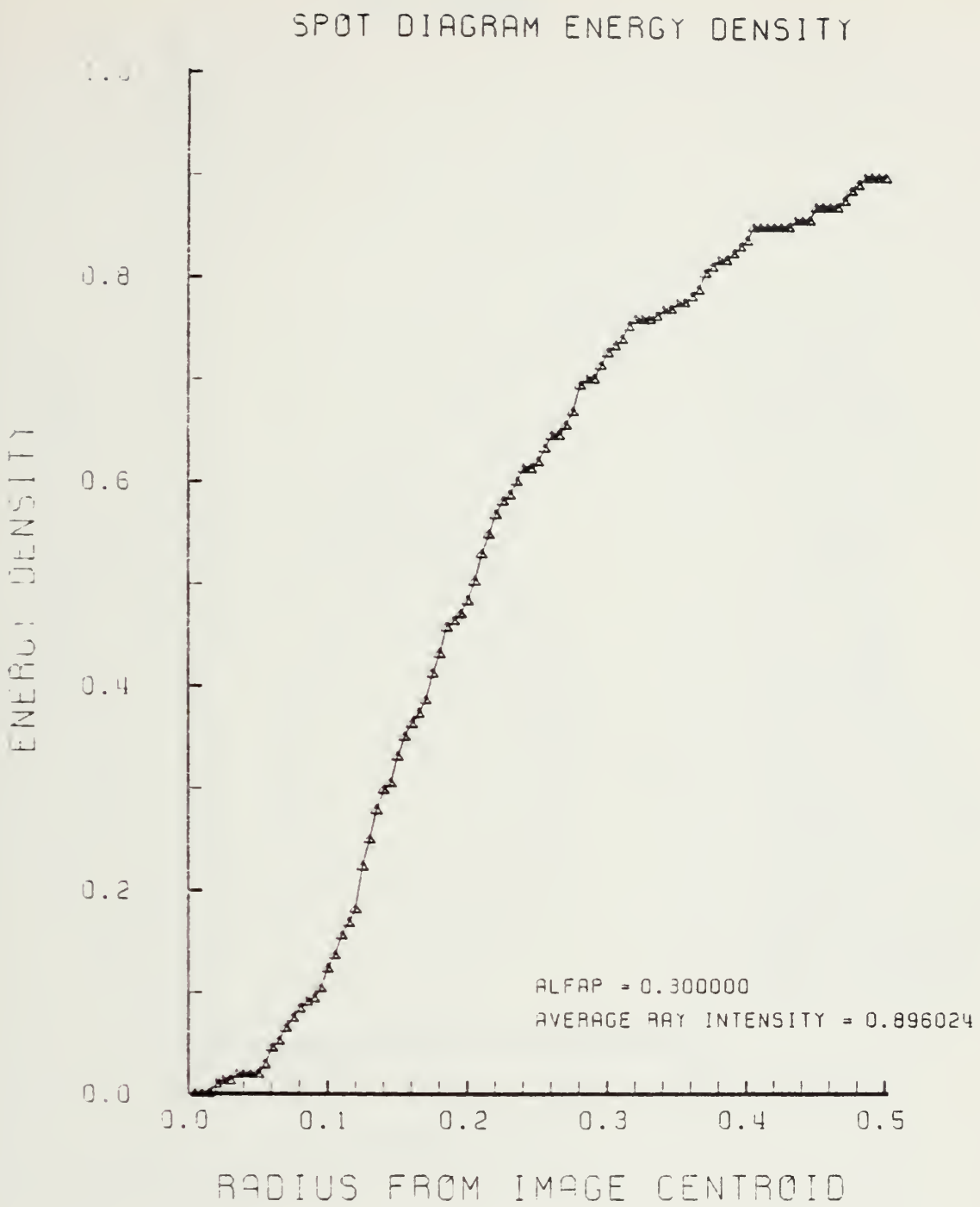

Figure E-40. Encircled Energy of Figure E-39

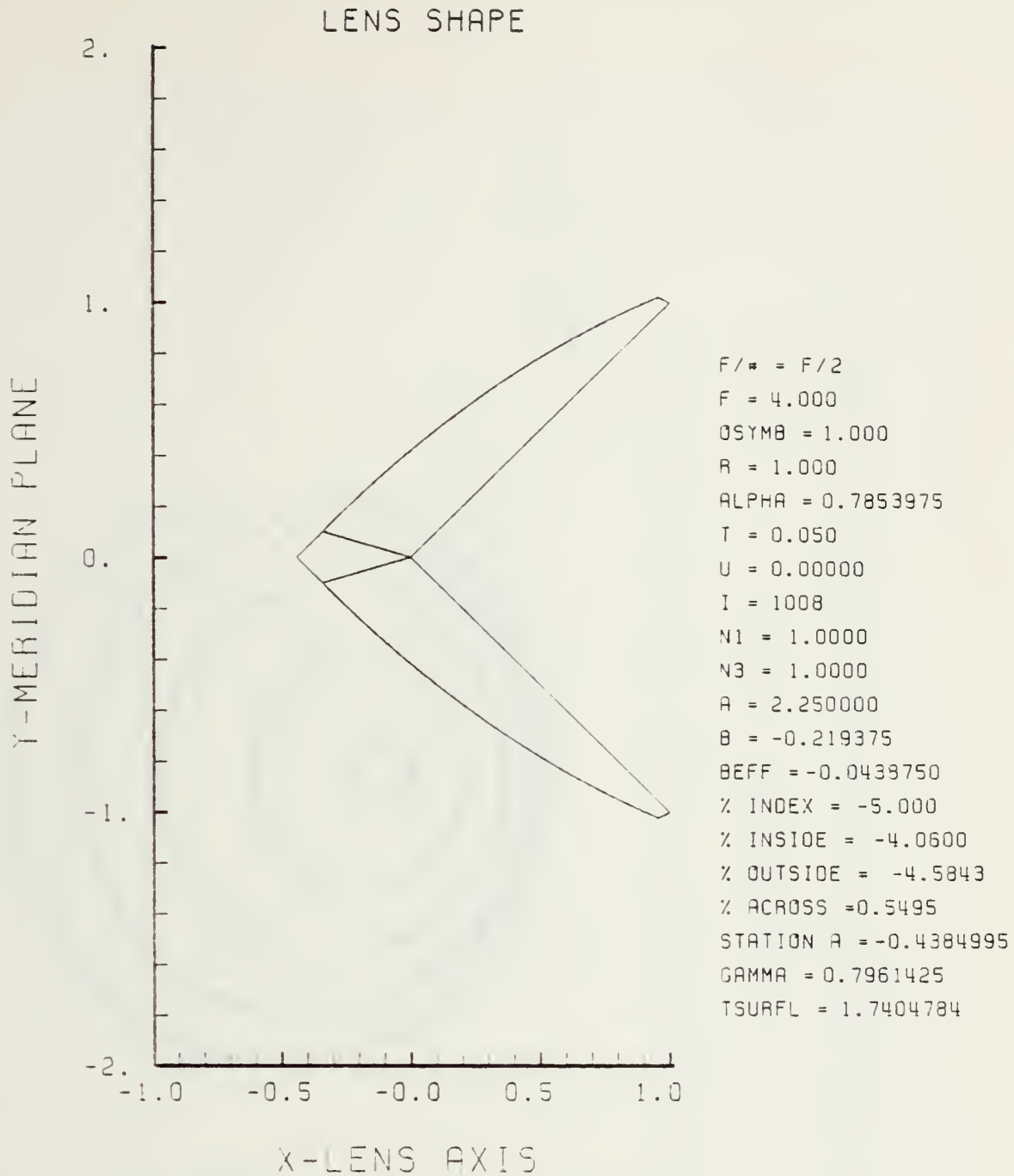

Figure E-41. GRIN Lens Shape at -5%, OB = 1.00, a = 2.25

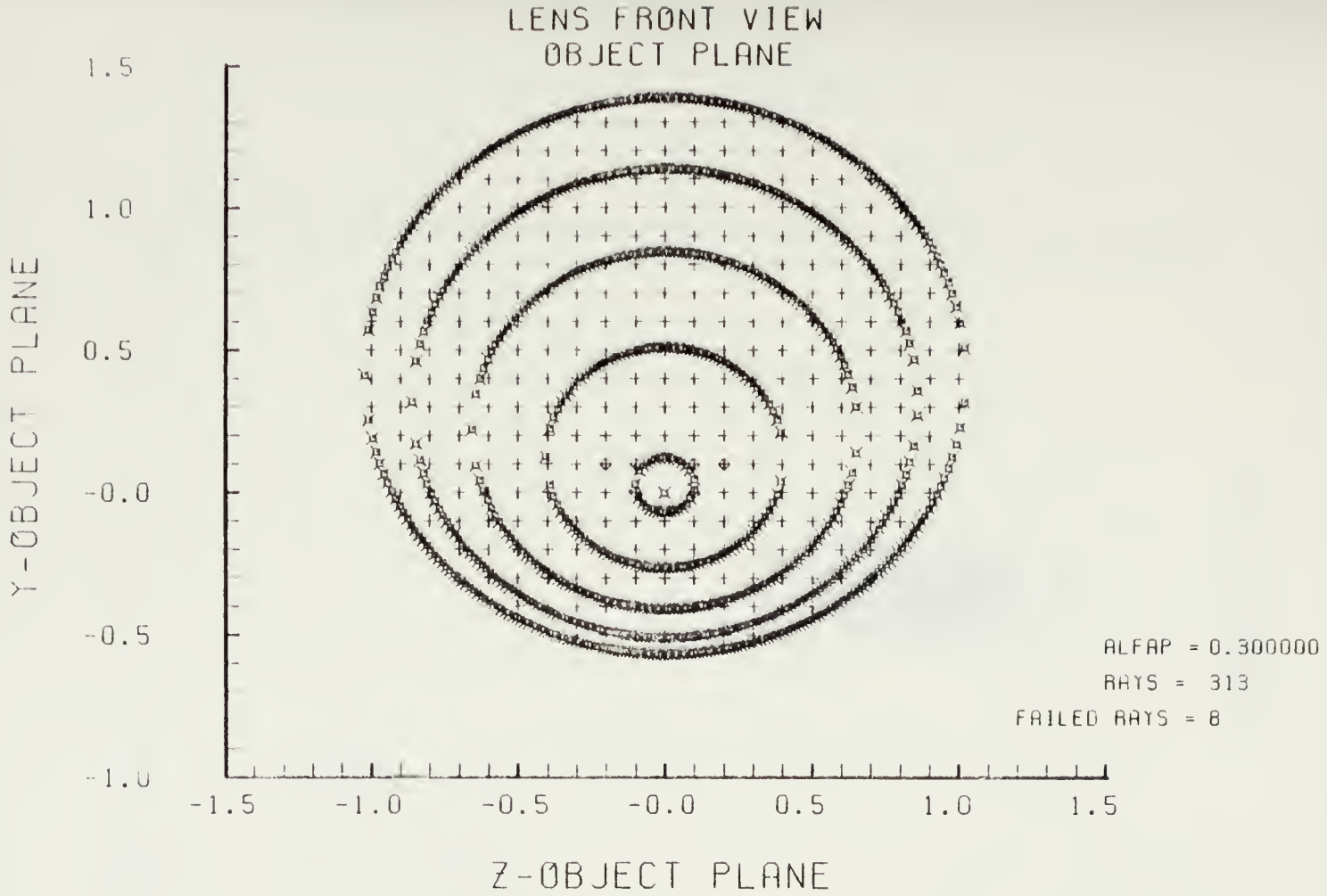

Figure E-42. Grid Plane at α_p = 0.3 for Lens of Figure E-41

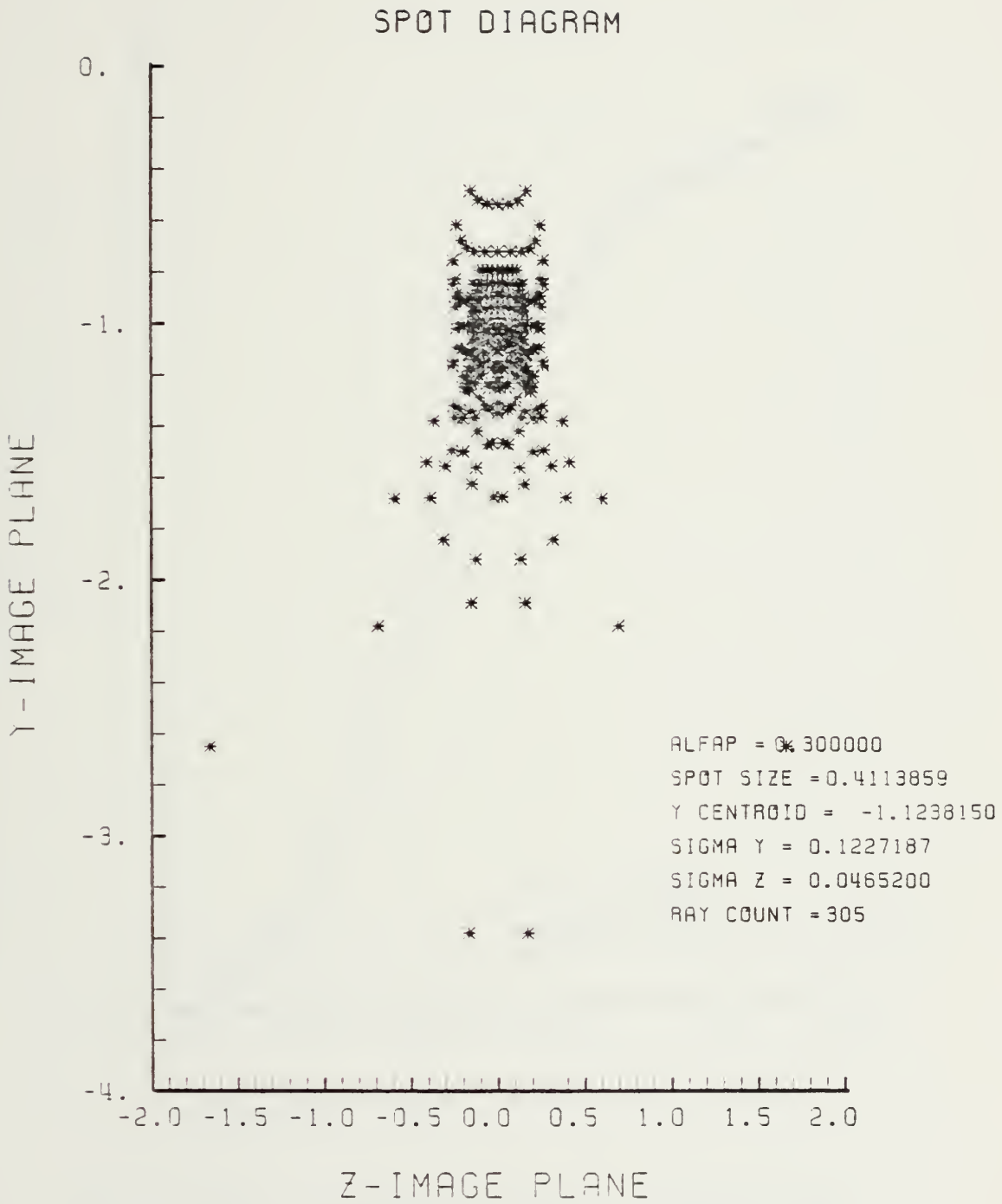

Figure E-43. Spot Diagram for Grid of Figure E-42

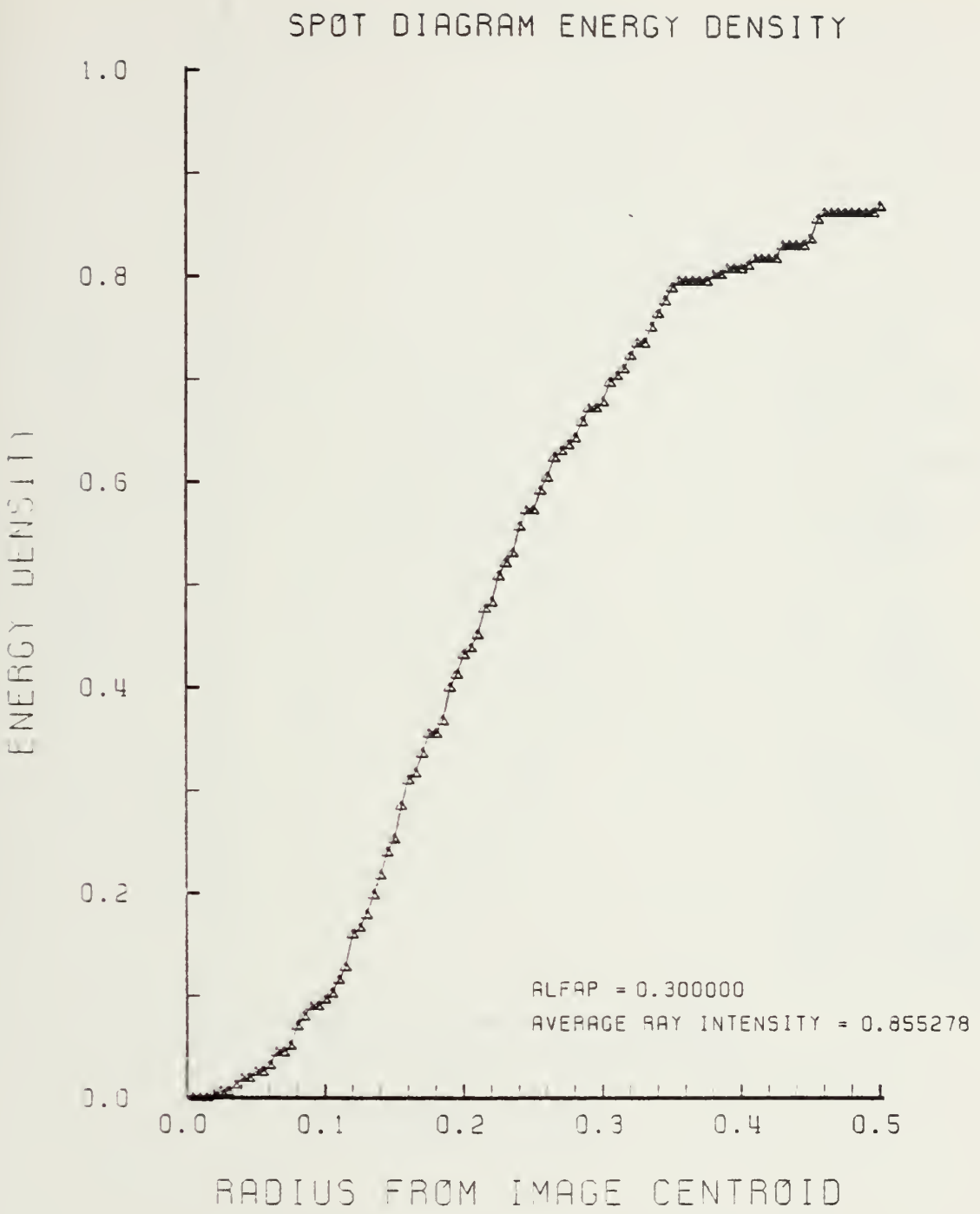

Figure E-44. Encircled Energy of Figure E-43

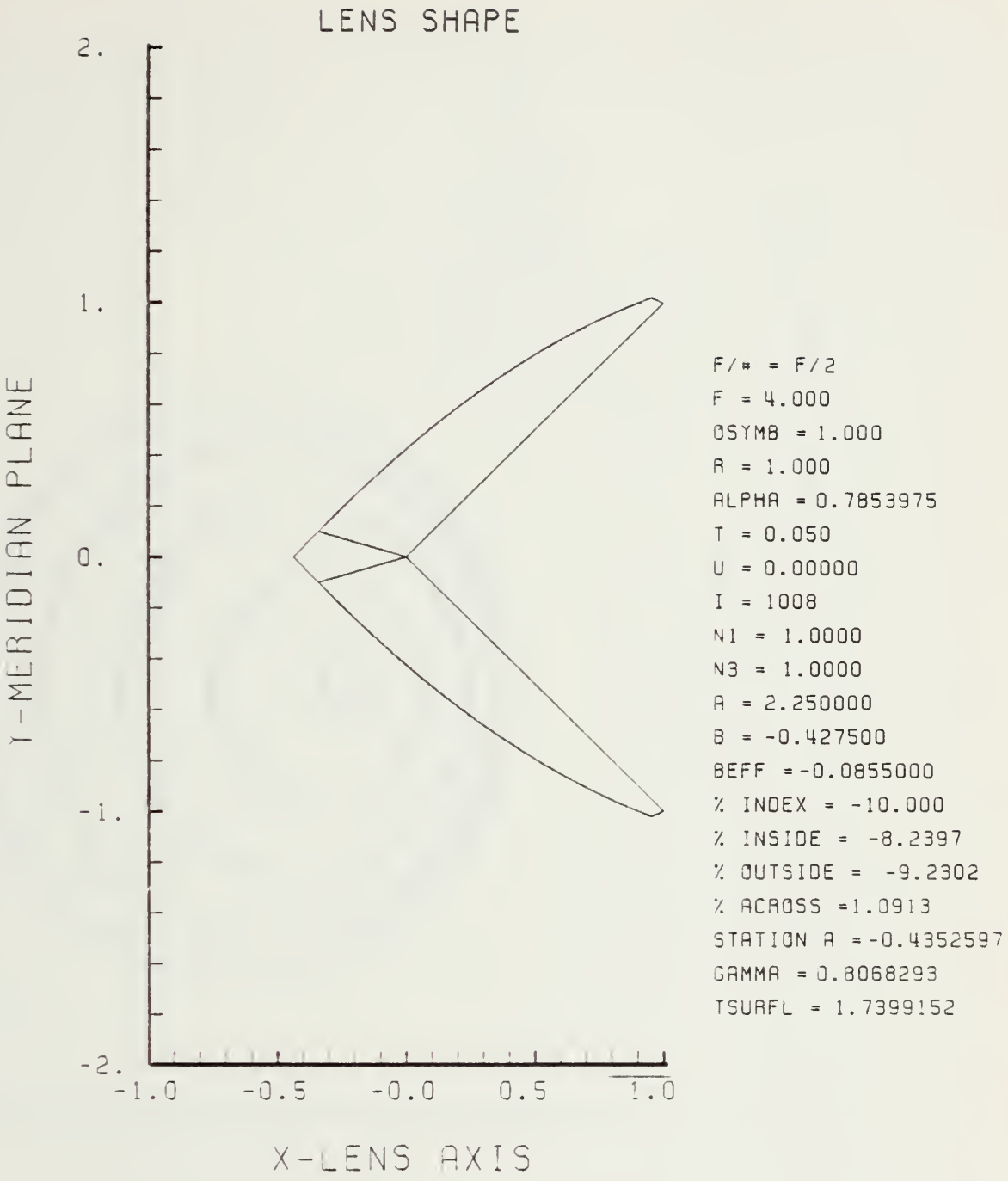

Figure E-45. GRIN Lens Shape at -10%, OB = 1.00
a = 2.25

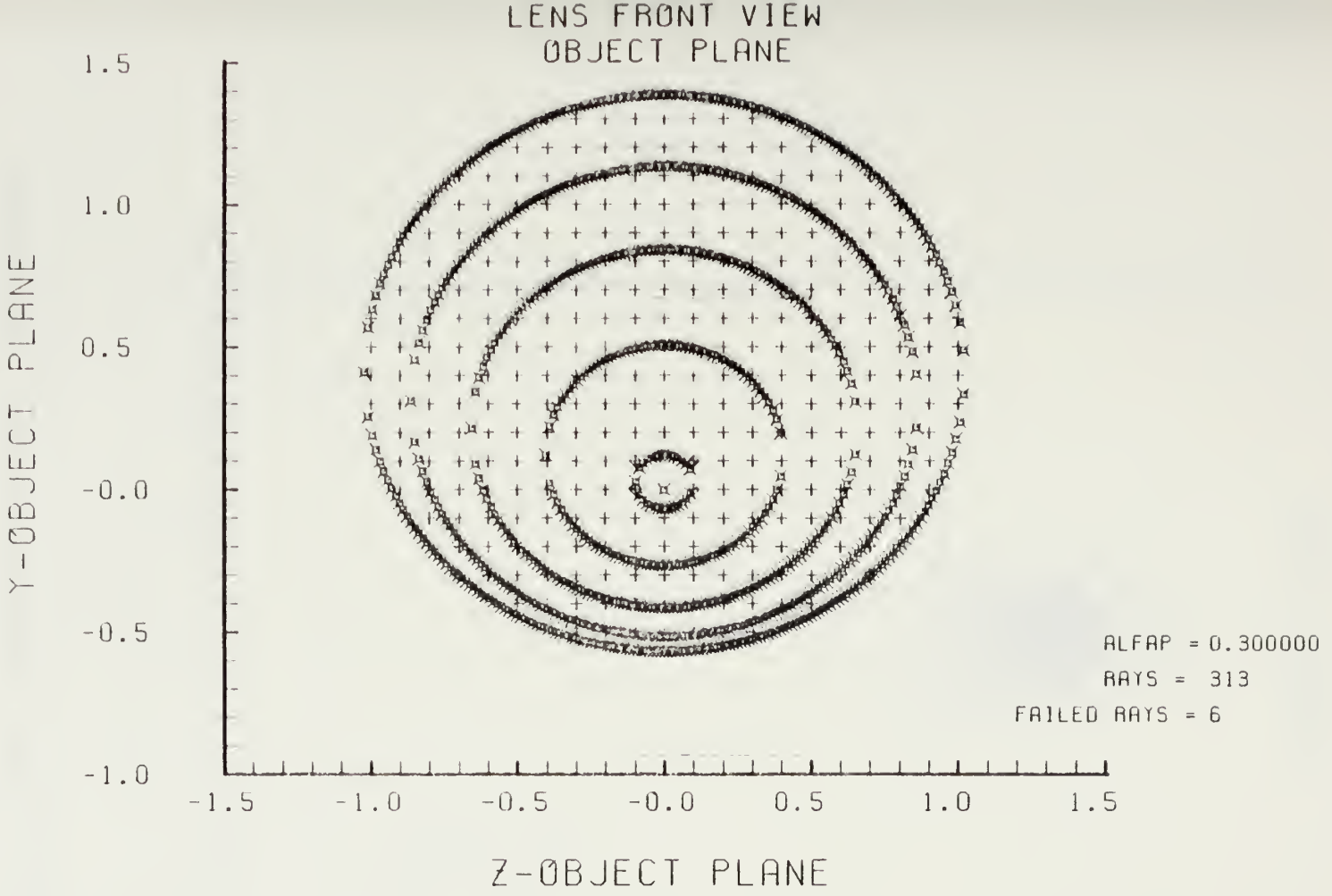

Figure E-46. Grid Plane at $\alpha_p = 0.3$ for Lens of Figure E-45

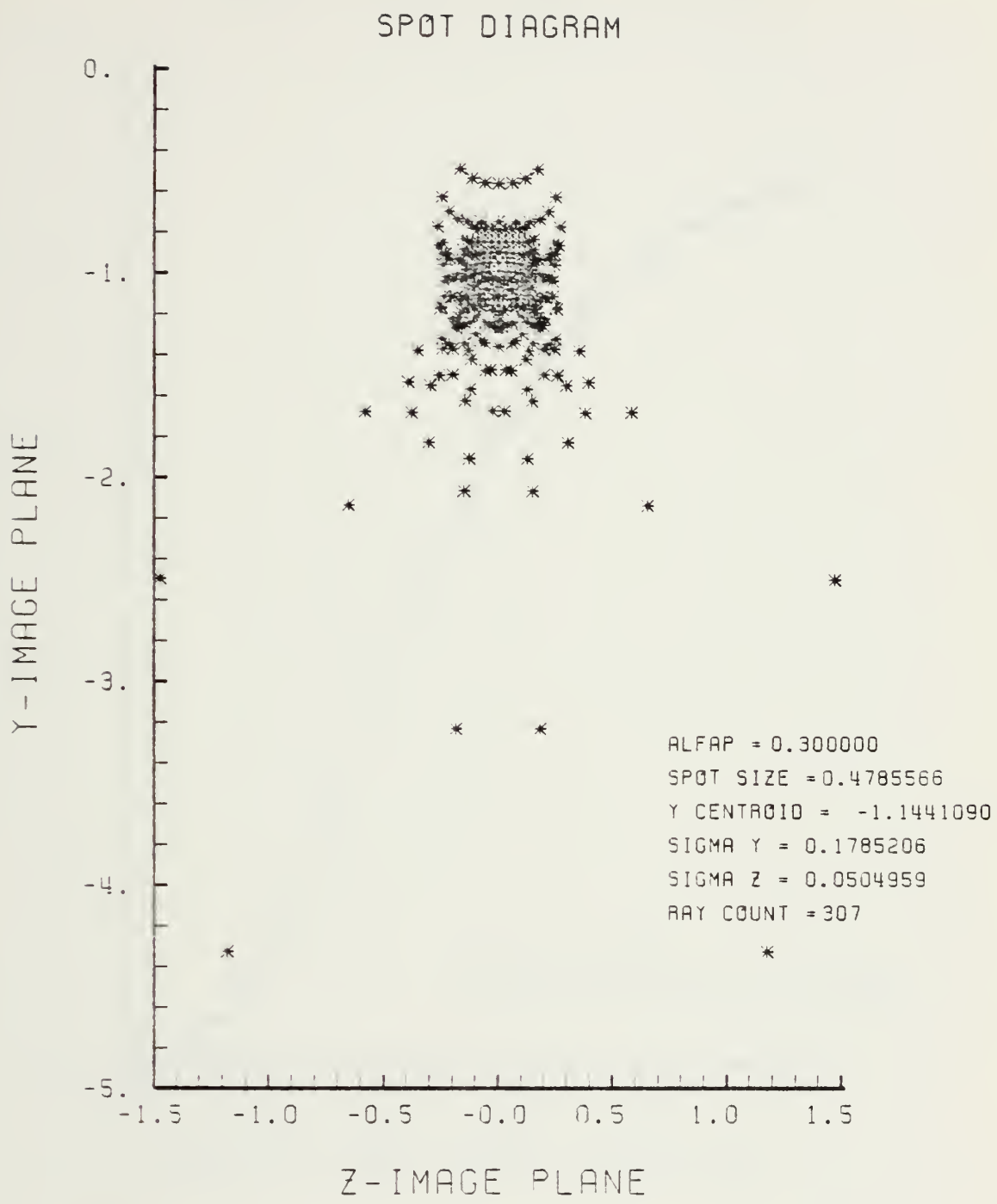

Figure E-47. Spot Diagram for Grid of Figure E-46

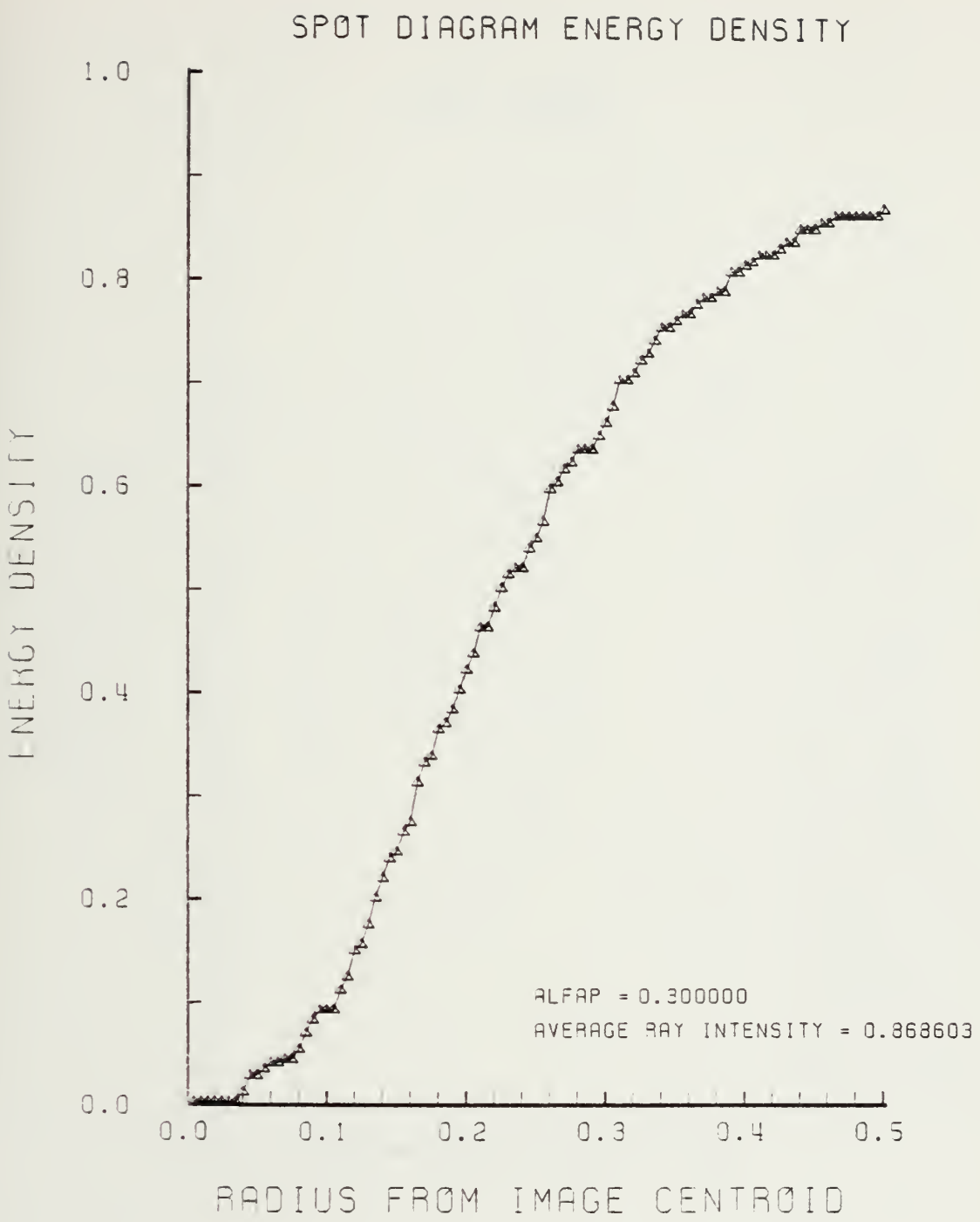

Figure E-48. Encircled Energy of Figure E-47

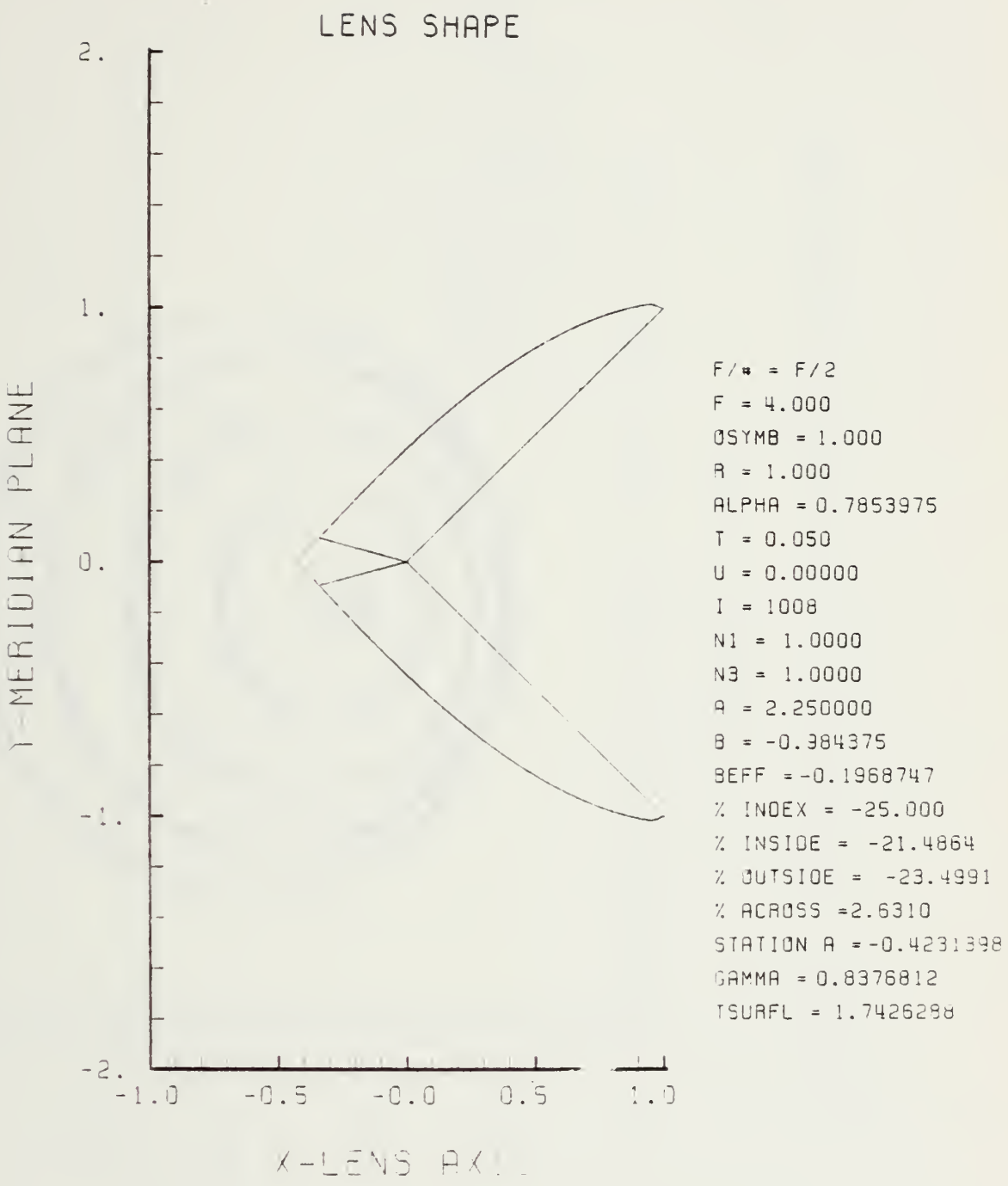

Figure E-49. GRIN Lens Shape at -25%, OB = 1.00, a = 2.25

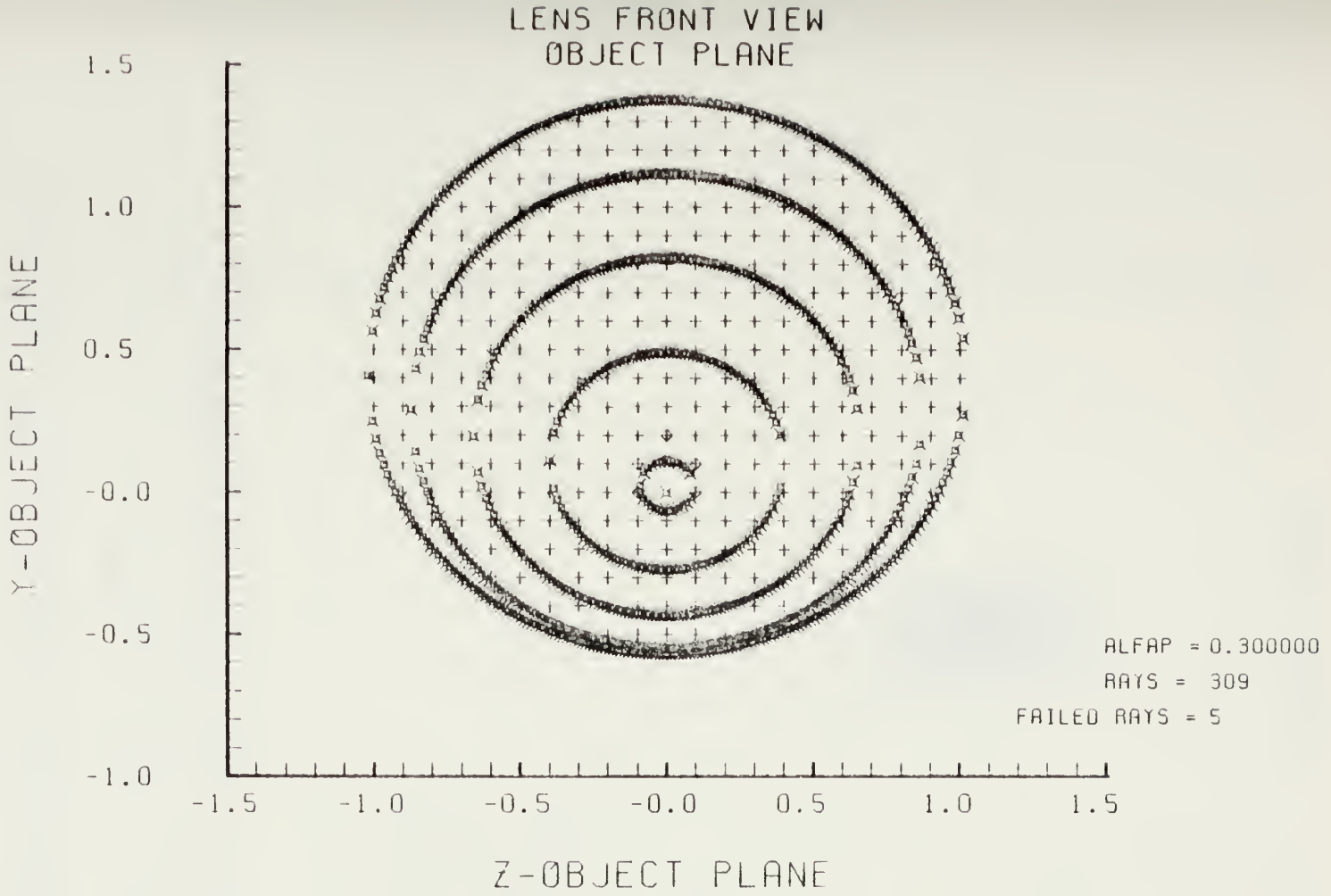

Figure E-50. Grid Plane at α_p = 0.3 for Lens of Figure E-49

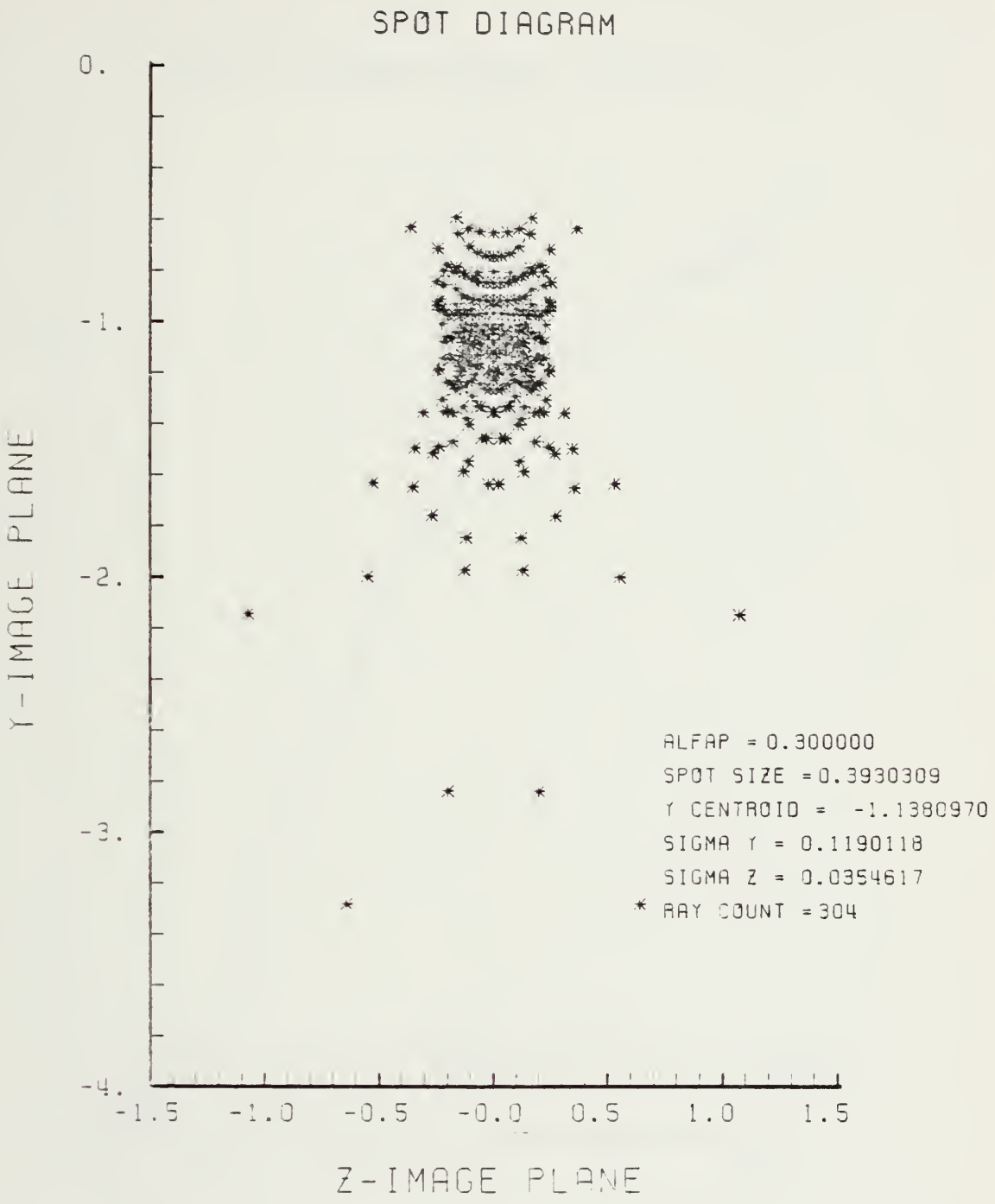

Figure E-51. Spot Diagram for Grid of Figure E-50

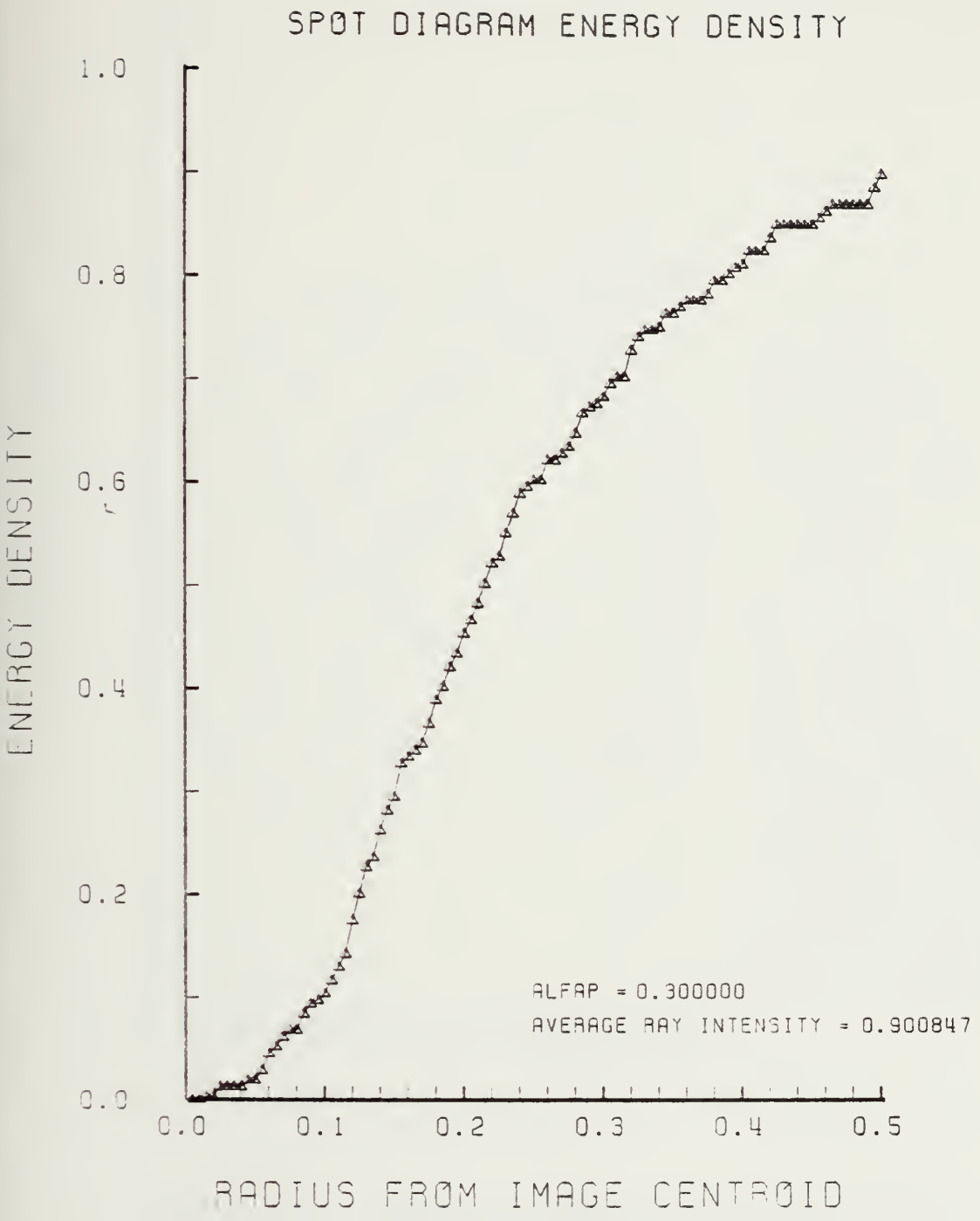

Figure E-52. Encircled Energy of Figure E-51

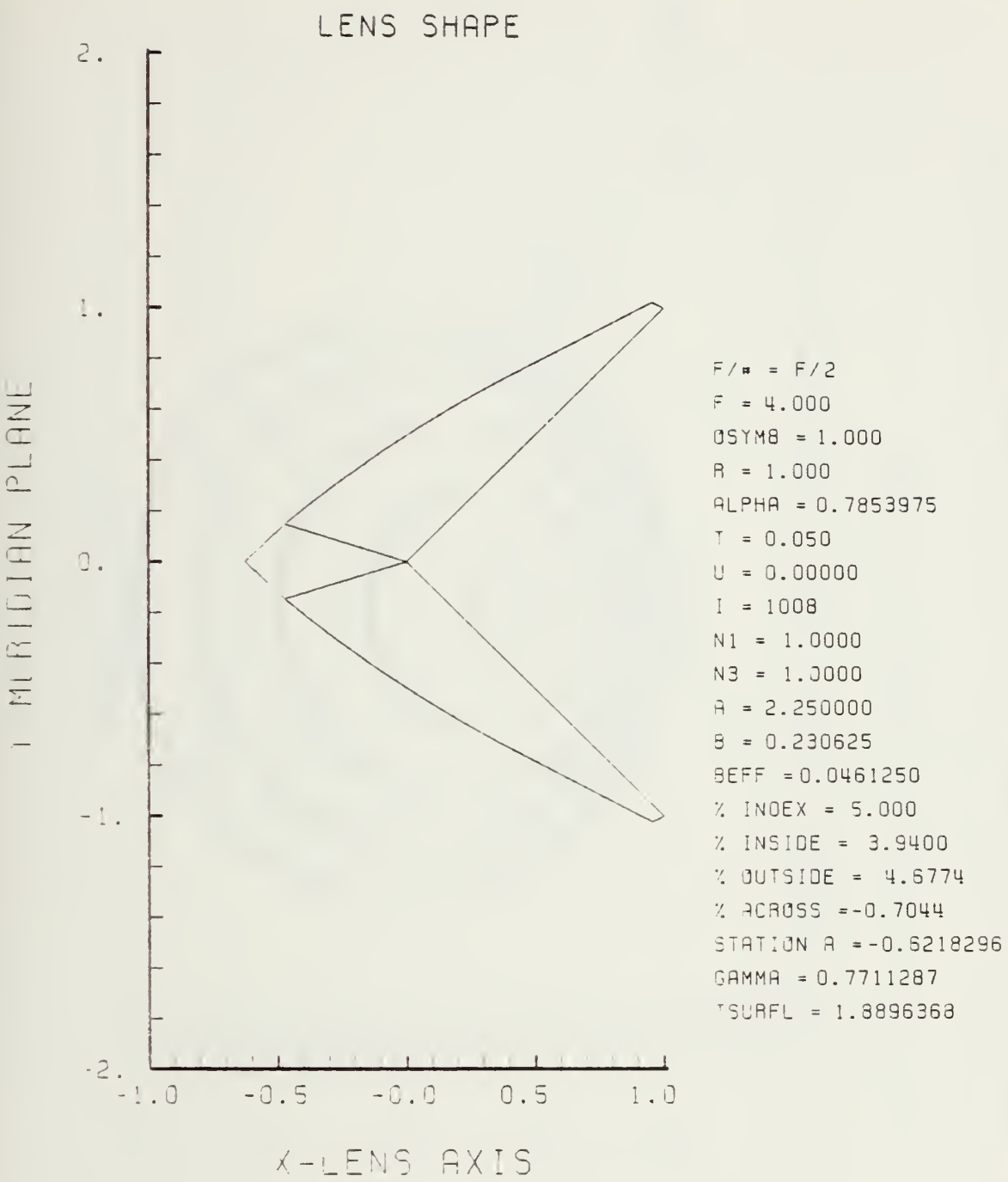

Figure E-53. GRIN Lens Shape at +5%, OB = 1.00, a = 2.25

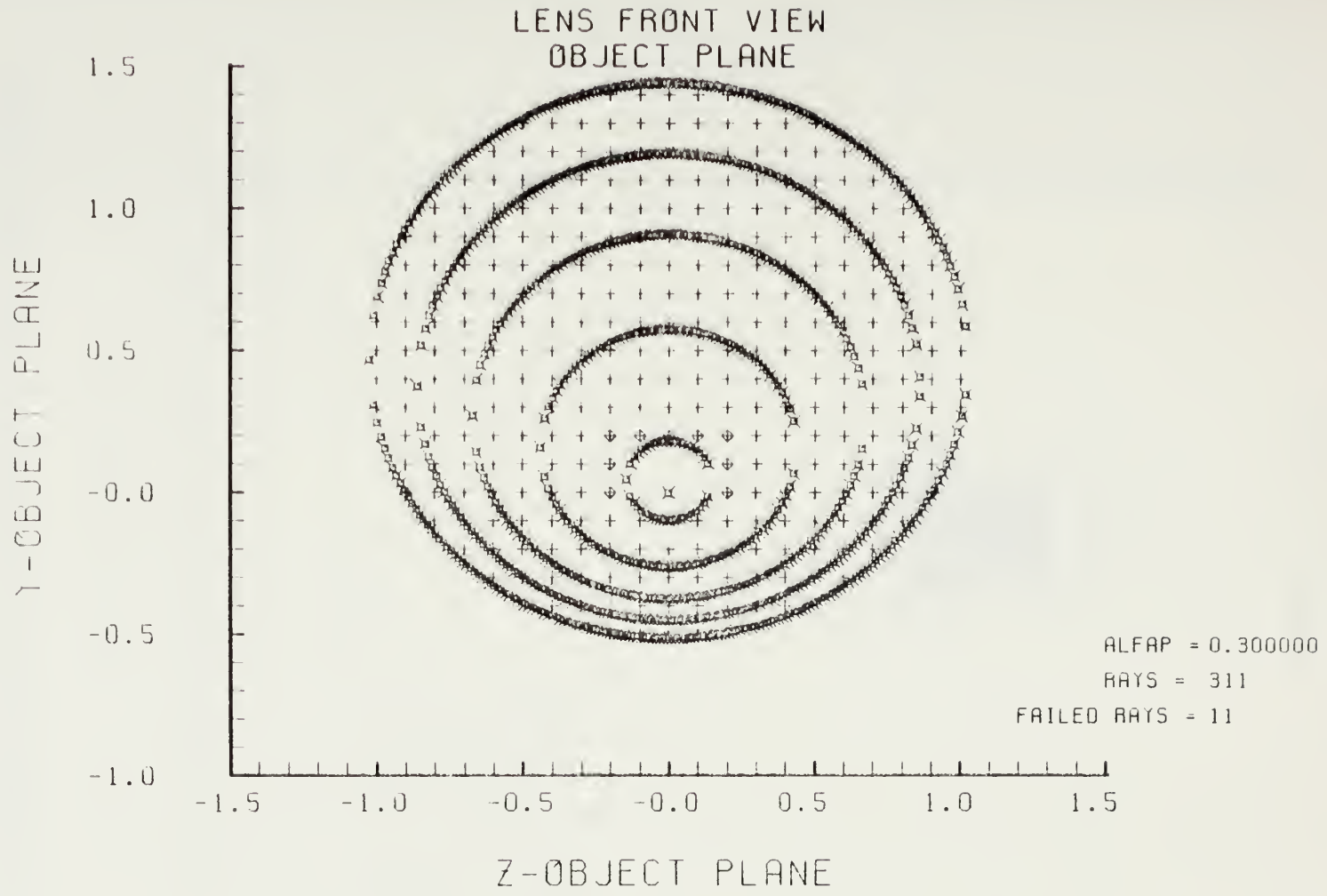

Figure E-54. Grid Plane at α_p = 0.3 for Lens of Figure E-53

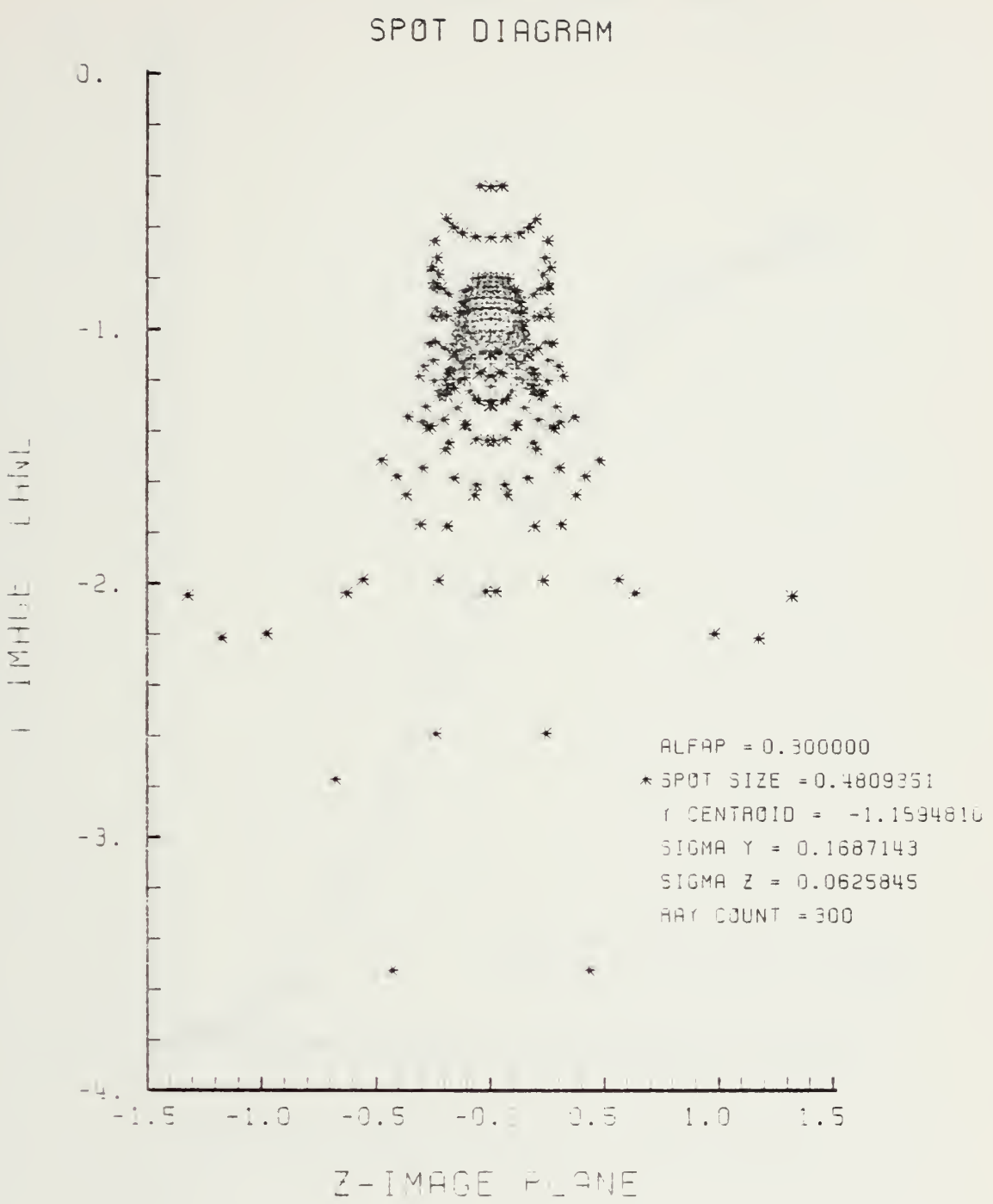

Figure E-55. Spot Diagram for Grid of Figure E-54

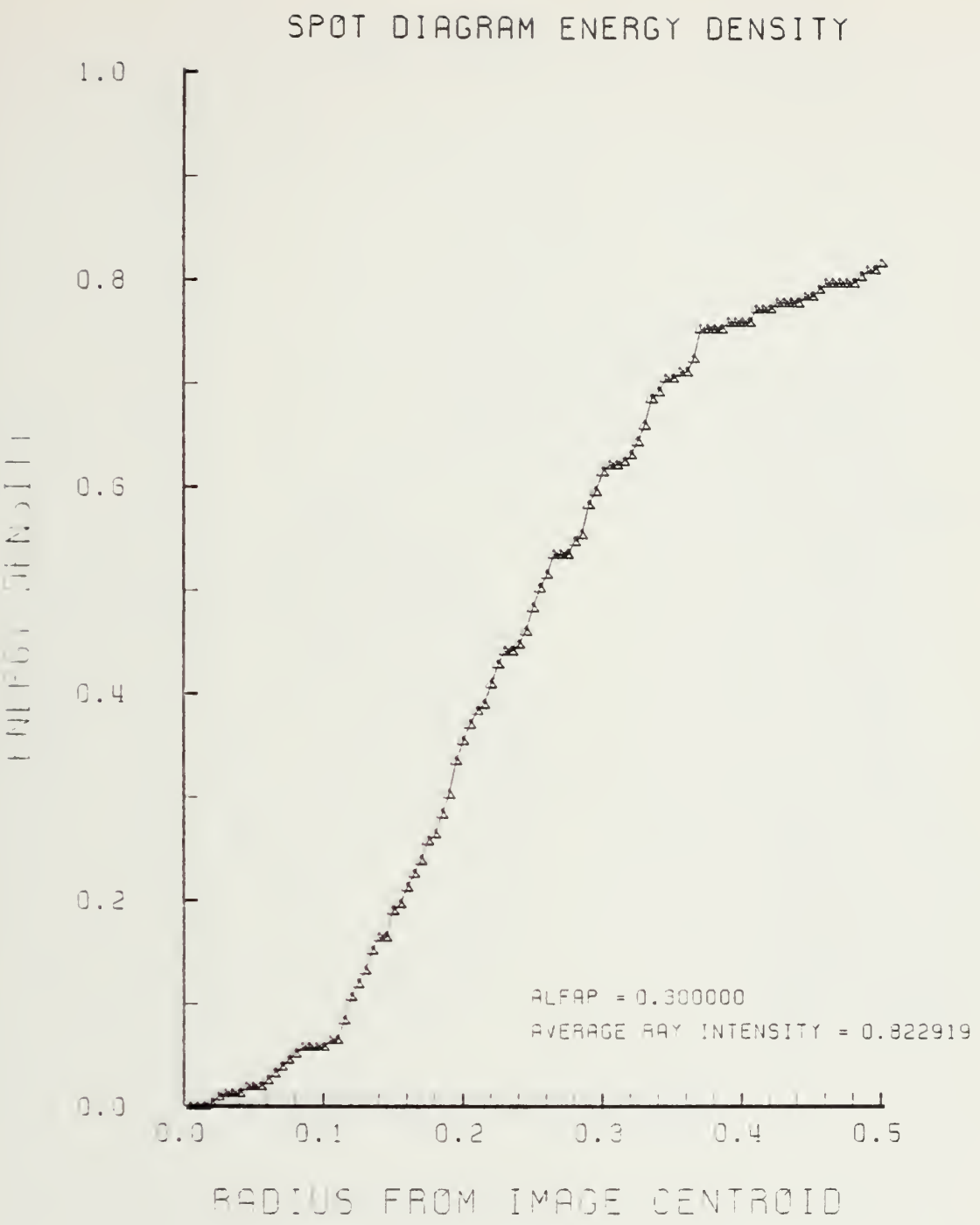

Figure E-56. Encircled Energy of Figure E-55

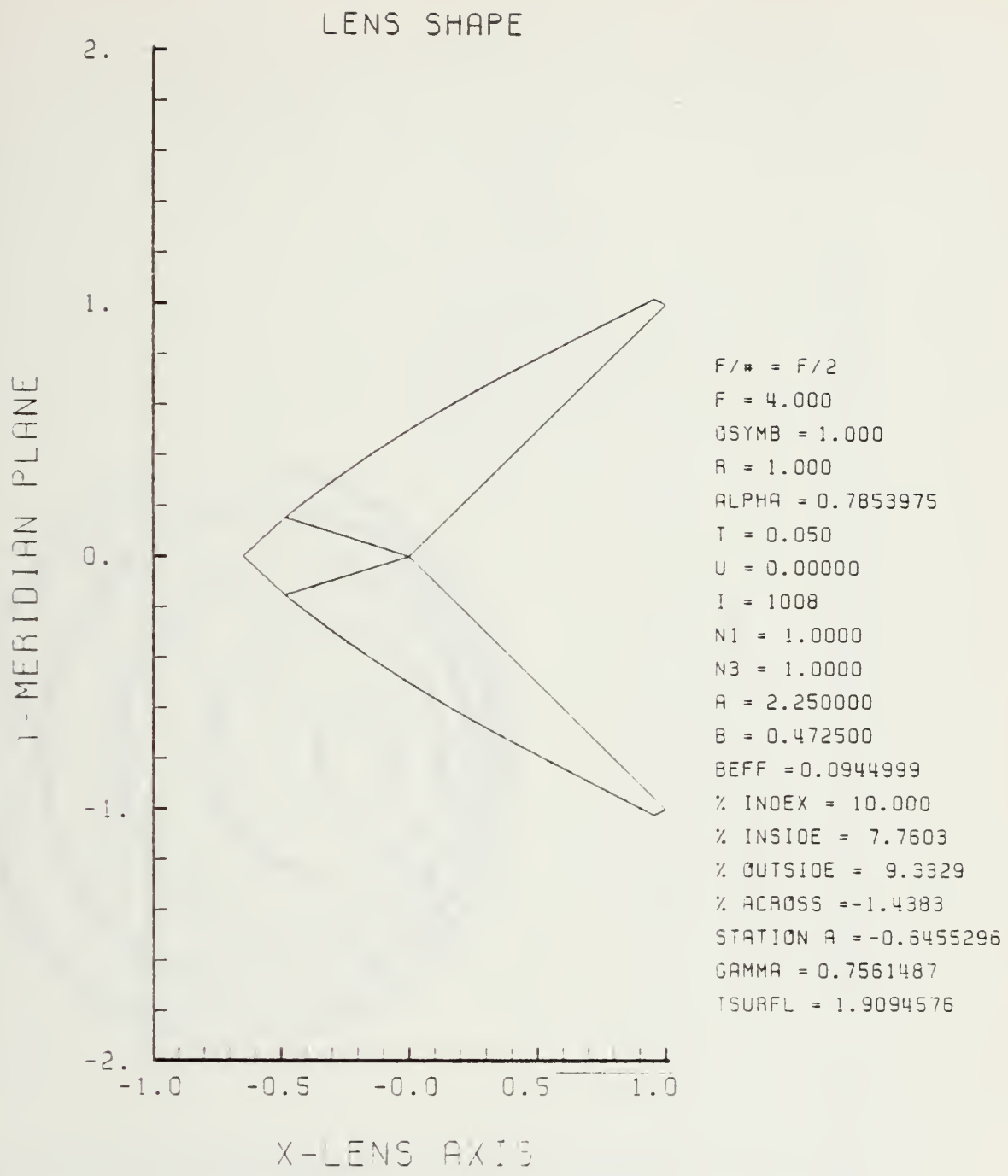

Figure E-57. GRIN Lens Shape at +10%, OB = 1.00, a = 2.25

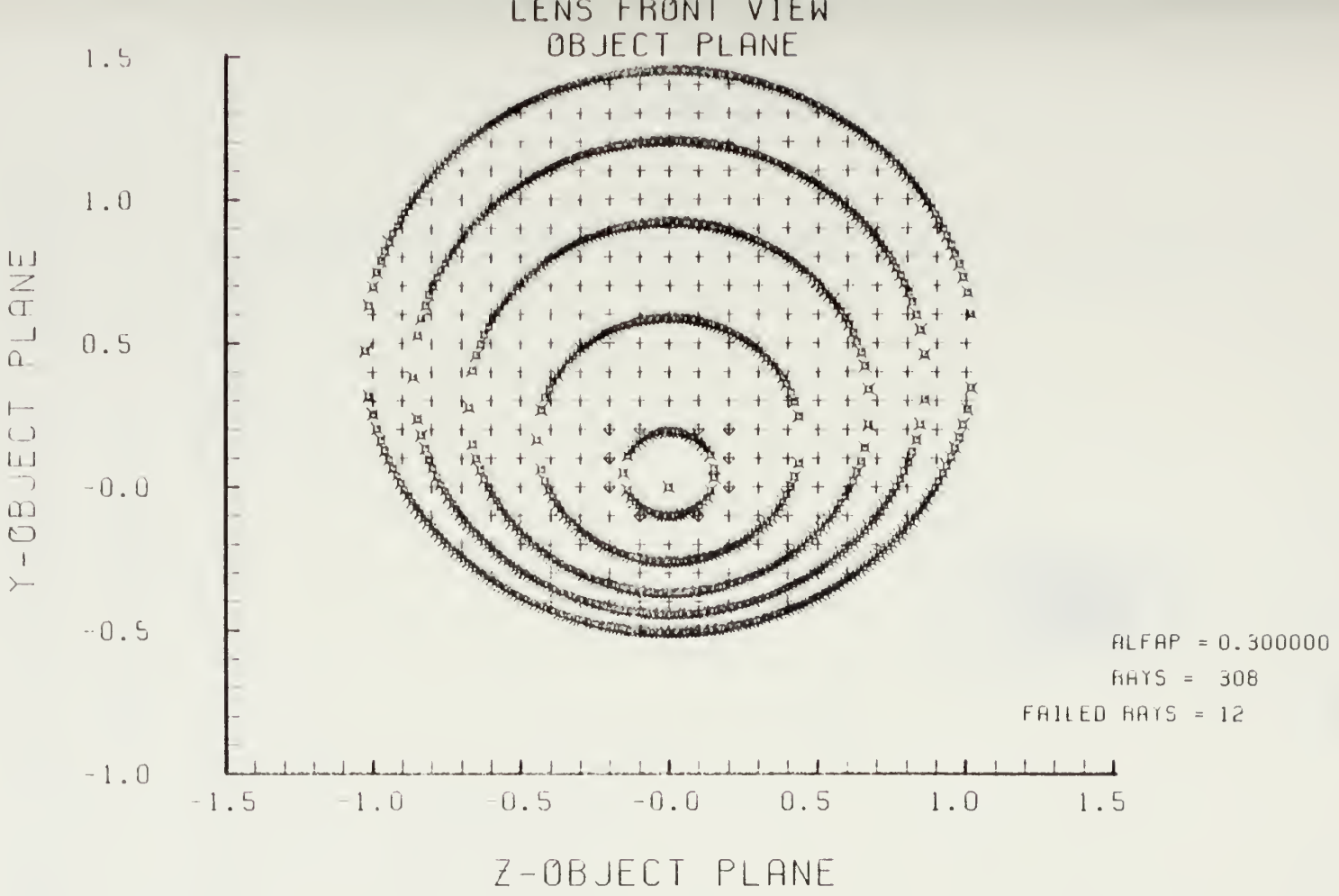

Figure E-58. Grid Plane at $\alpha_p = 0.3$ for Lens of Figure E-57

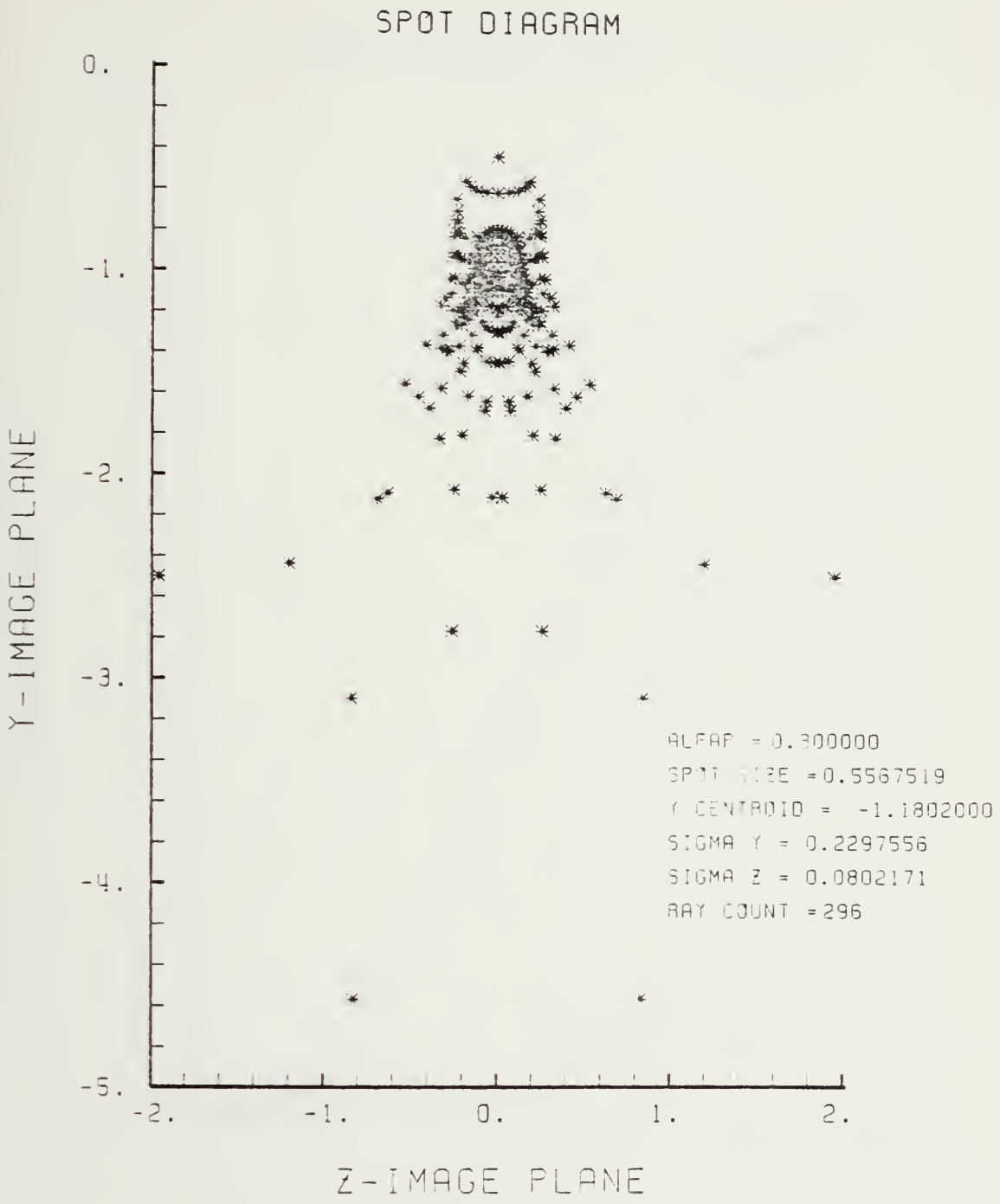

Figure E-59. Spot Diagram for Grid of Figure E-58

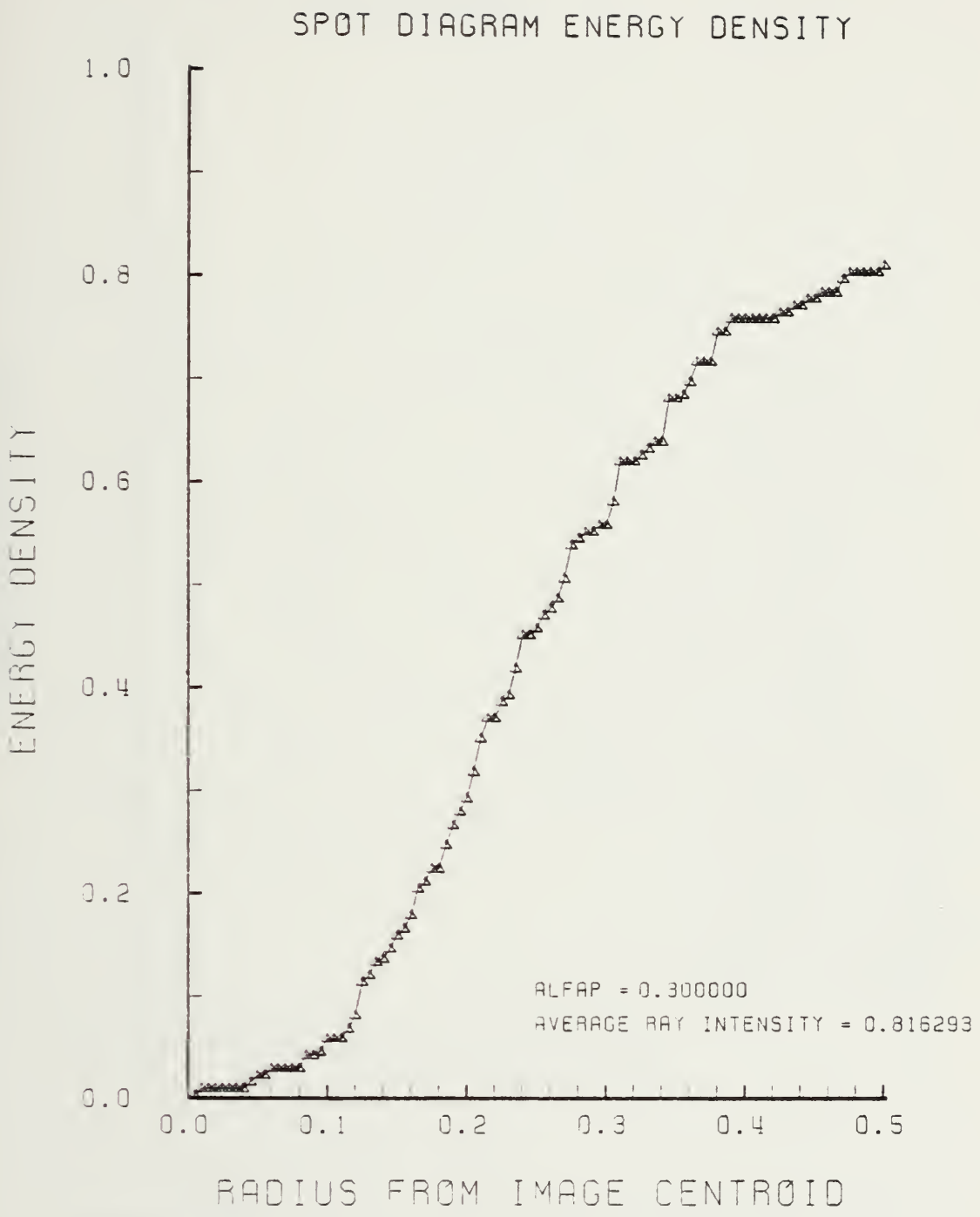

Figure E-60. Encircled Energy of Figure E-59

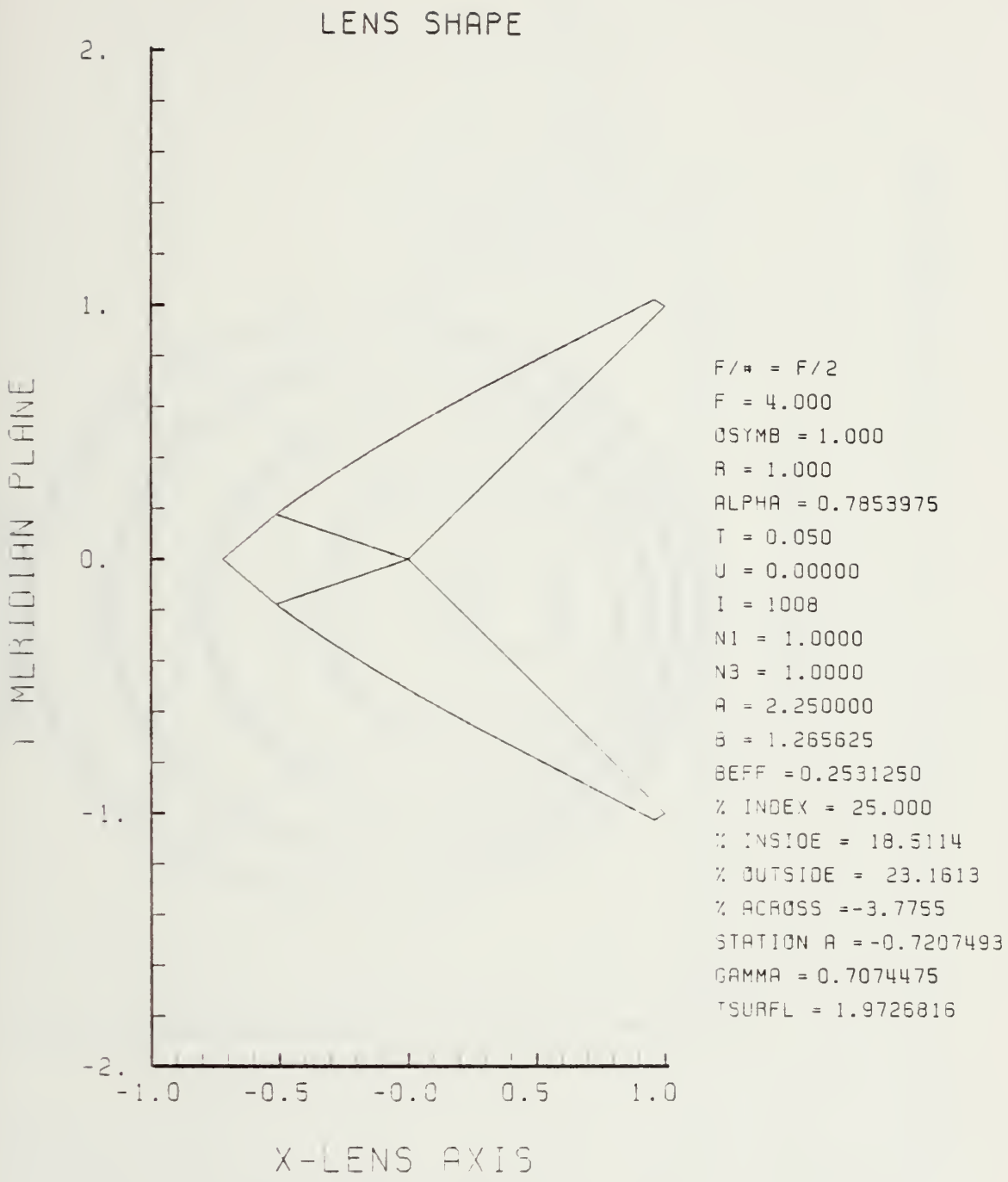

Figure E-61. GRIN Lens Shape at +25%, OB = 1.00, a = 2.25

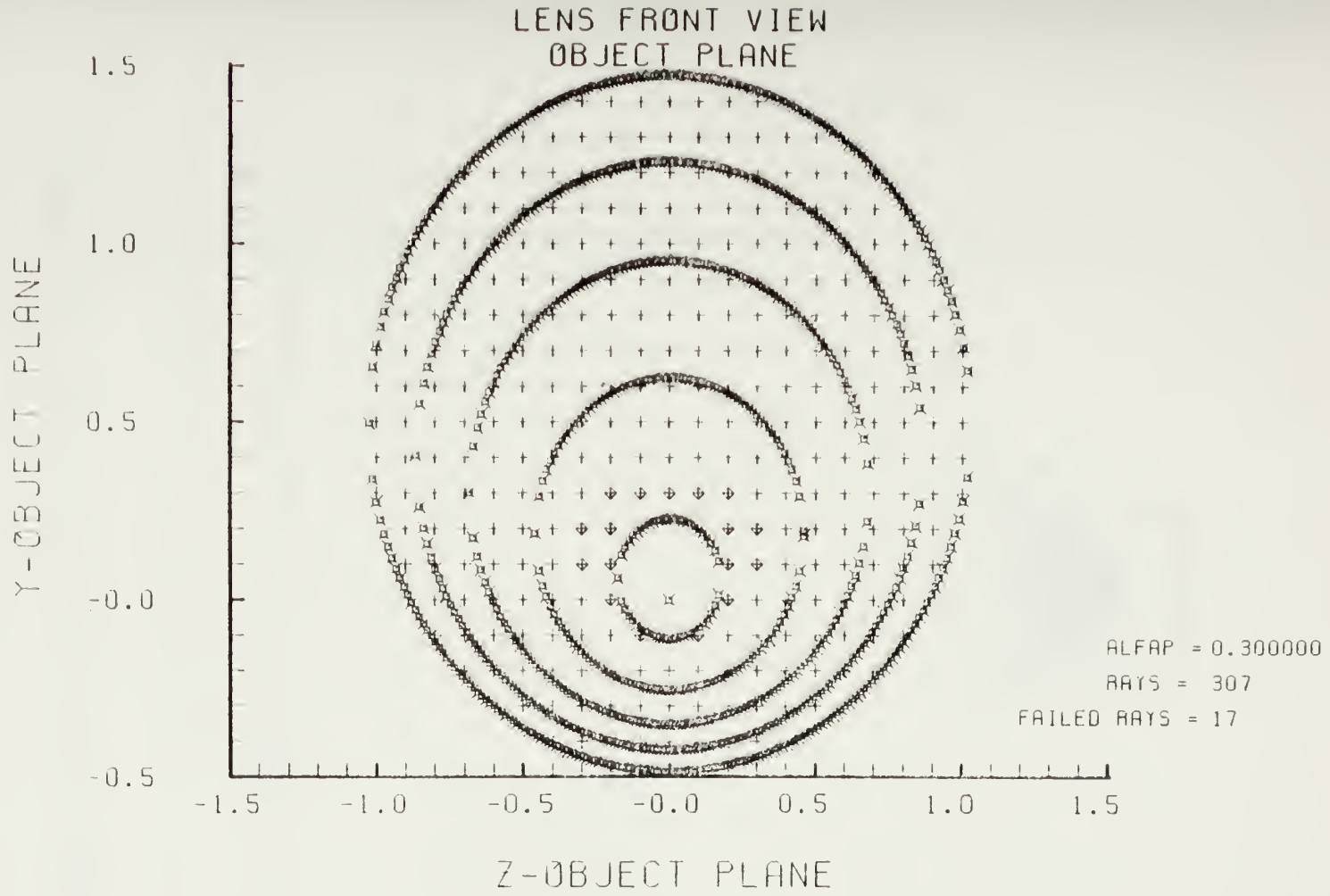

Figure E-62. Grid Plane at α_p = 0.3 for Lens of Figure E-61

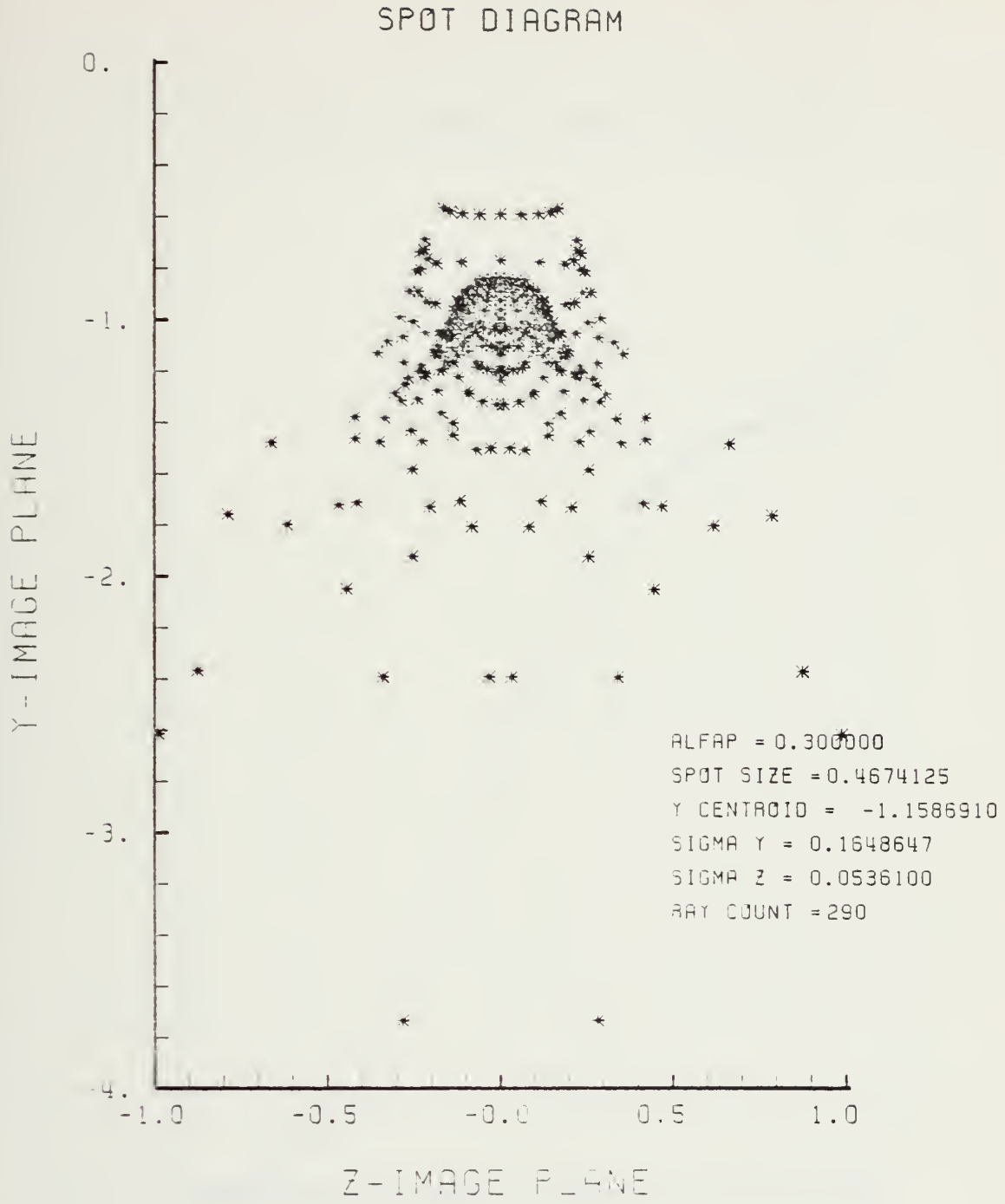

Figure E-63. Spot Diagram for Grid of Figure E-62

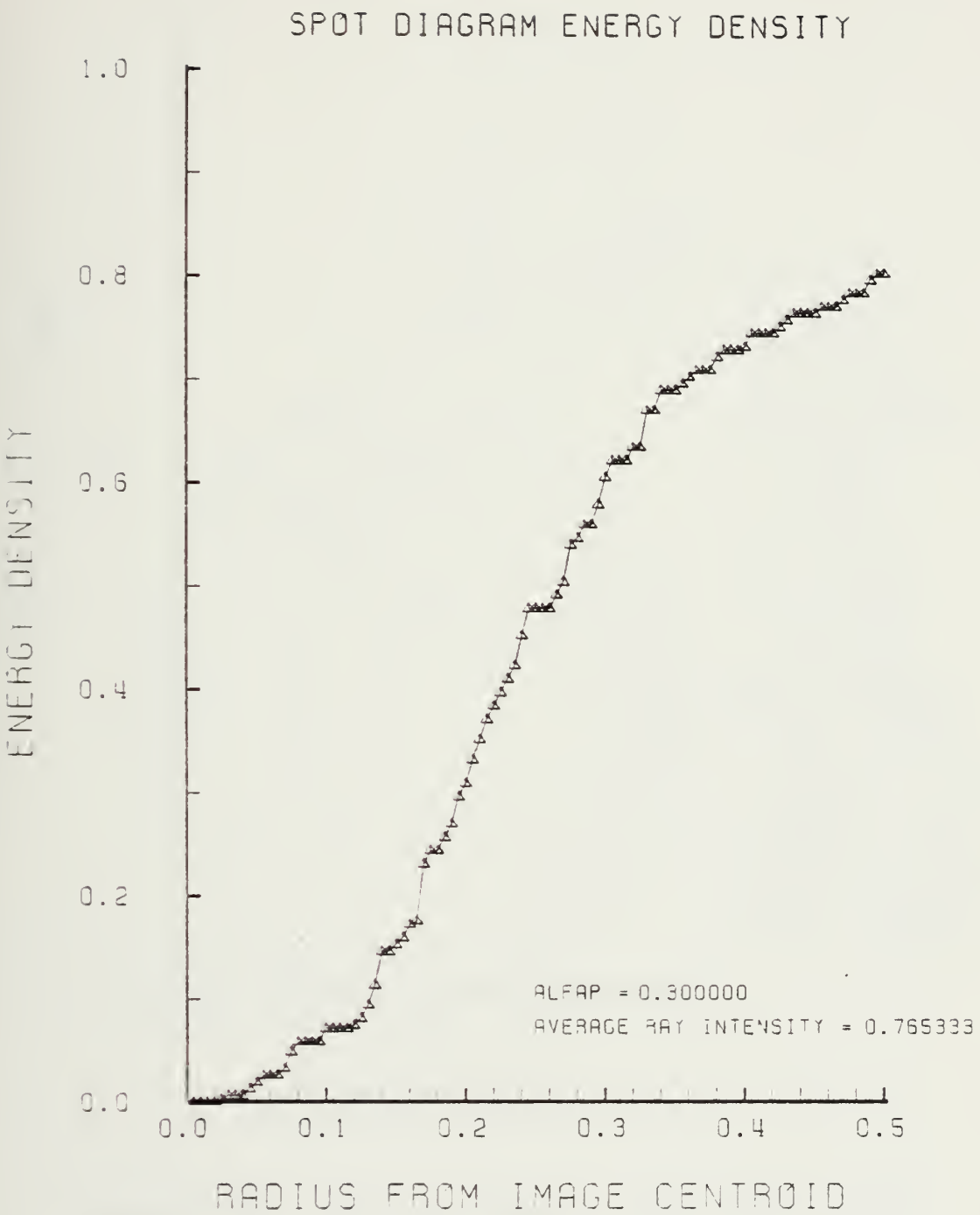

Figure E-64. Encircled Energy of Figure E-63

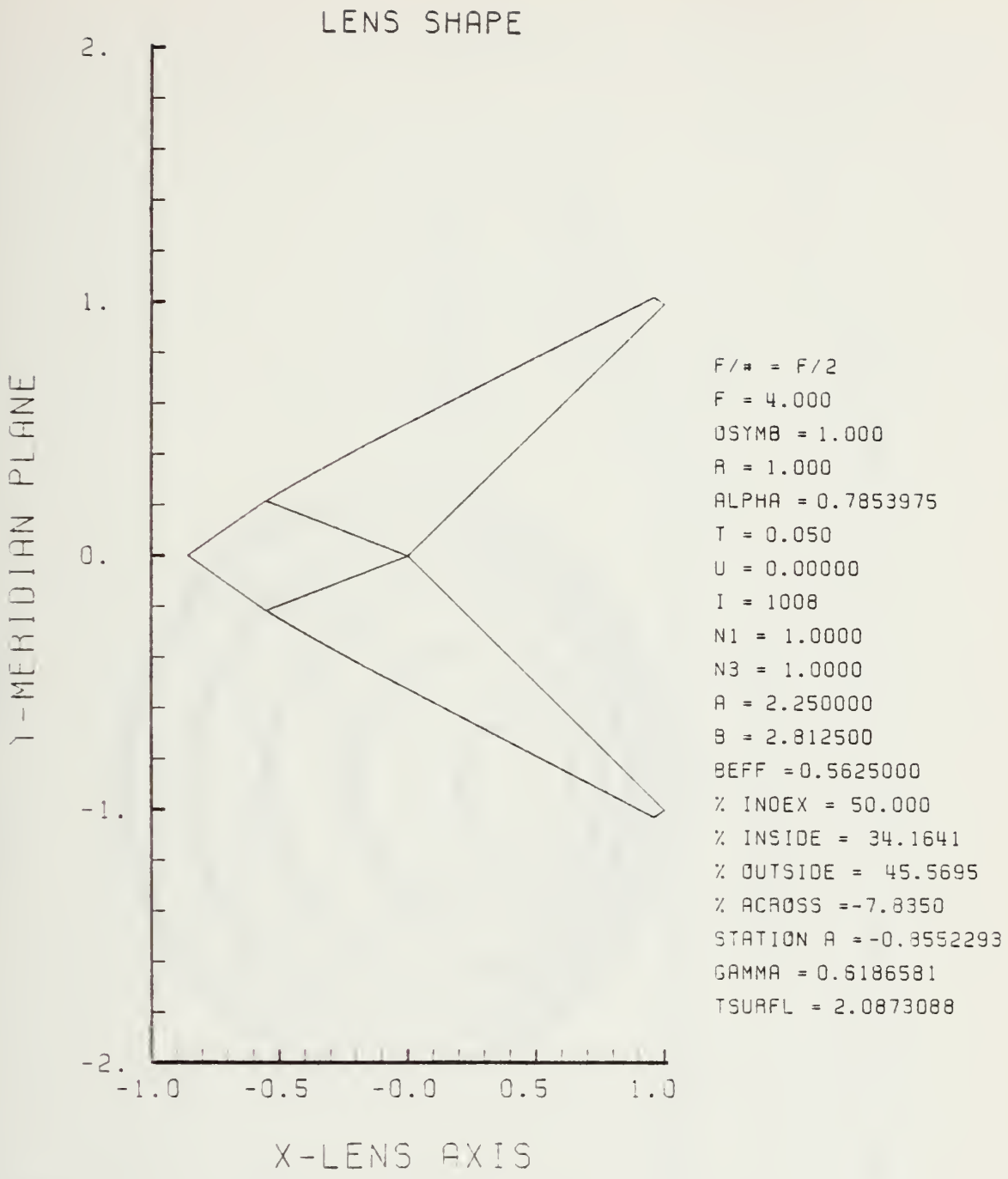

Figure E-65. GRIN Lens Shape at +50%, OB = 1.00, a = 2.25

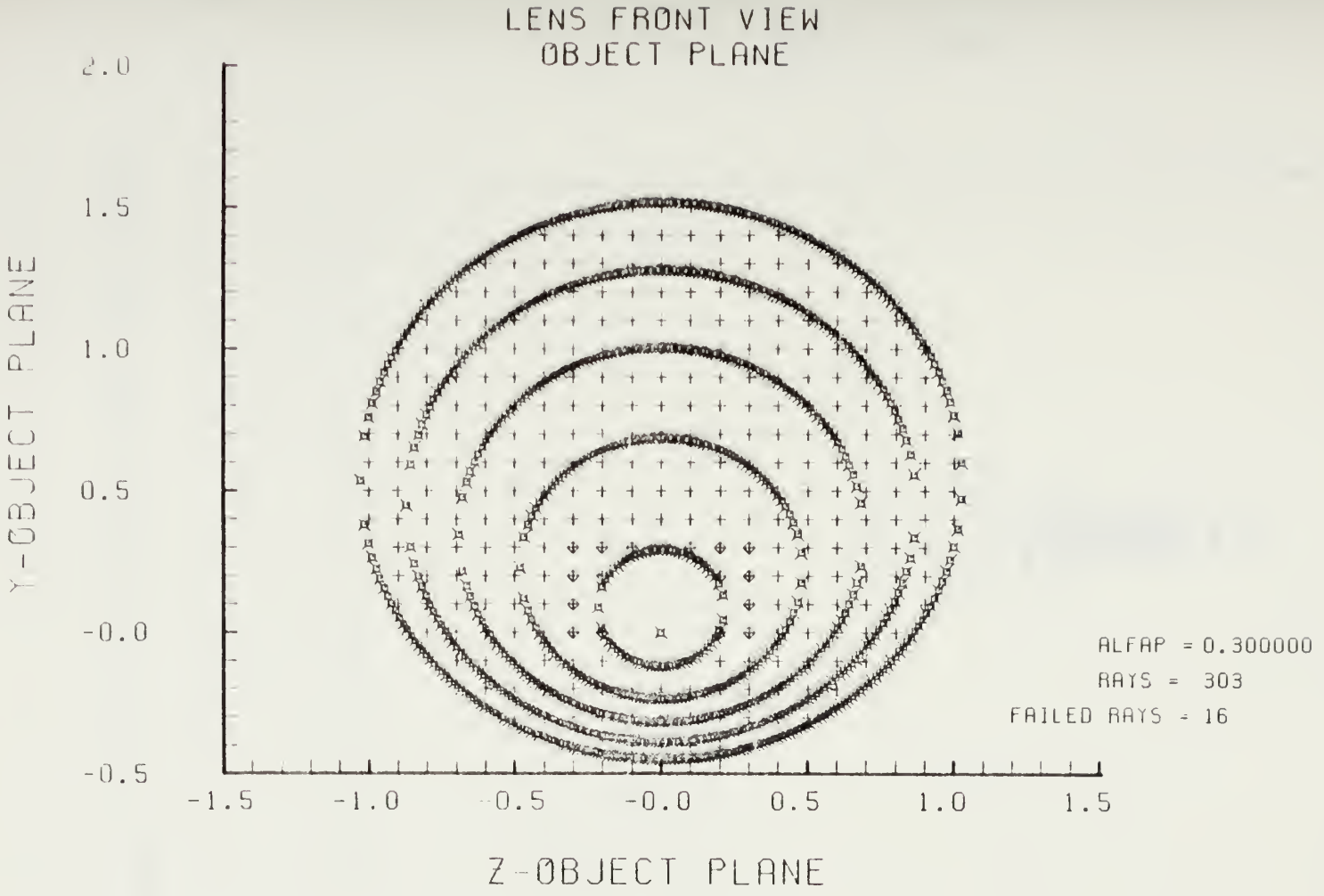

Figure E-66. Grid Plane at α_p = 0.3 for Lens of Figure E-65

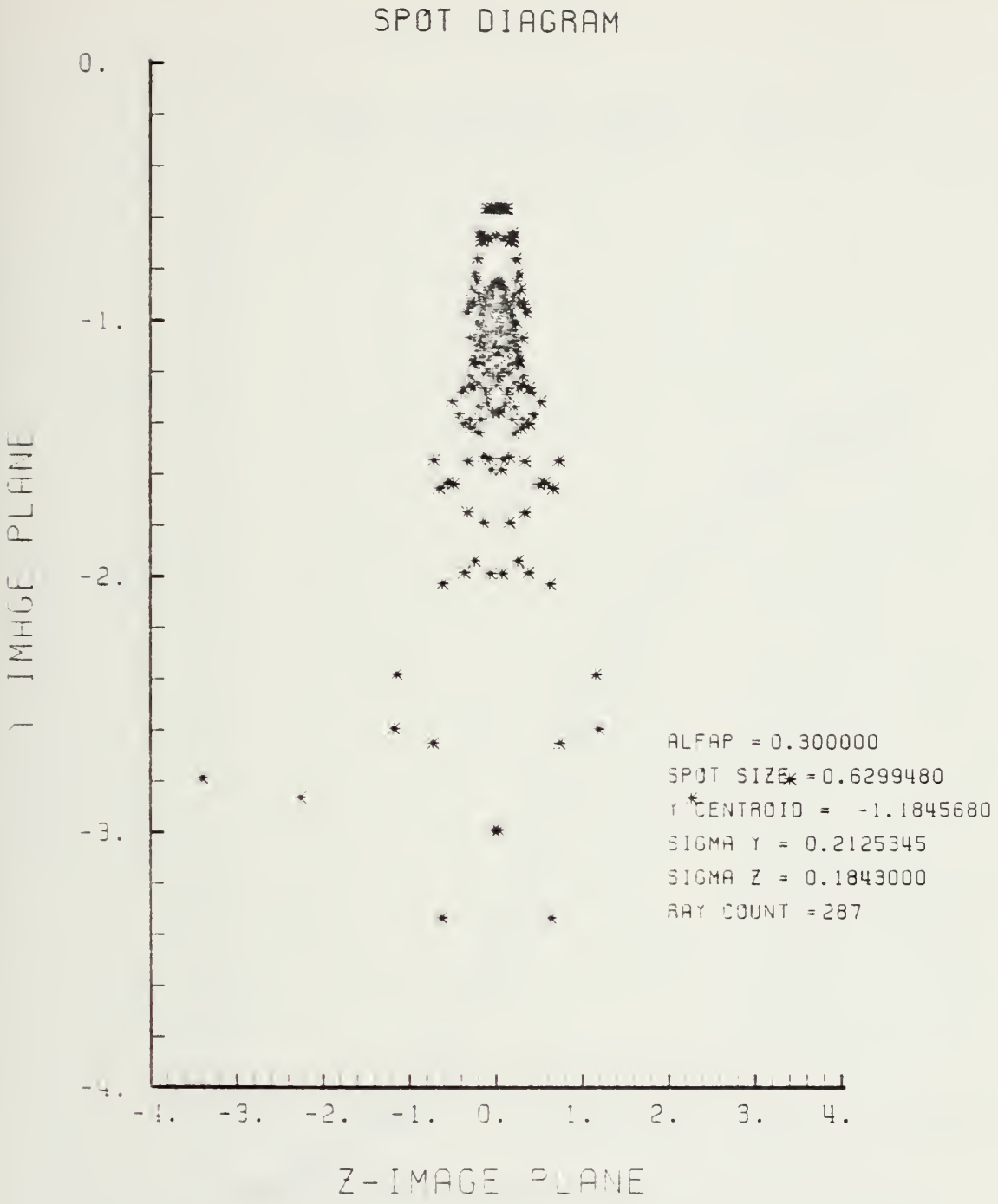

Figure E-67. Spot Diagram for Grid of Figure E-66

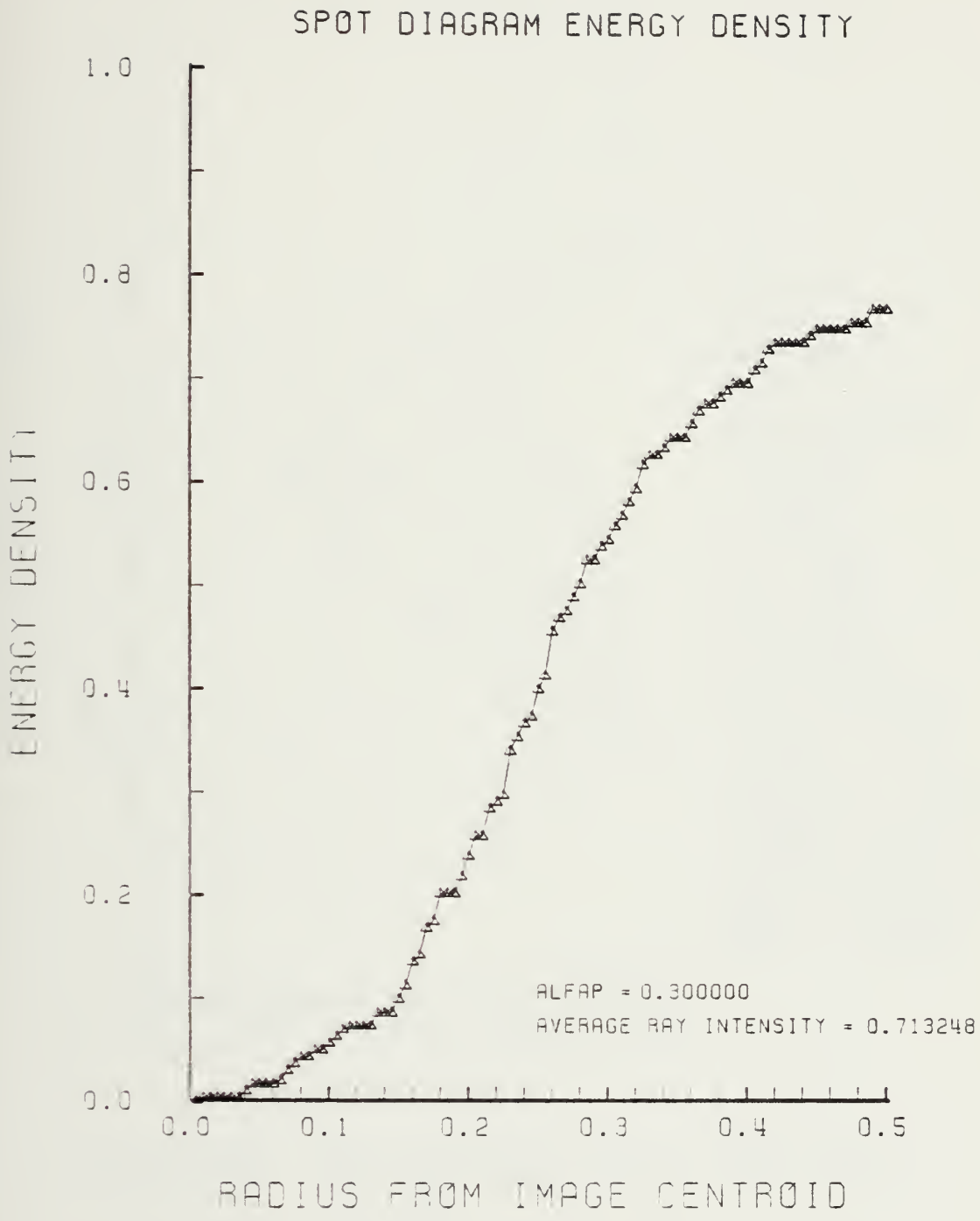

Figure E-68. Encircled Energy of Figure E-67

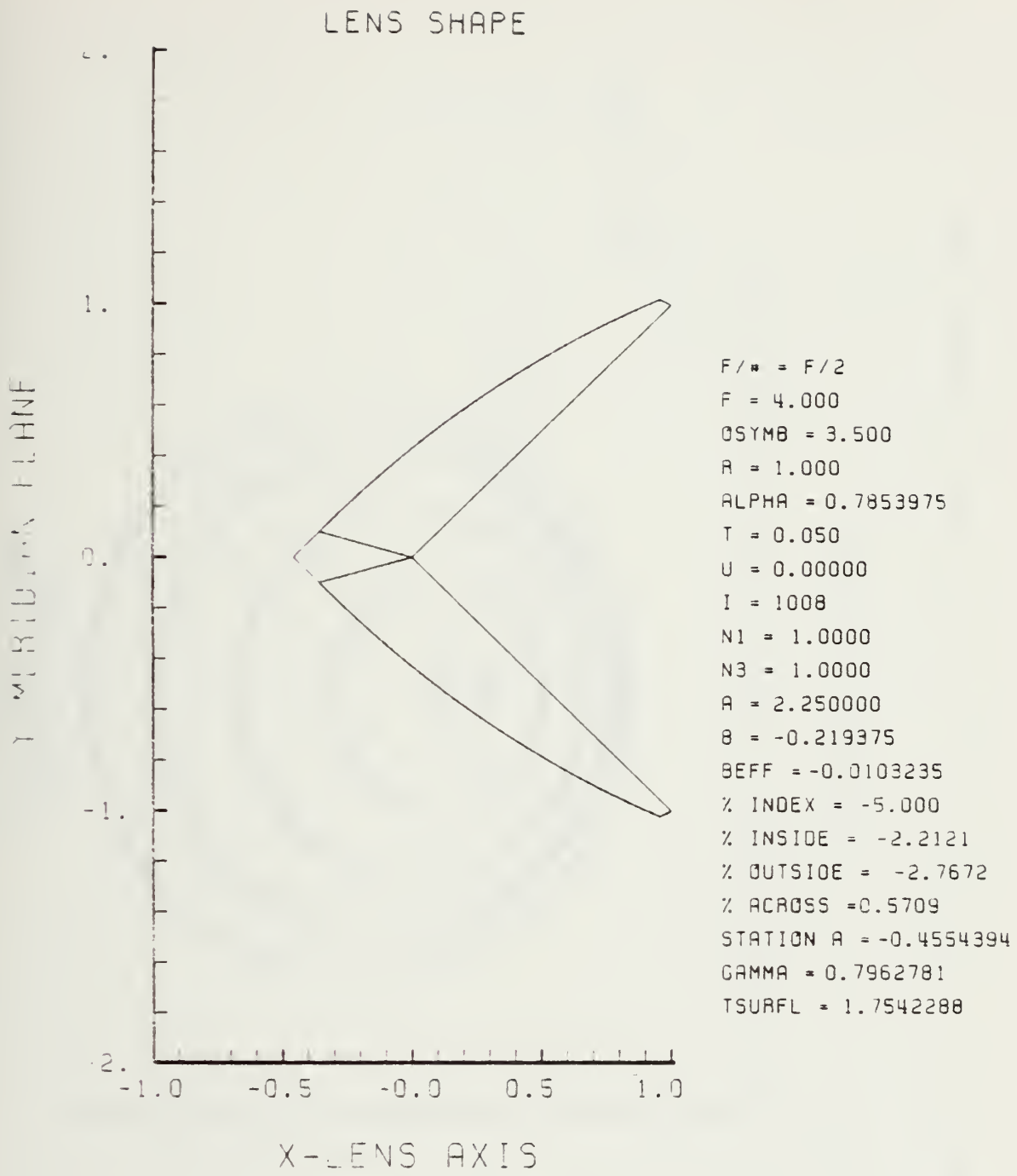

Figure E-69. GRIN Lens Shape at -5%, OB = 3.50, a = 2.25

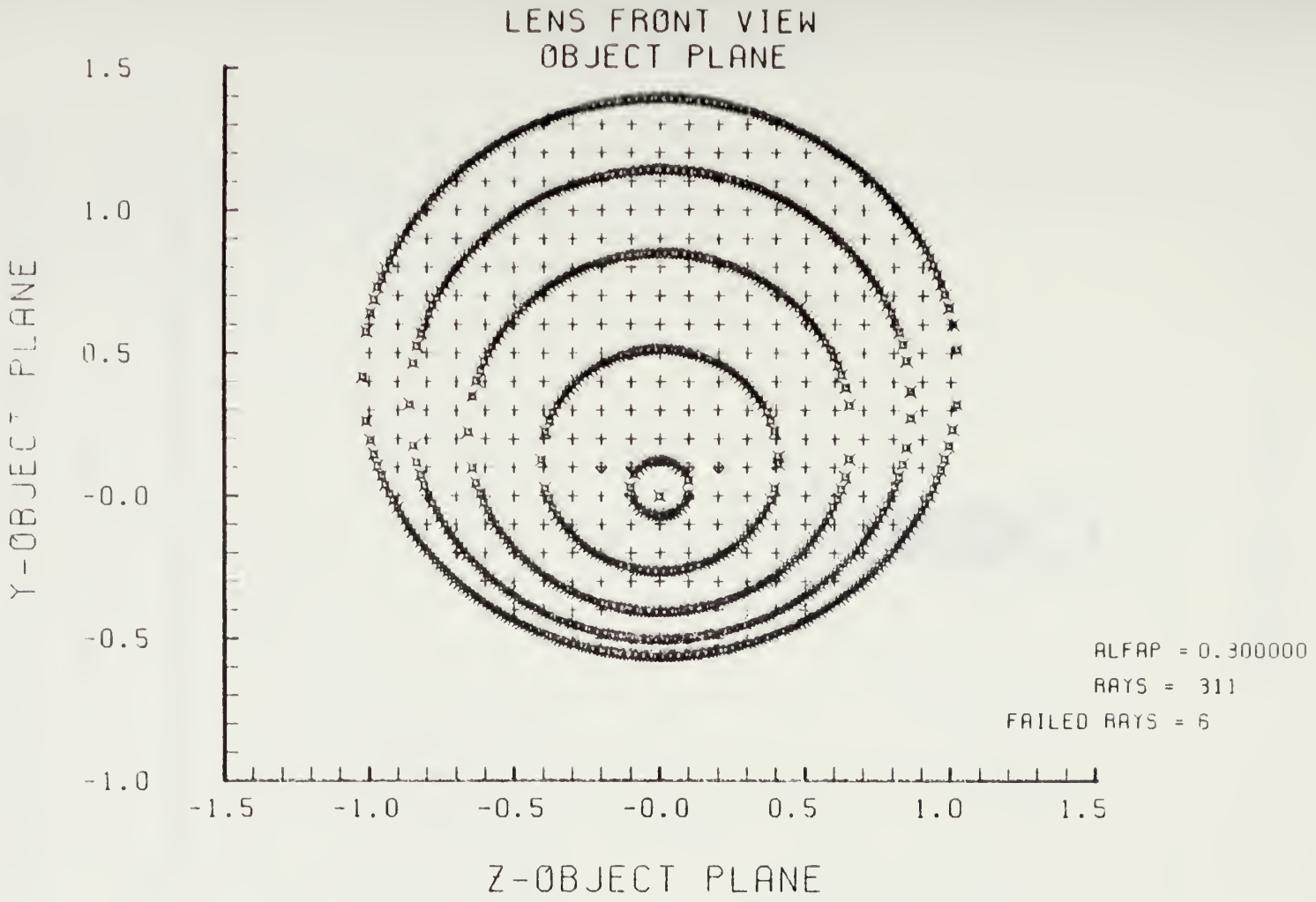

Figure E-70. Grid Plane at α_p = 0.3 for Lens of Figure E-69

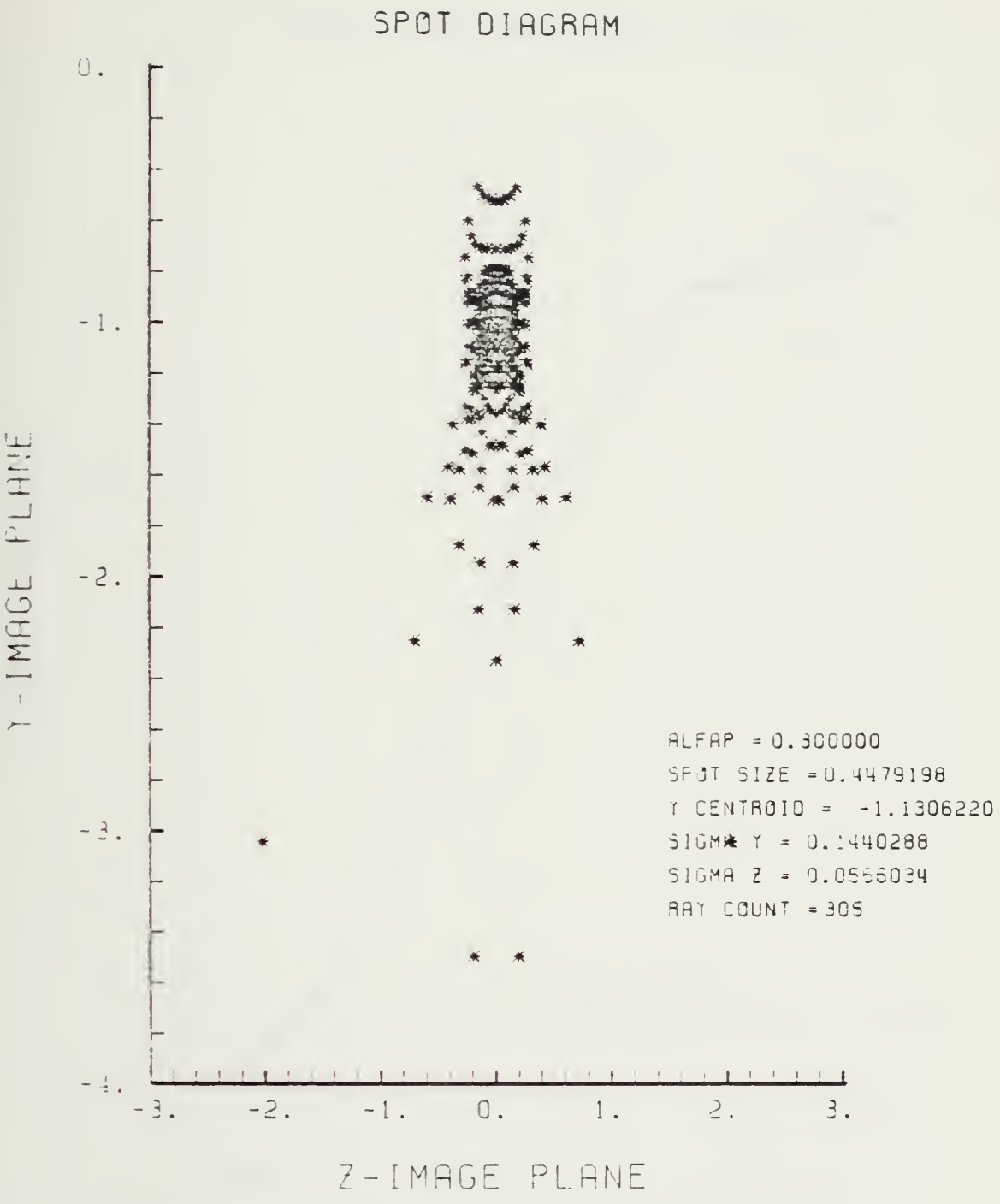

Figure E-71. Spot Diagram for Grid of Figure E-70

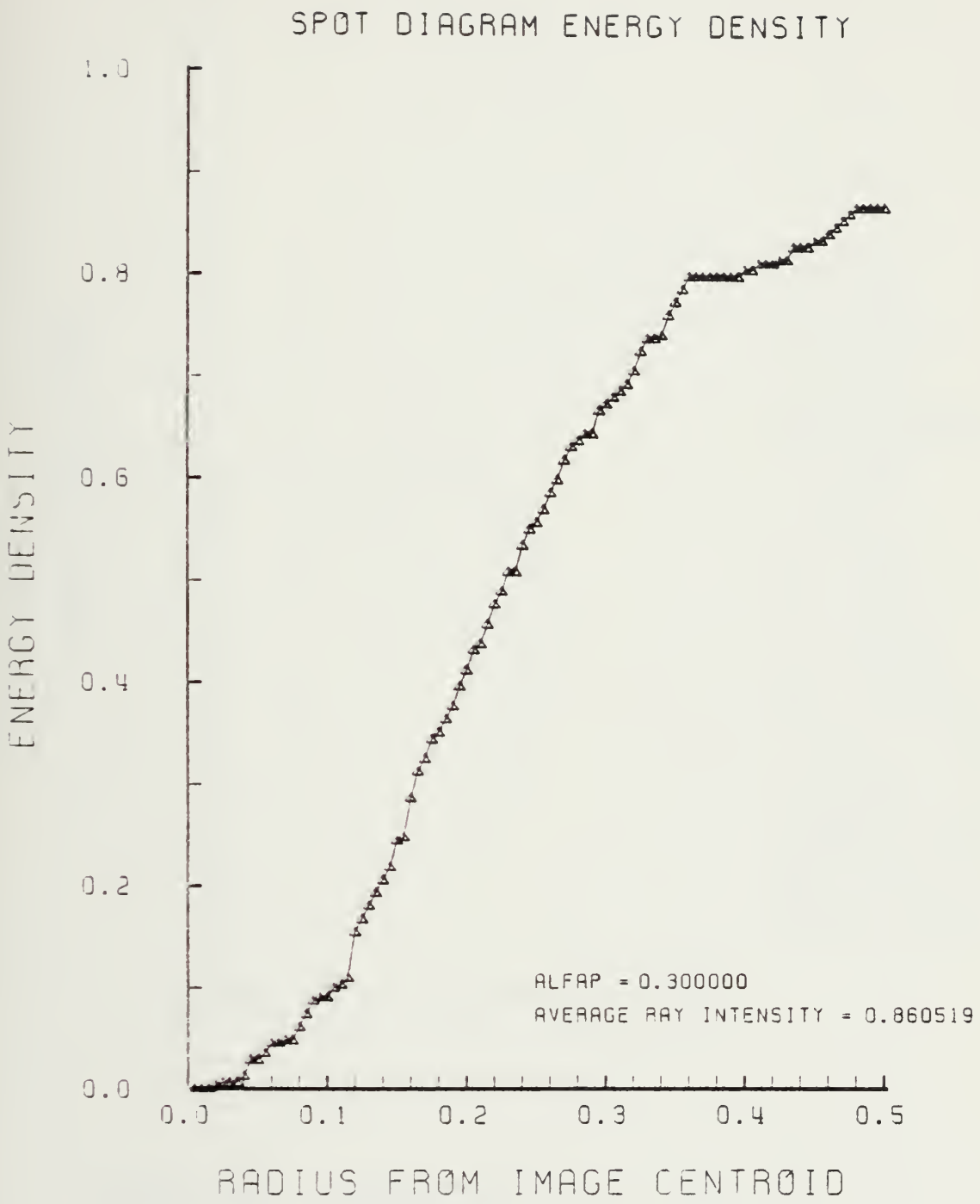

Figure E-72. Encircled Energy of Figure E-71

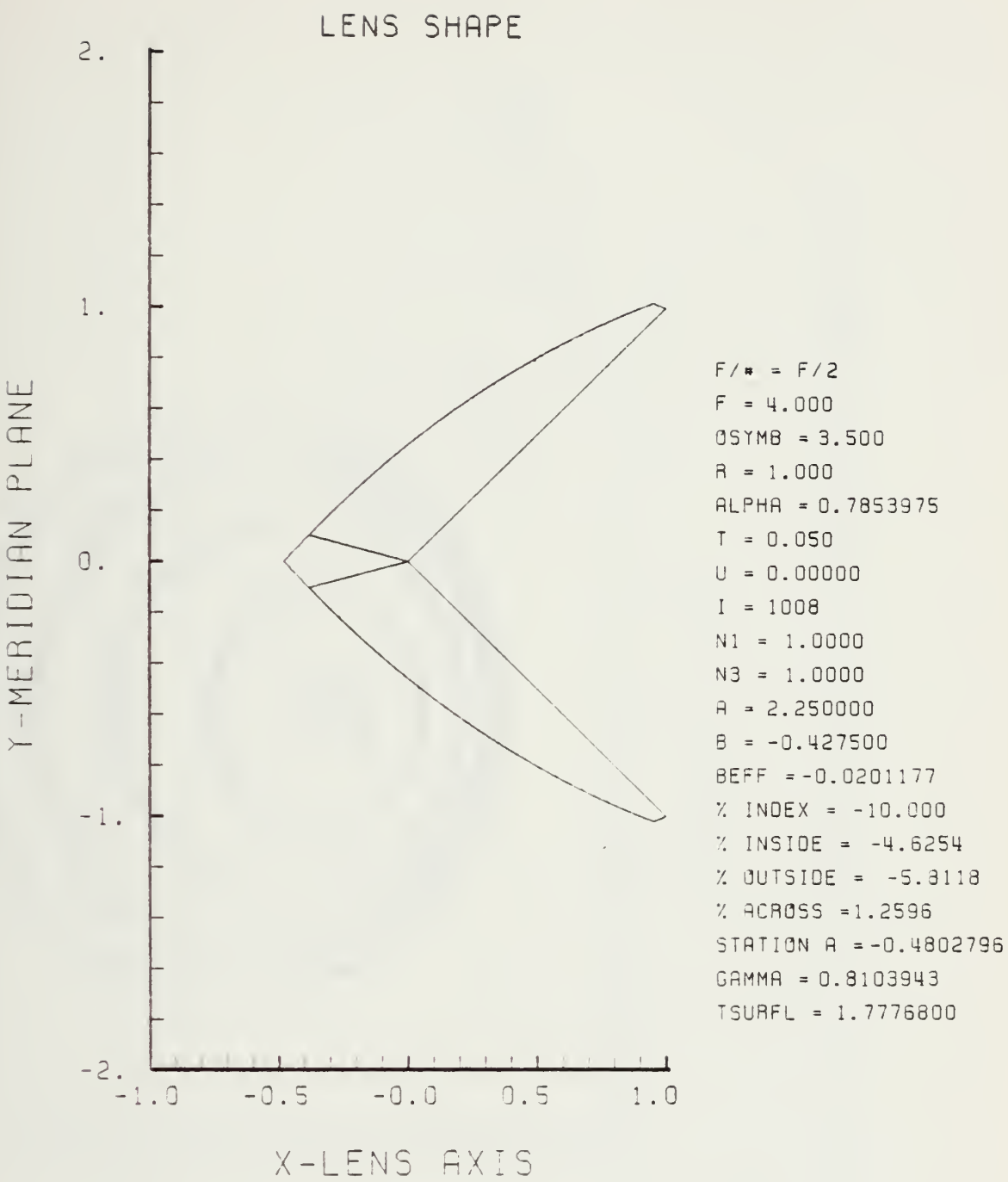

Figure E-73. GRIN Lens Shape at -10%, OB = 3.50, a = 2.25

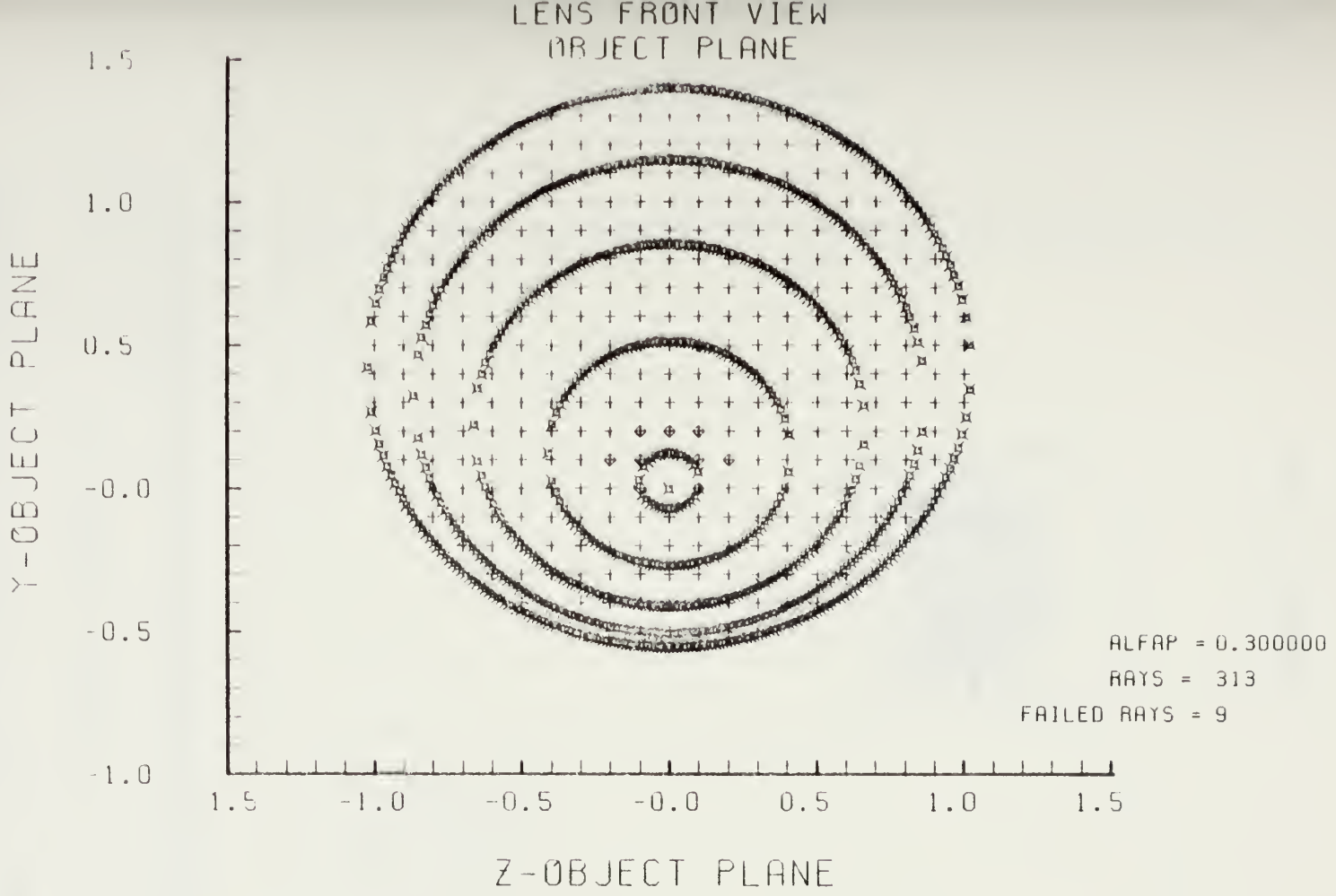

Figure E-74. Grid Plane at $\alpha_p = 0.3$ for Lens of Figure E-73

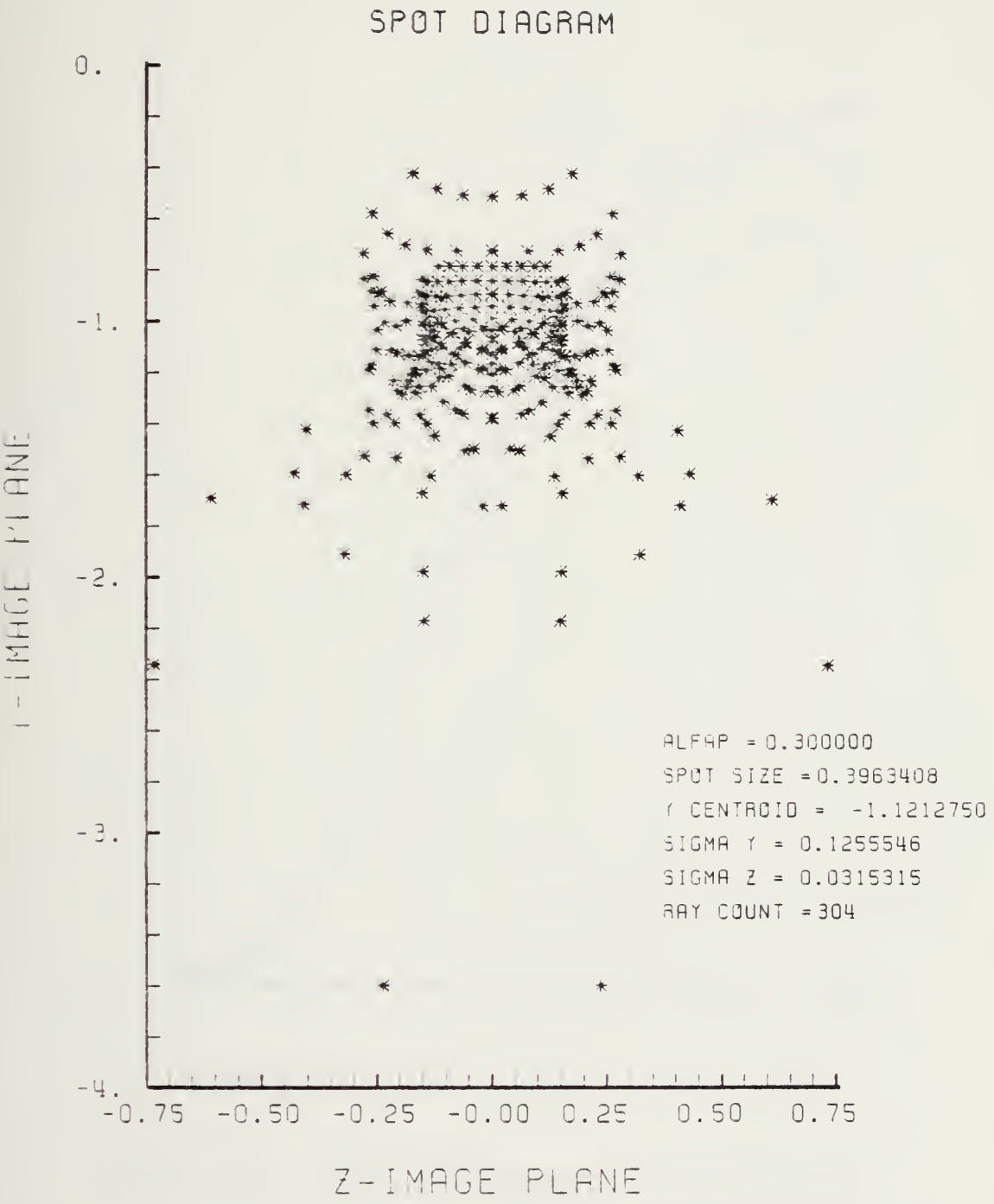

Figure E-75. Spot Diagram for Grid of Figure E-74

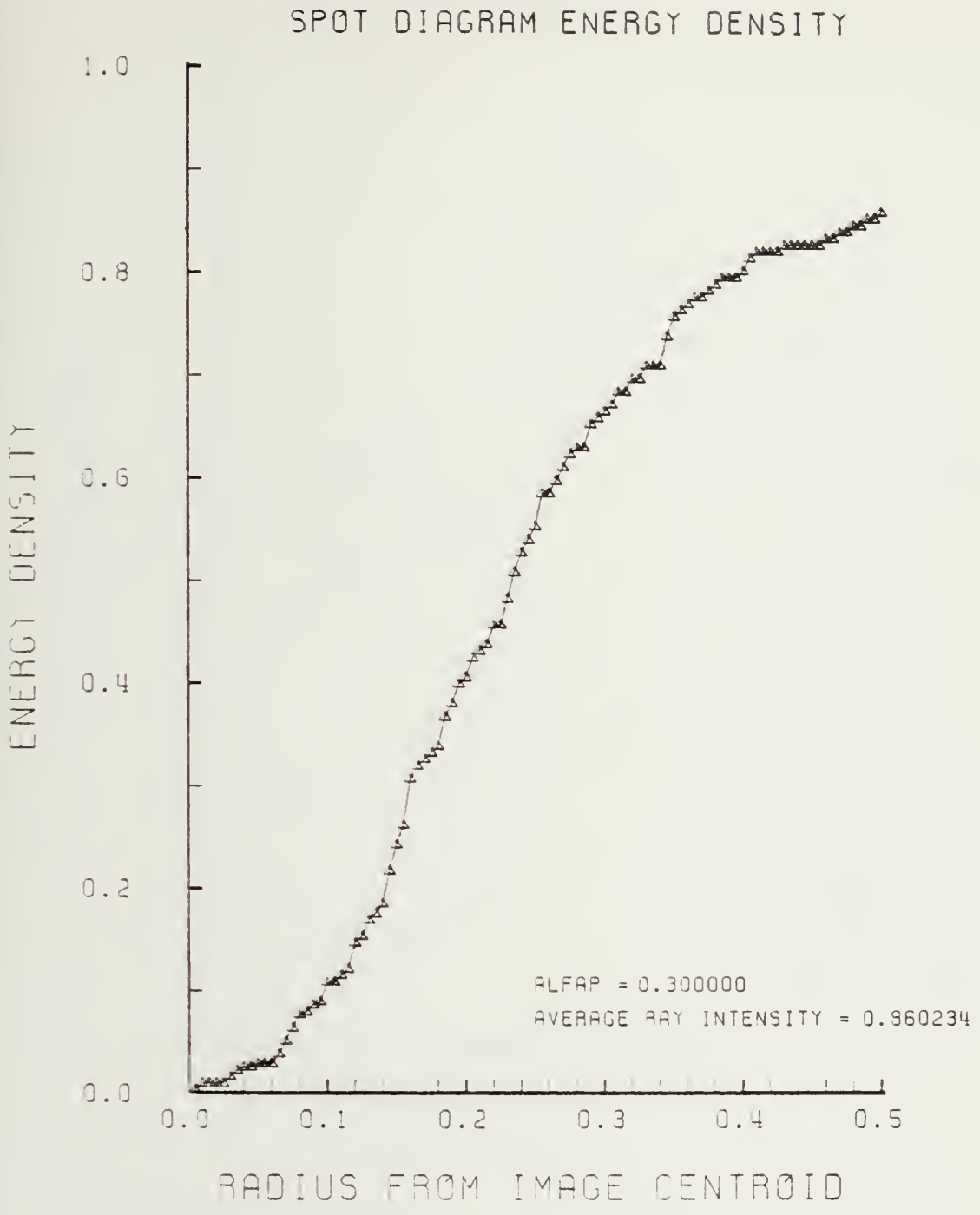

Figure E-76. Encircled Energy of Figure E-75

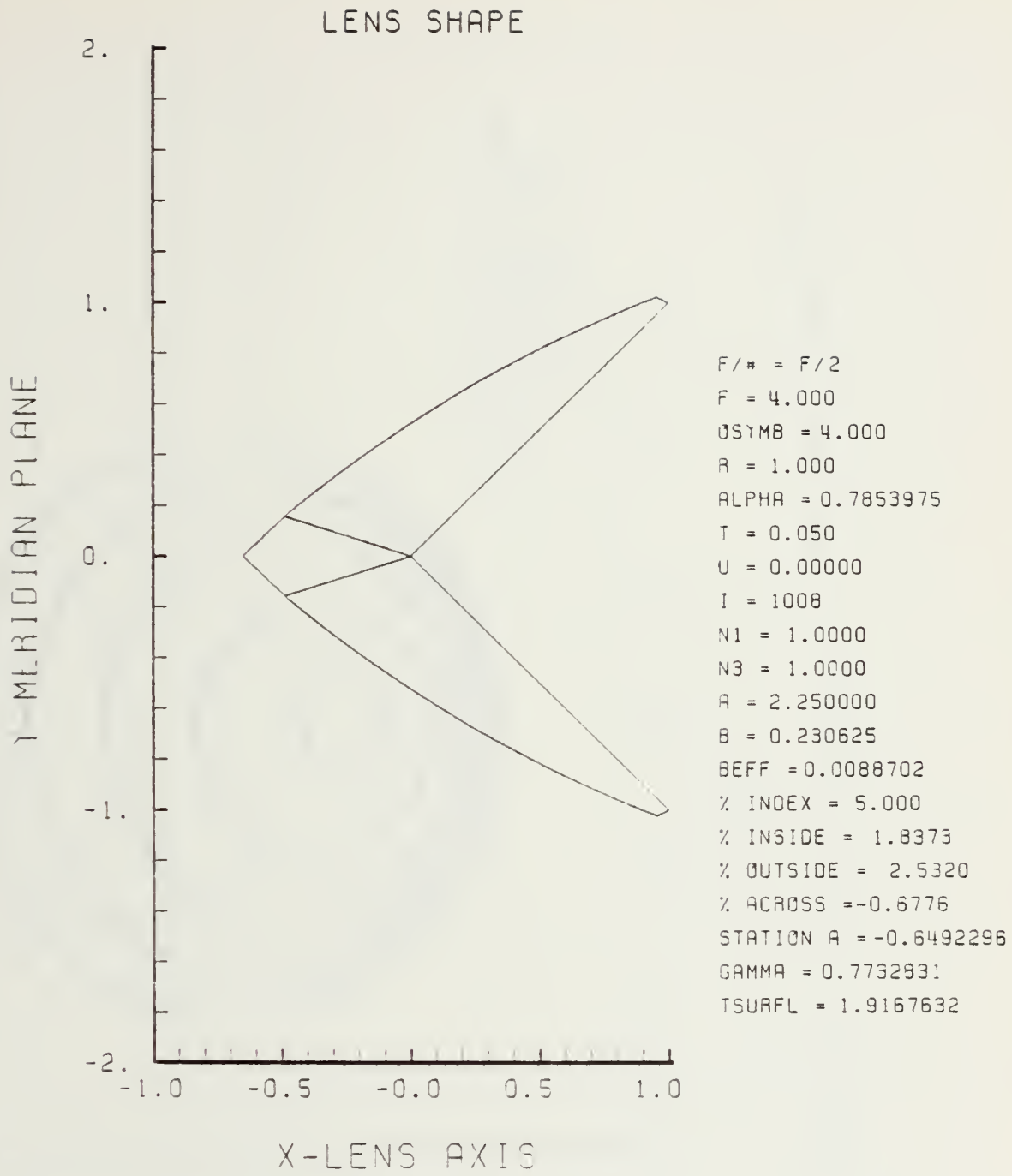

Figure E-77. GRIN Lens Shape at +5%, OB = 4.00, a = 2.25

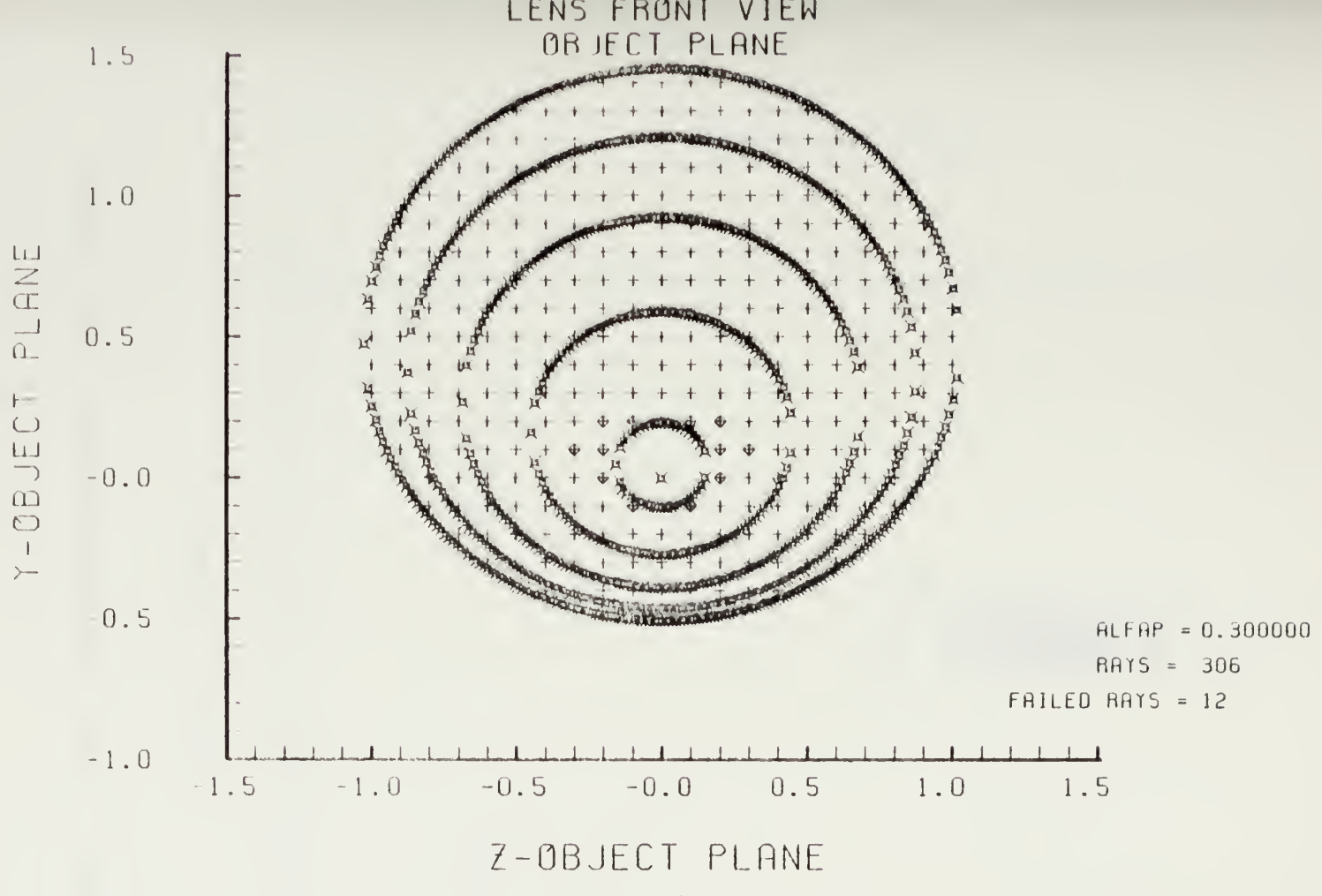

Figure E-78. Grid Plane at α_p = 0.3 for Lens of Figure E-77

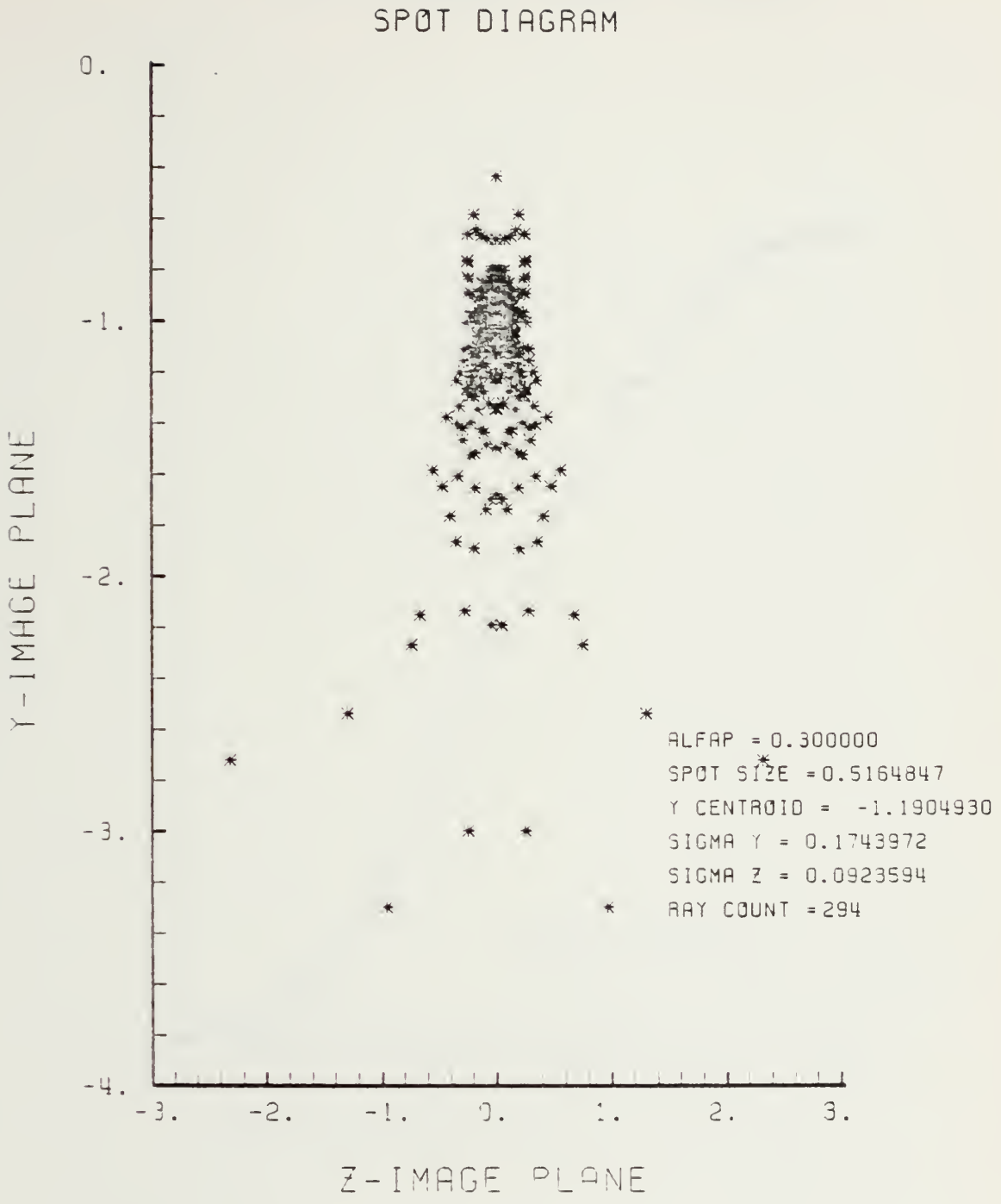

Figure E-79. Spot Diagram for Grid of Figure E-78

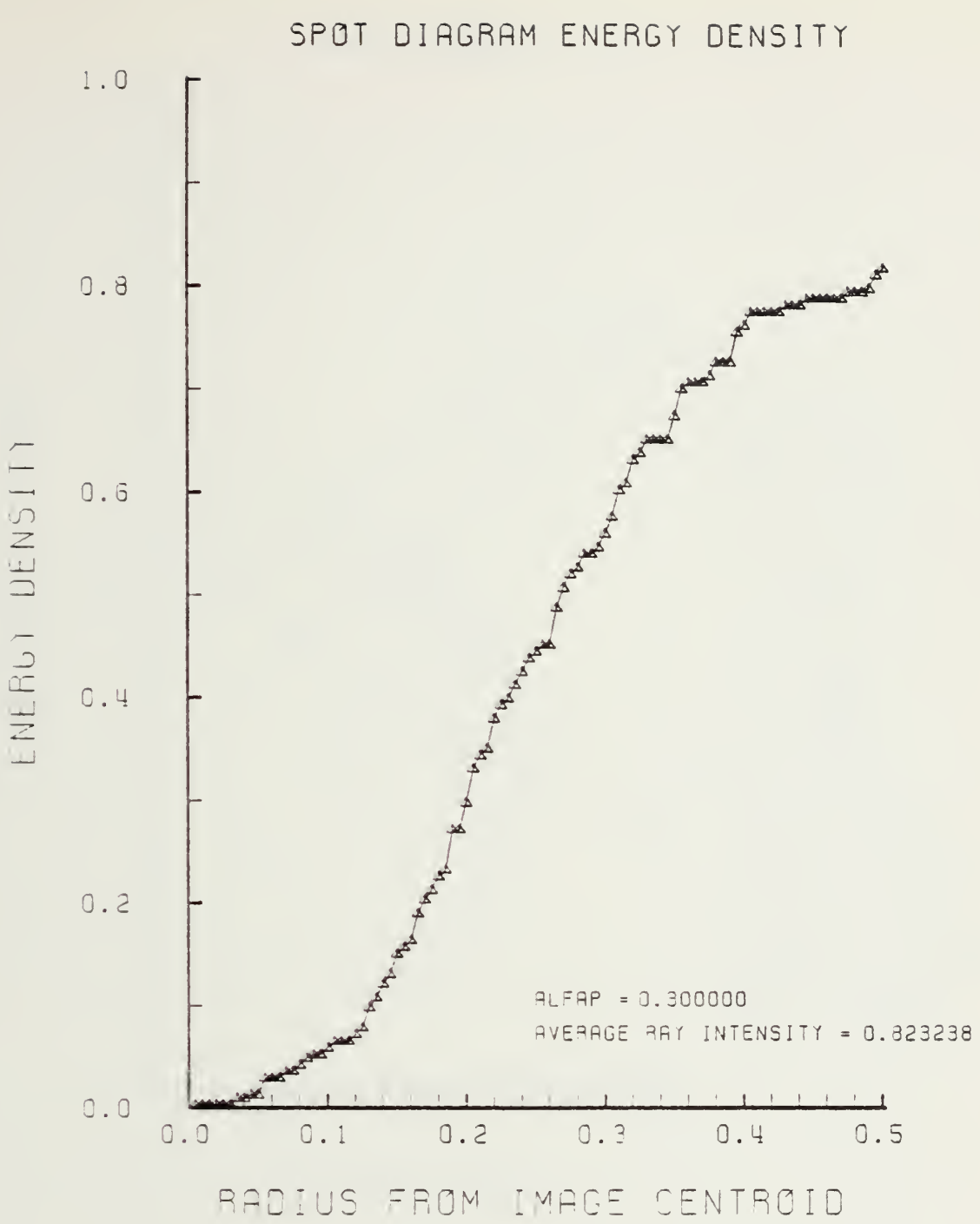

Figure E-80. Encircled Energy of Figure E-79

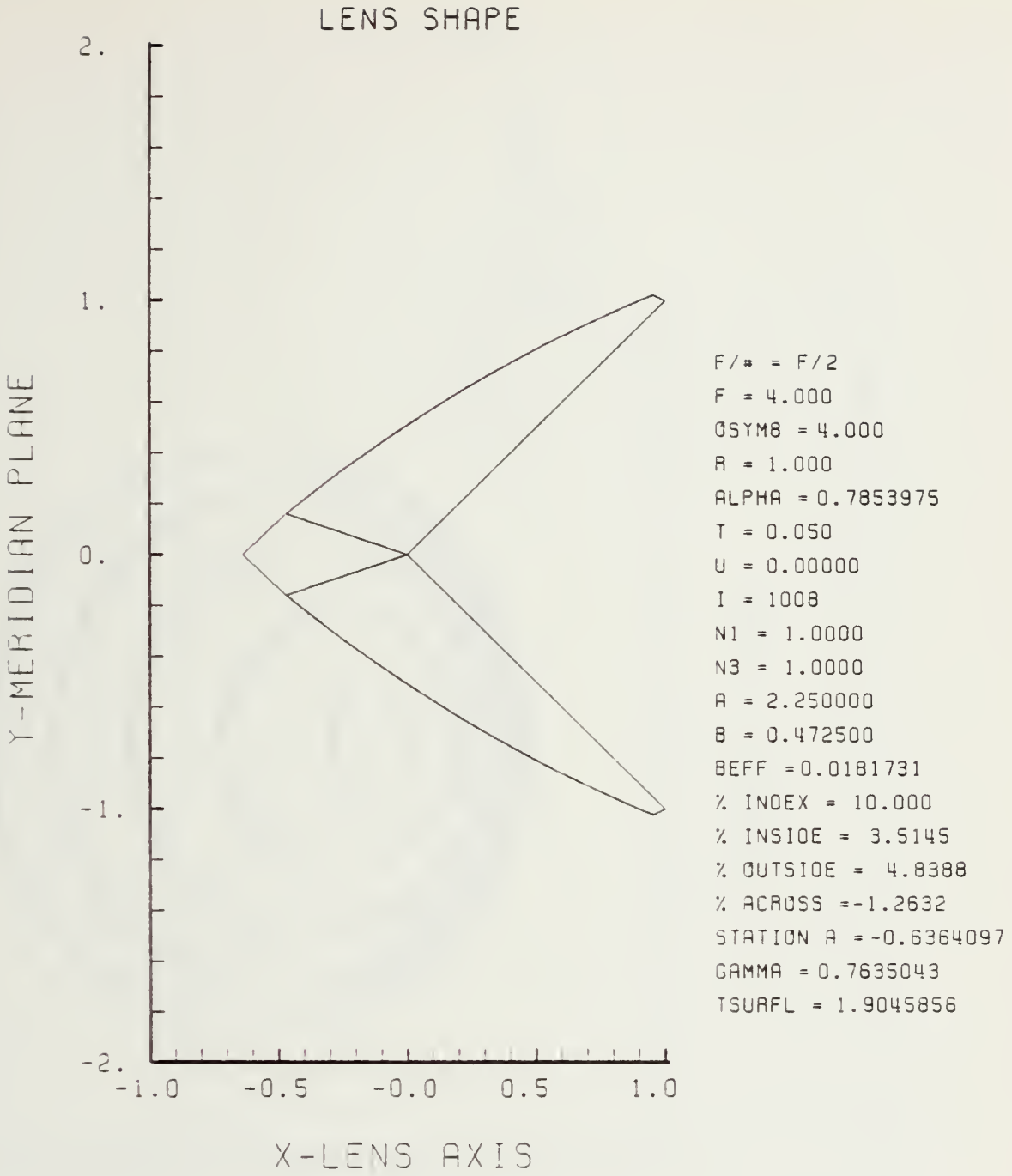

Figure E-81. GRIN Lens Shape at +10%, OB = 4.00, a = 2.25

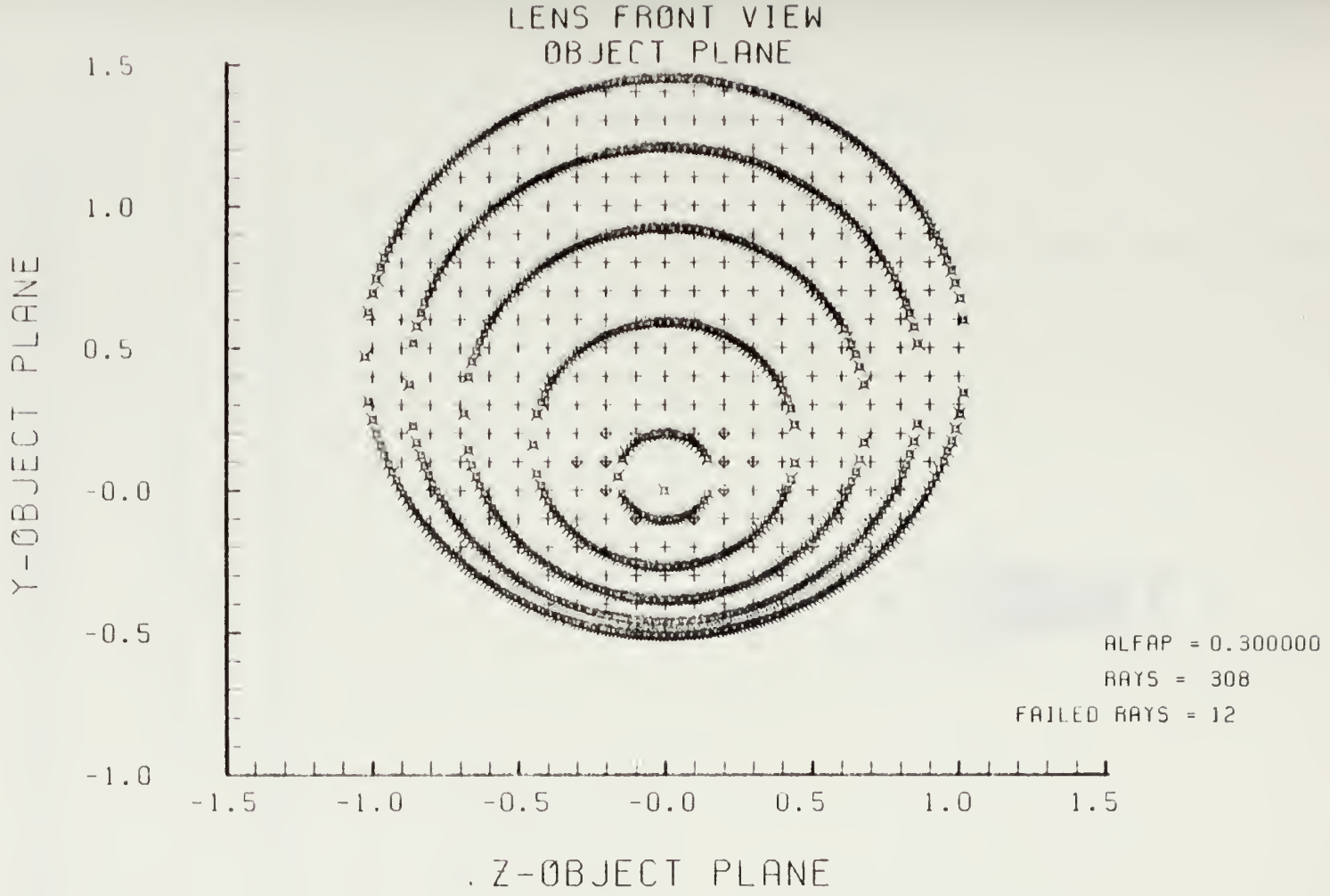

Figure E-82. Grid Plane at $\alpha_p = 0.3$ for Lens of Figure E-81

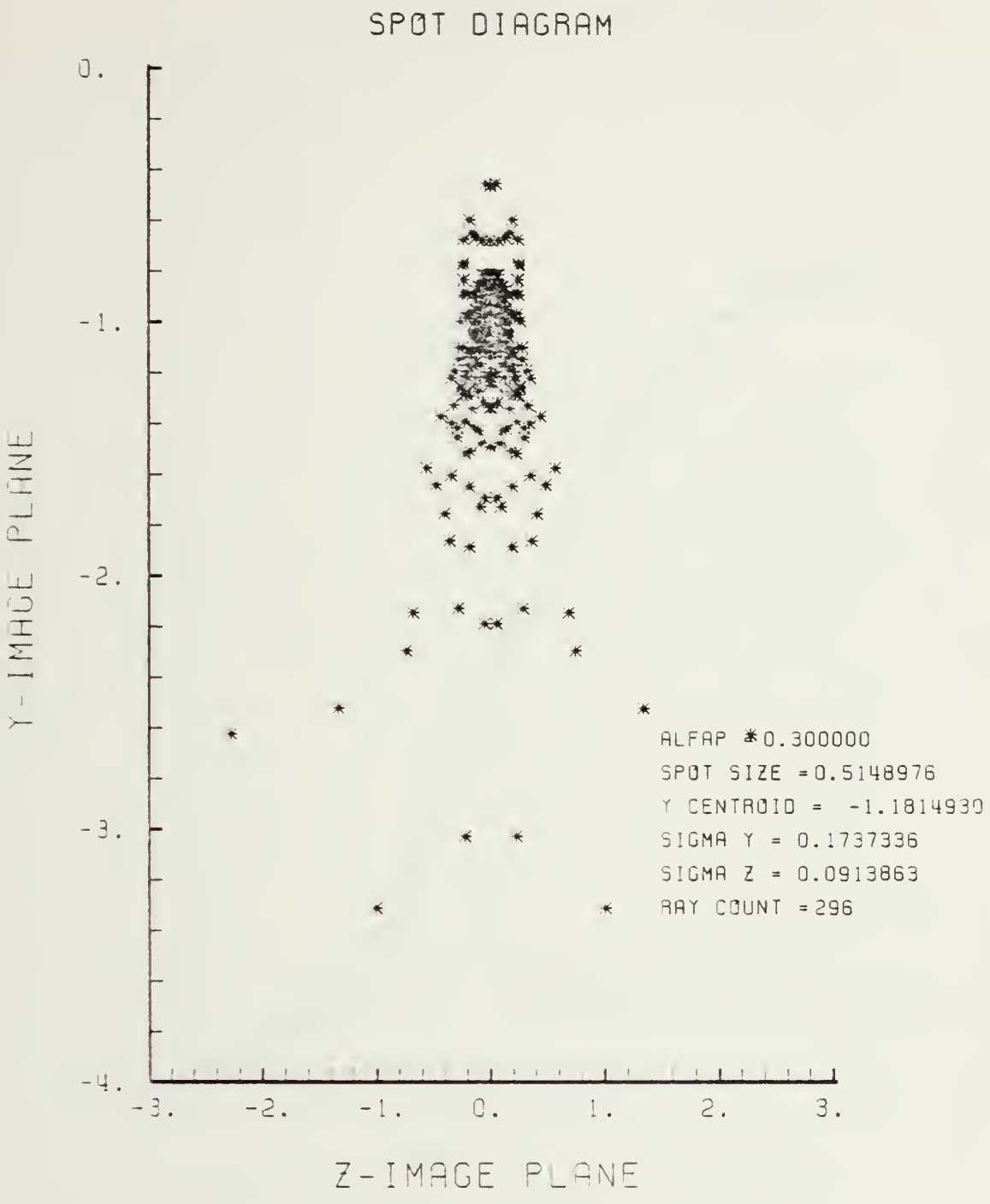

Figure E-83. Spot Diagram for Grid of Figure E-82

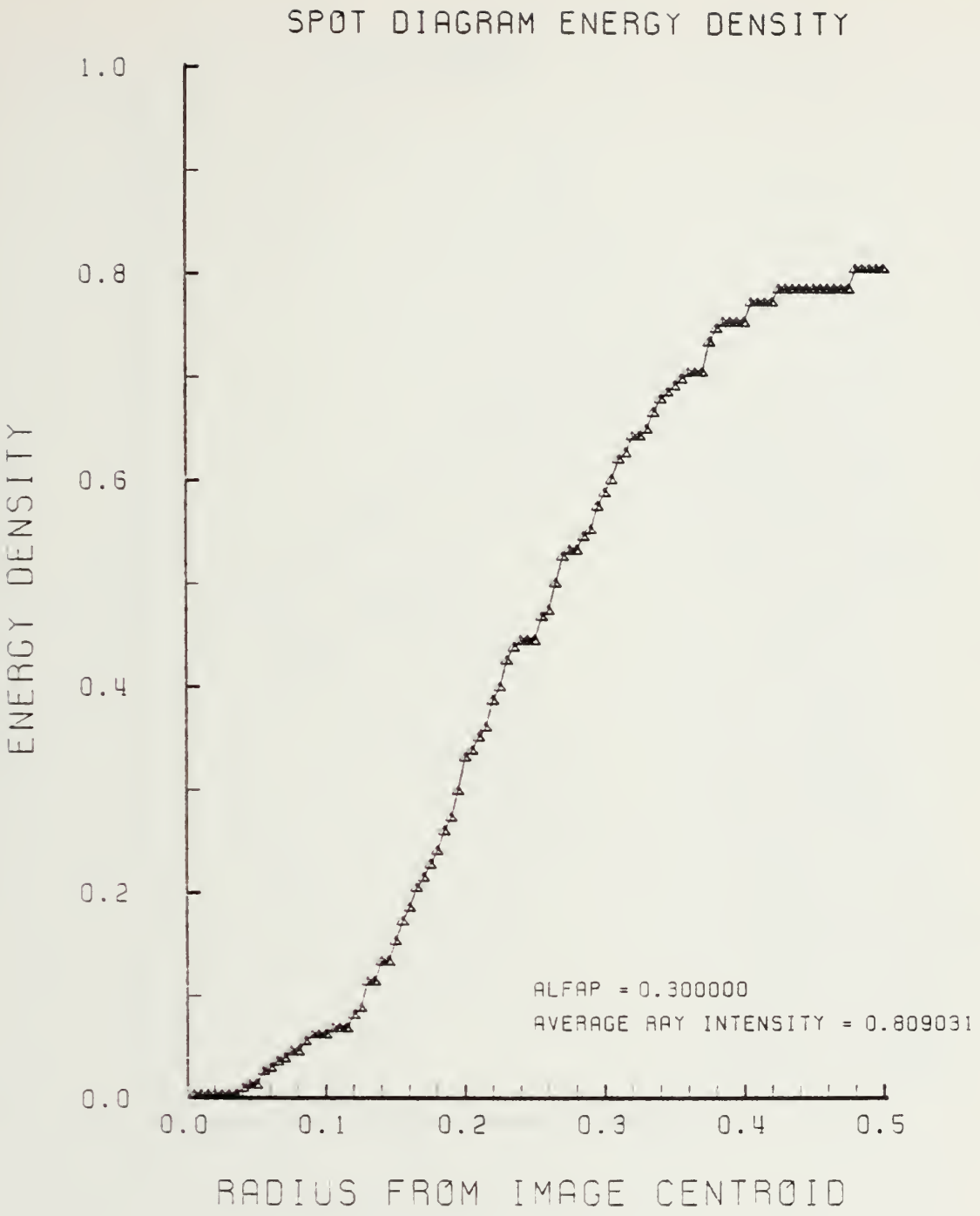

Figure E-84. Encircled Energy of Figure E-83

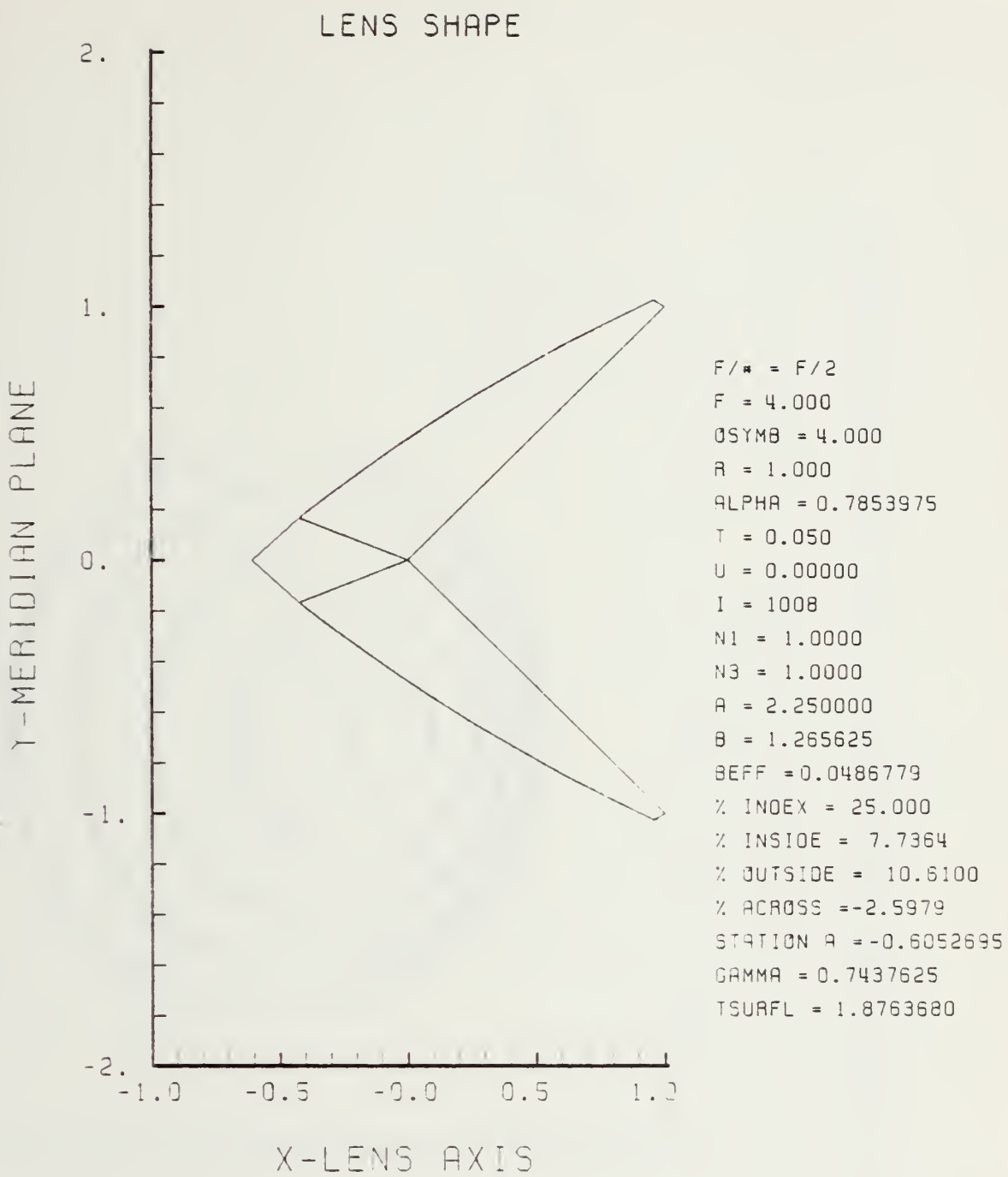

Figure E-85. GRIN Lens Shape at +25%, OB = 4.00, a = 2.25

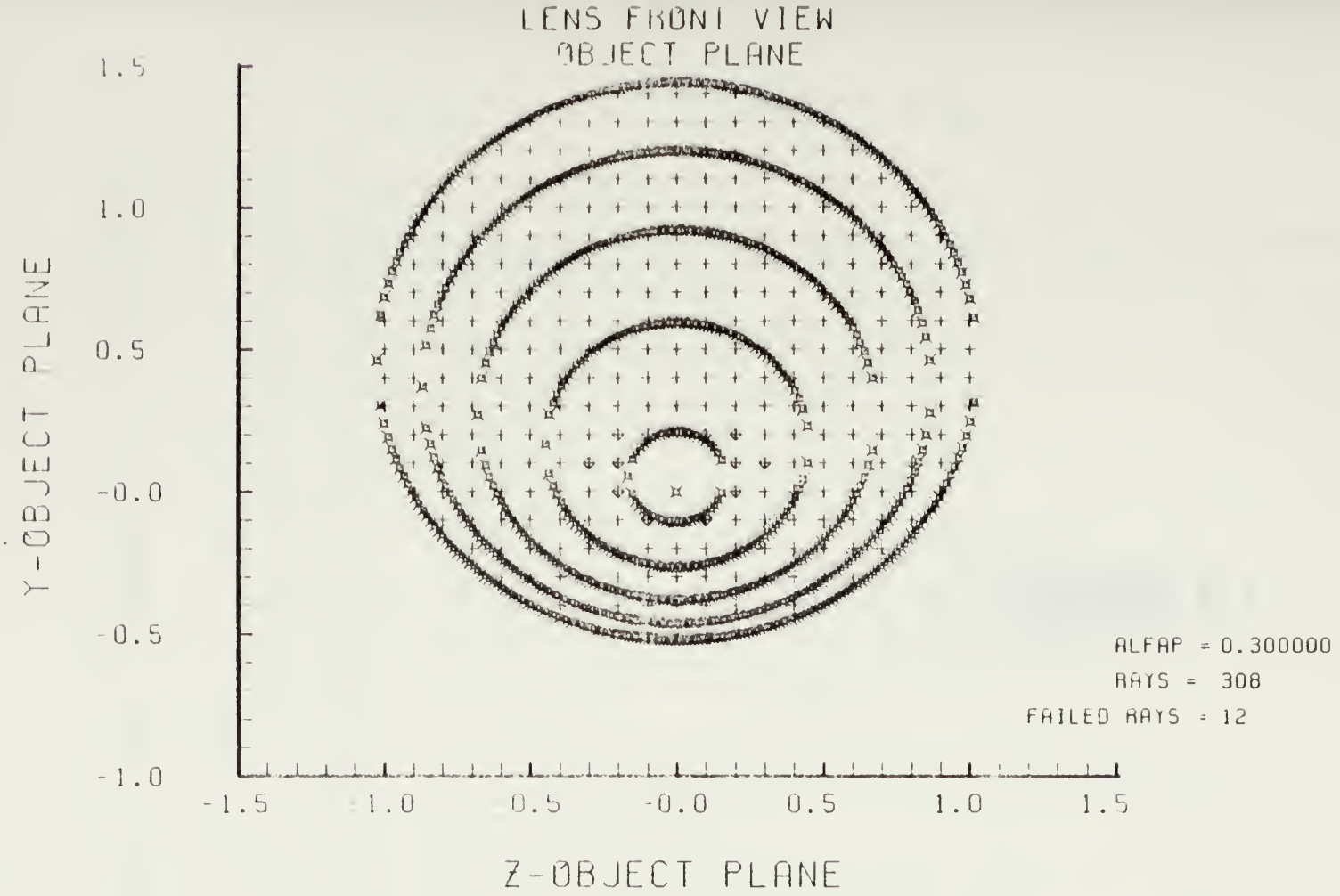

Figure E-86. Grid Plane at $\alpha_p = 0.3$ for Lens of Figure E-85

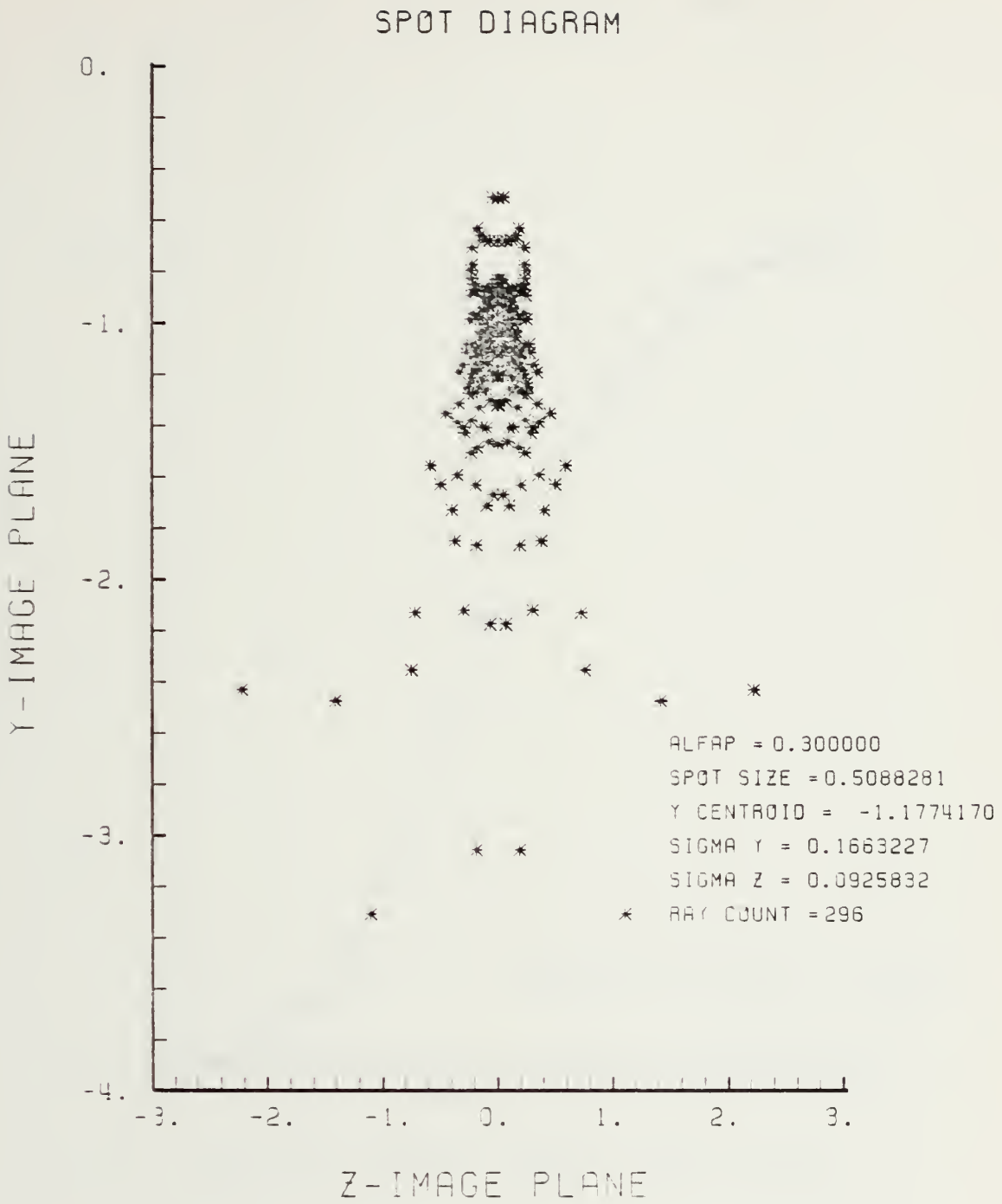

Figure E-87. Spot Diagram for Grid of Figure E-86

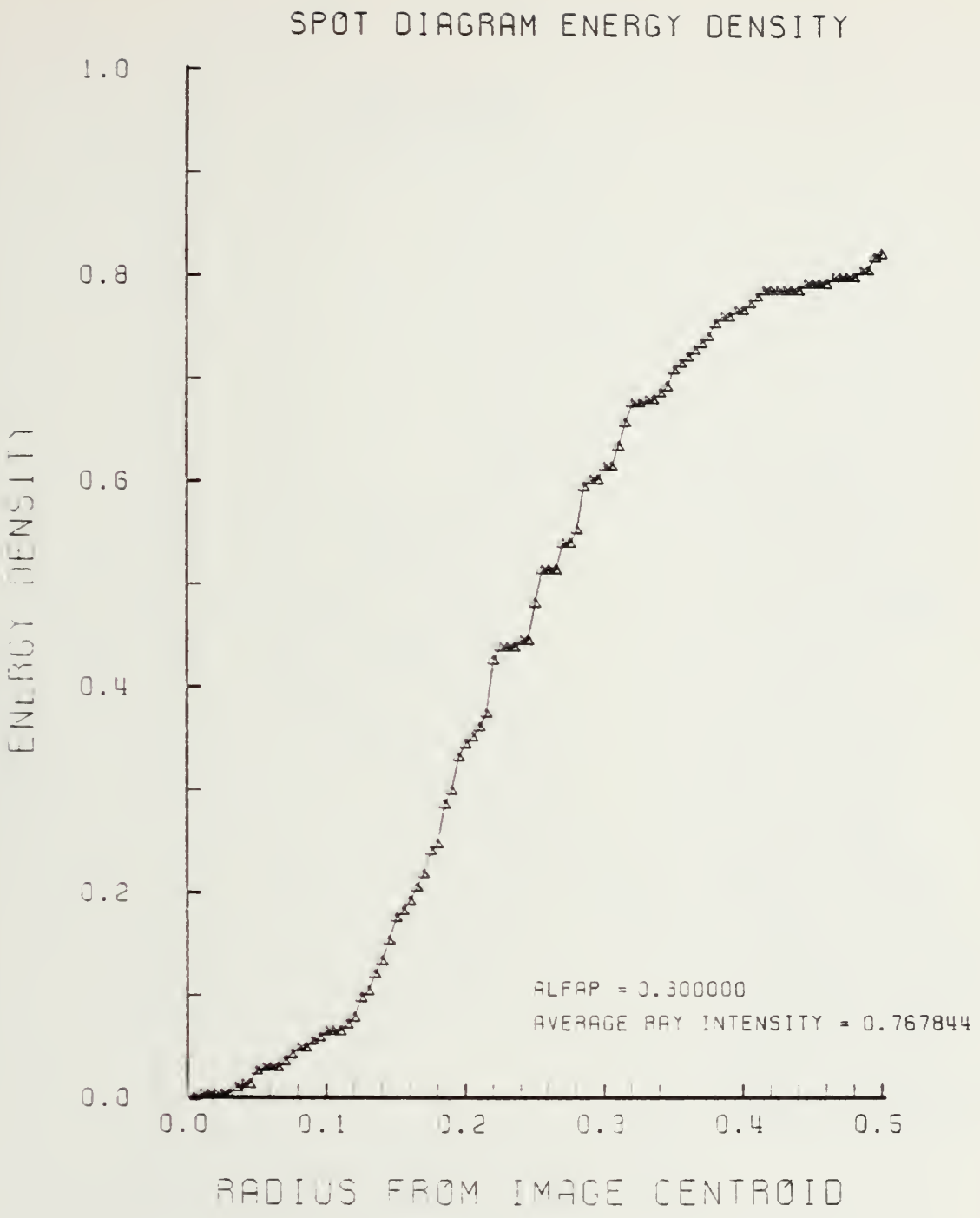

Figure E-88. Encircled Energy of Figure E-87

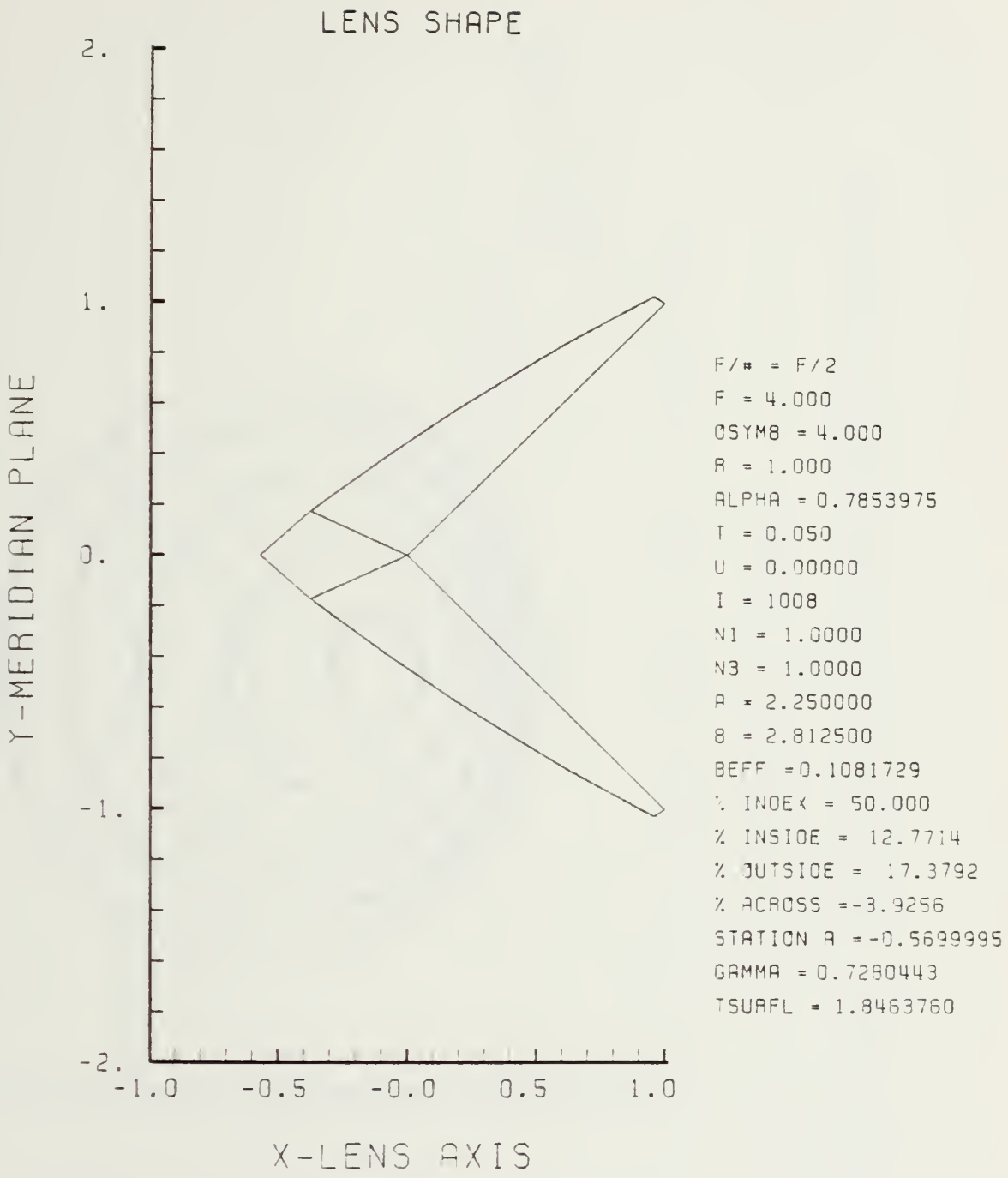

Figure E-89. GRIN Lens Shape at +50%, OB = 4.00, a = 2.25

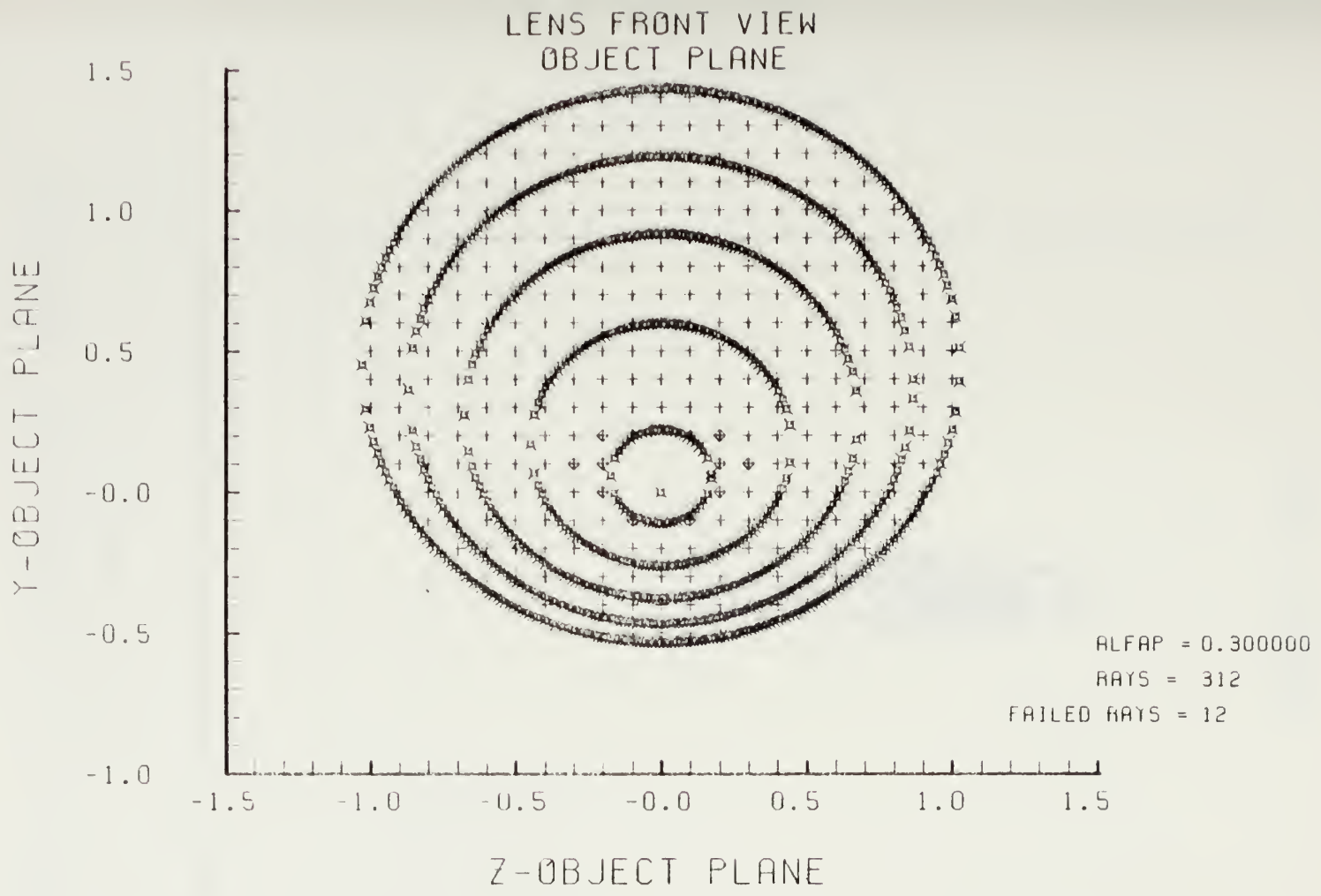

Figure E-90. Grid Plane at α_p = 0.3 for Lens of Figure E-89

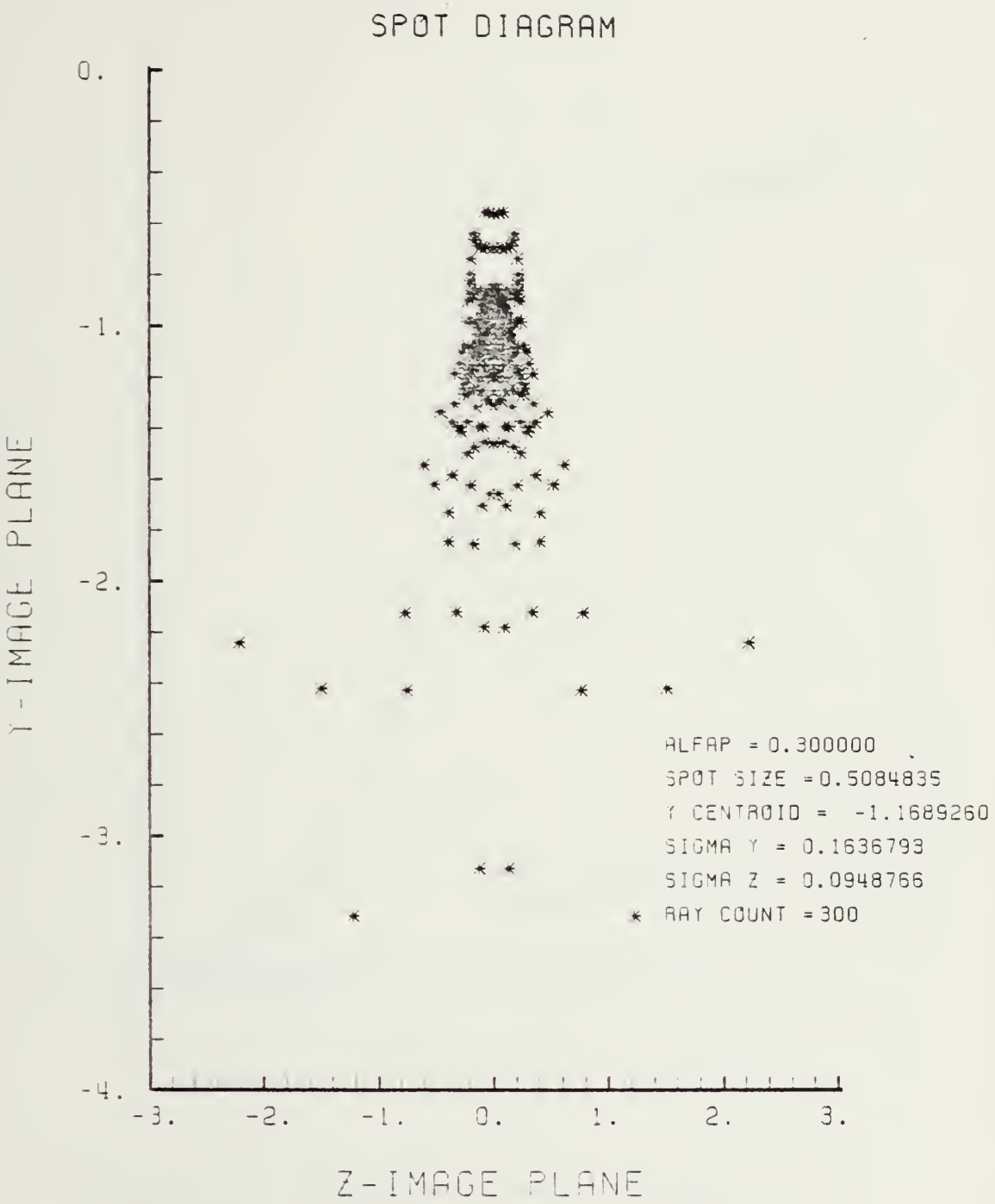

Figure E-91. Spot Diagram for Grid of Figure E-90

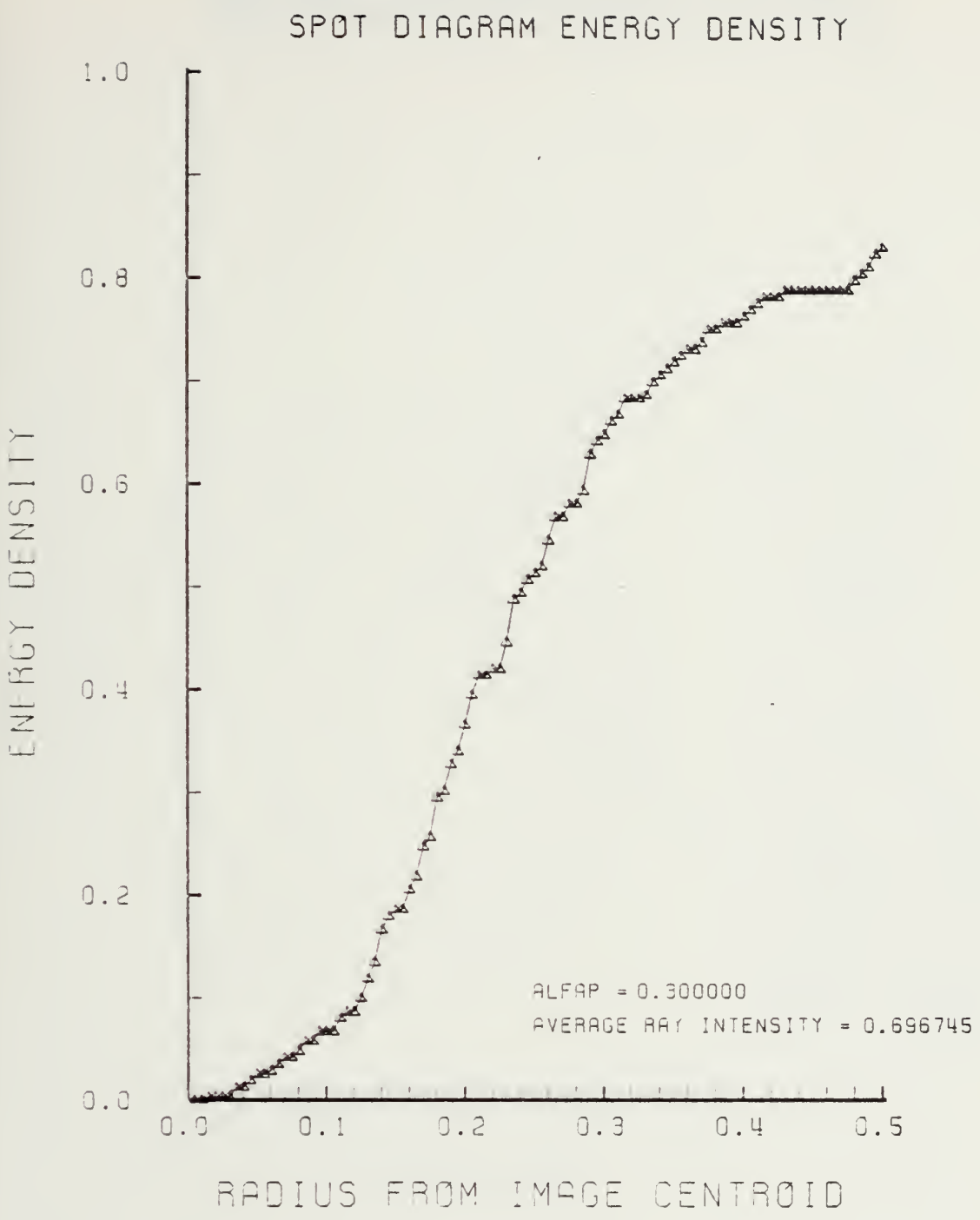

Figure E-92. Encircled Energy of Figure E-91

APPENDIX F

GRIN LENS PERFORMANCE PLOTS IN THE HIGH RANGE OF INDICES OF REFRACTION (a = 9.00)

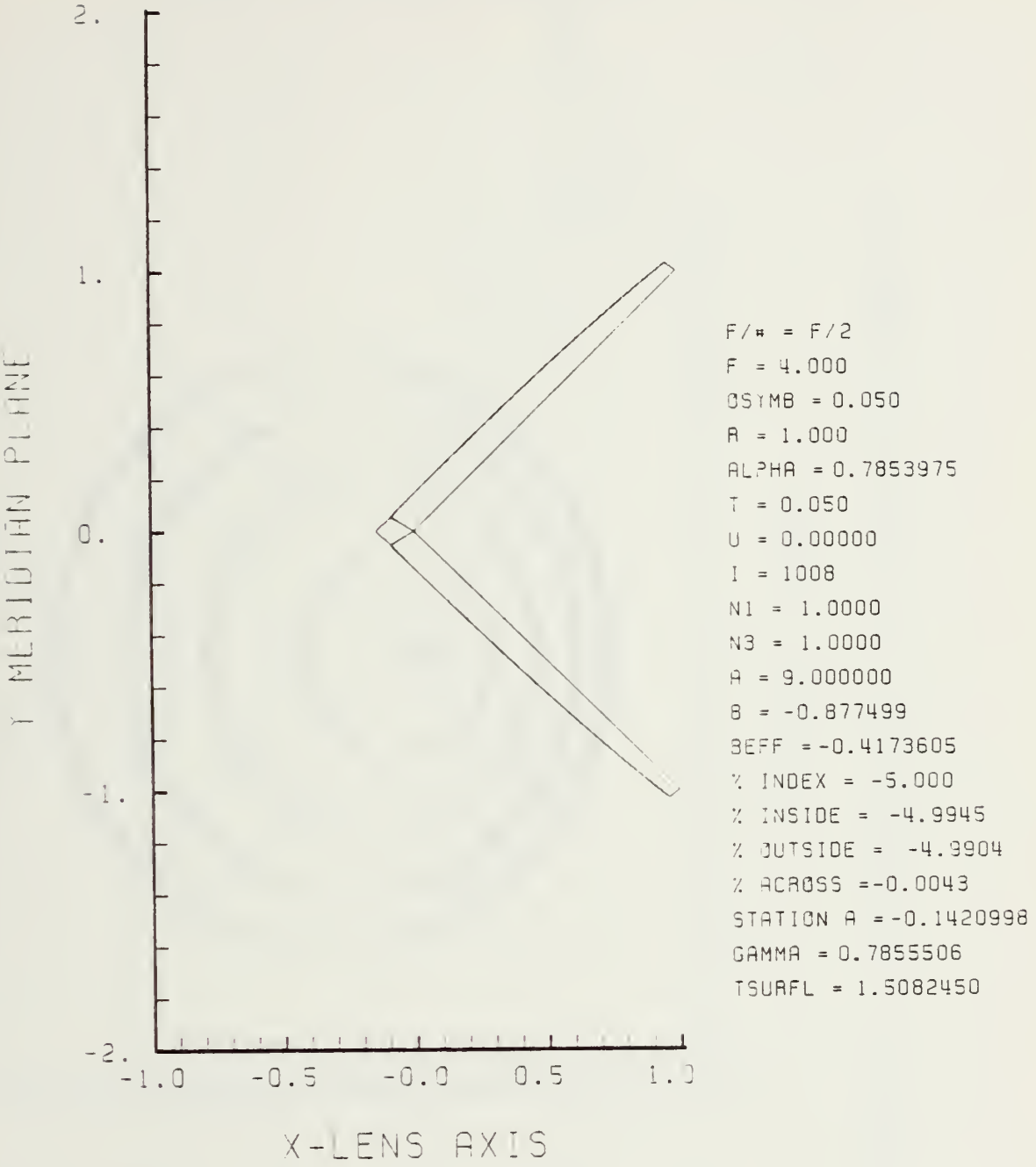

Figure F-1. GRIN Lens Shape at -5%, OB = 0.05, a = 9.00

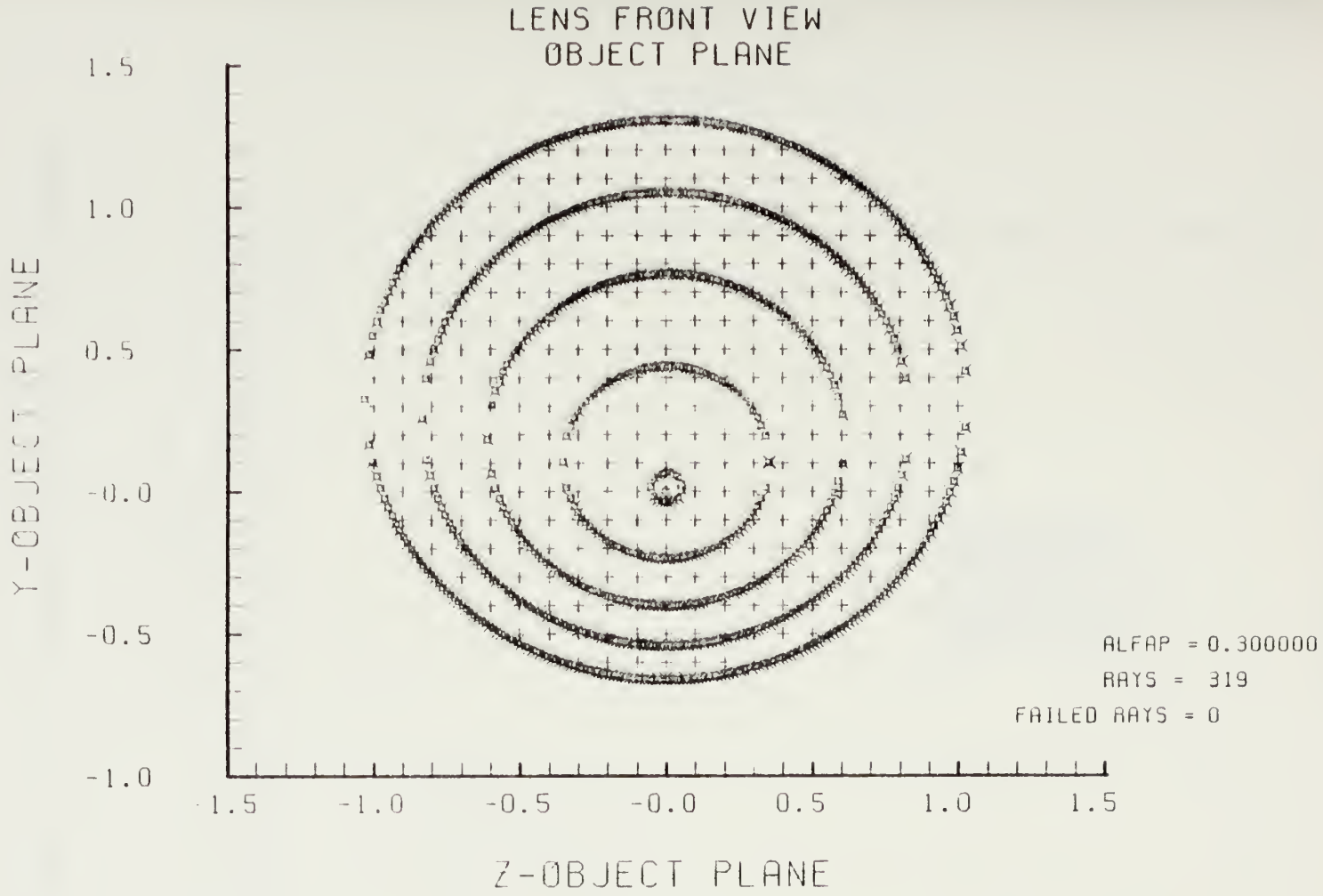

Figure F-2. Grid Plane at $\alpha_p = 0.3$ for Lens of Figure F-1

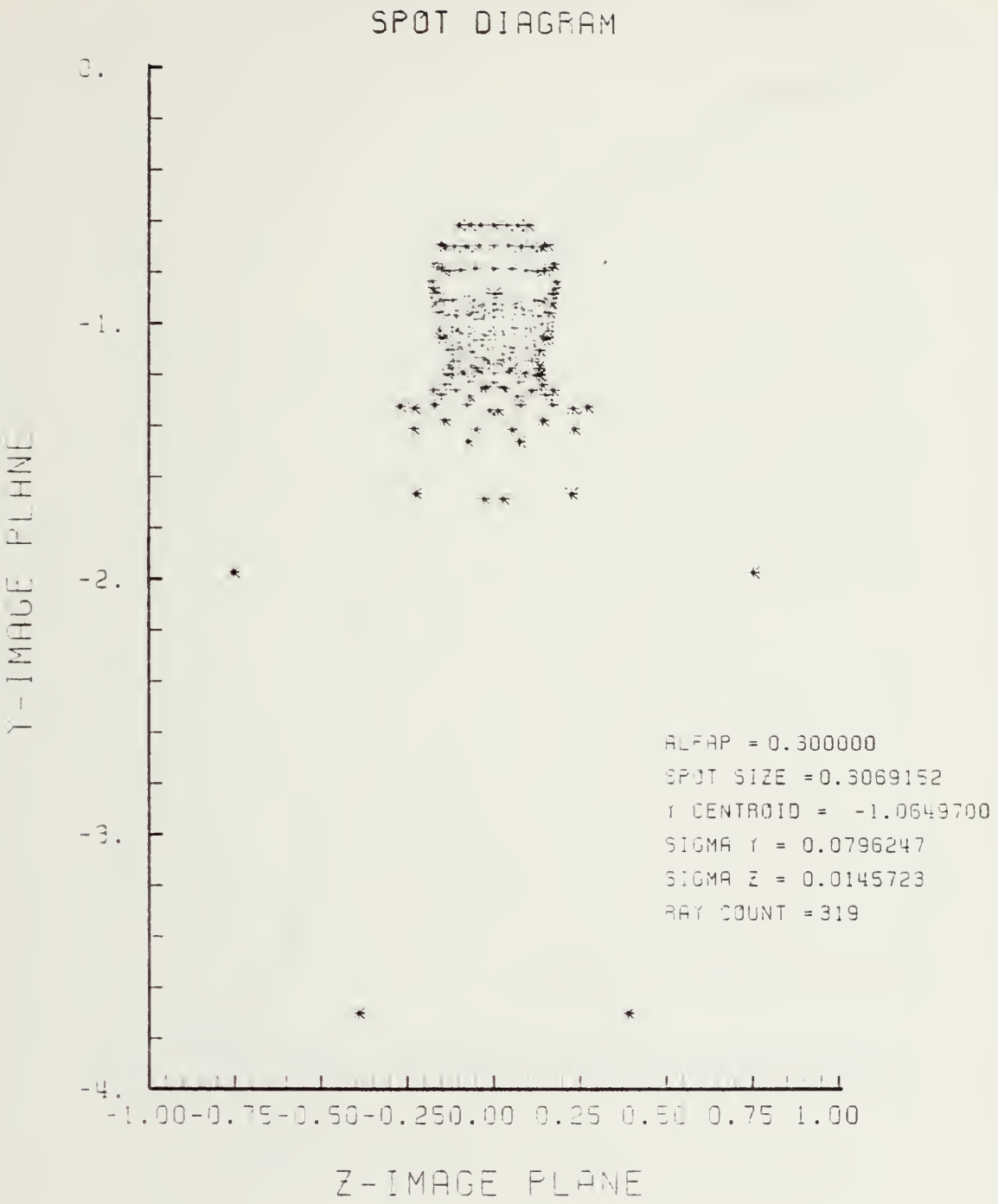

Figure F-3. Spot Diagram for Grid of Figure F-2

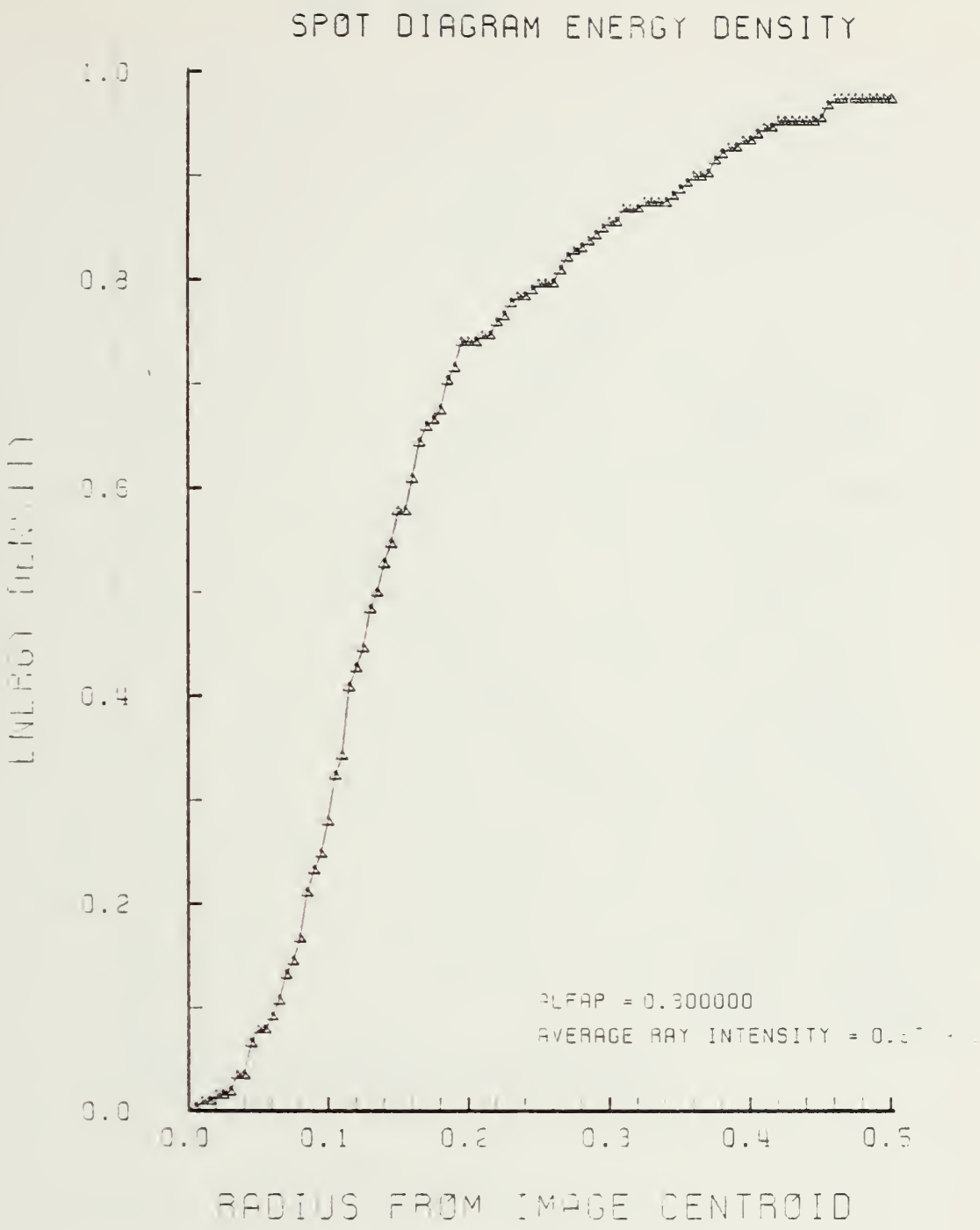

Figure F-4. Encircled Energy of Figure F-3

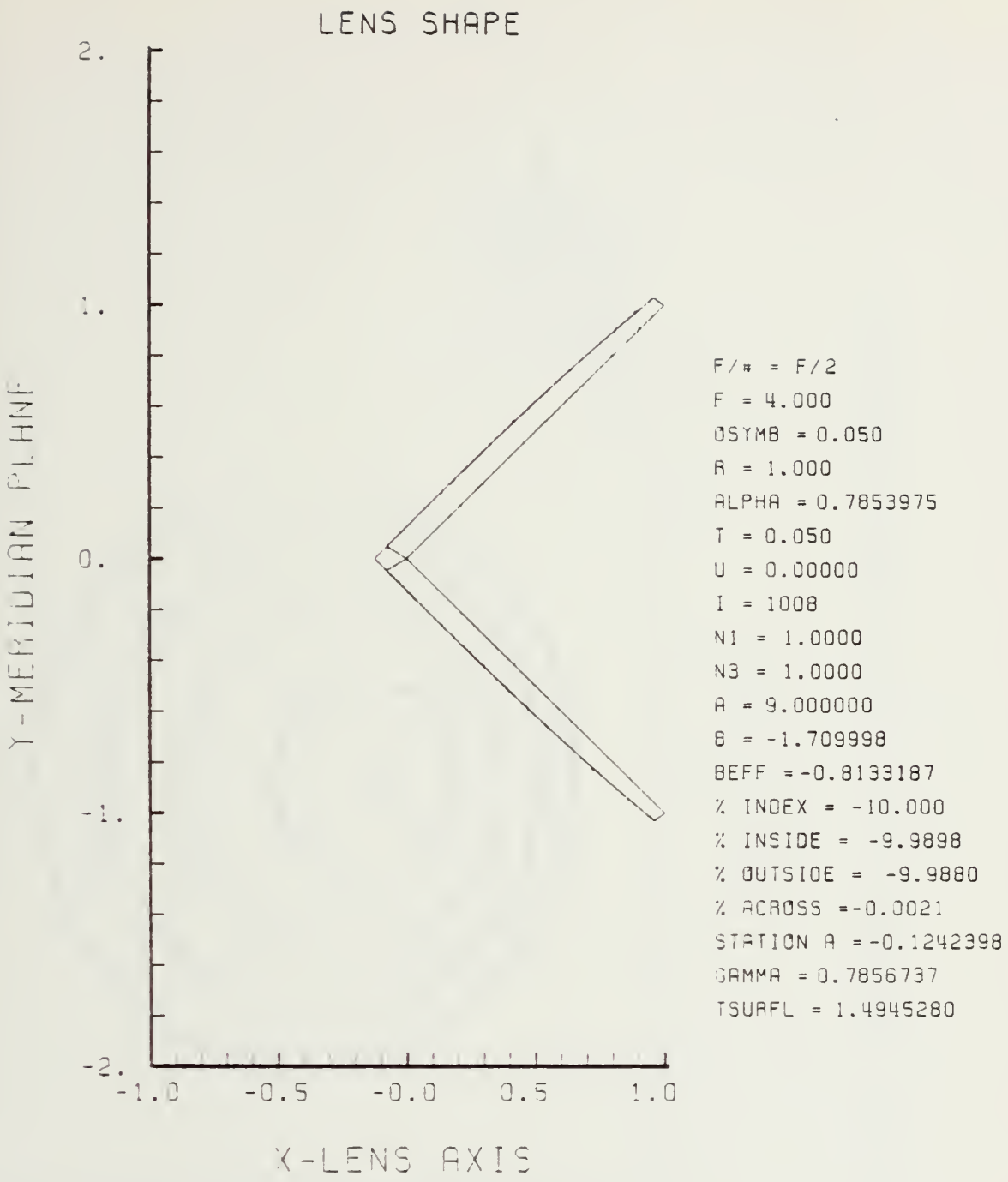

Figure F-5. GRIN Lens Shape at -10%, OB = 0.05, a = 9.00

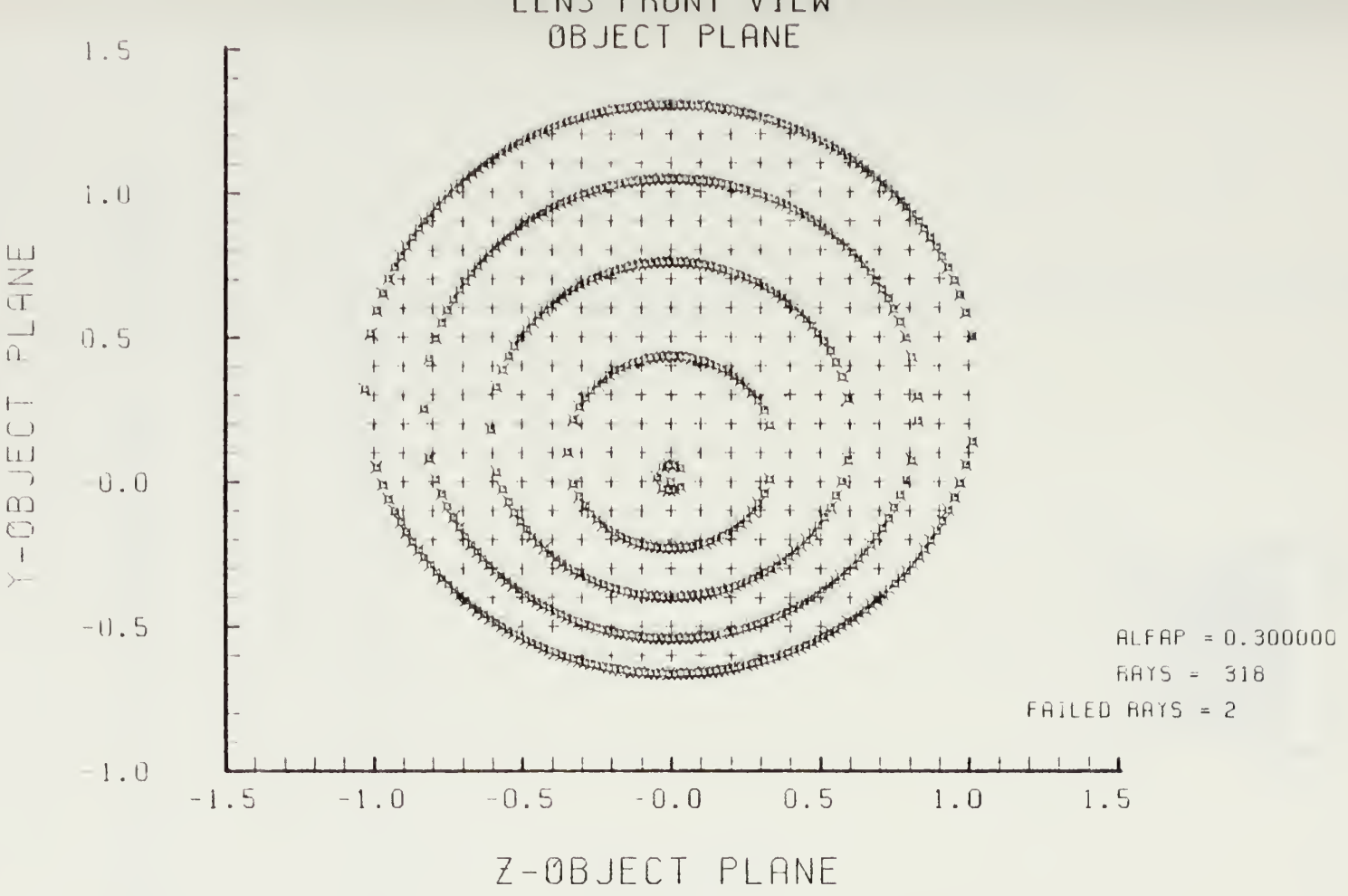

Figure F-6. Grid Plane at α_p = 0.3 for Lens of Figure F-5

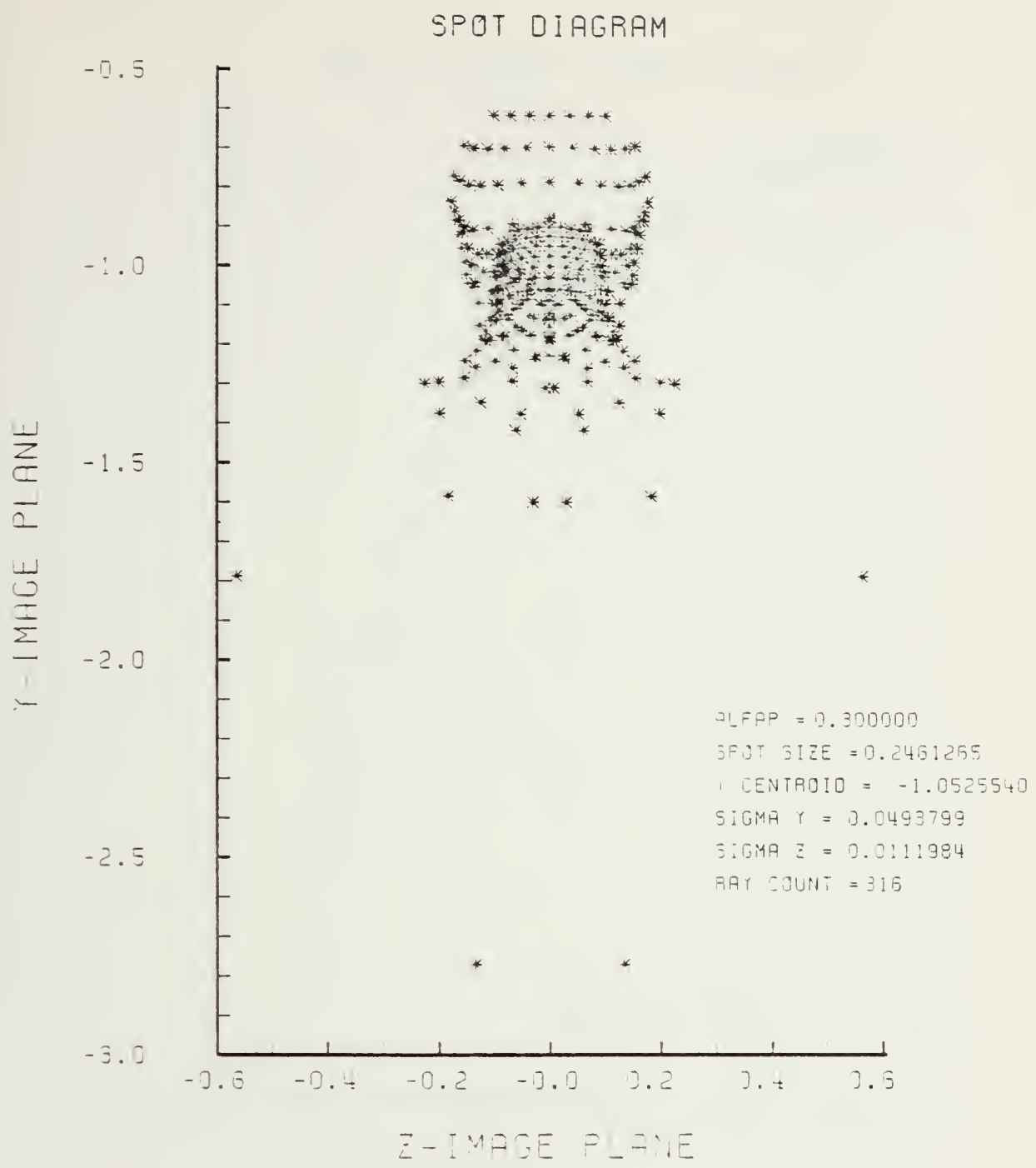

Figure F-7. Spot Diagram for Grid of Figure F-6

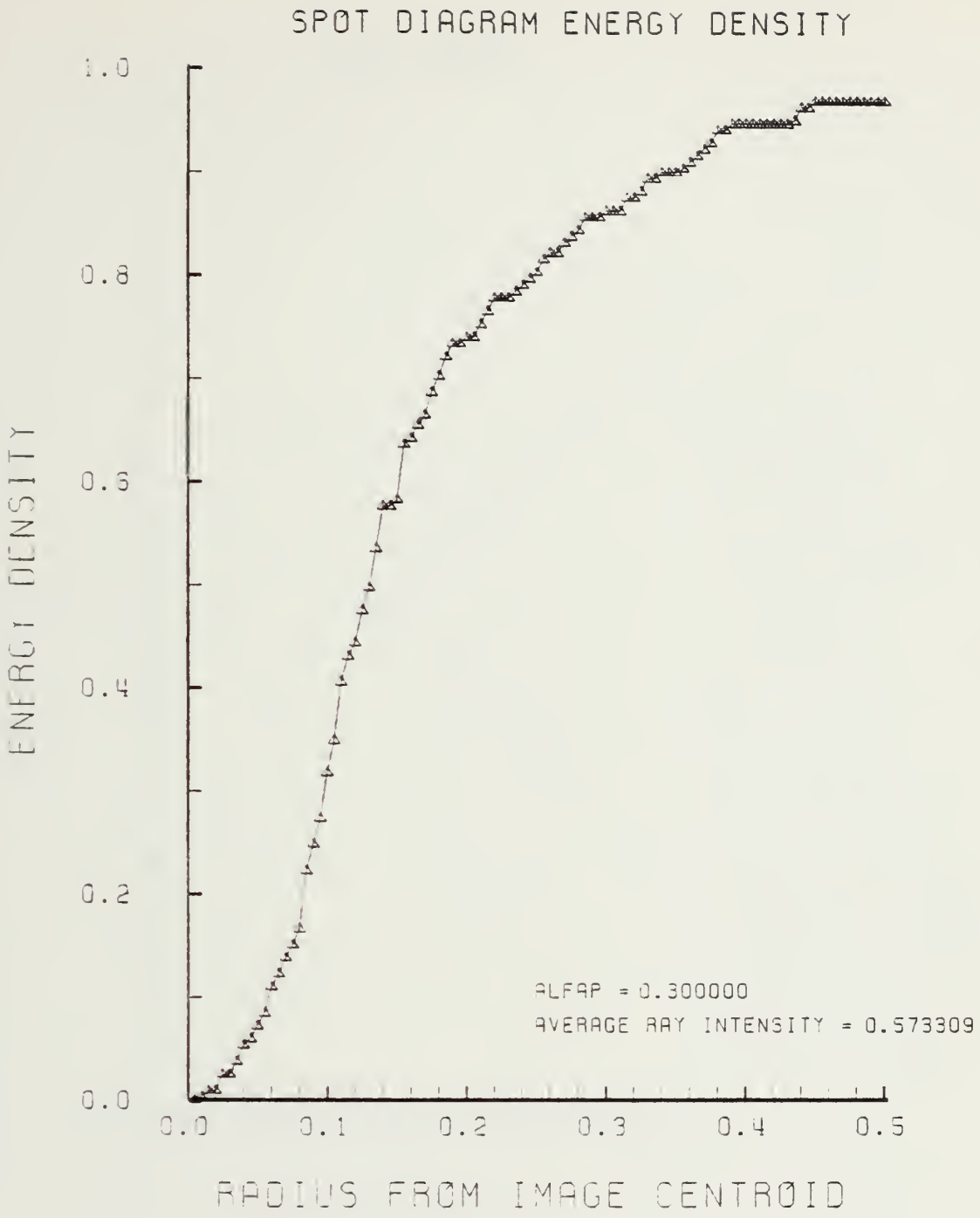

Figure F-8. Encircled Energy of Figure F-7

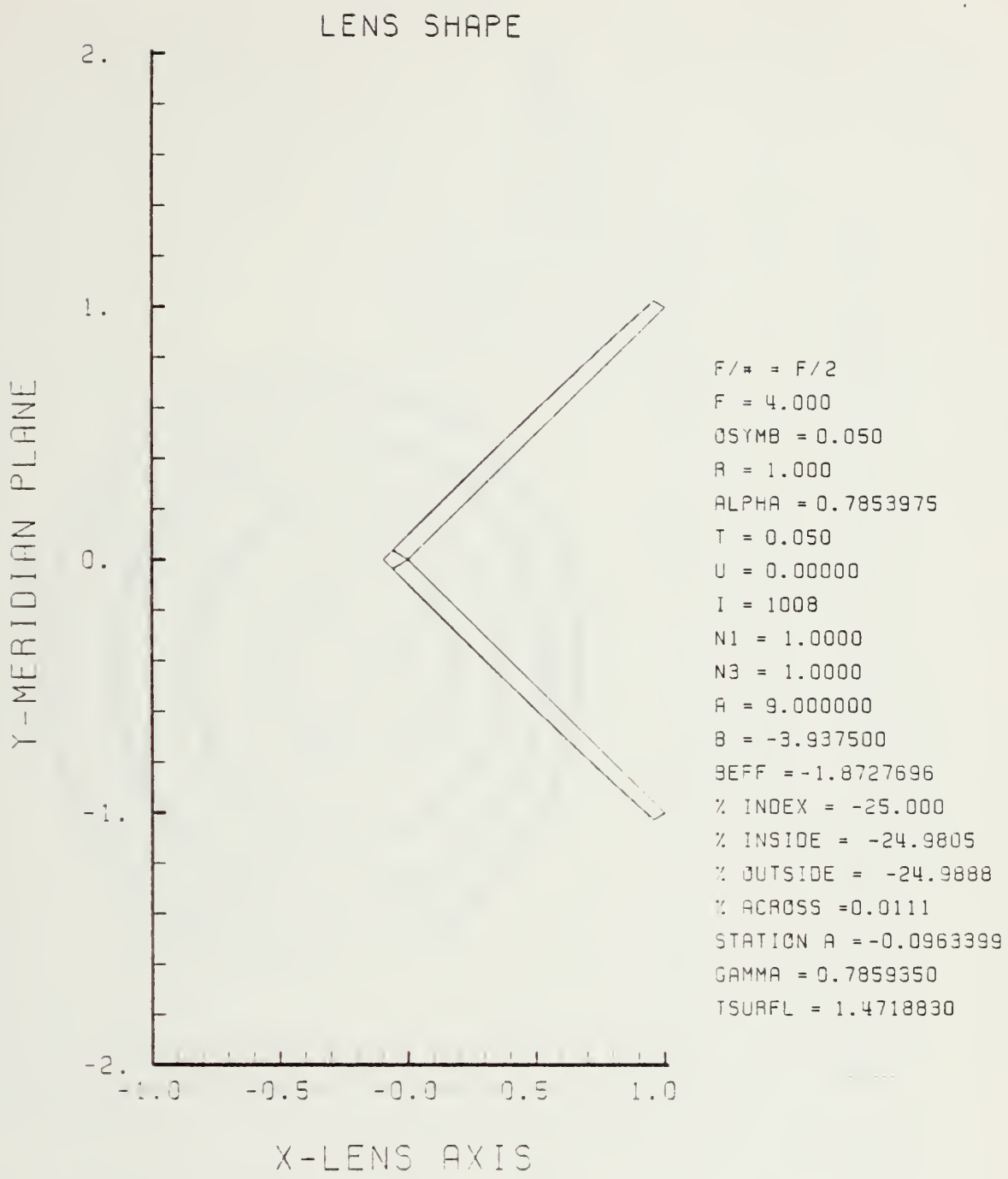

Figure F-9. GRIN Lens Shape at -25%, OB = 0.05, a = 9.00

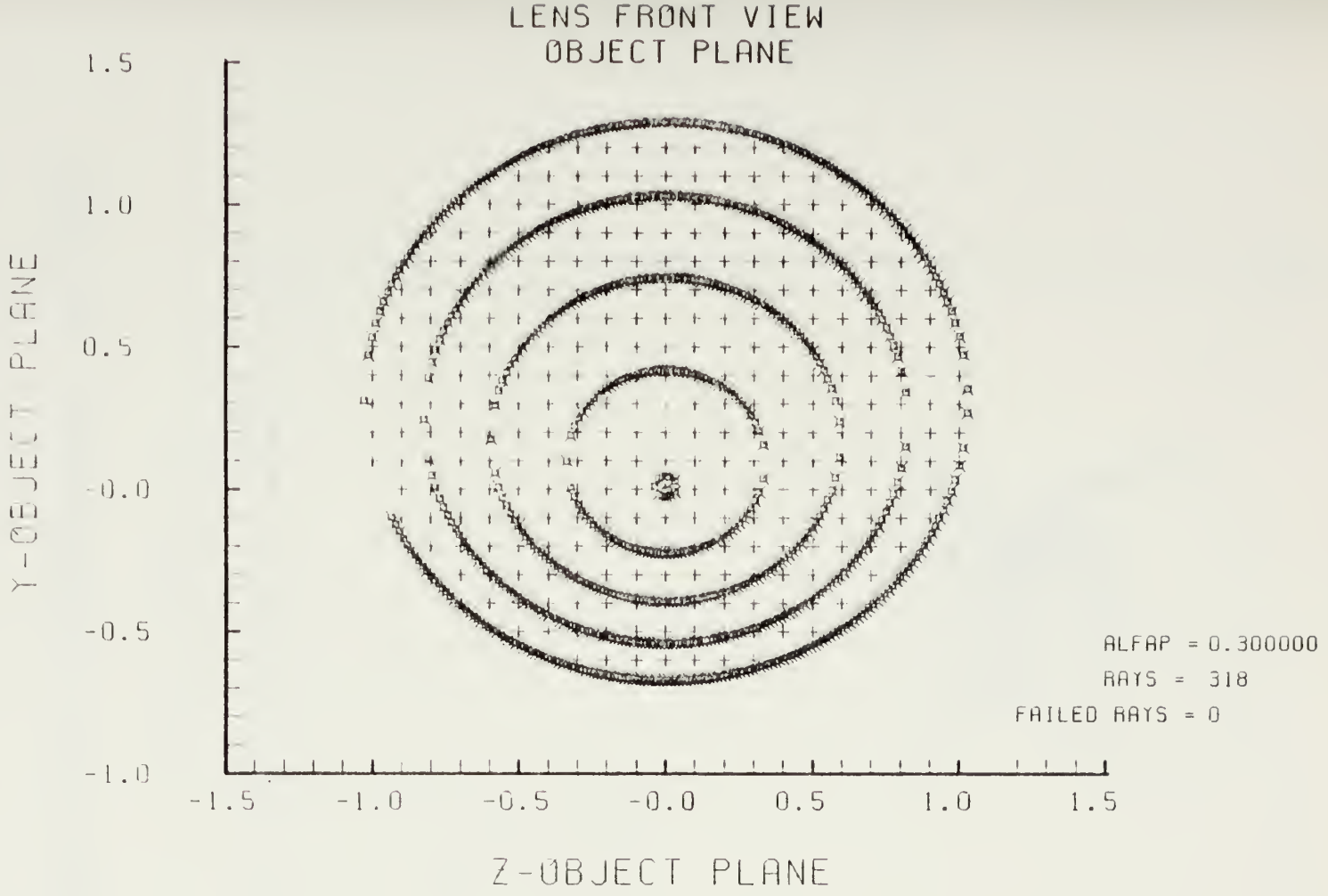

Figure F-10. Grid Plane at α_p = 0.3 for Lens of Figure F-9

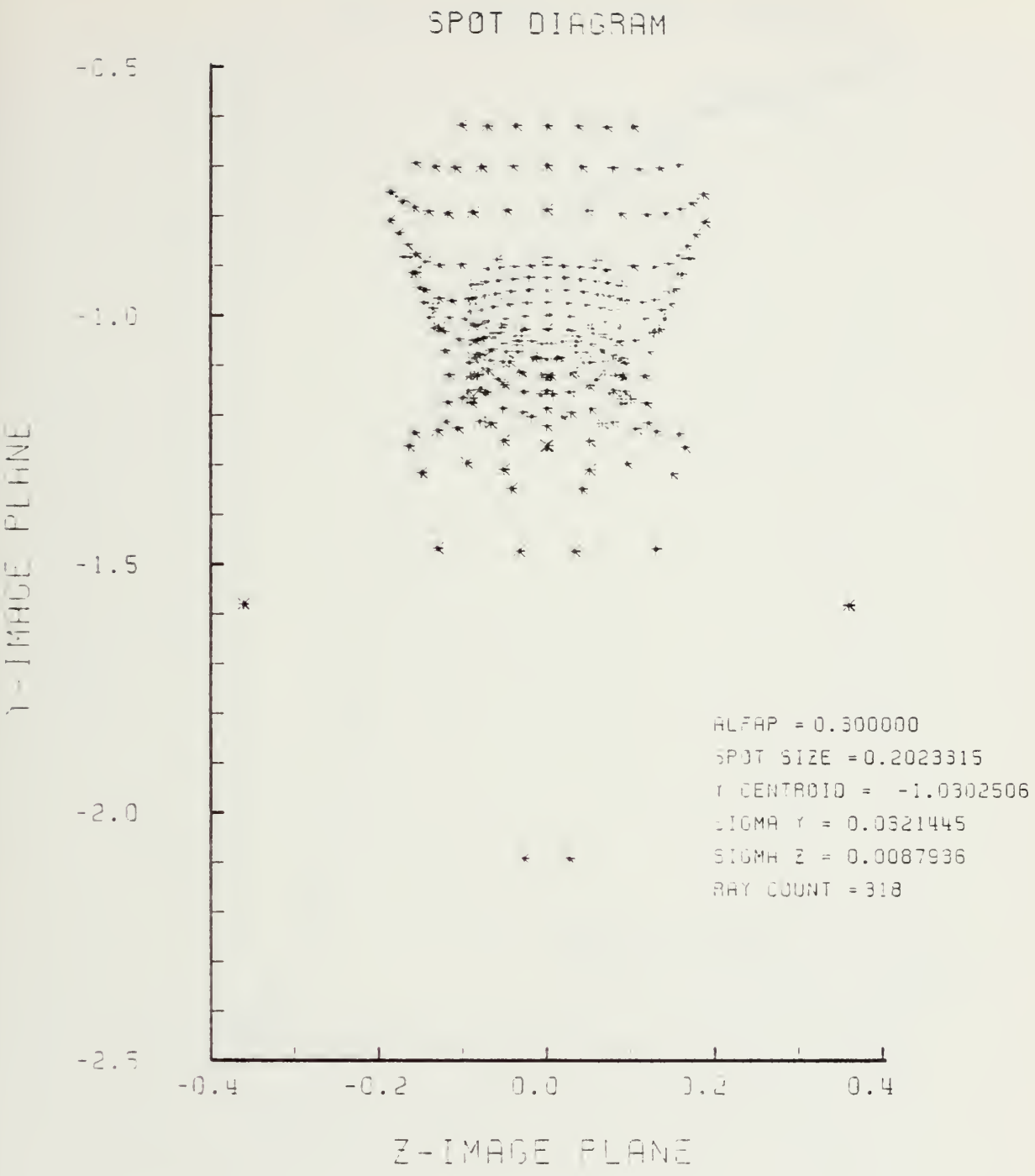

Figure F-11. Spot Diagram for Grid of Figure F-10

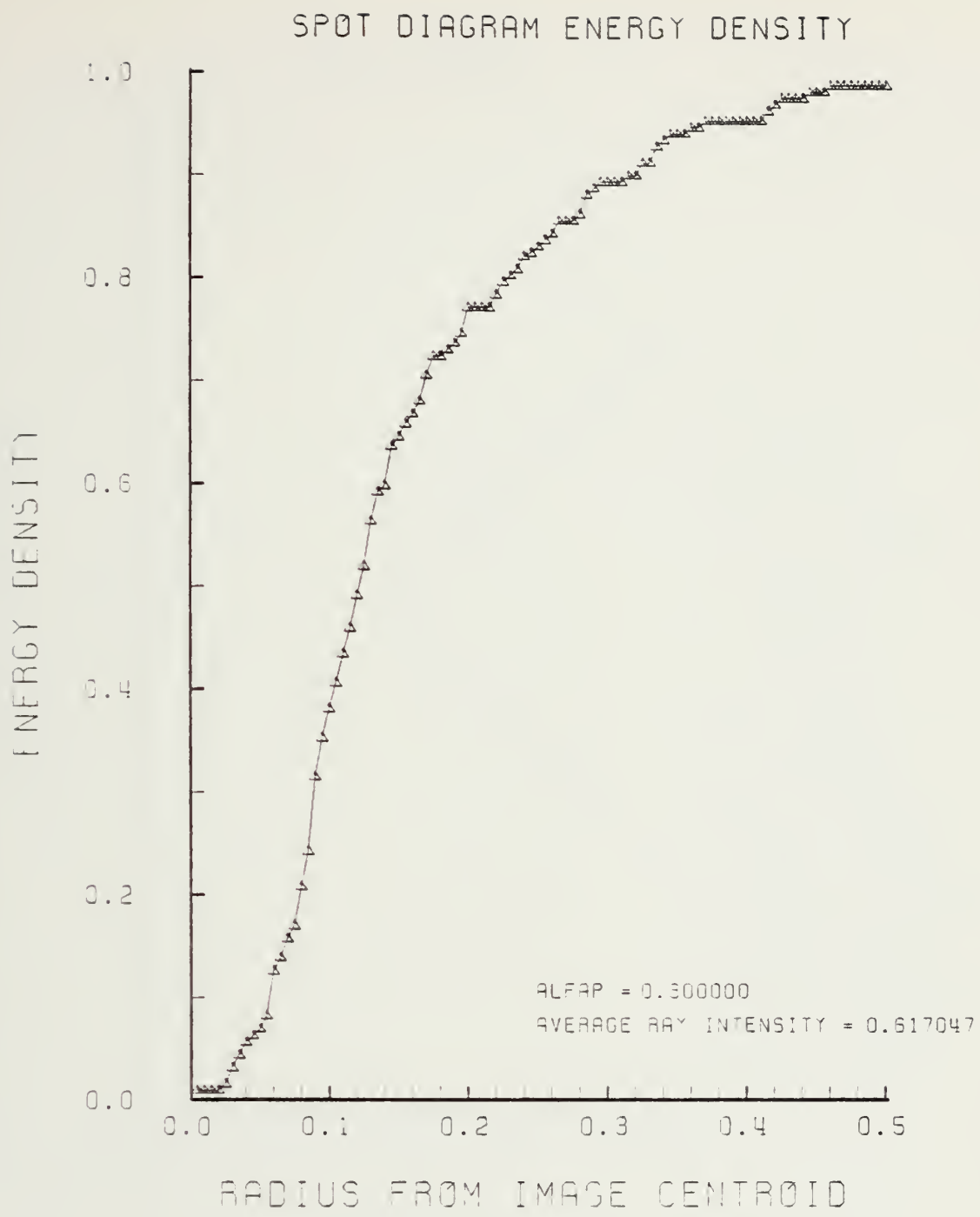

Figure F-12. Encircled Energy of Figure F-11

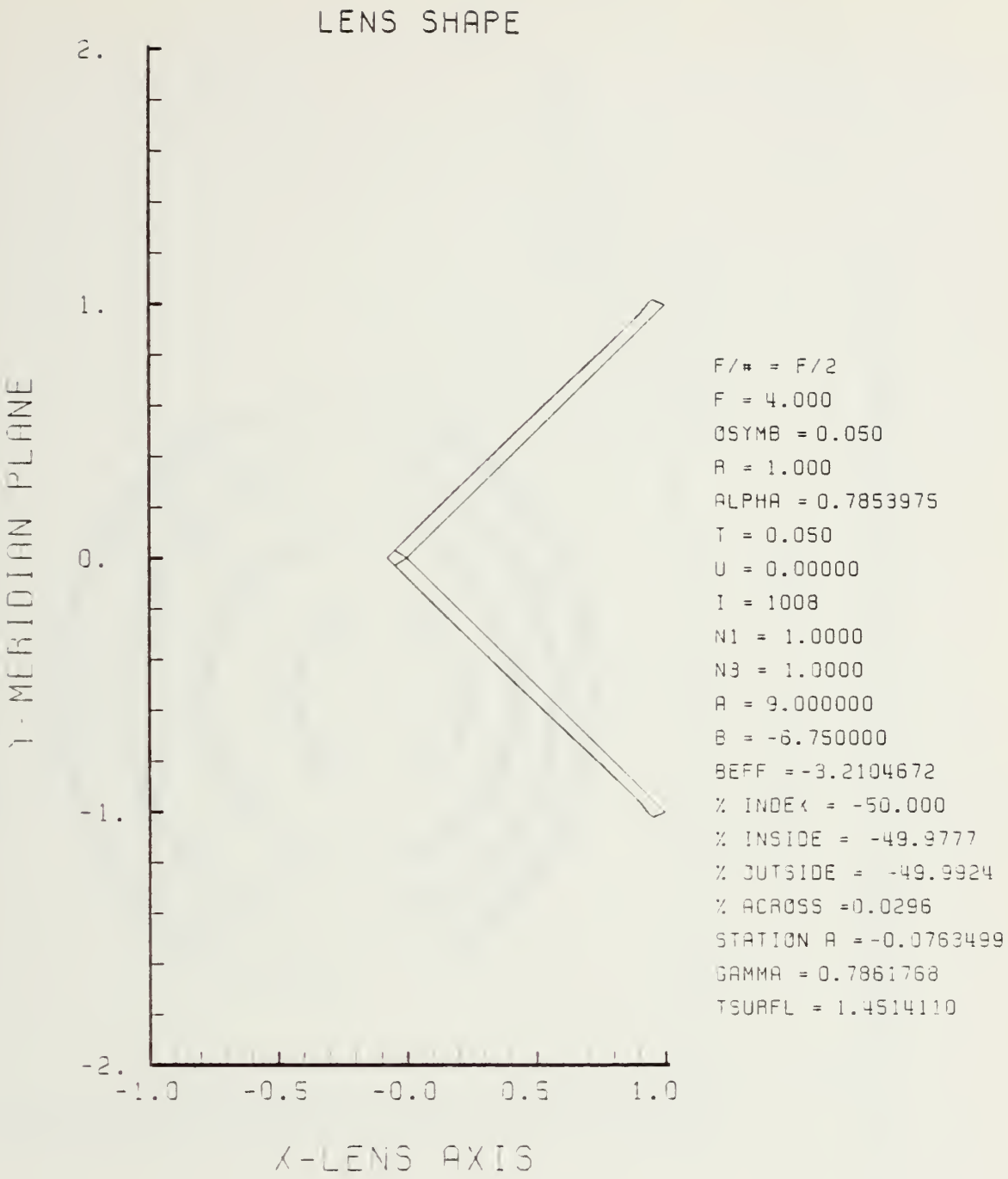

Figure F-13. GRIN Lens Shape at -50%, OB = 0.05, a = 9.00

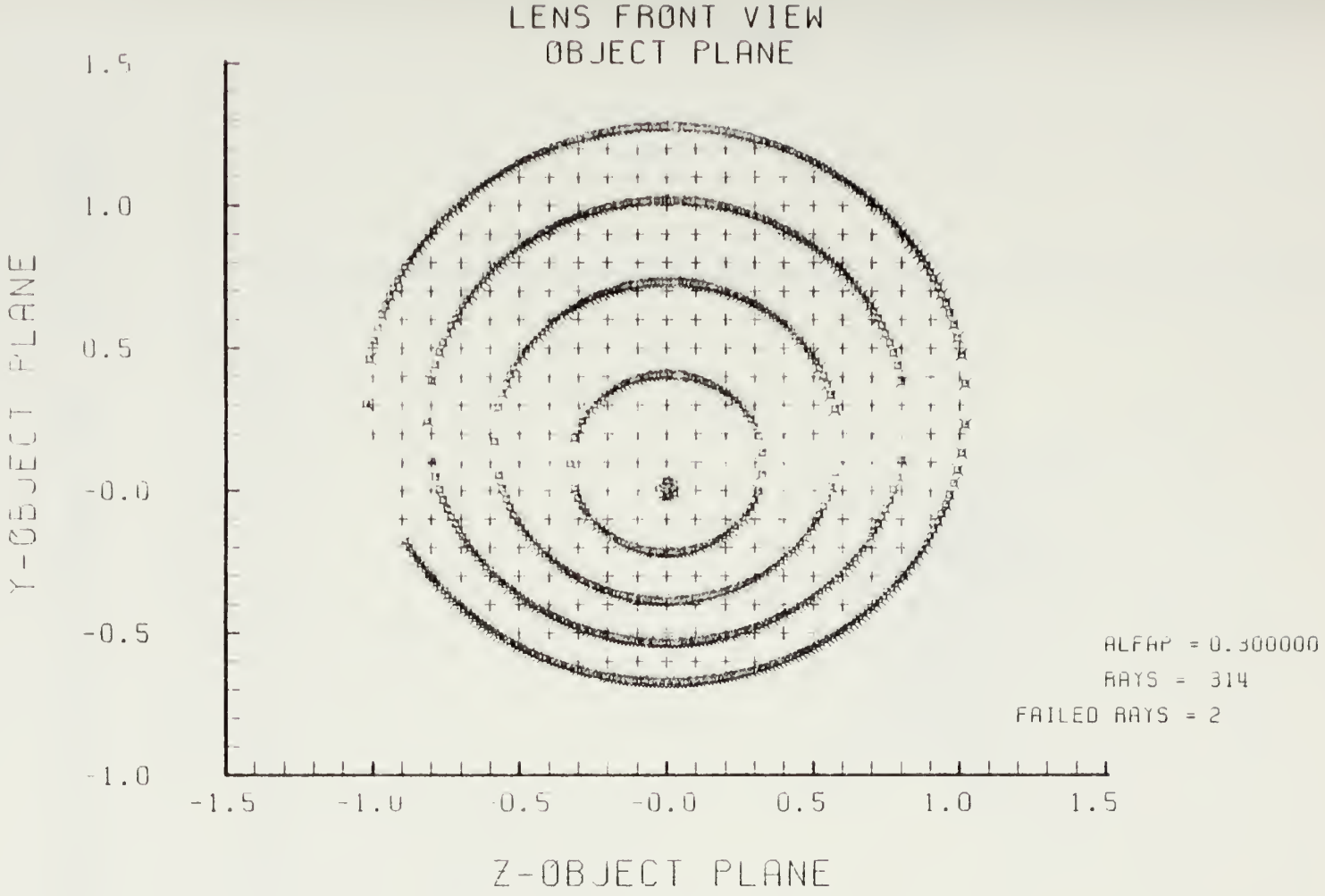

Figure F-14. Grid Plane at $\alpha_p = 0.3$ for Lens of Figure F-13

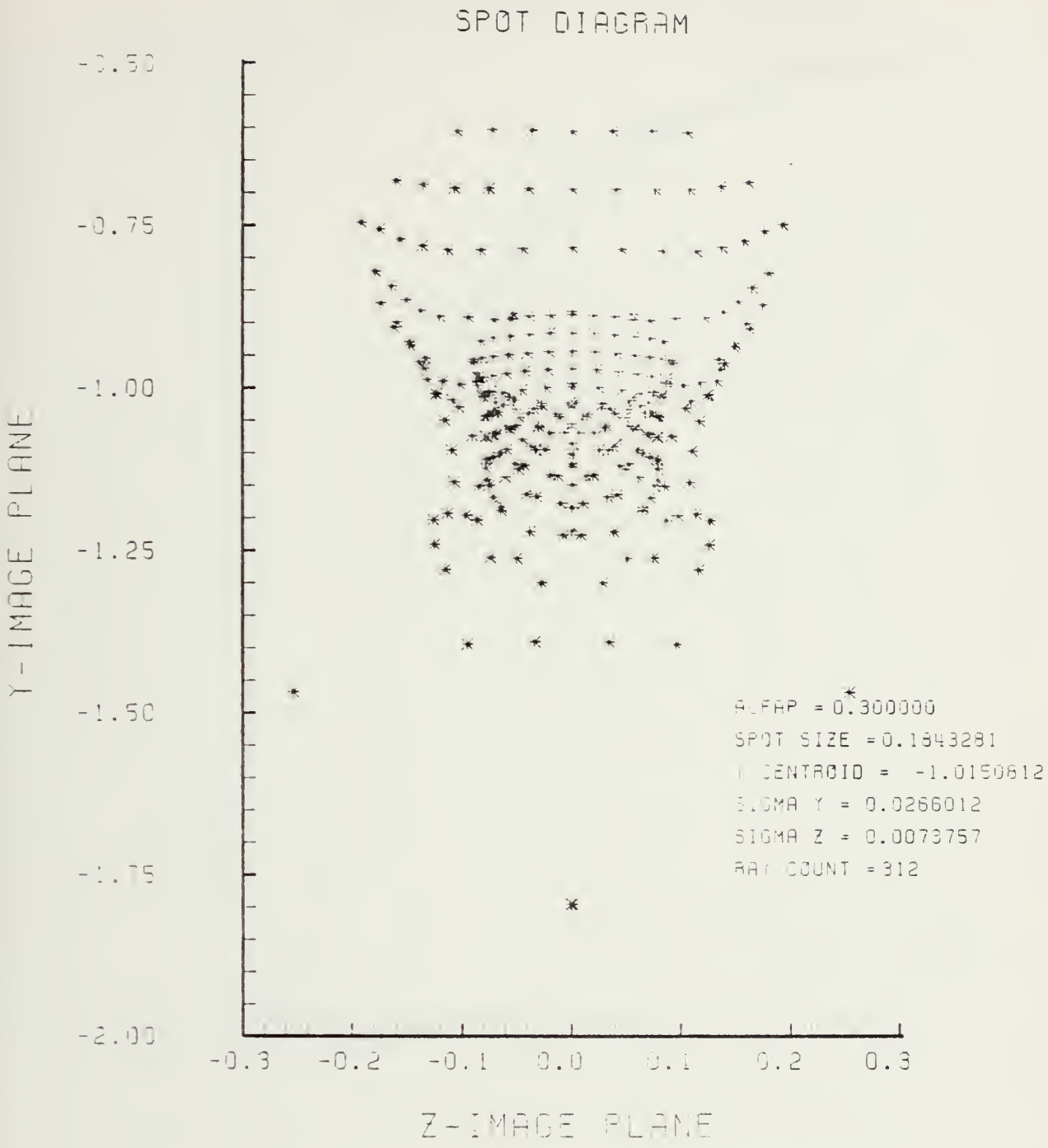

Figure F-15. Spot Diagram for Grid of Figure F-14

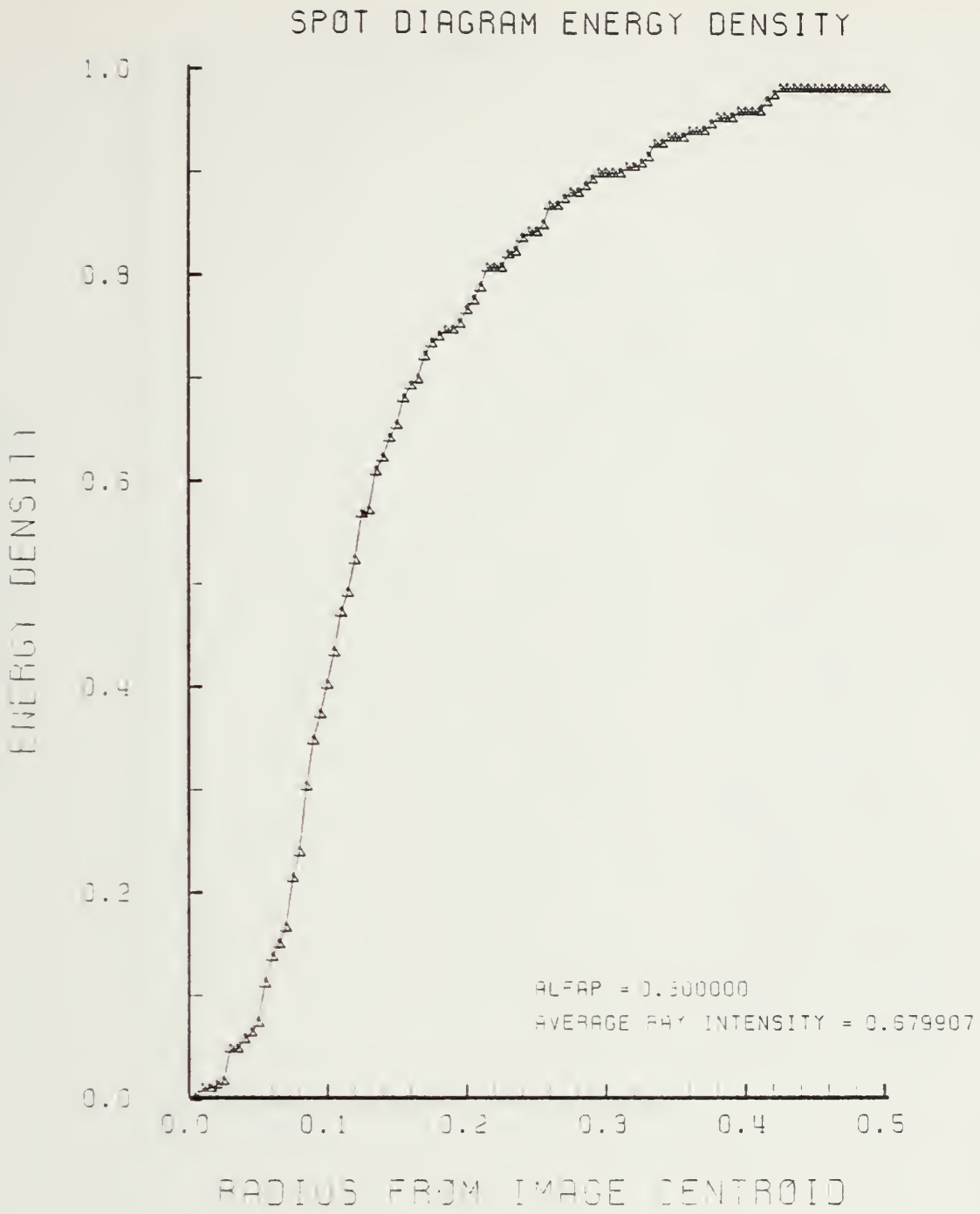

Figure F-16. Encircled Energy of Figure F-15

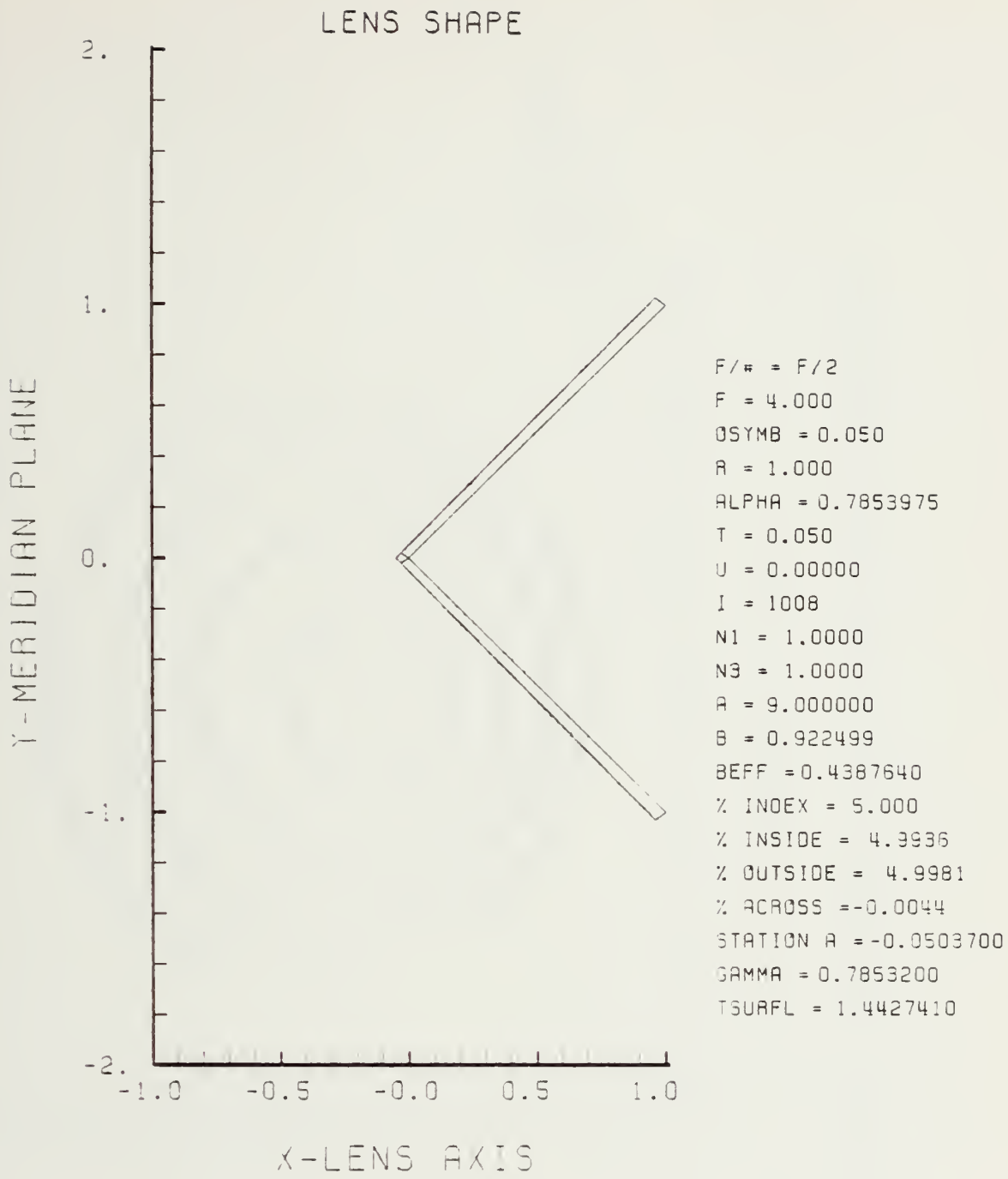

Figure F-17. GRIN Lens Shape at +5%, OB = 0.05, a = 9.00

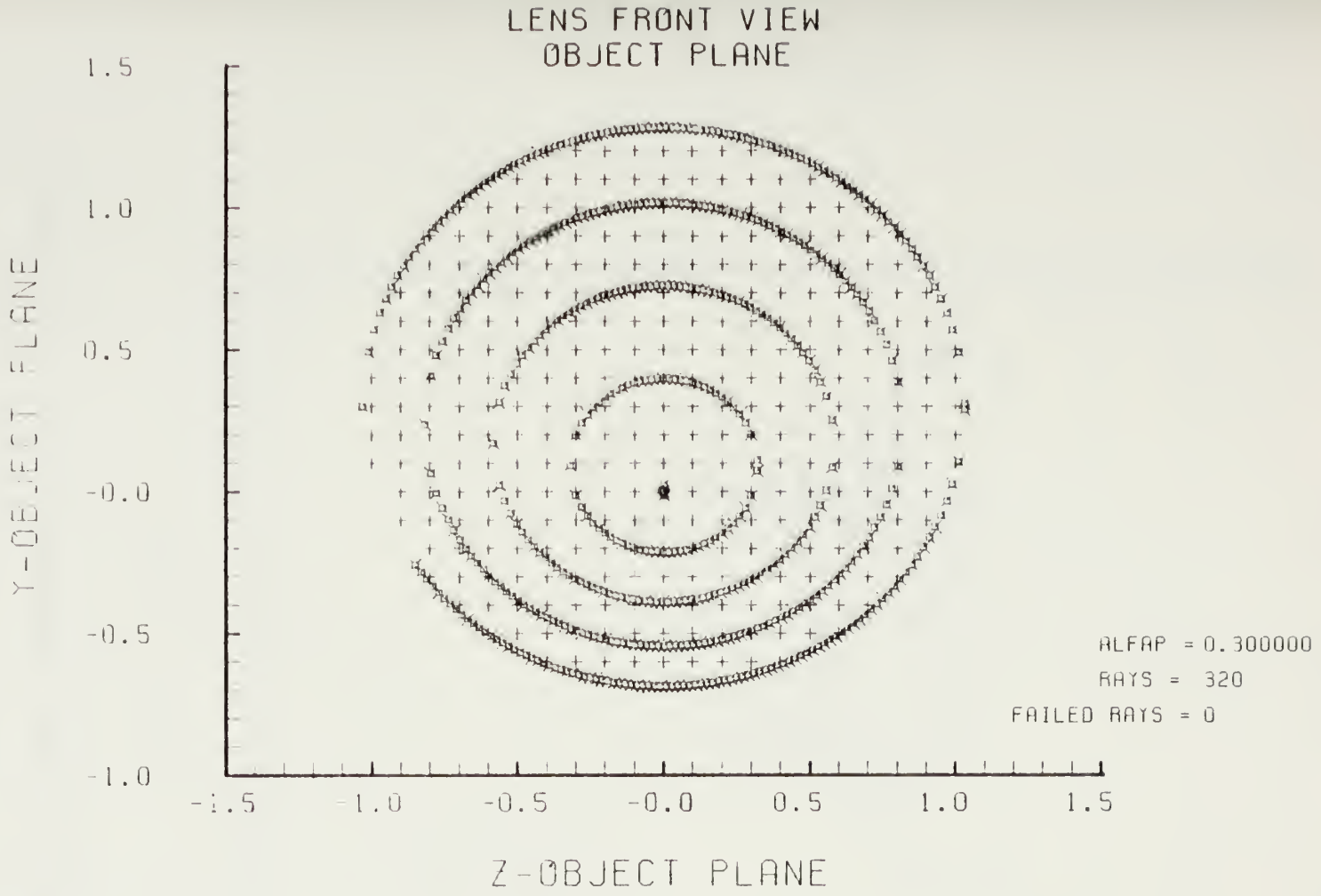

Figure F-18. Grid Plane at $\alpha_p = 0.3$ for Lens of Figure F-17

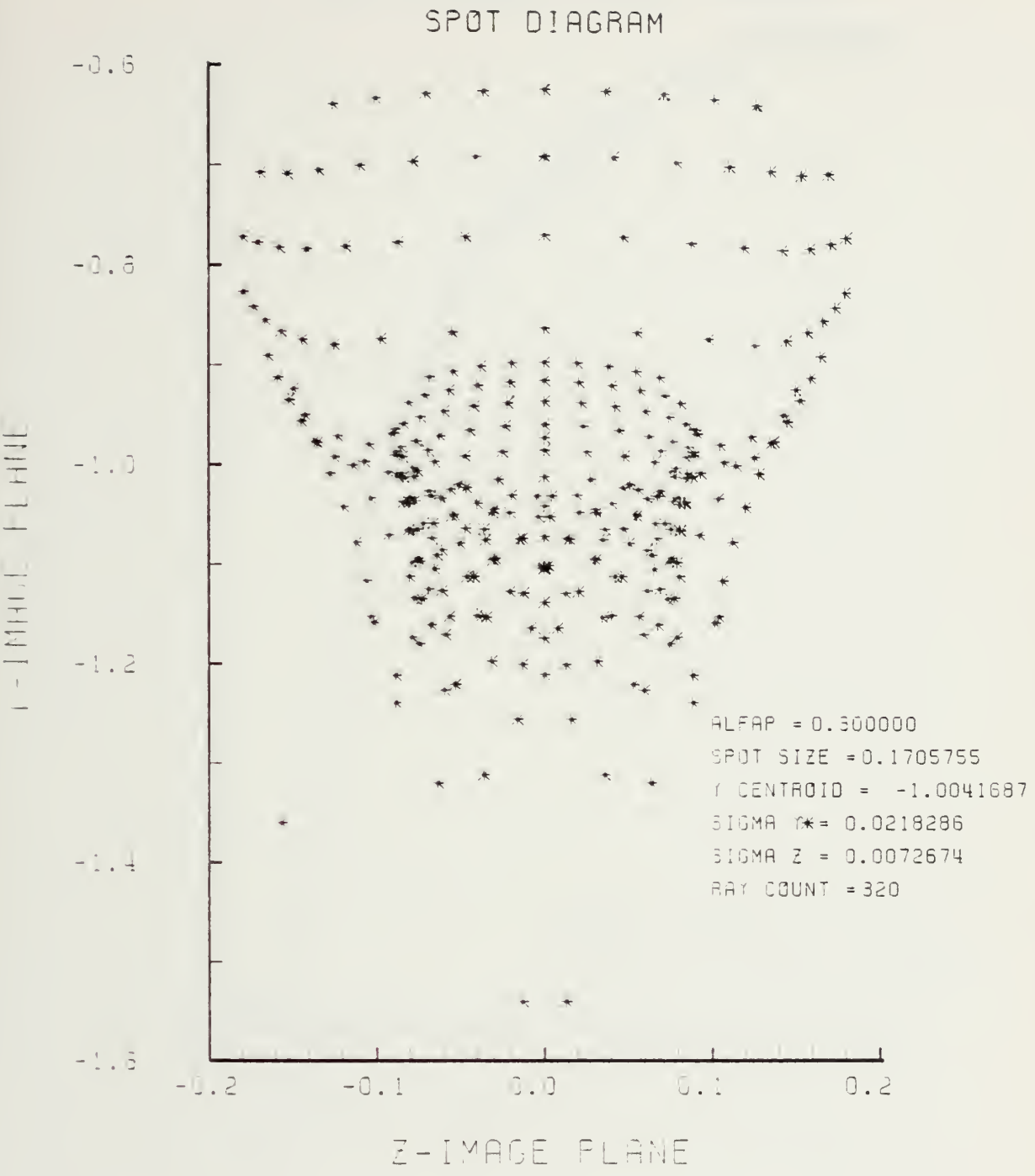

Figure F-19. Spot Diagram for Grid of Figure F-18

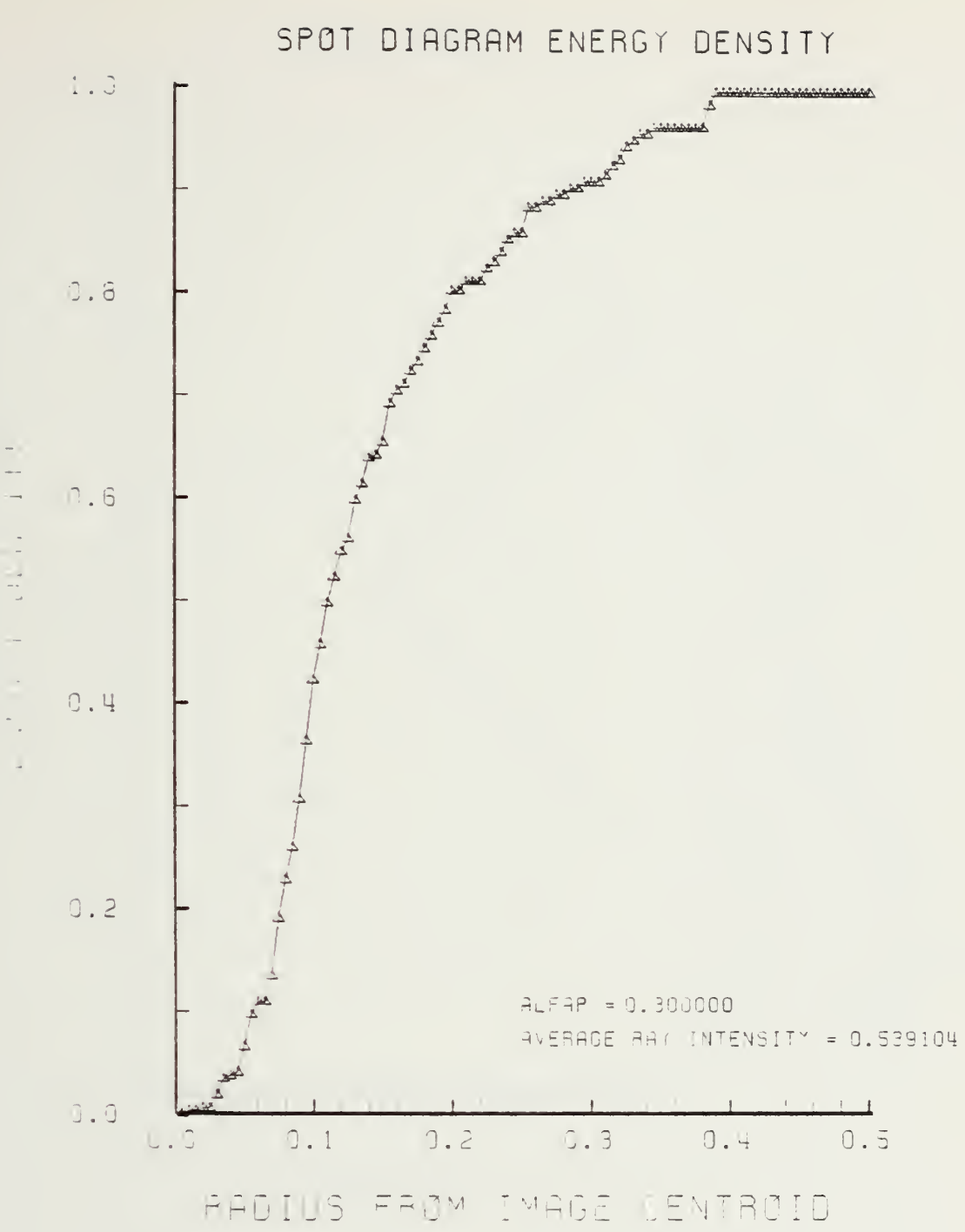

Figure F-20. Encircled Energy of Figure F-19

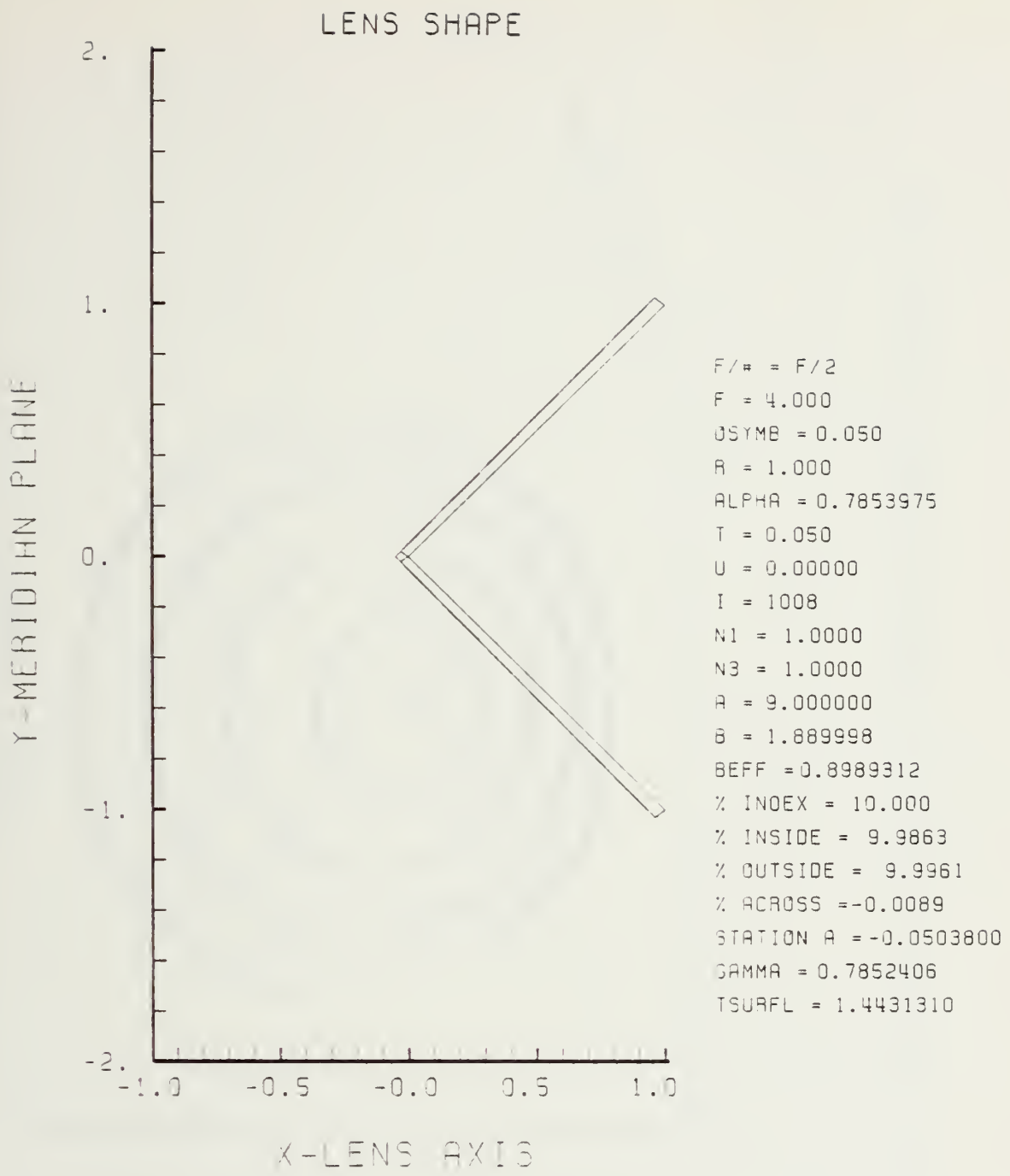

Figure F-21. GRIN Lens Shape for +10%, OB = 0.05, a = 9.00

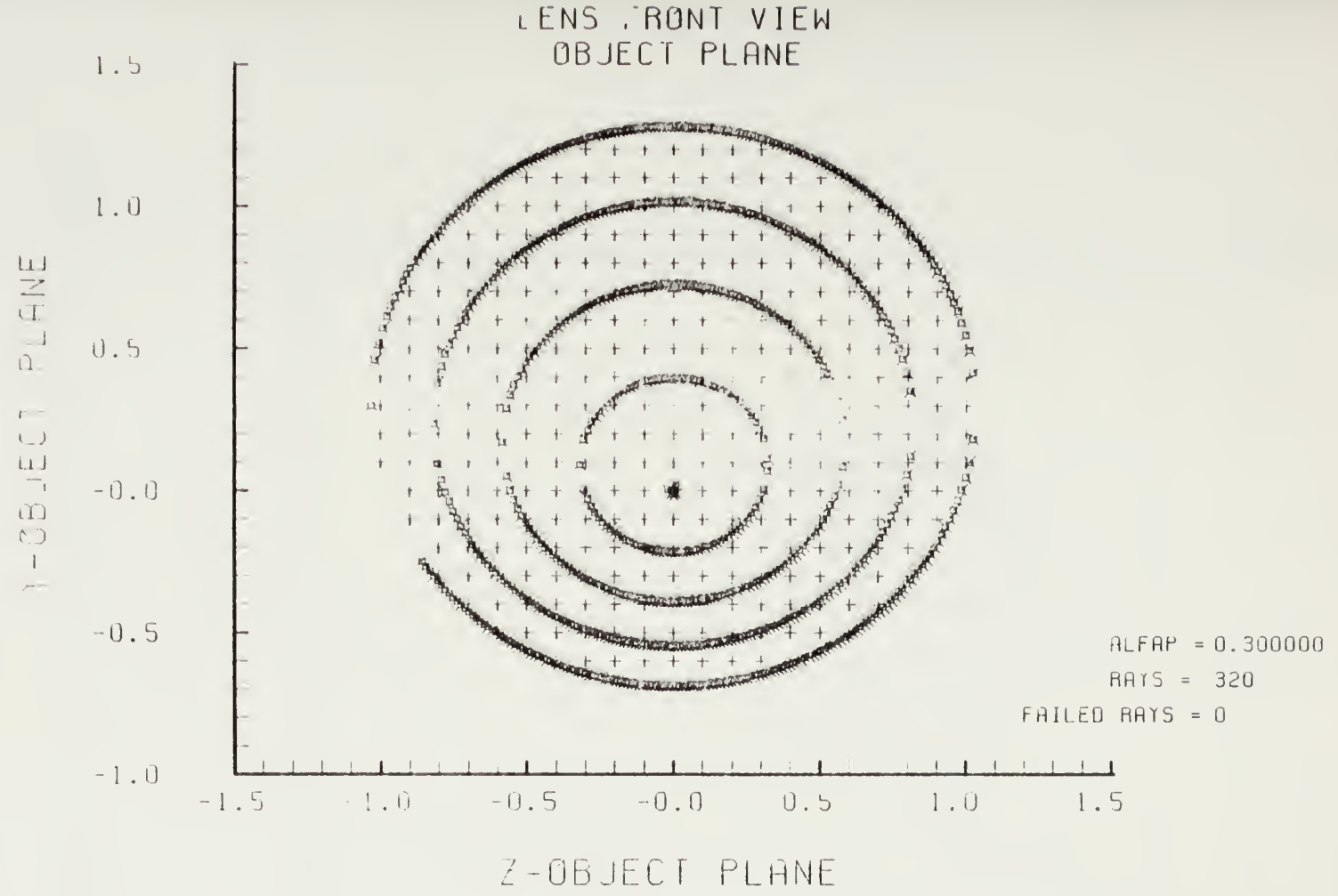

Figure F-22. Grid Plane at α_p = 0.3 Radians for Lens of Figure F-21

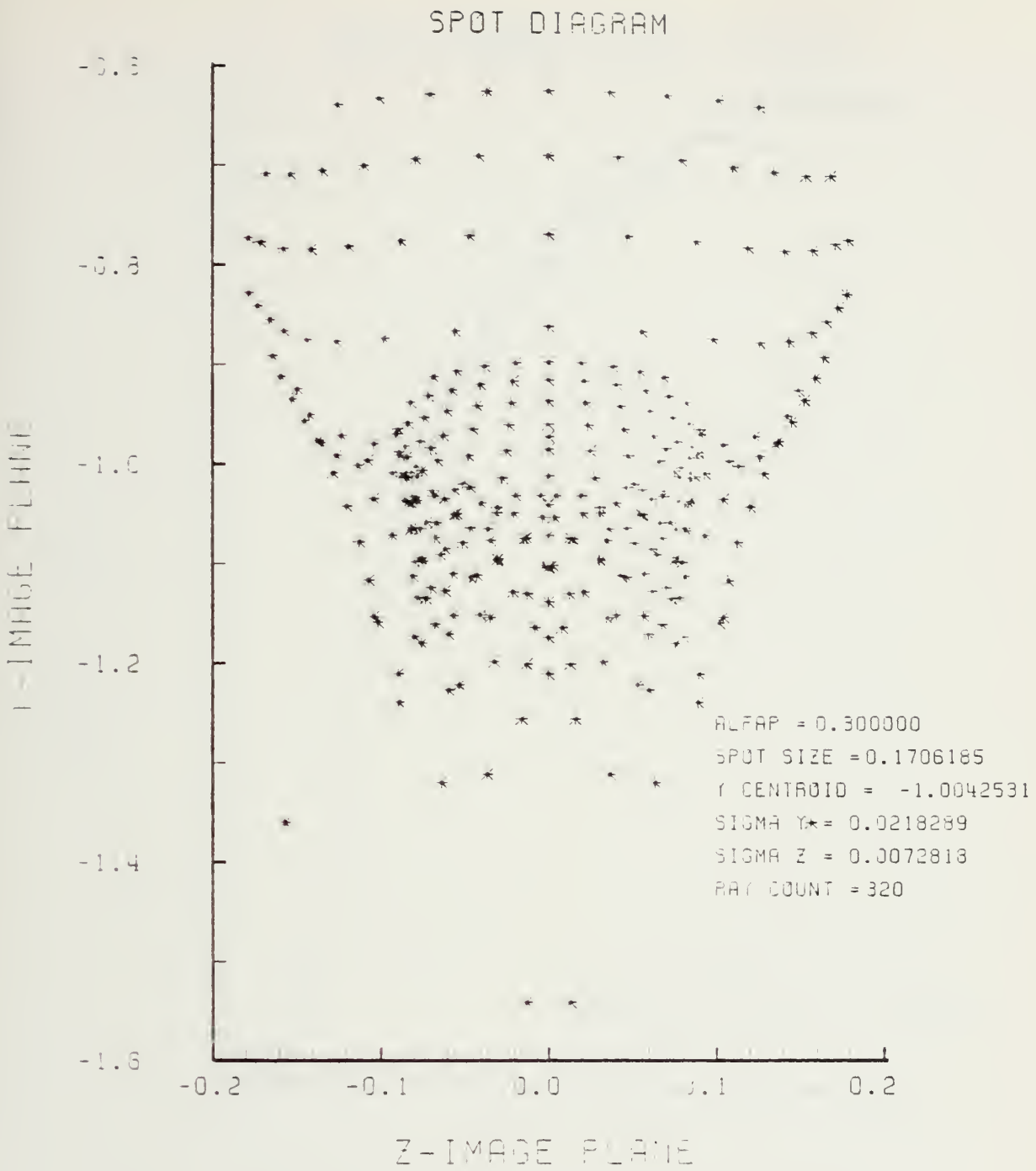

Figure F-23. Spot Diagram for Grid of Figure F-22

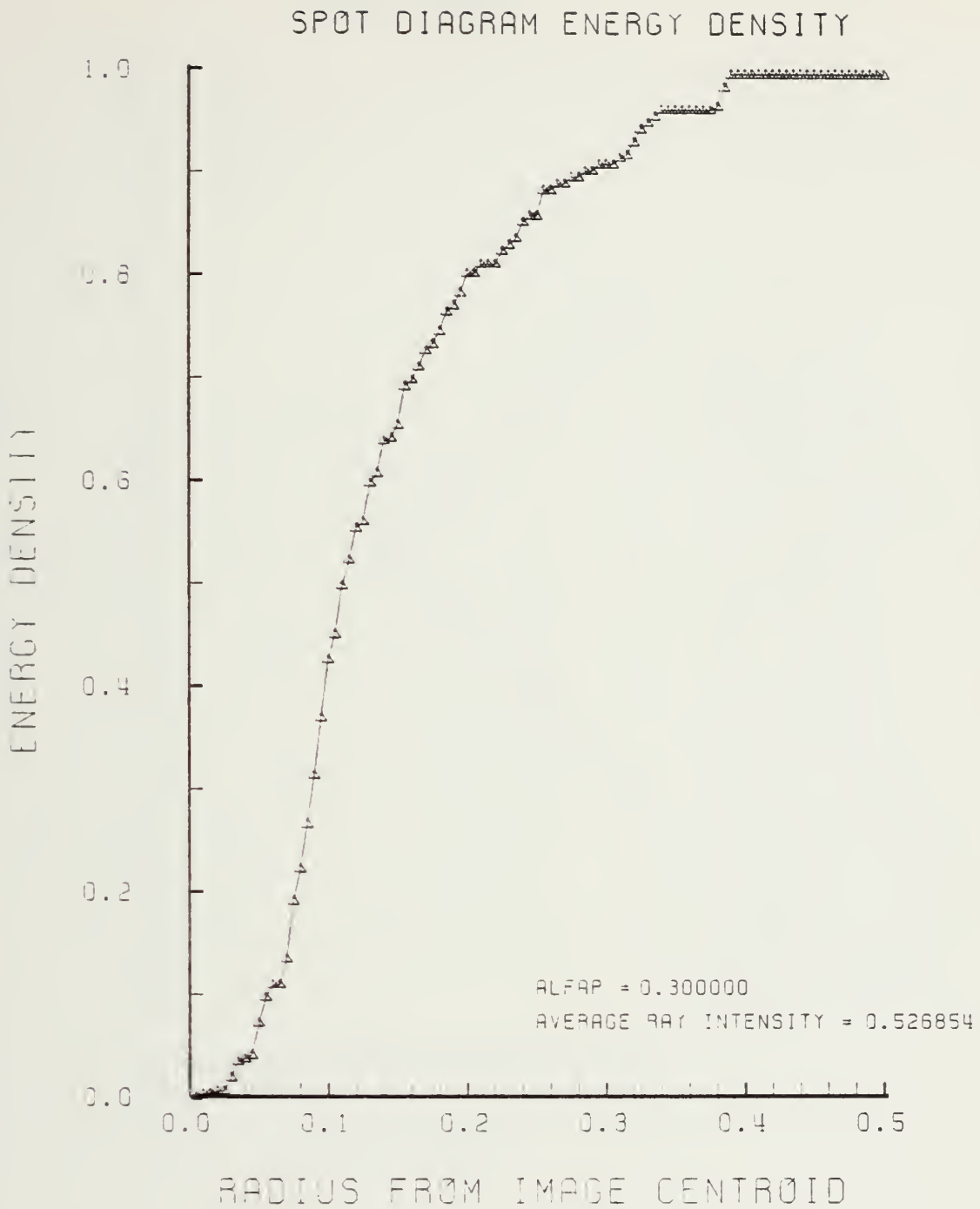

Figure F-24. Encircled Energy of Figure F-23

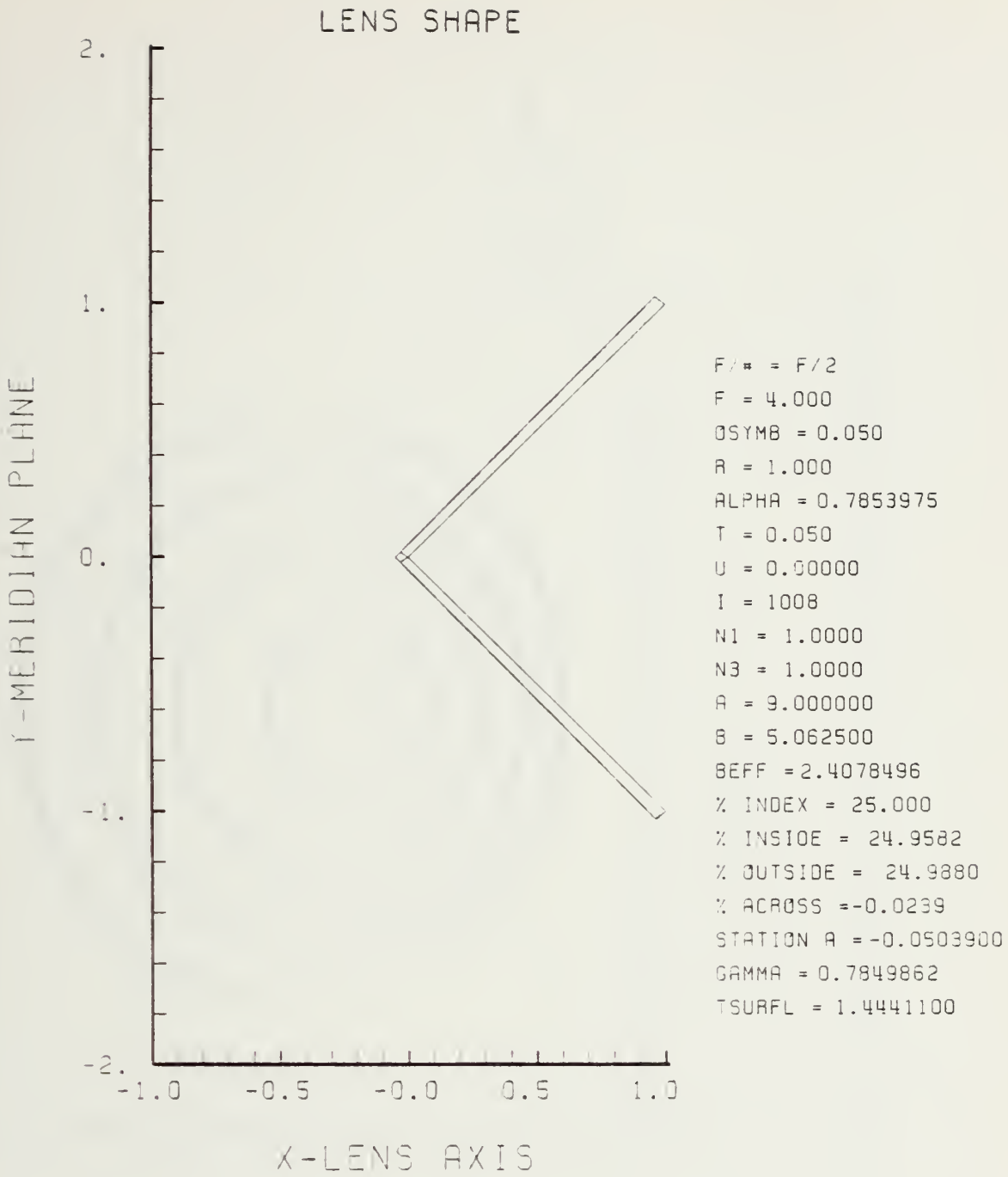

Figure F-25. GRIN Lens Shape for +25%, OB = 0.05, a = 9.00

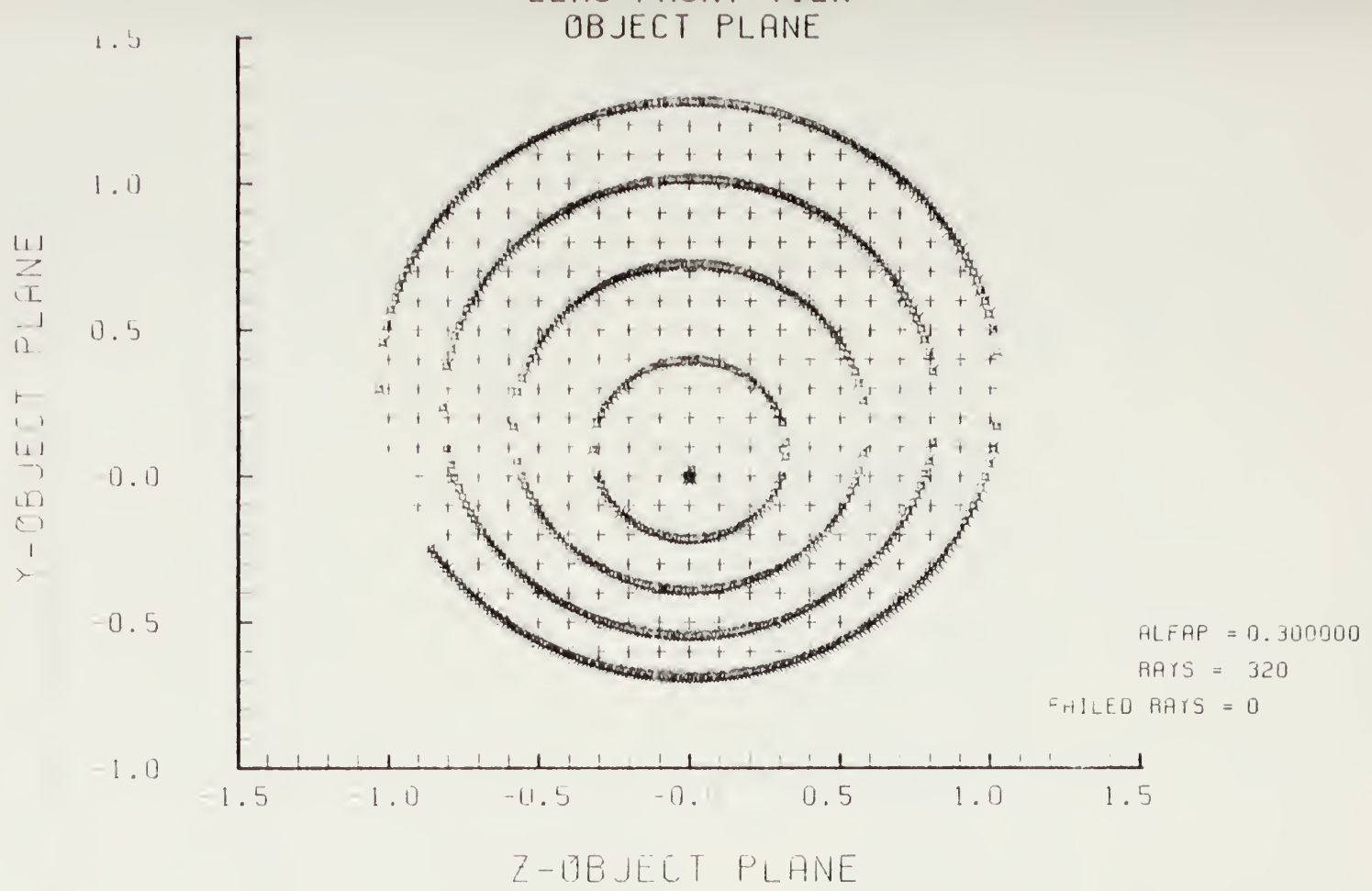

Figure F-26. Grid Plane at α_p = 0.3 for Lens of Figure F-25

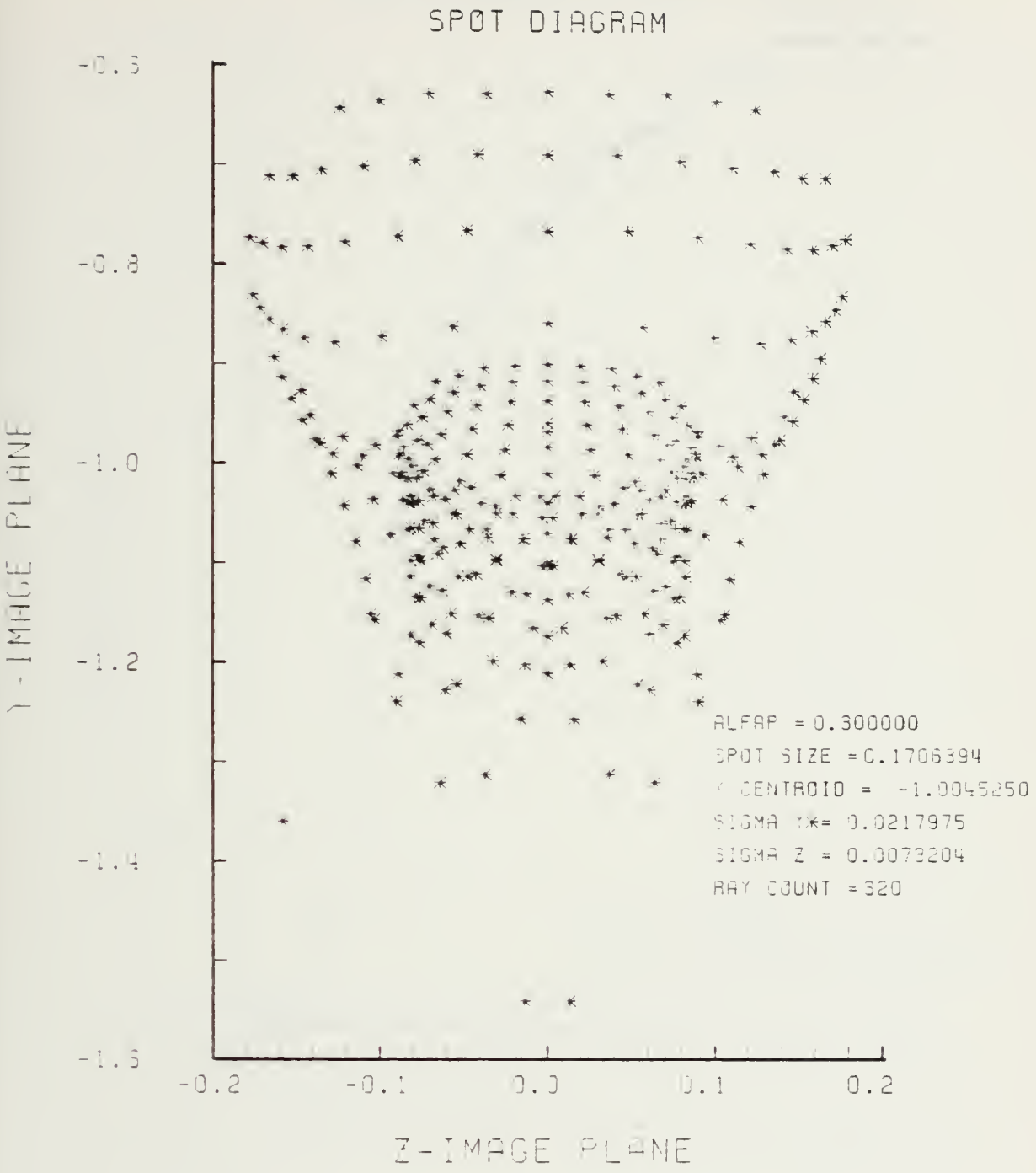

Figure F-27. Spot Diagram for Grid of Figure F-26

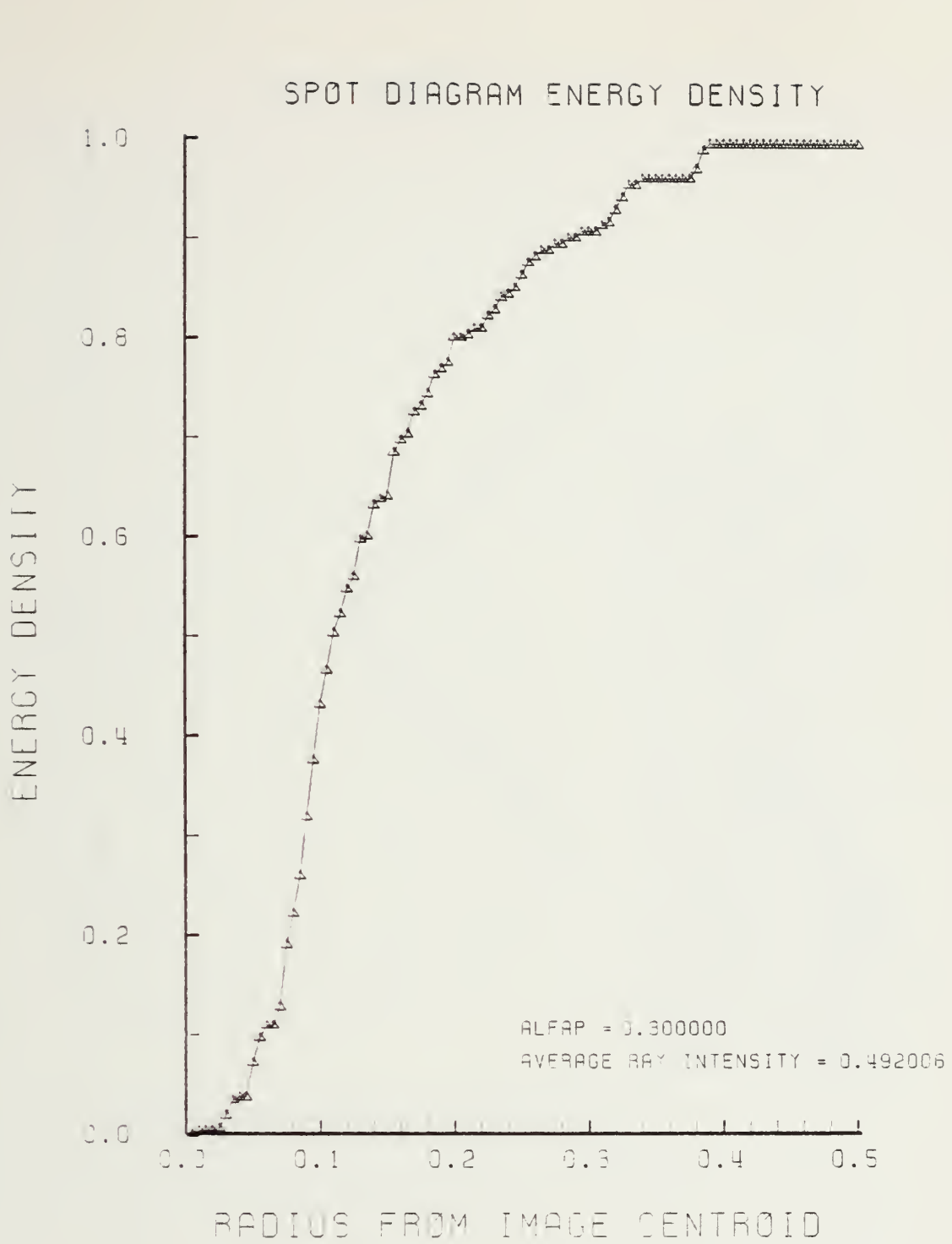

Figure F-28. Encircled Energy of Figure F-27

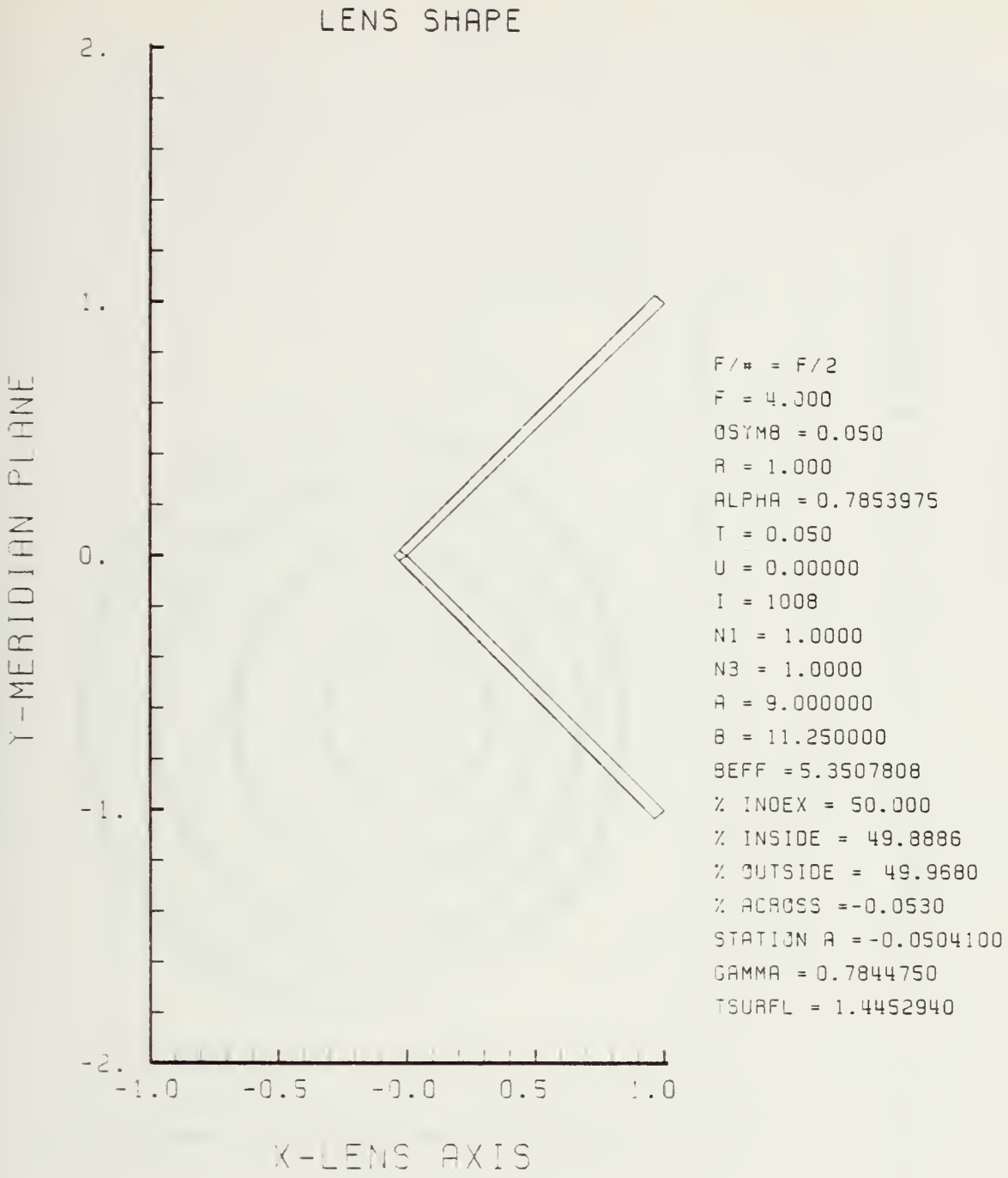

Figure F-29. GRIN Lens Shape at +50%, OB = 0.05, a = 9.00

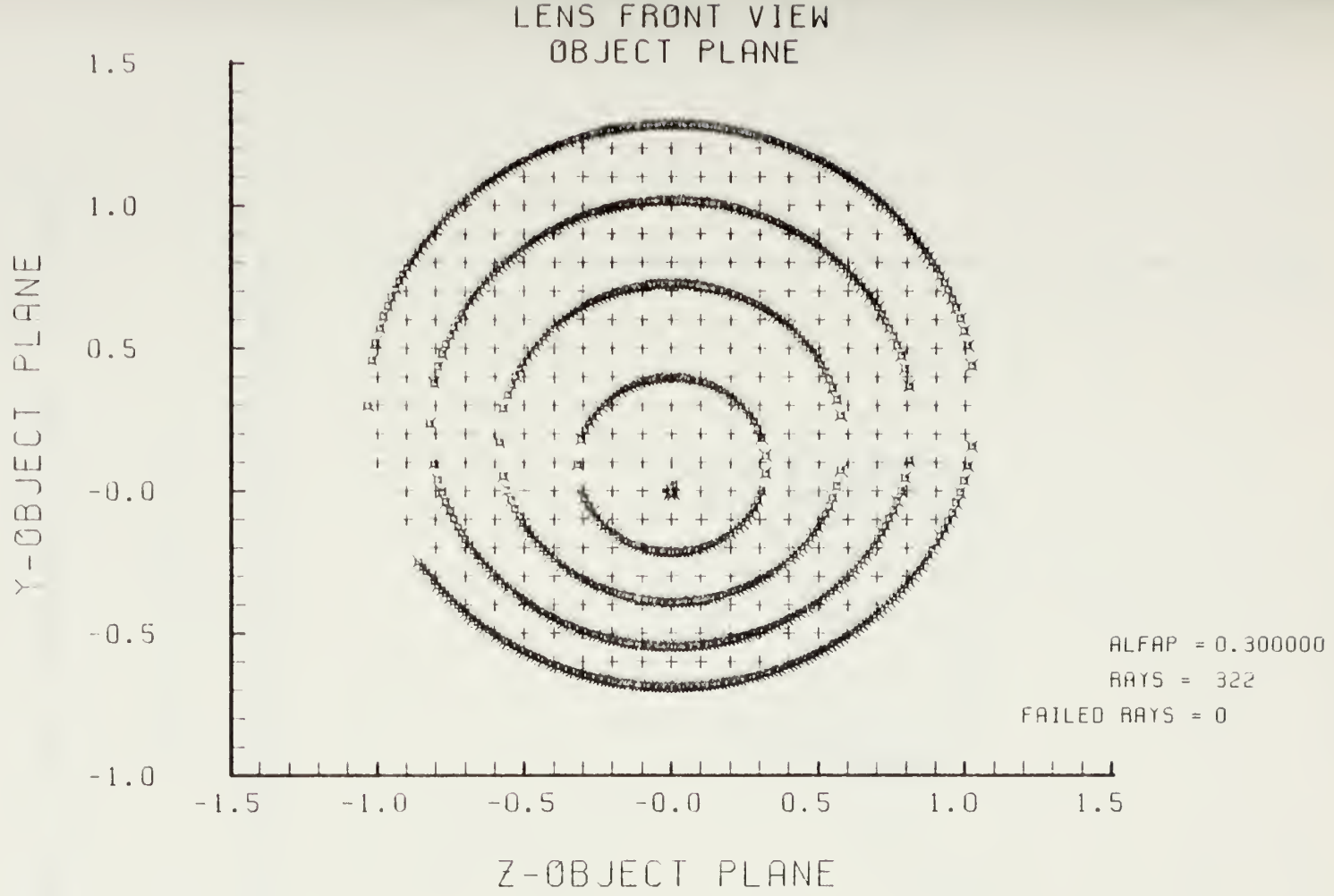

Figure F-30. Grid Plane at $\alpha_p = 0.3$ for Lens of Figure F-29

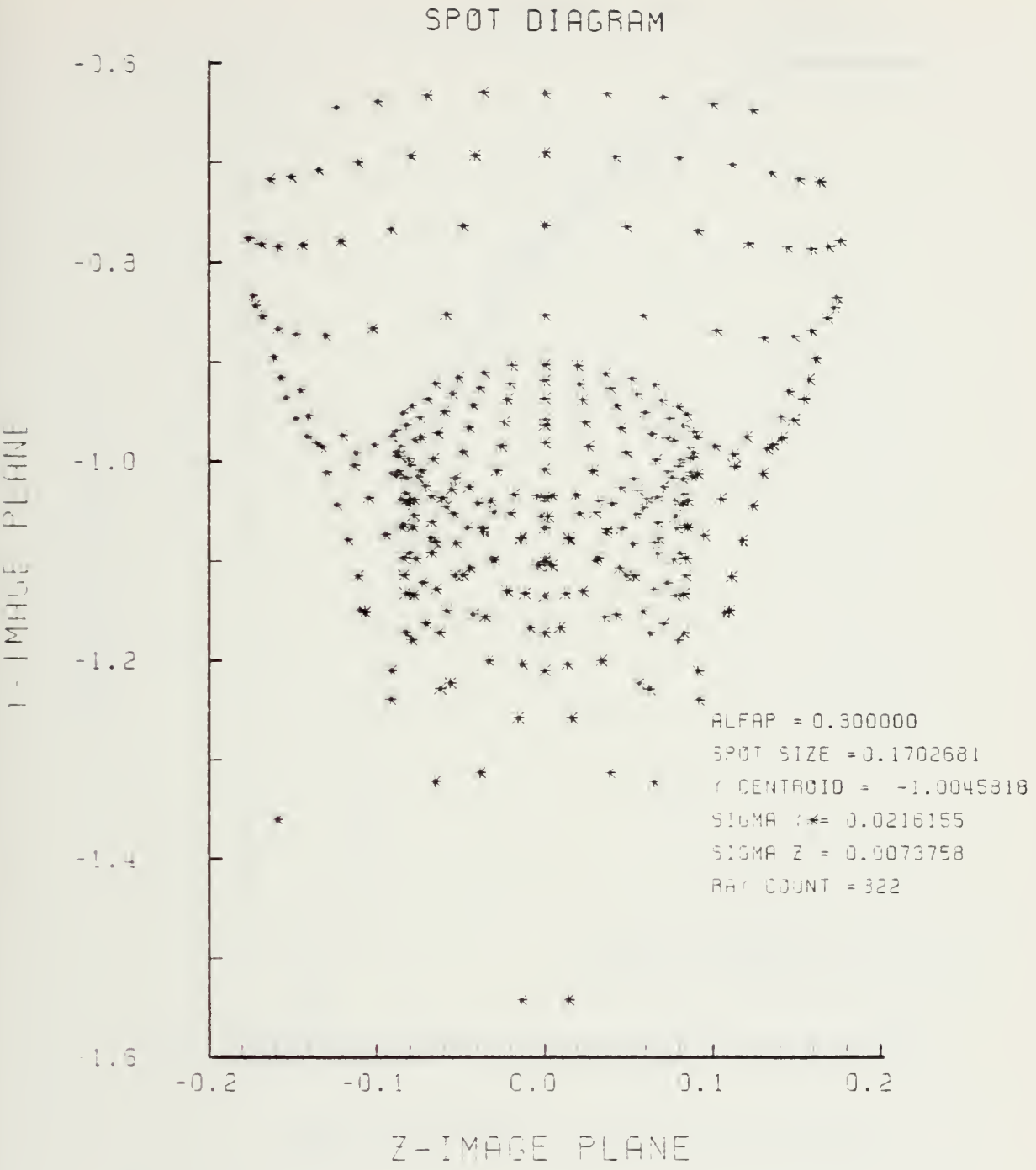

Figure F-31. Spot Diagram for Grid of Figure F-30

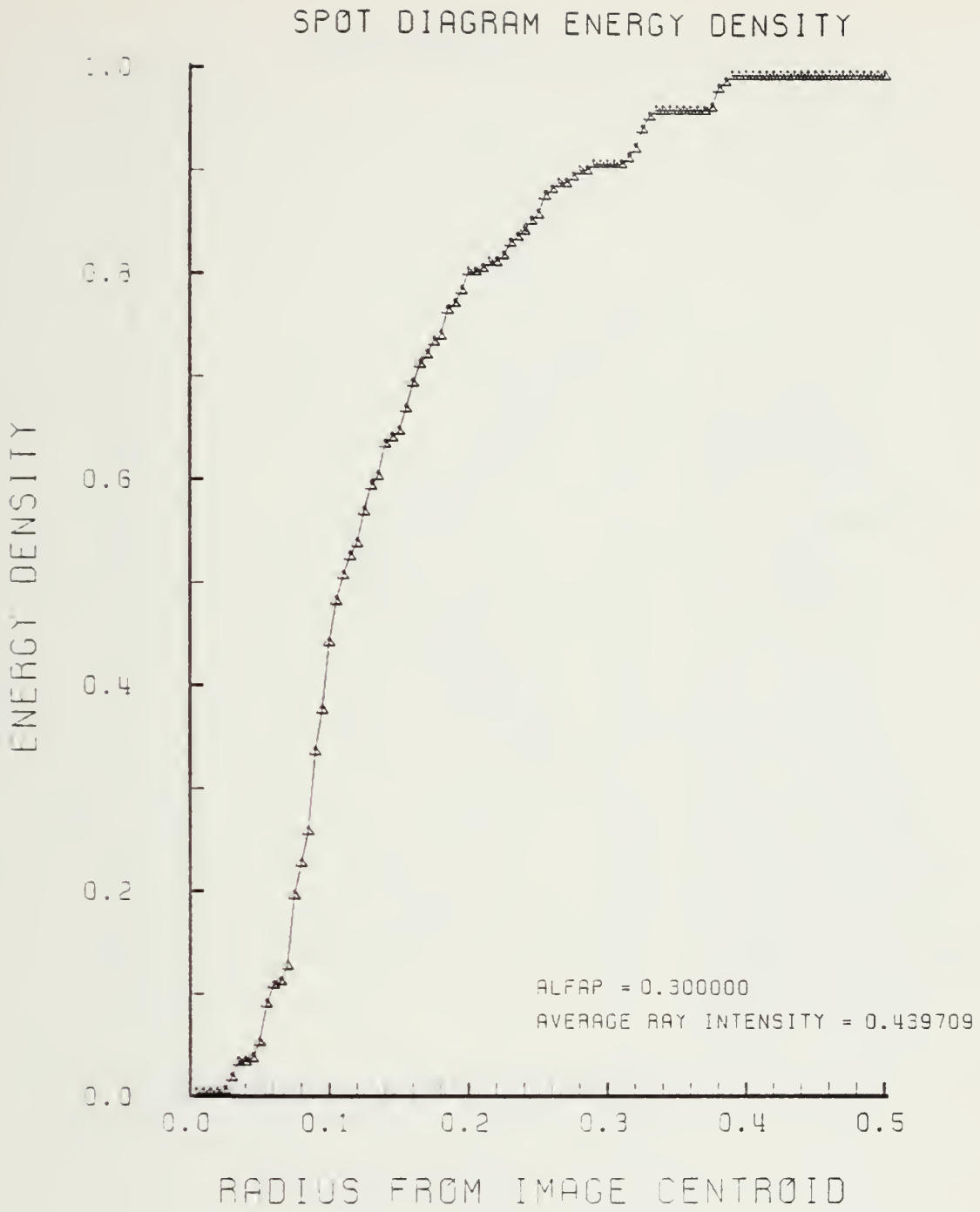

Figure F-32. Encircled Energy of Figure F-31

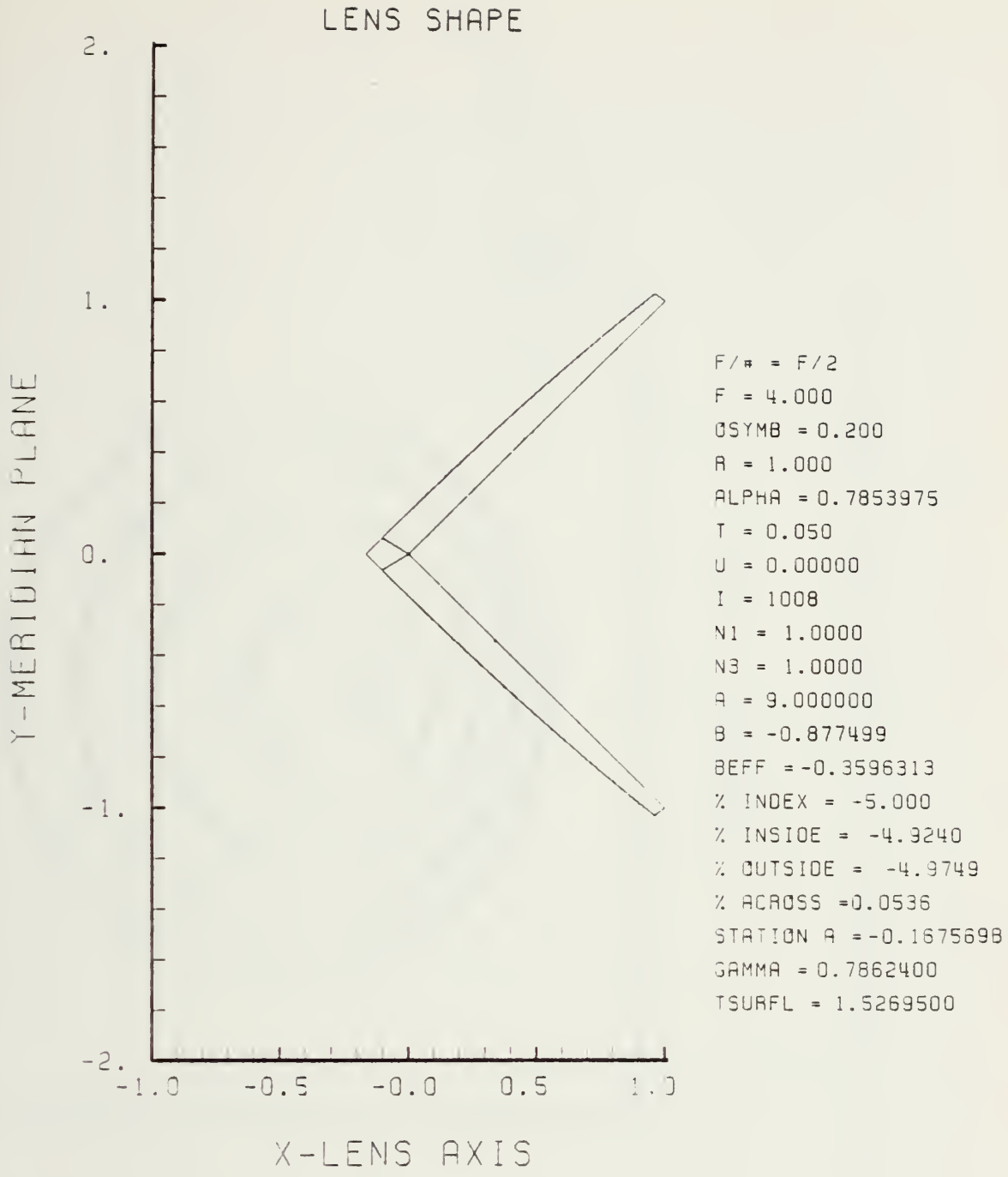

Figure F-33. GRIN Lens Shape at -5%, OB = 0.20, a = 9.00

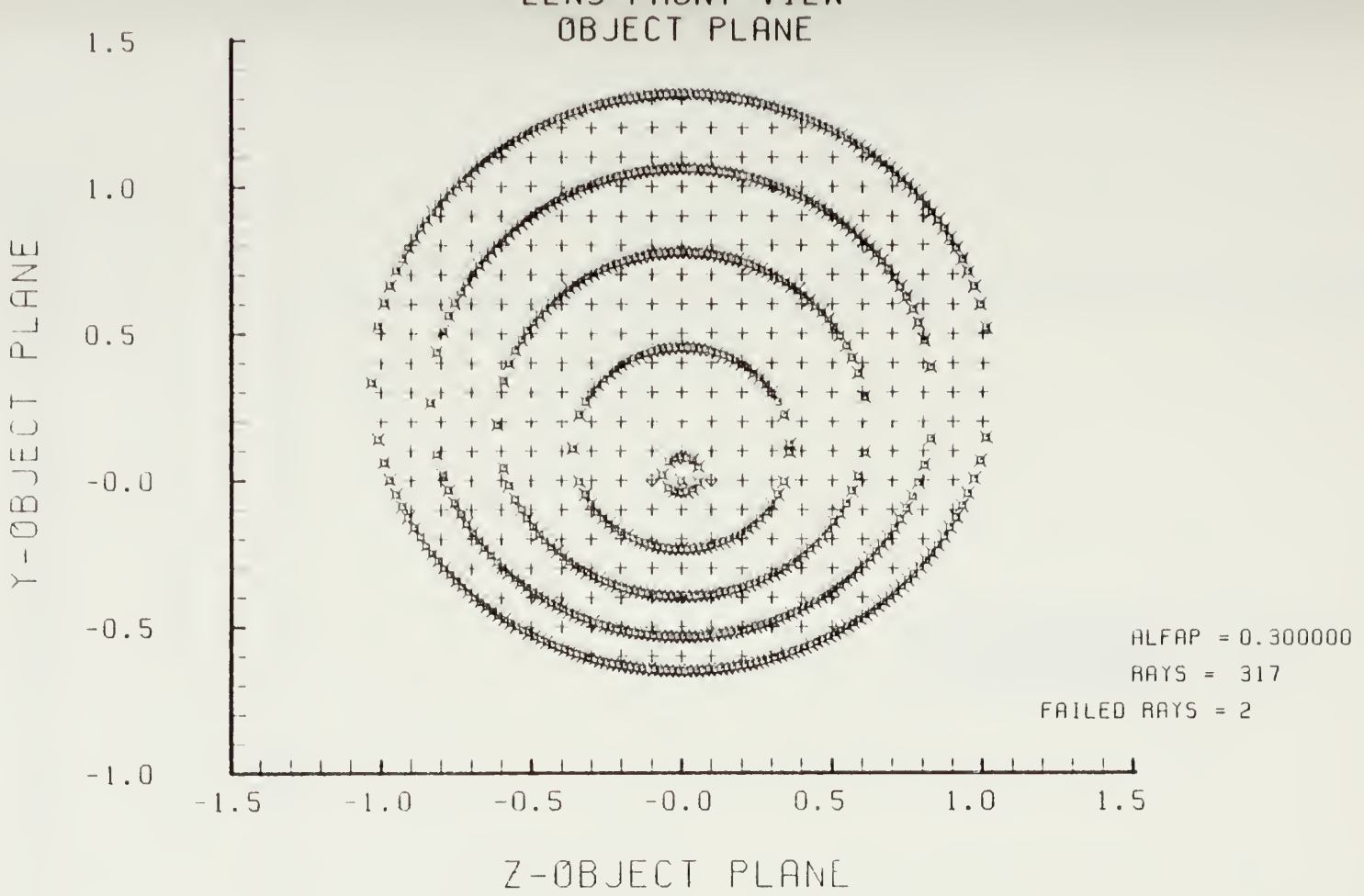

Figure F-34. Grid Plane at $\alpha_p = 0.3$ for Lens of Figure F-33

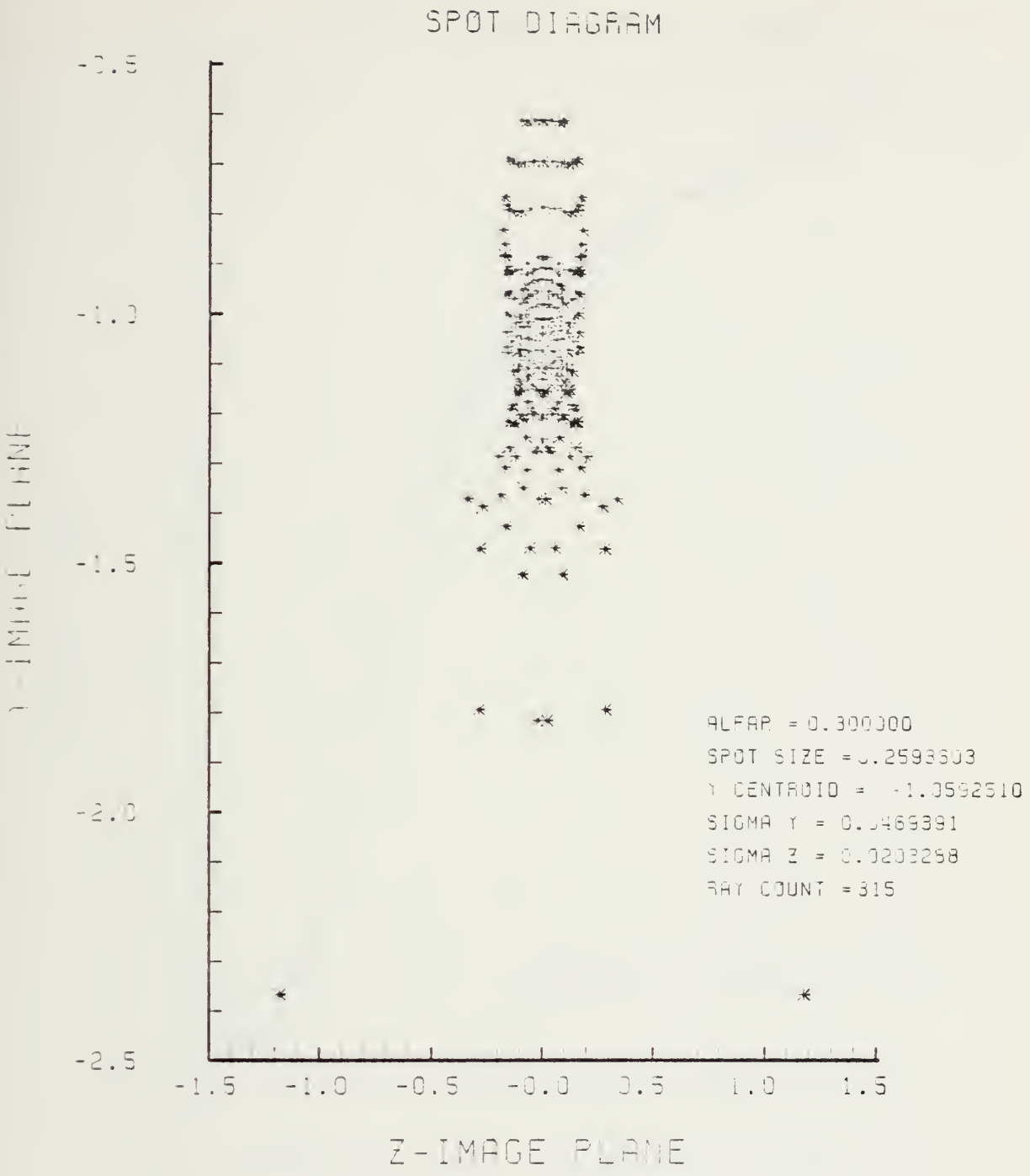

Figure F-35. Spot Diagram for Grid of Figure F-34

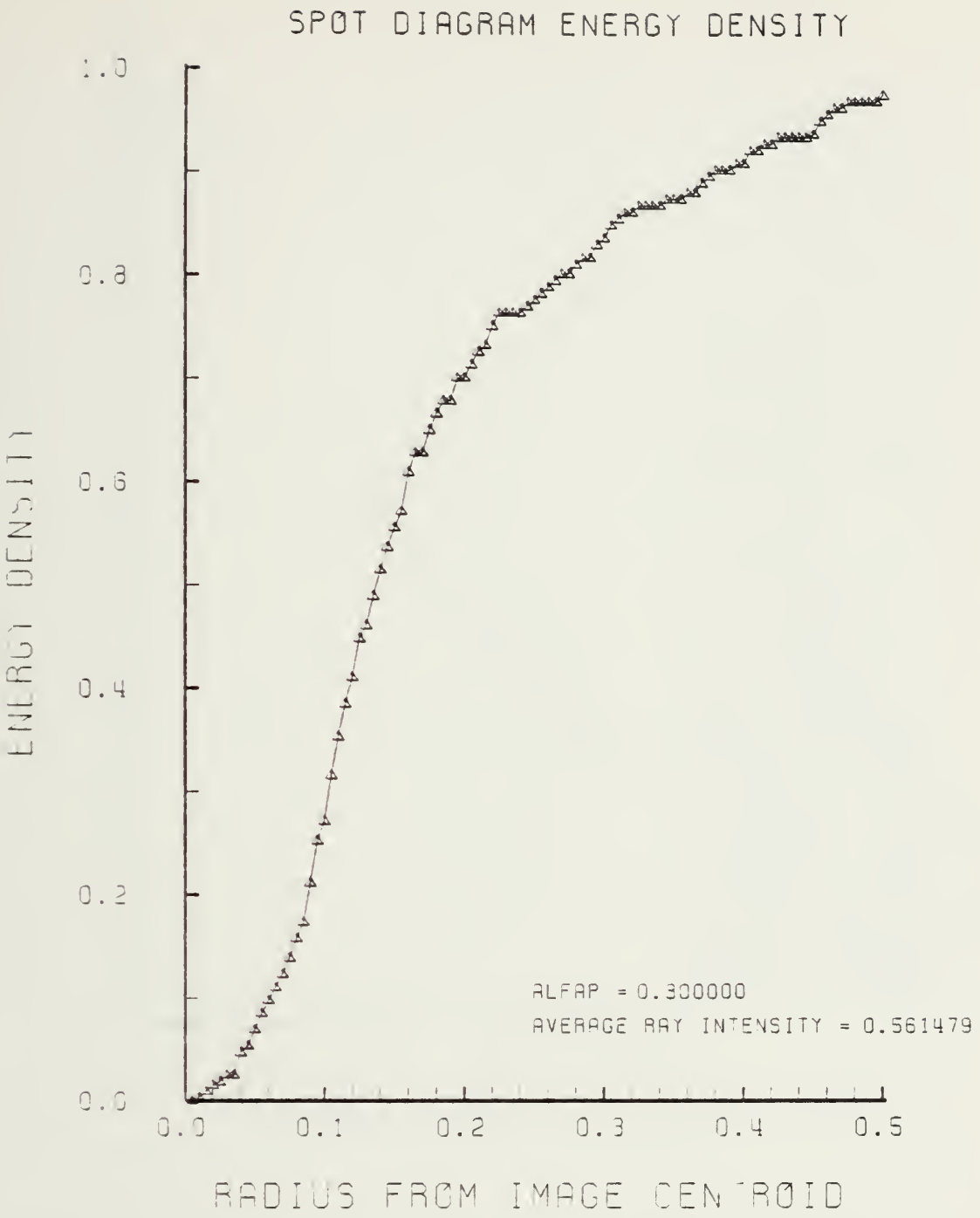

Figure F-36. Encircled Energy of Figure F-35

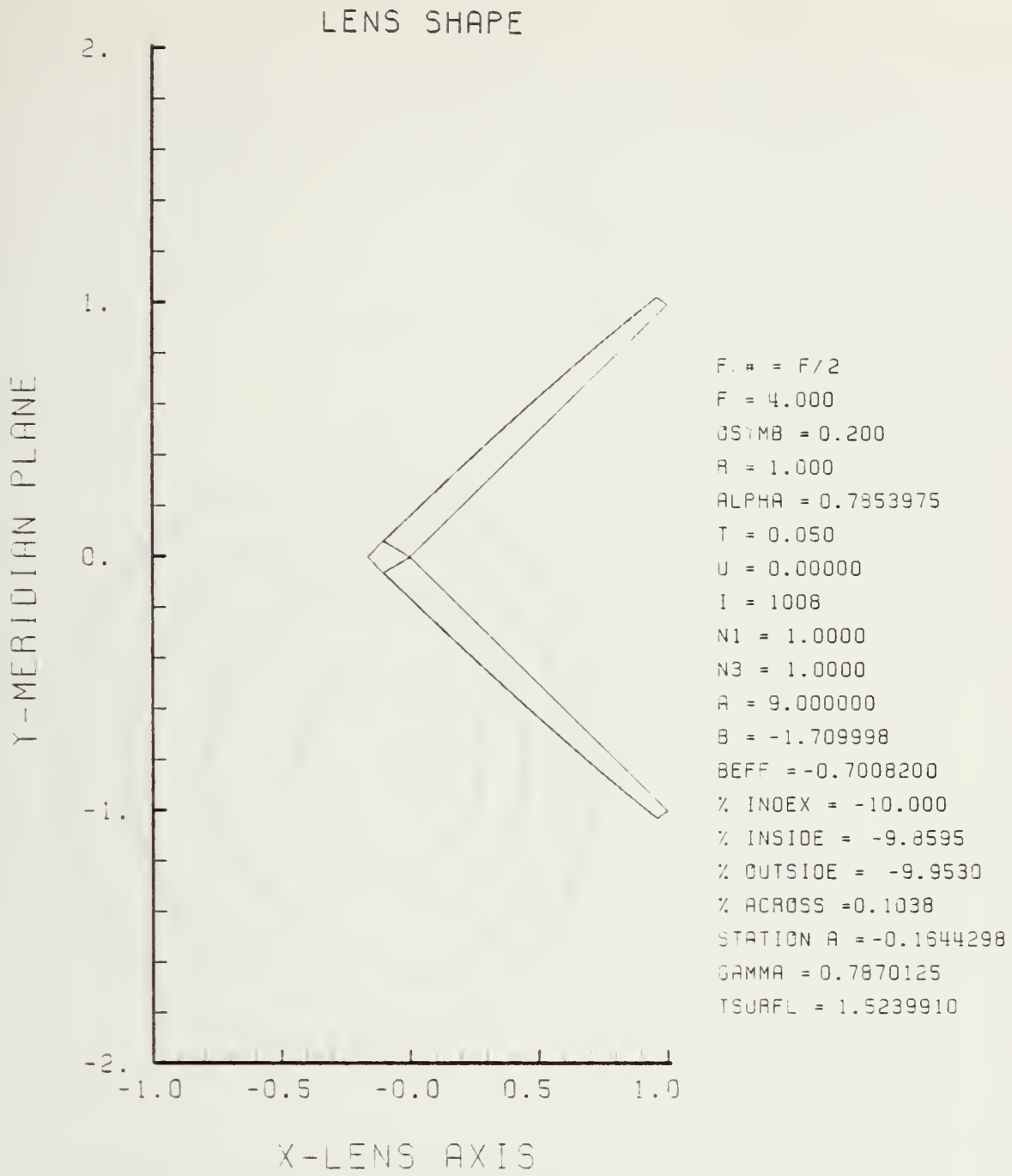

Figure F-37. GRIN Lens Shape at -10%, OB = 0.20, a = 9.00

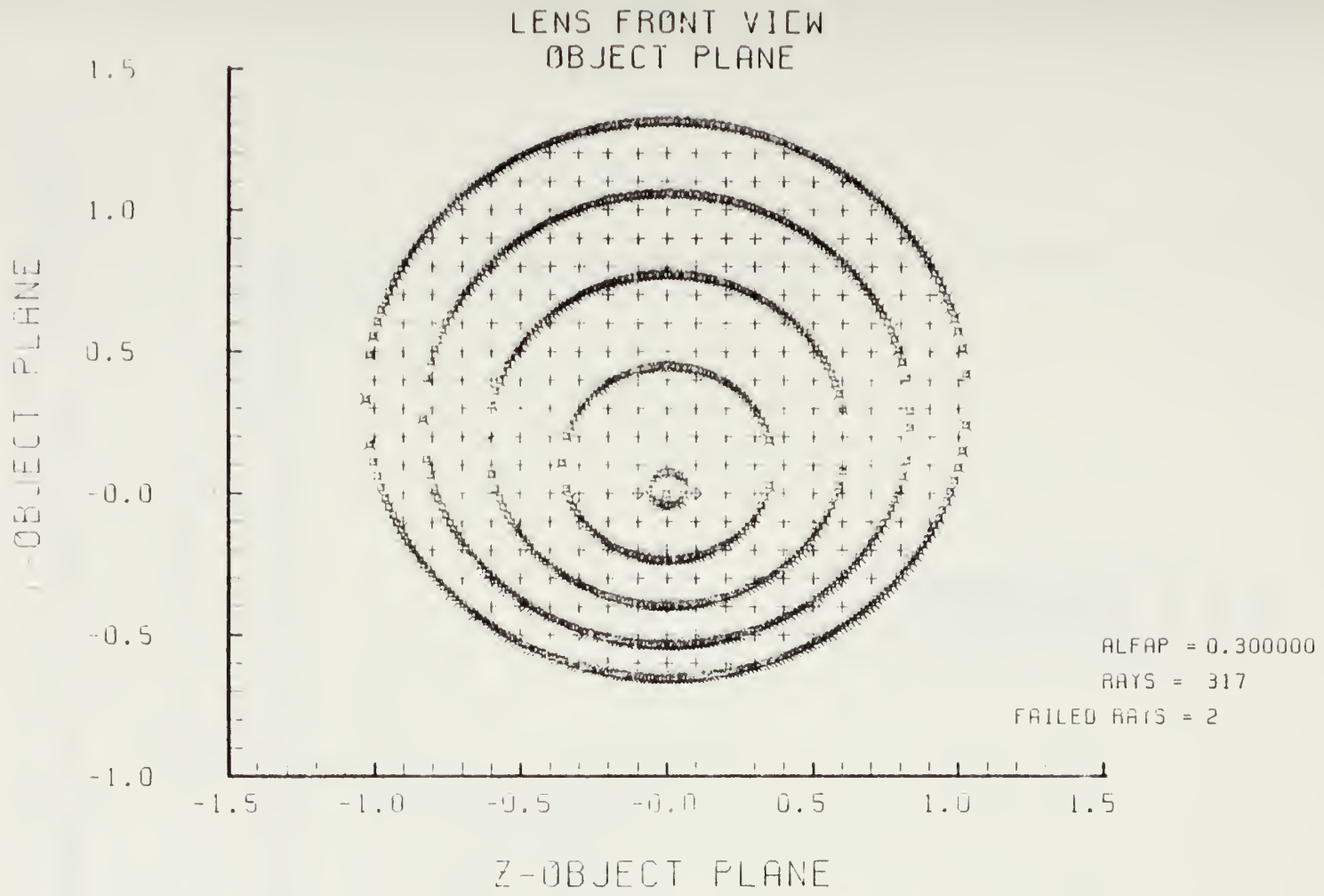

Figure F-38. Grid Plane at $\alpha_p = 0.3$ for Lens of Figure F-37

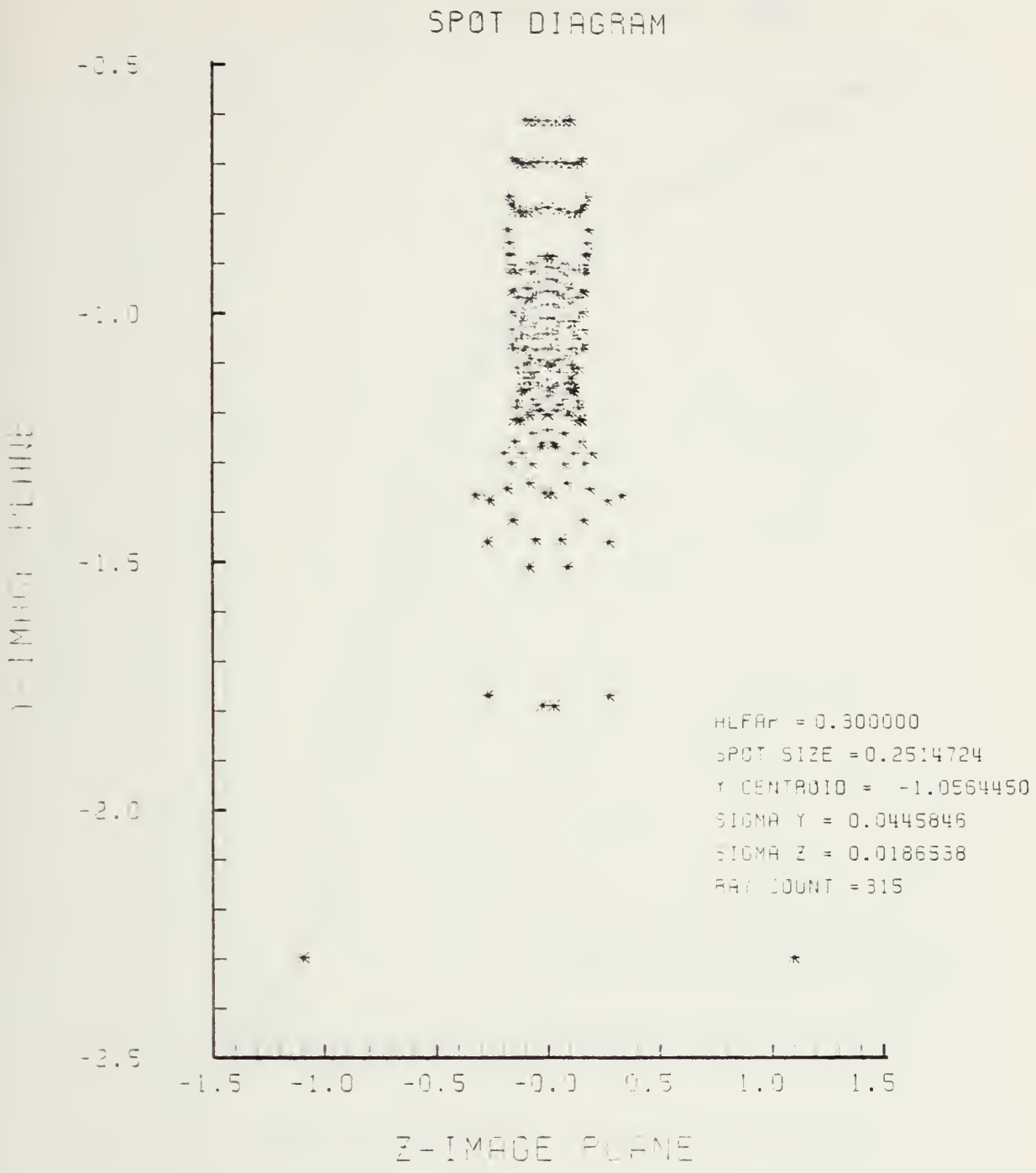

Figure F-39. Spot Diagram for Grid of Figure F-38

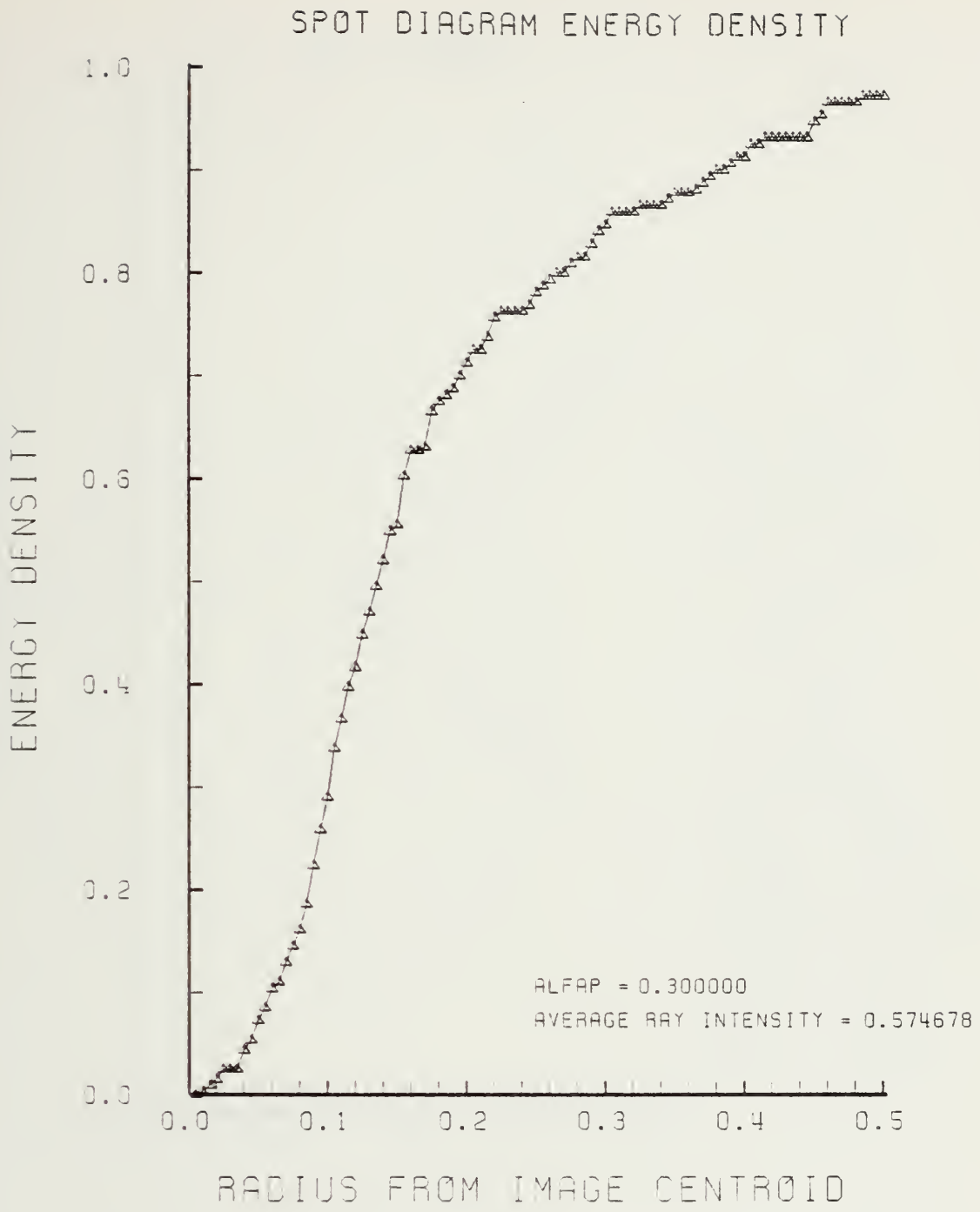

Figure F-40. Encircled Energy of Figure F-39

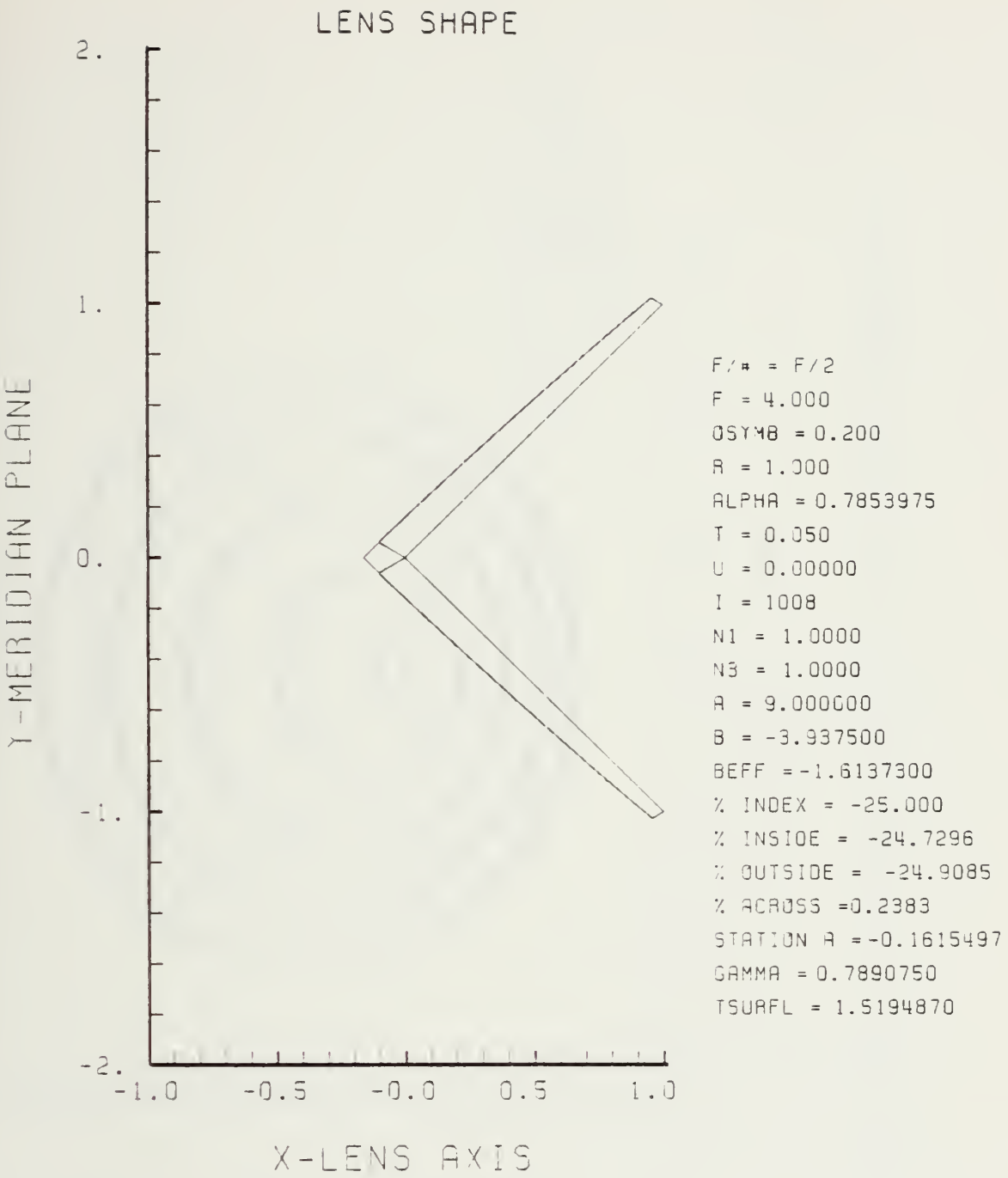

Figure F-41. GRIN Lens Shape at -25%, OB = 0.20, a = 9.00

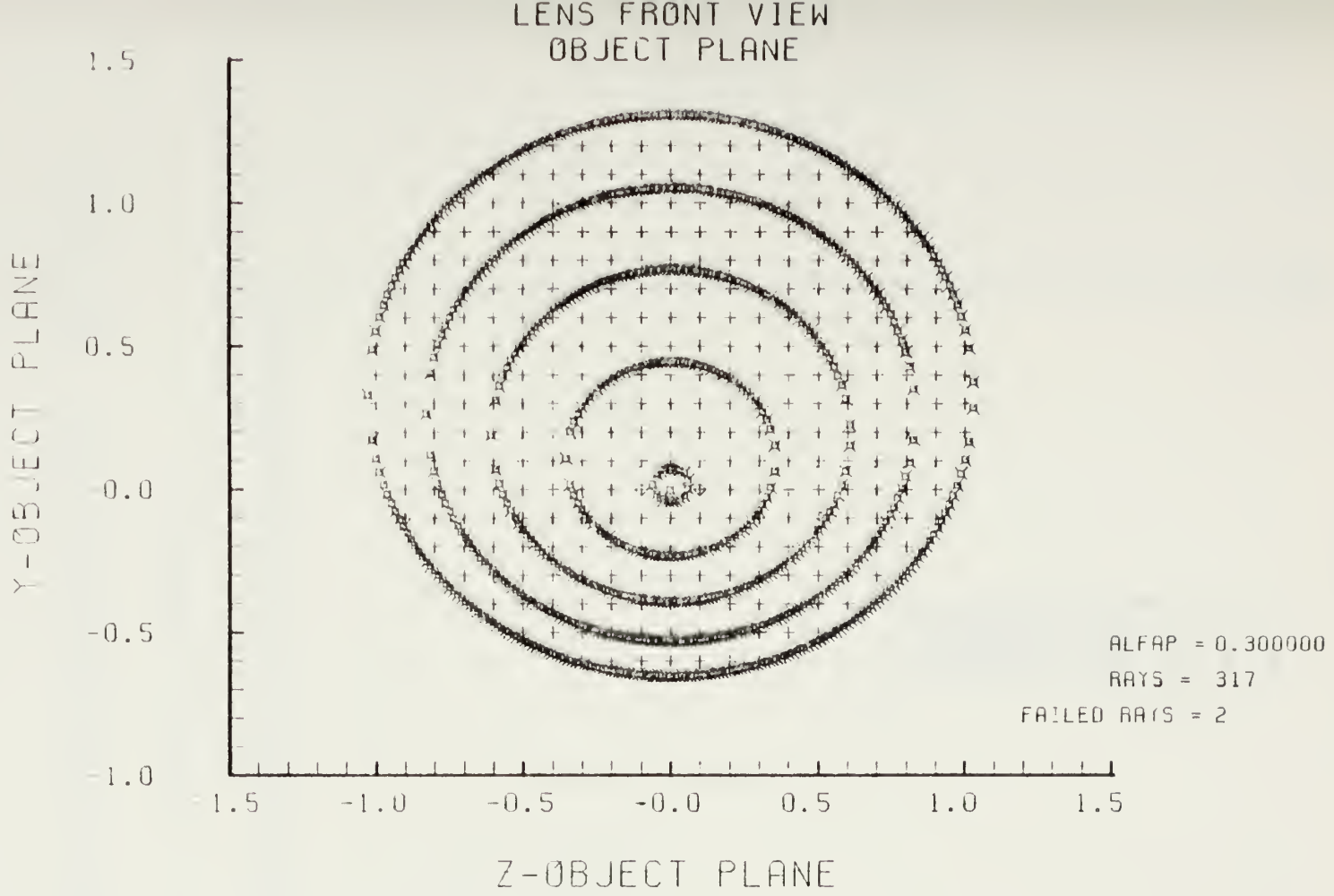

Figure F-42. Grid Plane at α_p = 0.3 for Lens of Figure F-41

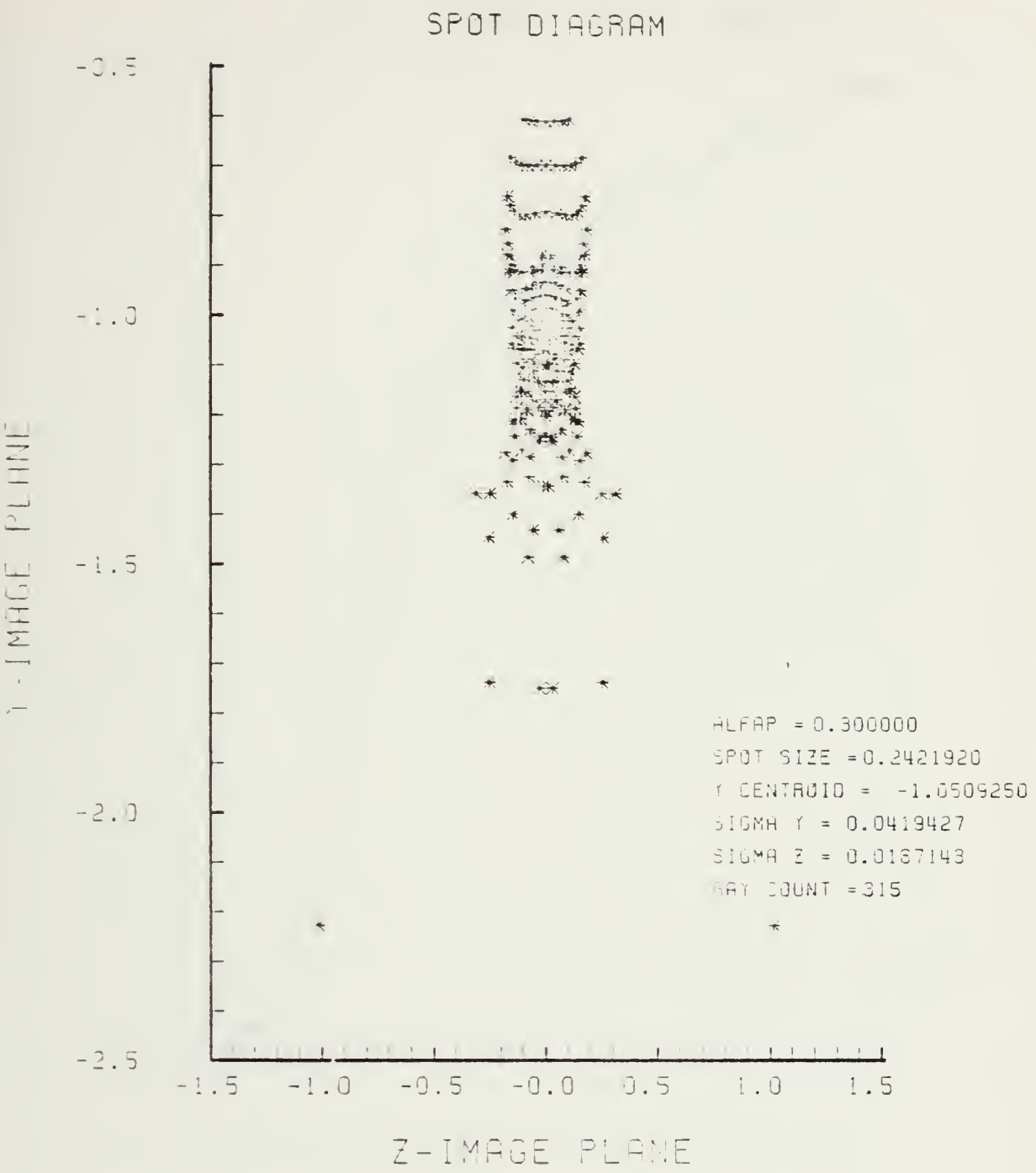

Figure F-43. Spot Diagram for Grid of Figure F-42

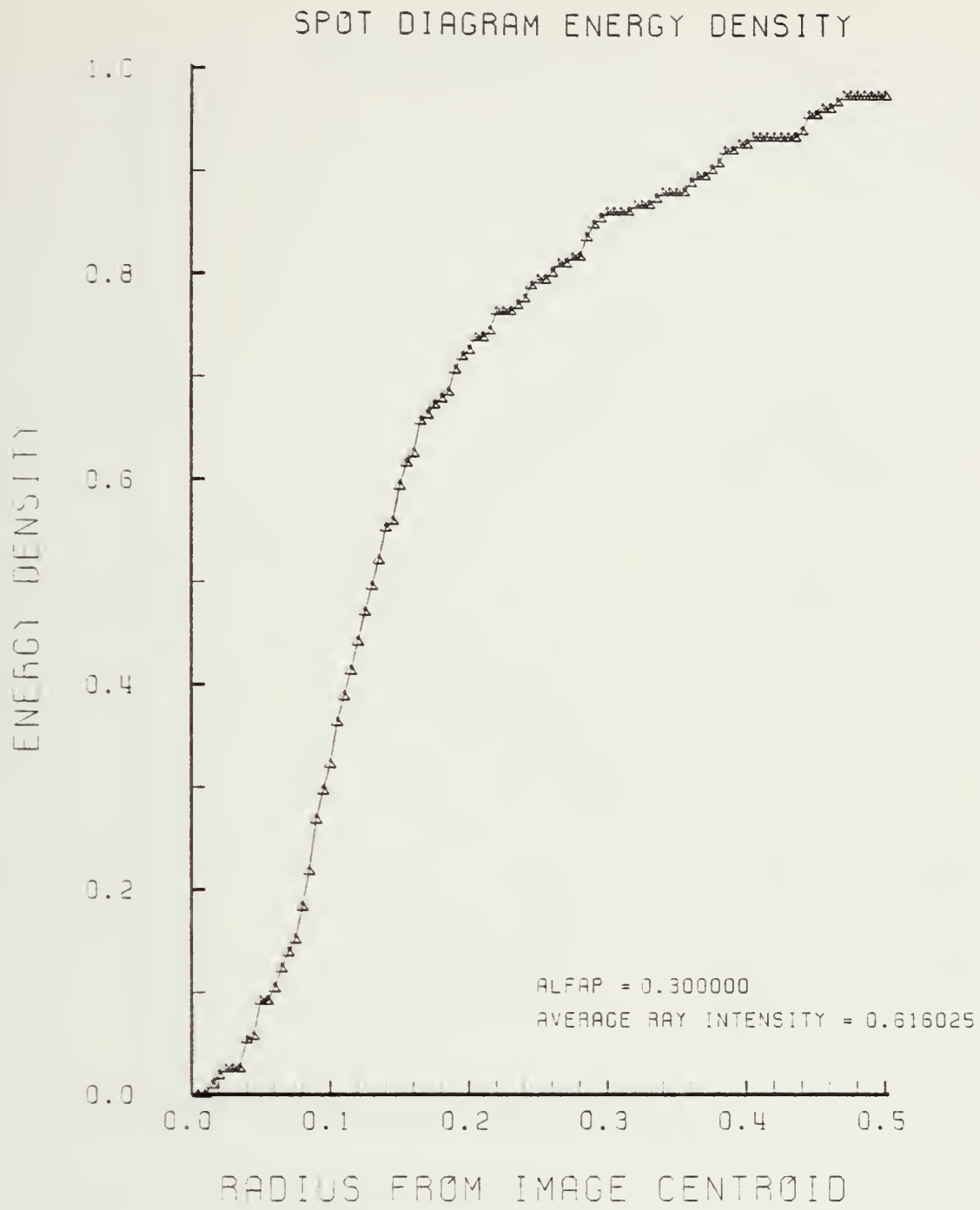

Figure F-44. Encircled Energy of Figure F-43

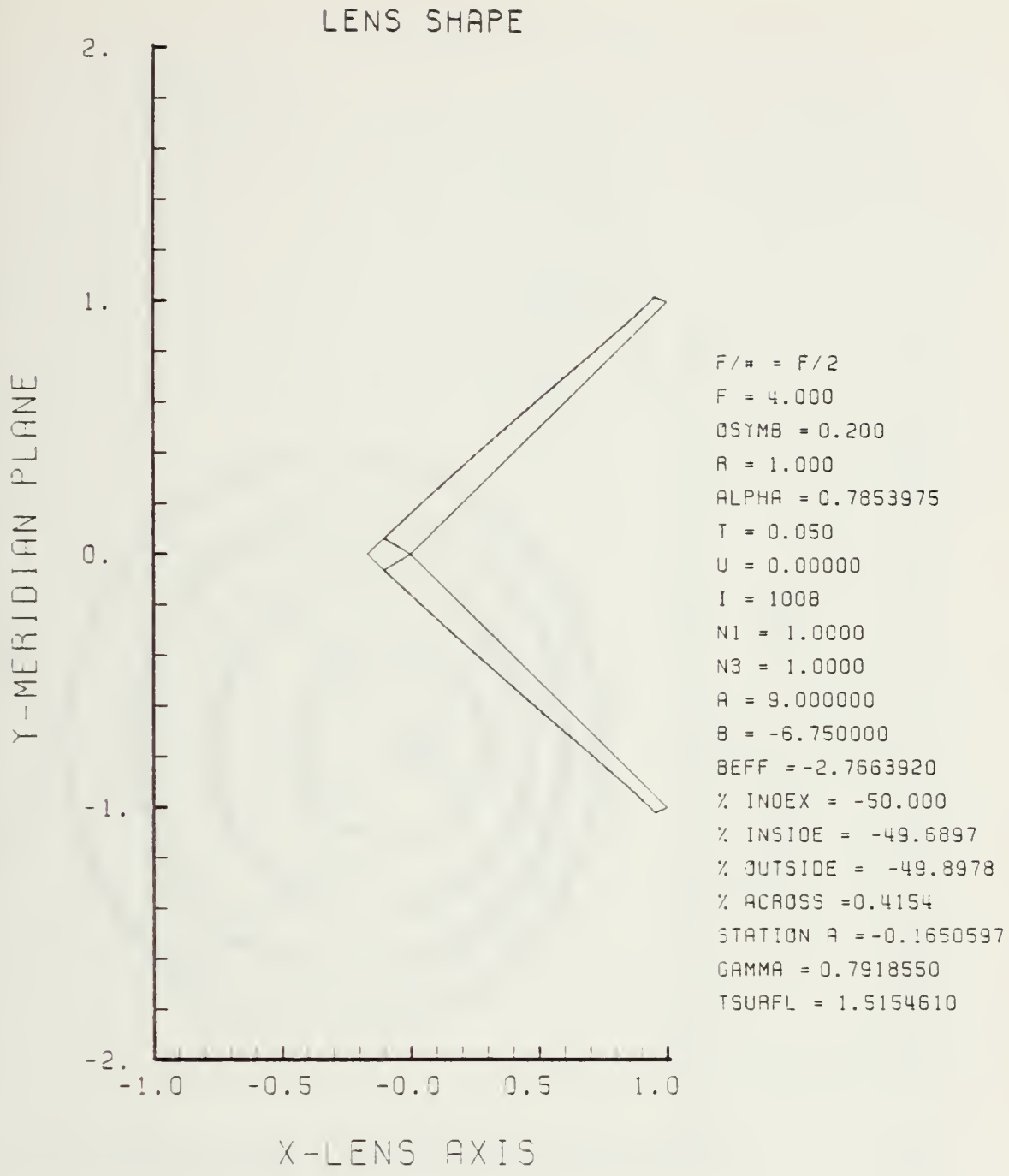

Figure F-45. GRIN Lens Shape for -50%, OB = 0.20, a = 9.00

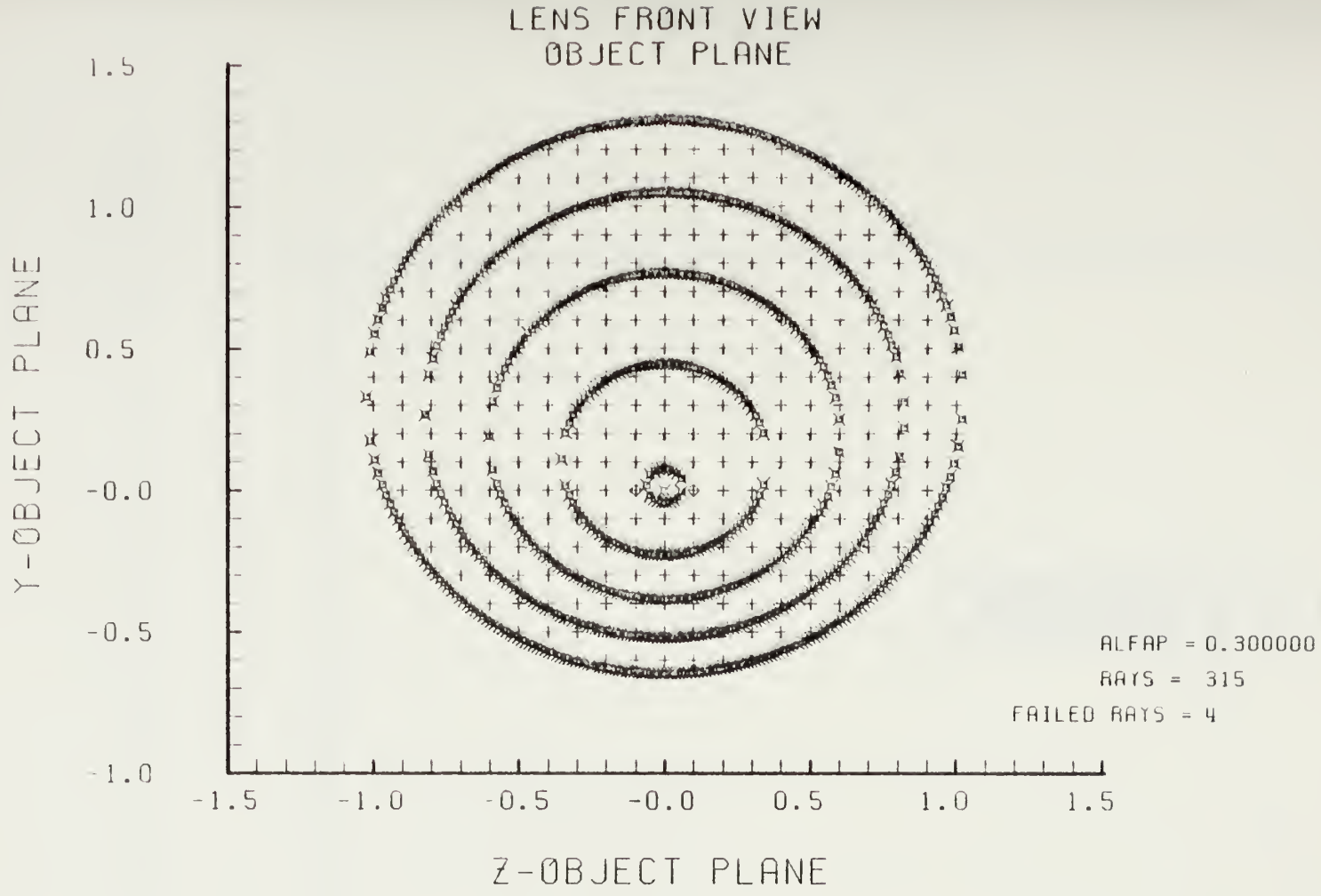

Figure F-46. Grid Plane at α_p = 0.3 for Lens of Figure F-45

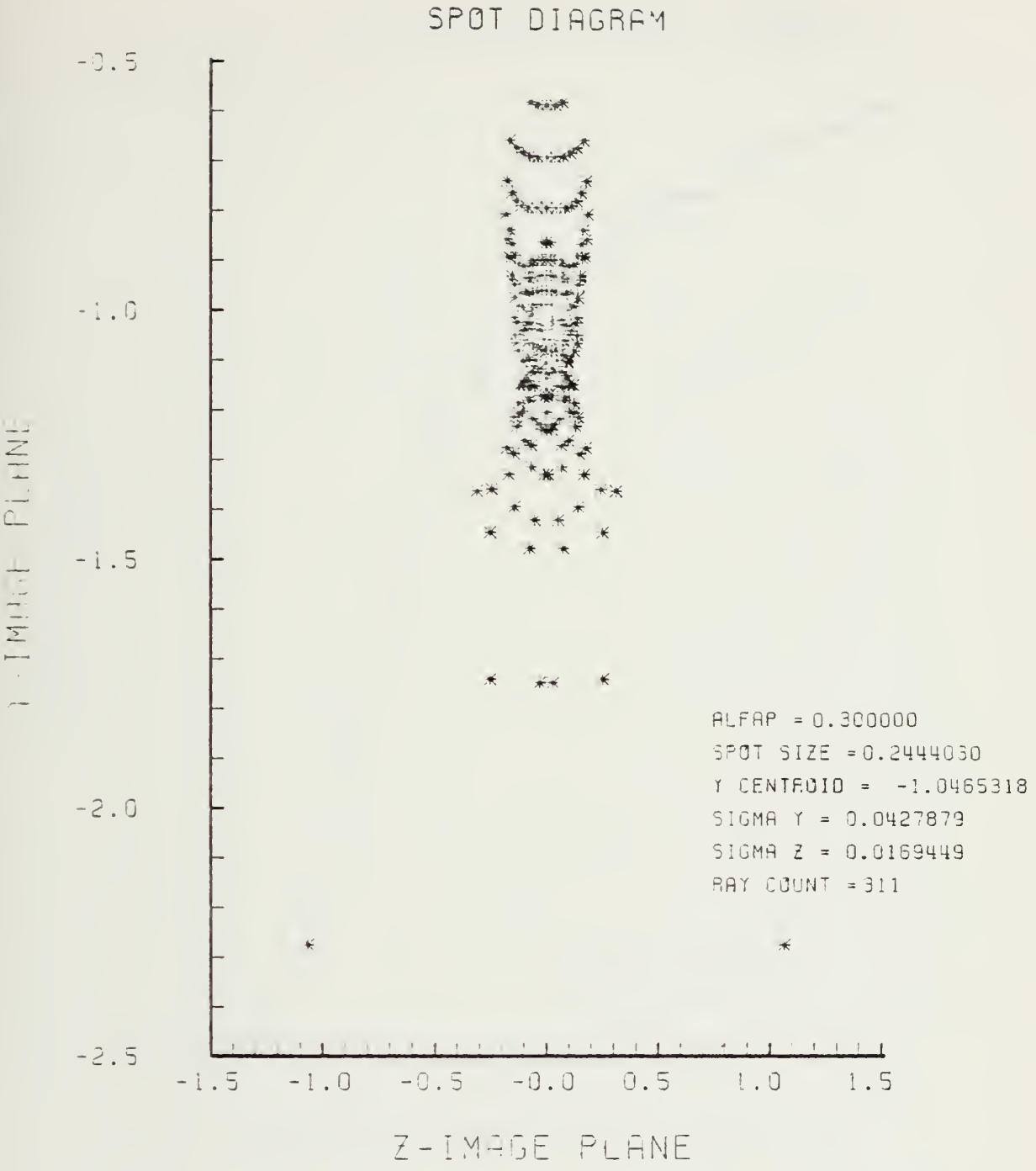

Figure F-47. Spot Diagram for Grid of Figure F-46

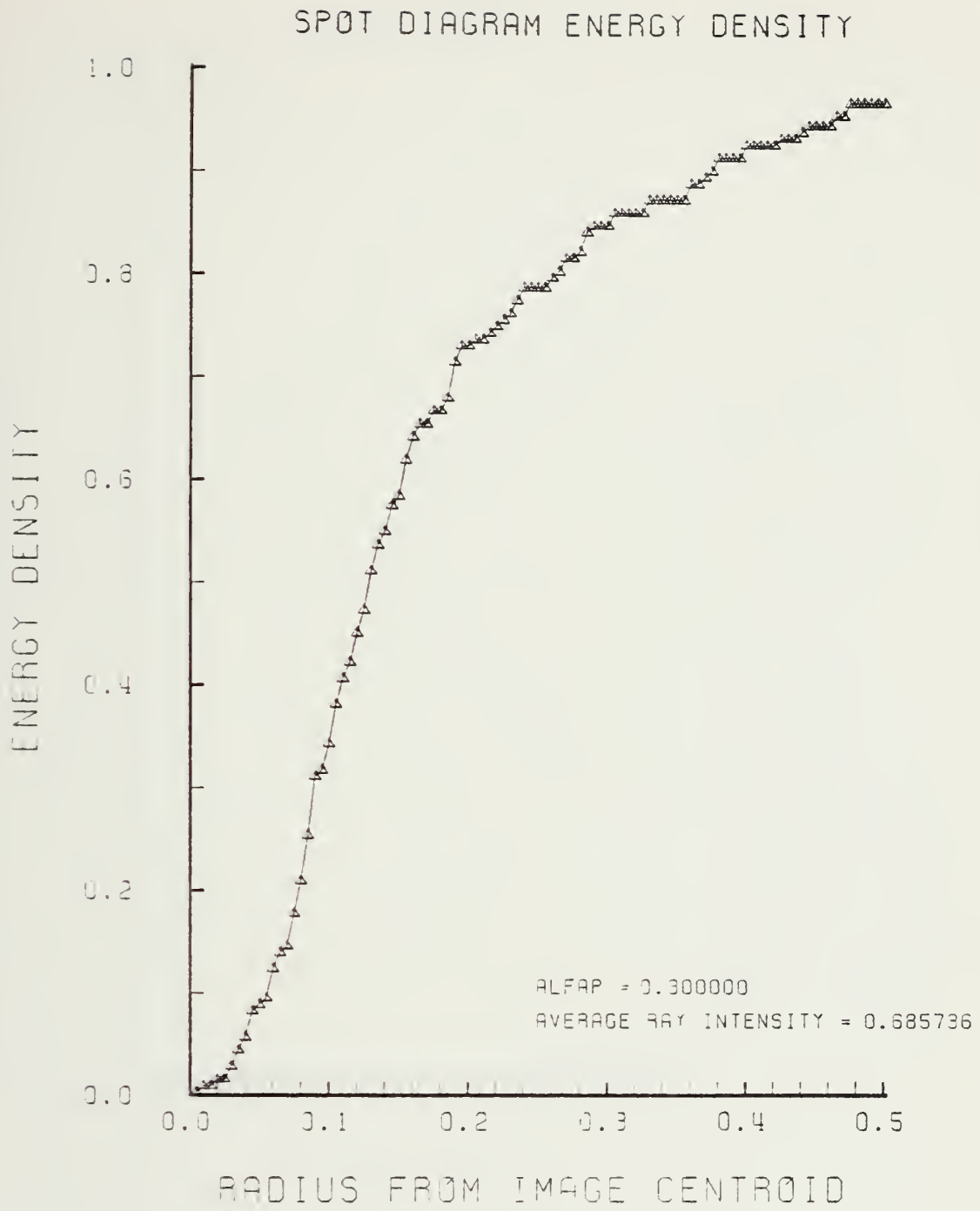

Figure F-48. Encircled Energy of Figure F-47

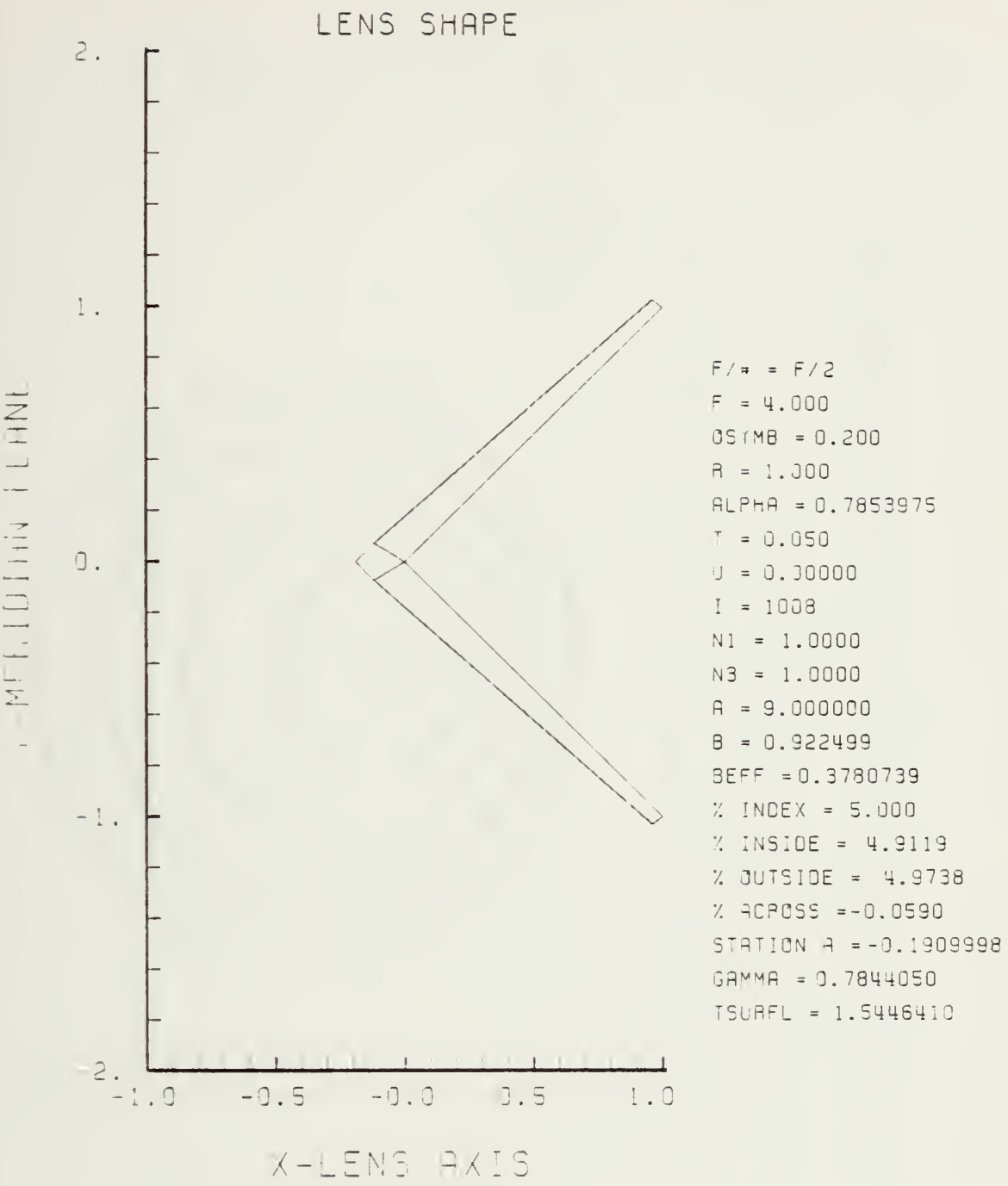

Figure F-49. GRIN Lens Shape for +5%, OB = 0.20, a = 9.00

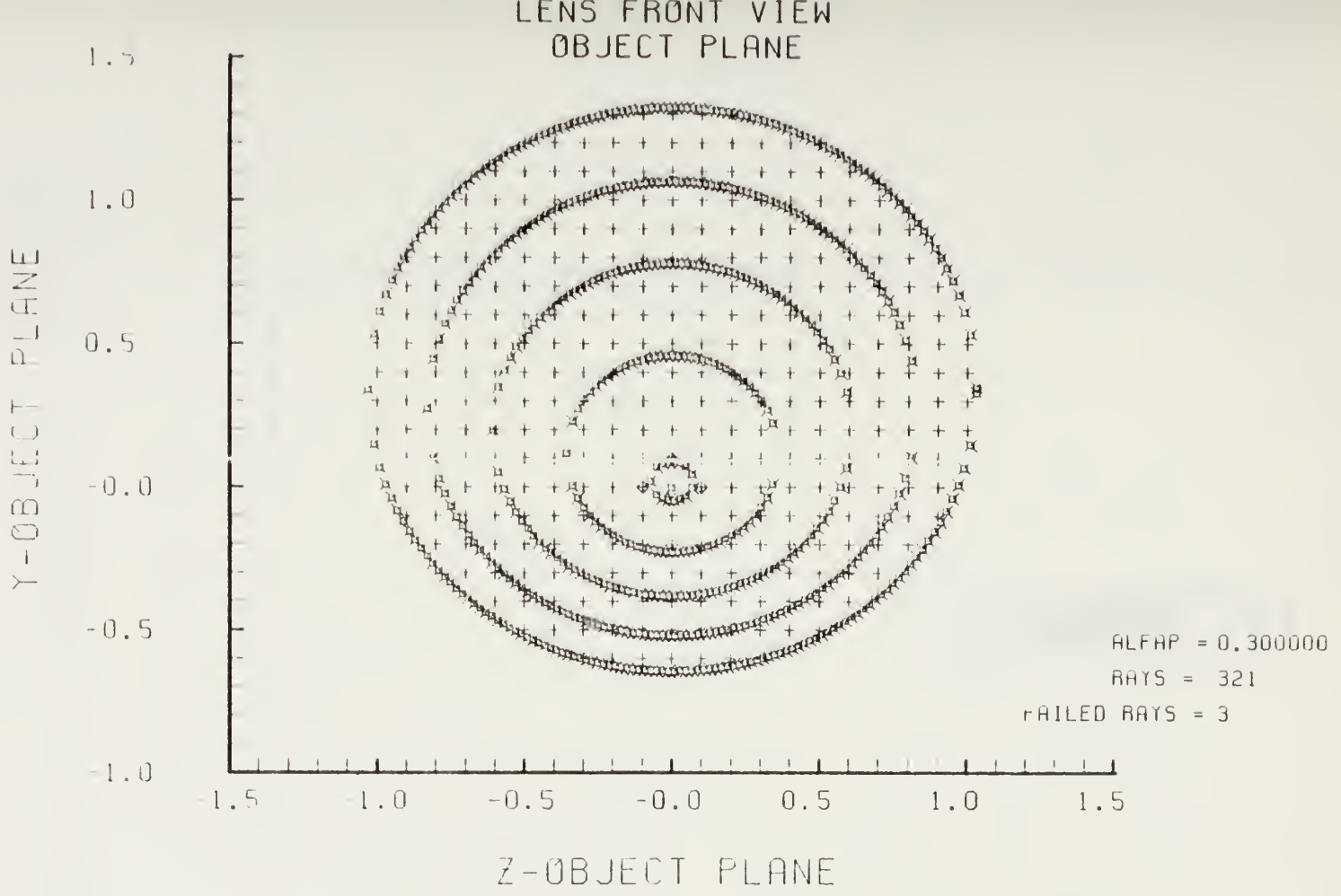

Figure F-50. Grid Plane at α_p = 0.3 for Lens of Figure F-49

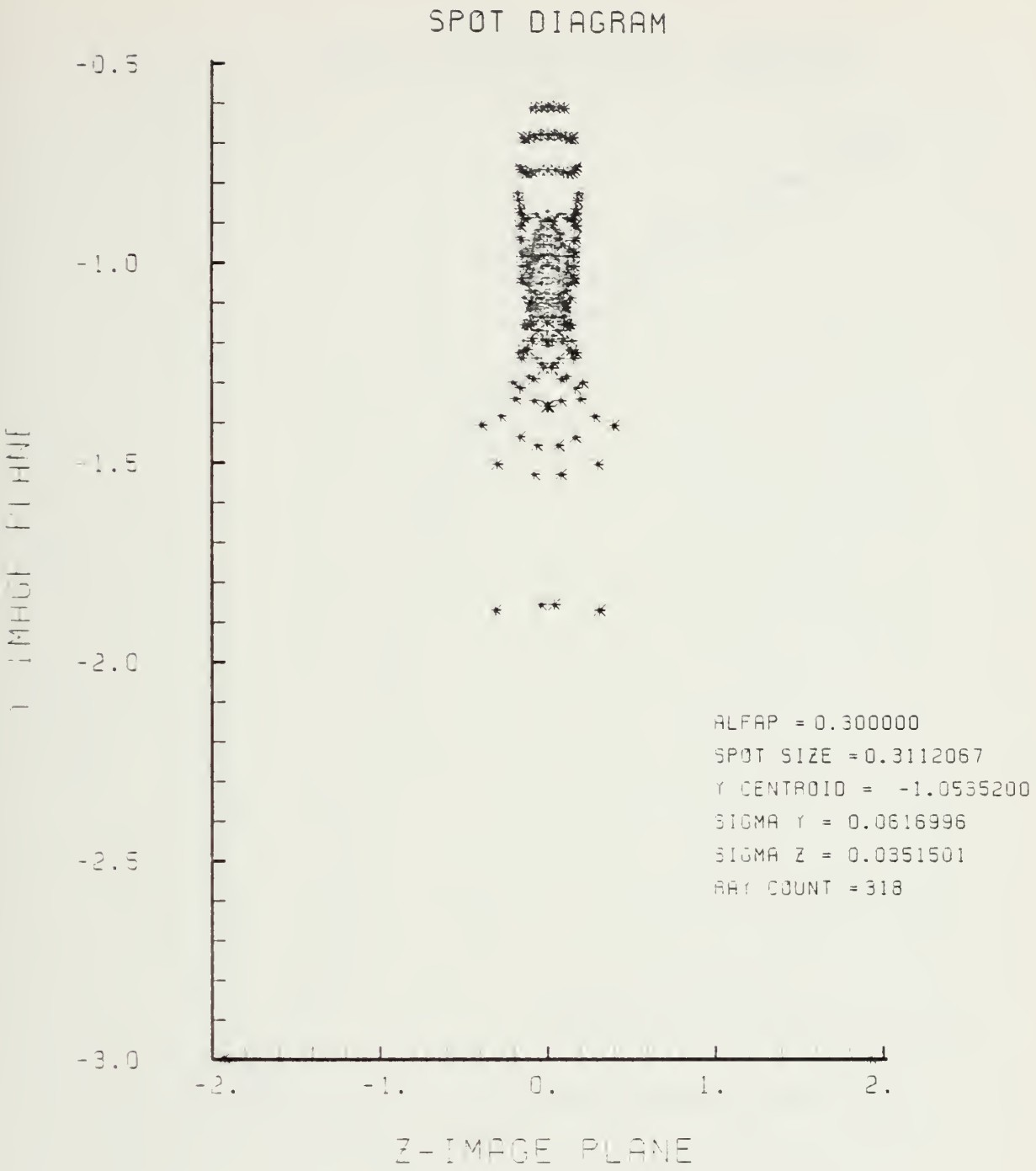

Figure F-51. Spot Diagram for Grid of Figure F-50

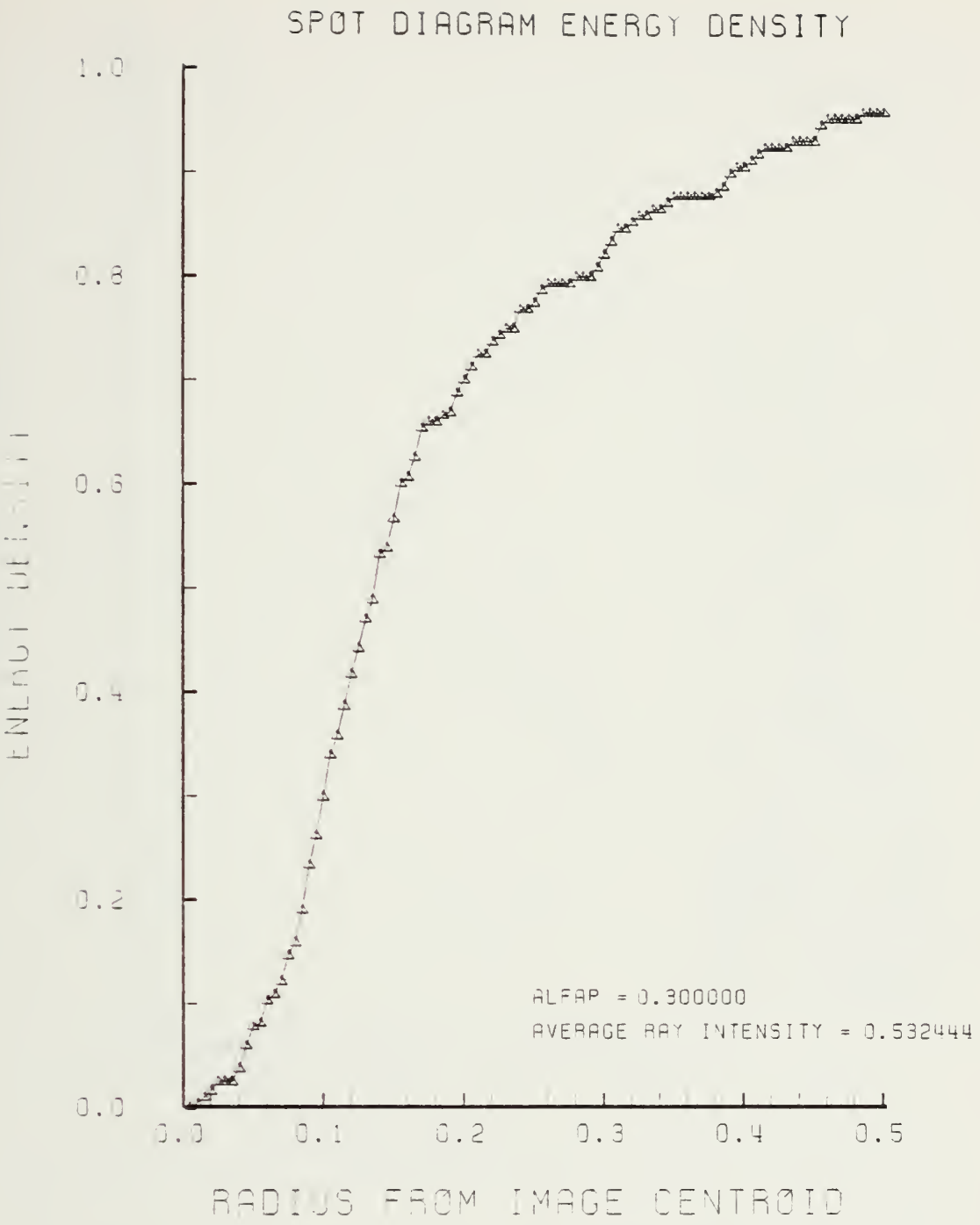

Figure F-52. Encircled Energy of Figure F-51

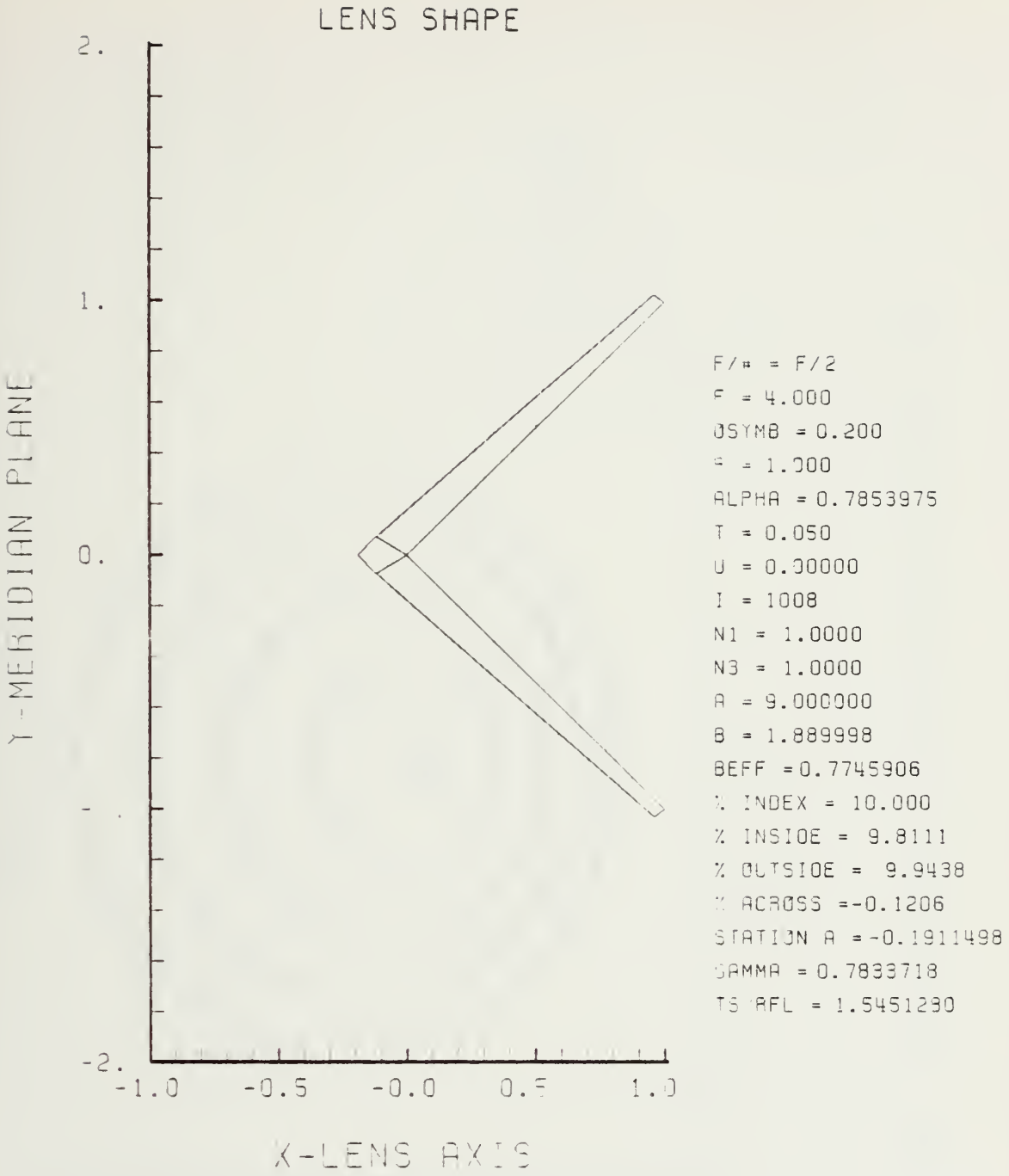

Figure F-53. GRIN Lens Shape at +10%, OB = 0.20, a = 9.00

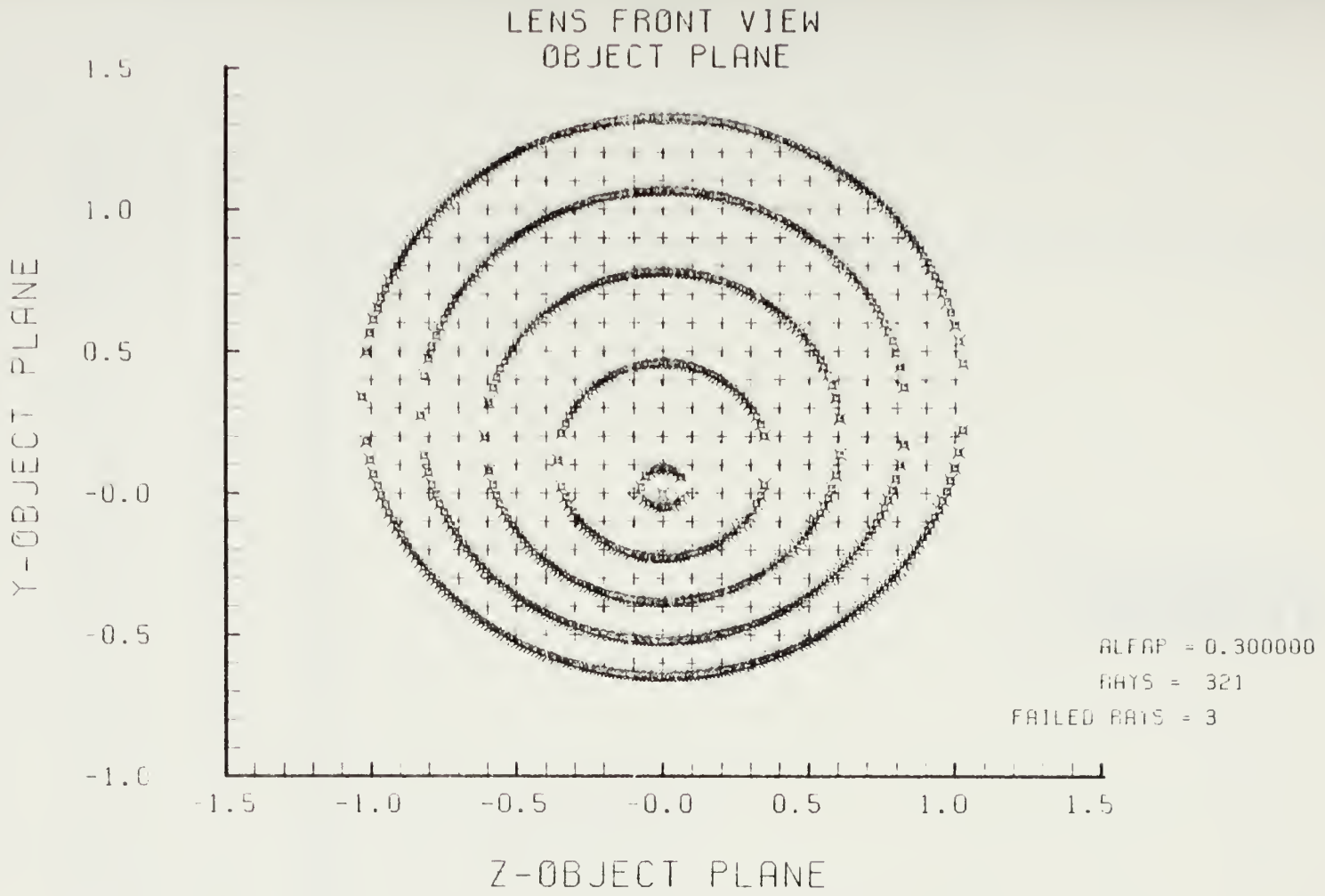

Figure F-54. Grid Plane at α_p = 0.3 for Lens of Figure F-53

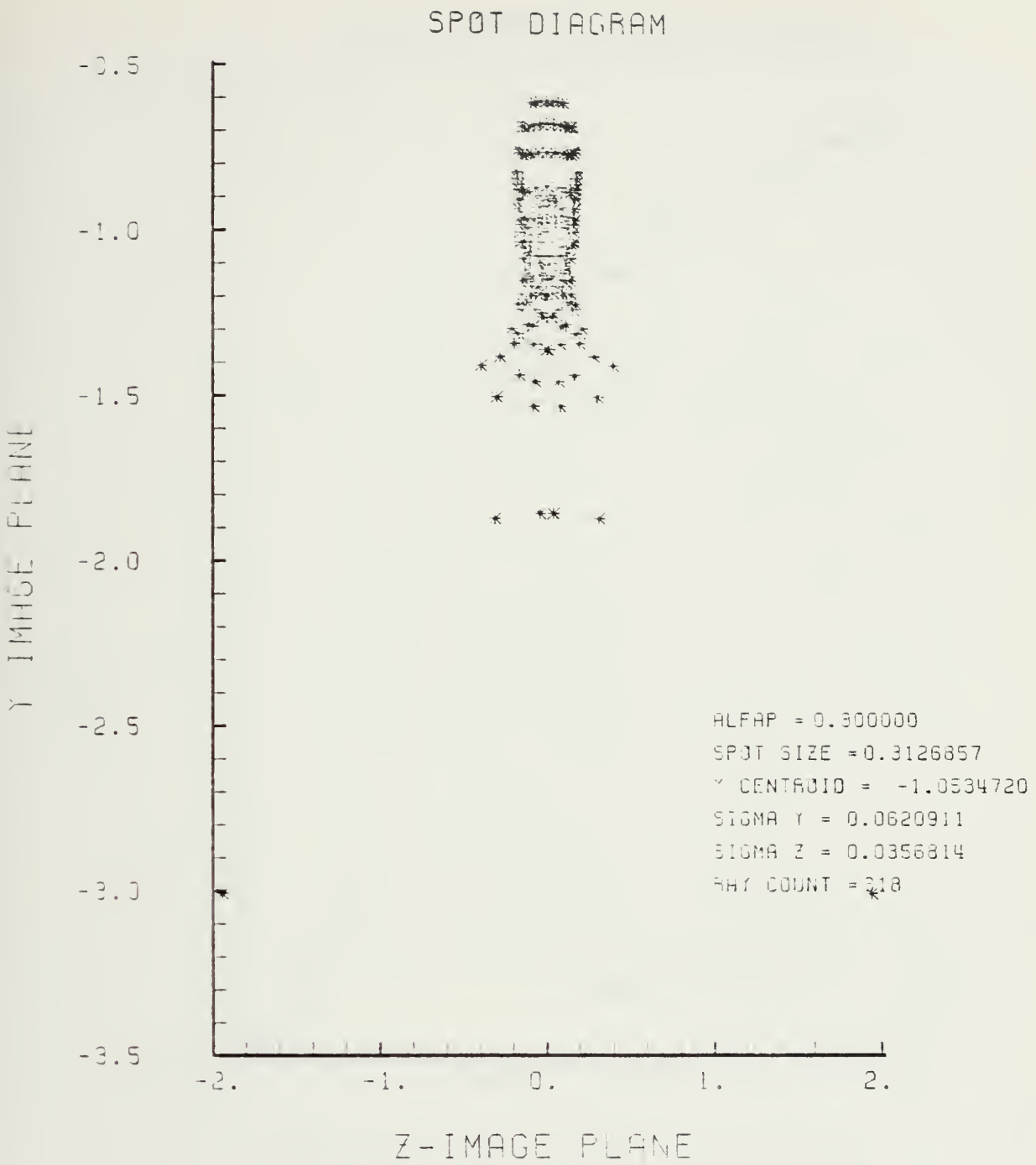

Figure F-55. Spot Diagram for Grid of Figure F-54

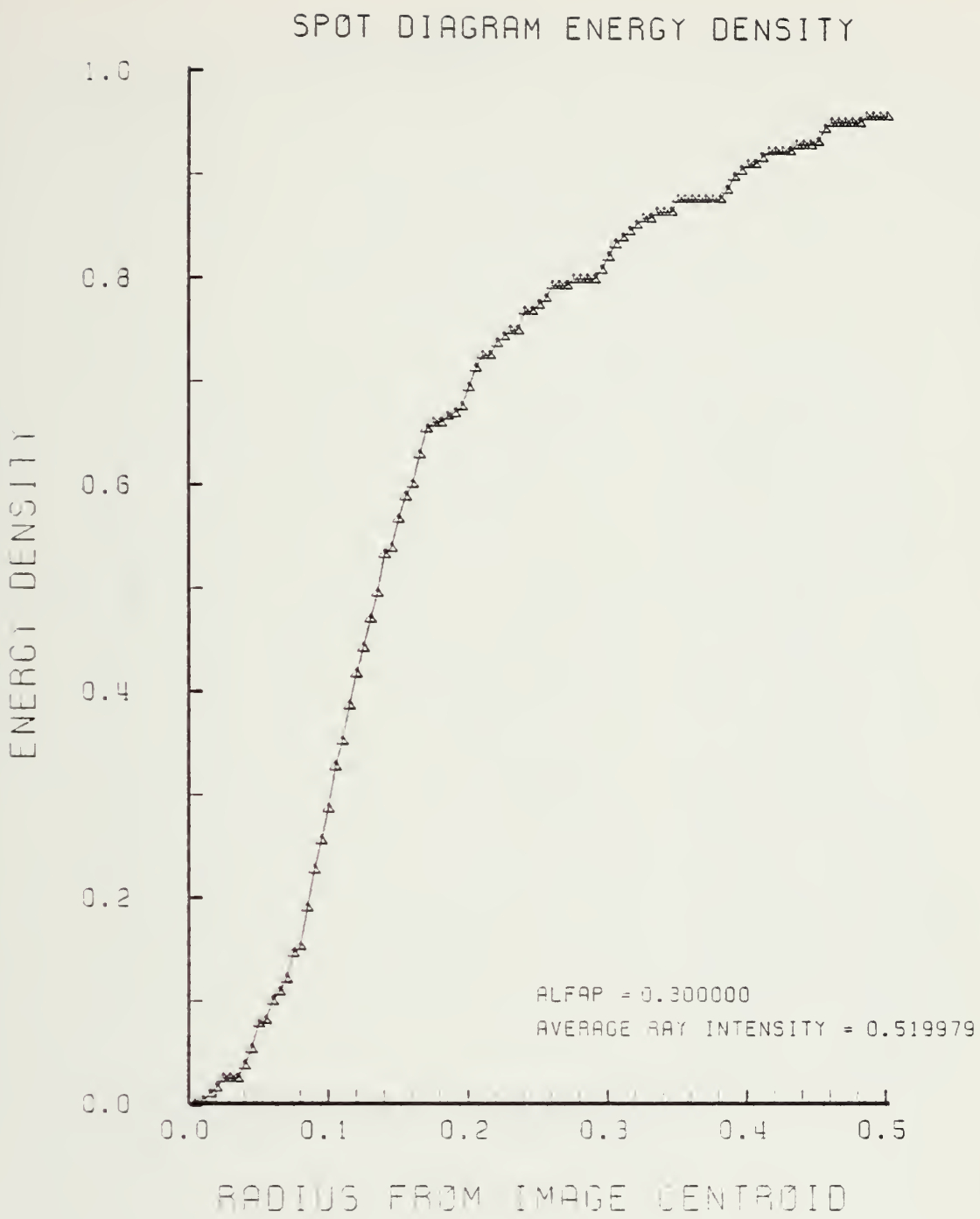

Figure F-56. Encircled Energy of Figure F-55

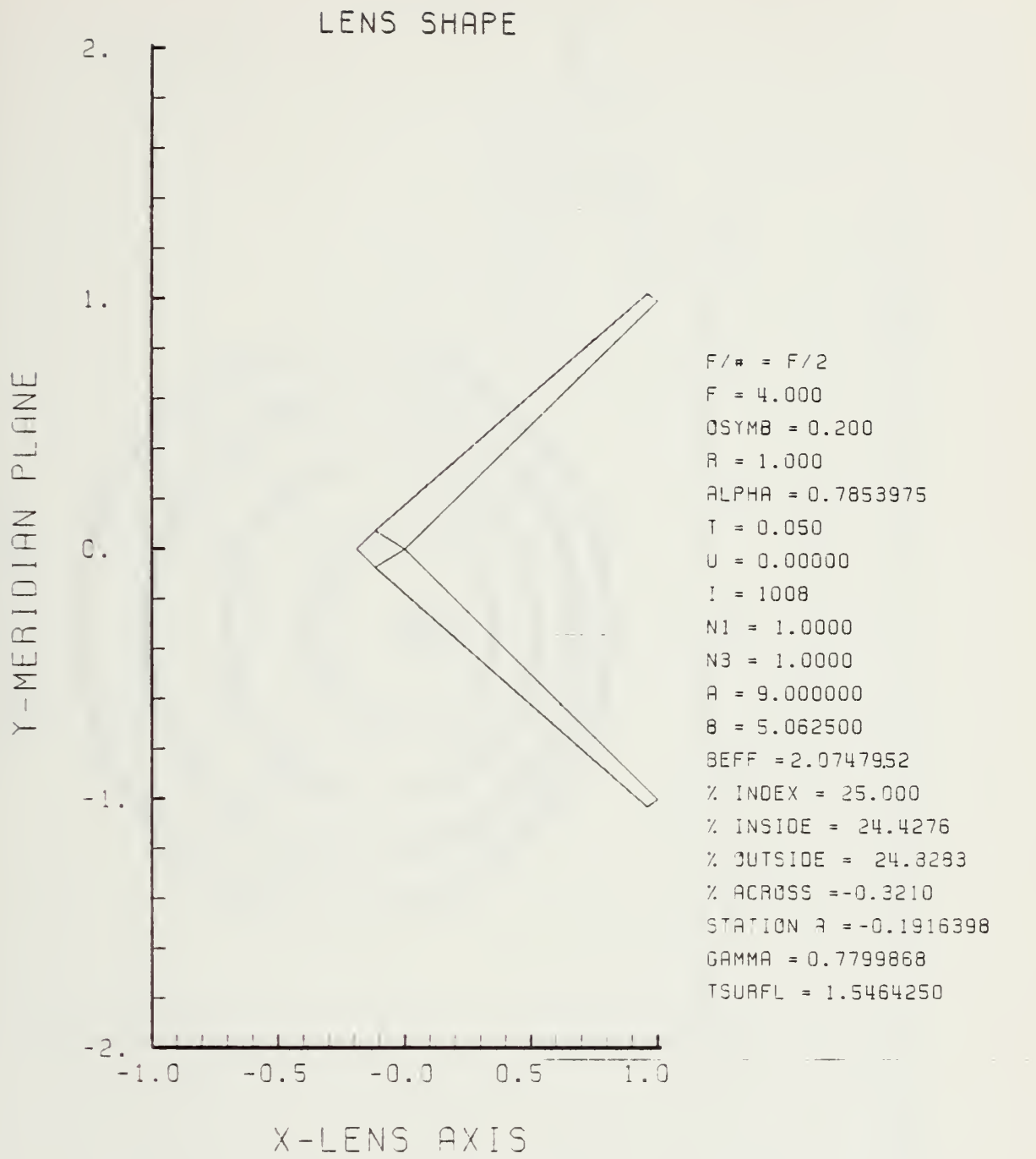

Figure F-57. GRIN Lens Shape at +25%, OB = 0.20, a = 9.00

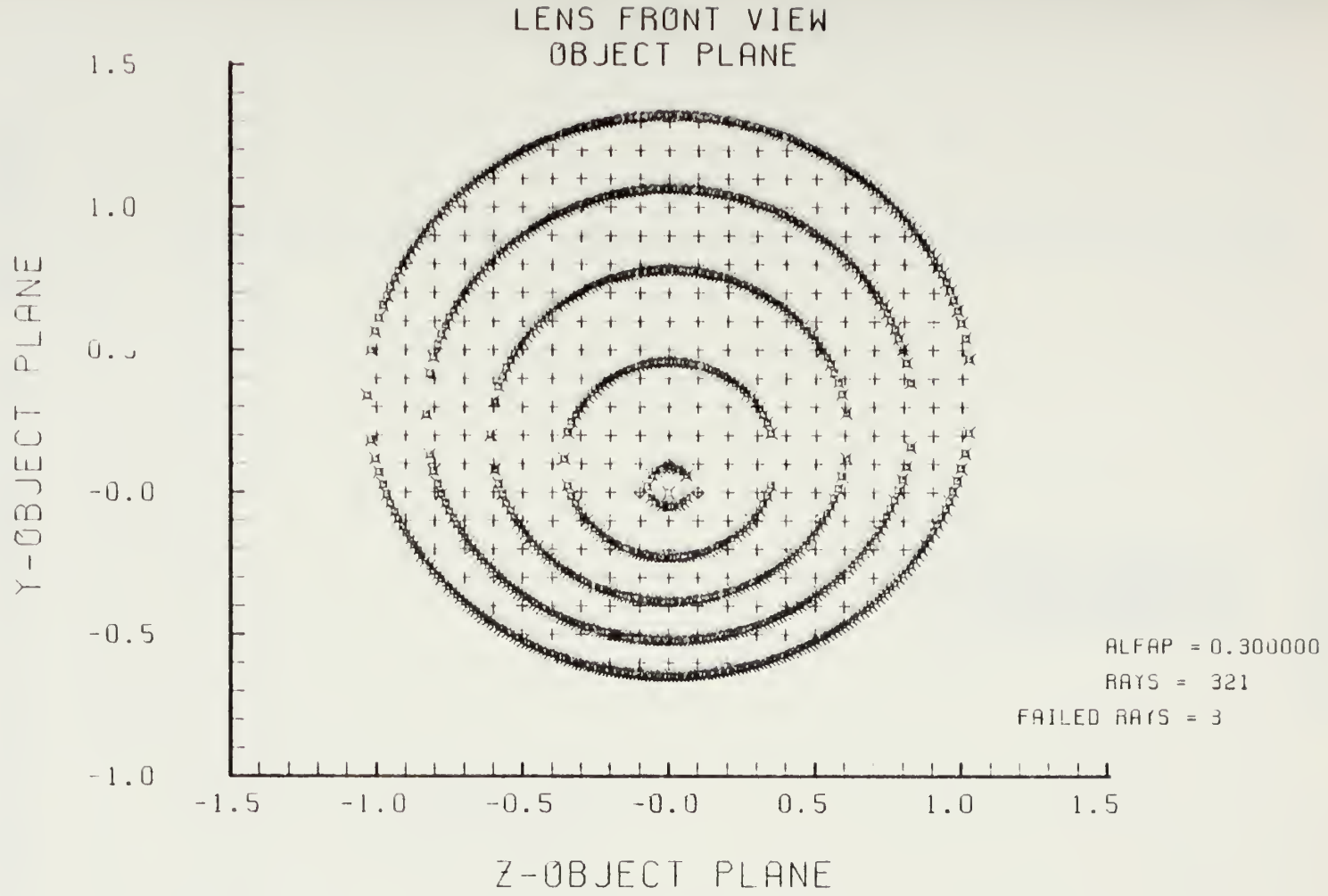

Figure F-58. Grid Plane at α_p = 0.3 for Lens of Figure F-57

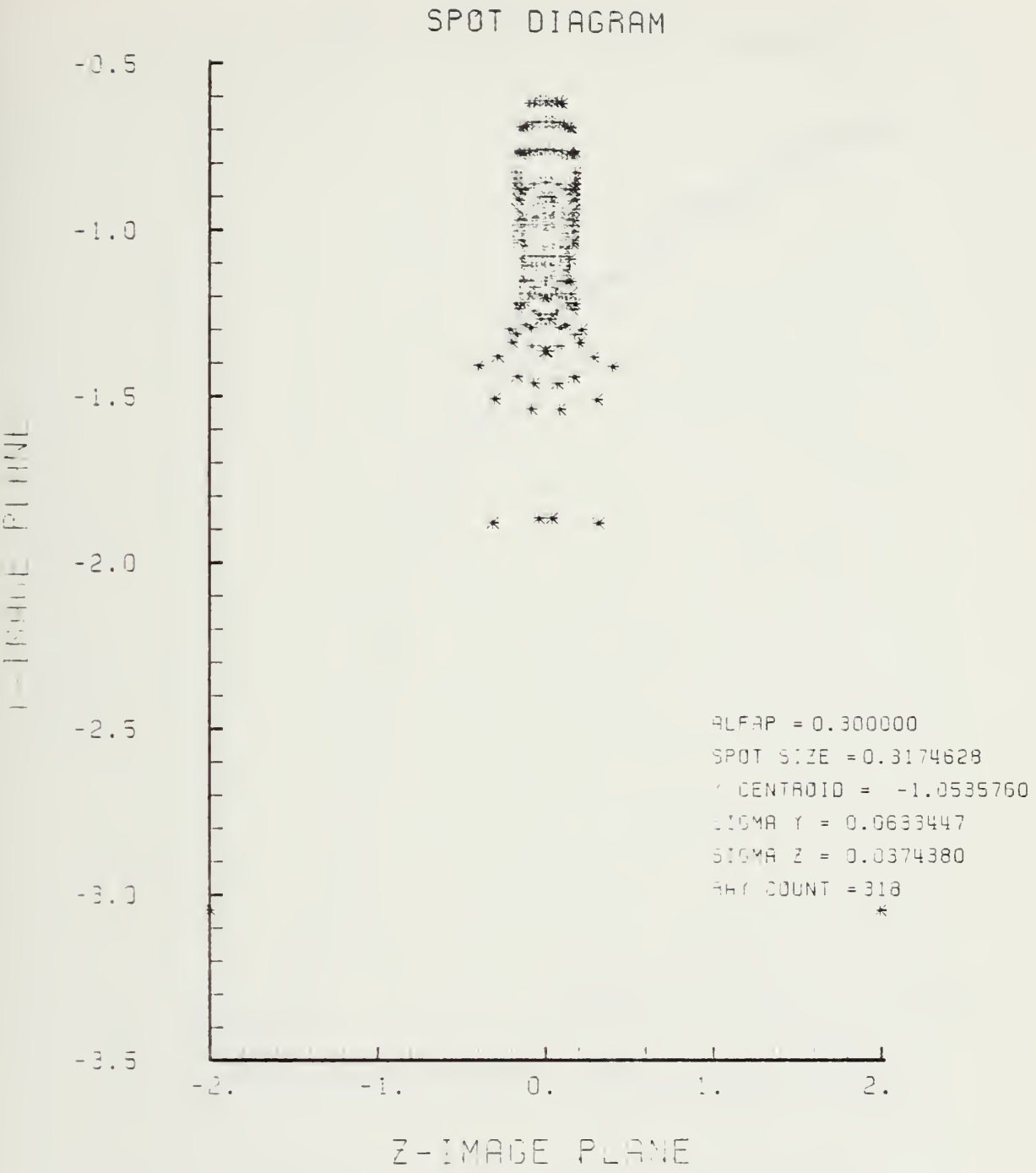

Figure F-59. Spot Diagram for Grid of Figure F-58

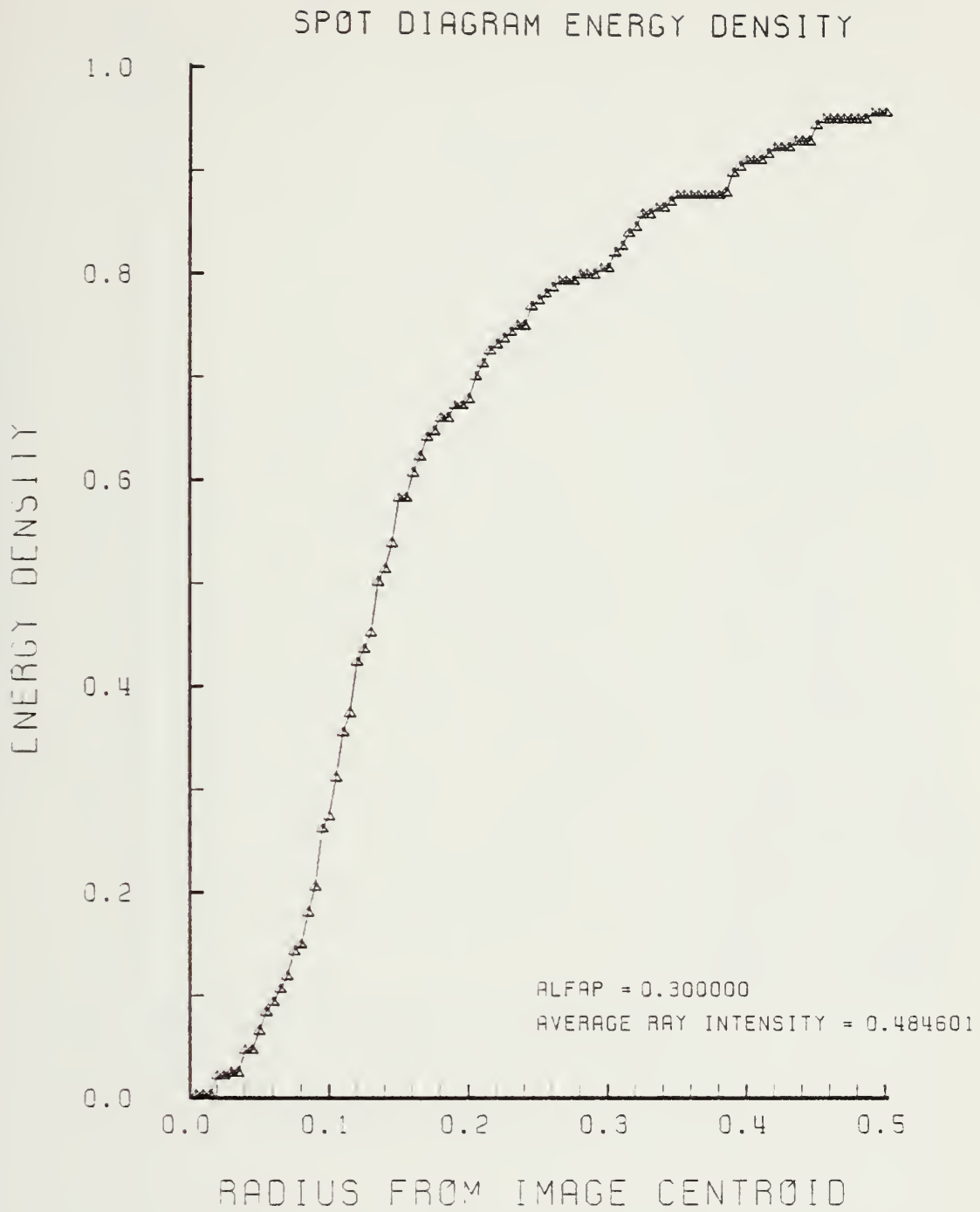

Figure F-60. Encircled Energy of Figure F-59

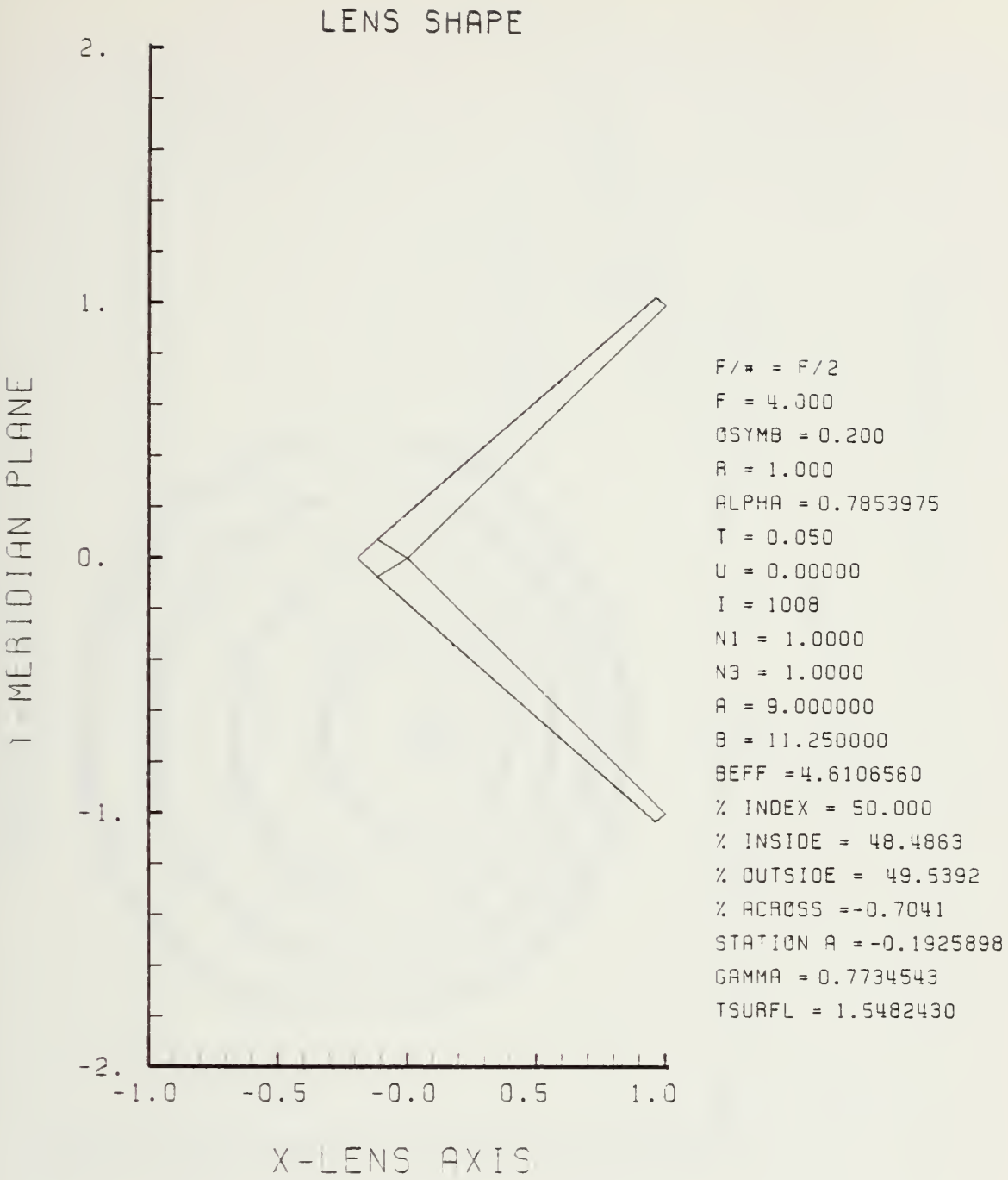

Figure F-61. GRIN Lens Shape at +50%, OB = 0.20, a = 9.00

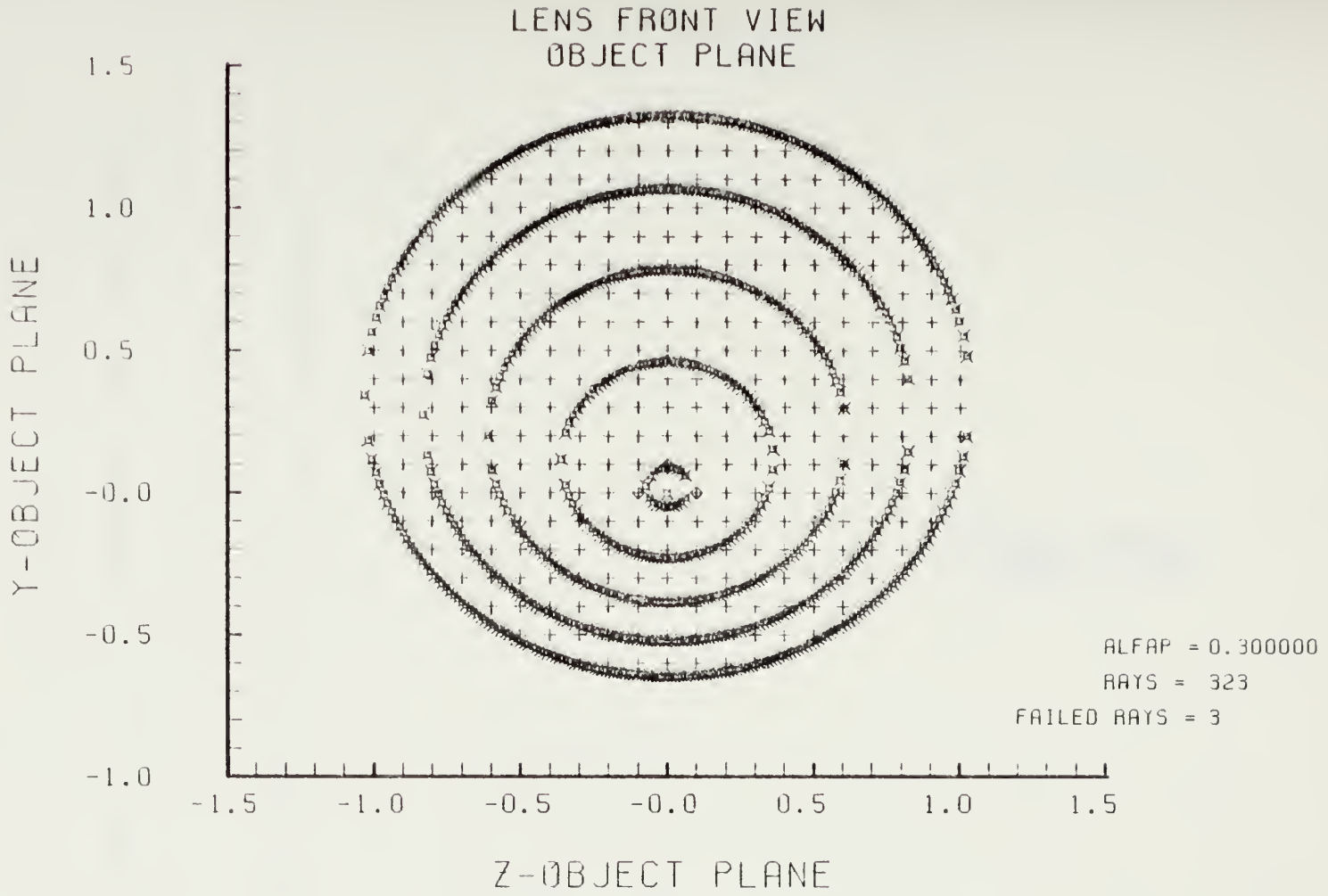

Figure F-62. Grid Plane at $\alpha_p = 0.3$ for Lens of Figure F-61

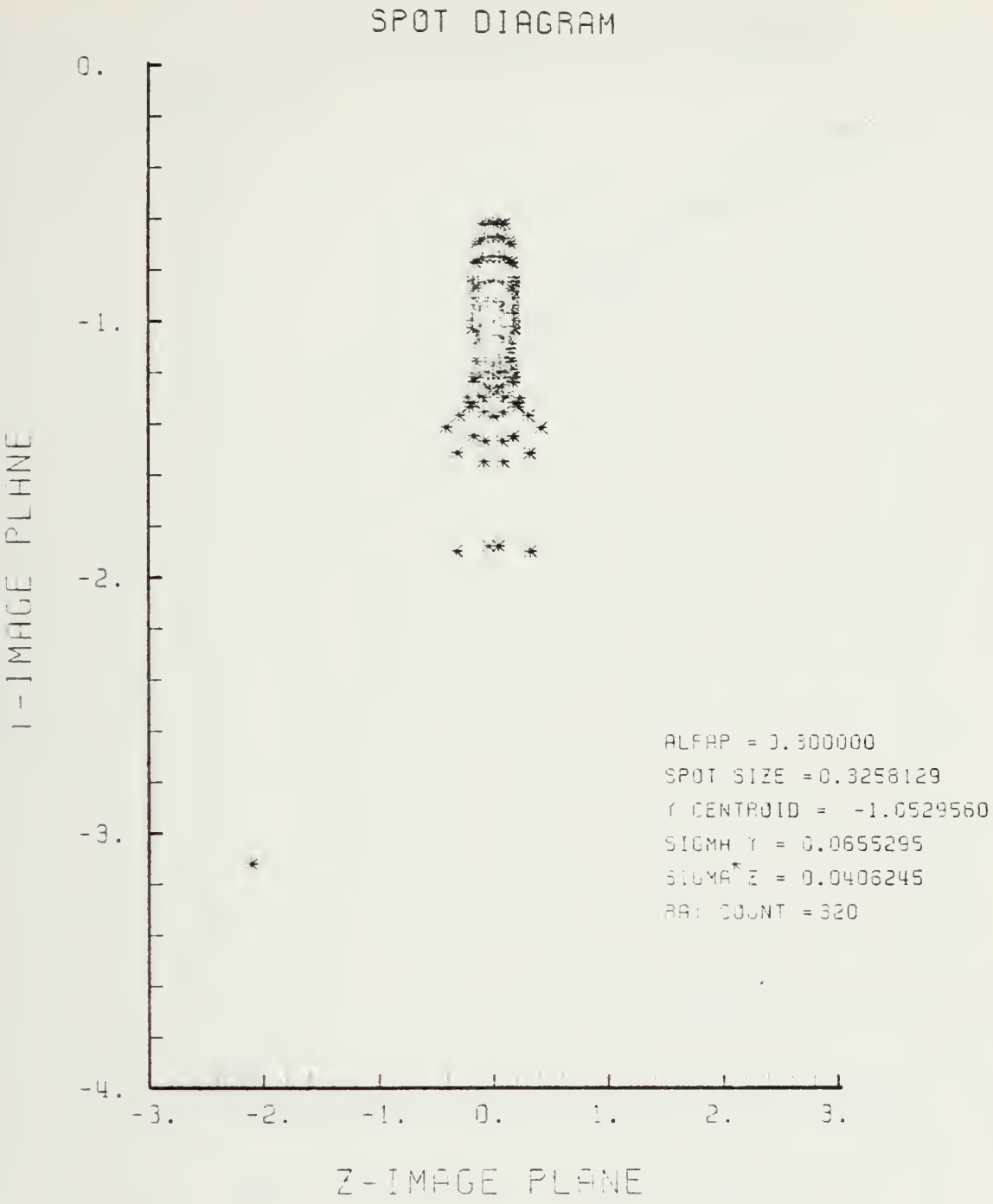

Figure F-63. Spot Diagram for Grid of Figure F-62

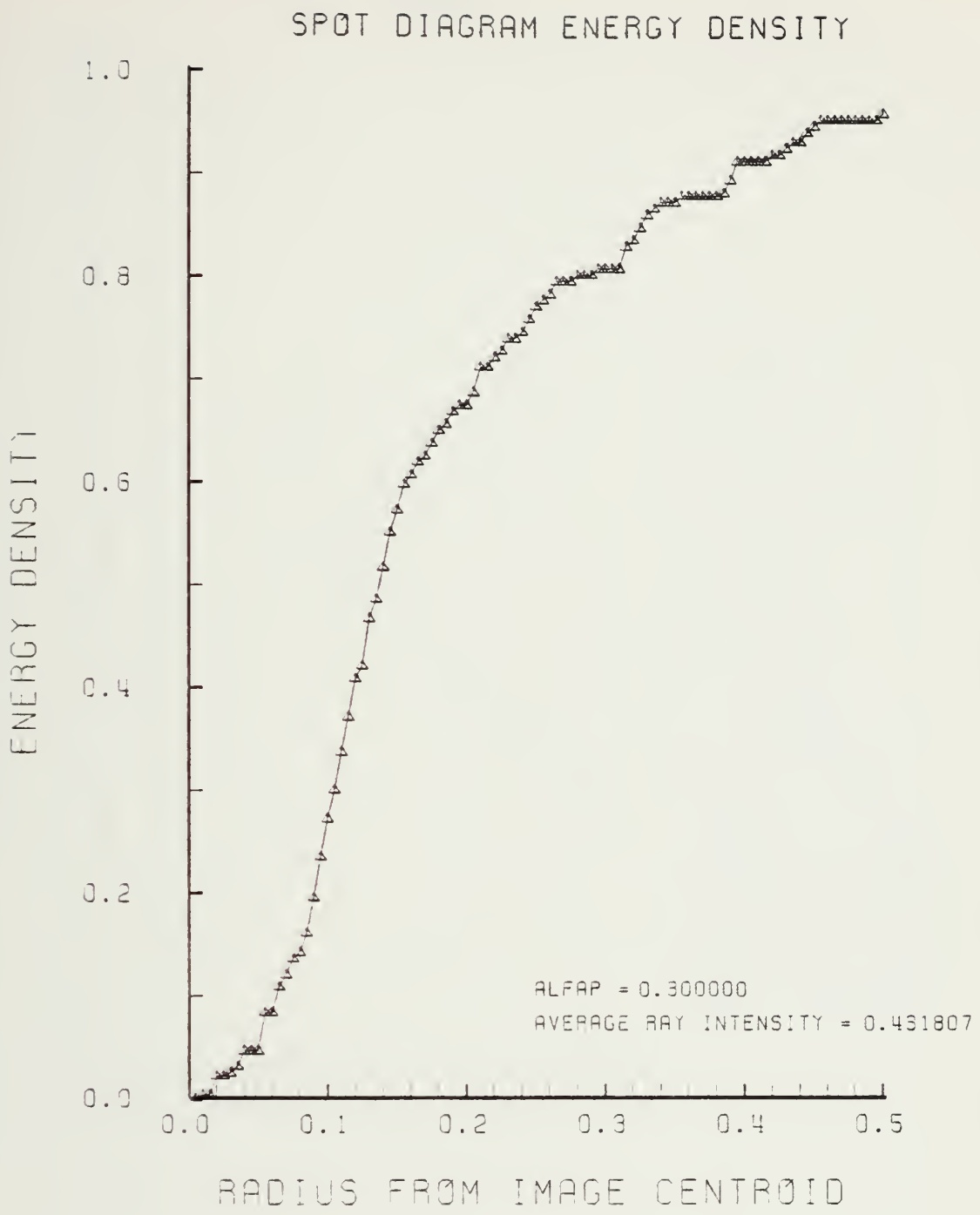

Figure F-64. Encircled Energy of Figure F-63

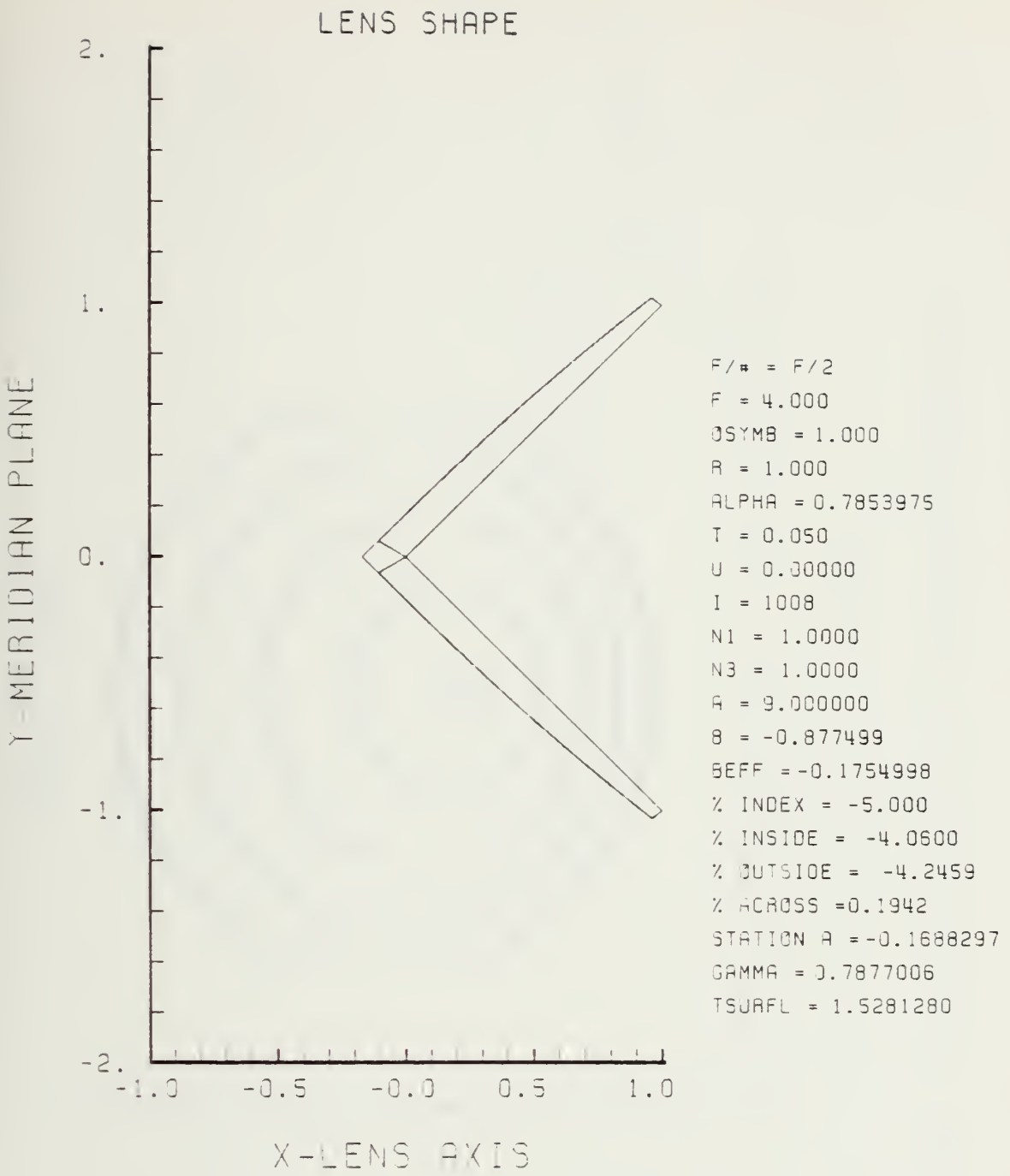

Figure F-65. GRIN Lens Shape at -5%, OB = 1.00, a = 9.00

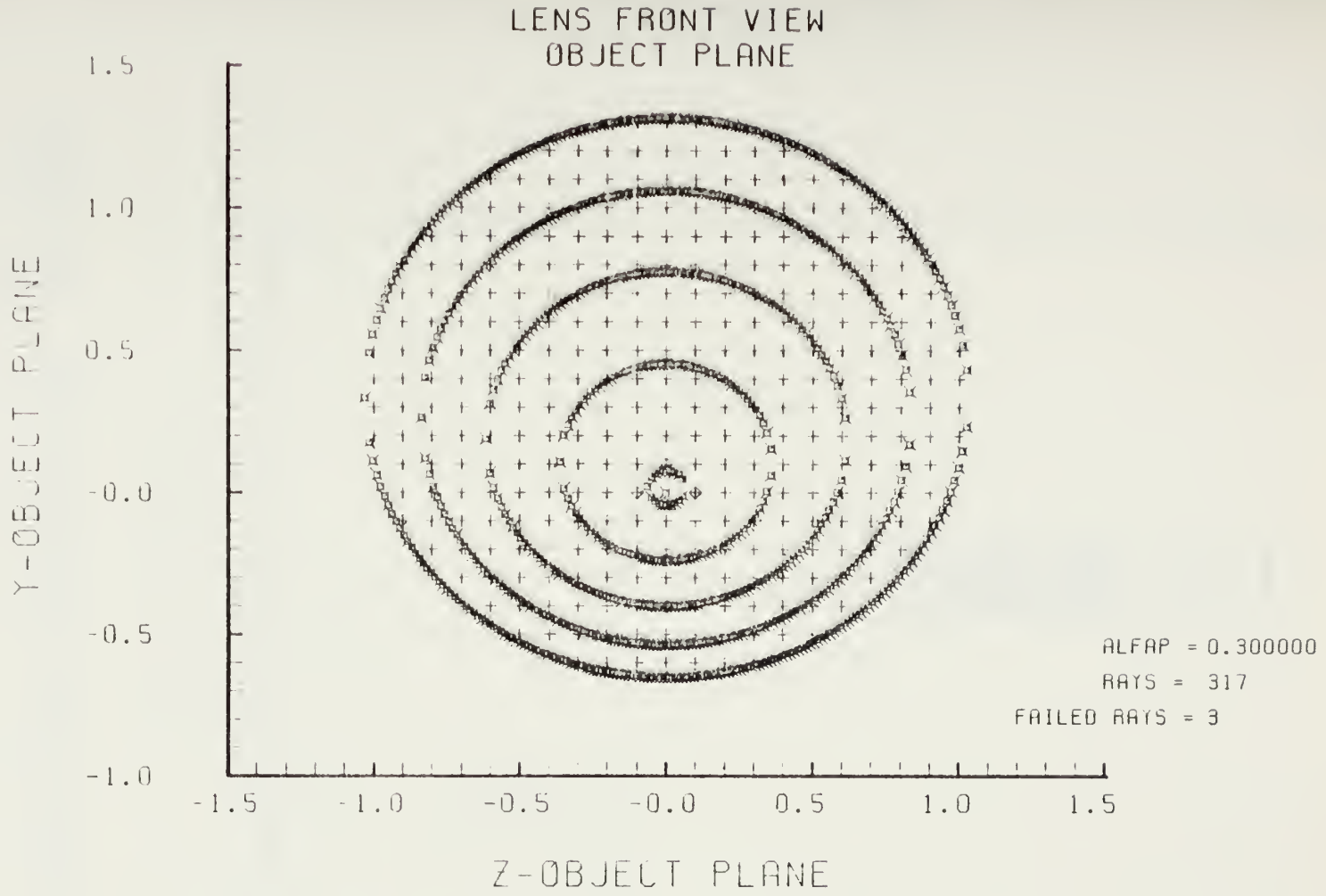

Figure F-66. Grid Plane at $\alpha_p = 0.3$ for Lens of Figure F-65

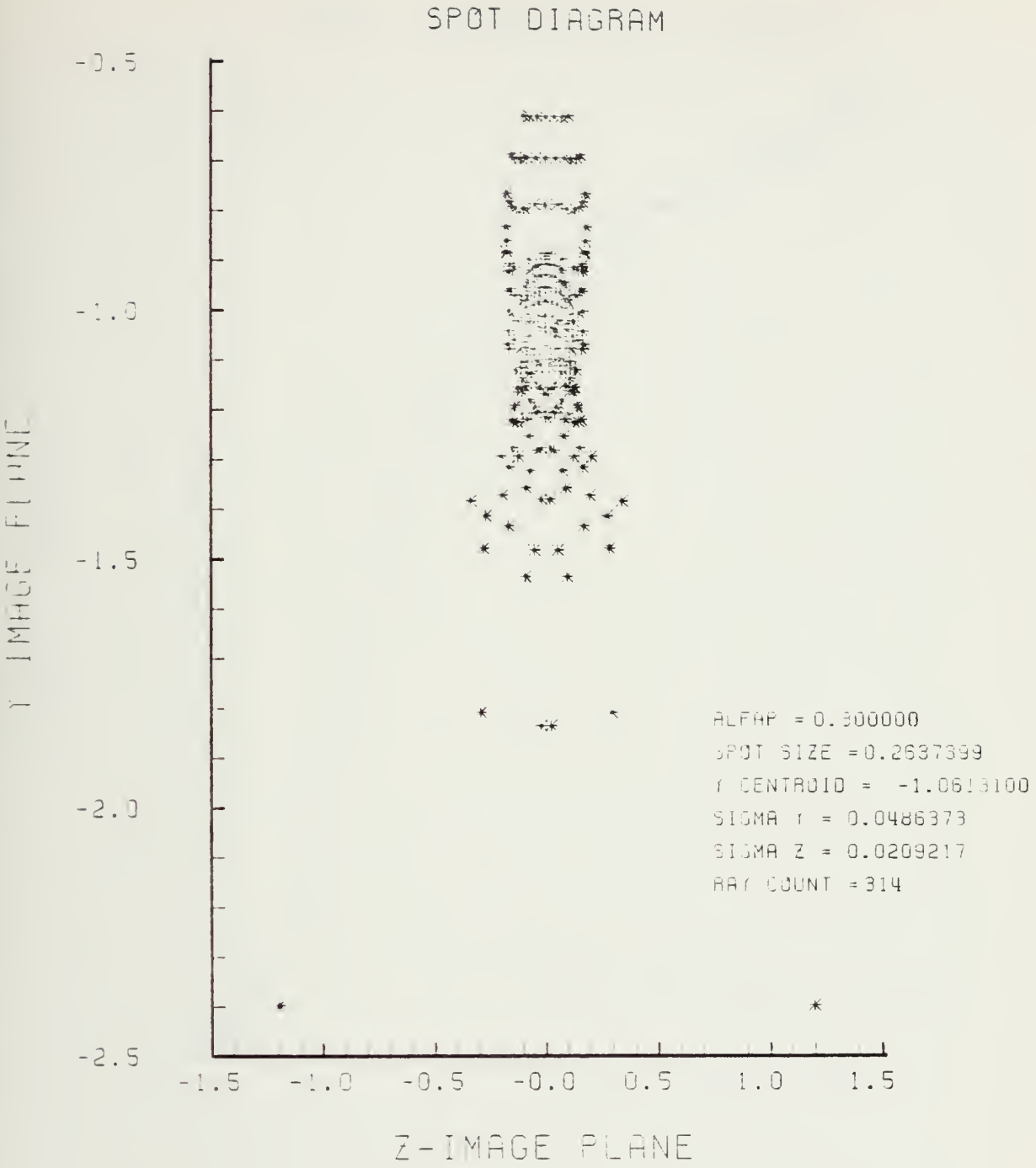

Figure F-67. Spot Diagram for Grid of Figure F-66

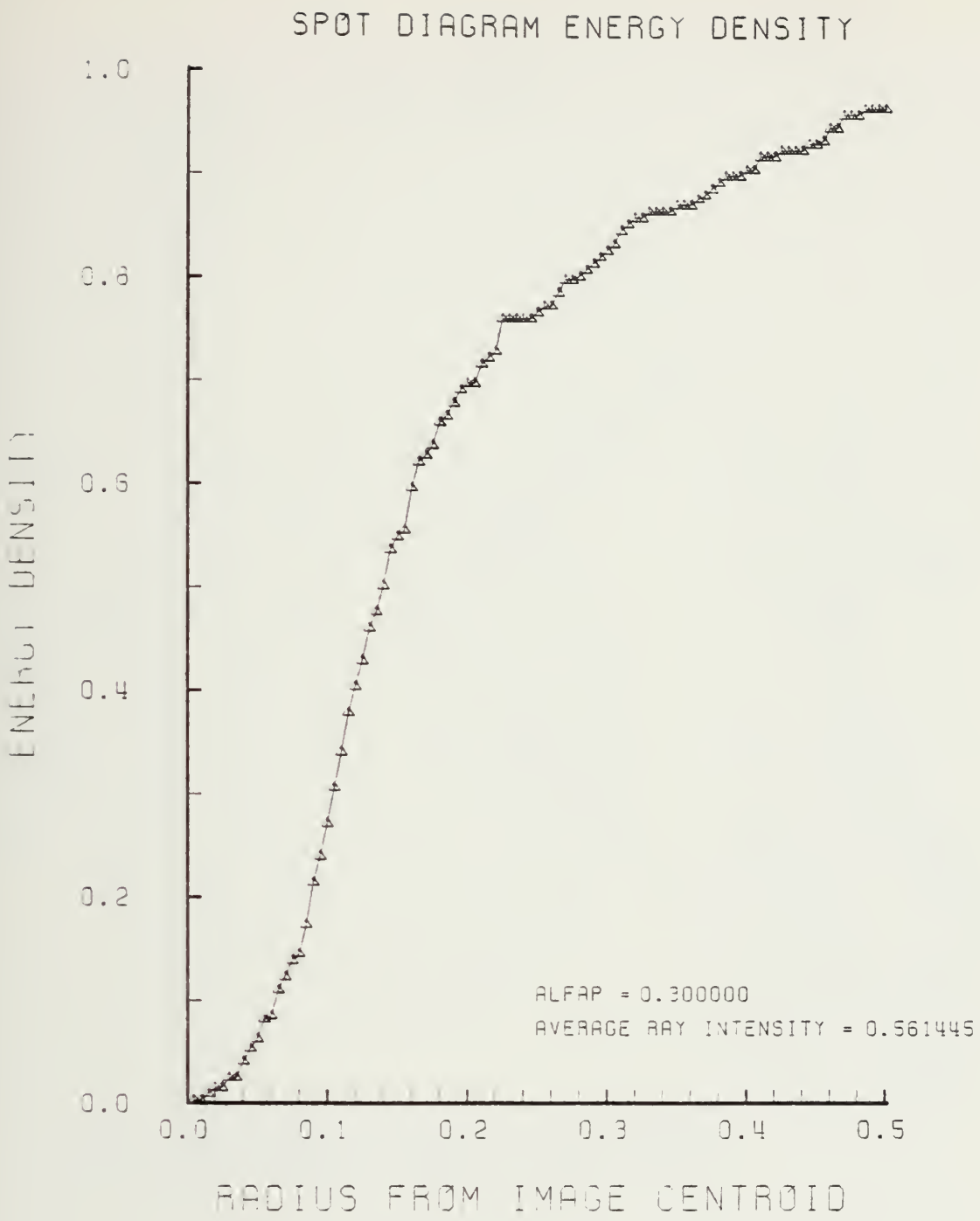

Figure F-68. Encircled Energy of Figure F-67

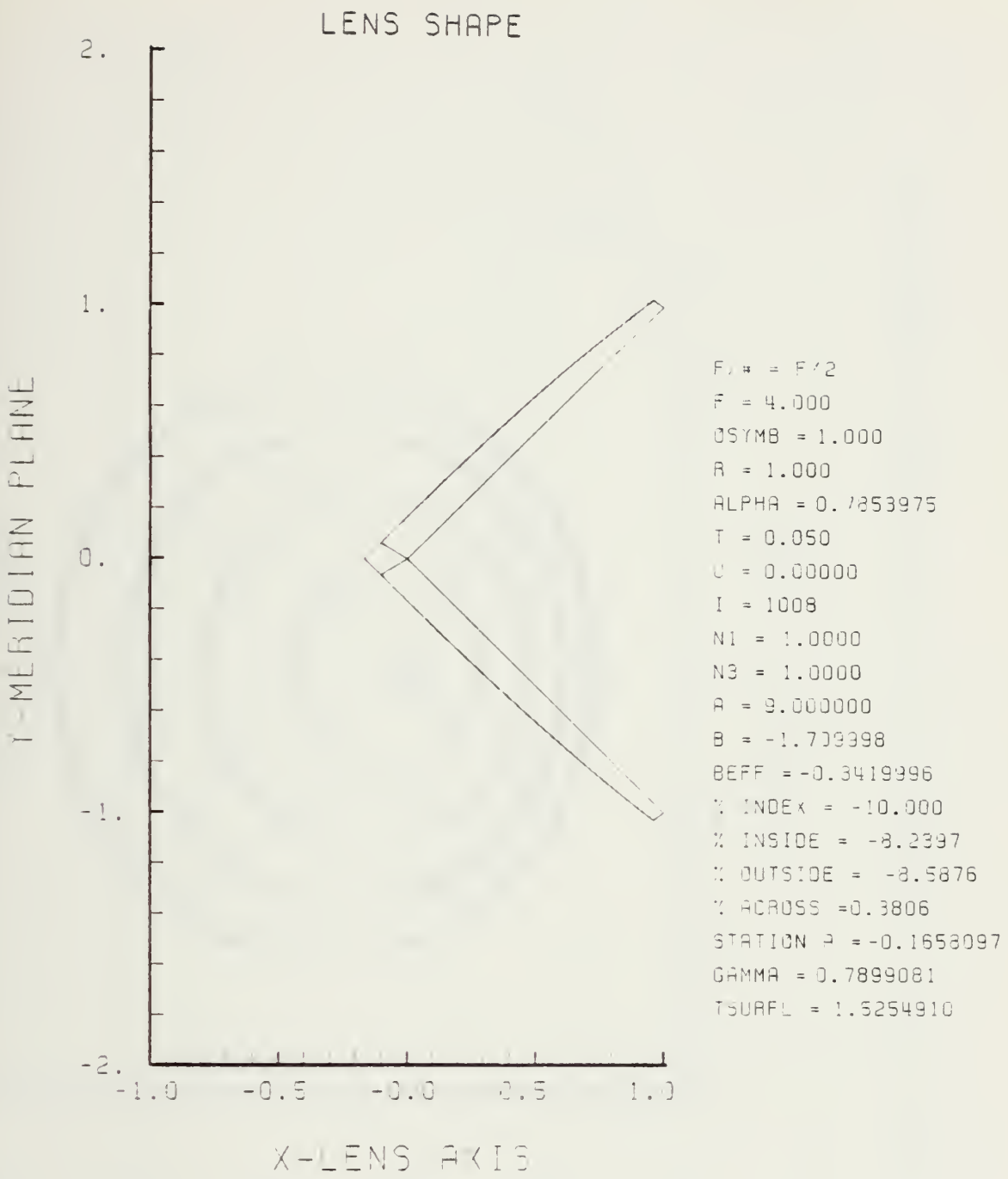

Figure F-69. GRIN Lens Shape at -10%, OB = 1.00, a = 9.00

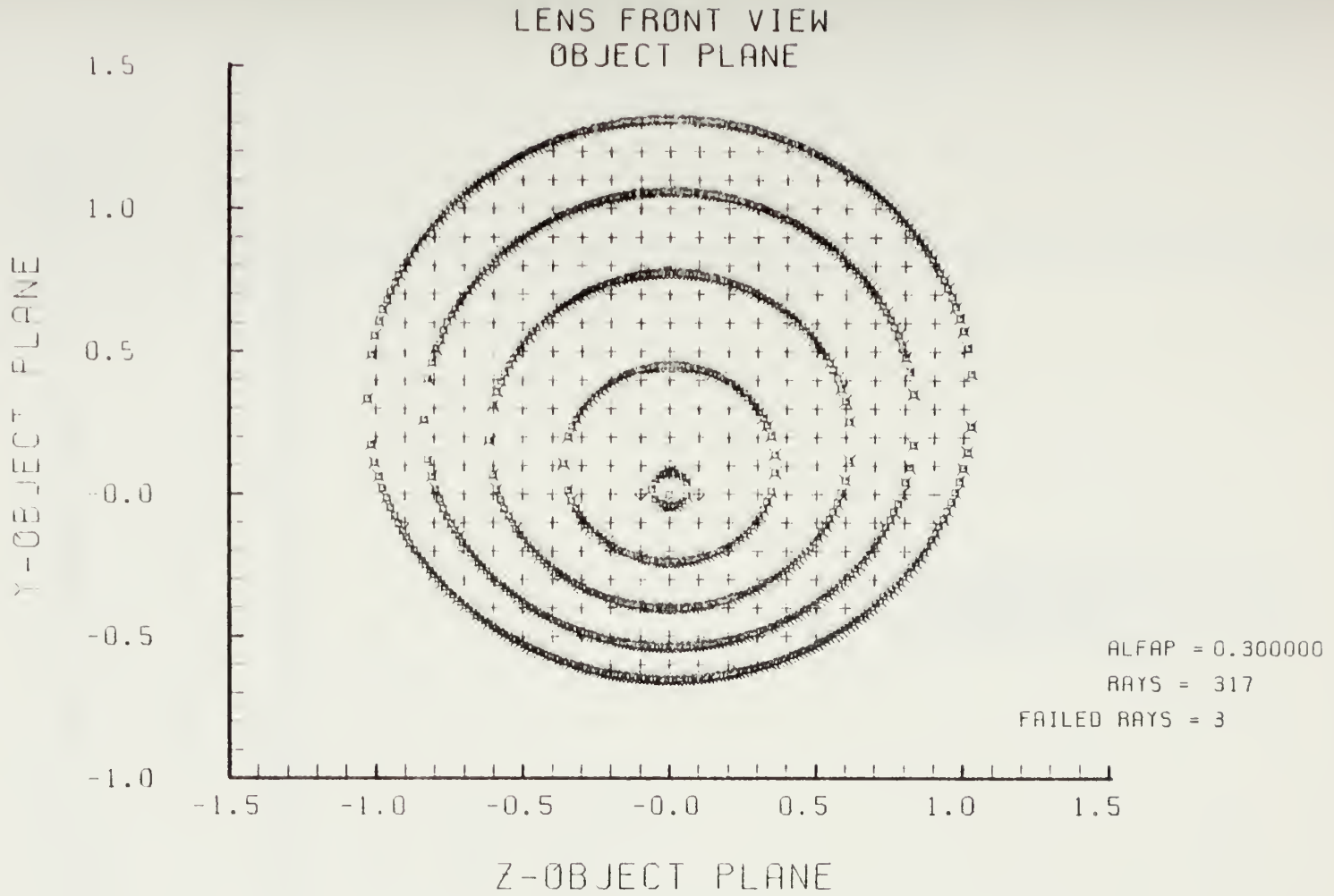

Figure F-70. Grid Plane at α_p = 0.3 for Lens of Figure F-69

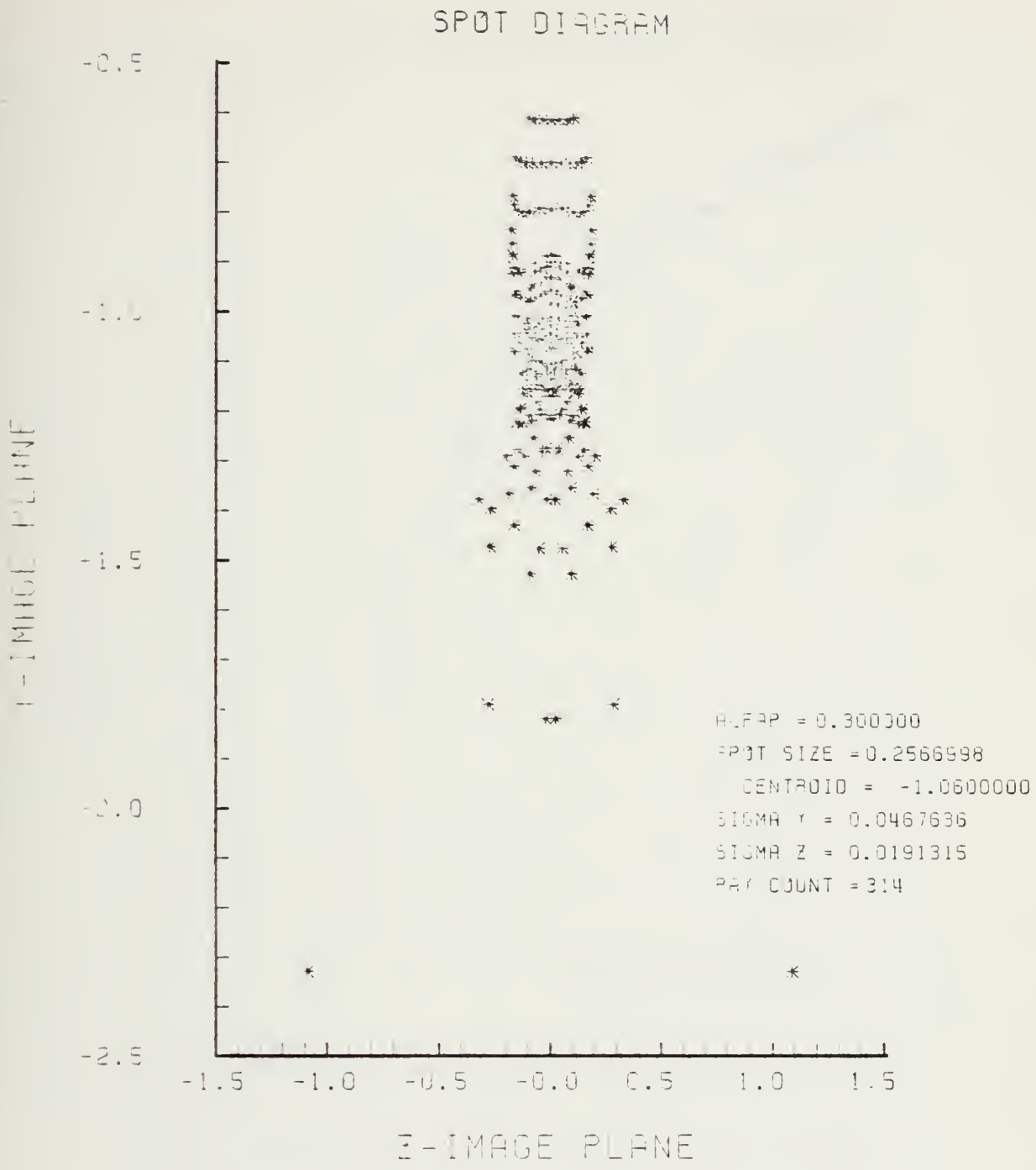

Figure F-71. Spot Diagram for Grid of Figure F-70

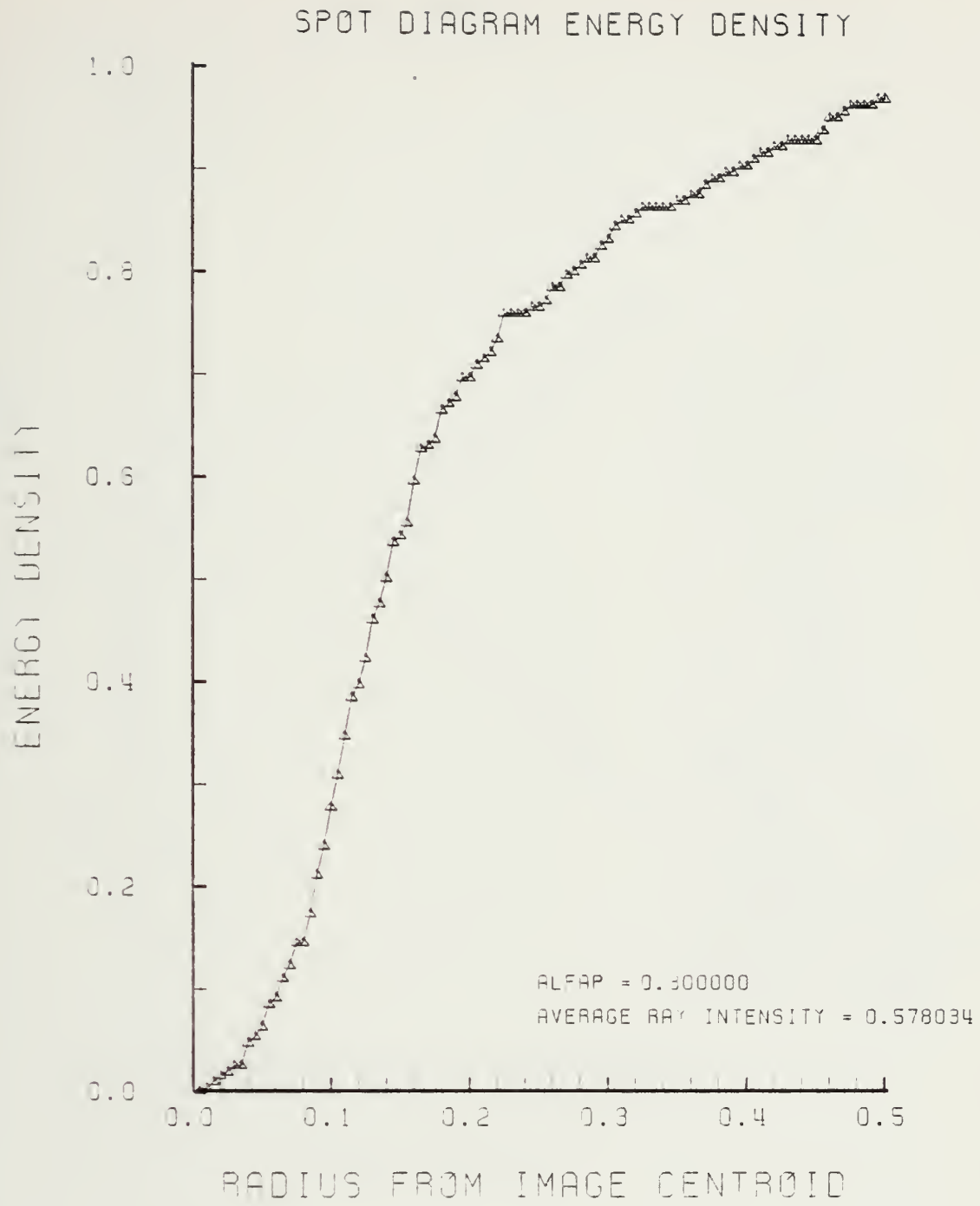

Figure F-72. Encircled Energy of Figure F-71

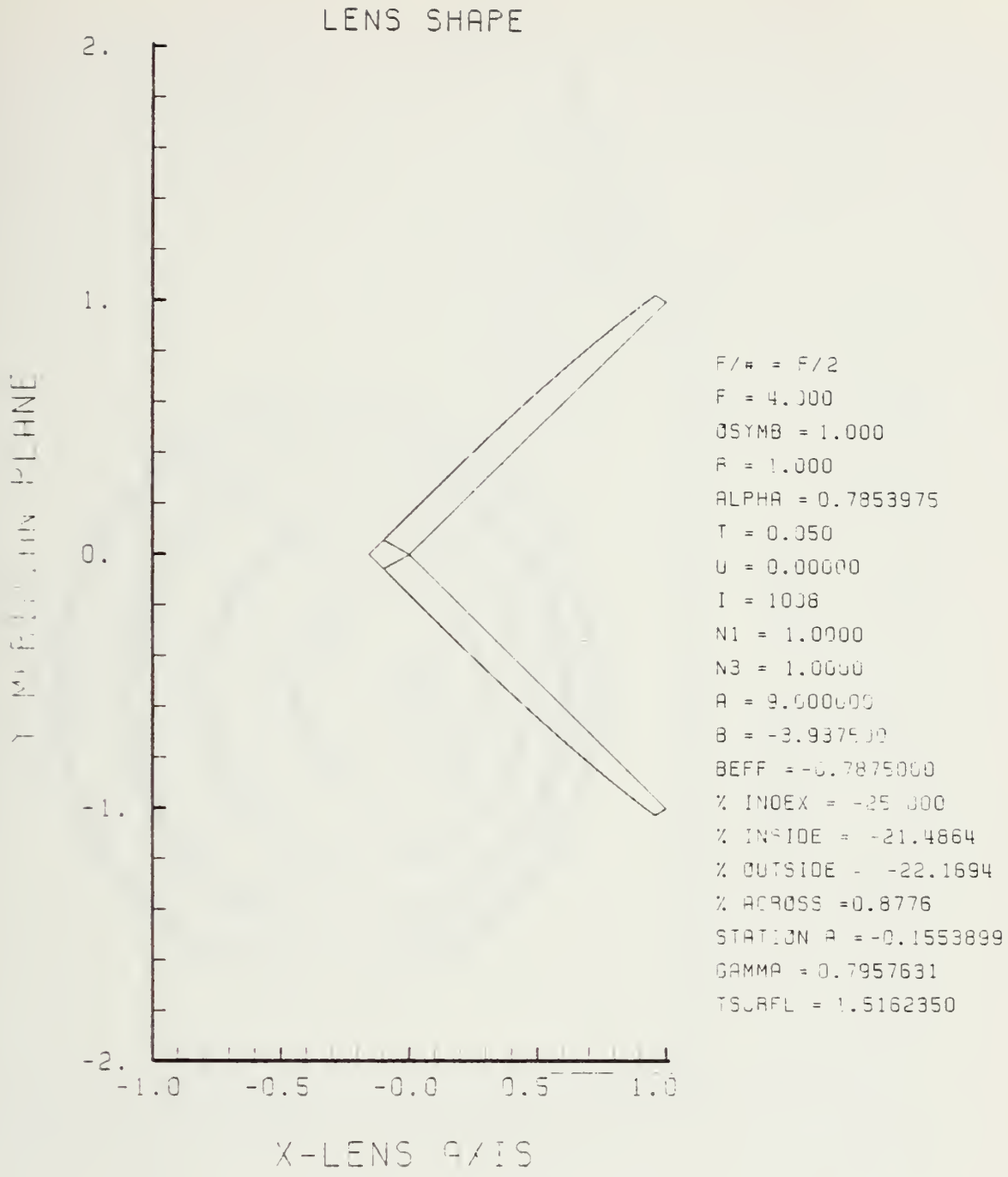

Figure F-73. GRIN Lens Shape at -25%, OB = 1.00, a = 9.00

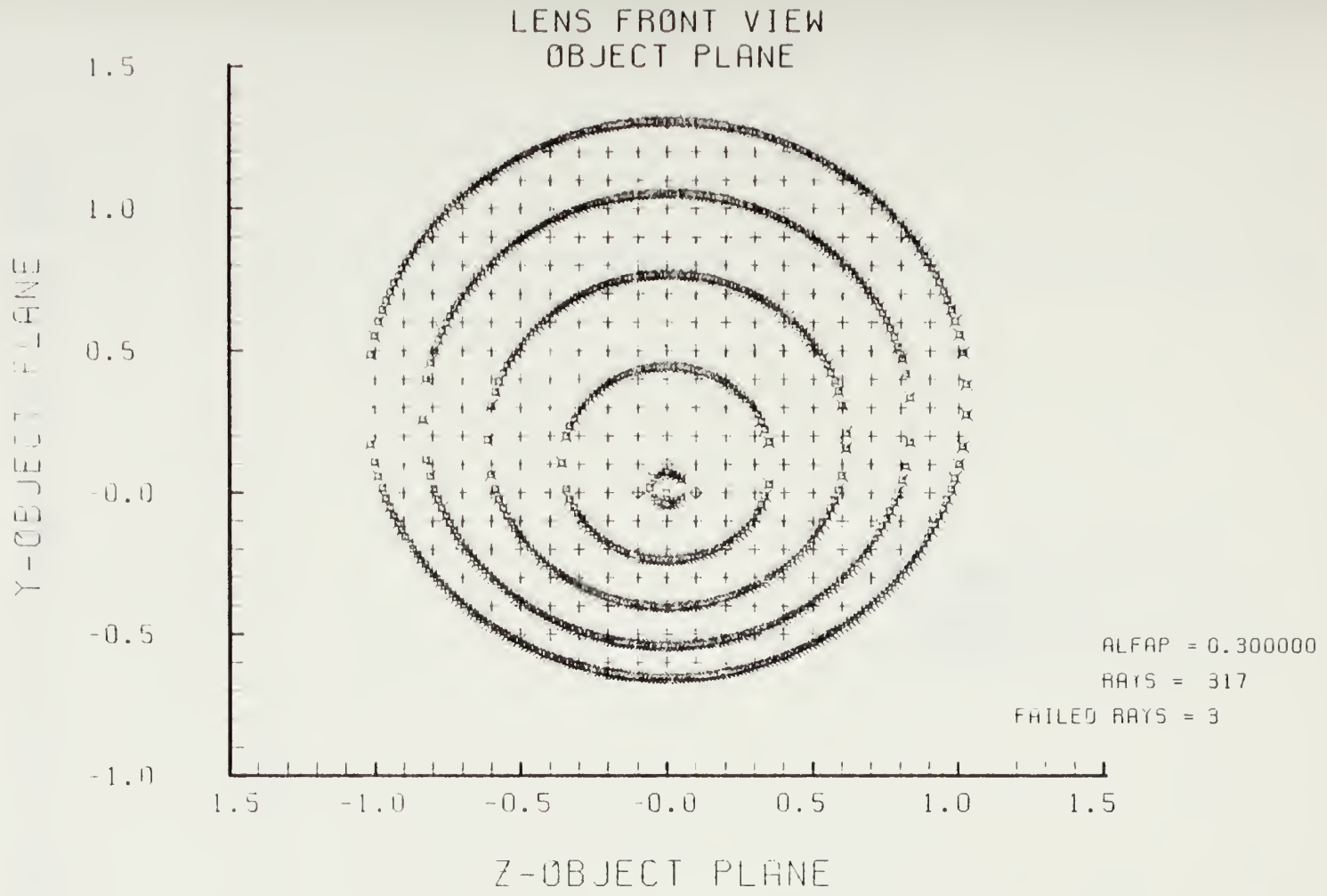

Figure F-74. Grid Plane at α_p = 0.3 for Lens of Figure F-73

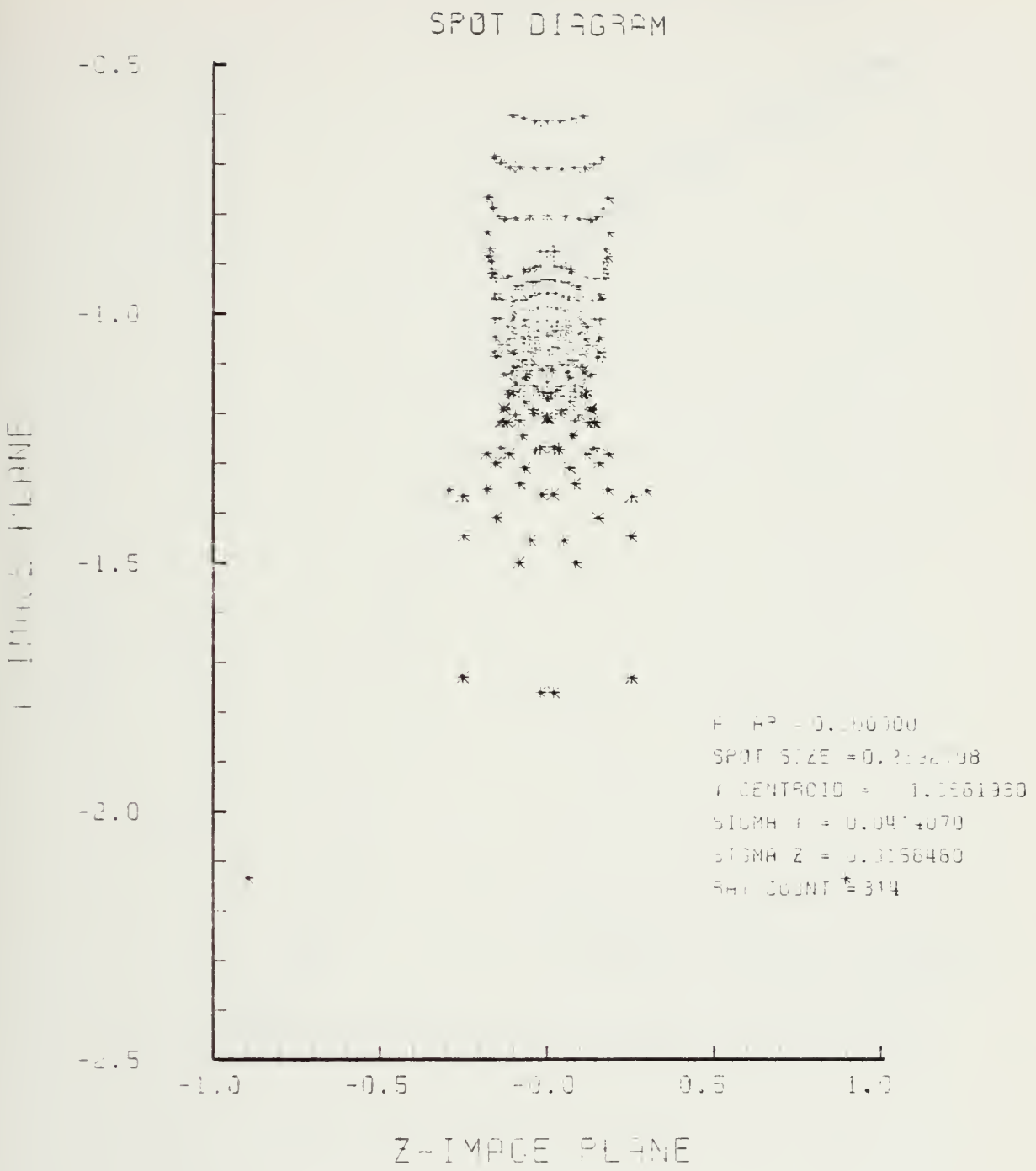

Figure F-75. Spot Diagram for Grid of Figure F-74

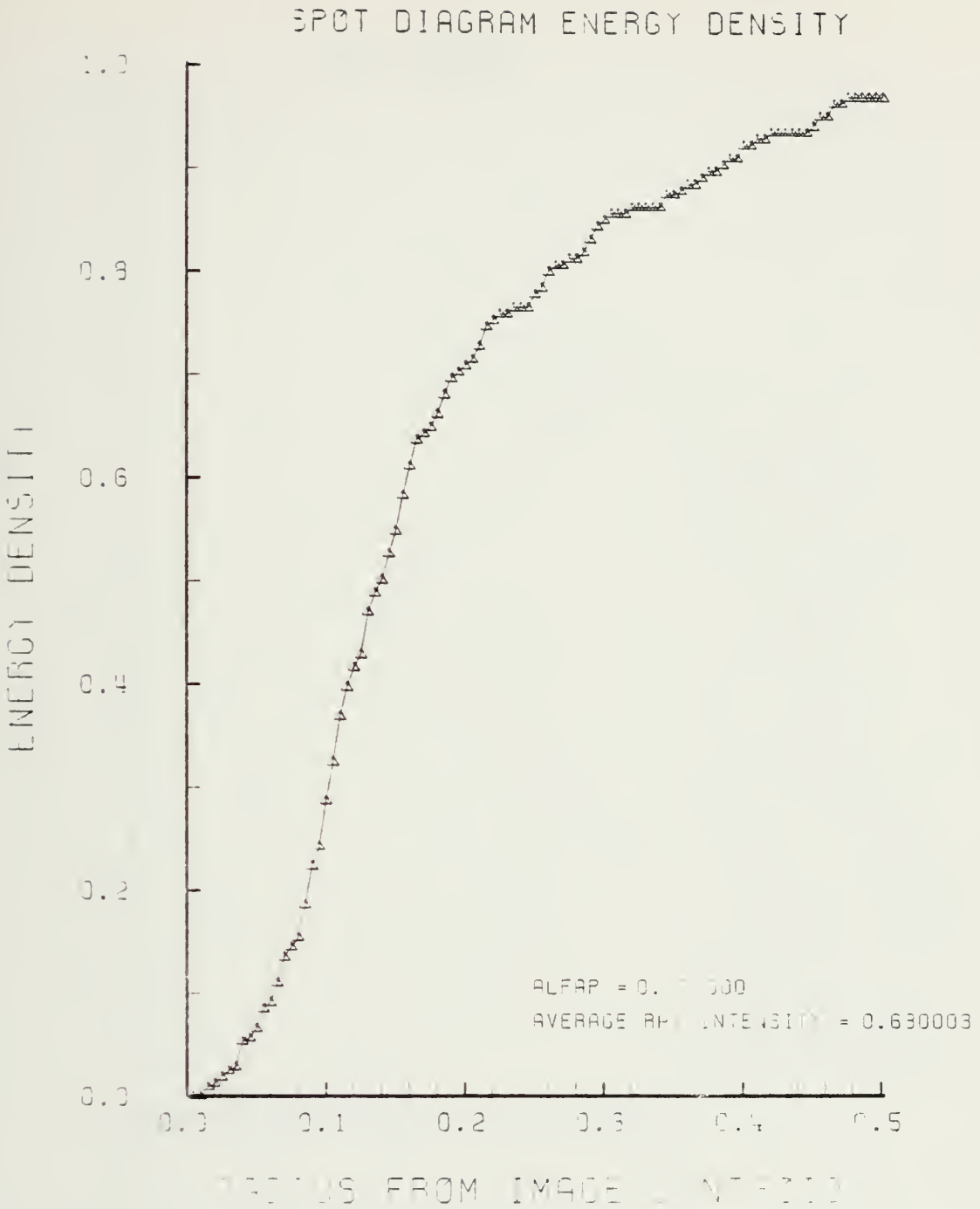

Figure F-76. Encircled Energy of Figure F-75

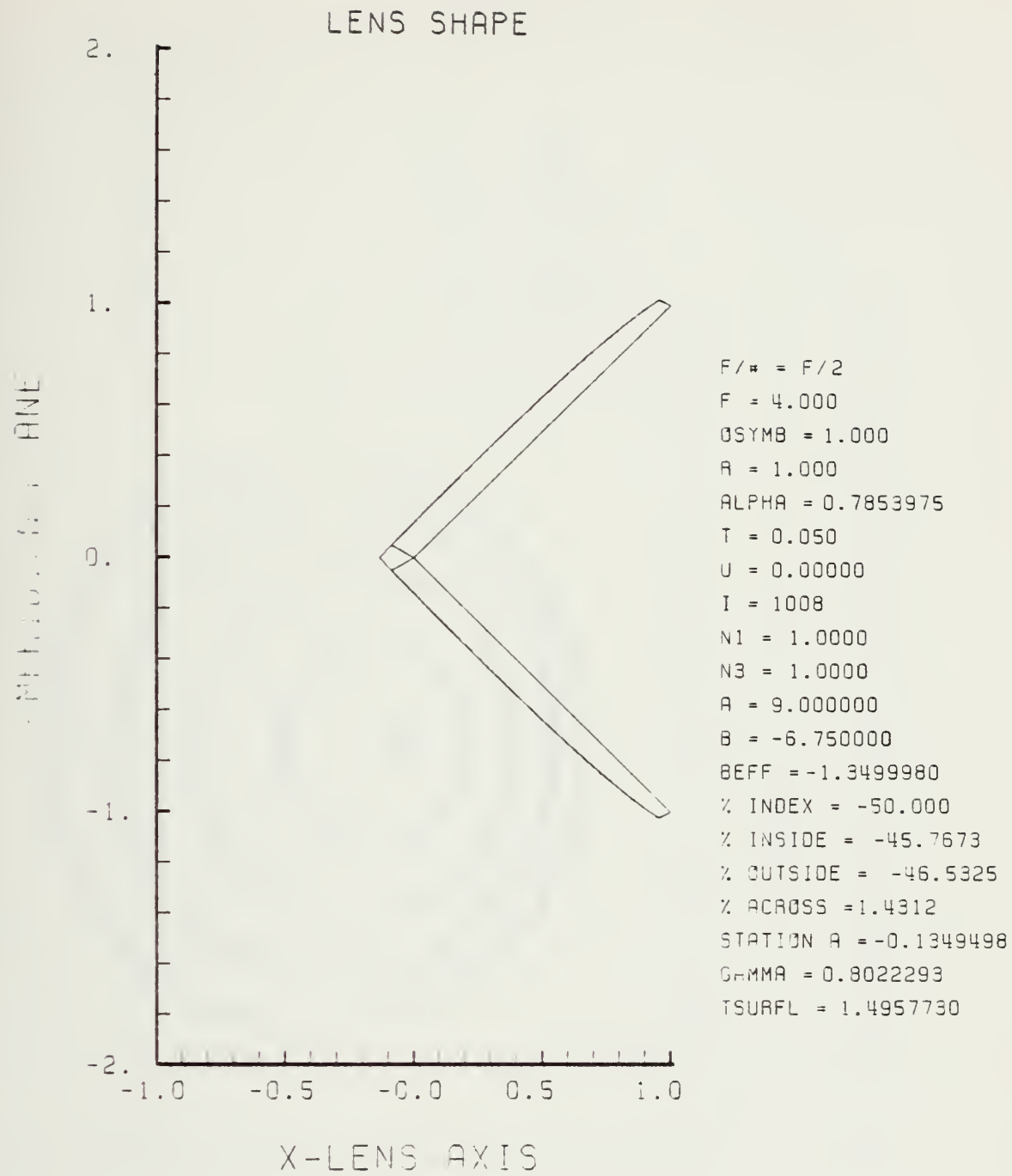

Figure F-77. GRIN Lens Shape at -50%, OB = 1.00, a = 9.00

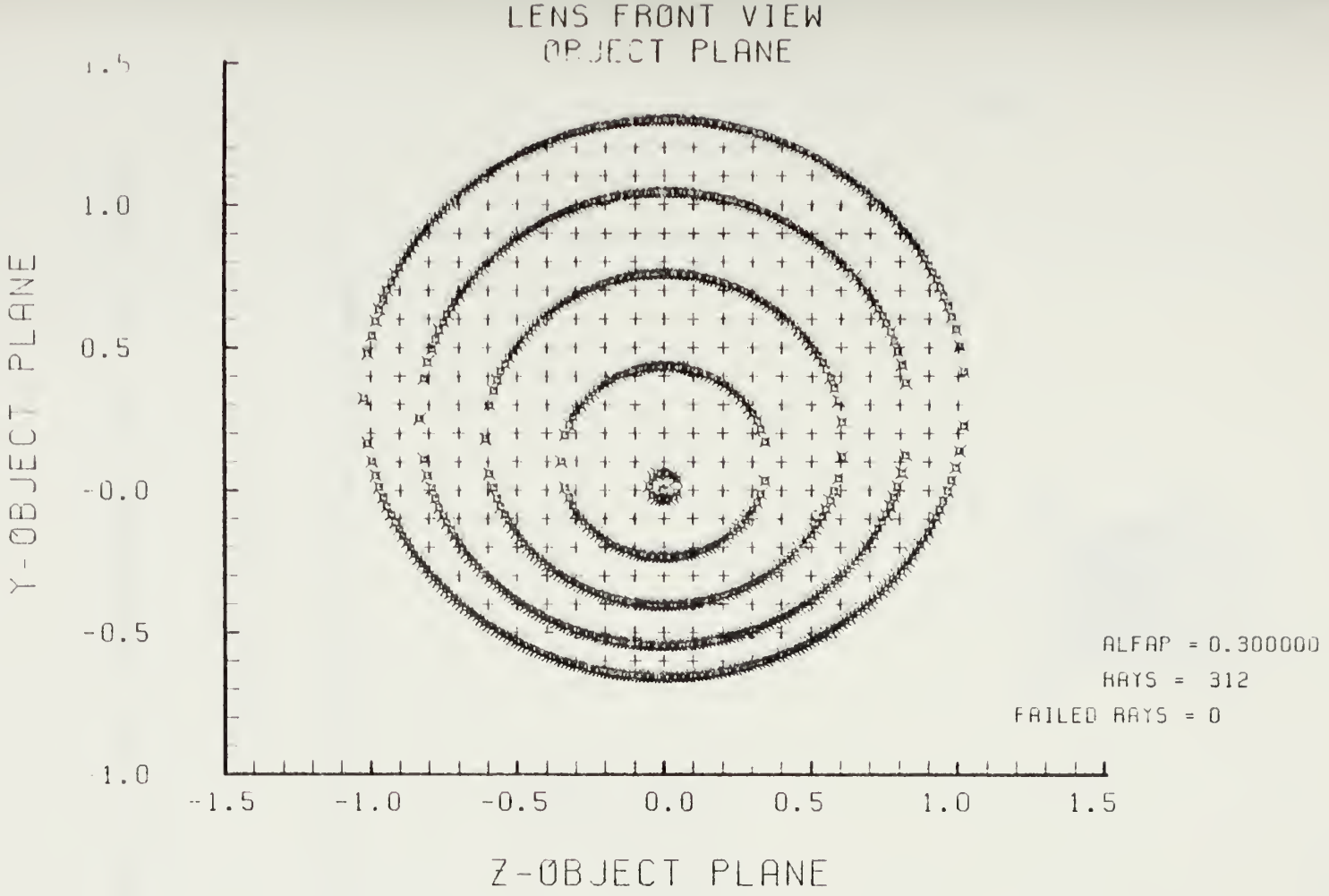

Figure F-78. Grid Plane at α_p = 0.3 for Lens of Figure F-77

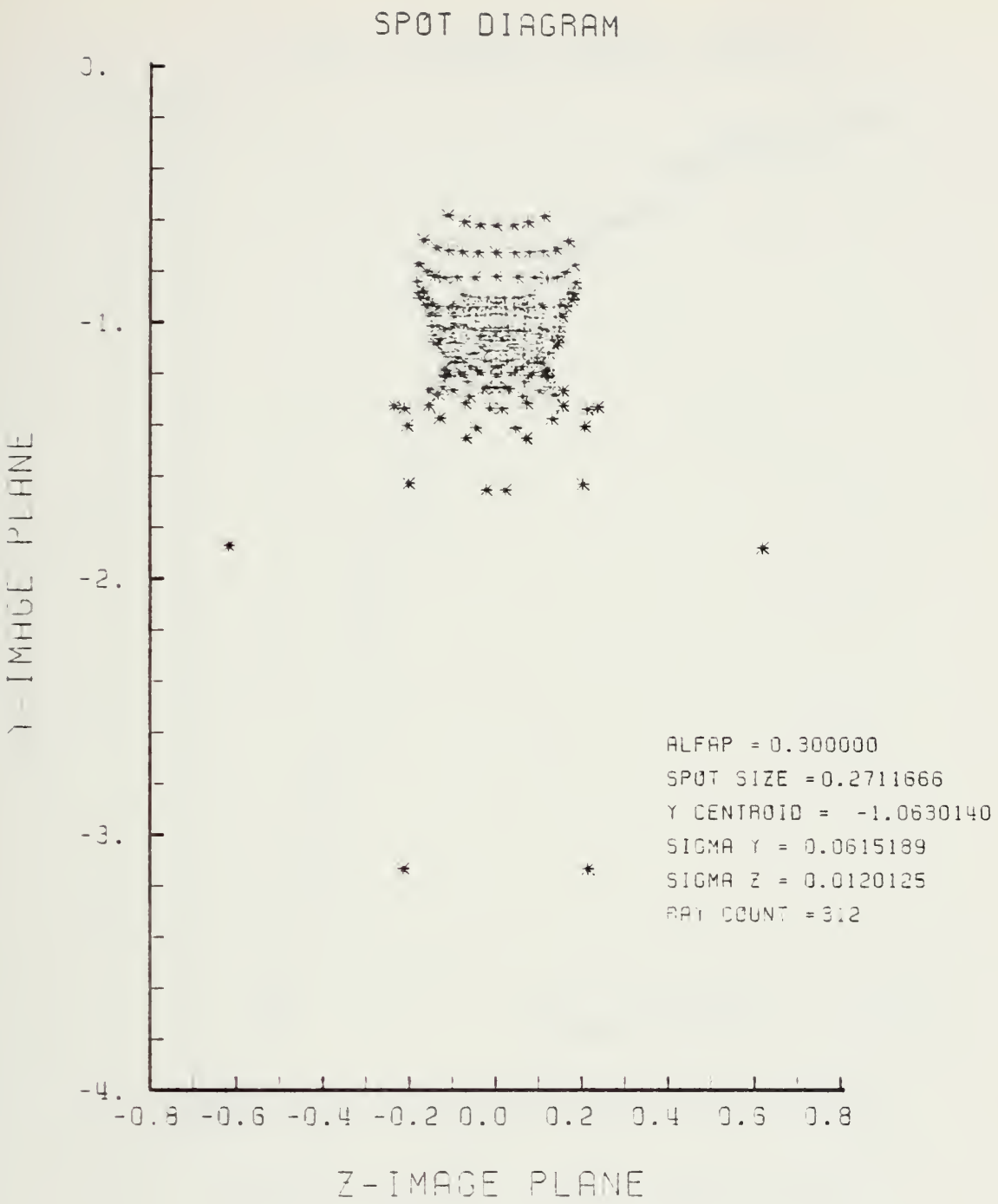

Figure F-79. Spot Diagram for Grid of Figure F-78

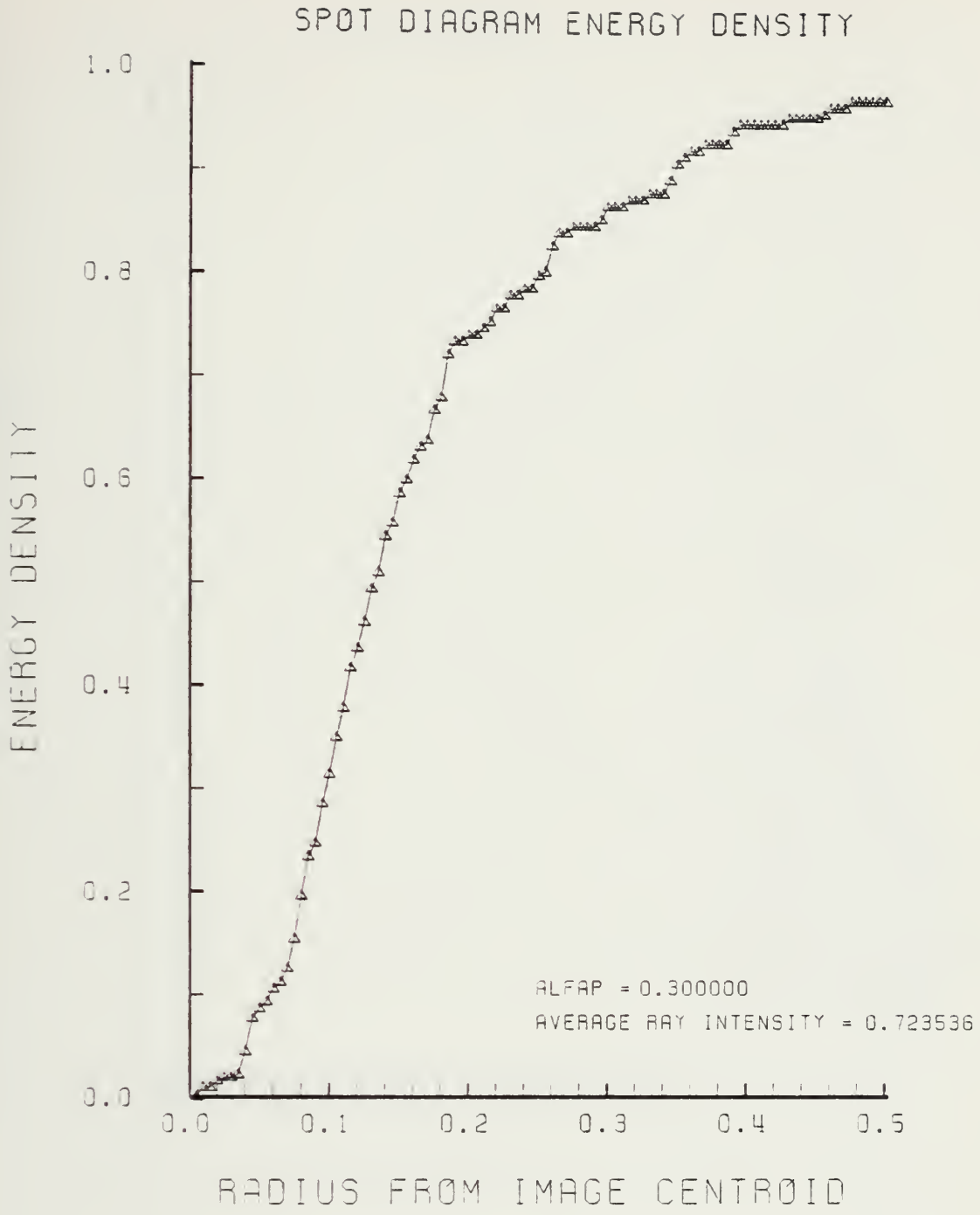

Figure F-80. Encircled Energy of Figure F-79

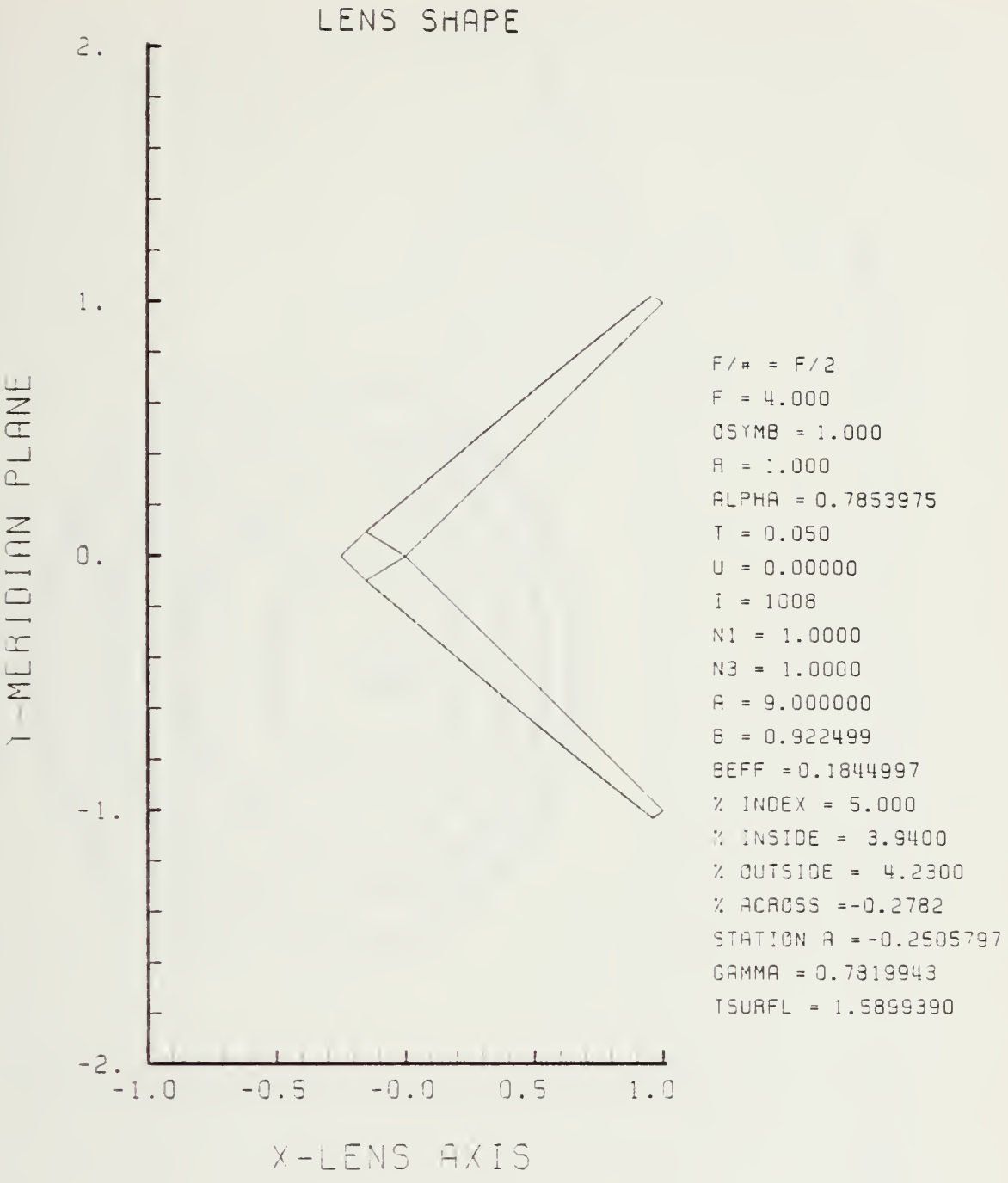

Figure F-81. GRIN Lens Shape at +5%, OB = 1.00, a = 9.00

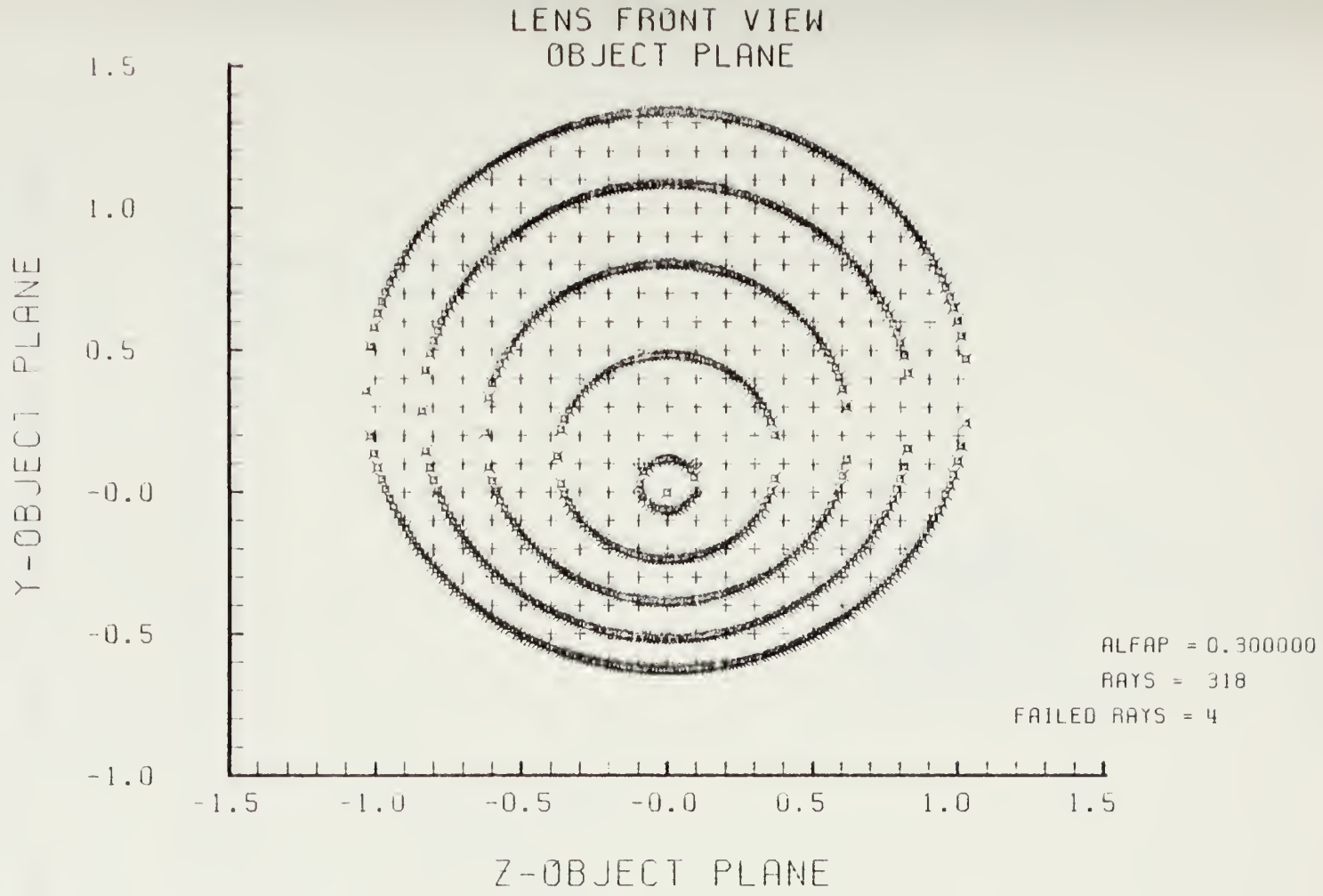

Figure F-82. Grid Plane at α_p = 0.3 for Lens of Figure F-81

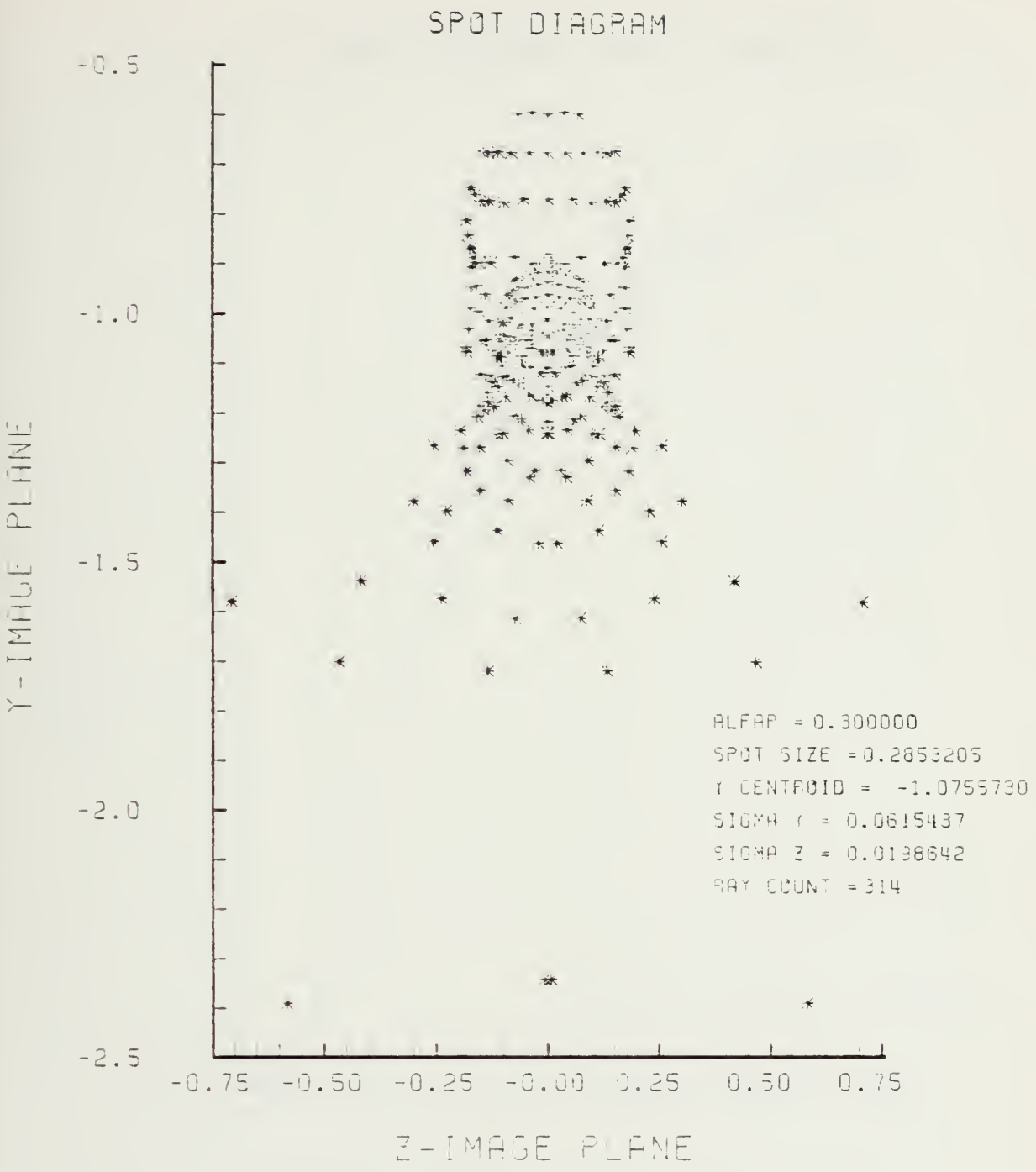

Figure F-83. Spot Diagram for Grid of Figure F-82

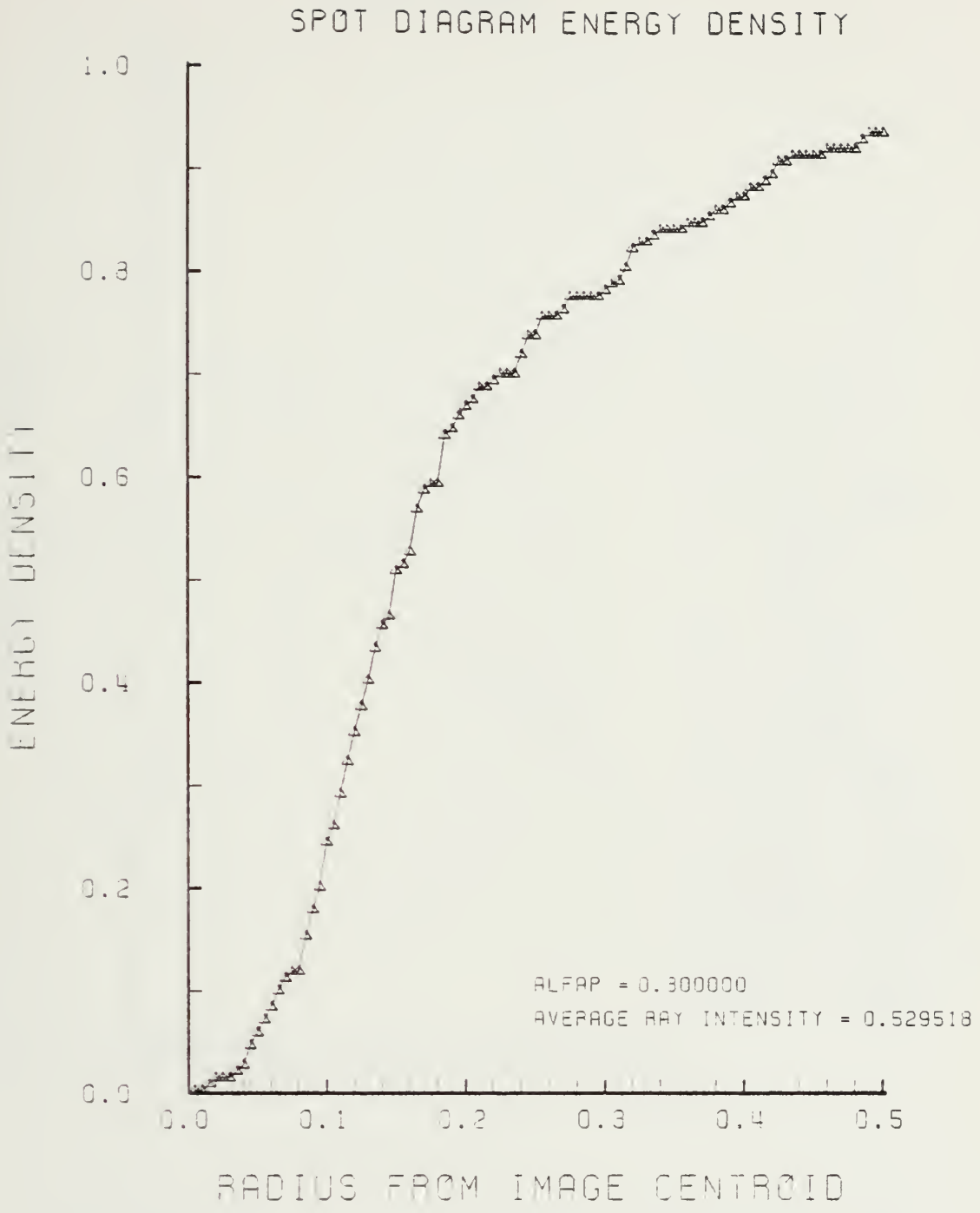

Figure F-84. Encircled Energy of Figure F-83

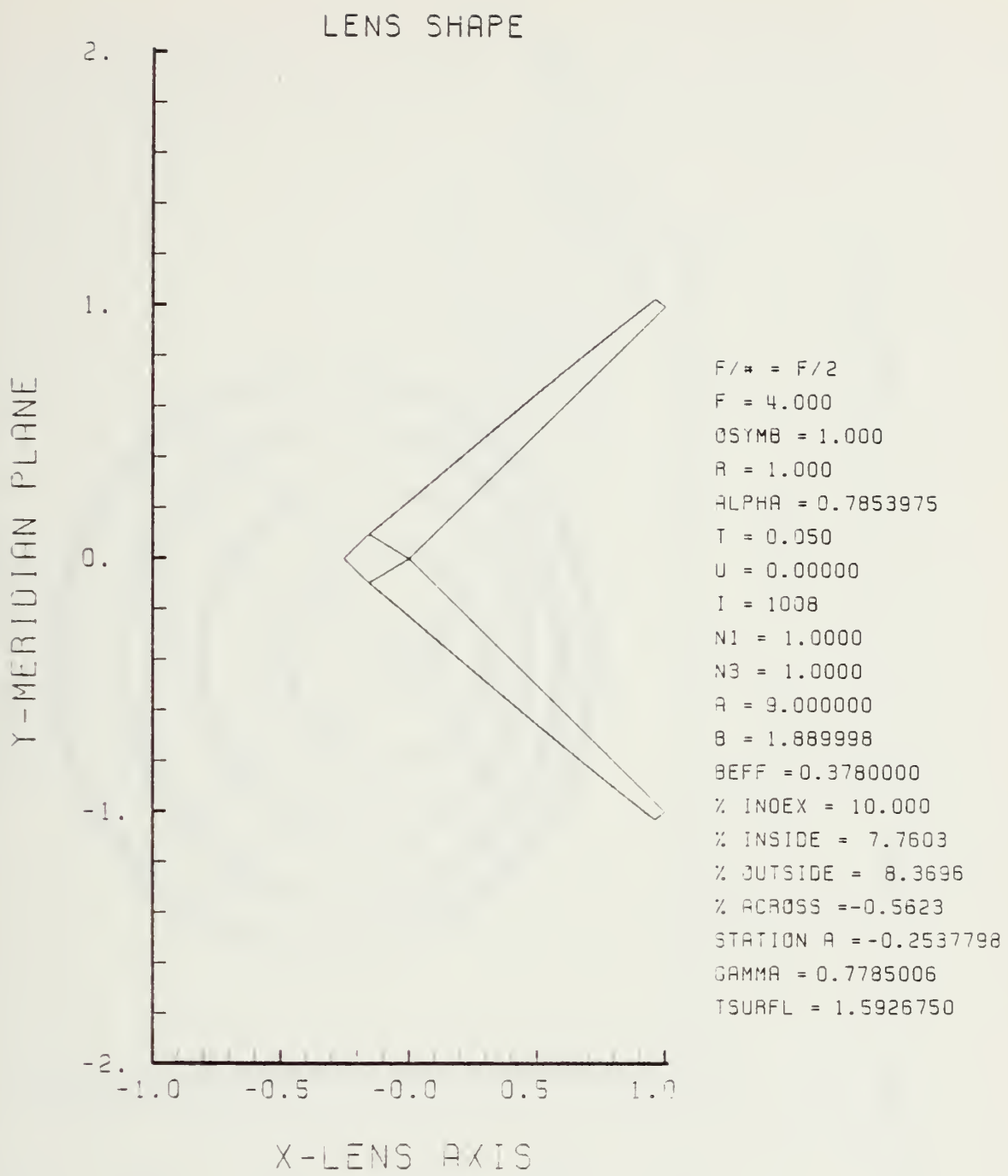

Figure F-85. GRIN Lens Shape at +10%, OB = 1.00, a = 9.00

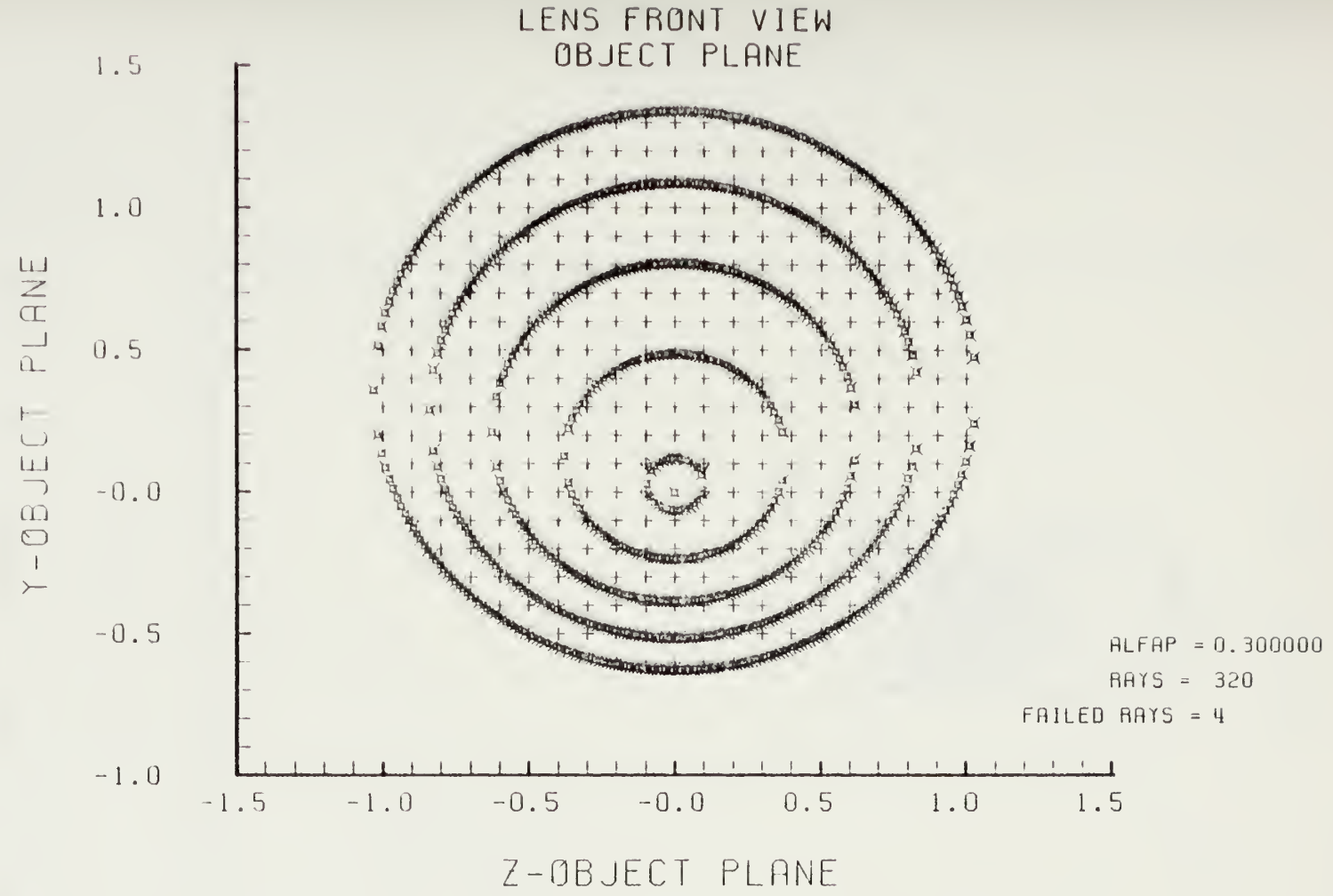

Figure F-86. Grid Plane at $\alpha_p = 0.3$ for Lens of Figure F-85

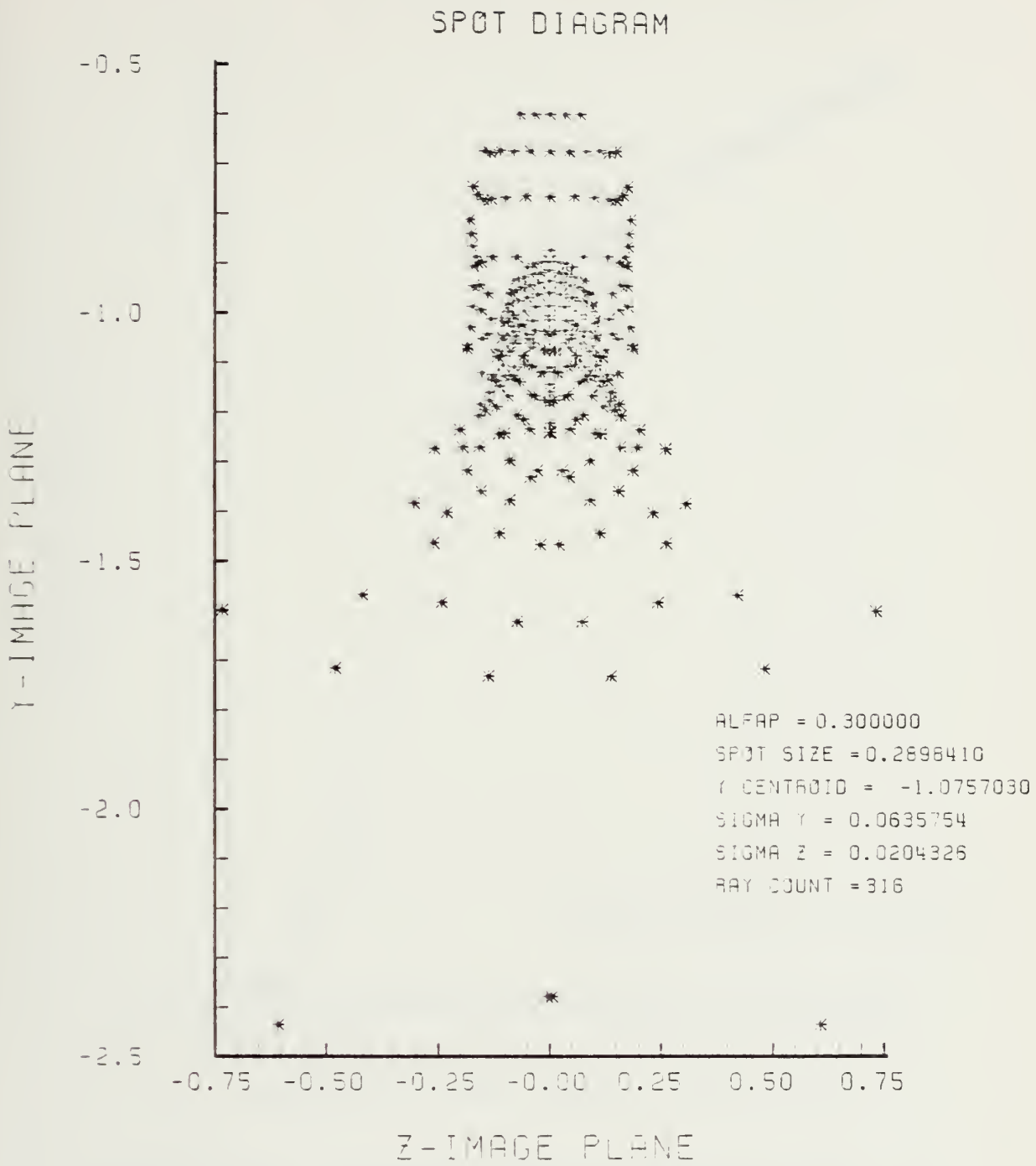

Figure F-87. Spot Diagram for Grid of Figure F-86

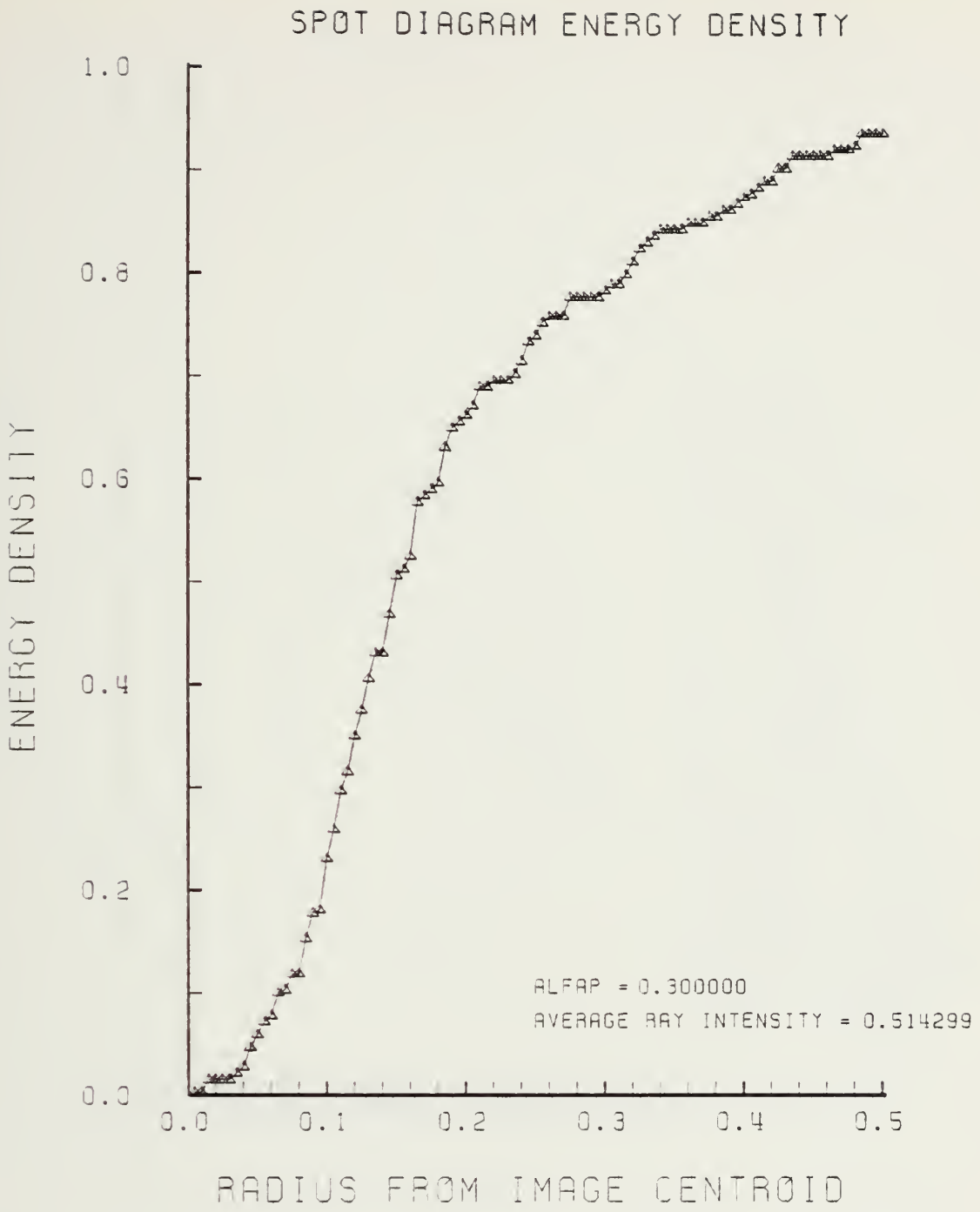

Figure F-88. Encircled Energy of Figure F-87

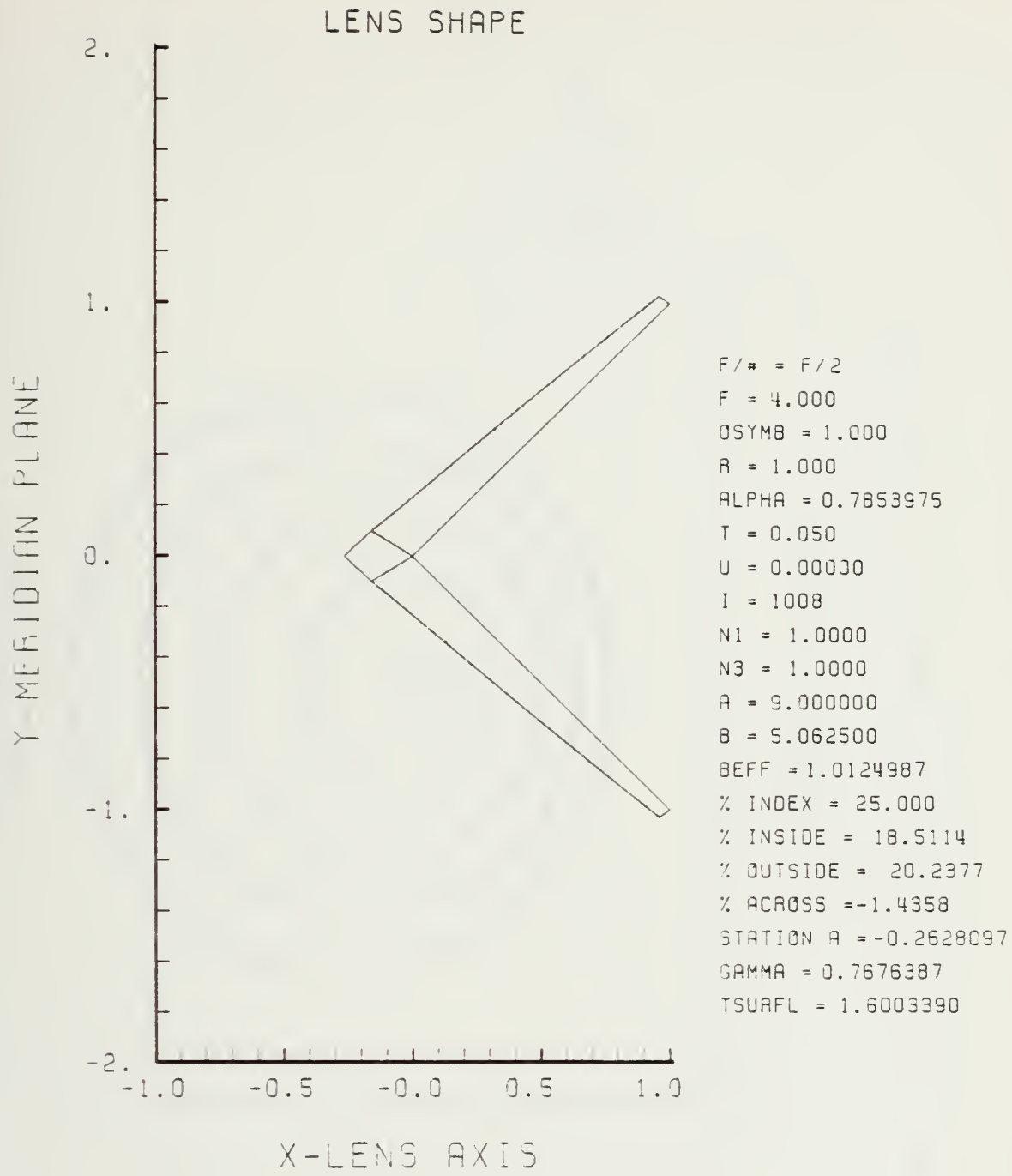

Figure F-89. GRIN Lens Shape at +25%, OB = 1.00, a = 9.00

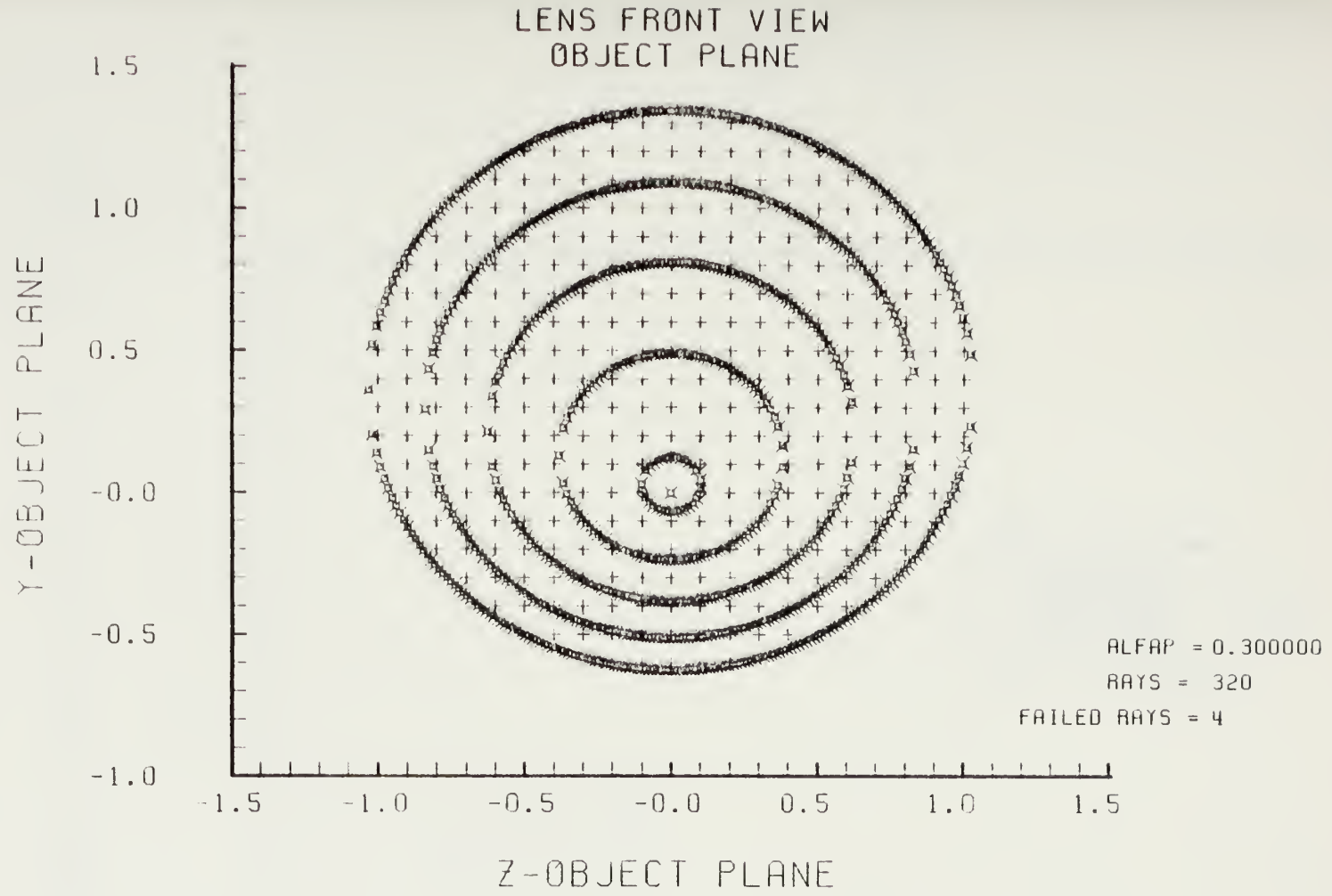

Figure F-90. Grid Plane at α_p = 0.3 for Lens of Figure F-89

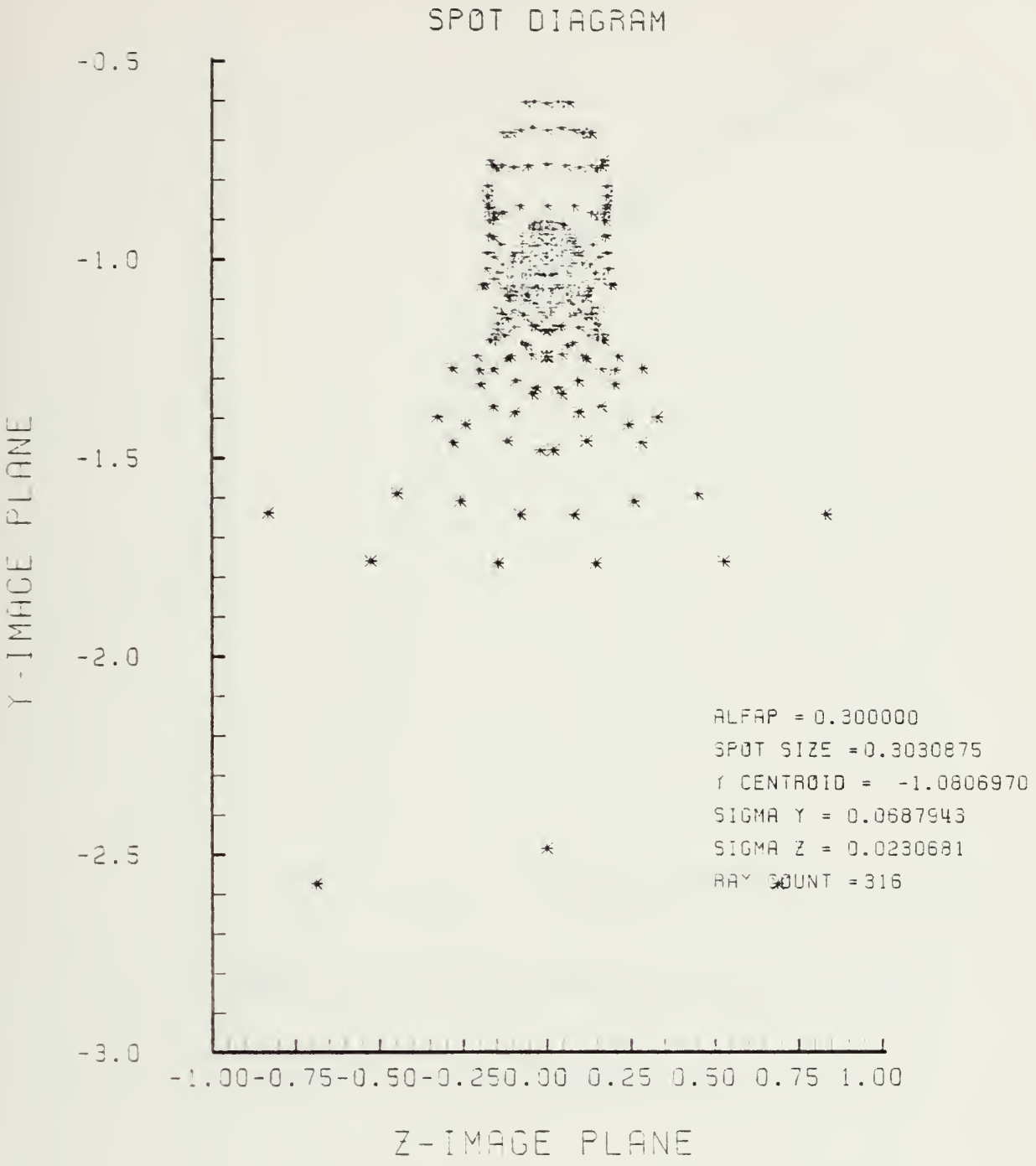

Figure F-91. Spot Diagram for Grid of Figure F-90

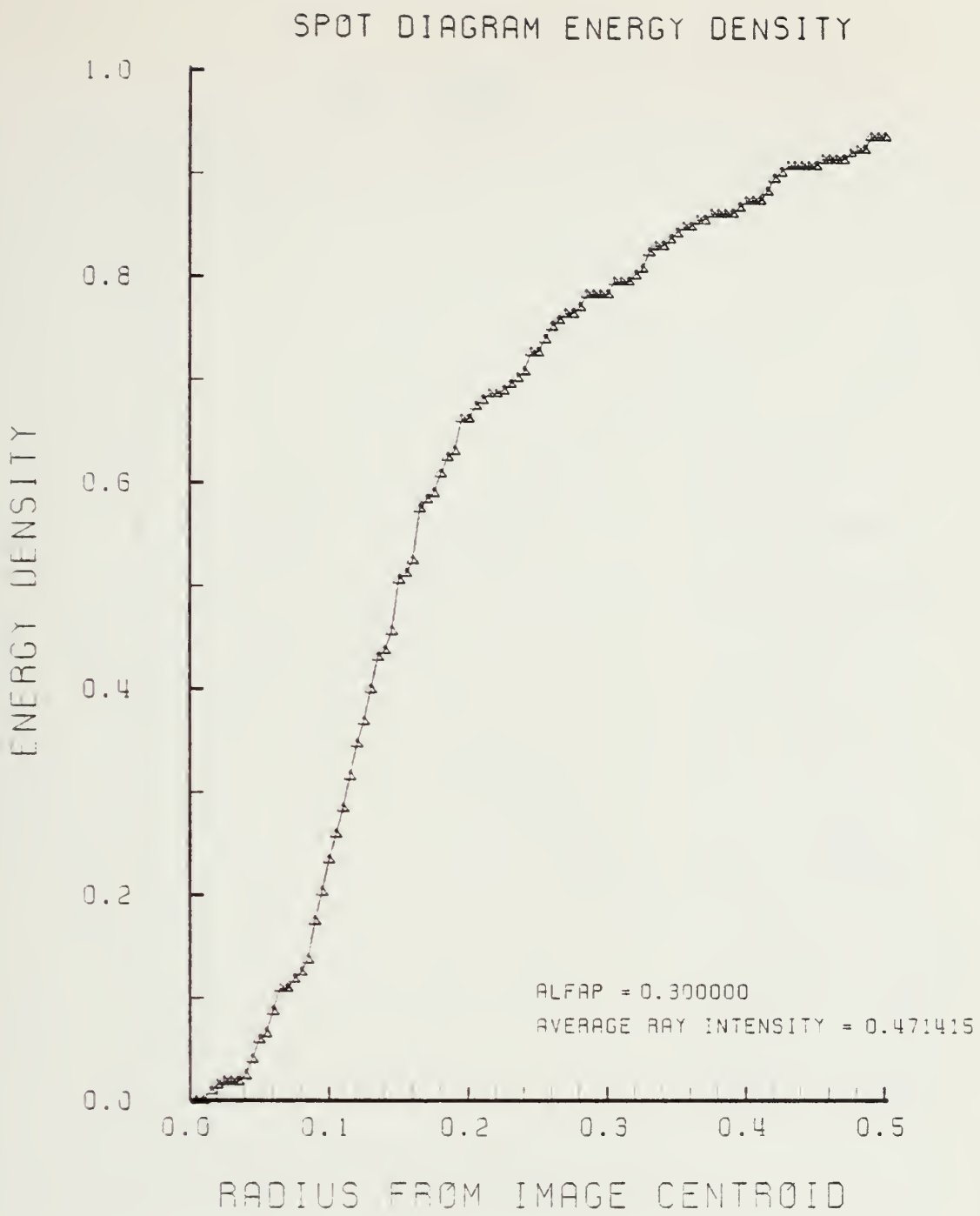

Figure F-92. Encircled Energy of Figure F-91

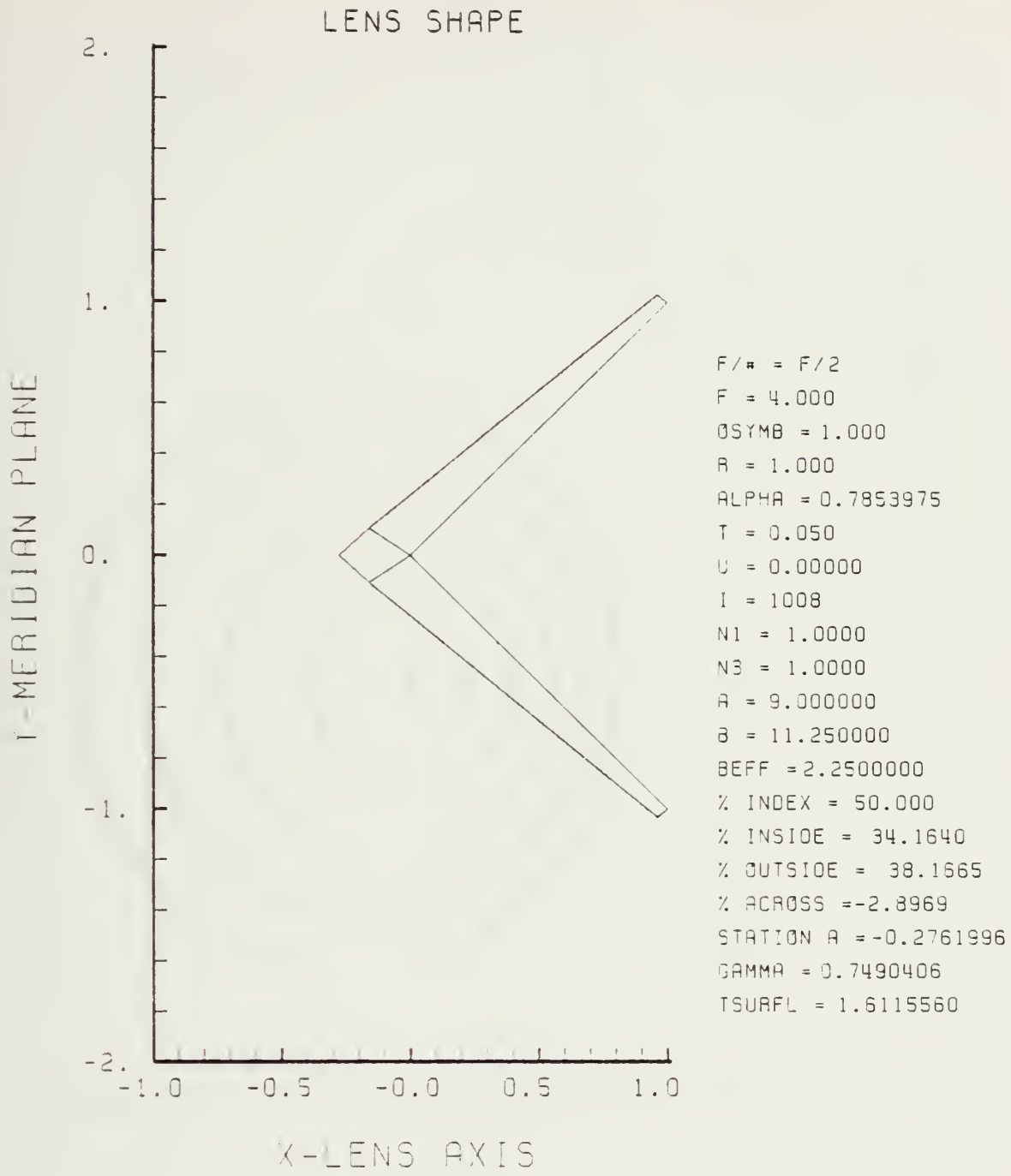

Figure F-93. GRIN Lens Shape at +50%, OB = 1.00, a = 9.00

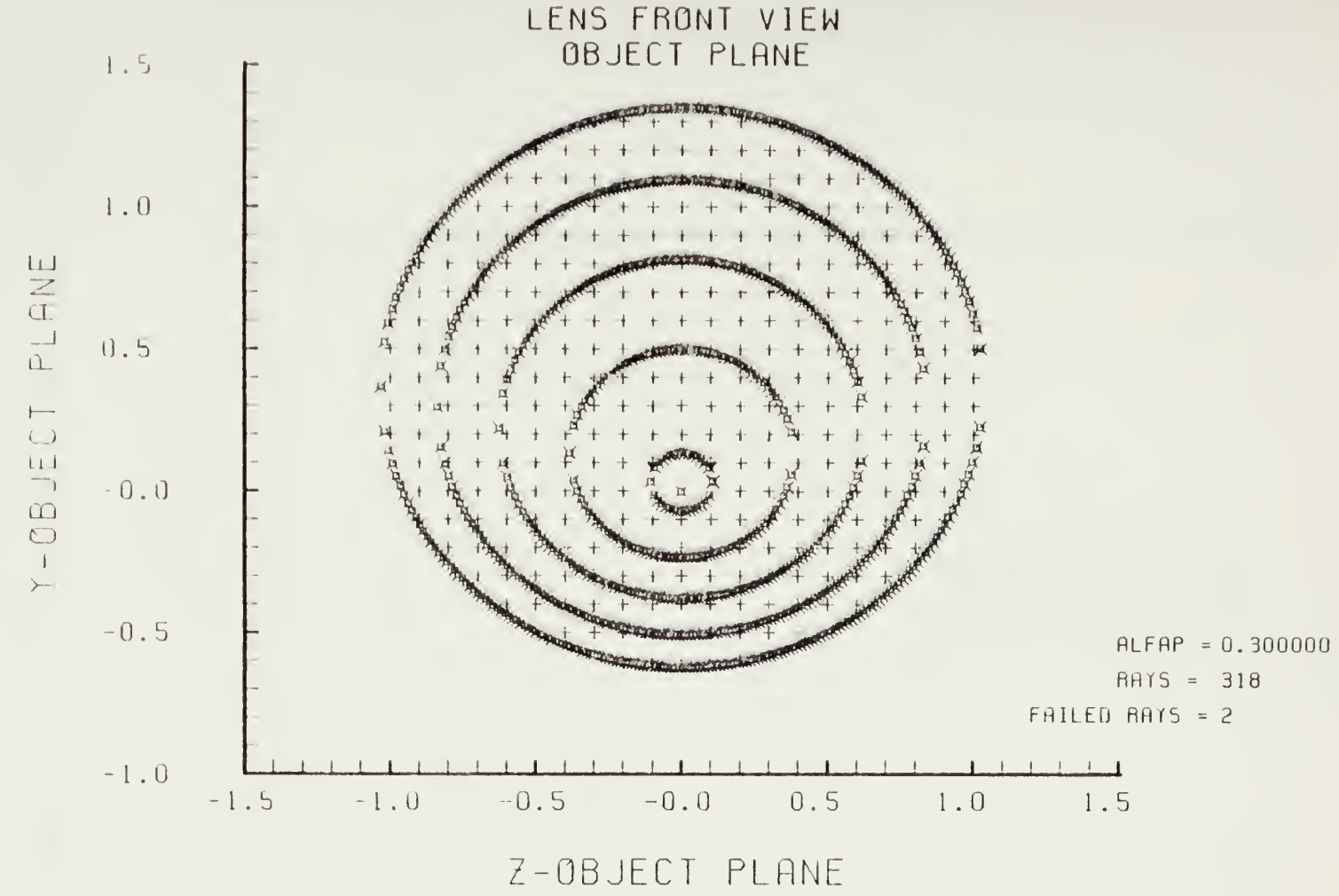

Figure F-94. Grid Plane at $\alpha_p = 0.3$ for Lens of Figure F-93

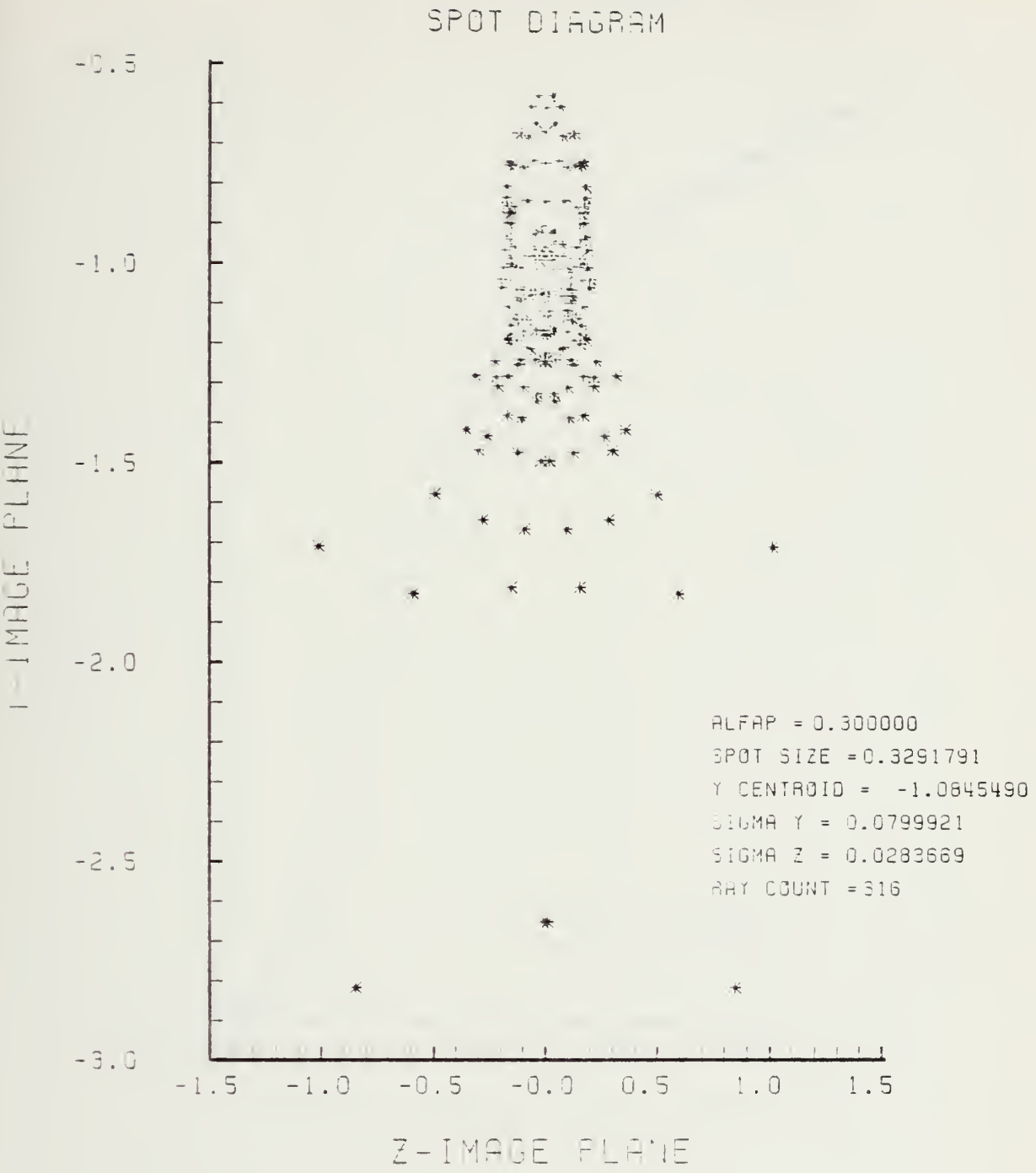

Figure F-95. Spot Diagram for Grid of Figure F-94

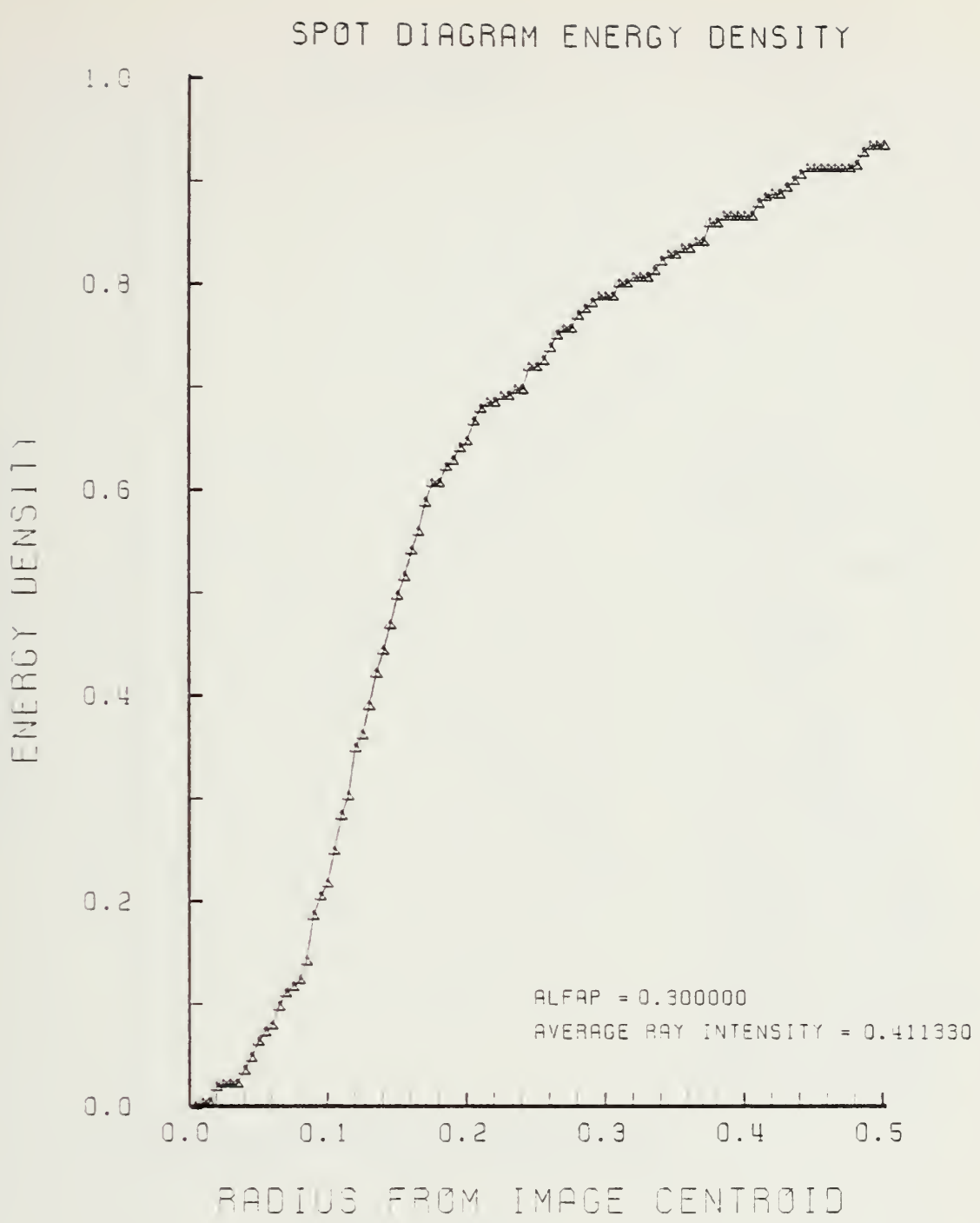

Figure F-96. Encircled Energy of Figure F-95

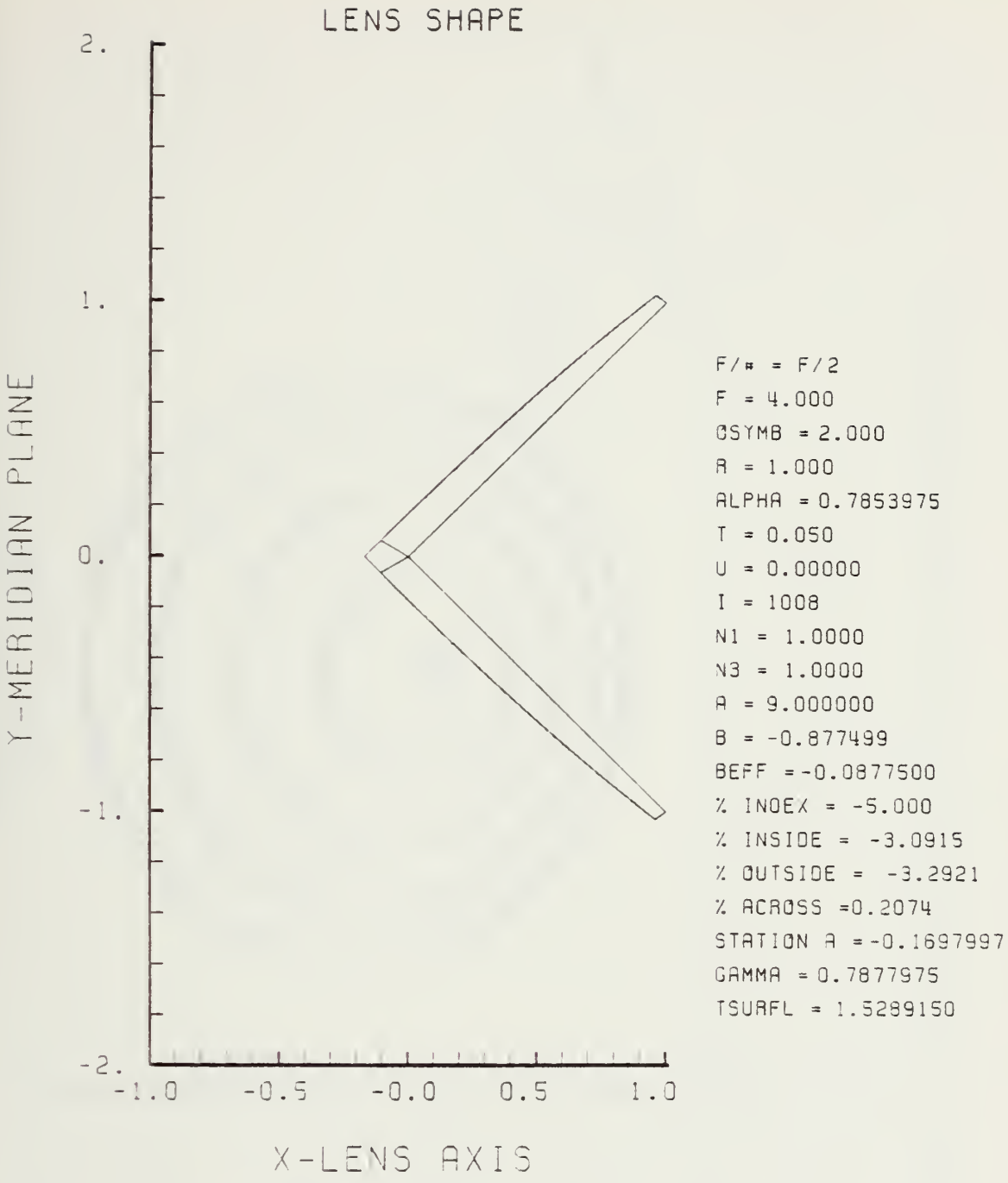

Figure F-97. GRIN Lens Shape at -5%, OB = 2.00, a = 9.00

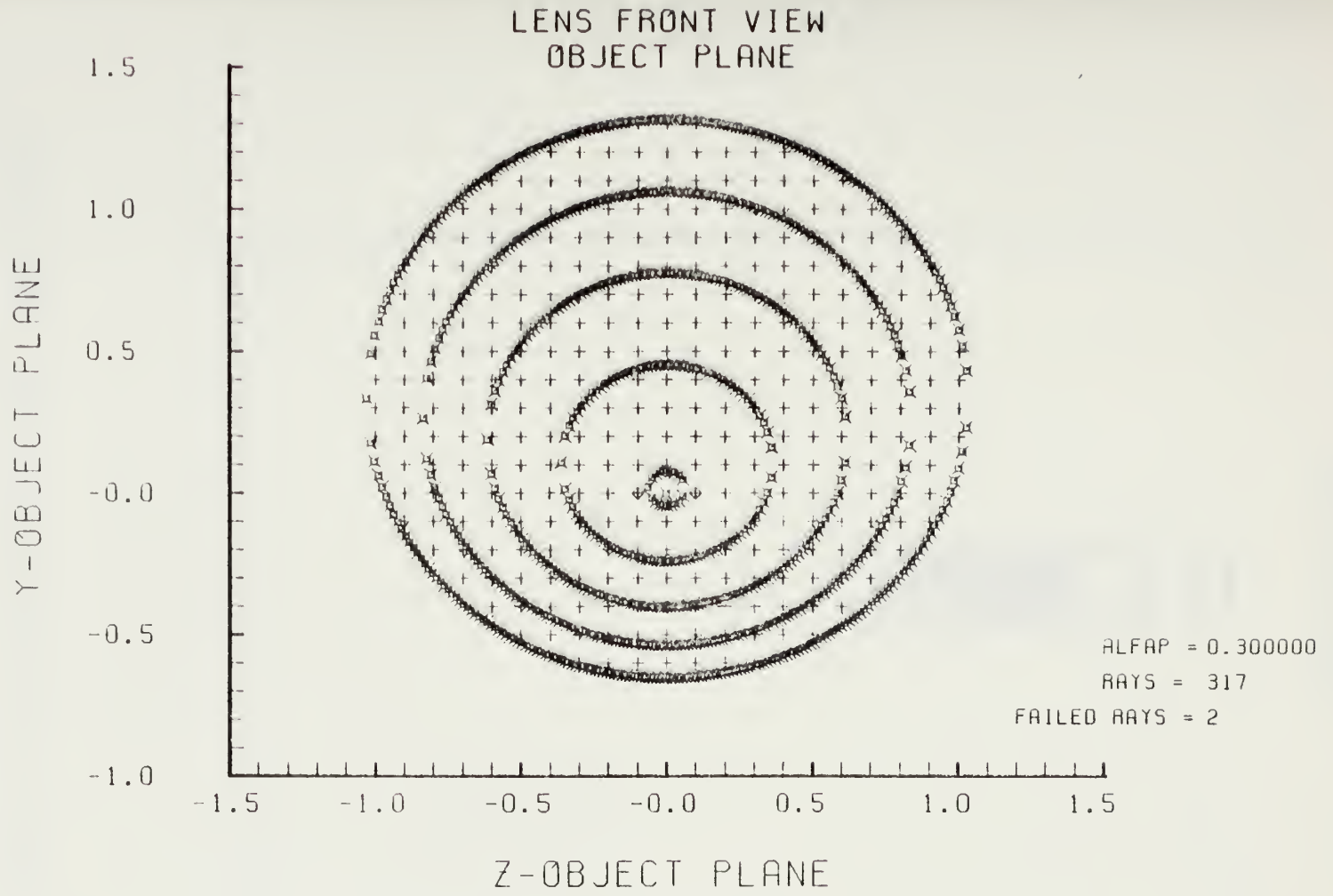

Figure F-98. Grid Plane at α_p = 0.3 for Lens of Figure F-97

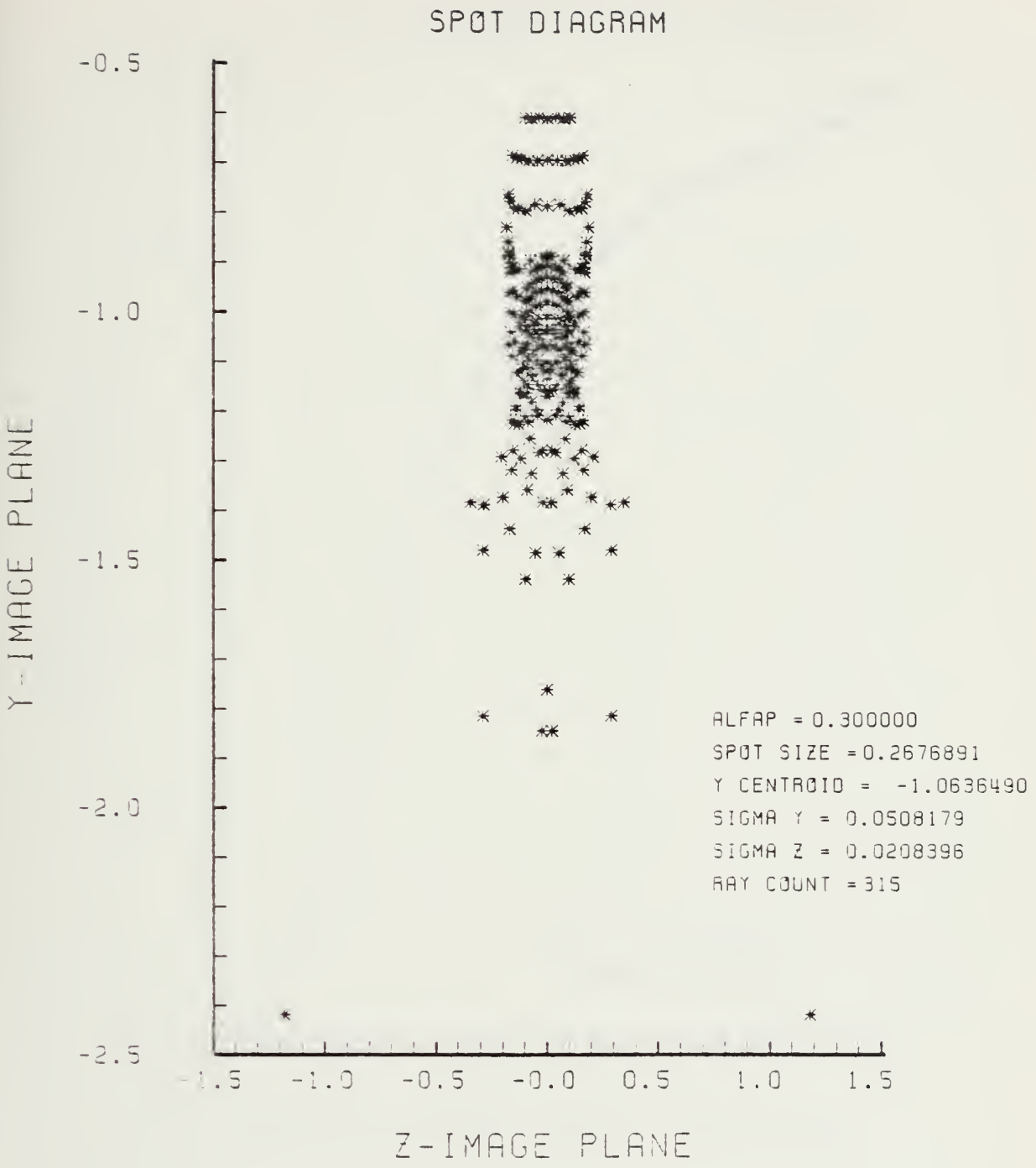

Figure F-99. Spot Diagram for Grid of Figure F-98

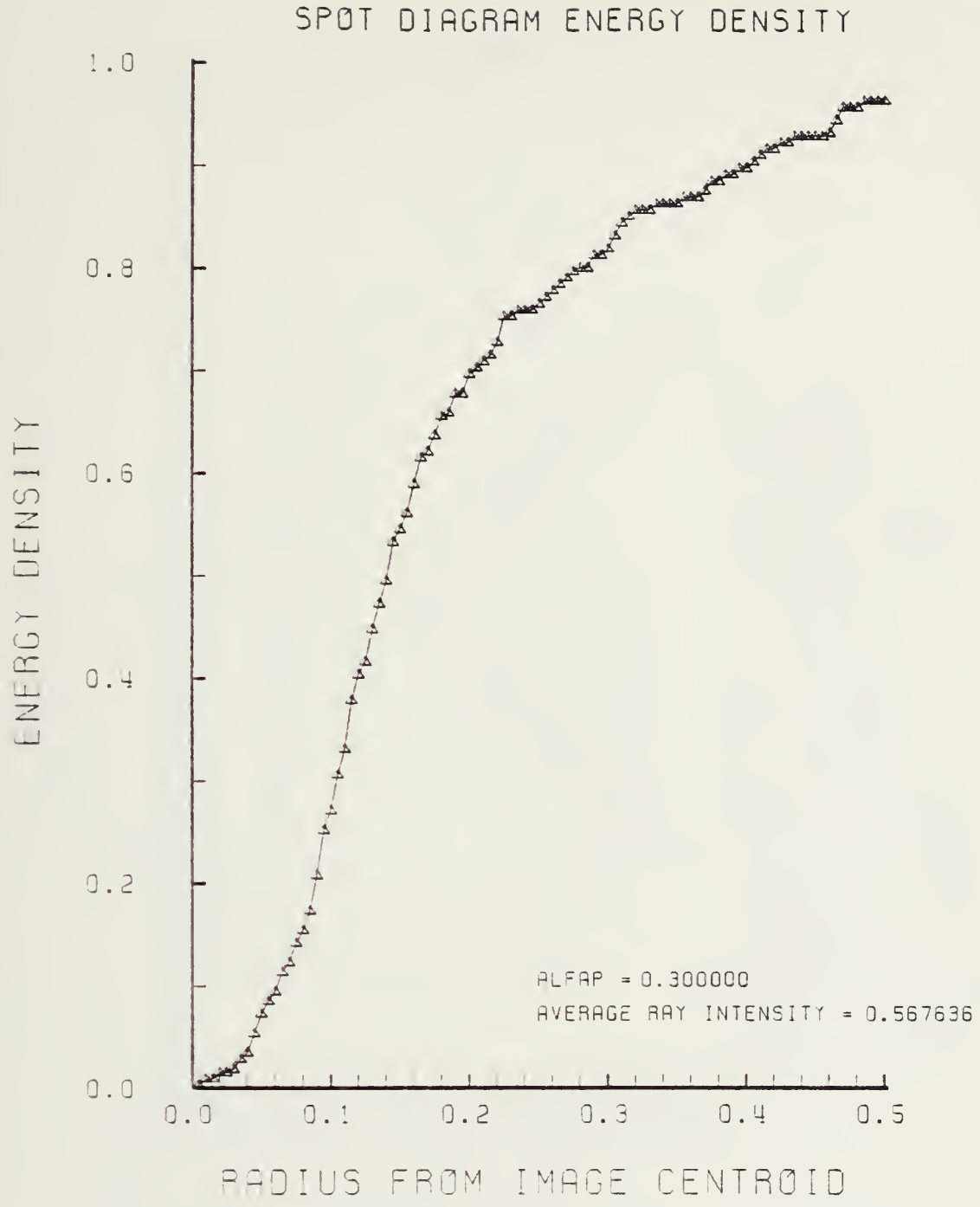

Figure F-100. Encircled Energy of Figure F-99

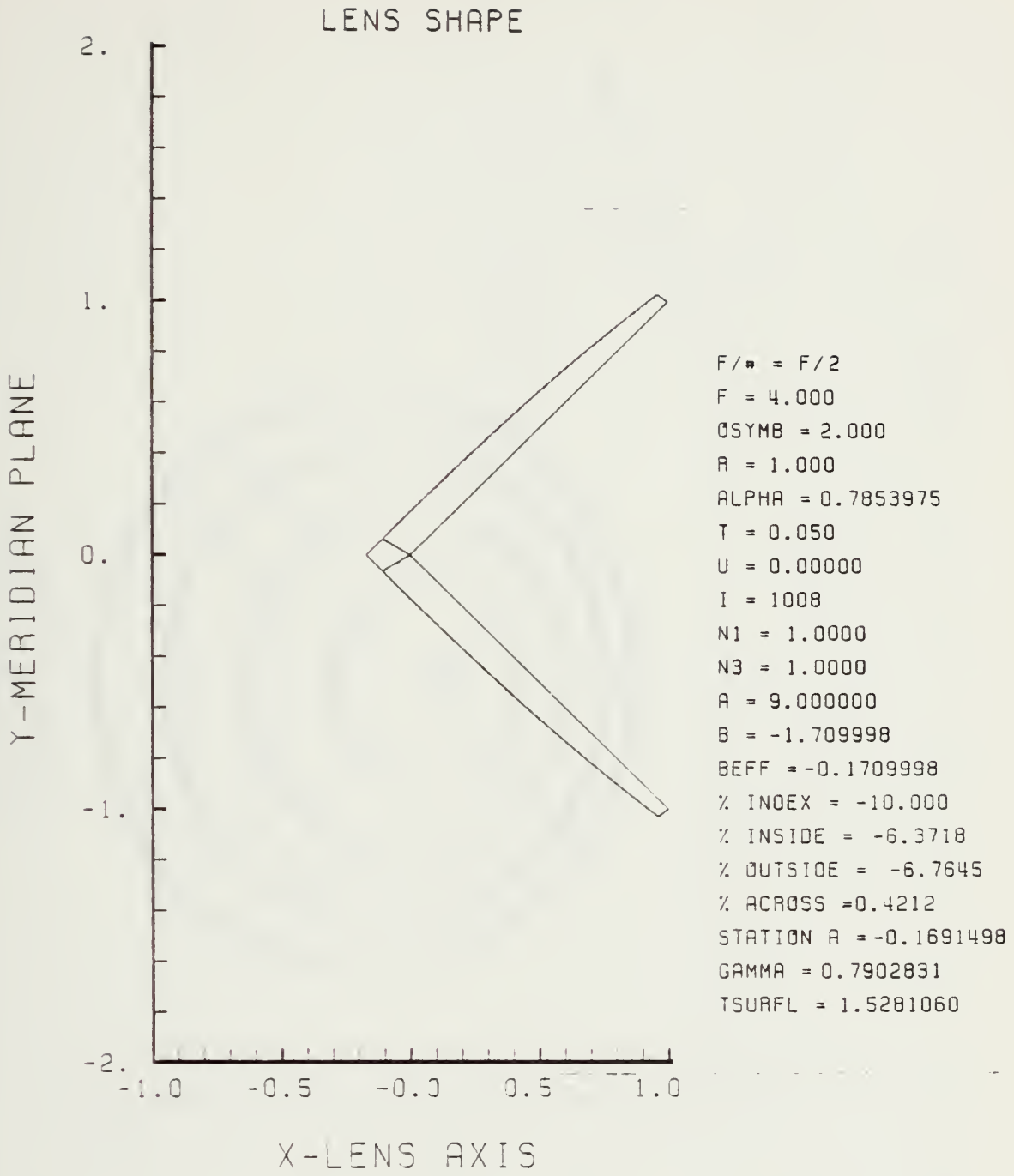

Figure F-101. GRIN Lens Shape at -10%, OB = 2.00, a = 9.00

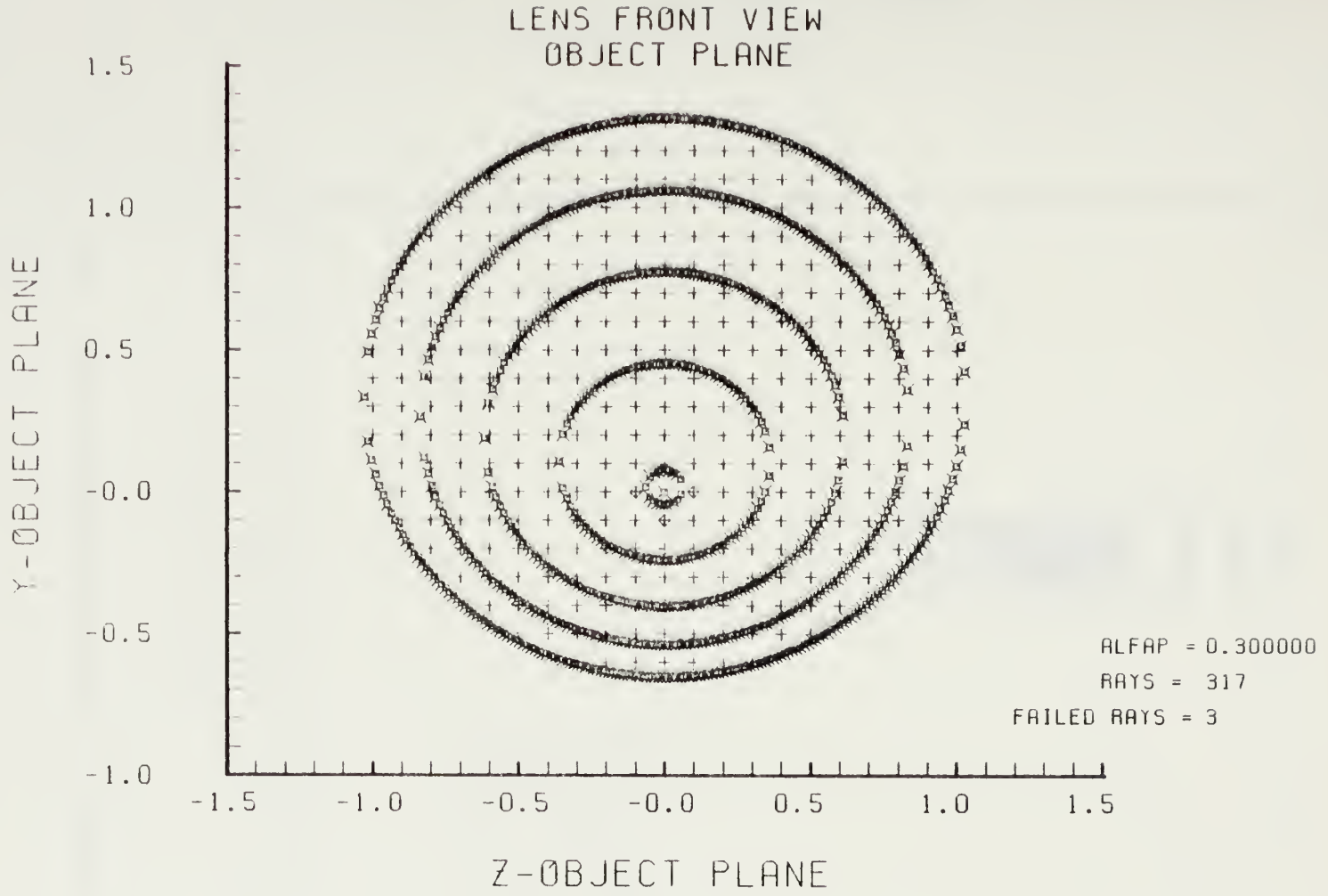

Figure F-102. Grid Plane at α_p = 0.3 for Lens of Figure F-101

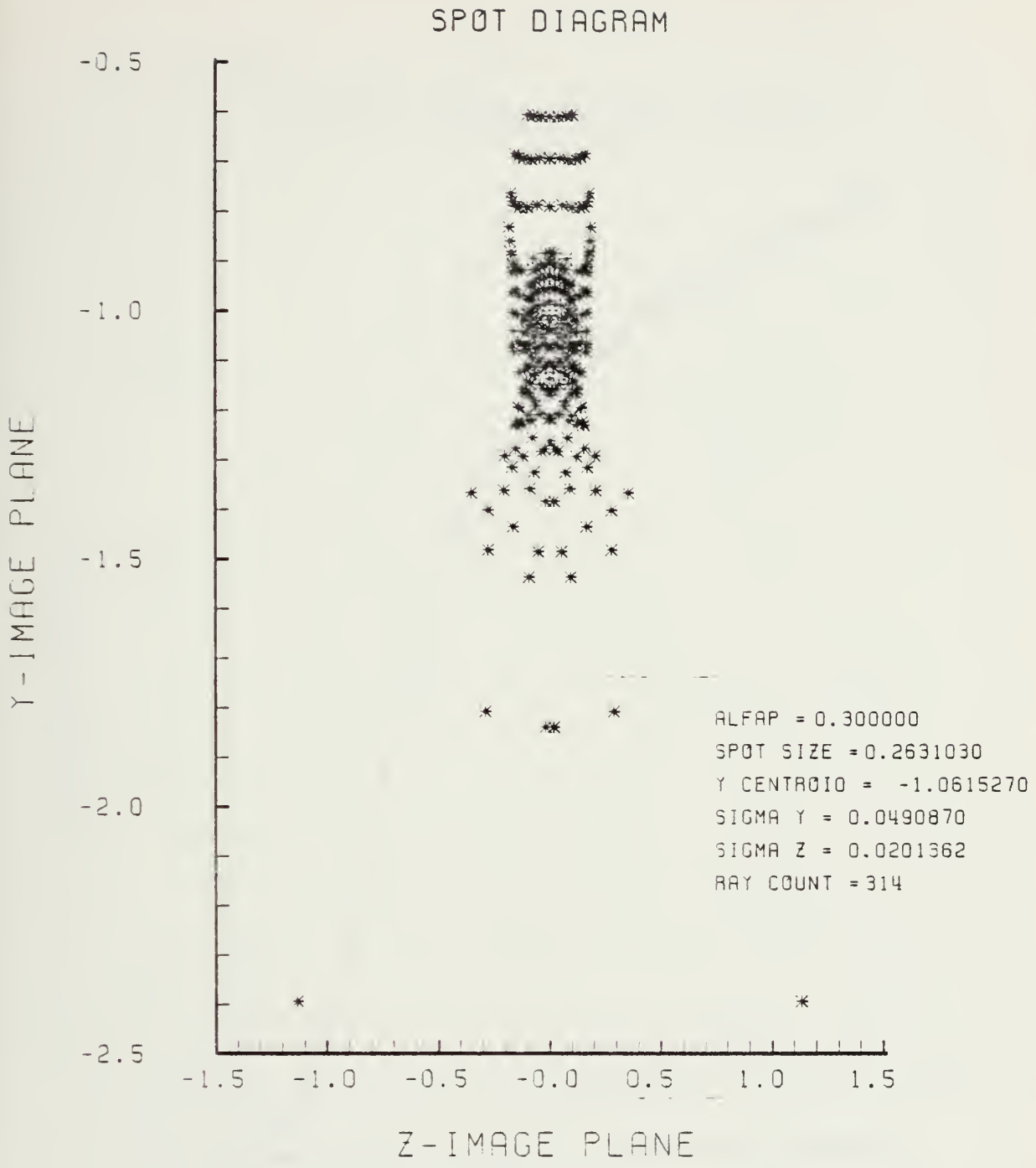

Figure F-103. Spot Diagram for Grid of Figure F-102

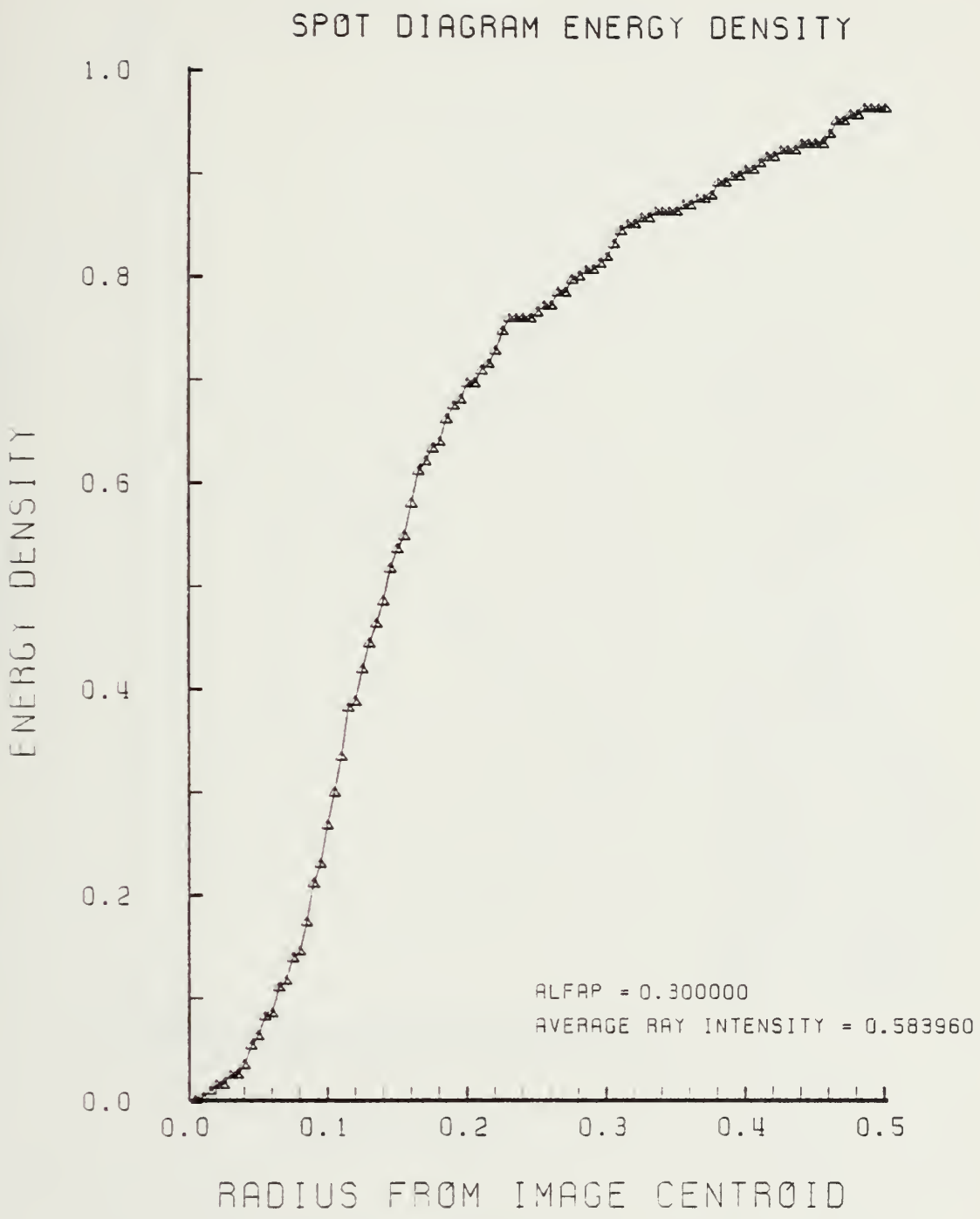

Figure F-104. Encircled Energy of Figure F-103

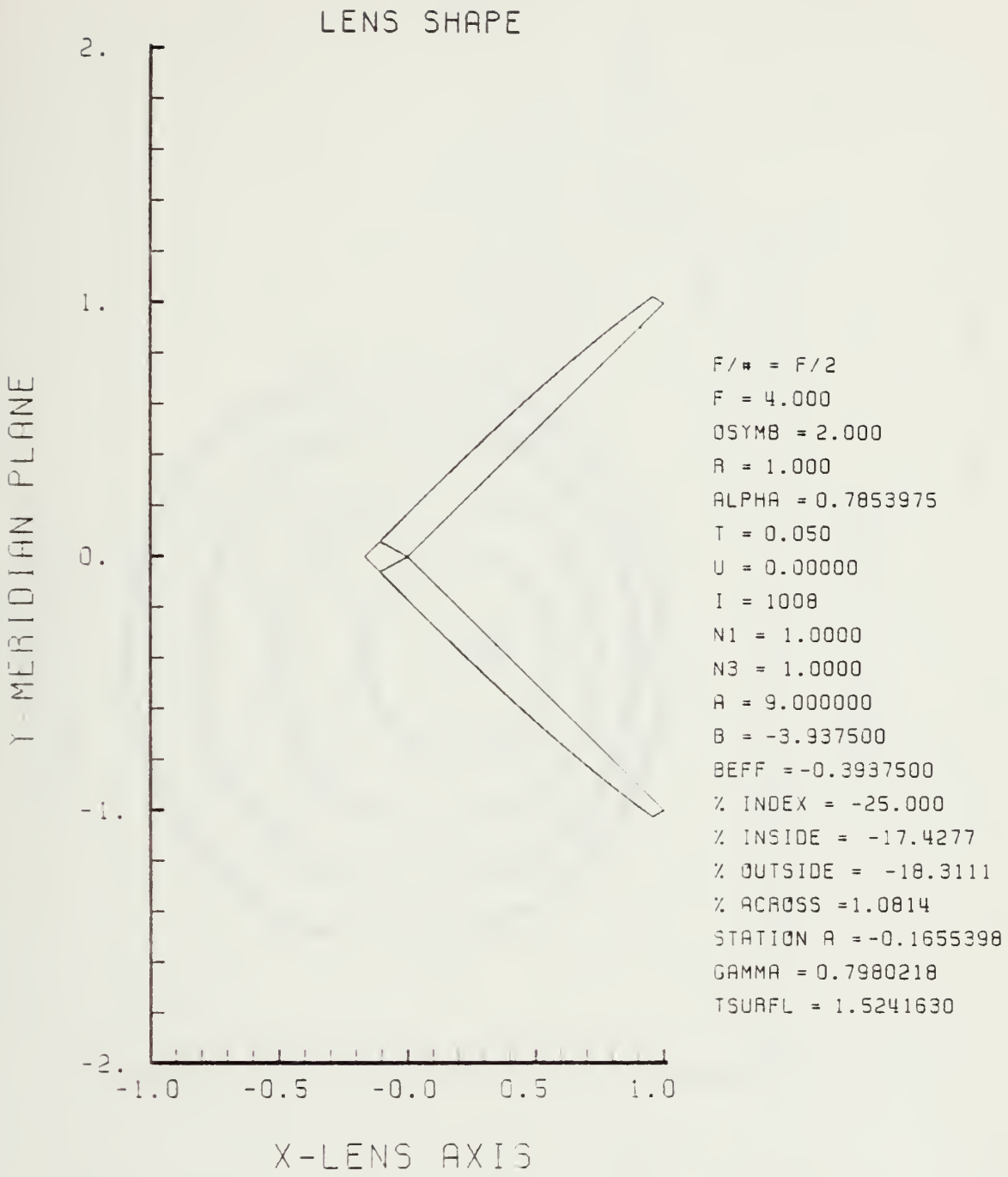

Figure F-105. GRIN Lens Shape at -25%, OB = 2.00, a = 9.00

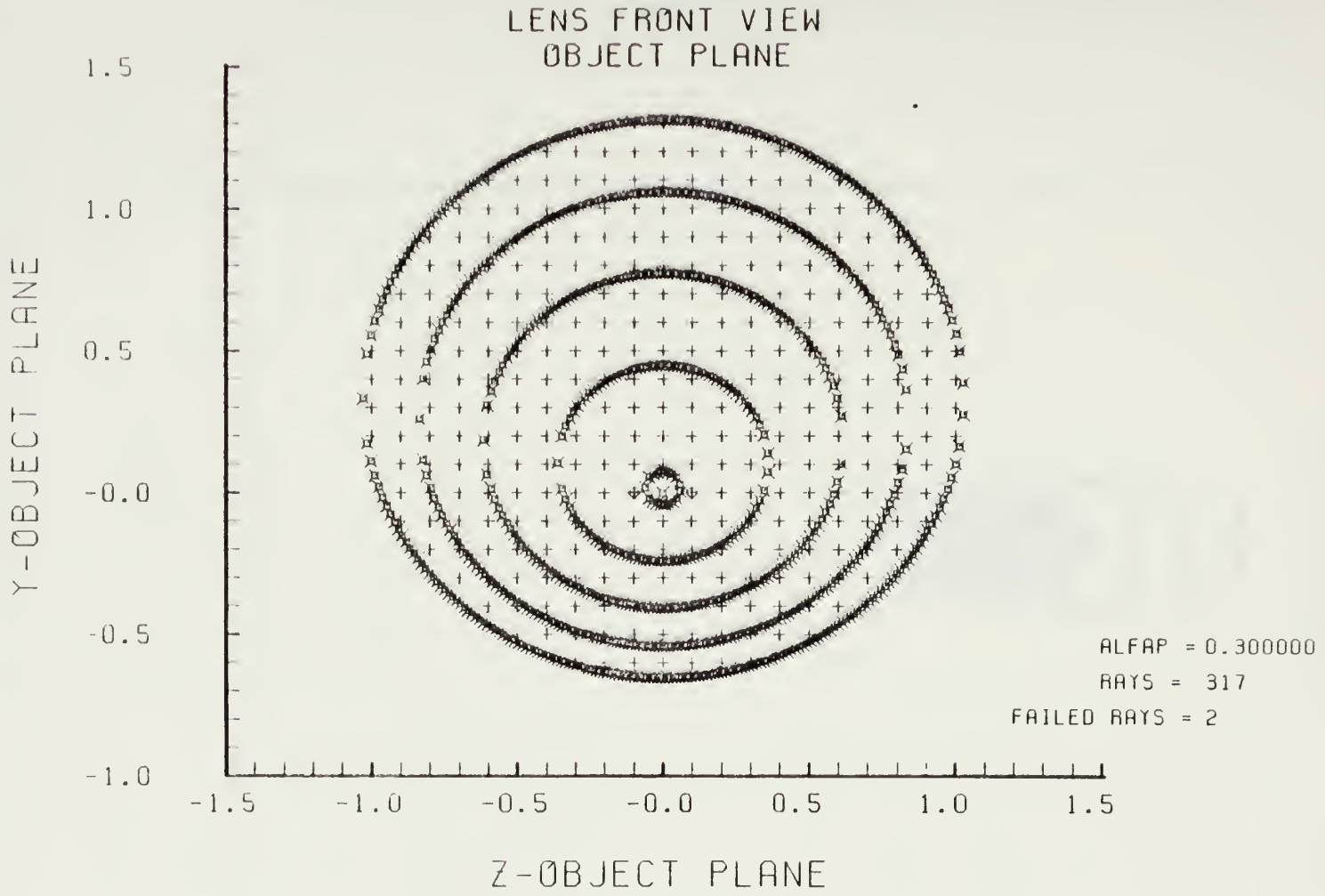

Figure F-106. Grid Plane at α_p = 0.3 for Lens of Figure F-105

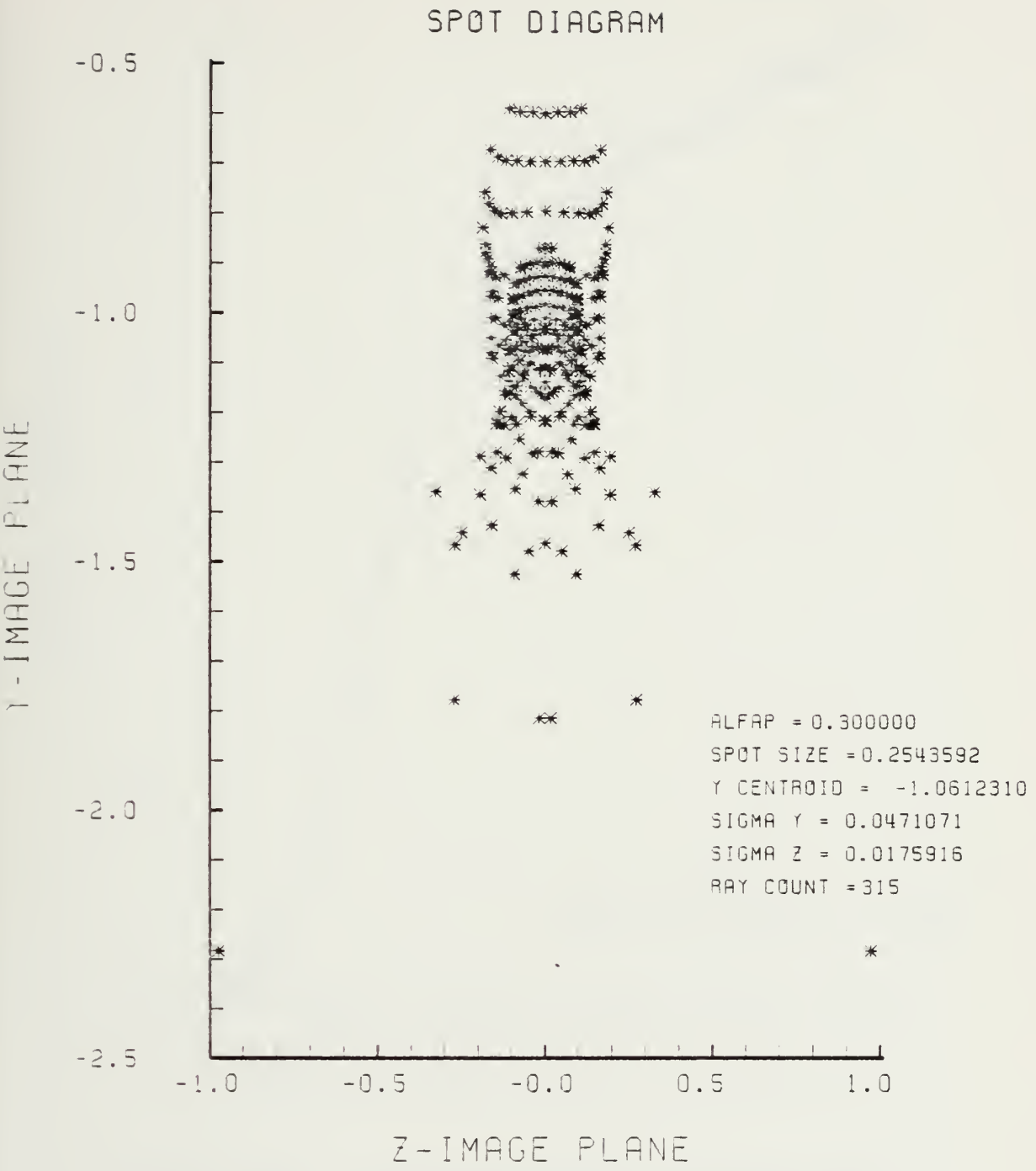

Figure F-107. Spot Diagram for Grid of Figure F-106

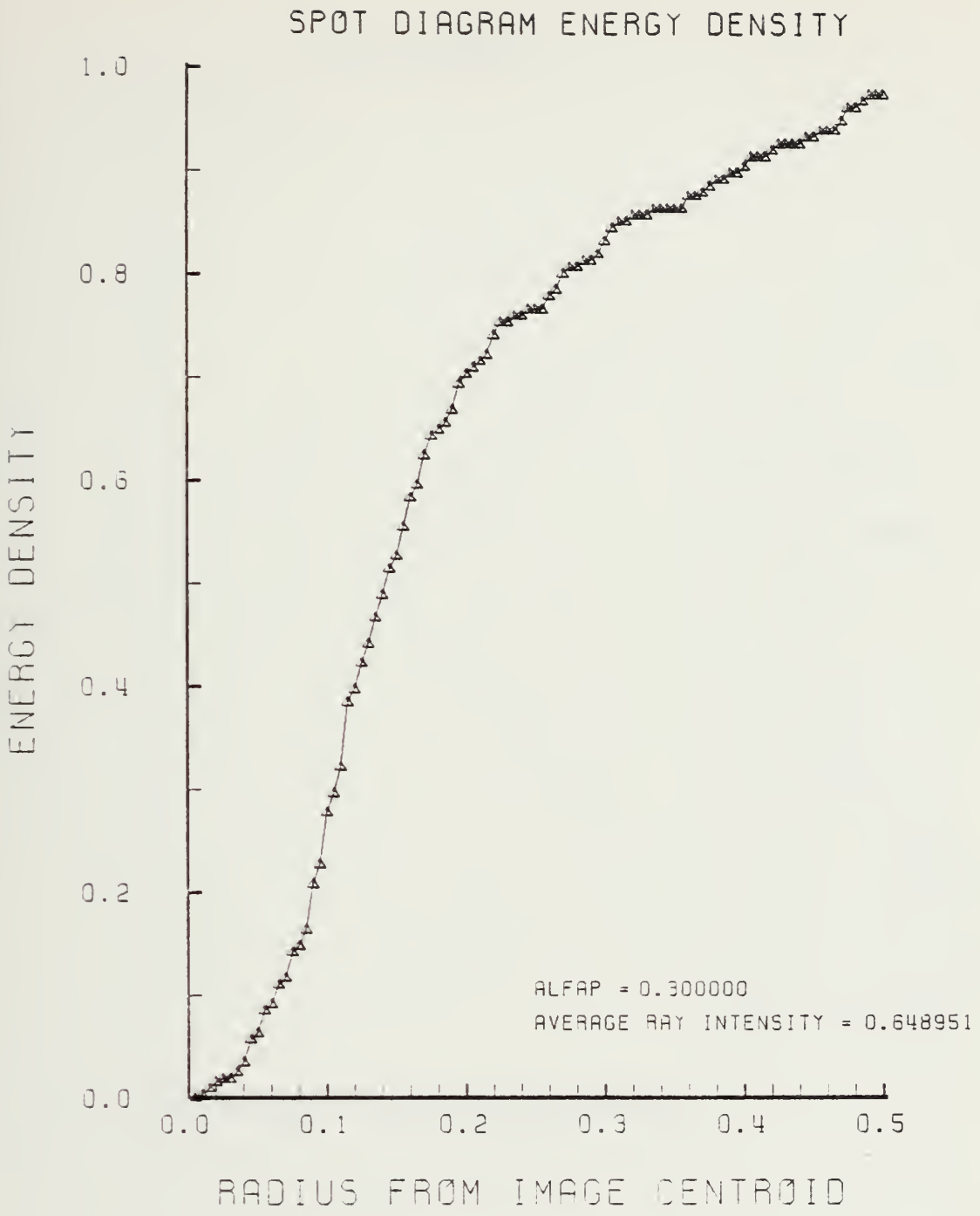

Figure F-108. Encircled Energy of Figure F-107

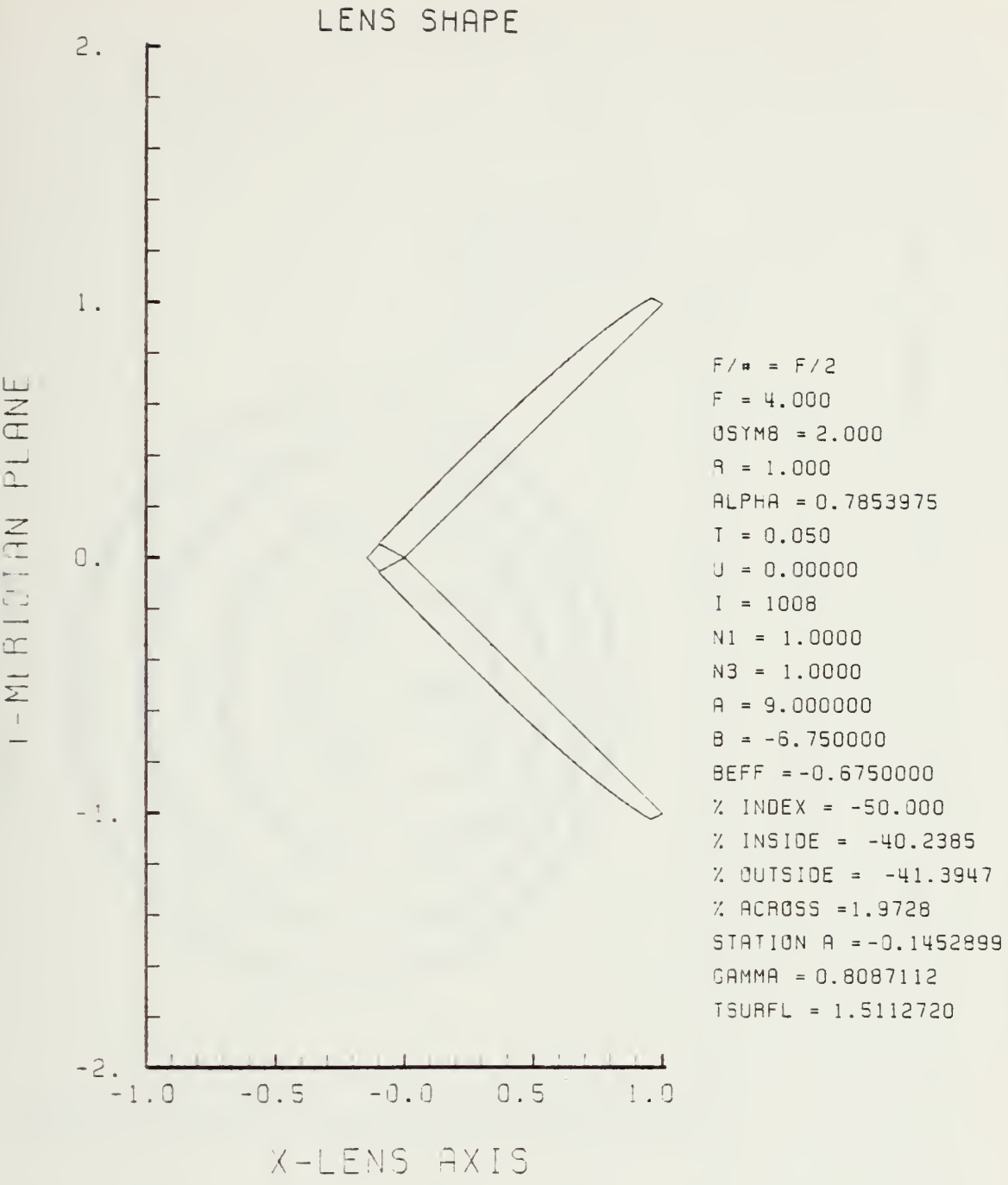

Figure F-109. GRIN Lens Shape at -50%, OB = 2.00, a = 9.00

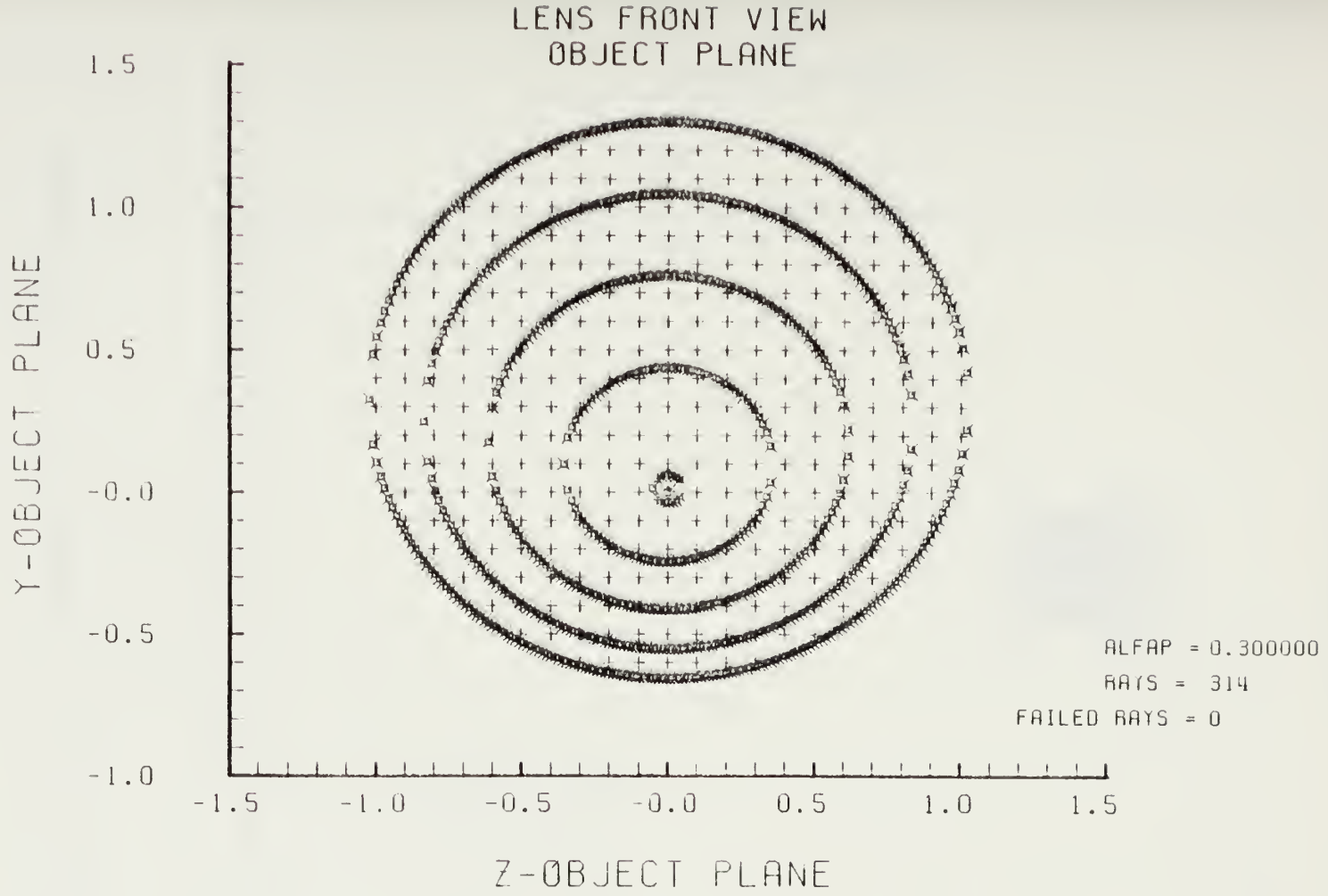

Figure F-110. Grid Plane at α_p = 0.3 for Grid of Figure F-109

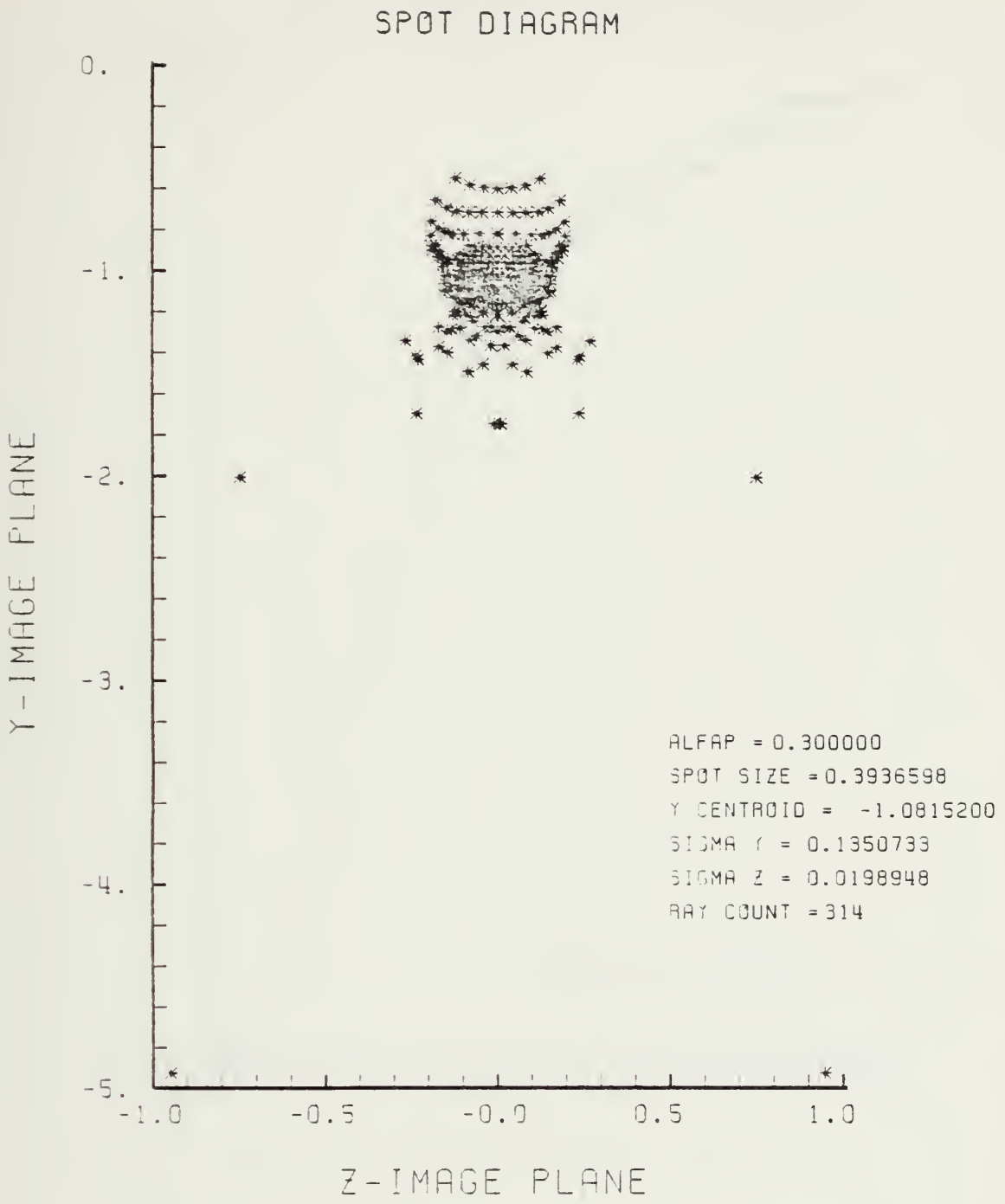

Figure F-111. Spot Diagram for Grid of Figure F-110

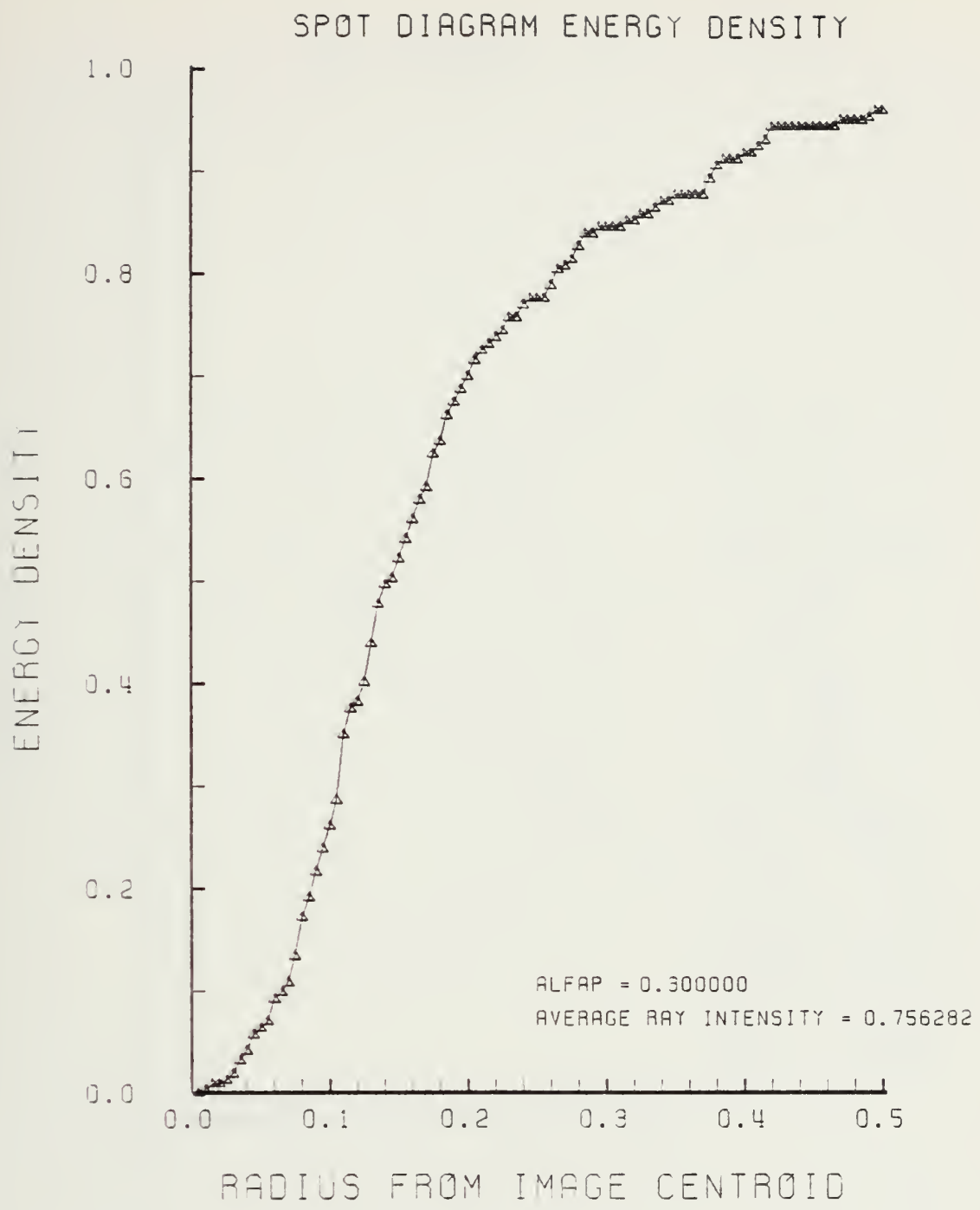

Figure F-112. Encircled Energy of Figure F-111

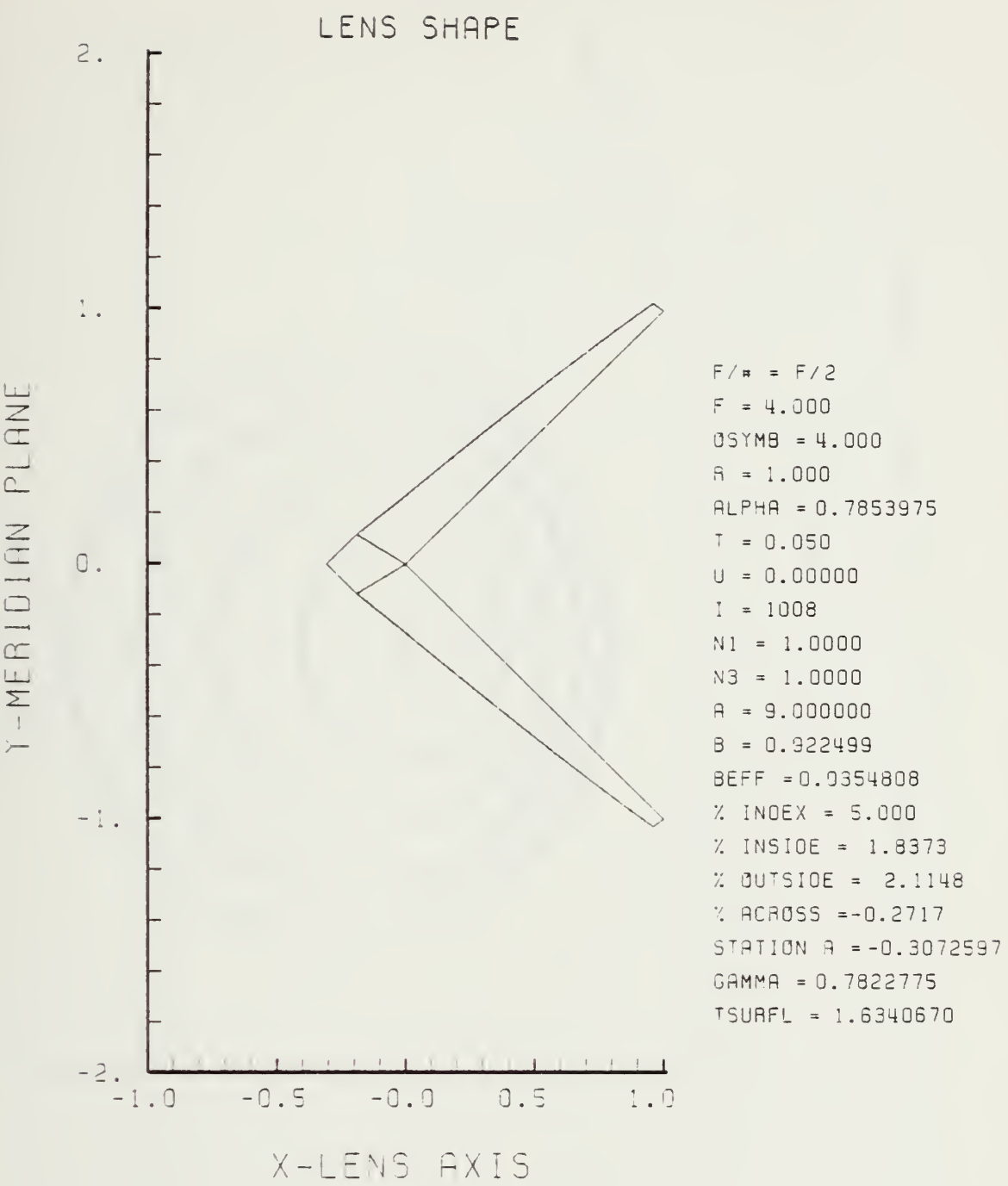

Figure F-113. GRIN Lens Shape at +5%, OB = 4.00, a = 9.00

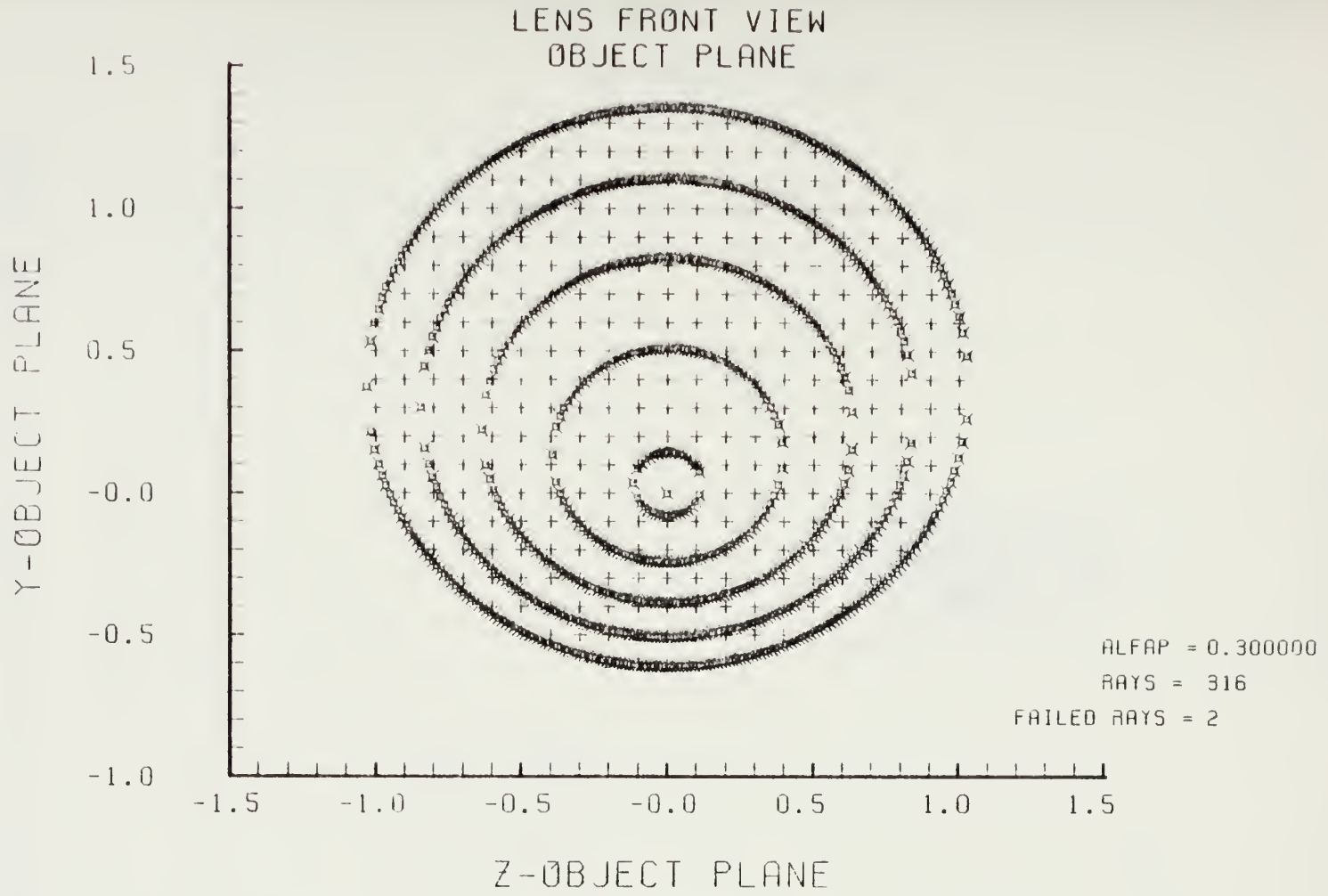

Figure F-114. Grid Plane at α_p = 0.3 for Lens of Figure F-113

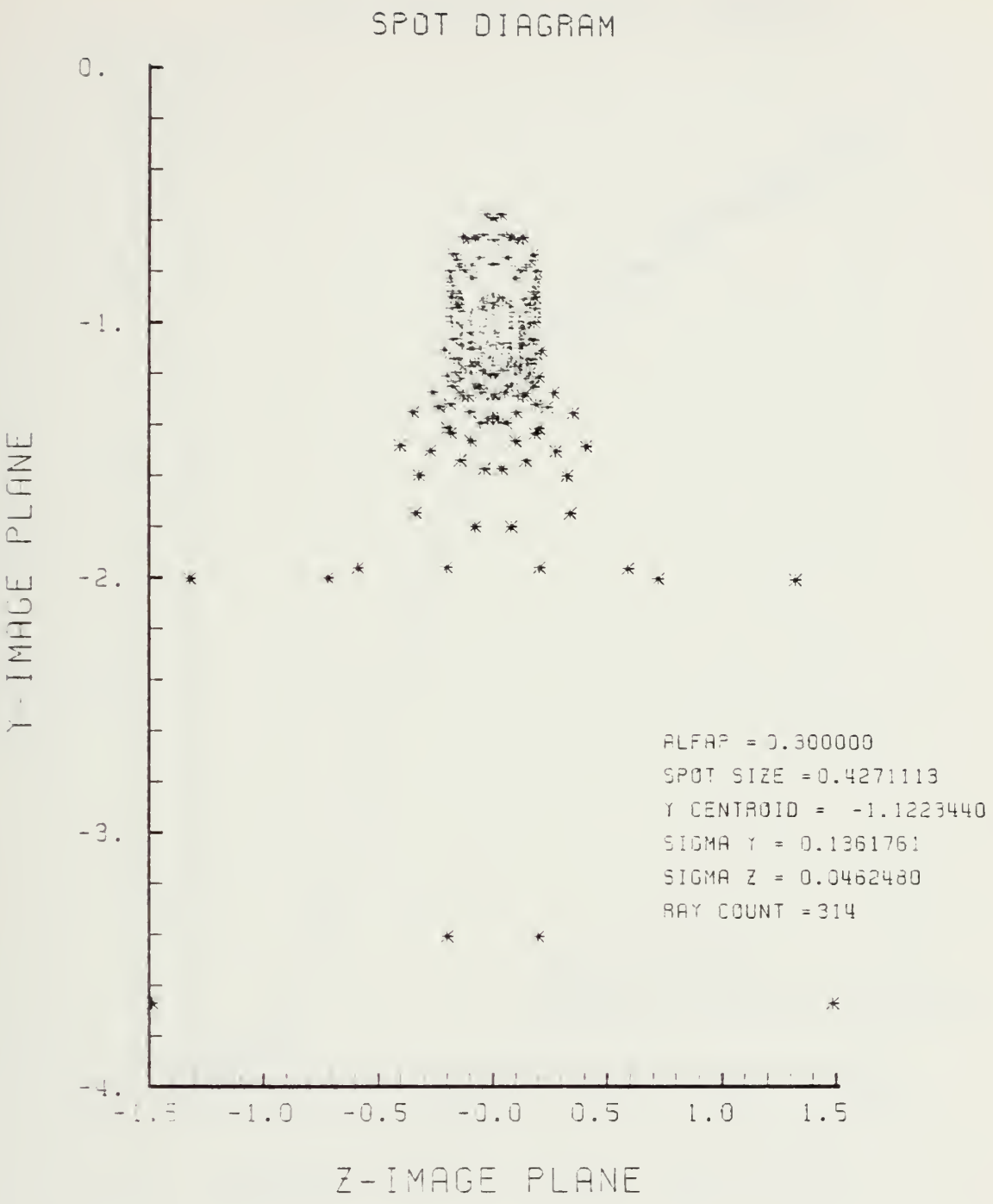

Figure F-115. Spot Diagram for Grid of Figure F-114

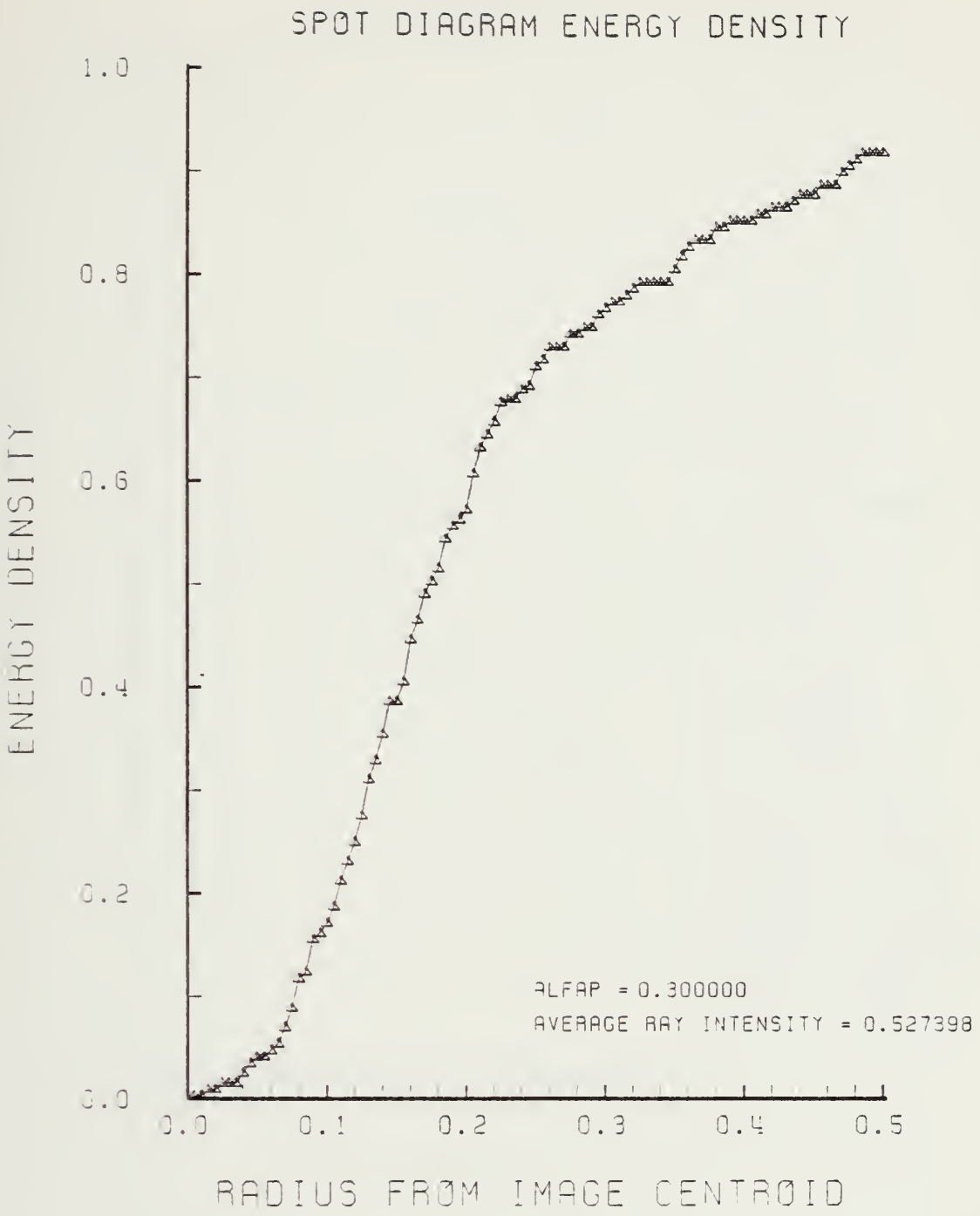

Figure F-116. Encircled Energy of Figure F-115

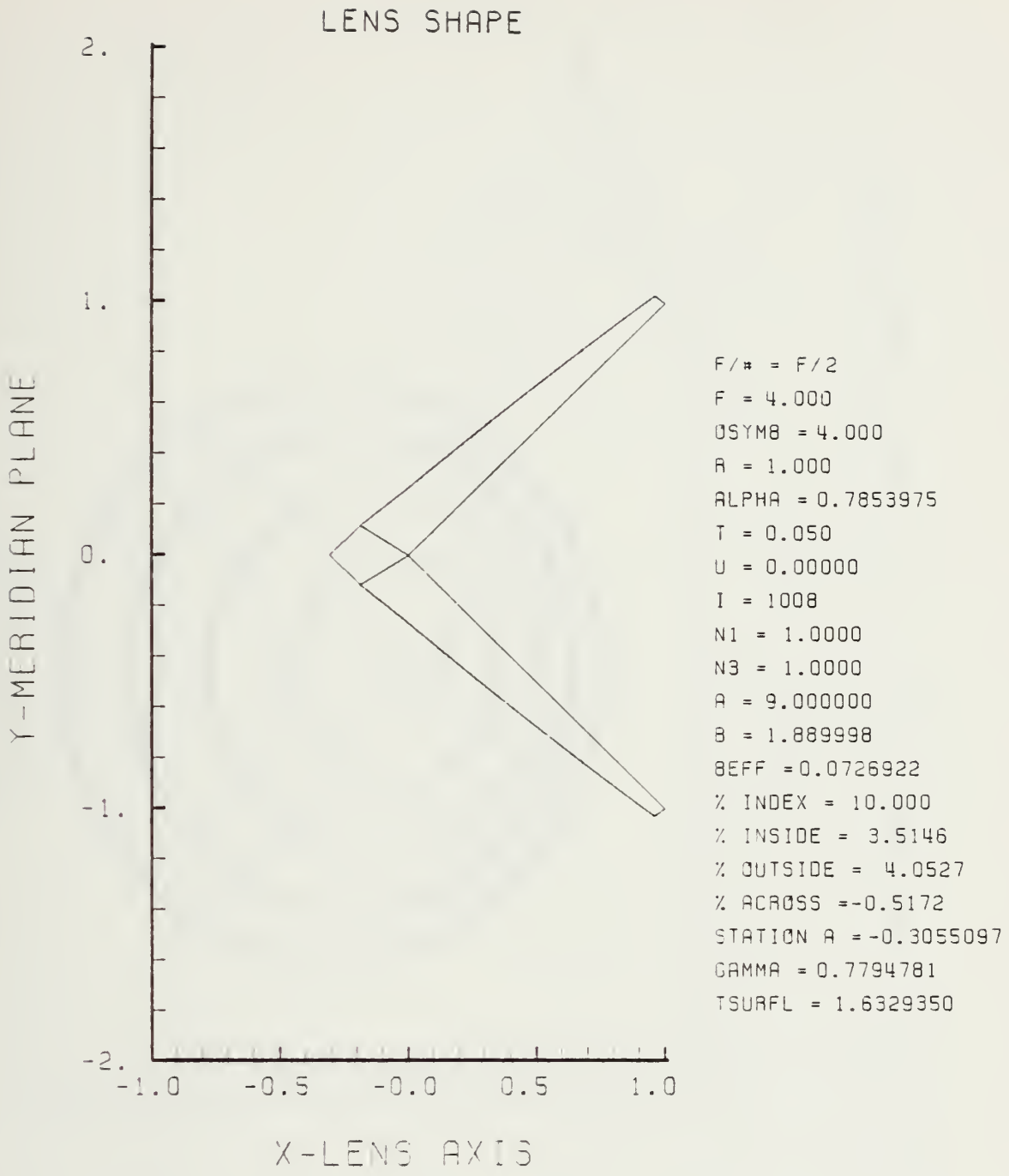

Figure F-117. GRIN Lens Shape at +10%, OB = 4.00, a = 9.00

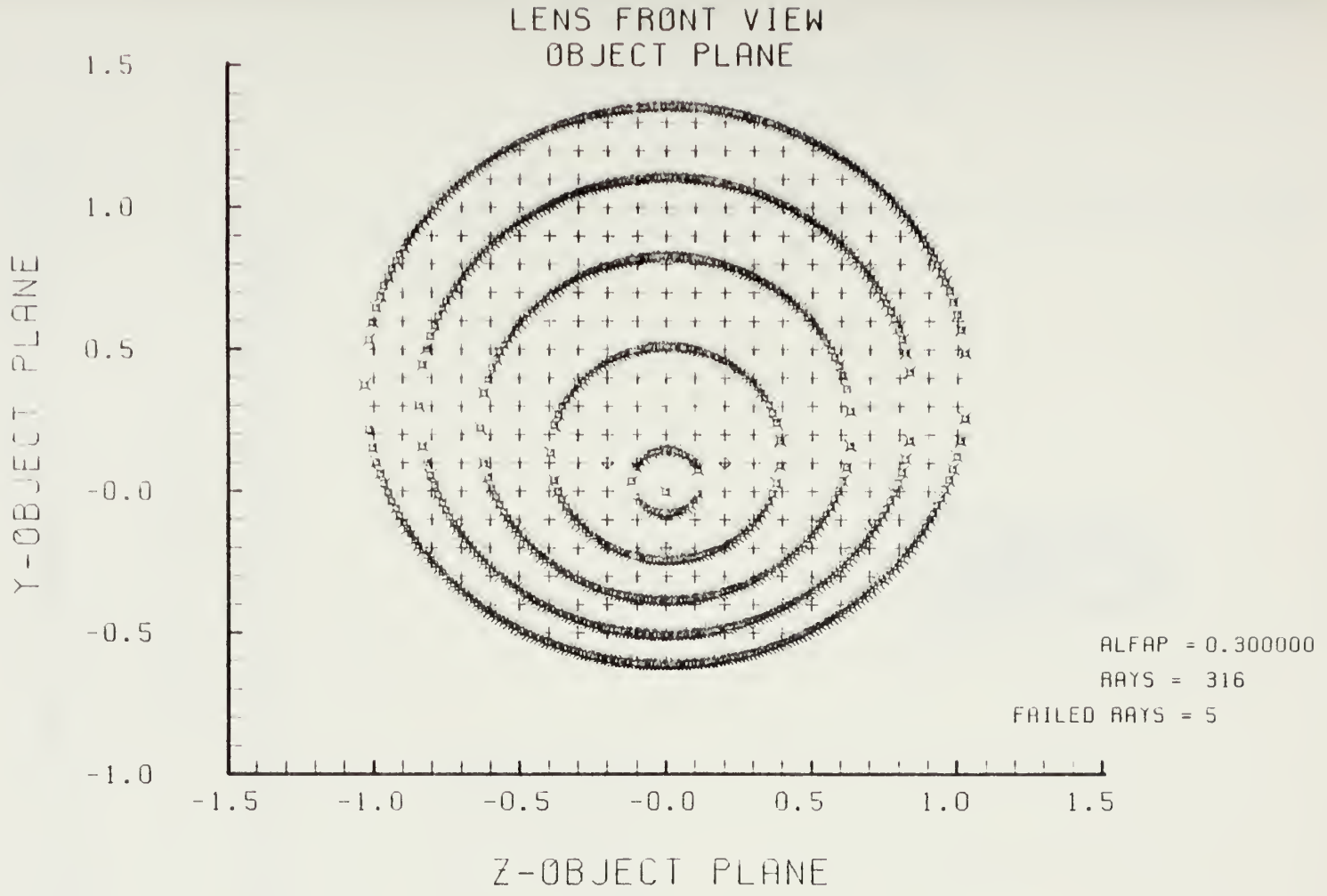

Figure F-118. Grid Plane at α_p = 0.3 for Lens of Figure F-117

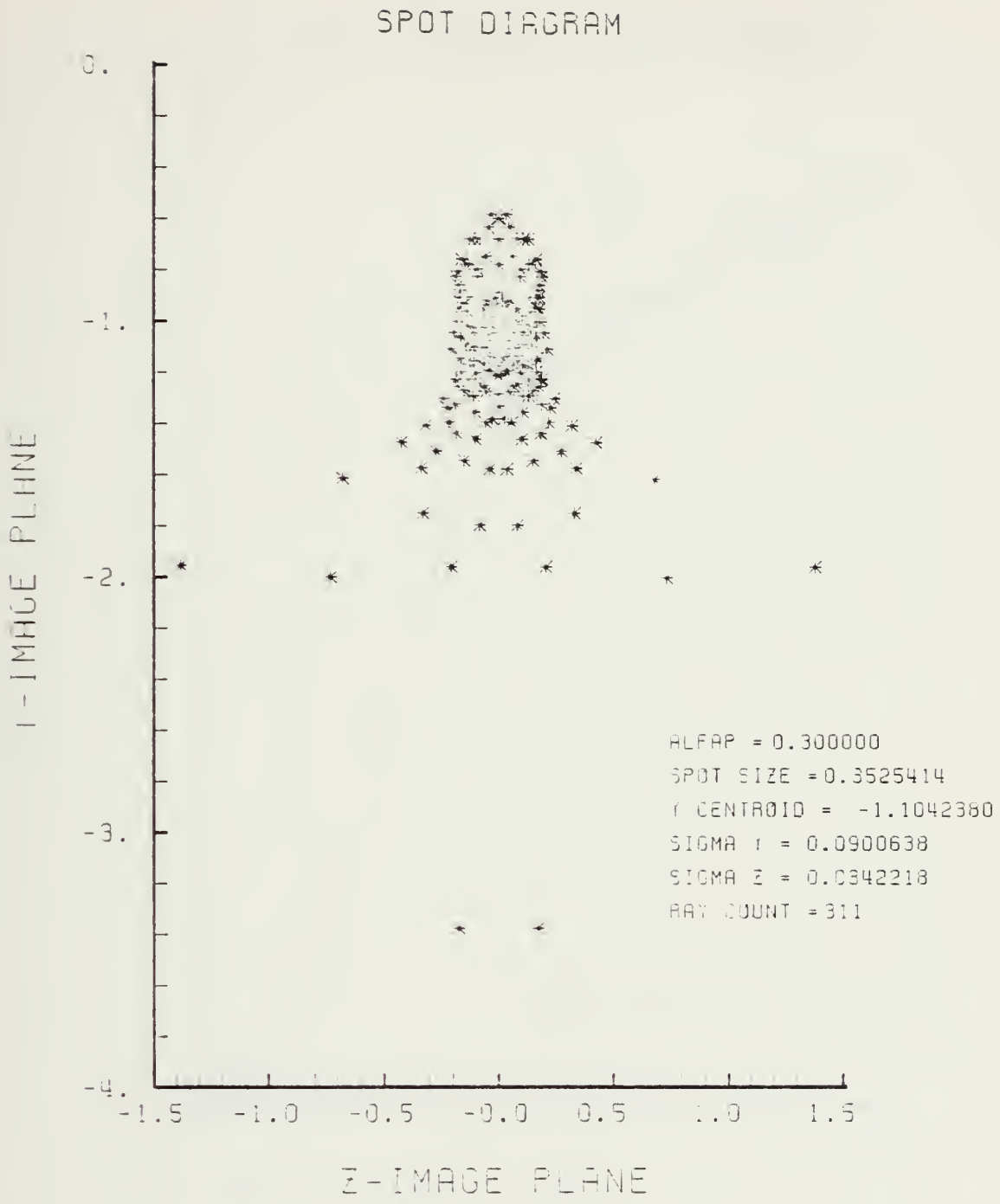

Figure F-119. Spot Diagram for Grid of Figure F-118

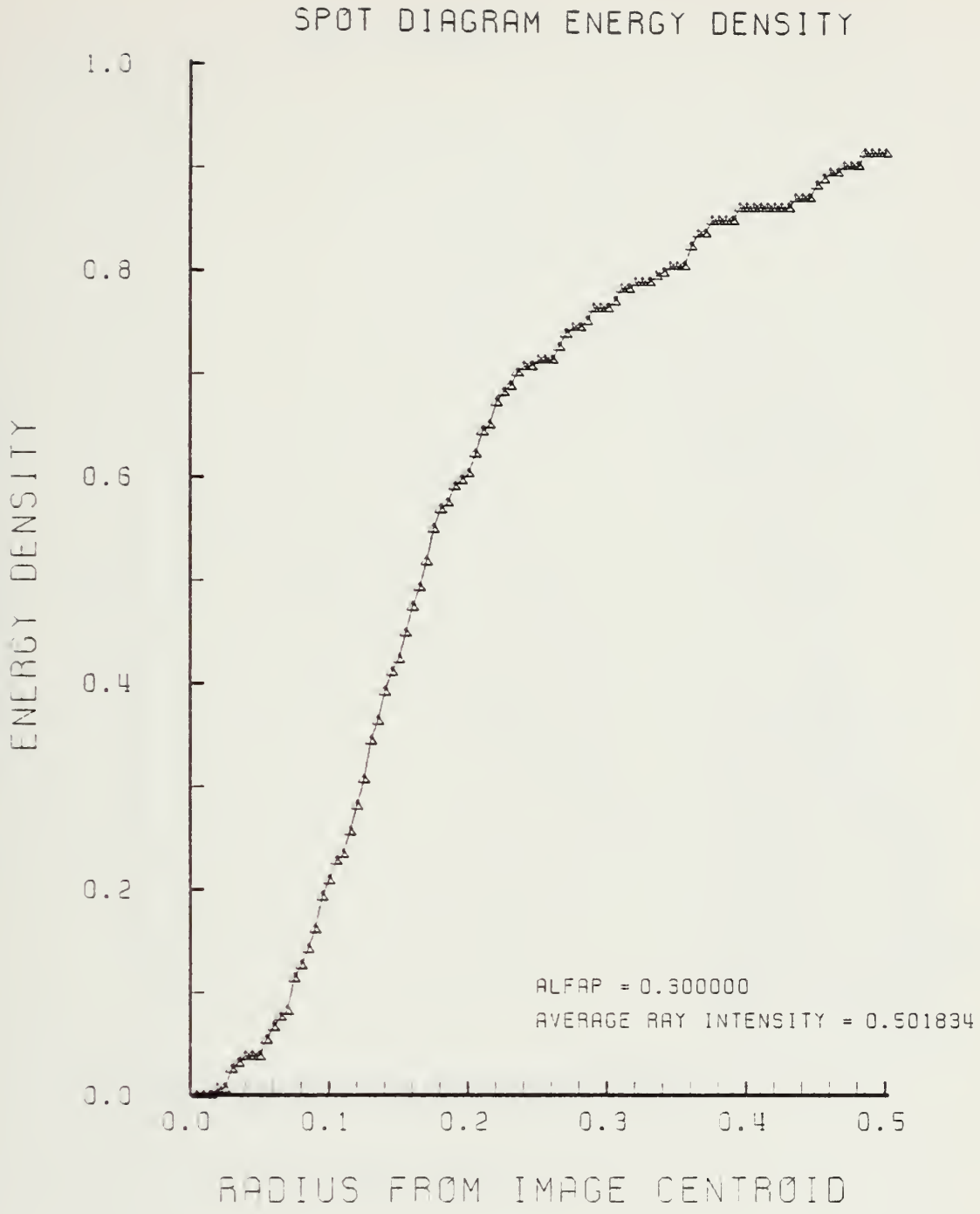

Figure F-120. Encircled Energy of Figure F-119

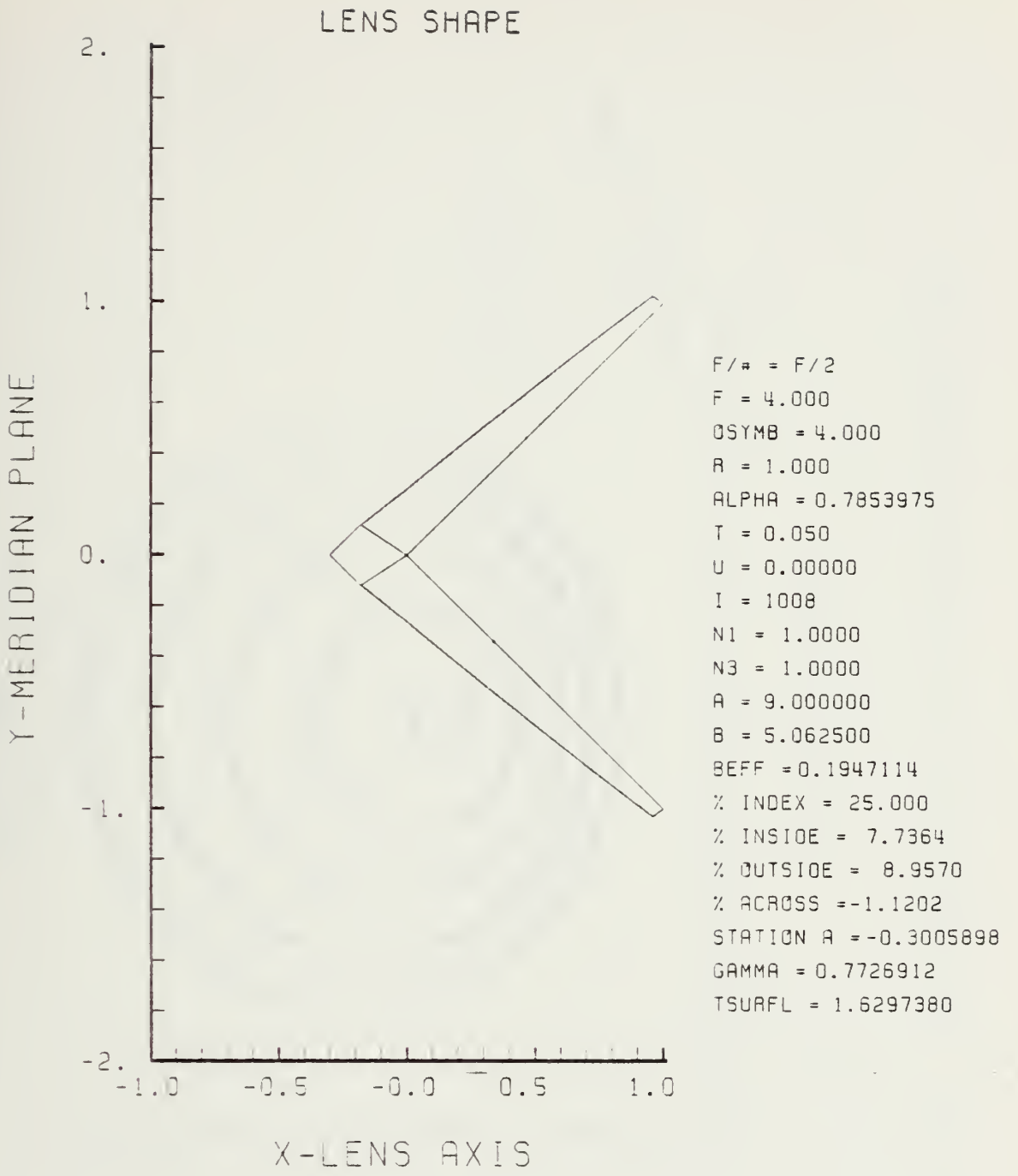

Figure F-121. GRIN Lens Shape at +25%, OB = 4.00, a = 9.00

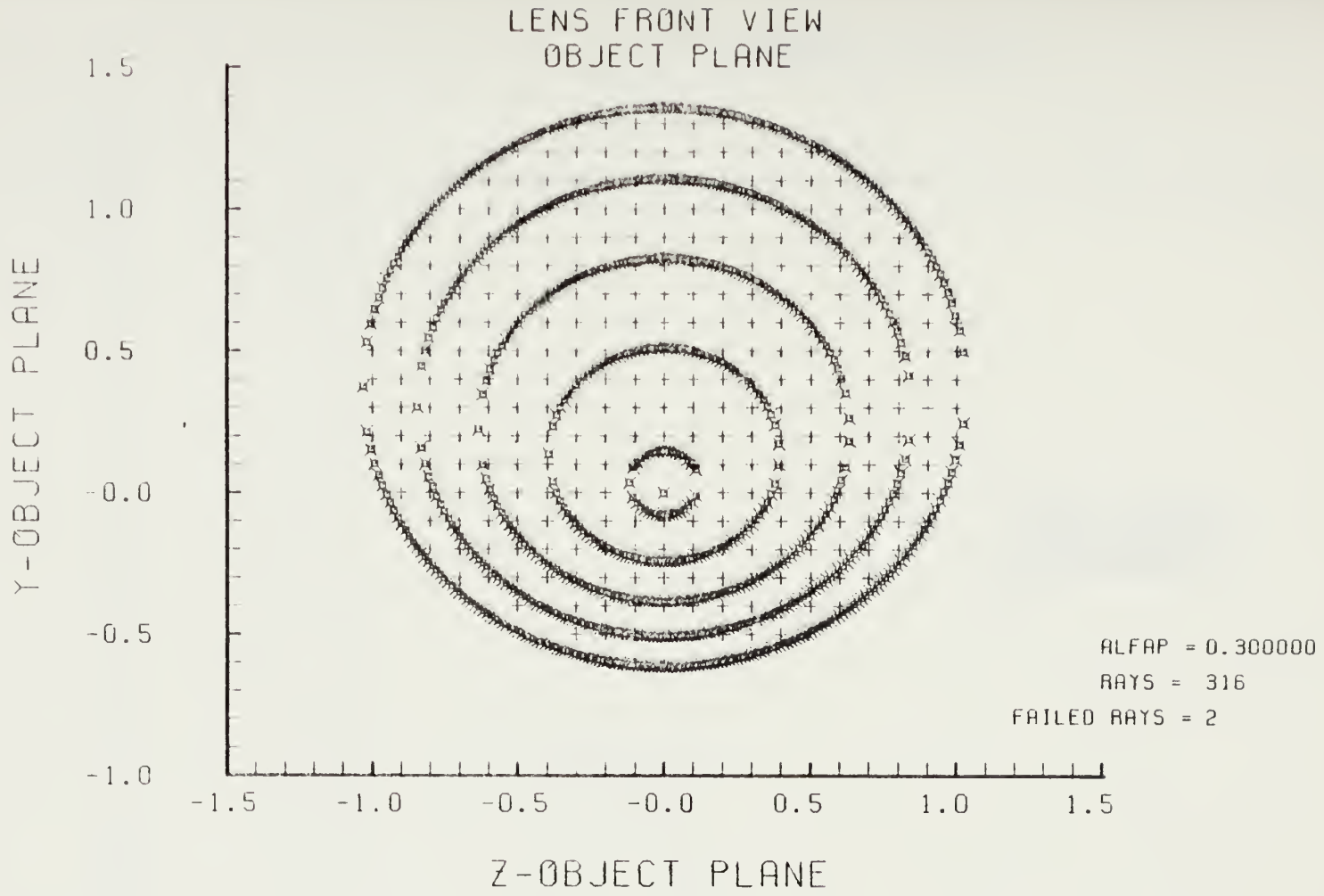

Figure F-122. Grid Plane at α_p = 0.3 for Lens of Figure F-121

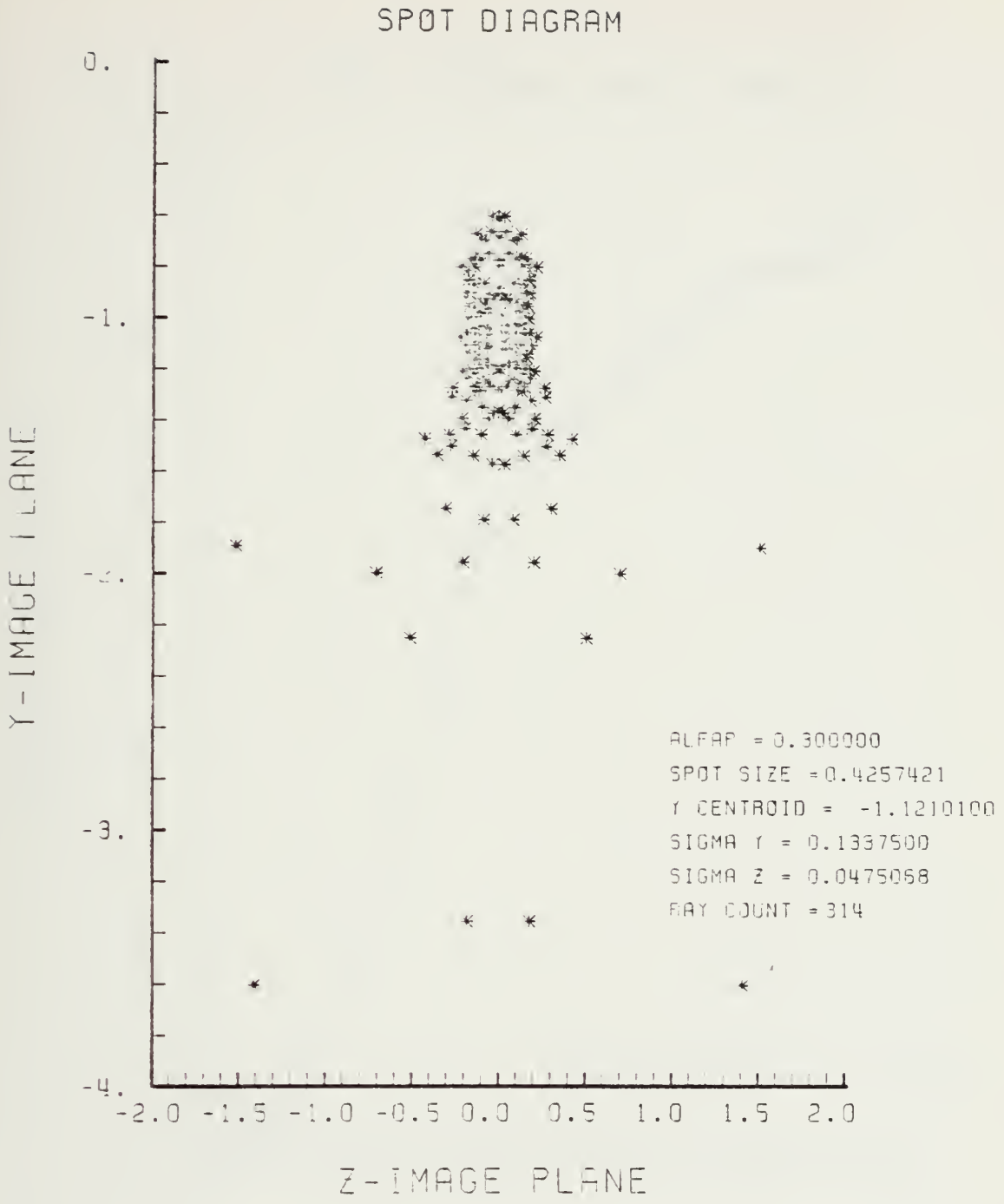

Figure F-123. Spot Diagram for Grid of Figure F-122

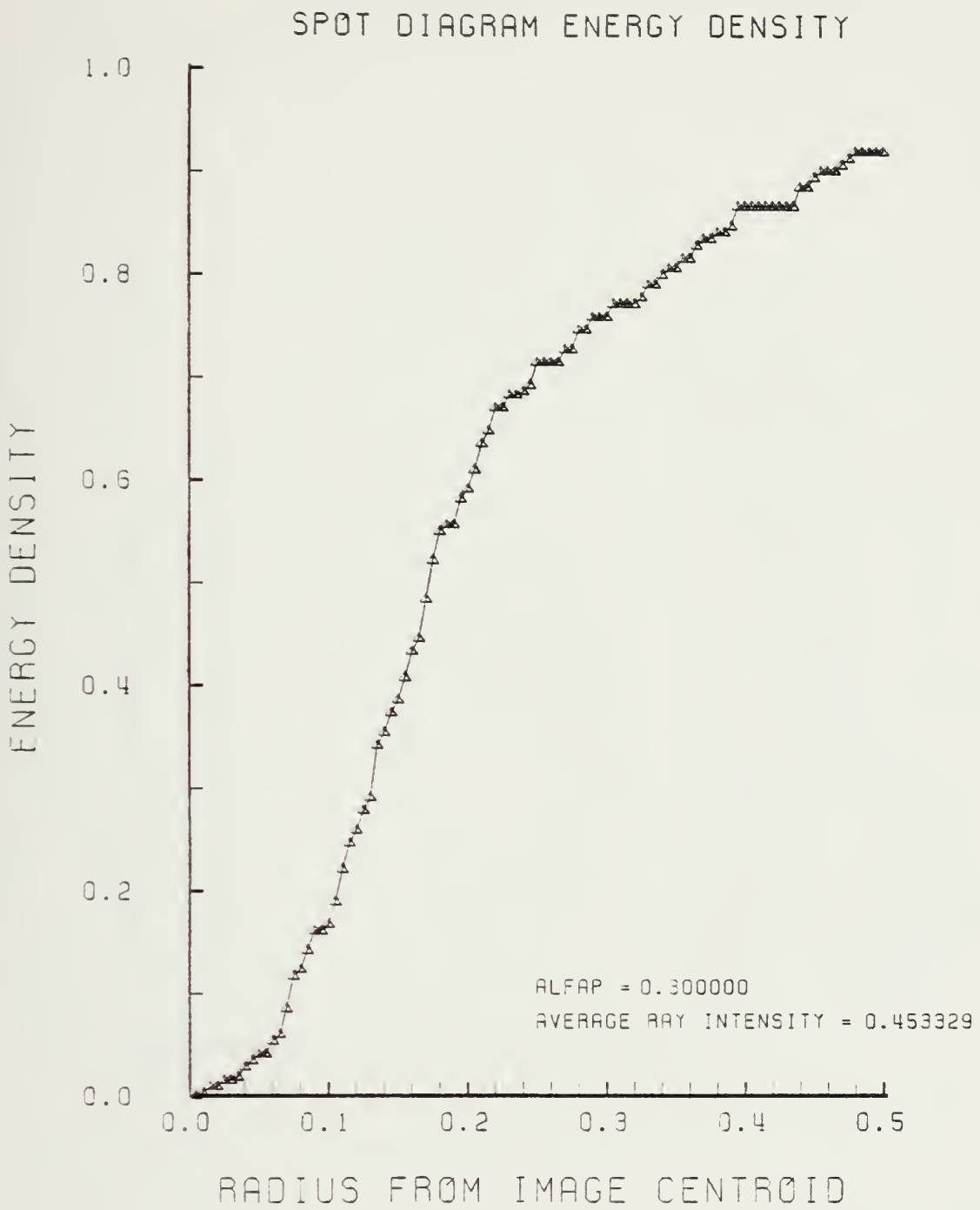

Figure F-124. Encircled Energy of Figure F-123

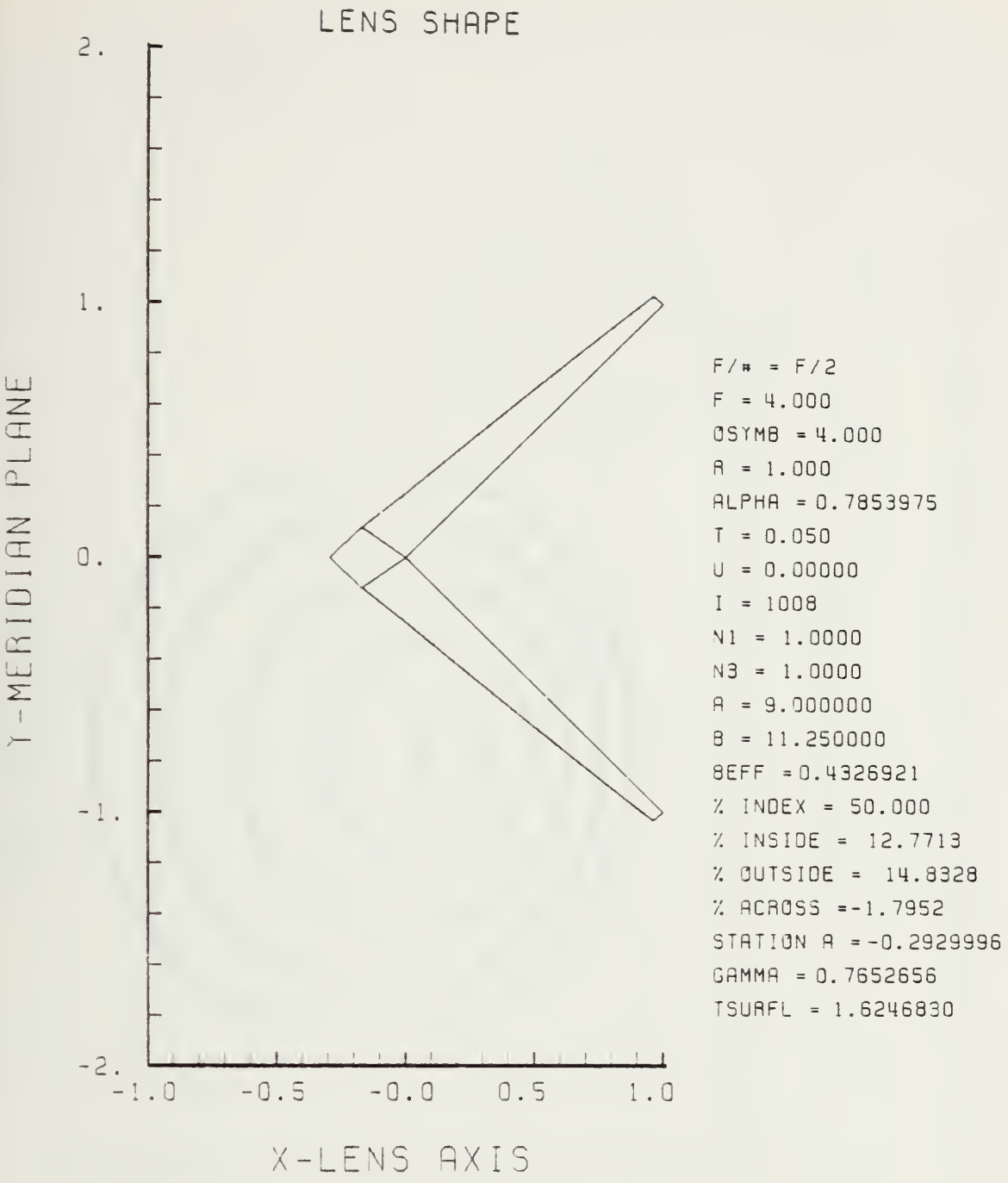

Figure F-125. GRIN Lens Shape at +50%, OB = 4.00, a = 9.00

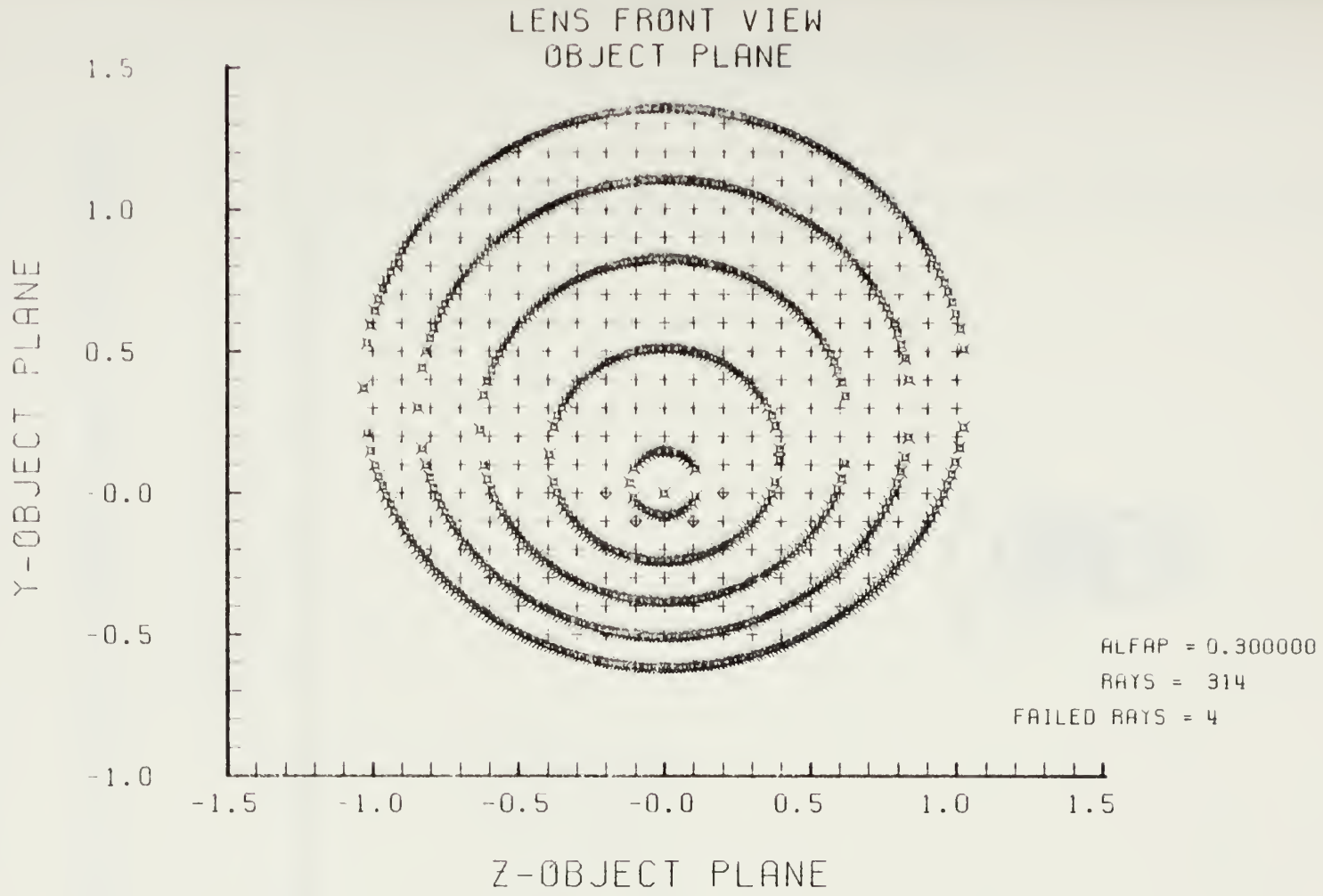

Figure F-126. Grid Plane at α_p = 0.3 for Lens of Figure F-125

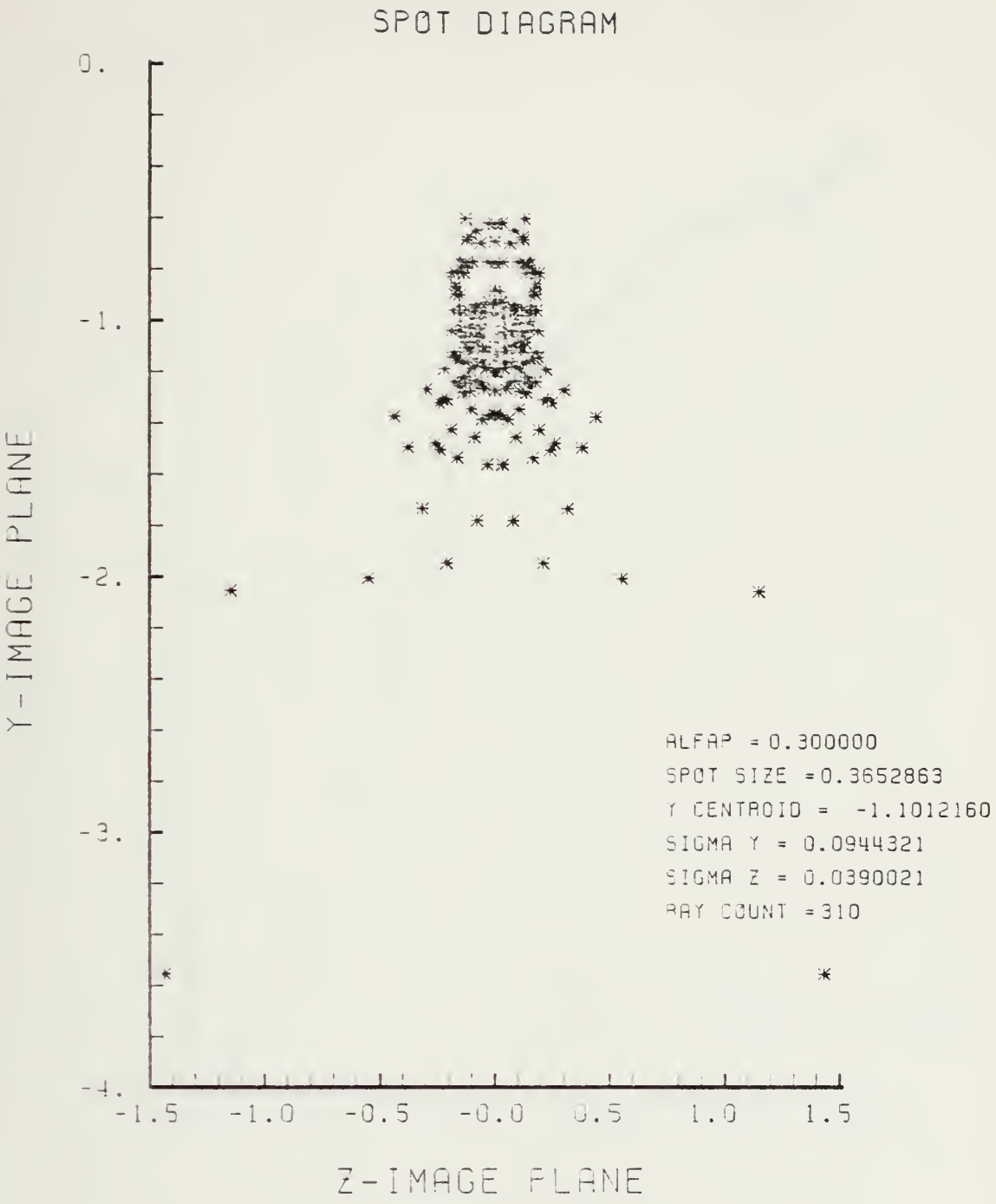

Figure F-127. Spot Diagram for Grid of Figure F-126

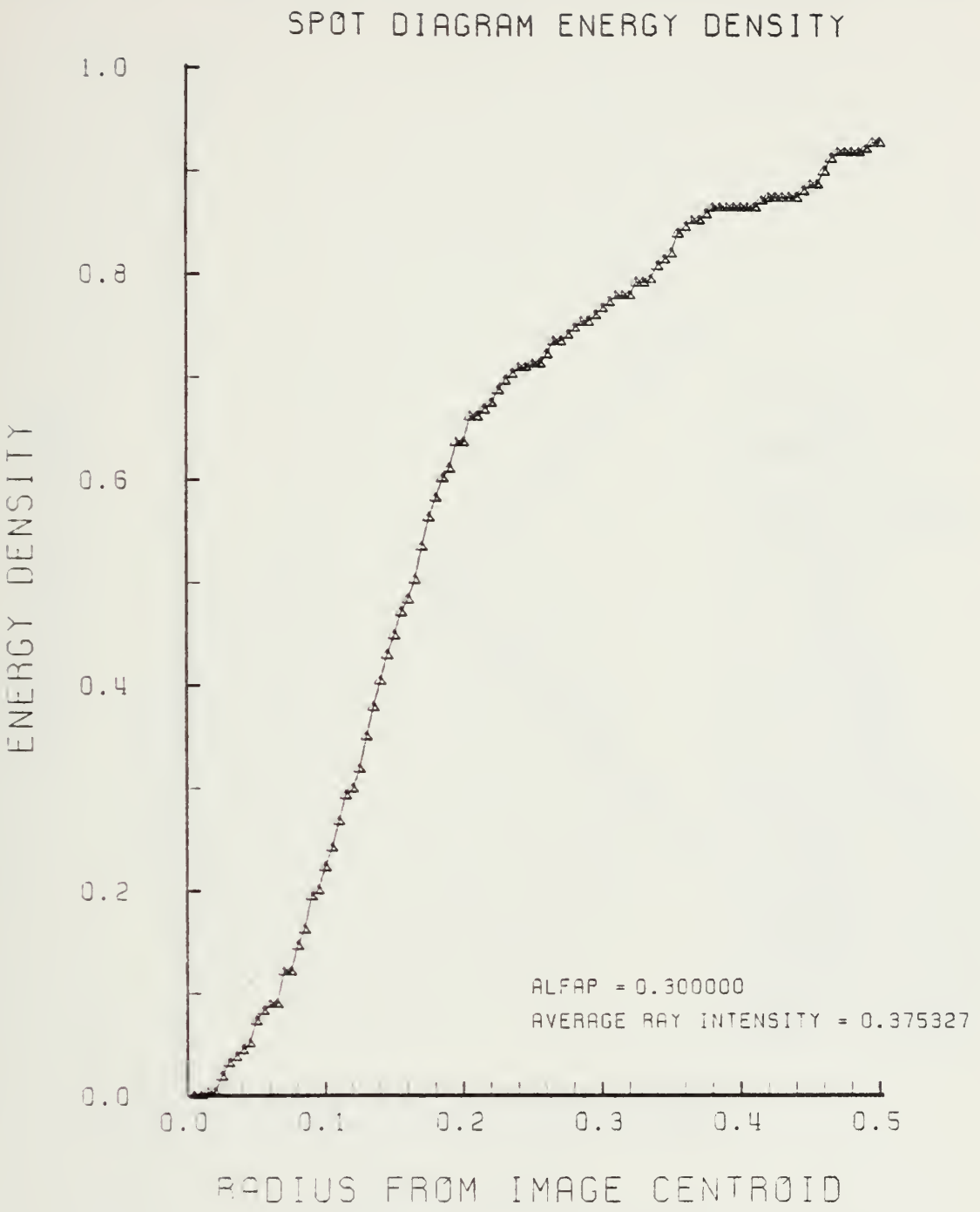

Figure F-128. Encircled Energy of Figure F-127

APPENDIX G

"BEST" GRIN LENS PERFORMANCE PLOTS IN THE F/2 CONFIGURATION

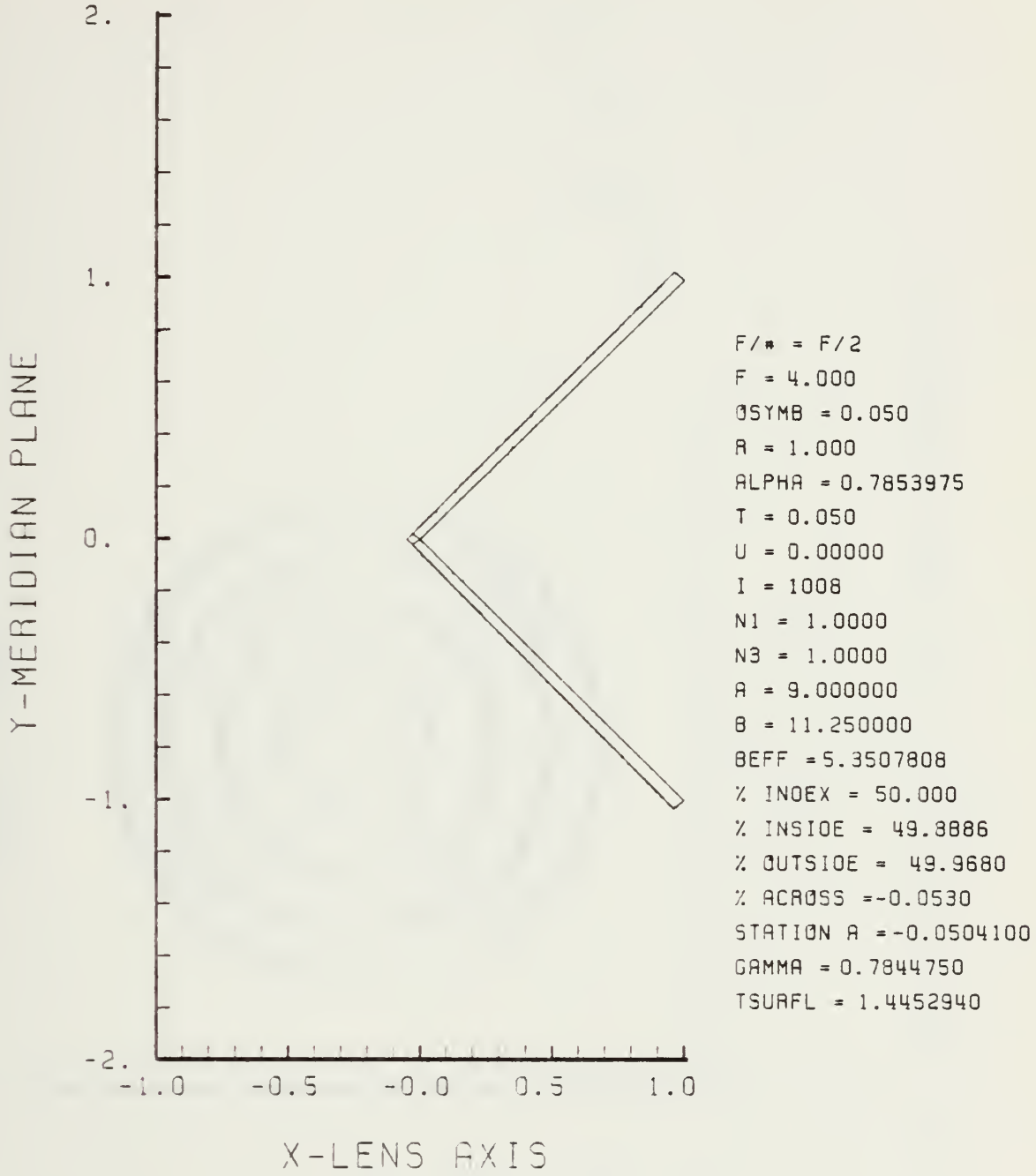

Figure G-1. "Best" GRIN Lens Shape with 50% Gradient, OB = 0.05 and a = 9.00 in the F/2 Configuration

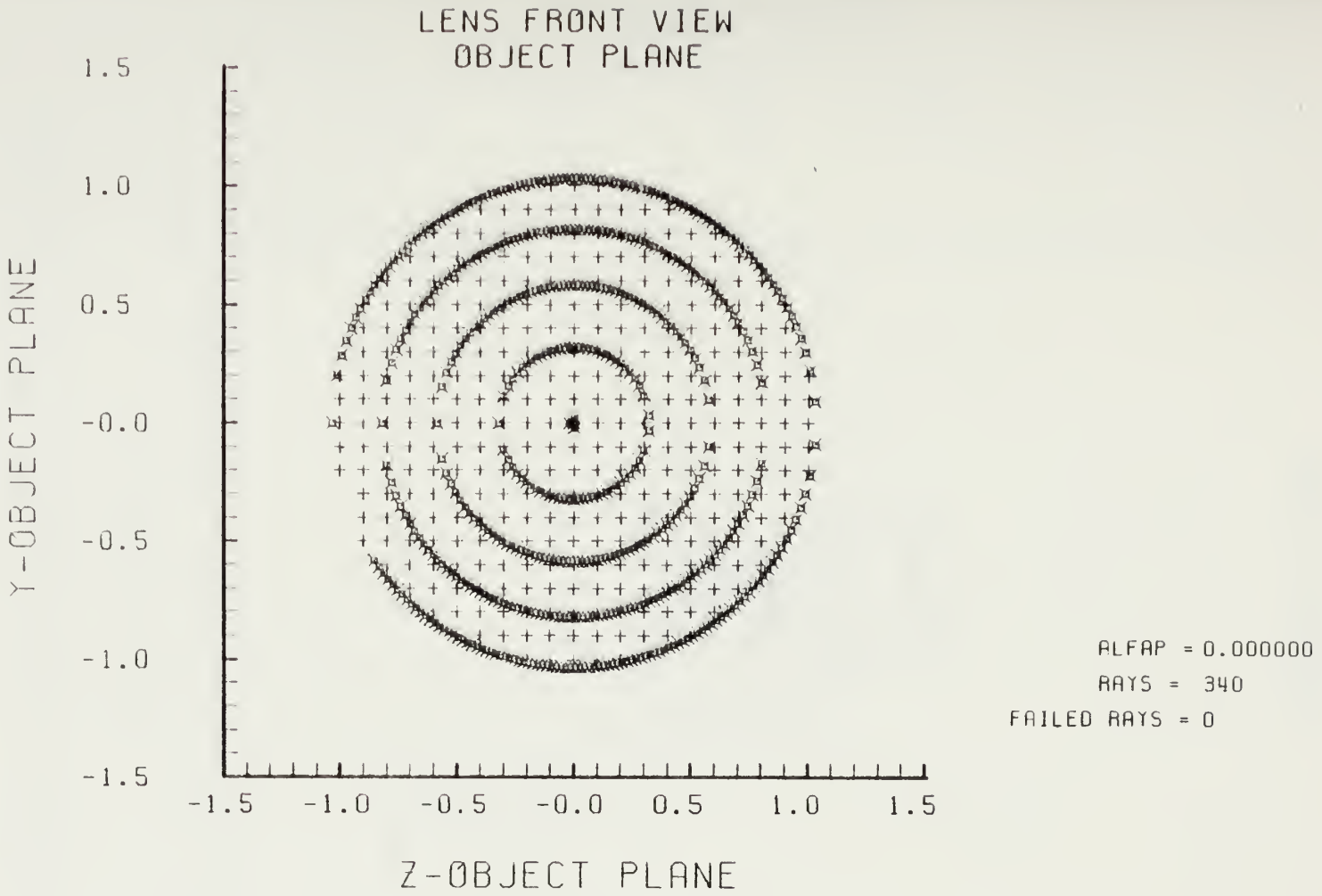

Figure G-2. Grid Plane at $\alpha_p = 0.0$ for Lens of Figure G-1

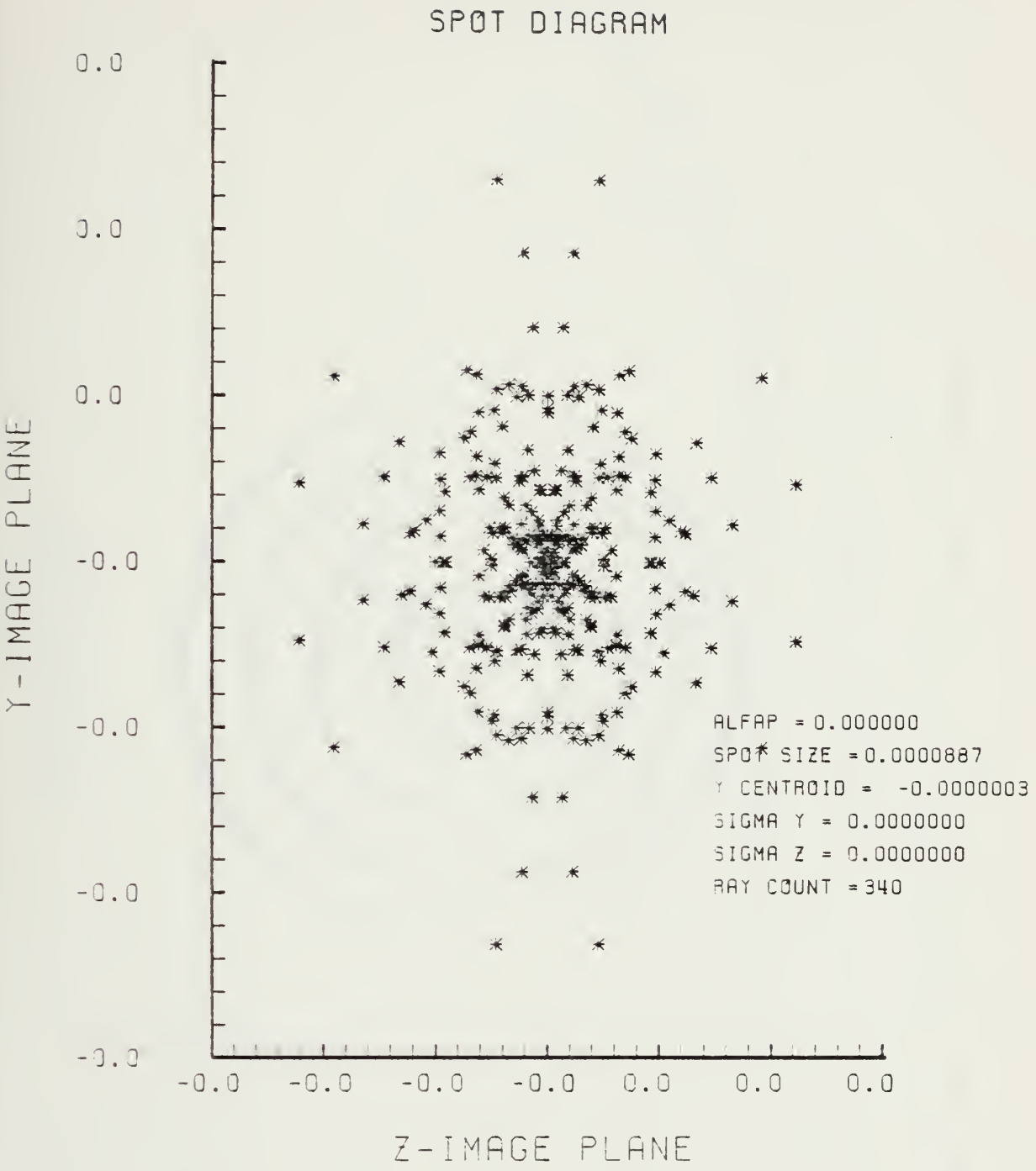

Figure G-3. Spot Diagram for Grid of Figure G-2

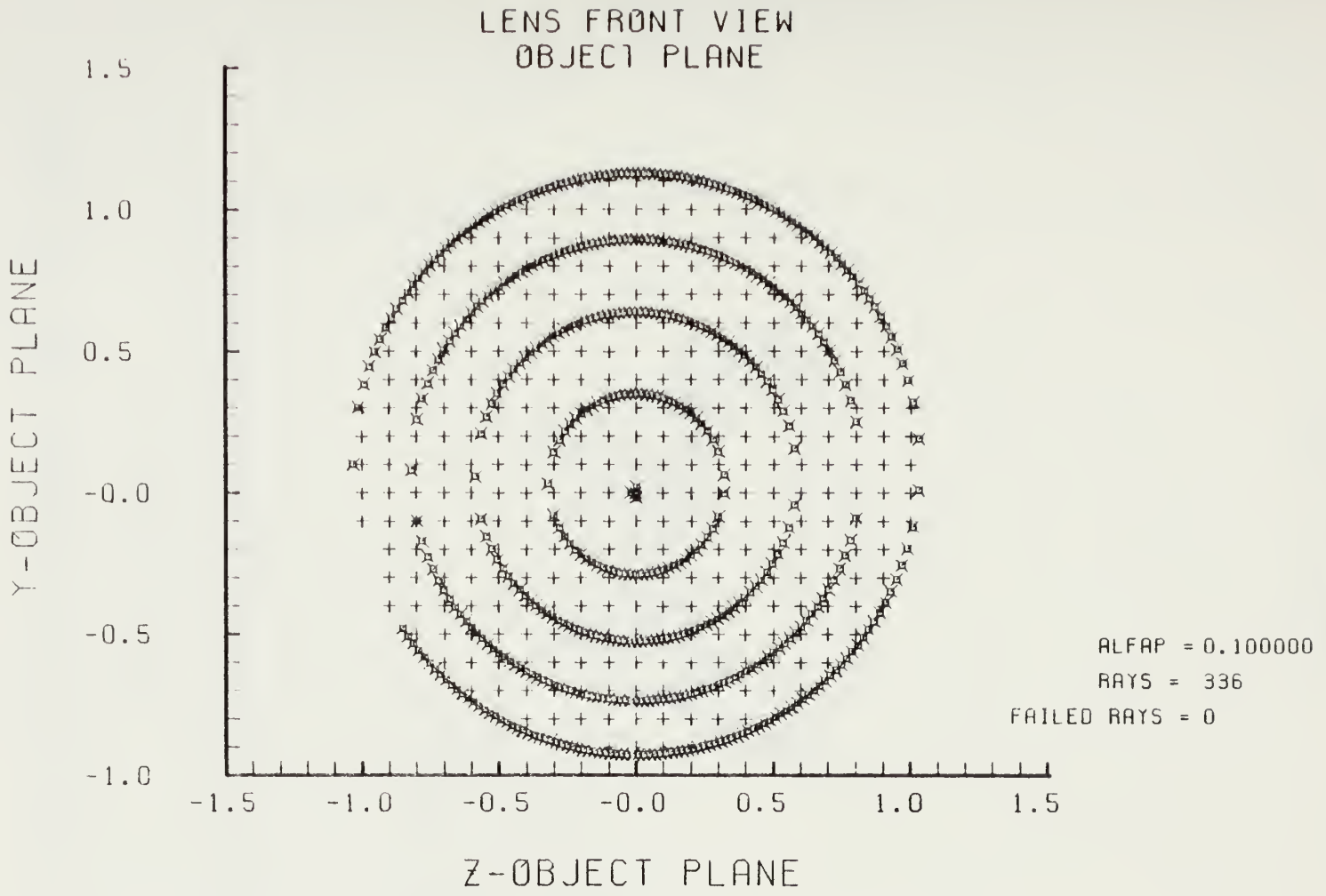

Figure G-4. Grid Plane at α_p = 0.1 for Lens of Figure G-1

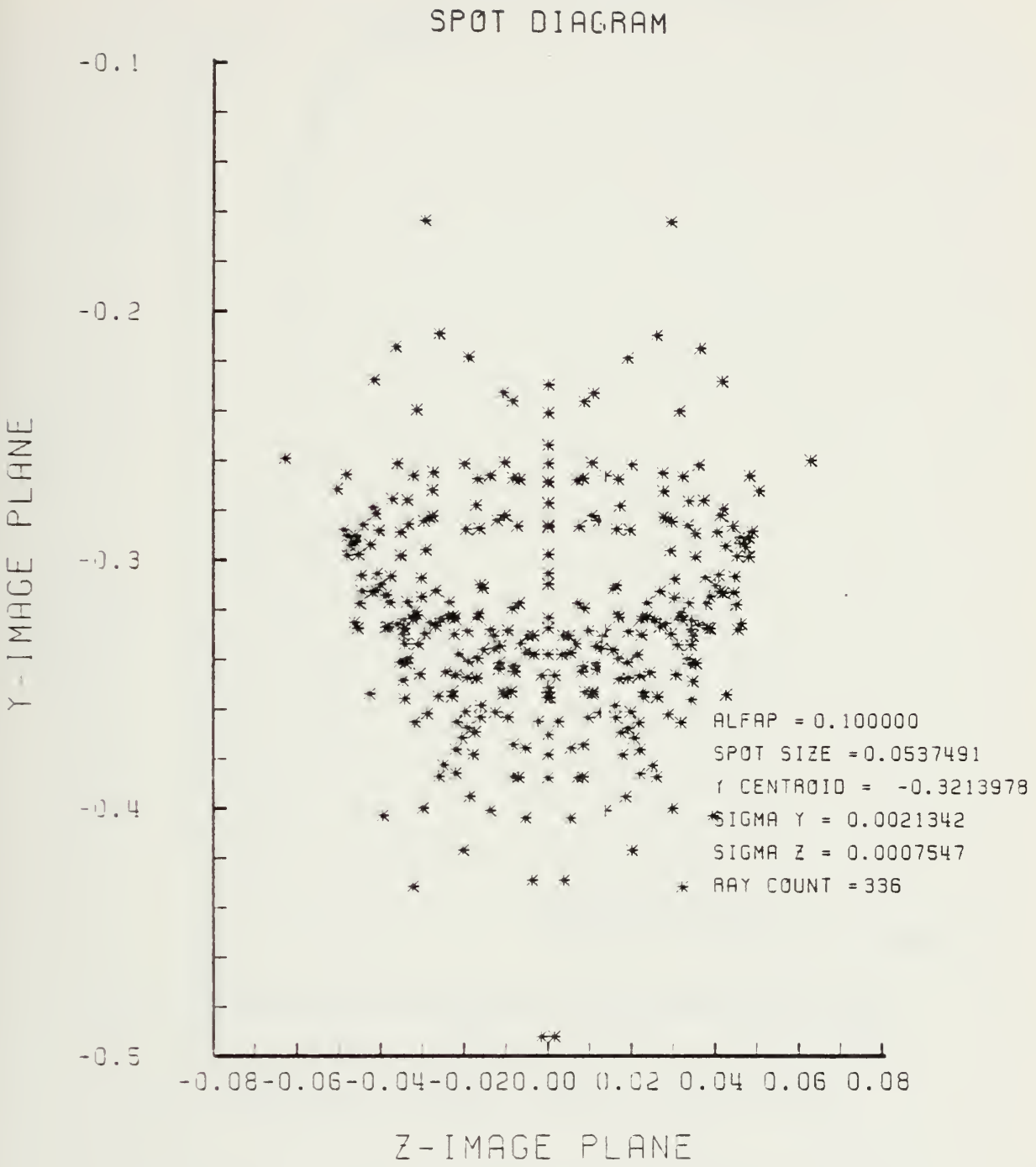

Figure G-5. Spot Diagram for Grid of Figure G-4

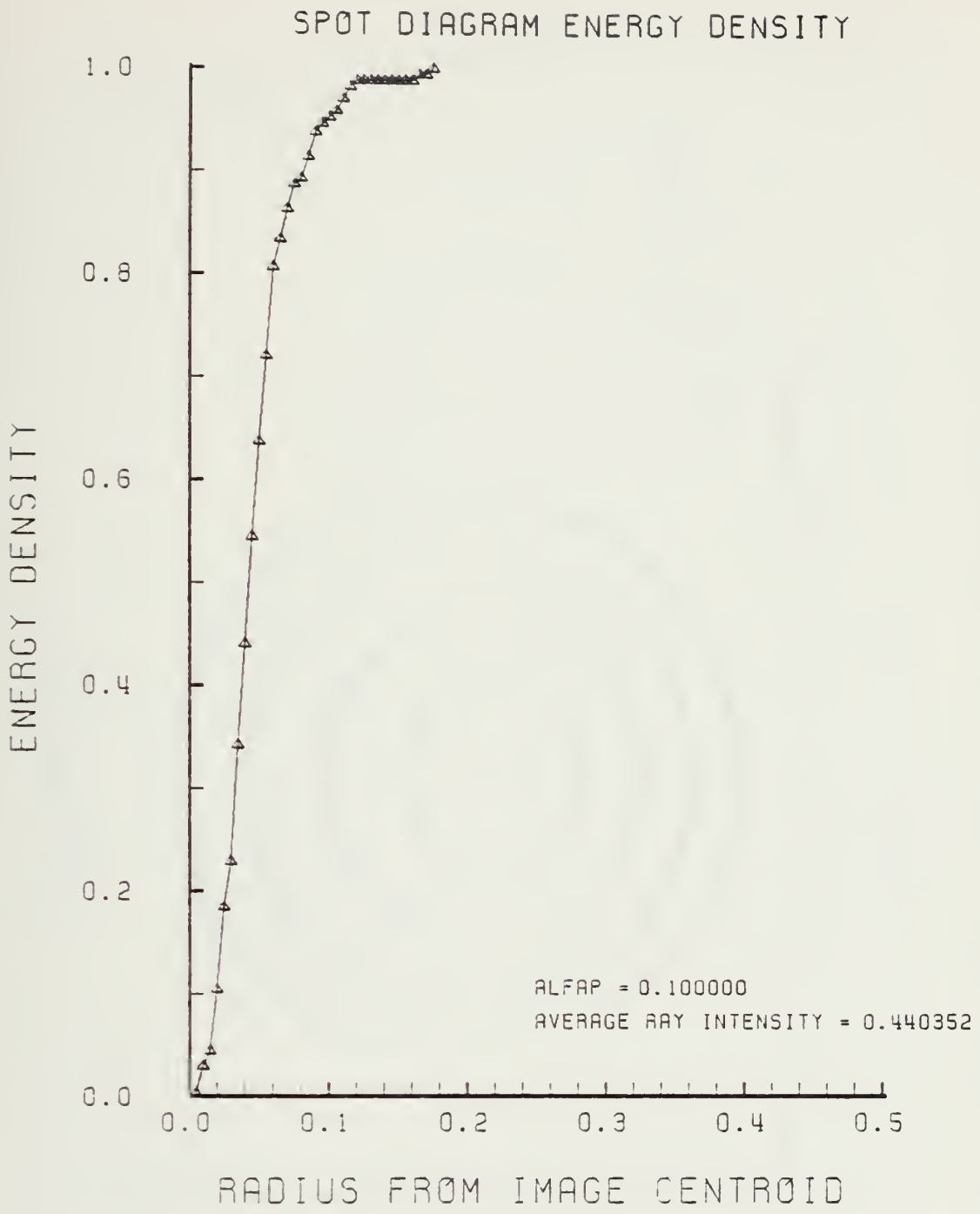

Figure G-6. Encircled Energy of Figure G-5

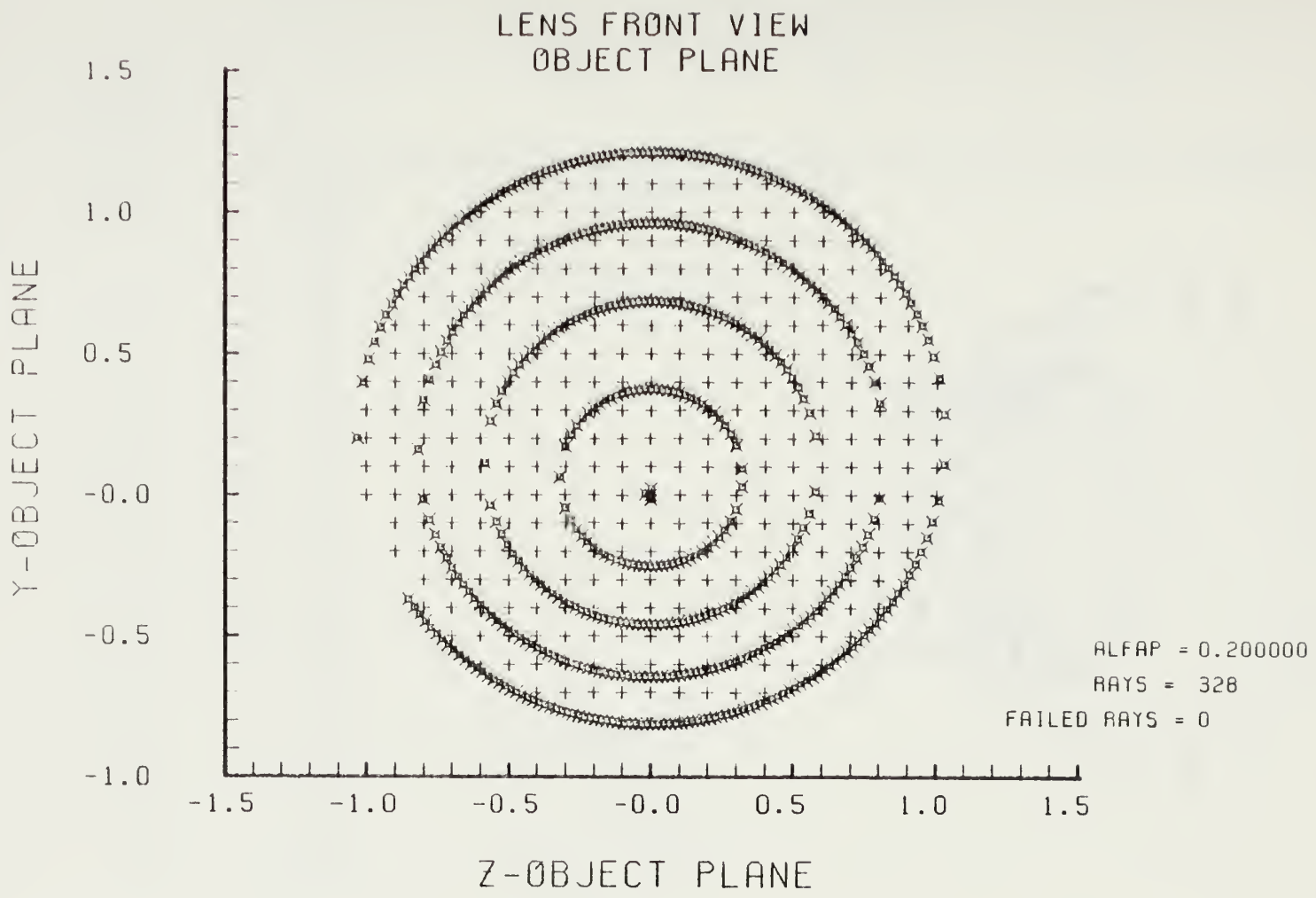

Figure G-7. Grid Plane at α_p = 0.2 for Lens of Figure G-1

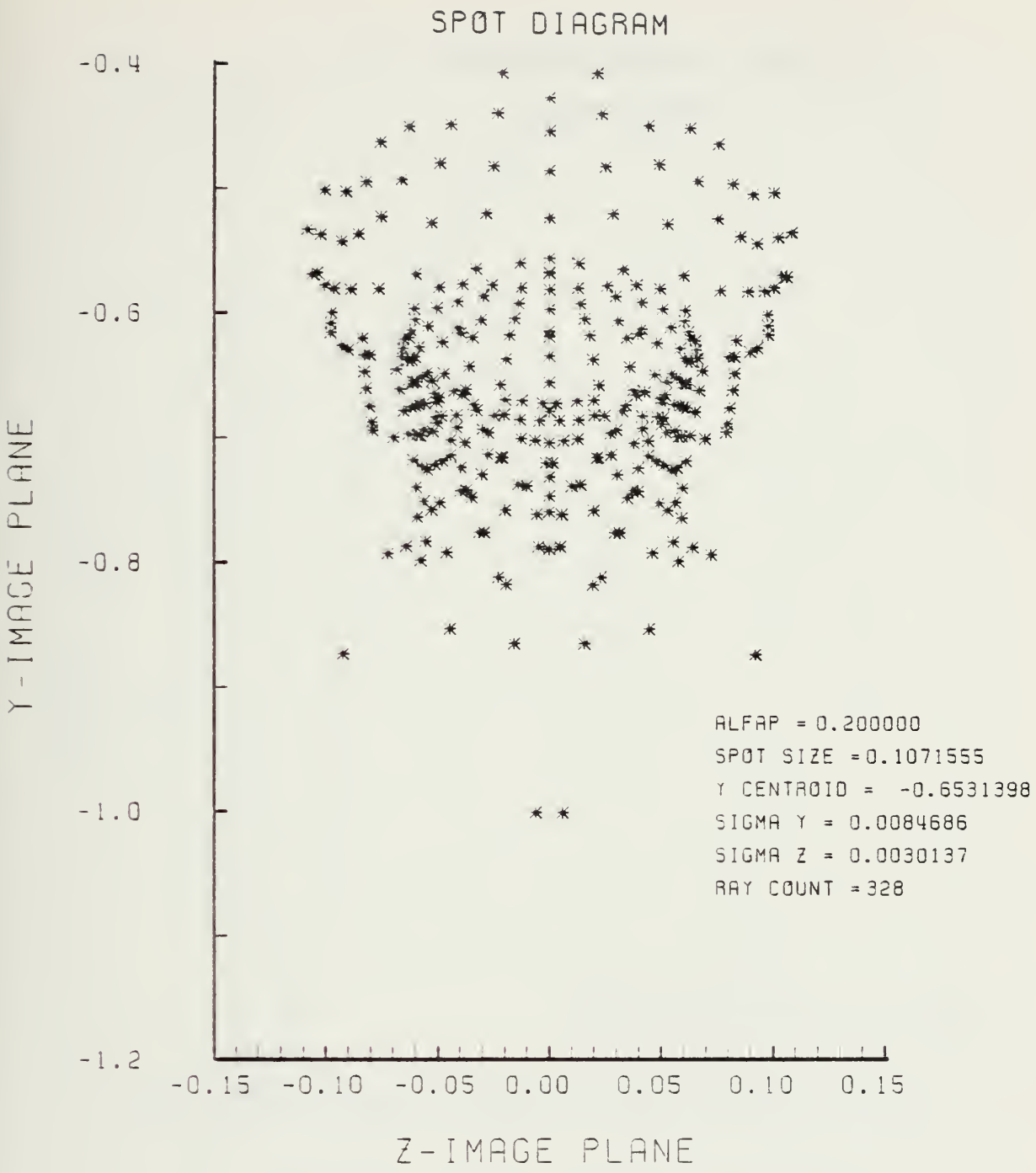

Figure G-8. Spot Diagram for Grid of Figure G-7

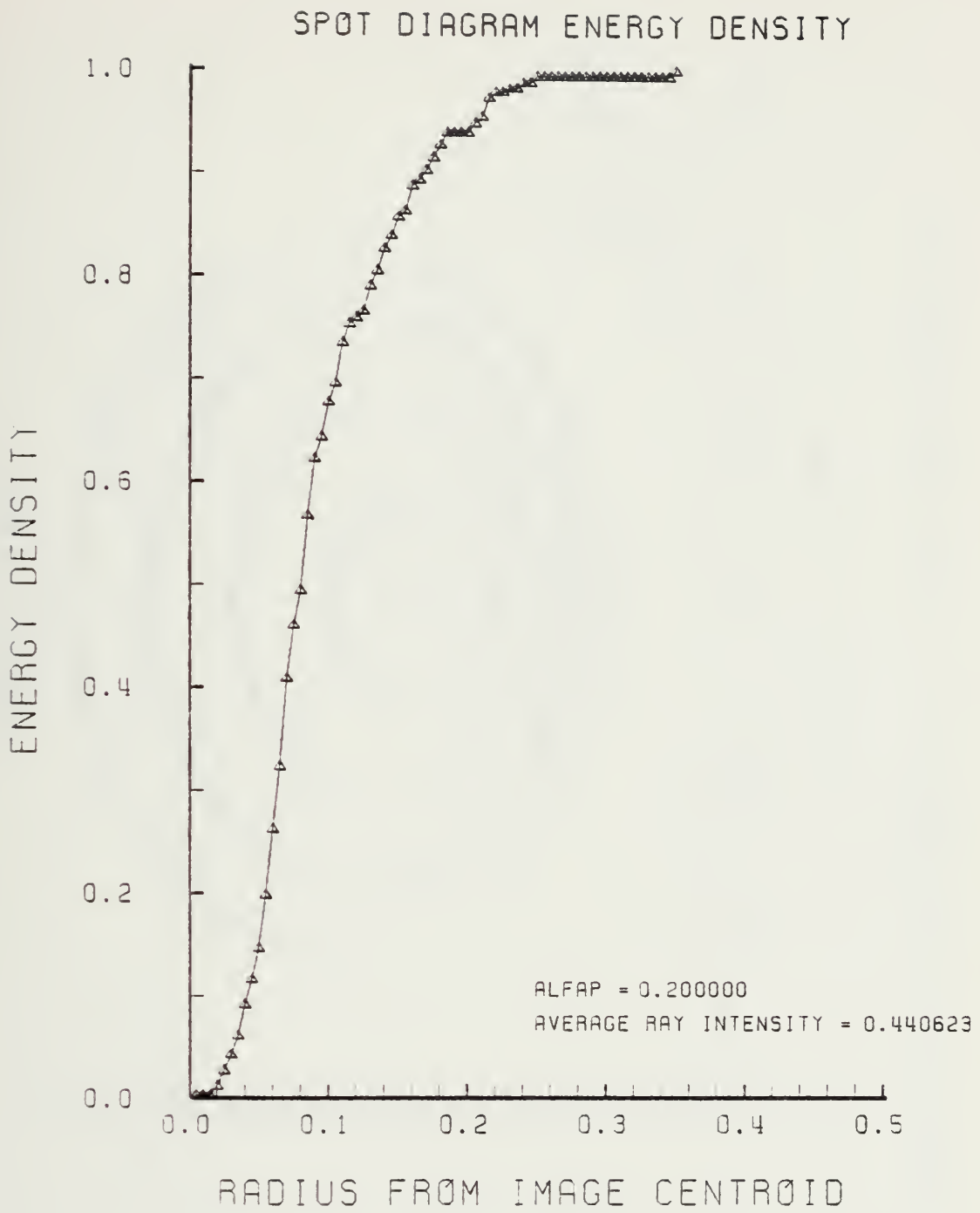

Figure G-9. Encircled Energy of Figure G-8

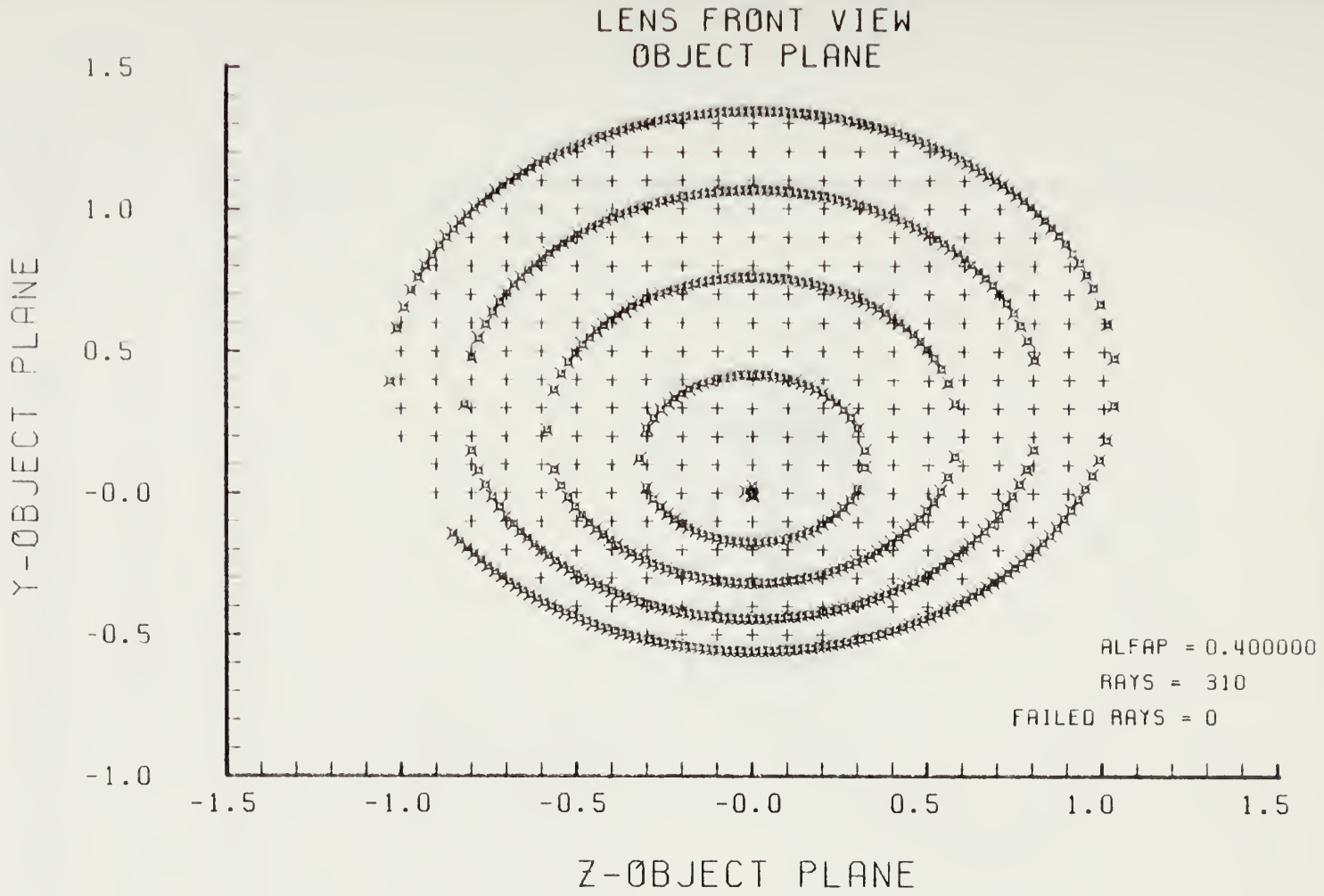

Figure G-10. Grid Plane at $\alpha_p = 0.4$ for Lens of Figure G-1

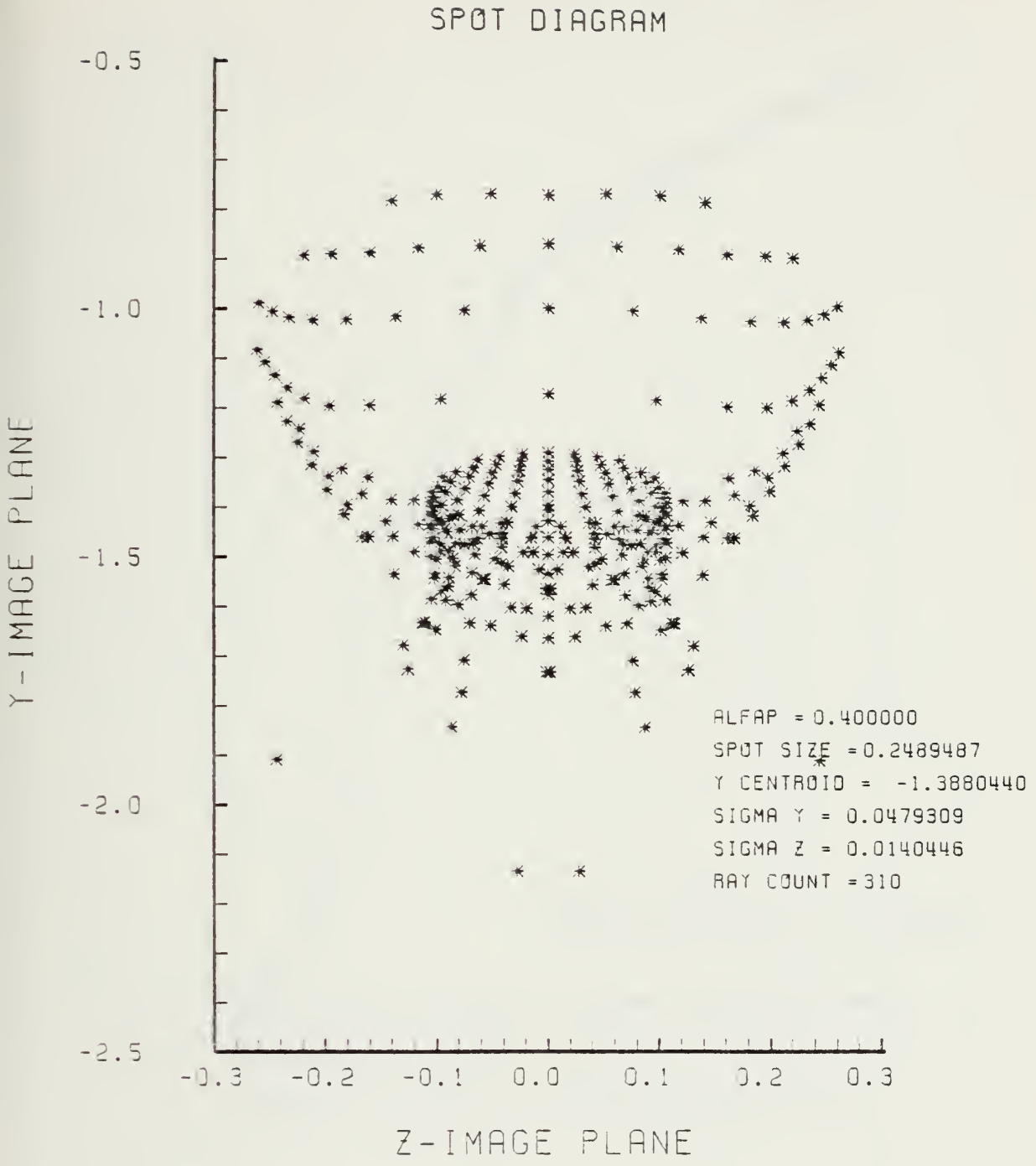

Figure G-11. Spot Diagram for Grid of Figure G-10

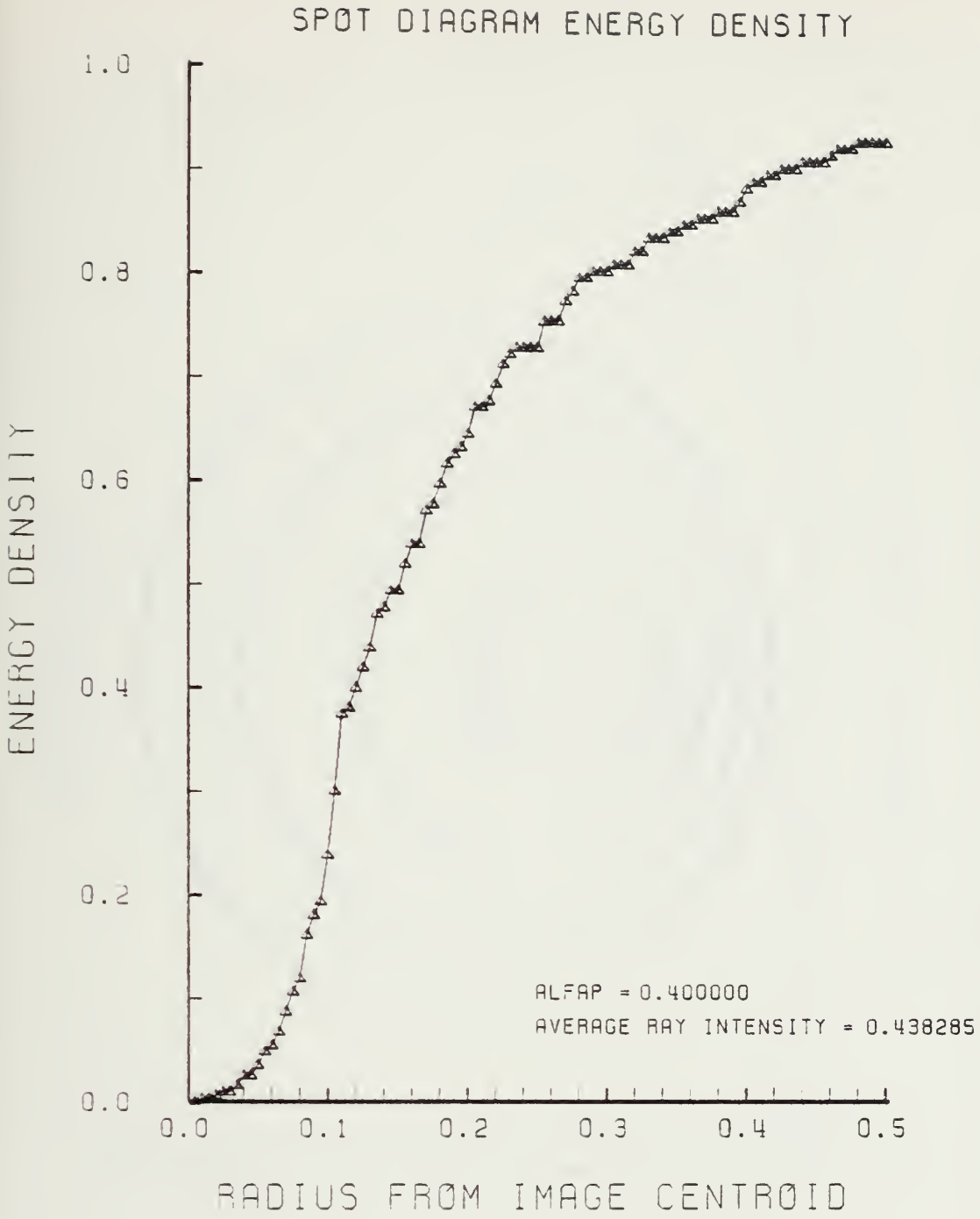

Figure G-12. Encircled Energy of Figure G-11

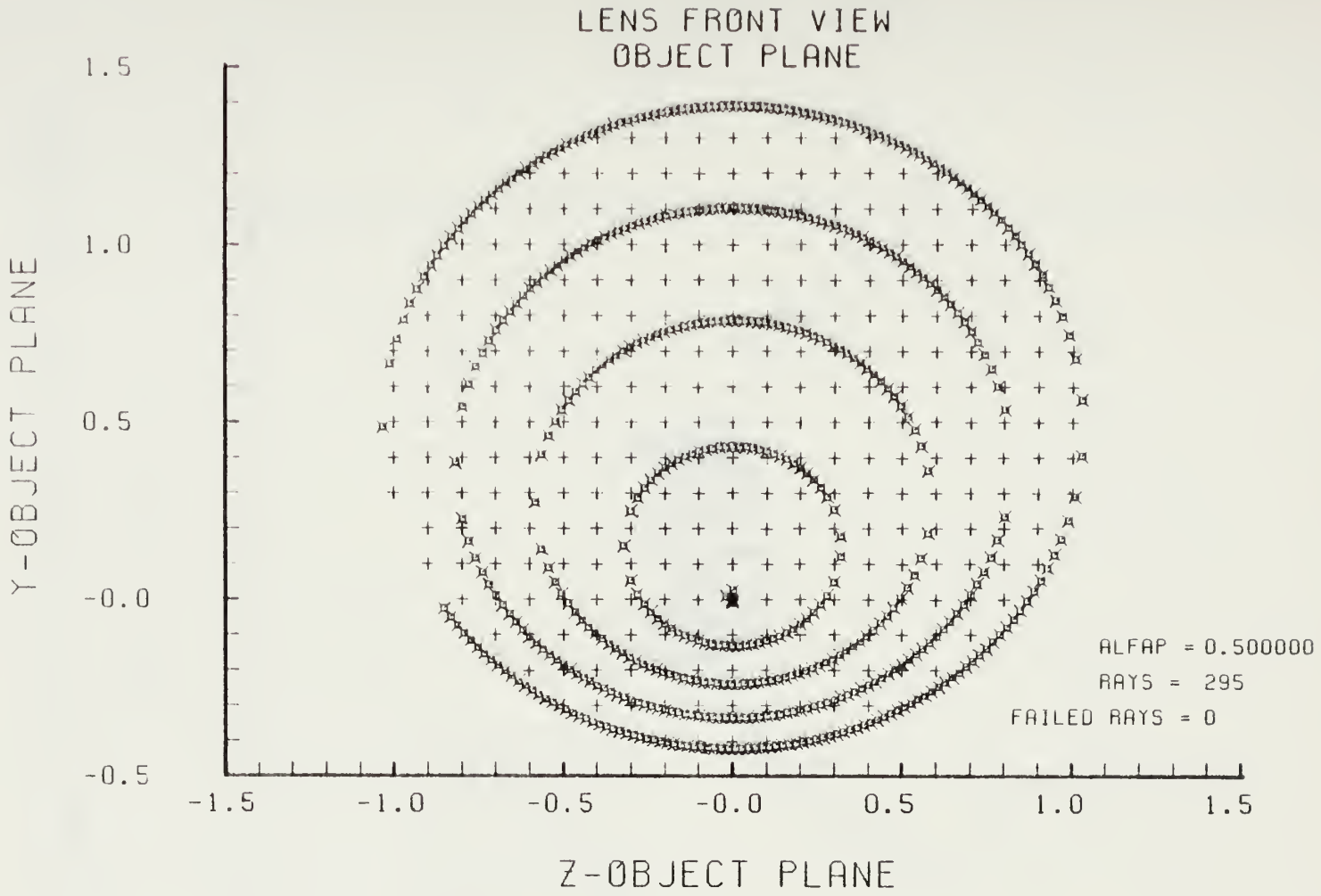

Figure G-13. Grid Plane at α_p = 0.5 for Lens of Figure G-1

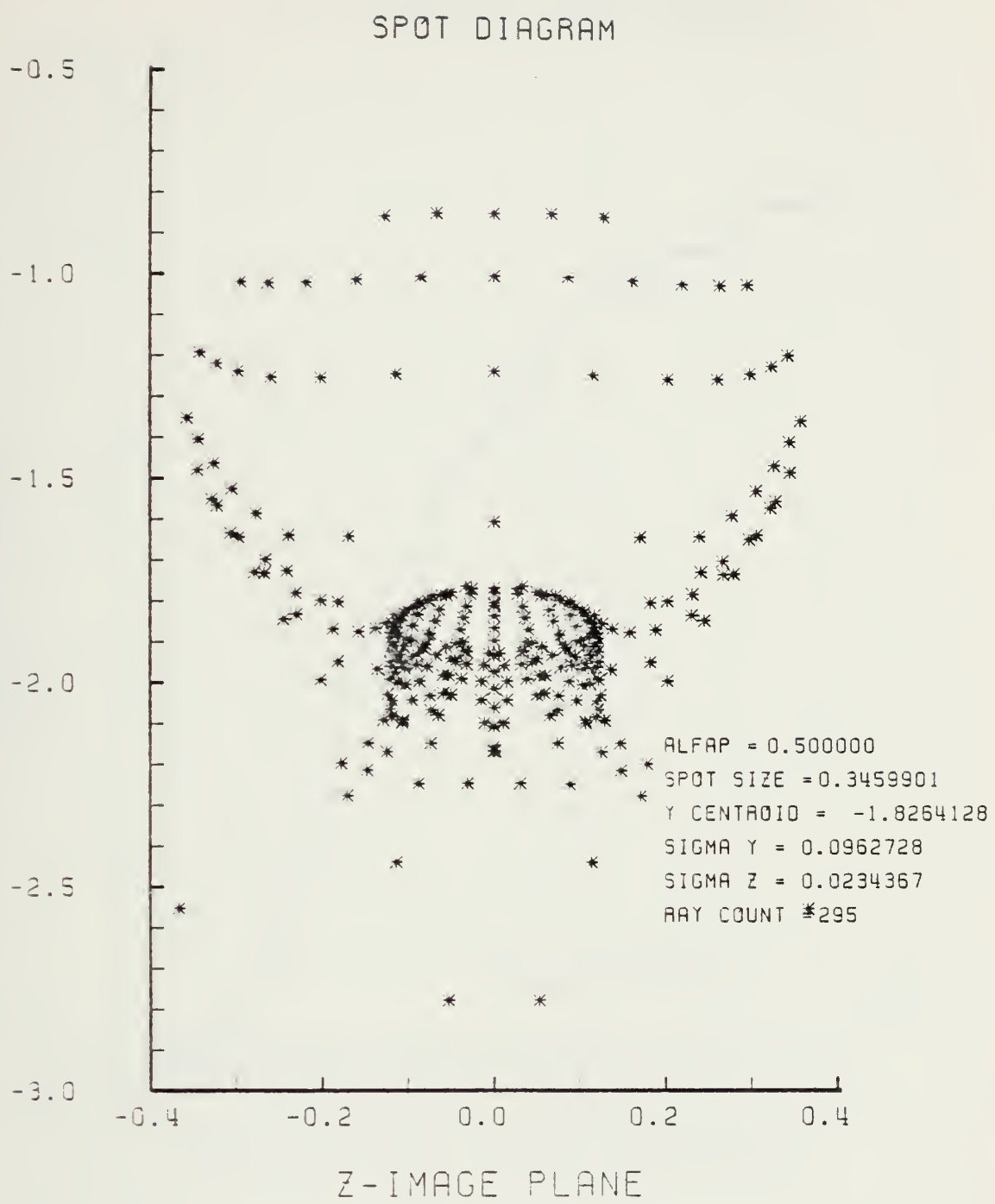

Figure G-14. Spot Diagram for Grid of Figure G-13

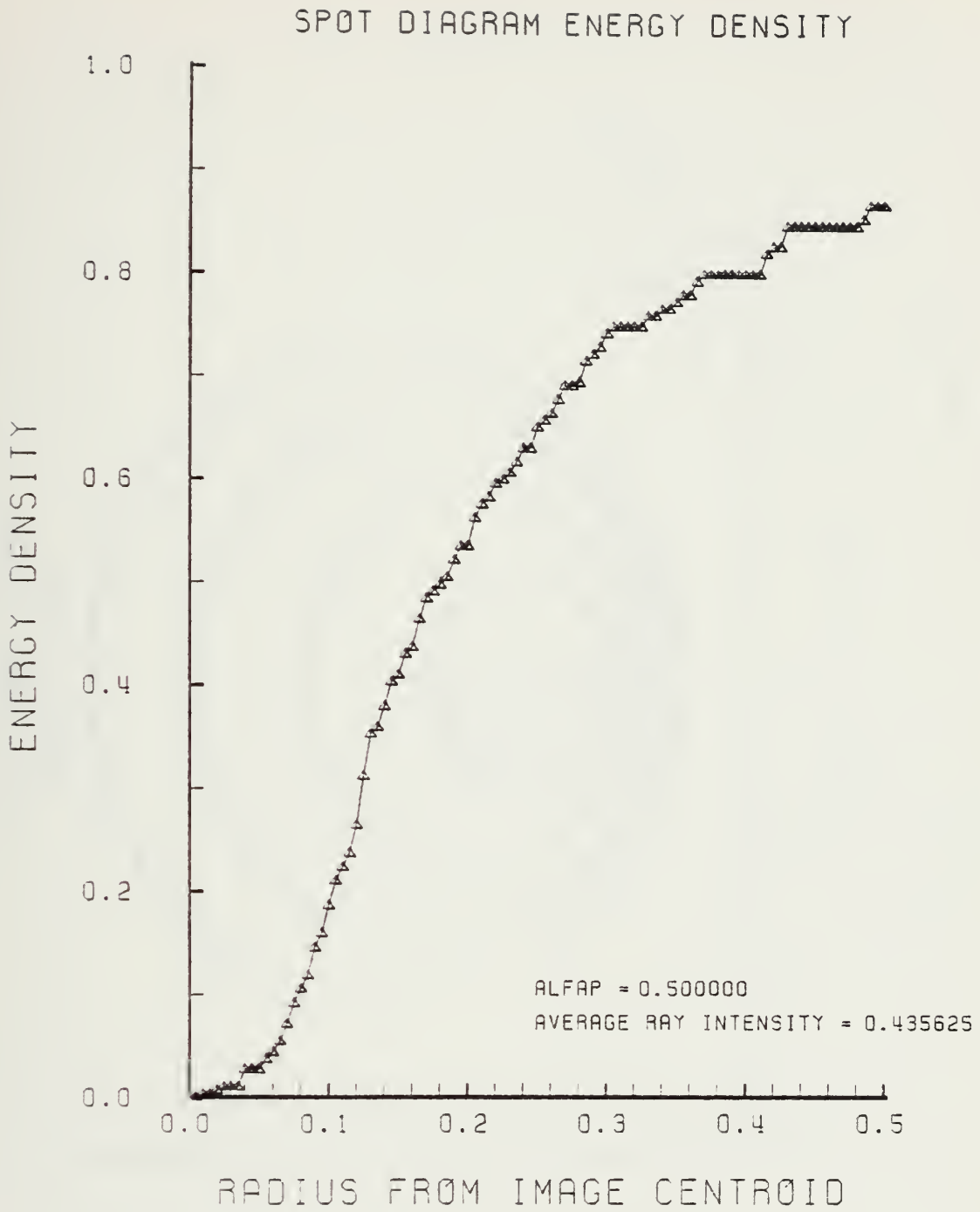

Figure G-15. Encircled Energy of Figure G-14

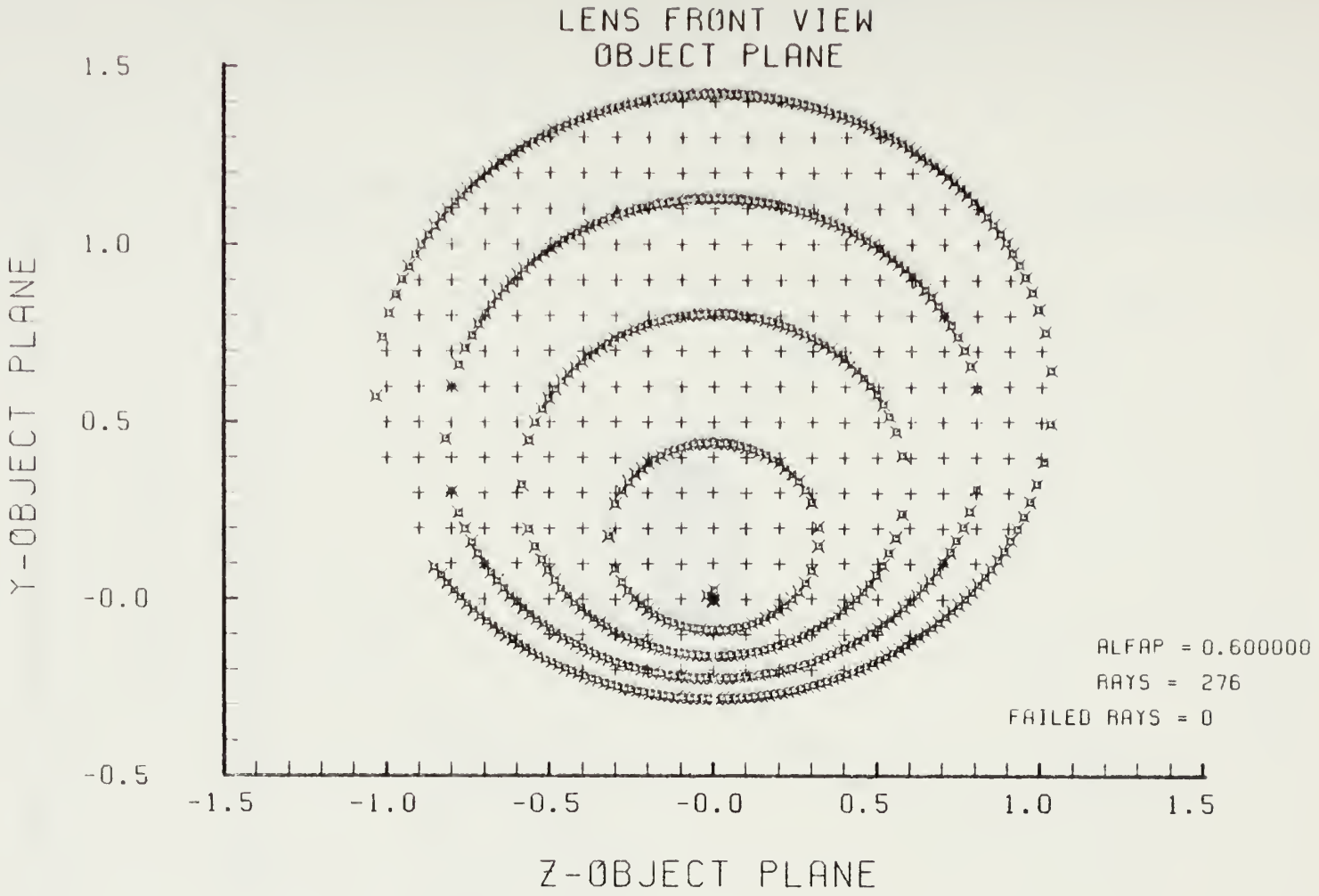

Figure G-16. Grid Plane at $\alpha_p = 0.7$ for Lens of Figure G-1

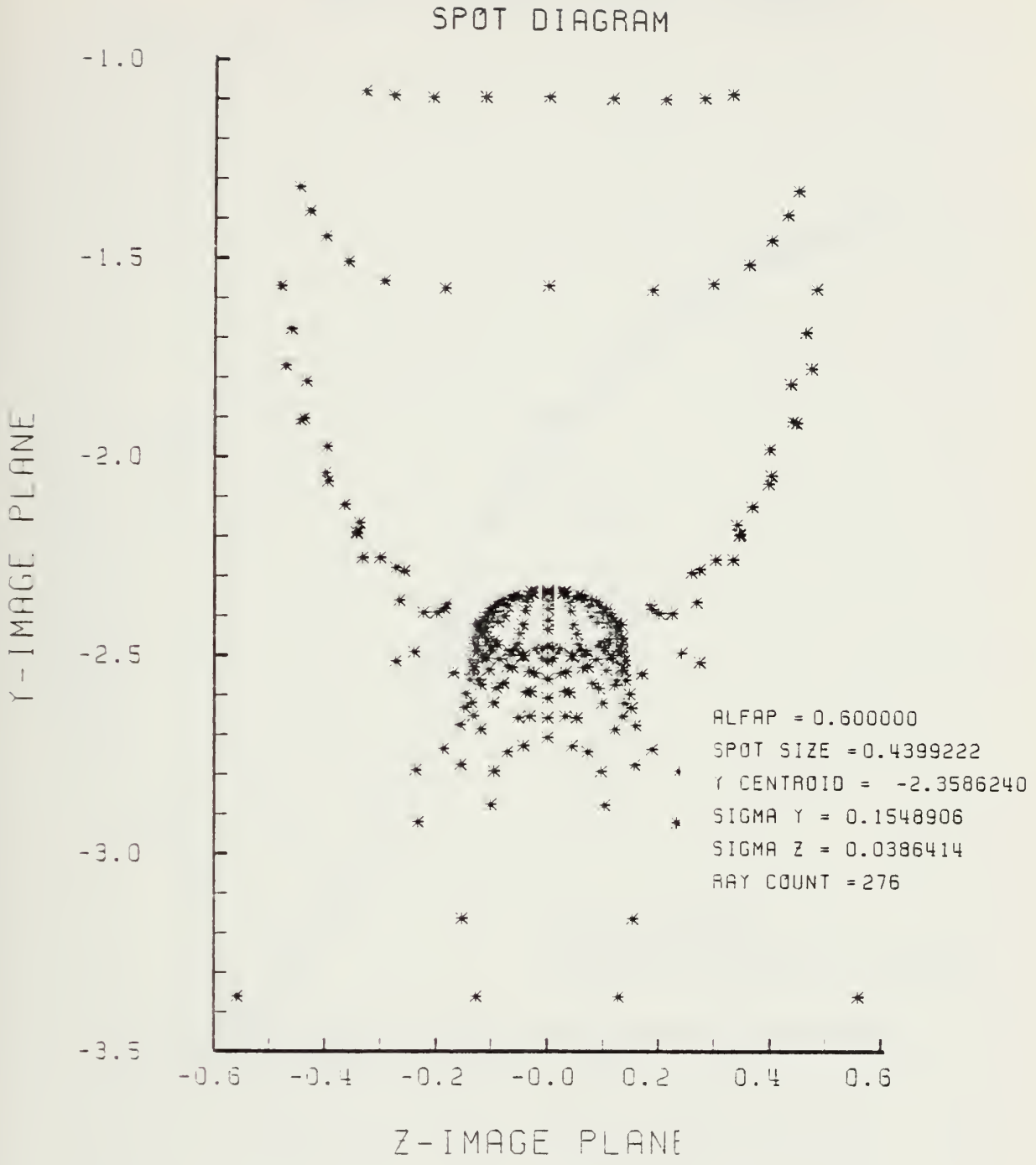

Figure G-17. Spot Diagram for Grid of Figure G-16

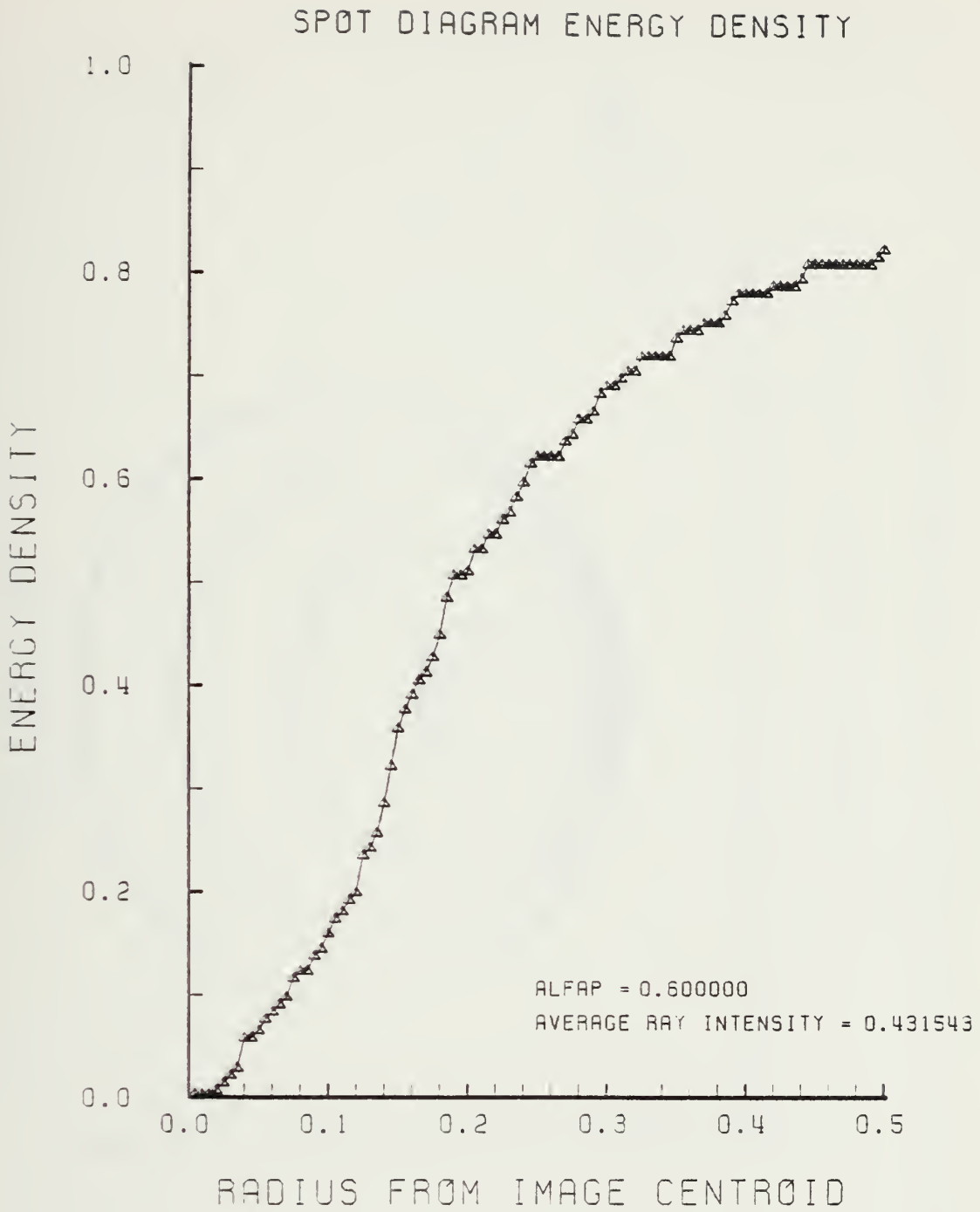

Figure G-18. Encircled Energy of Figure G-17

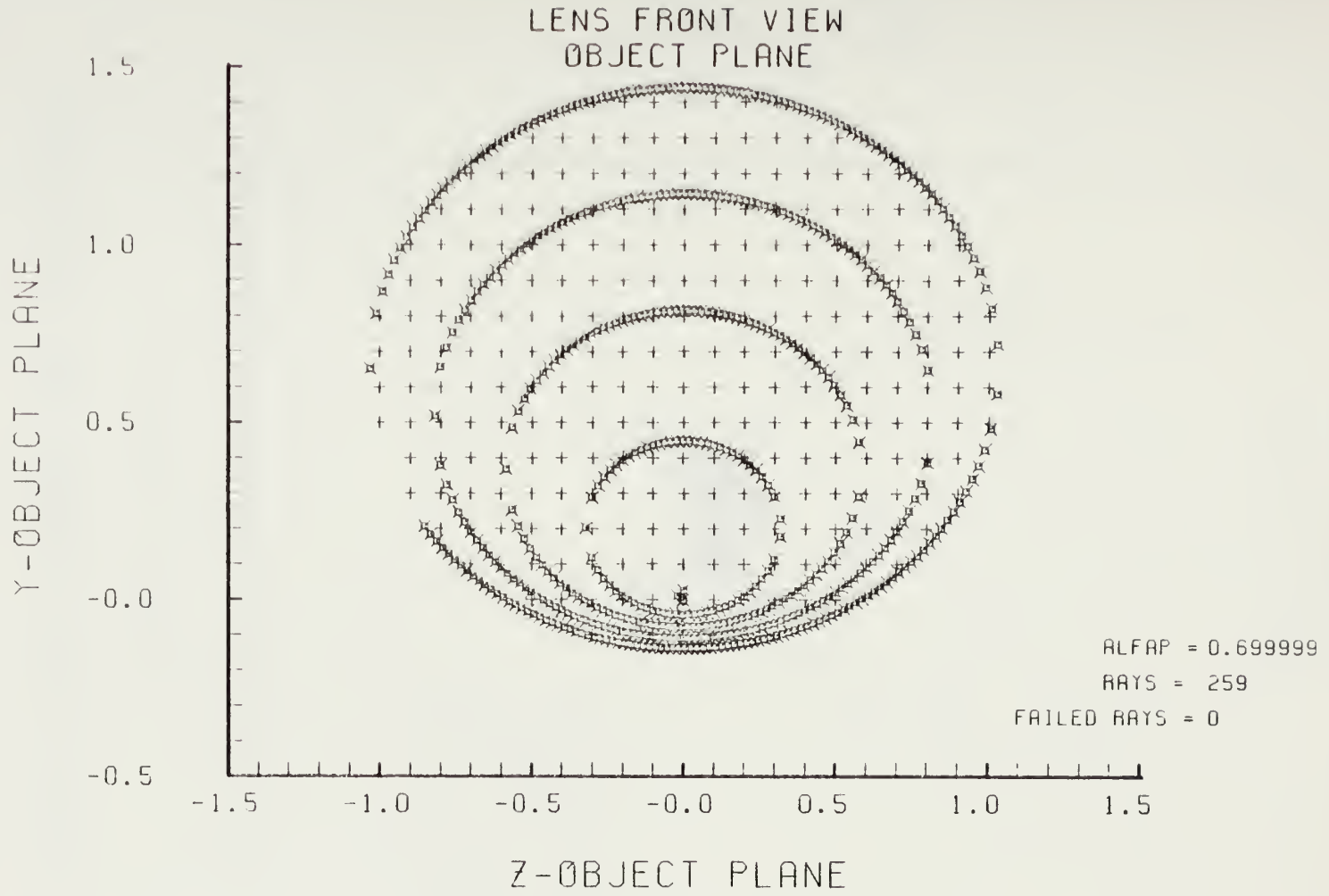

Figure G-19. Grid Plane at α_p = 0.7 for Lens of Figure G-1

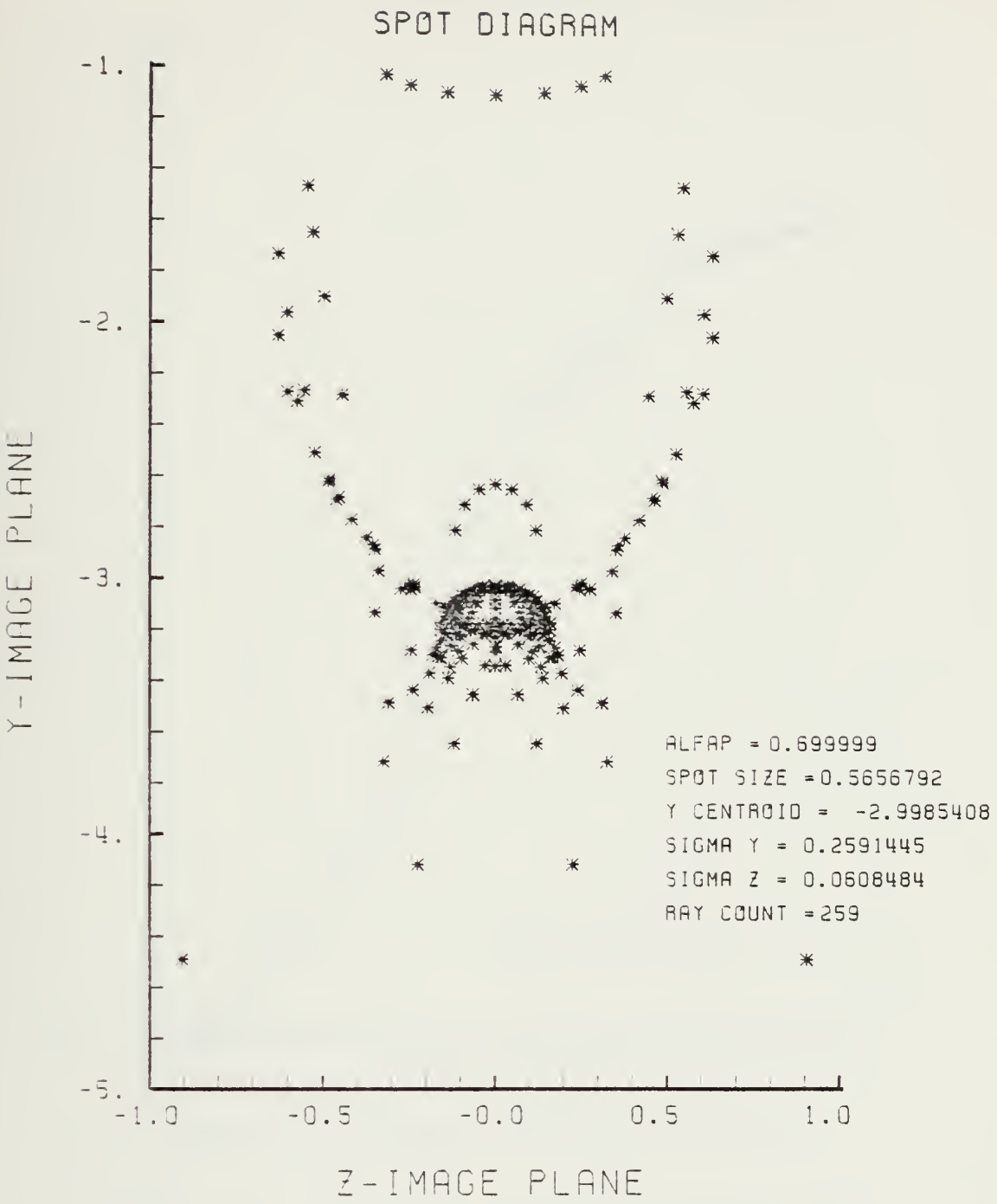

Figure G-20. Spot Diagram for Grid of Figure G-19

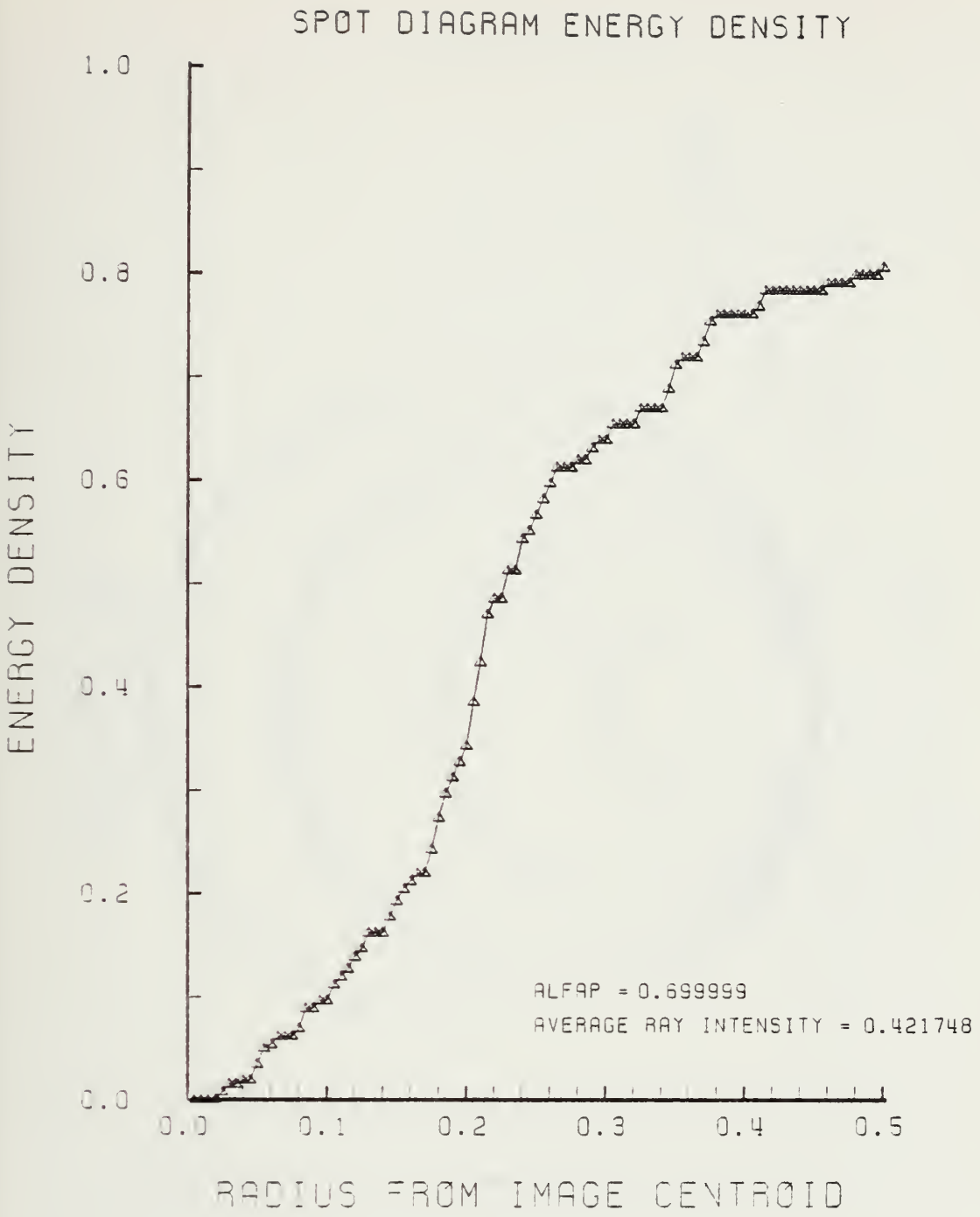

Figure G-21. Encircled Energy of Figure G-20

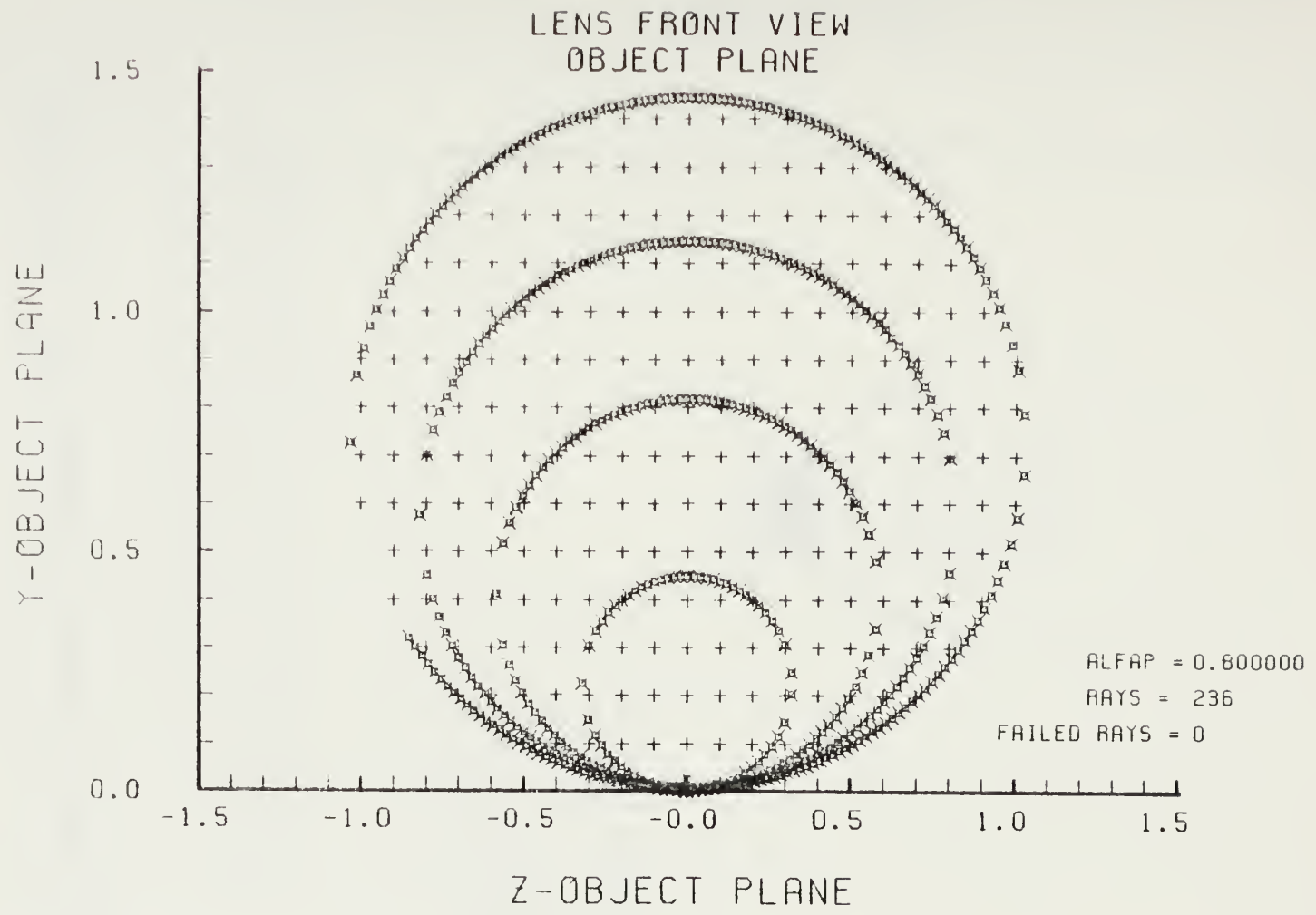

Figure G-22. Grid Plane at $\alpha_p = 0.8$ for Lens of Figure G-1

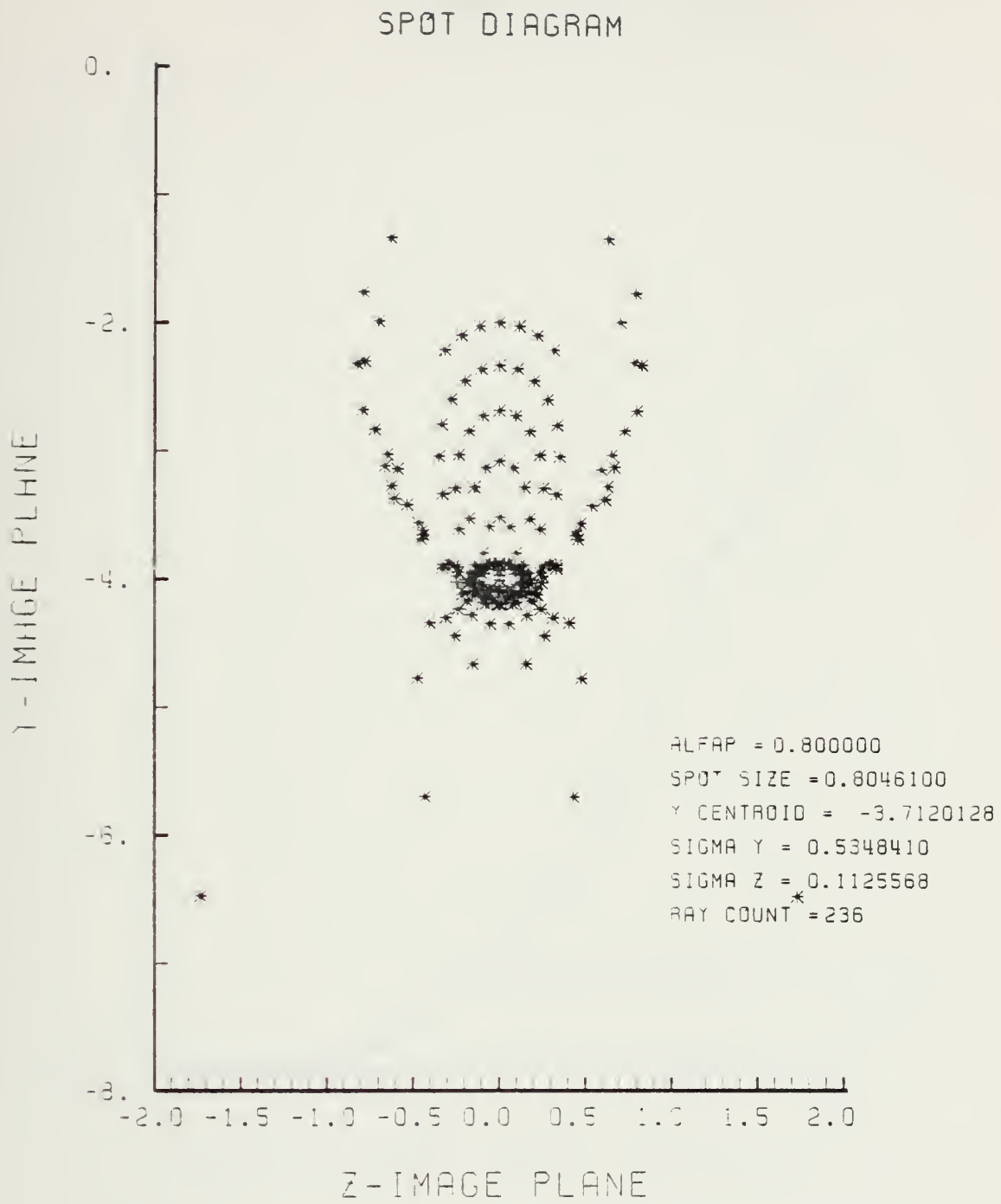

Figure G-23. Spot Diagram for Grid of Figure G-22

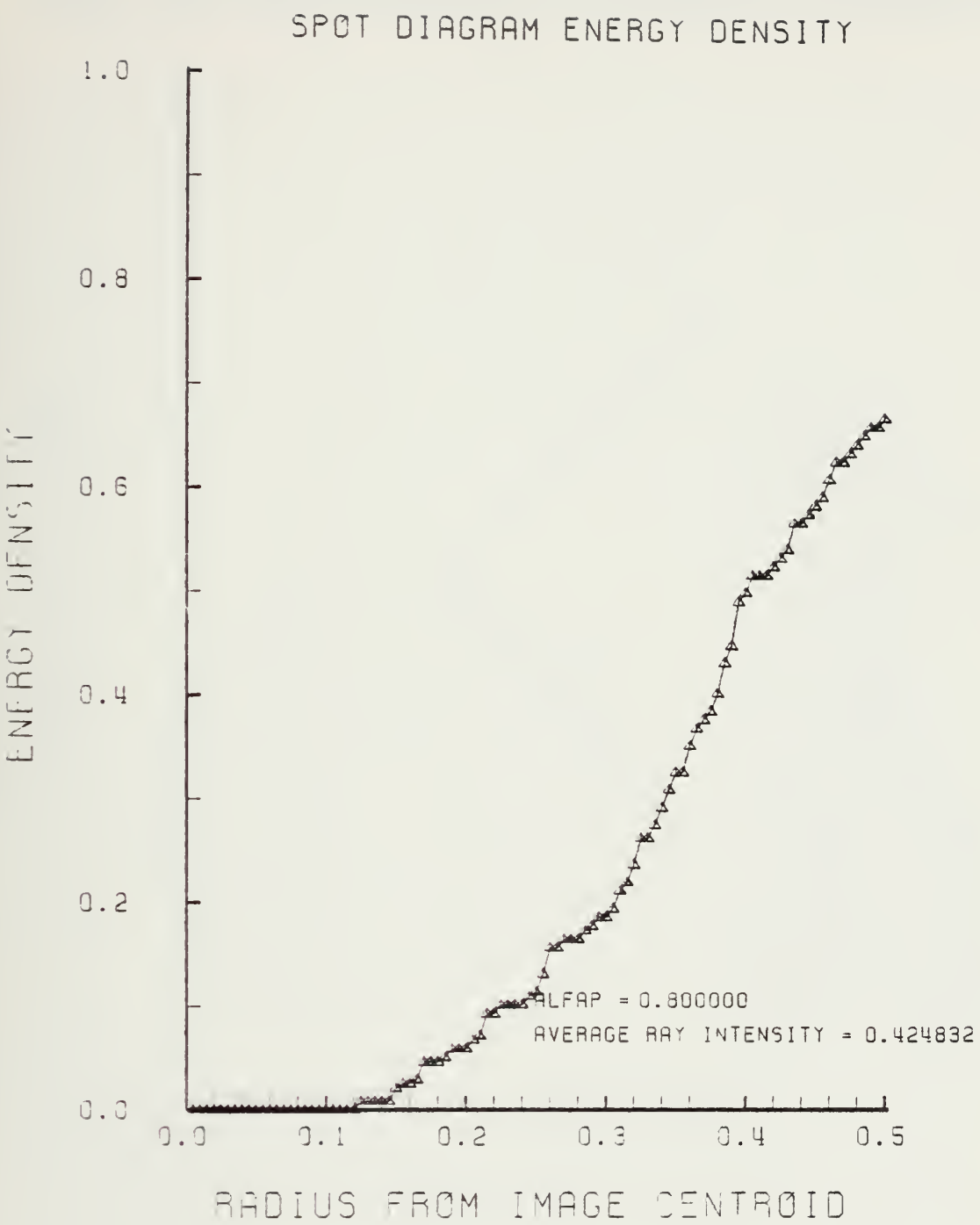

Figure G-24. Encircled Energy of Figure G-23

APPENDIX H

"BEST" GRIN LENS PERFORMANCE PLOTS IN THE F/1 CONFIGURATION

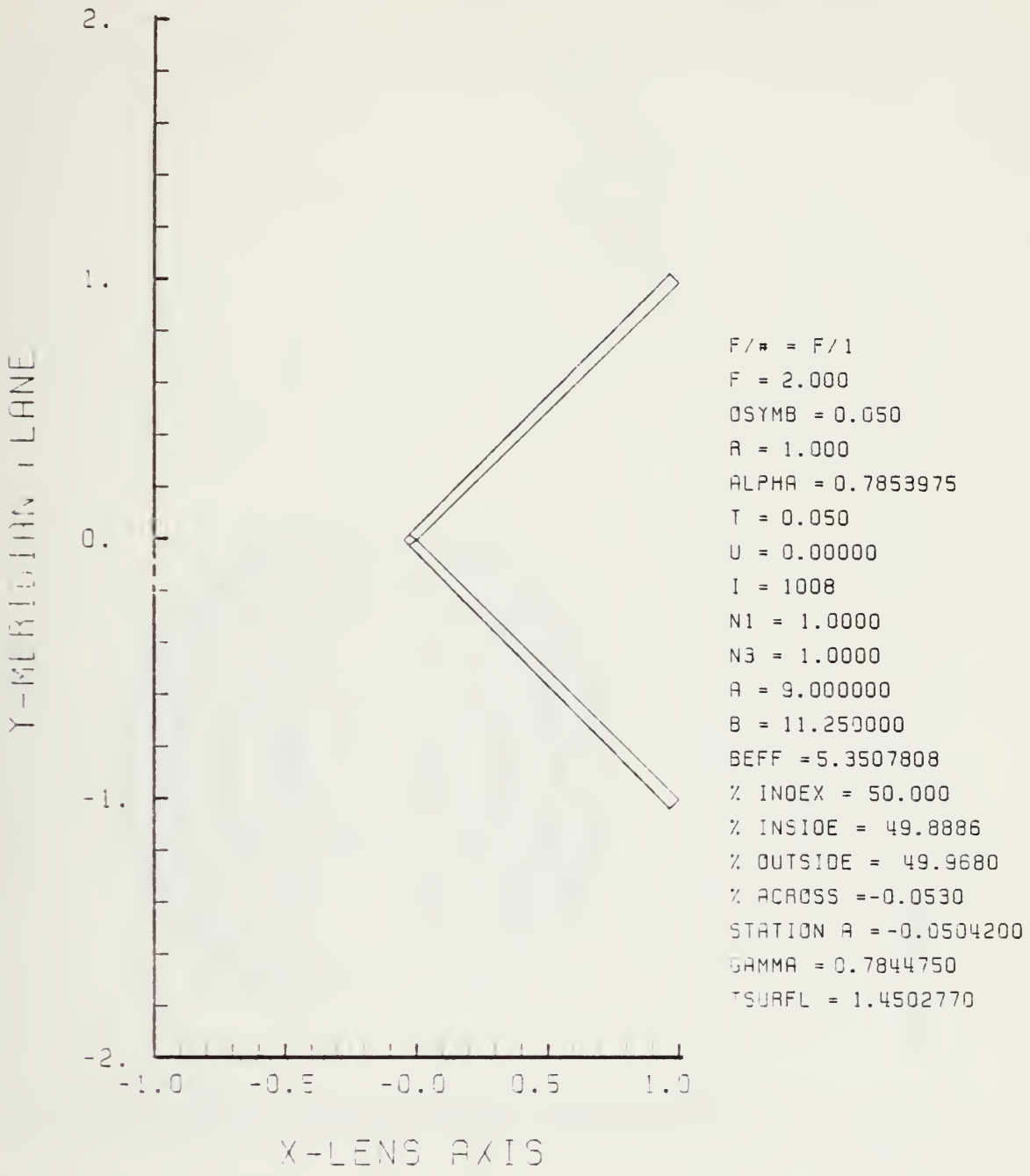

Figure H-1. "Best" GRIN Lens Shape with 50% Gradient, OB = 0.05, and a = 9.00 in the F/1 Configuration

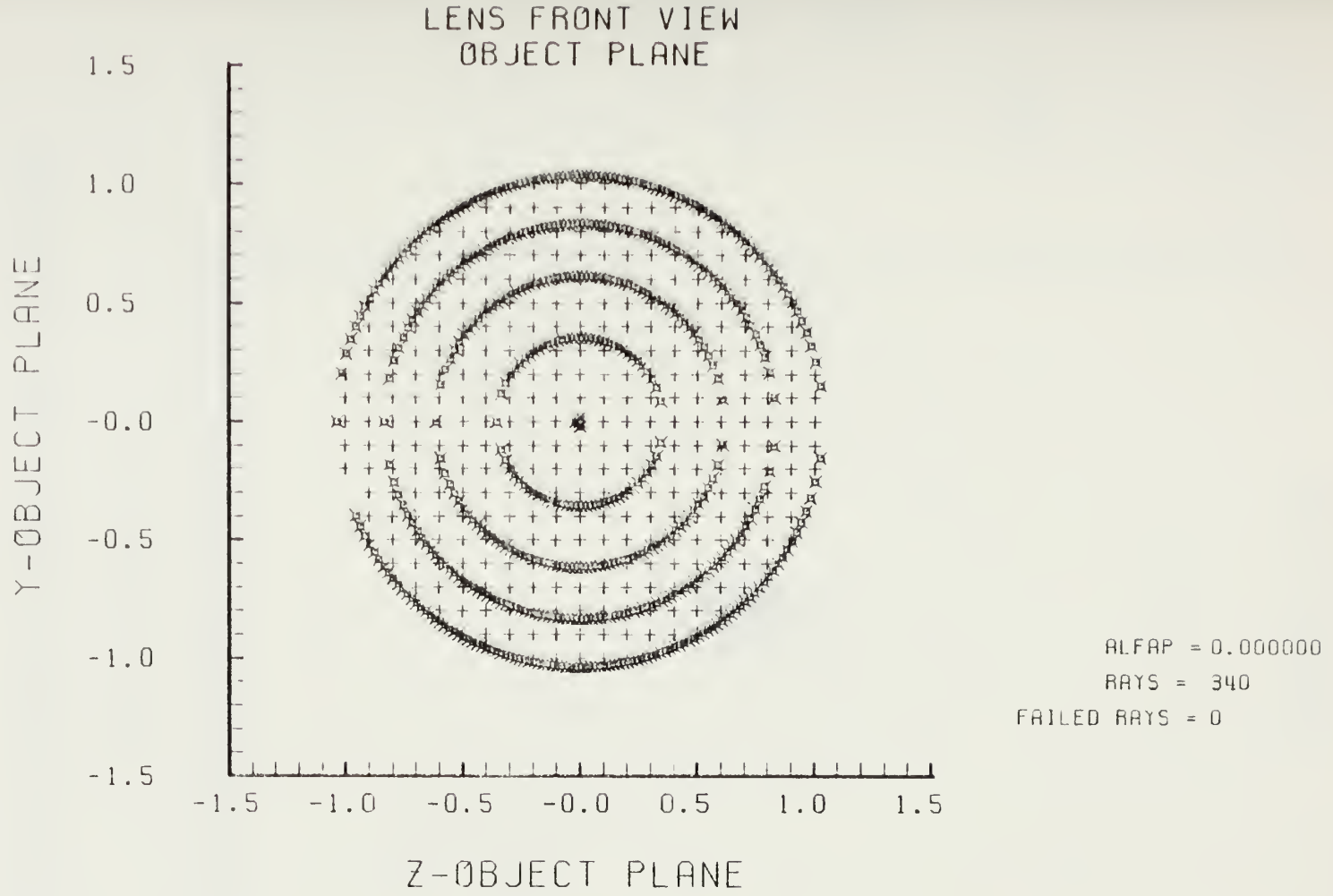

Figure H-2. Grid Plane at $\alpha_p = 0.0$ for Lens of Figure H-1

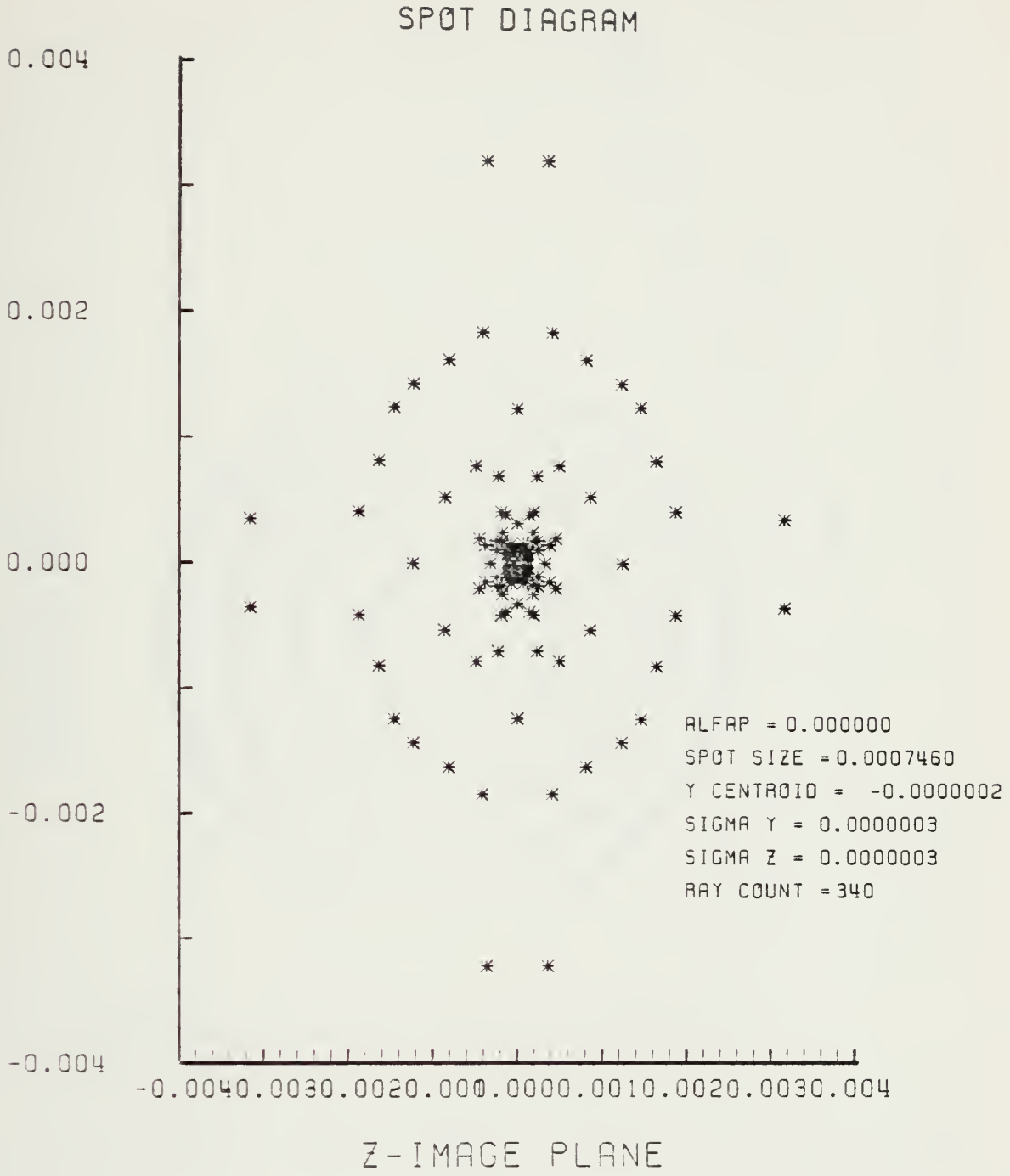

Figure H-3. Spot Diagram for Grid of Figure H-2

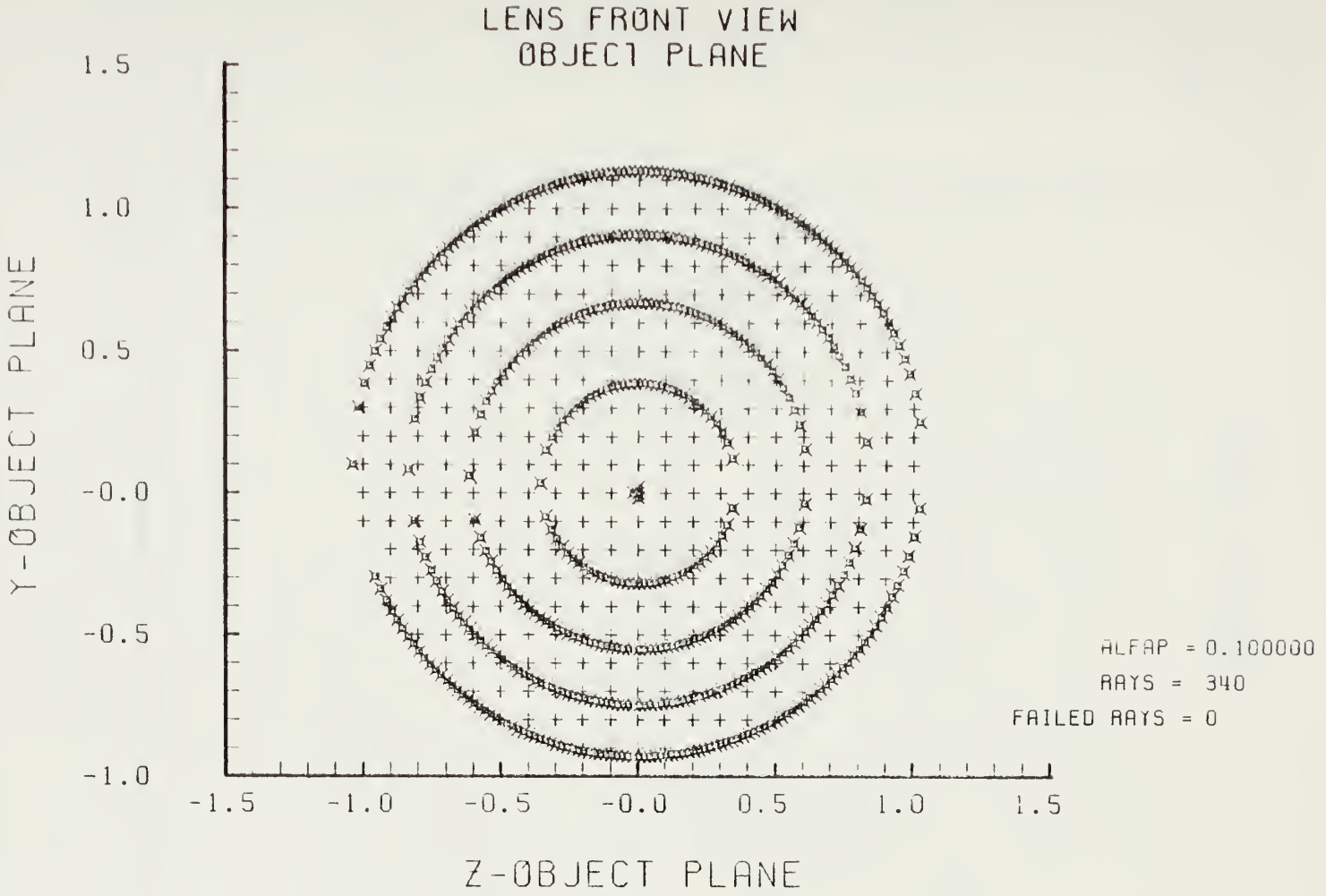

Figure H-4. Grid Plane at α_p = 0.1 for Lens of Figure H-1

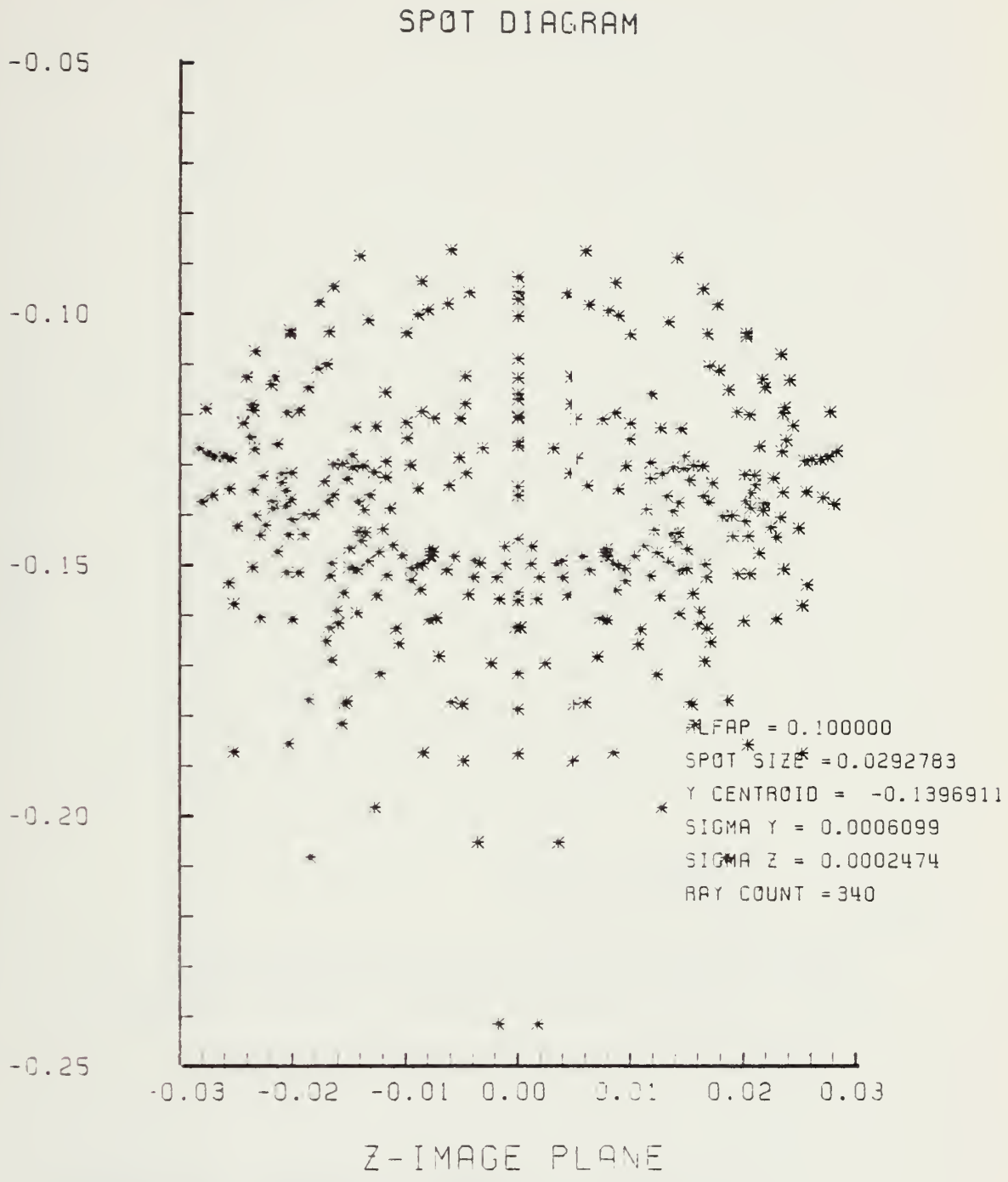

Figure H-5. Spot Diagram for Grid of Figure H-4

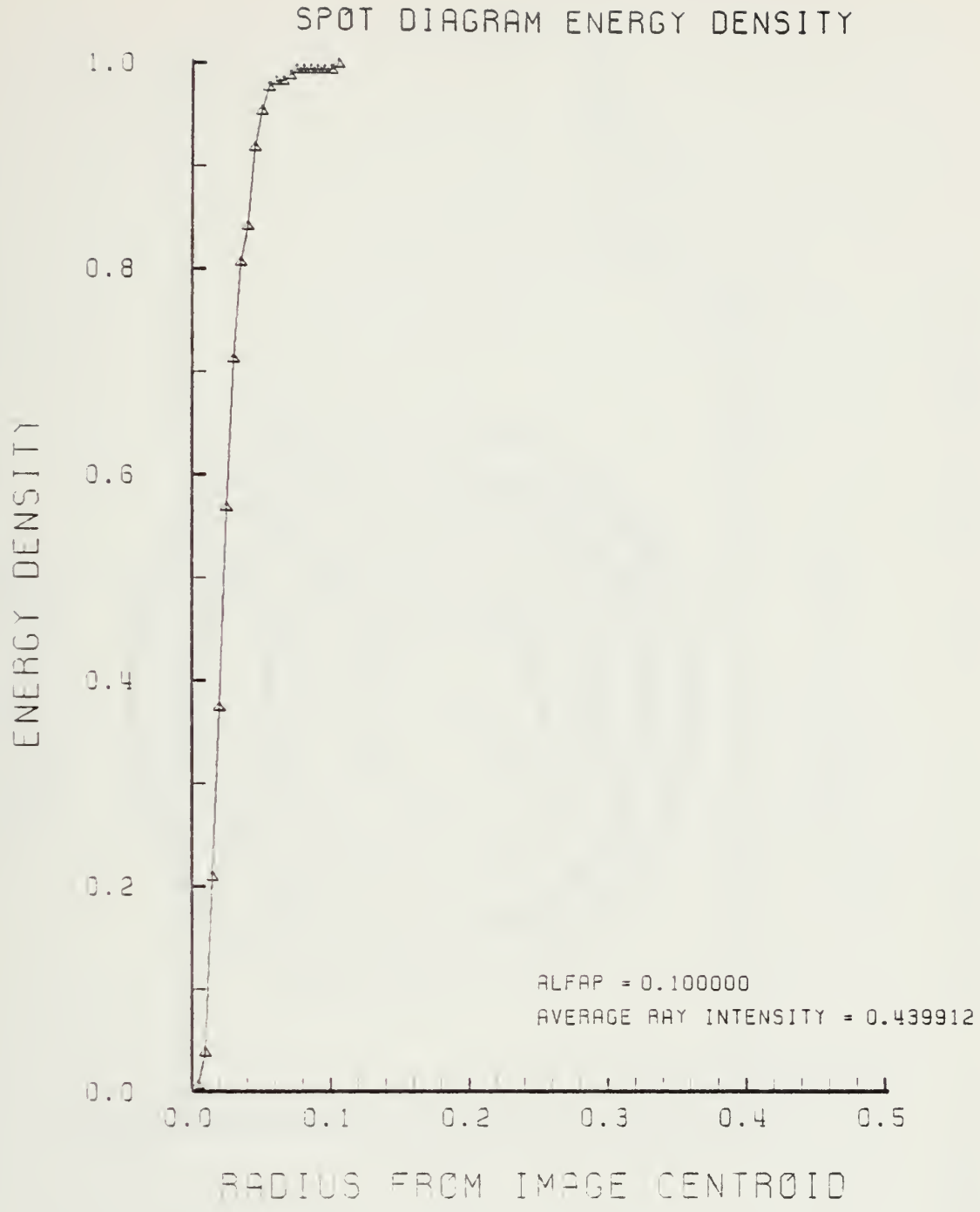

Figure H-6. Encircled Energy of Figure H-5

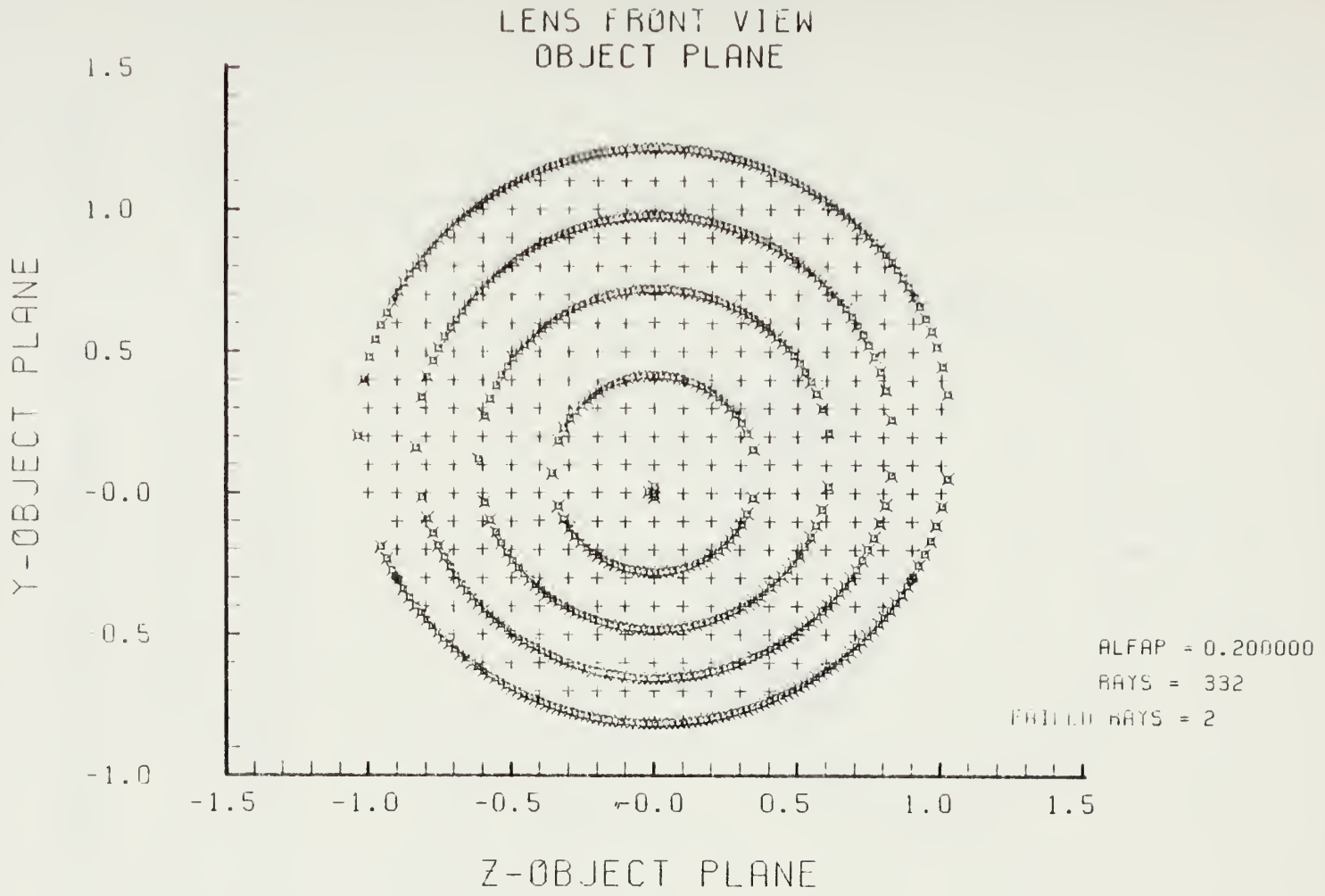

Figure H-7. Grid Plane at α_p = 0.2 for Lens of Figure H-1

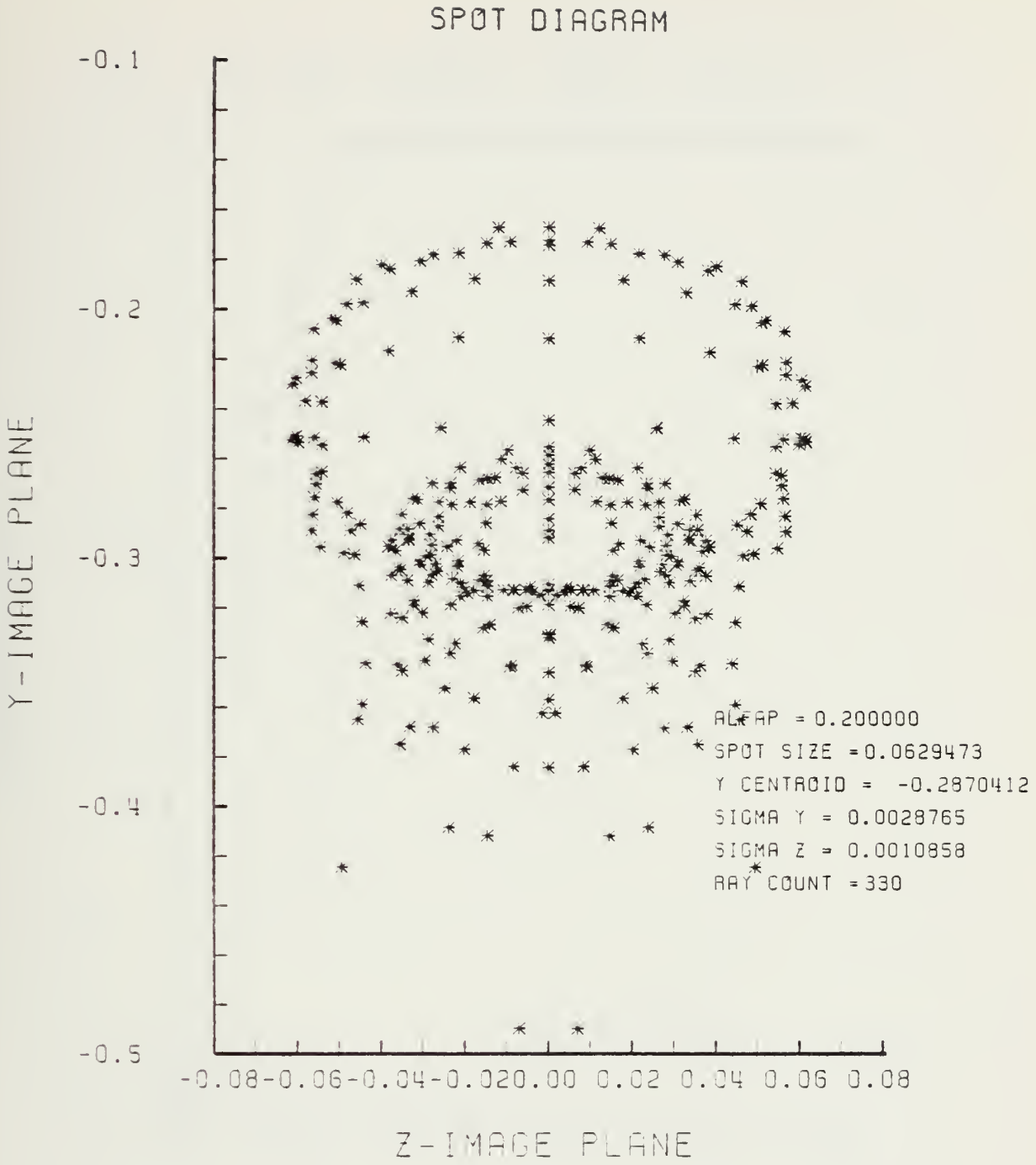

Figure H-8. Spot Diagram for Grid of Figure H-7

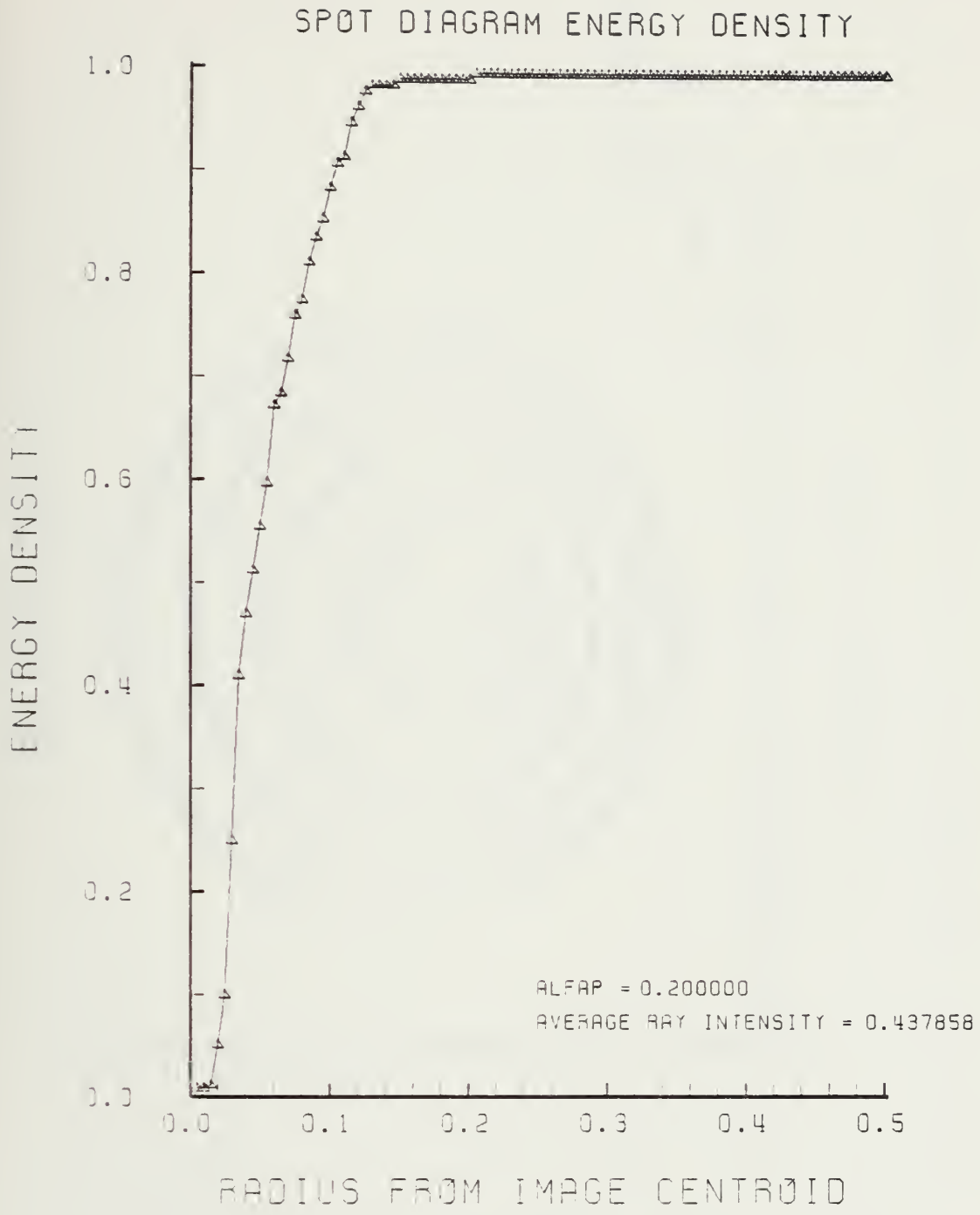

Figure H-9. Encircled Energy of Figure H-8

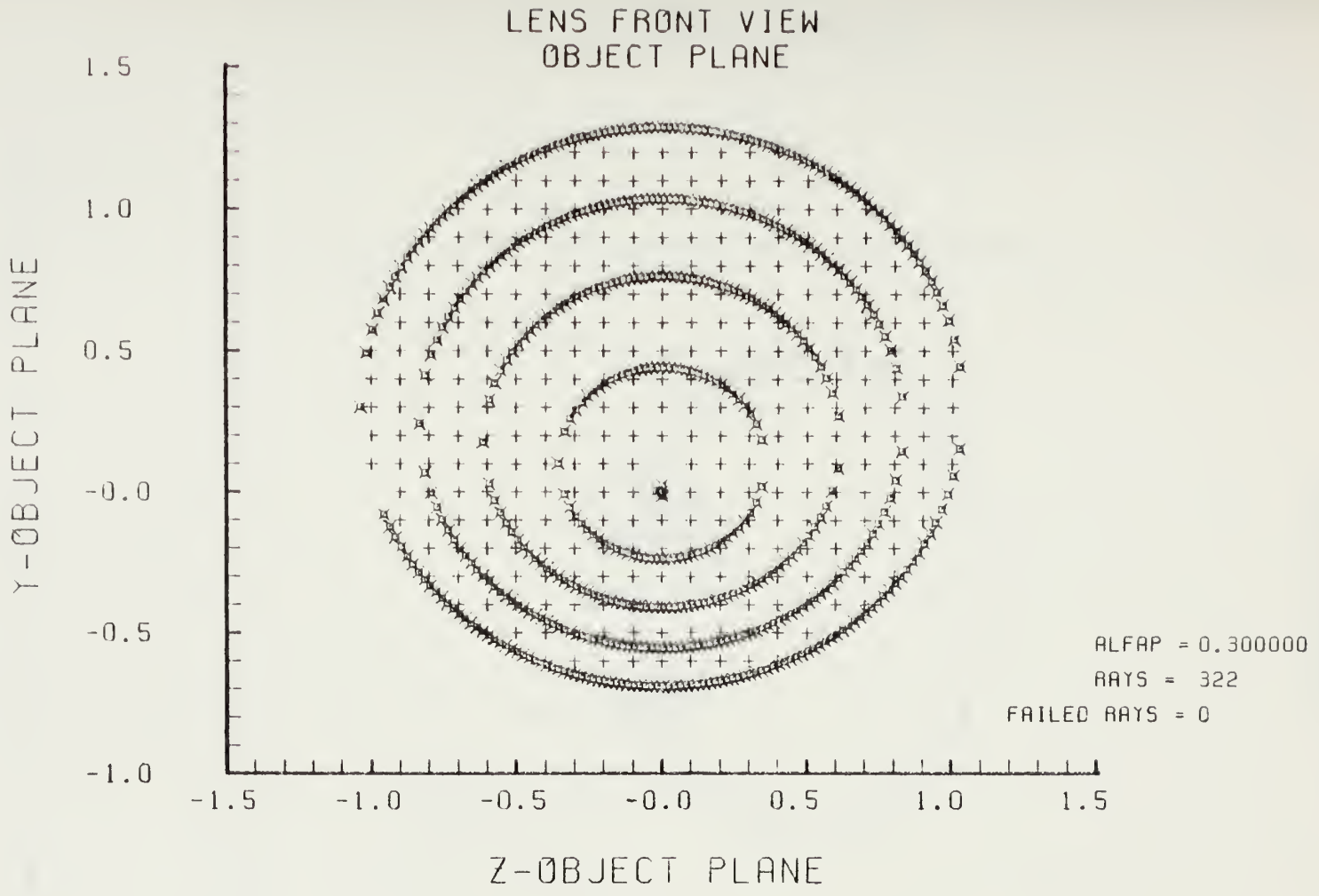

Figure H-10. Grid Plane at $\alpha_p = 0.3$ for Lens of Figure H-1

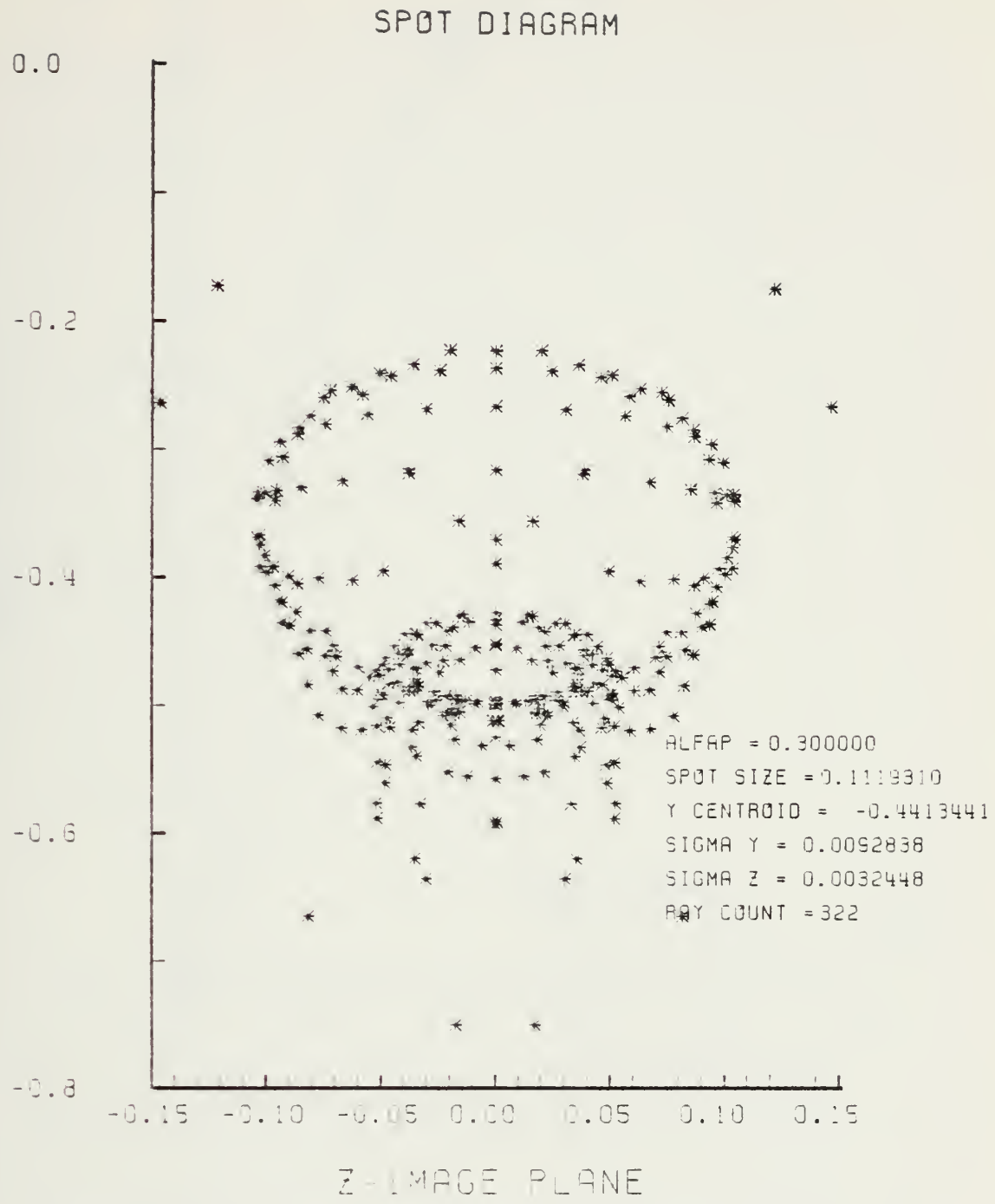

Figure H-11. Spot Diagram for Grid of Figure H-10

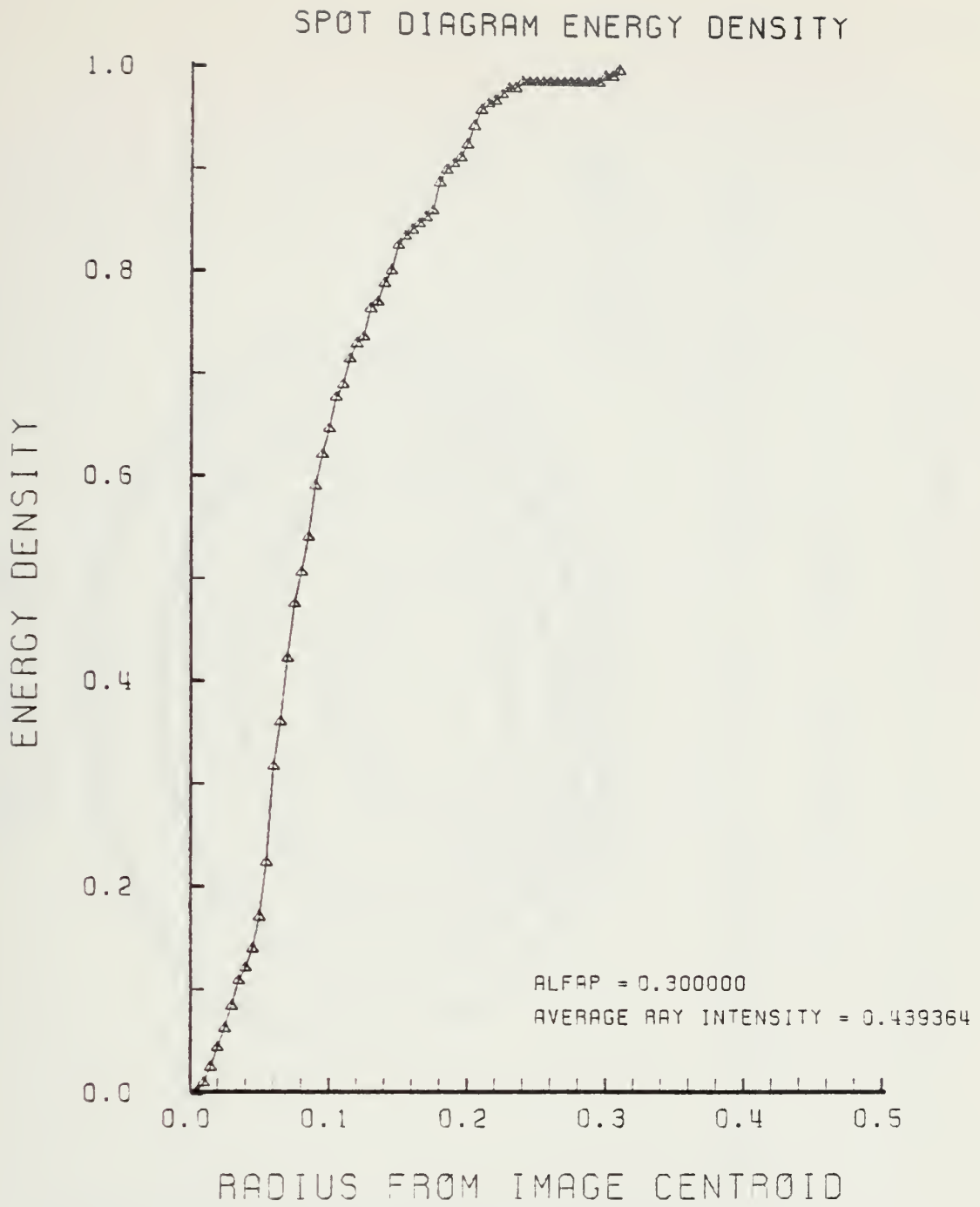

Figure H-12. Encircled Energy of Figure H-11

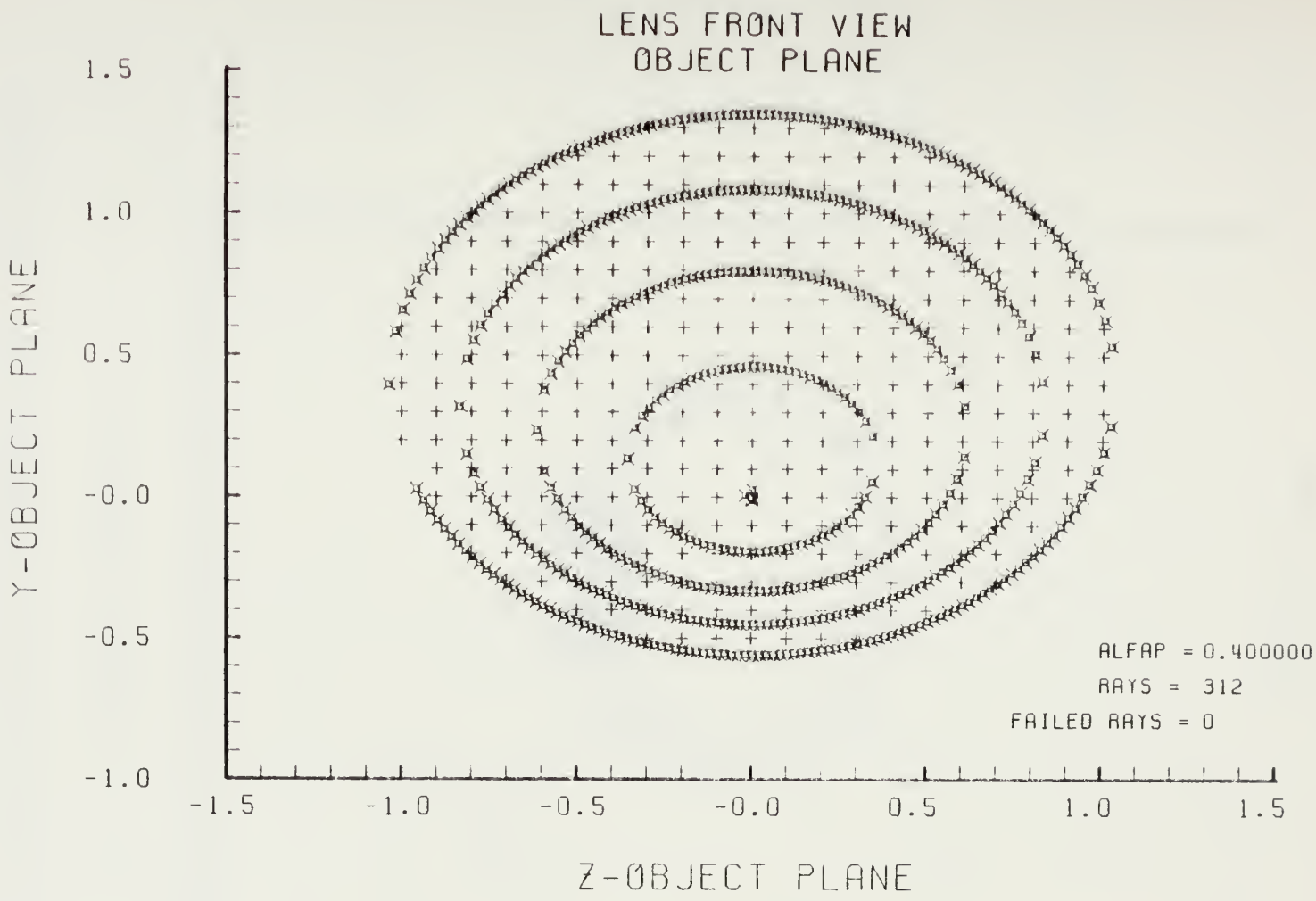

Figure H-13. Grid Plane at $\alpha_p = 0.4$ for Lens of Figure H-1

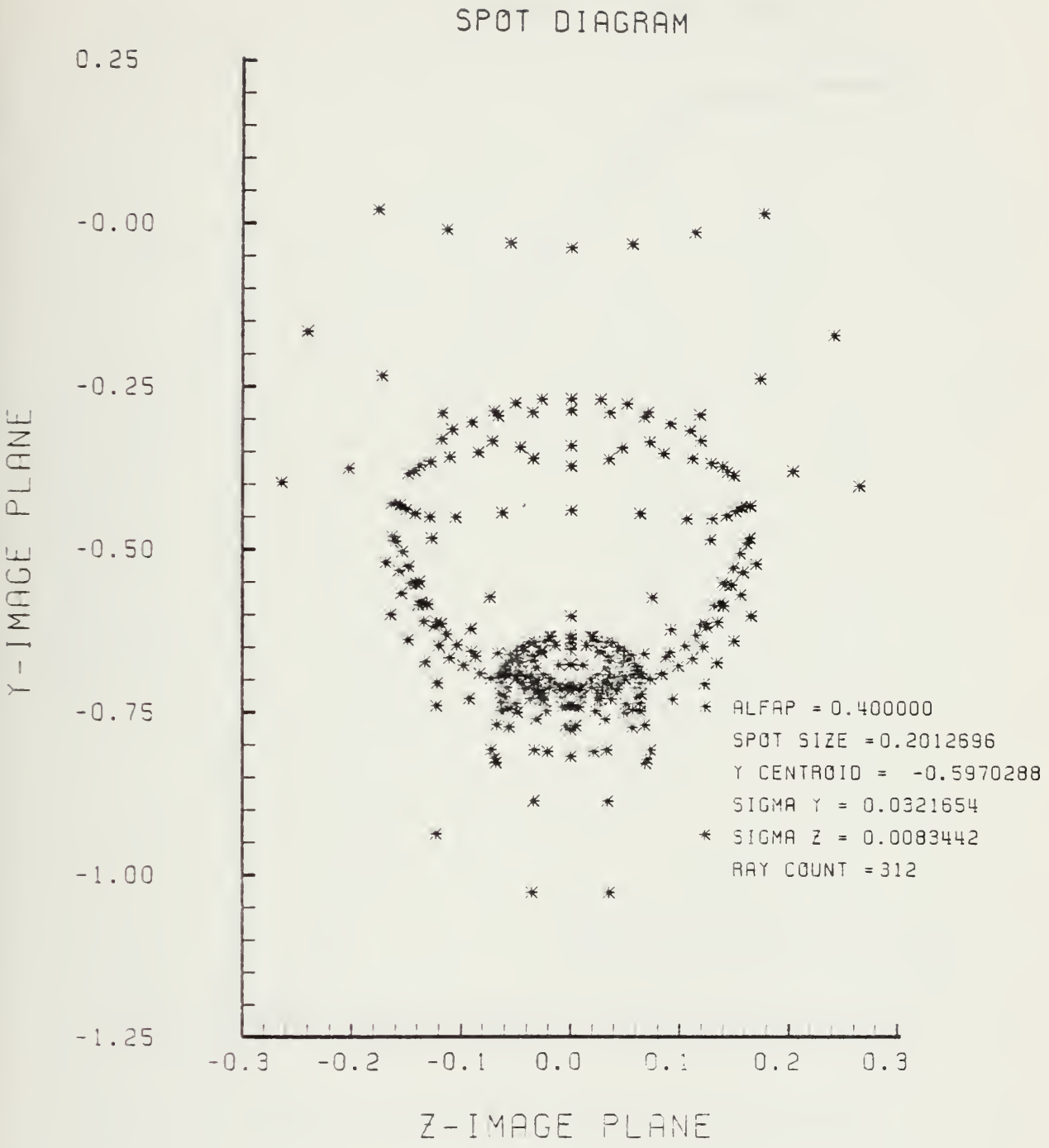

Figure H-14. Spot Diagram for Grid of Figure H-13

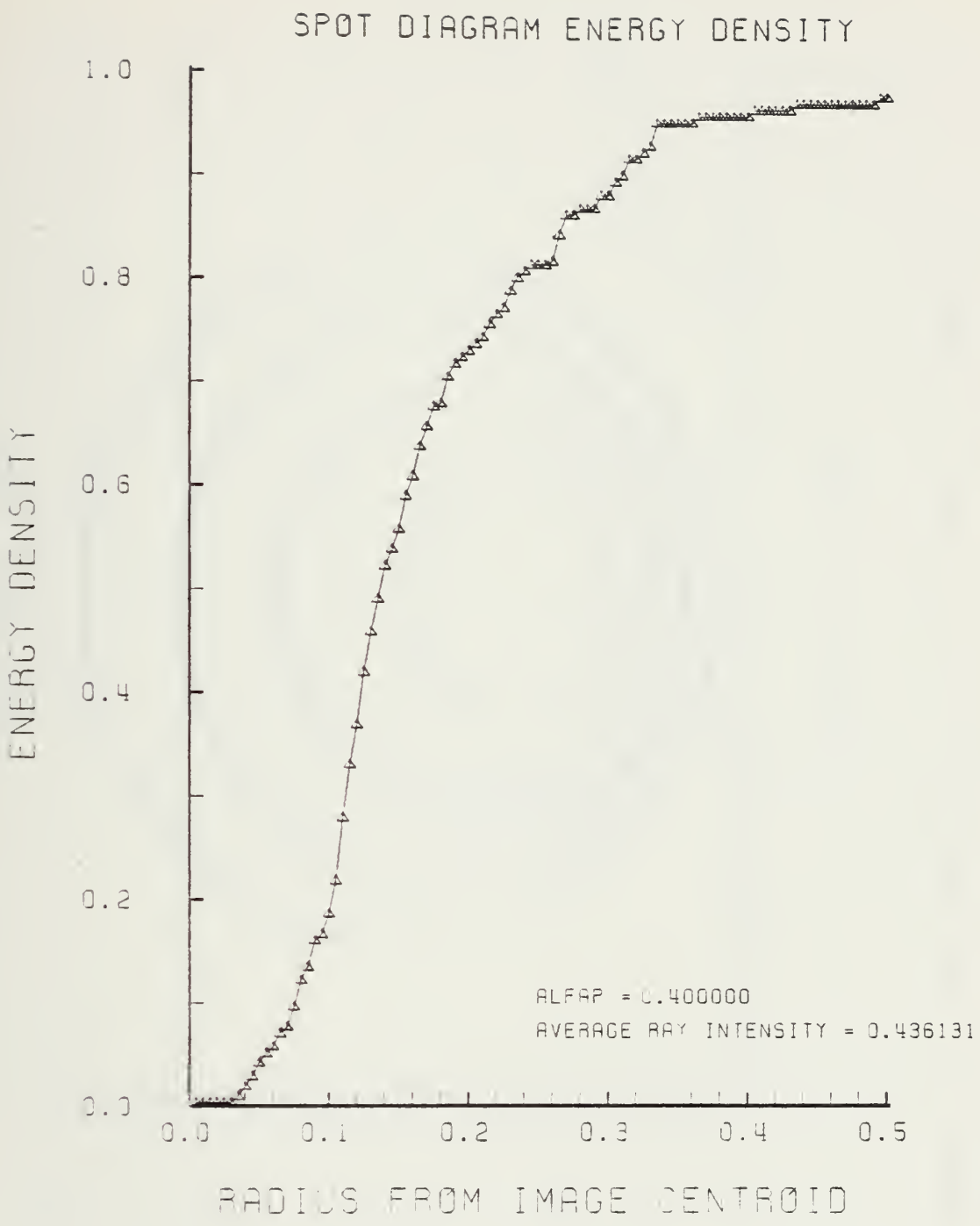

Figure H-15. Encircled Energy of Figure H-14

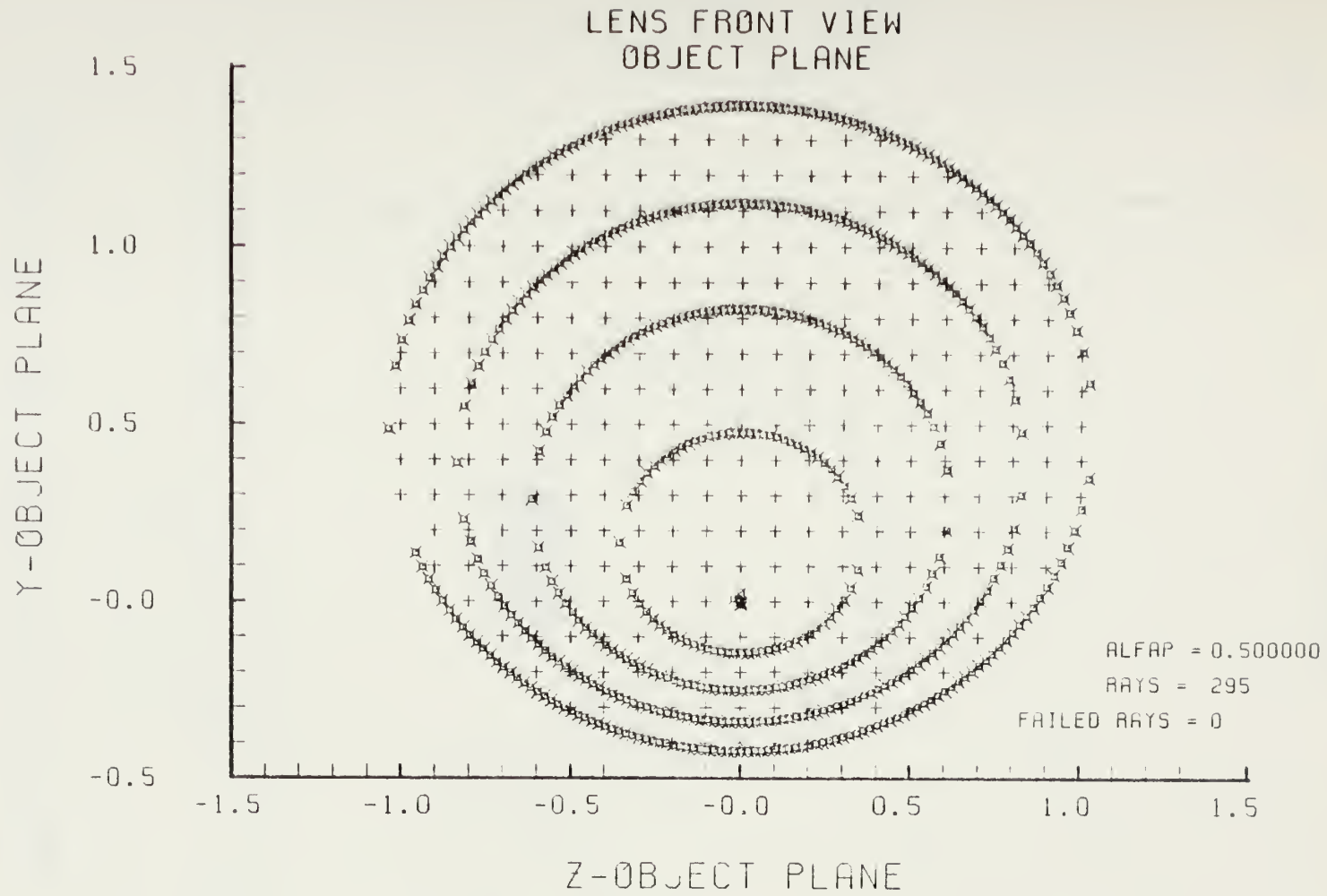

Figure H-16. Grid Plane at $\alpha_p = 0.5$ for Lens of Figure H-1

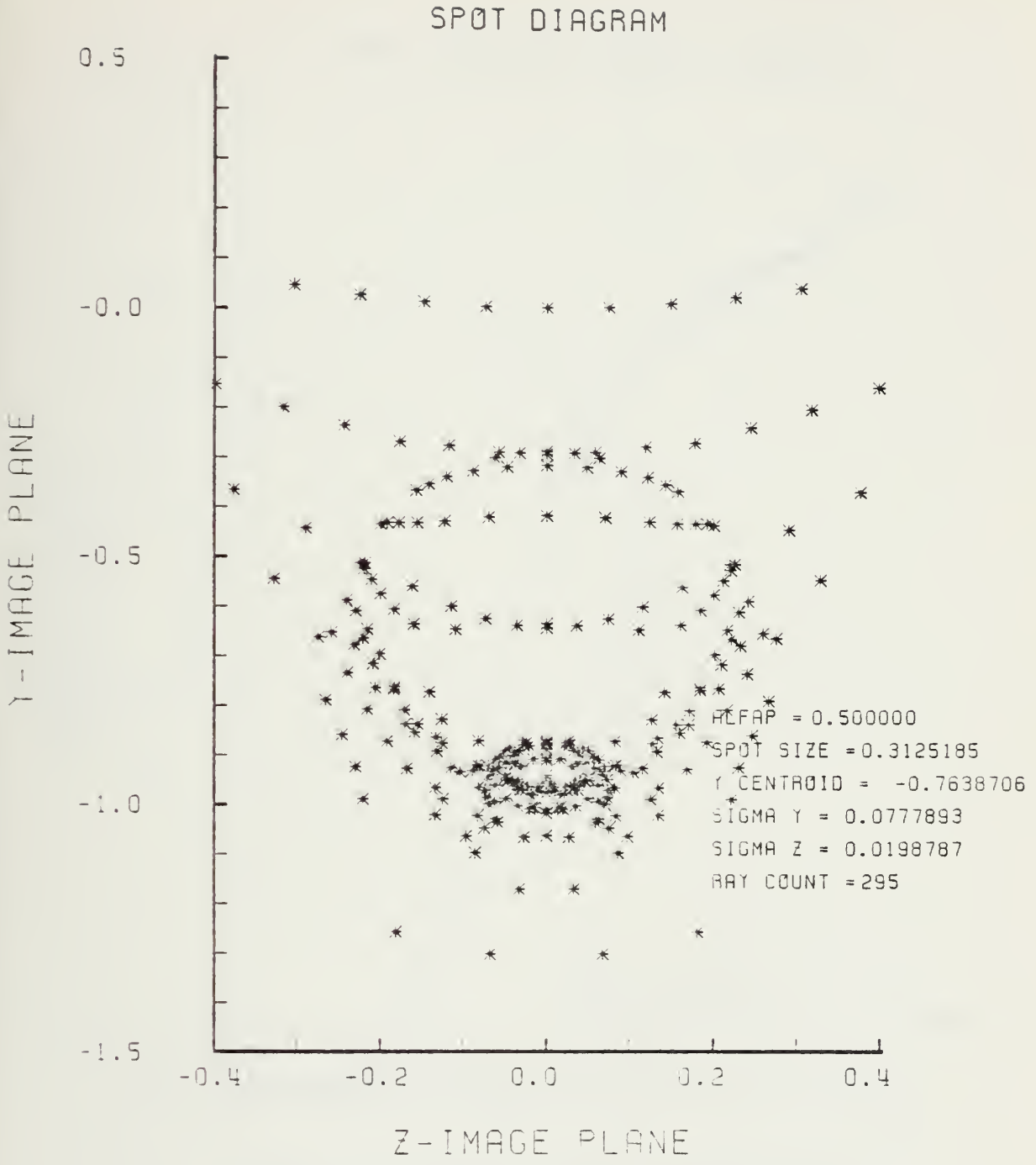

Figure H-17. Spot Diagram for Grid of Figure H-16

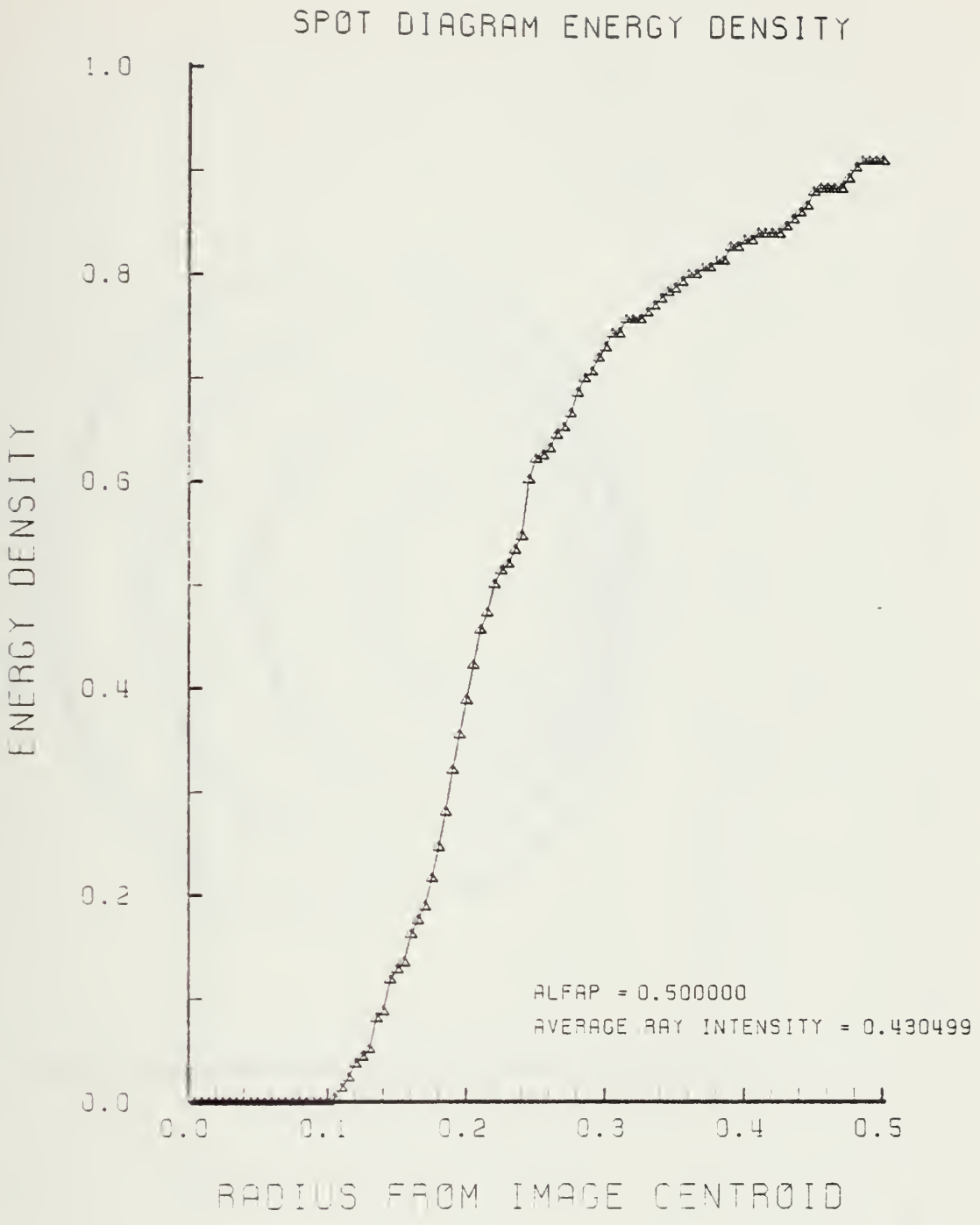

Figure H-18. Encircled Energy of Figure H-17

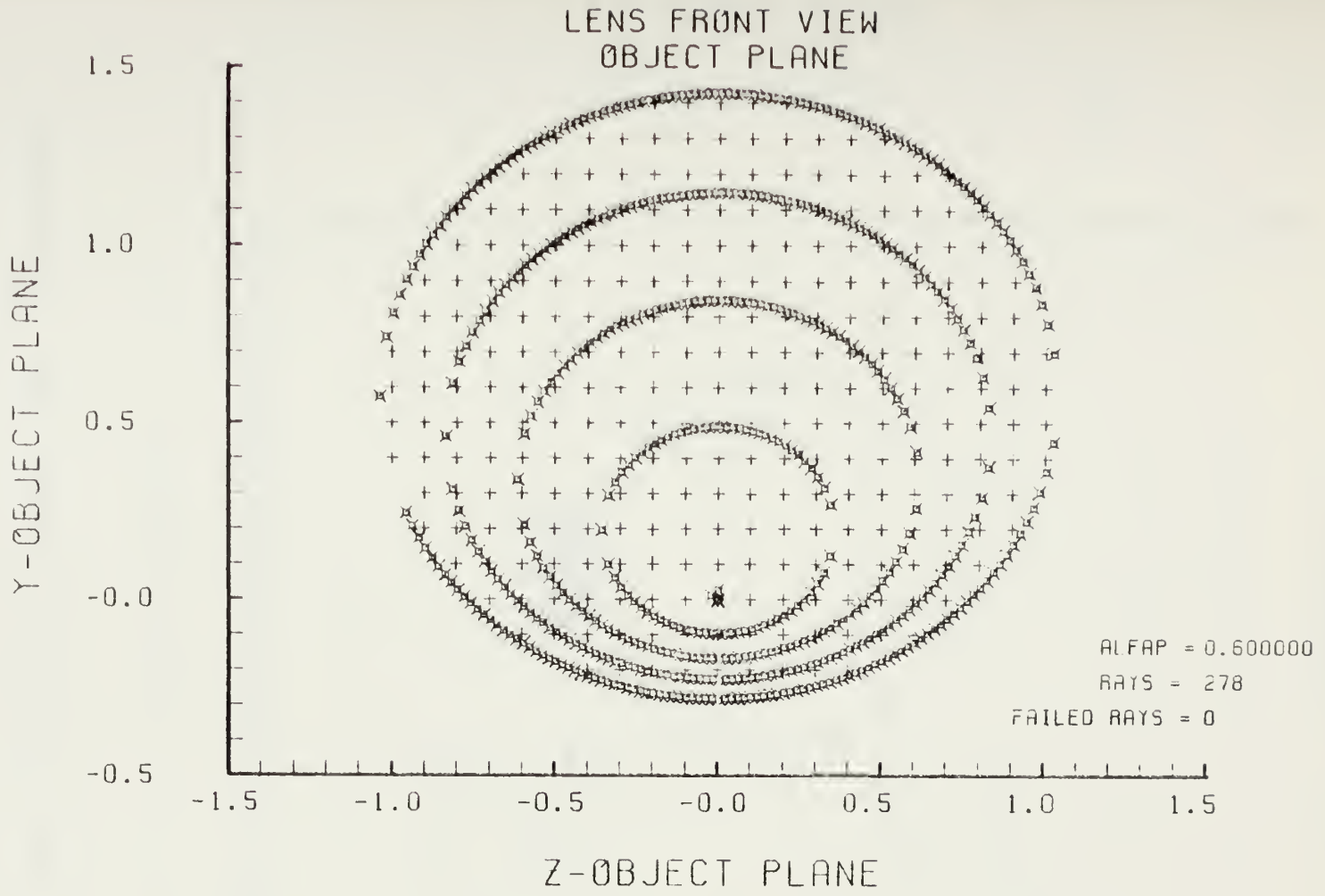

Figure H-19. Grid Plane at $\alpha_p = 0.6$ for Lens of Figure H-1

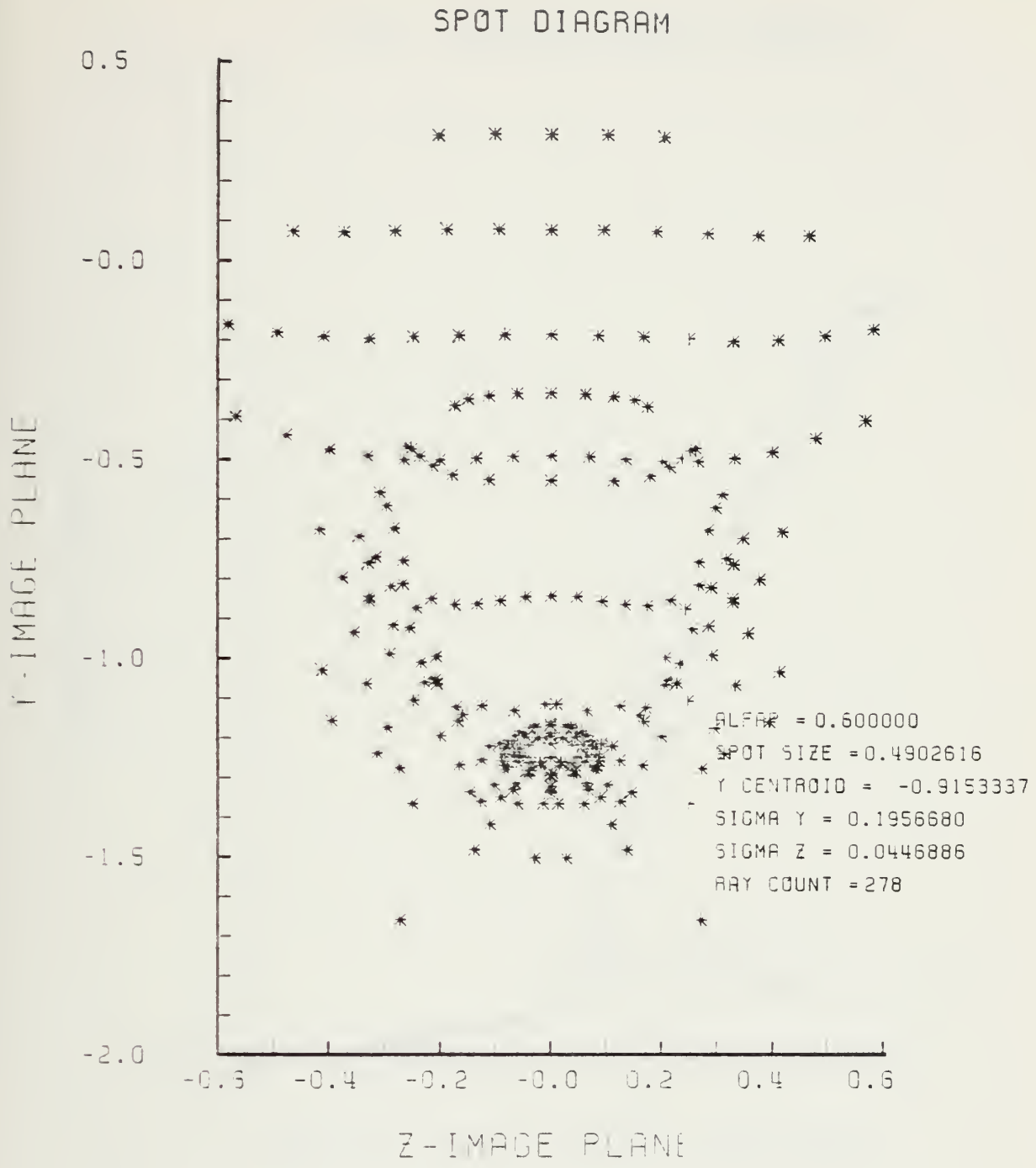

Figure H-20. Spot Diagram for Grid of Figure H-19

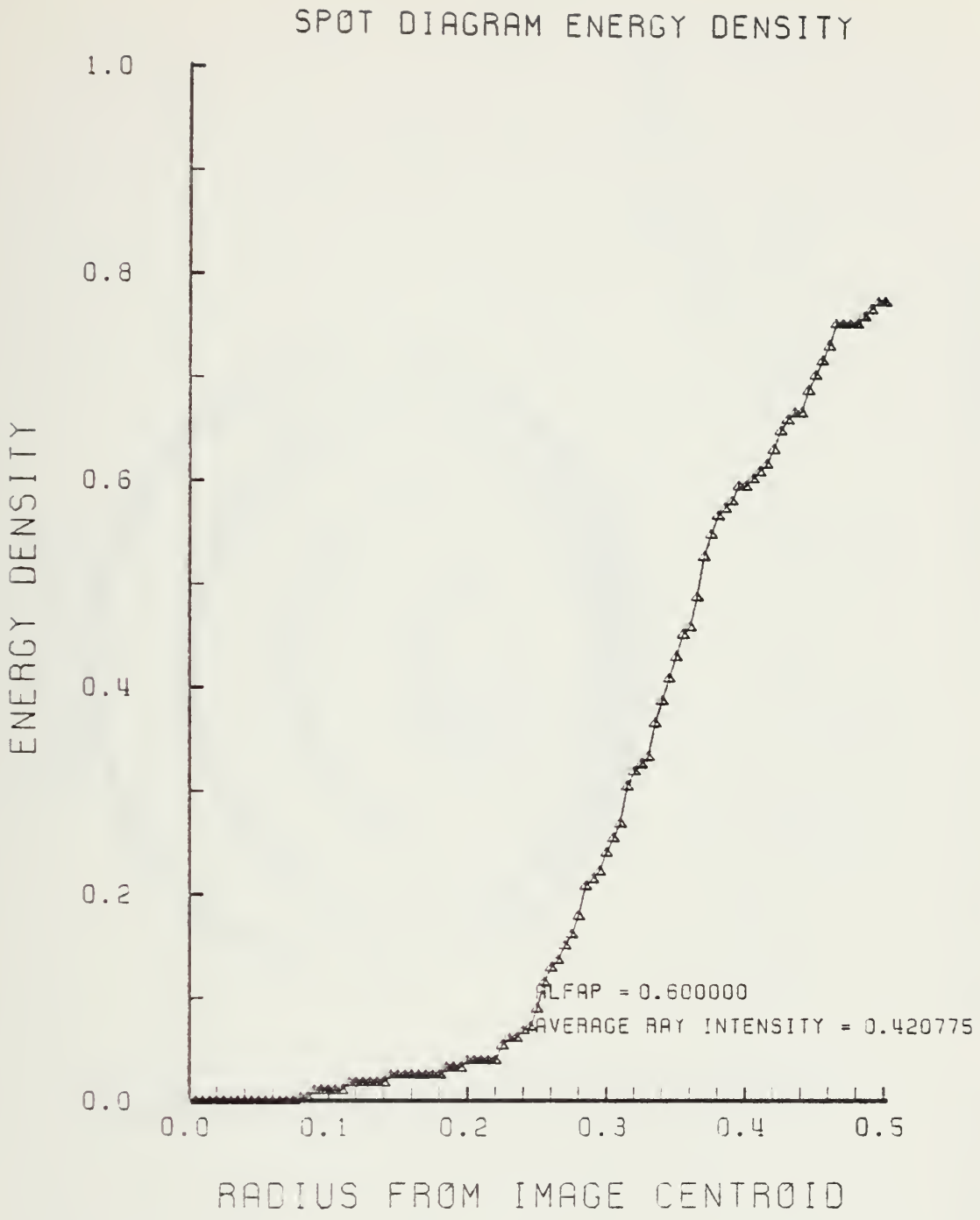

Figure H-21. Encircled Energy of Figure H-20

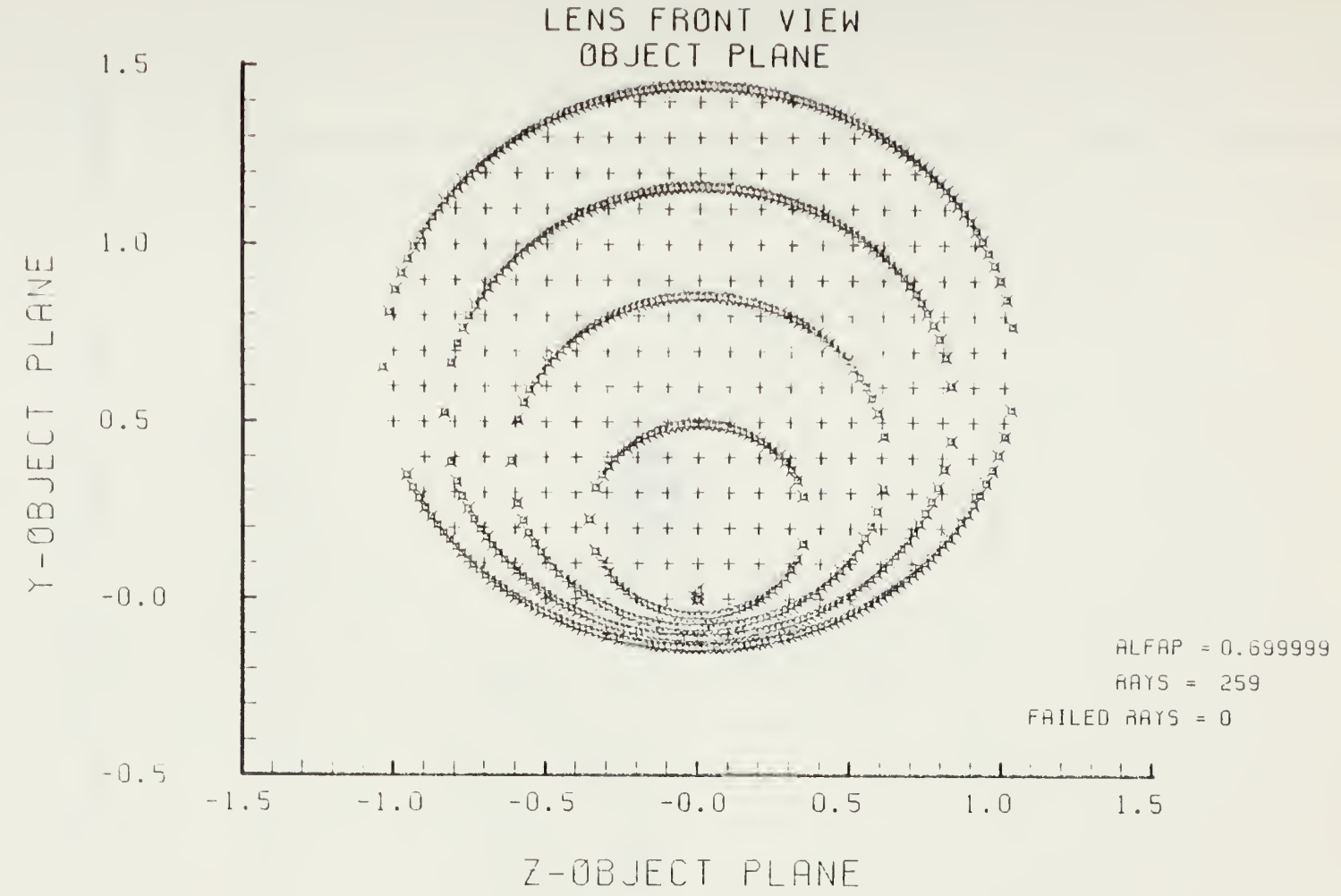

Figure H-22. Grid Plane at $\alpha_p = 0.7$ for Lens of Figure H-1

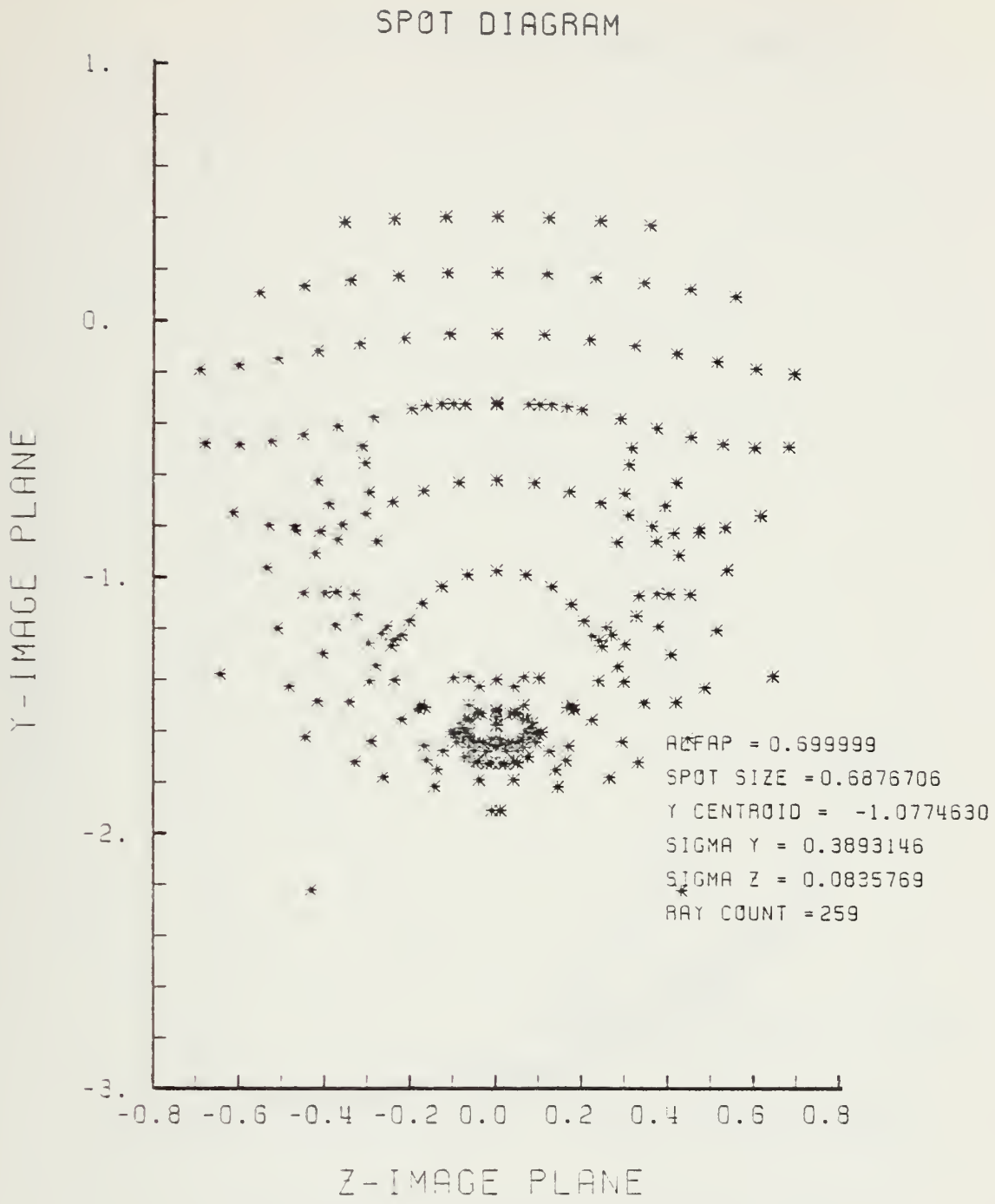

Figure H-23. Spot Diagram for Grid of Figure H-22

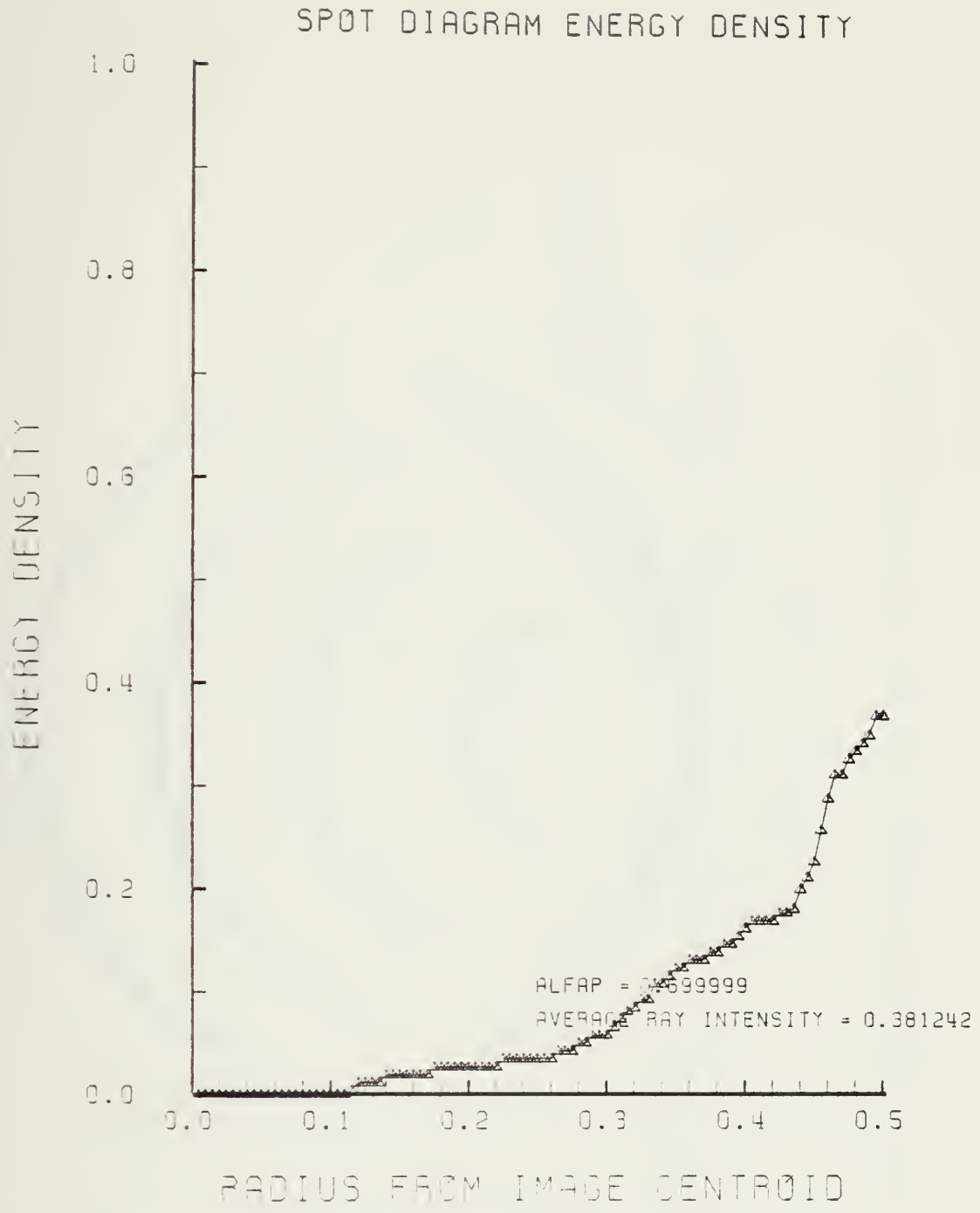

Figure H-24. Encircled Energy of Figure H-23

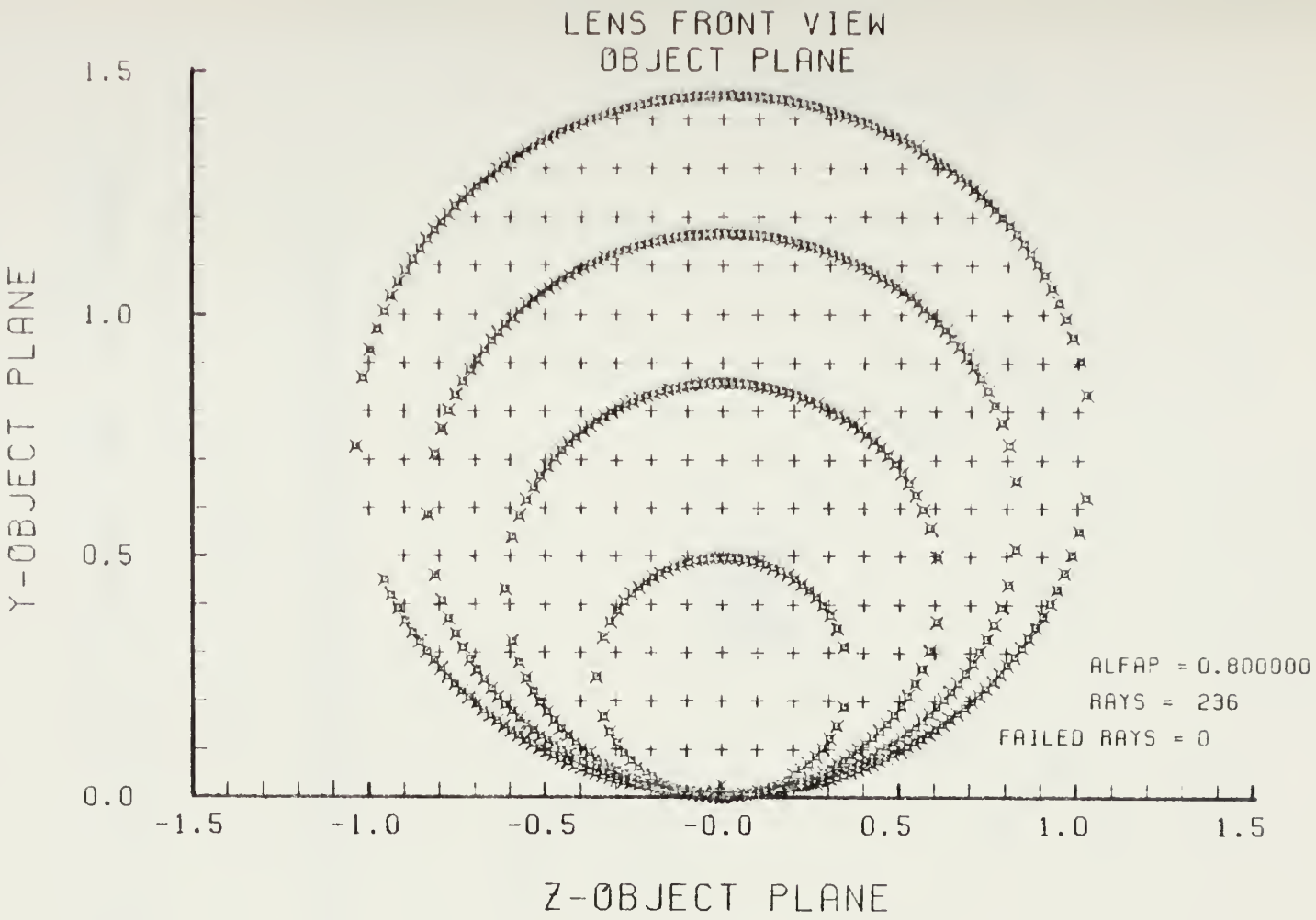

Figure H-25. Grid Plane at $\alpha_p = 0.8$ for Lens of Figure H-1

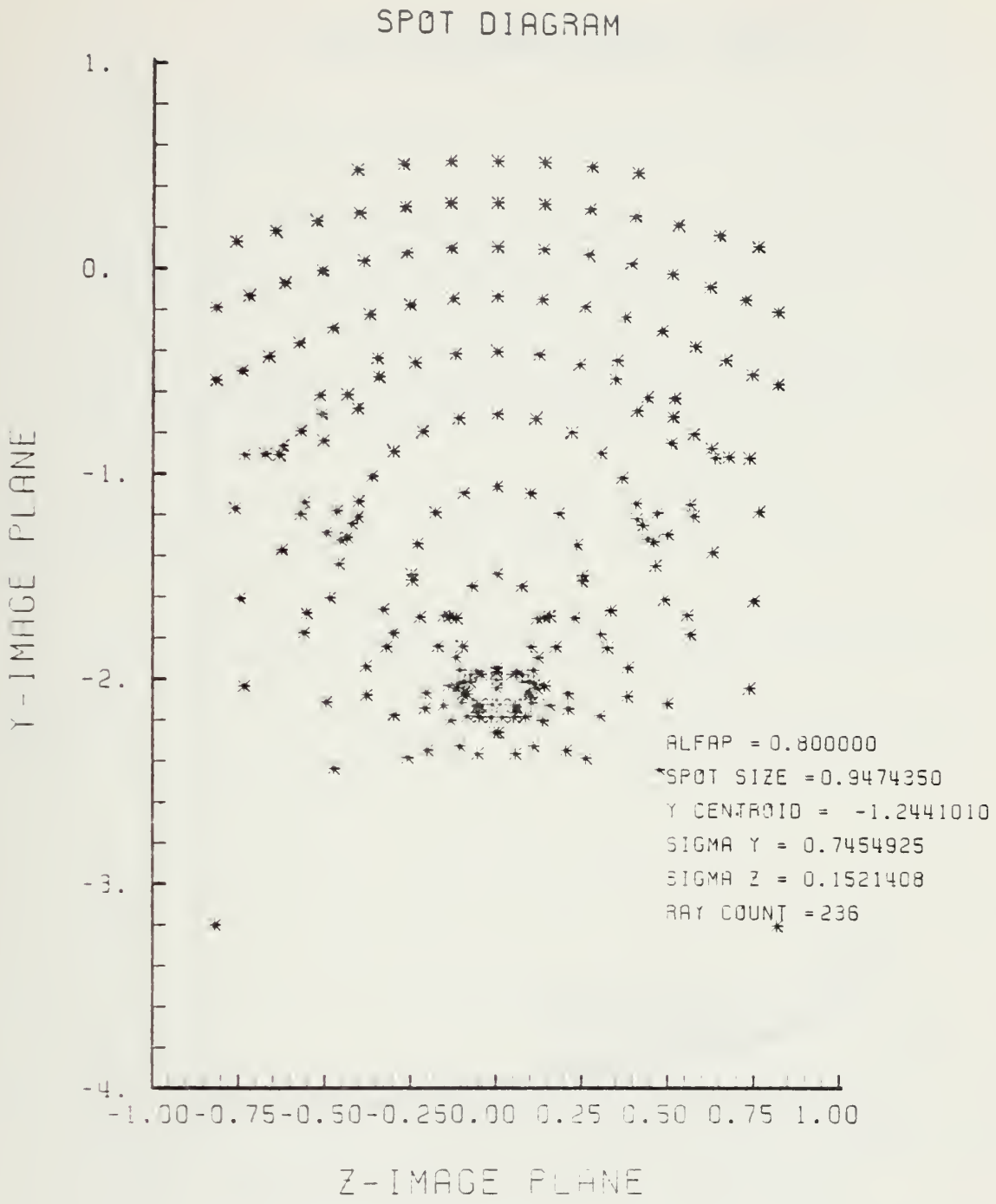

Figure H-26. Spot Diagram for Grid of Figure H-25

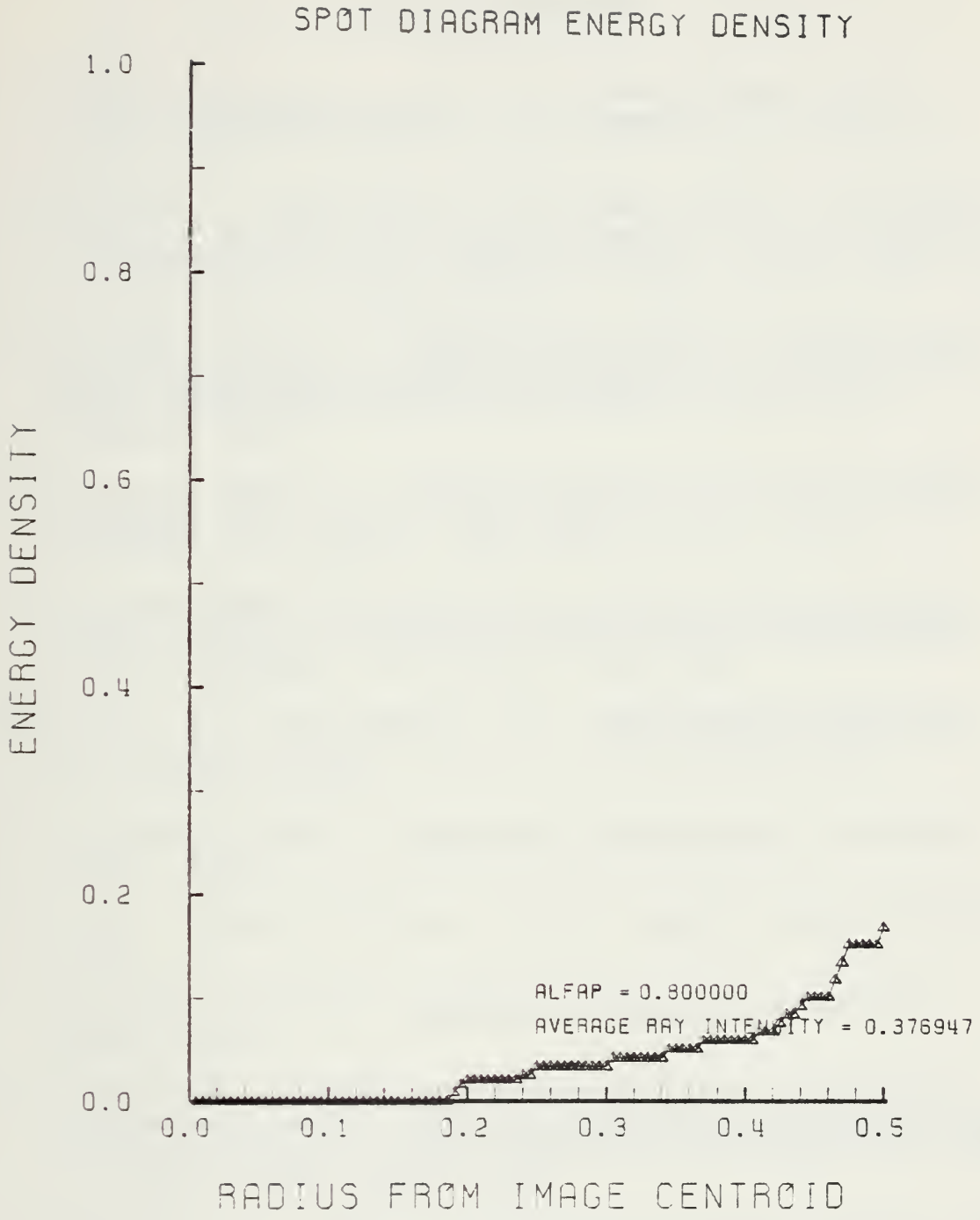

Figure H-27. Encircled Energy of Figure H-26

LIST OF REFERENCES

1. Marchand, Erich W., "Gradient-index imaging optics today", Applied Optics, V. 21, number 6, p. 983, 15 March 1982.

2. Kitano, I., Nishigawa, K., and Momokita, A., "Diffusion behavior of doped polarizable ions in glass during the ion-exchange process", Applied Optics, V. 21, number 6, p. 1017-1020, 15 March 1982.

3. Frazier, Robert L., Exterior Ballastics, Guidance Laws and Optics for a Gun-Launched Missile, M.S. Thesis, Naval Postgraduate School, Monterey, California, December 1980.

4. Terrell, James M., Conical Lens for 5"/54 Gun Launched Missile, M.S. Thesis, Naval Postgraduate School, Monterey, California, June 1981.

5. Amichai, Oded, Sharp Nose Lens Design Using Refractive Index Gradient, Contractor Report, Naval Postgraduate School, Monterey, California, June 1982.

6. Otten, L.J. and Gilbert, K.G., Aero-Optical Phenomena, V. 80, AIAA Progress Series in Astronautics and Aeronautics, 1982.

7. Kingslake, Rudolf, Lens Design Fundamentals, Academic Press, 1978.

8. Hecht, Eugene and Zajac, Alfred, Optics, Addison-Wesley, 1979.

9. Marchand, Erich W., Gradient Index Optics, Academic Press, 1978.

10. Curcio, M.E., "Precision-machined optics for reducing system complexity", Infrared Imaging Systems Technology, Society of Photo-Optical Instrumentation Engineers (SPIE), V. 226, p. 91-97, April 1980.

11. Harney, R.C., "Dual active/passive infrared imaging systems", Infrared Imaging Systems Technology, Society of Photo-Optical Instrumentation Engineers (SPIE), V. 226, p. 74-82, April 1980.

12. Robb, Paul N., "Lens design using optical aberration coefficients", Proceedings of 1980 International Lens Design Conference (OSA), Society of Photo-Optical Instrumentation Engineers (SPIE), V. 237, p. 109-118, 1980.

13. Sharma, Anurog, Kumar, D.A. Vizia, and Ghatak, A.K., "Tracing rays through graded-index media: a new method", Applied Optics, V. 21, number 6, p. 984-987, 15 March 1982.

14. Moore, Duncan T., and Stagaman, Joan M., "Ray tracing in anamorphic gradient-index media", Applied Optics, V. 21, number 6, p. 999-1003, 15 March 1982.

INITIAL DISTRIBUTION LIST

		No. Copies
1.	Defense Technical Information Center Cameron Station Alexandria, Virginia 22314	2
2.	Library, Code 0142 Naval Postgraduate School Monterey, California 93940	2
3.	Department Chairman, Code 67 Department of Aeronautics Naval Postgraduate School Monterey, California 93940	1
4.	Distinguished Professor A. E. Fuhs Code 67Fu Department of Aeronautics Naval Postgraduate School Monterey, California 93940	4
5.	LTC Rene Larriva, USMC Defense Advanced Research Projects Agency 1400 Wilson Blvd. Arlington, Virginia 22209	2
6.	Commander, Naval Sea Systems Command Naval Sea Systems Command Headquarters Attn: Code 62YC Washington, D.C. 20362	1
7.	Mr. Conrad Brandts Naval Surface Weapons Center Dahlgren, Virginia 22448	1
8.	Dr. Fred Billig Applied Physics Lab Johns Hopkins Road Laurel, Maryland 20810	1
9.	Commander, U.S. Army Armament Research and Development Command (ARRAD COM) Attn: Mr. Lou Marino Dover, N.J. 07801	1
10.	Deputy Chief of Staff for Research Development and Studies Headquarters USMC Washington, D.C. 20370	1

11.	Commander Development Command USMC Base Quantico, Virginia 22134	1
12.	Commander Artillery Development Command Fort Sill, Oklahoma 73503	1
13.	Captain Herbert M. Carr 2100 Raleigh Ave. Austin, TX 78703	3
14.	Dr. Lloyd Smith Code 3205 Naval Weapons Center China Lake, California 93555	1
15.	Dr. Harold L. Bennett Code 3272 Naval Weapons Center China Lake, California 93555	1
16.	Dr. T. G. Bergman Code 3941 Naval Weapons Center China Lake, California 93555	1
17.	Dr. Oded Amichai Ministry of Defense P.O.B. 2250 Haifa, ISRAEL	1
18.	Research Administration Code 012A Naval Postgraduate School Monterey, California 93940	1
19.	Deputy Under Secretary of the Army for Operations Research Room 2E261, Pentagon Washington, D.C. 20310	1
20.	LT James Terrell, USN Code 290 Supervisor of Shipbuilding, Conversion, and Repair, USN Pascagoula, MS 39567	1